

Dissertation zur Erlangung des Doktorgrades
der Fakultät für Chemie und Pharmazie
der Ludwig-Maximilians-Universität München

Energetic Organo-Silicon Compounds —Silicon Makes the Difference—

Anian Peter Nieder

aus

Hünfeld

2013

Erklärung

Diese Dissertation wurde im Sinne von §7 der Promotionsordnung vom 28. November 2011 von Herrn Prof. Dr. Thomas M. Klapötke betreut.

Eidesstattliche Versicherung

Diese Dissertation wurde eigenständig und ohne unerlaubte Hilfe erarbeitet.

München, den 6. September 2013

Dissertation eingereicht am 17. Sept. 2013

1. Gutachter: Prof. Dr. T. M. Klapötke

2. Gutachter: Prof. Dr. K. Karaghiosoff

Mündliche Prüfung am 22. Oktober 2013

„Ich wusste ja gar nicht, daß Hirten lesen können,“
bemerkte eine weibliche Stimme an seiner Seite. [...]

„Weile Schafe mehr lehren können als Bücher,“
erwiderte der Jüngling.

Der Alchimist, Paulo Coelho, 1991.

Danksagung

Mein Dank gilt zuallererst meinem Doktorvater Herrn Prof. Dr. Thomas M. Klapötke für die jahrelange Unterstützung, auch schon vor meiner Dissertation, die Möglichkeit der Teilnahme an vielen Tagungen und Fortbildungen, sowie die gute fachliche und finanzielle Unterstützung. Darüber hinaus möchte ich mich für das spannende und einzigartige Thema meiner Arbeit bedanken.

Herrn Prof. Dr. Konstantin Karaghiosoff möchte ich für die fachlichen und auch außerdisziplinären Diskussionen und Hilfestellungen danken, aber ganz besonders für die gemeinsamen Erlebnisse bei verschiedensten Gelegenheiten.

Herrn Akad. ORat. Dr. Burkhard Krumm gilt ebenfalls ein besonderer Dank für die Zeit und Geduld, die hervorragende Unterstützung und Anleitung seit meiner Diplomarbeit und den botanisch und kulinarischem Austausch.

Ich danke „der guten Seele“ Frau Irene Scheckenbach für ihr unermüdliches Engagement für den gesamten Arbeitskreis.

An dieser Stelle möchte ich mich für die gute und erfolgreiche Zusammenarbeit bei meinen Kooperationspartnern Dr. Dennis Troegel und Prof. Dr. Reinhold Tacke, sowie Dr. Stuart Hayes, Dr. Raphael Berger und Prof. Dr. Norbert Mitzel und zu guter Letzt Dr. Jane Murray und Dr. Peter Politzer bedanken. Camilla Evangelisti gebührt ein besonderer Dank, nicht nur für zahlreiche Rechnungen, die sie für mich durchgeführt hatte, sondern auch für die täglichen Vorführungen ihrer italienischen Kochkünste.

Ein ganz besonderer Dank gilt meinem langjährigen Laborkollegen Dr. Franz Martin für die vielen arbeitsreichen Stunden im Labor, für das Vertrauen und das Gefühl der Sicherheit, sowie die Unterstützung bei allen aufgetretenen Schwierigkeiten und Risiken. Dies gilt auch für Marcos Kettner, der zudem mit einem guten Tropfen und sehr viel Obst, lange Abende und Wochenenden im Labor zu einem fruchtigen Vergnügen machte. Meinen Kollegen Sebastian Rest, Andreas Preimesser, Carolin Pflüger, Quirin Axthammer, Regina Scharf, Magdalena Rusan und dem „Hadesche“ Vera Hartdegen möchte ich für die Zeit und Zusammenarbeit danken. Auch ein Dankeschön an Stefan Huber für Fachsimpeleien, zahlreichen Messungen und die schnelle und zuverlässige Versorgung

mit Chemikalien. Alexander Dippold und Stefanie Schönberger für die Korrekturen und Feedbacks zu meiner Arbeit und darüber hinaus.

Meinen ehemaligen Kollegen und Doktoros Jan Welch, Matthias Scherr, Jörg Stierstorfer, Hendrik Radies, Karin Lux, Stefan Sproll, Norbert Mayr, Karina Tarantik, Franziska Betzker, Niko Fischer und Alexander Penger danke ich für die fachlichen Diskussionen für angenehme Atmosphäre im Arbeitskreis und im Besonderen für die schöne Zeit.

Bei meinen fleißigen Praktikanten möchte ich mich für ihre Bemühungen besonders bedanken und wünsche Andreas Nordheider, Michael Hörmannsdorfer, Julia Nagy, Regina Scharf, Ksenia Fominykh, Julia Nafe, Matthias Trunk, Oliver Richter, Christian Schütz, Laura Ascherl und Lisa Göpfert viel Erfolg für Ihre Zukunft.

Ein besonderer Dank gilt meiner Familie, die durch ihre jahrelange Unterstützung und den Rückhalt, die Ausbildung bis zu diesem Punkt möglich gemacht hat.

Table of Content

I.	Introduction	3
	Introduction	4
	Role of Silicon in the Field of Energetic Materials	8
	Theoretical Background	9
	Goals	11
II.	Summary	15
III.	Sila-Substitution of Alkyl Nitrates	28
	Introduction	29
	Results and Discussion	31
	Conclusion	54
	Experimental Section	55
	Acknowledgment	65
IV.	Azidomethyl Silane	70
	Introduction	71
	Results and Discussion	72
	Conclusion	76
	Experimental Section	77
	Acknowledgment	80
V.	Hexa-Substituted Disiloxanes	83
	Introduction	84
	Results and Discussion	86
	Conclusion	105
	Experimental Section	105
	Acknowledgment	110

VI.	Reaction Force Analysis and the Role of σ-Hole	113
	Introduction	114
	Results/Approach	120
	Discussion and summary	128
	Acknowledgment	129
VII.	Phenylsilanes and Siloxanes	134
	Introduction	135
	Results and Discussion	136
	Conclusion	157
	Experimental Section	157
	Acknowledgment	164
VIII.	Azole and Nitro Silanes	167
	Introduction	168
	Results and Discussion	169
	Conclusion	184
	Experimental Section	185
	Acknowledgment	190
IX.	Theoretical Approach of Energetic Silane	195
	Introduction	196
	Results and Discussion	201
	Conclusion	226
	Acknowledgment	228
	Supporting Information	S-1
	V. Hexa-Substituted Disiloxanes	S-1
	IX. Theoretical Approach of Energetic Silane	S-7

I. Introduction

Energetic silanes

AnianNieder3 – 14

Introduction



General approaches to the characteristics and design of common energetic materials. In addition, an abridgment of recent application and research of silicon and silanes in the topic of

energetic materials is given. The thermo-dynamic and theoretic computation background of detonation and impulse values are illustrated in an overview.

Introduction

The topic of energetic materials comprises materials with high energy content which can be released by an exothermic decomposition reaction. In a thermodynamic point of view the energy can be accumulated by chemical moieties with positive heat of formation in an optimized case.[1,2] Furthermore in chemical point of view, mixing an energy releasing component (fuel) in combination with an oxidizing substance (oxidizers) are the general building strategy for most of the energetic materials.[1–4] In addition, which is the main decision to call a compound high energetic is the way and kind of releasing the molecular stored energy and especially the time scale of the process (usually in a range of 10^{-2} to 10^{-6} sec).[1,2] In general, the topic can be divided into several subsections of rapid decomposing materials: the section of explosives[1,5], propellants[5] and pyrotechnics[5] is focused on the following.[1,2,4,6,7]

Explosive materials involve mainly primary and secondary explosives. An easy ignitability by heat, flame, radiation and/or mechanical manipulation (high sensitivity[5] is typical for primary explosives, for example lead azide $\text{Pb}(\text{N}_3)_2$).[5,7] The most important property of primary explosives is the occurrence of a deflagration (sub-sonic burning)[5] to detonation (super-sonic burning)[4,5] transition during the first microseconds after ignition. This process is called deflagration-to-detonation transition (DDT).[4,7,8] However the energy release and the performance are relatively low. The release of high amounts of energy and the capability of establishing a propagating shock front. This shock front should lead to the possibility to introduce the detonative decomposition into other materials, which are able to sustain the propagating shock front and increase the detonation performance.[4–7] These types of compounds are called secondary explosives.[5,7,8,9] They are not as easy to ignite as primary explosives by external stimuli (low sensitivity) and even more safe in handling. In general, they release much more energy as primary explosives.[7] The energy release is primarily due to pressure-volume work, which leads to

shattering effects to the surrounding area. The processes during detonation are complex and chemical and physical descriptions are found from many different authors.[1,2,4,7,8]

The decomposition of propellants and pyrotechnics is in the range of sub-sonic burning, deflagration[1,5,7] respectively. In the case of pyrotechnics, the requirements are focused onto specifically designed effects, like heat, special light emission spectra, smokes (for example coloured smokes) or sounds.[7] They are mostly mixtures by different kinds of components, whereupon each component has individual tasks to design the properties of the pyrotechnical mixture. For example the colorant and sparkling for fireworks, the heat and radiation imitation of the exhausted of turbines or other engines for decoy flare or the smoke generating properties are individually designed by special additives.[7] The most famous example is black powder.[5] Usually the oxidizer and the fuel are not combined in one molecule, in contrast to many primary and secondary explosives. The same for pyrotechnics is true for propellants. But in contrast to the former, a fast and high amount of gaseous exhaust (preferable light gaseous molecules) and a high combustion temperature are the main topics to increased the impulse of an propellant.[3]

From a chemical point of view the requirements for energetic materials are a positive heat of formation, an energy delivering backbone and an oxygen source. The main challenge is the simultaneous fulfilment of high performance, low producing costs, high safety and stability of the compound to ensure safe synthesis and handling. Recently, the interest in environmentally friendly compounds and also for its decomposition products is increased. Just focusing onto compound design, alkane backbones combine several advantages. First of all a good energy release by oxidation to CO/CO₂ ($\Delta_f H^\circ(\text{g}): -111/-394 \text{ kJ/mol}$) and H₂O ($\Delta_f H^\circ(\text{g/l}): -242/-286 \text{ kJ/mol}$),[4] the chemical flexibility, structural manifoldness and the stability of structures also in cooperation with other elements and structures turn carbon-hydrogen moieties into an almost ideal building block/fuel for energetic materials (compare given structures in Figure 1.1). In addition, the obtained volume of gas by CO/CO₂ and water has a positive influence into the desired energetic values (see below). Oxidation with environmental oxygen is first of all slow and the amount of oxygen is too low for releasing the energy of the oxidized molecule efficiently. To oxidize the carbon-hydrogen backbone, oxygen carriers like nitro and nitrate moieties are introduced at the backbone

structure (like in NG, TNT or RDX). Due to the increased oxygen content in comparison to the content in air and the independence

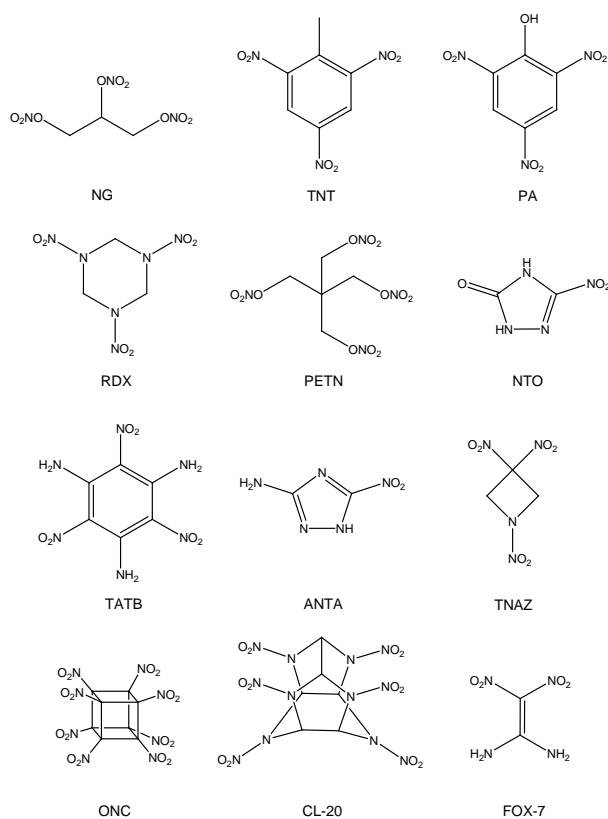


Figure 1.1. Molecular structure of several high energetic compounds (NG: glycerine trinitrate[5], TNT: 2,4,6-trinitrotoluene[5], PA: picric acid[5], RDX: 1,3,5-trinitro-1,3,5-triazine[5], PETN: pentaerythrityl tetranitrate[5], NTO: 3-nitro-1,2,4-triazol-5-on[5], TATB: 2,4,6-triamino-1,3,5-trinitrobenzene[5], ANTA: 5-amino-3-nitro-1,2,4-triazole[2], TNAZ: 1,3,3-trinitroazetidine[5], ONC: octanitrocubane[7], CL-20: 2,4,6,8,10,12-hexanitro-2,4,6,8,10,12-hexaazaisowurtzetane[7] and FOX-7: 1,1-diamino-2,2-dinitroethene[7]).

of the environmental nature (underwater, in solid materials etc.), increase the reaction rate, efficiency and also the energy output.[2–4] In addition to the already mentioned advantages of the nitro and nitrate moieties, the reduction of nitrogen into molecular N_2 strongly boost the energy release[2,3] and increases the gas volume. Ideally this happens without the need of oxygen (sometimes creating small amounts of NO), which consequently stays available for reacting with carbon and hydrogen. Moreover, nitrogen rich moieties like azides or the thermodynamically stable nitrogen heterocycles like tetrazoles, triazoles and tetrazines lift the performance (like in NTO and ANTA).[2,3] Modern energetic materials increase the energy output by using ring or cage strained backbone structures (like TNAZ, ONC and CL-

20). In addition, poly-chained and caged structures have typically higher densities as acyclic structures, due to a higher amount of tertiary and quaternary atoms like C and N.[2,3] The often laborious syntheses of these compounds raise the costs, which results in an unprofitable commercial use (for example in the case of ONC). In addition to the energetic moieties, conjugational functional structures can stabilize the molecule by mesomery, inductive effects or by intra- or intermolecular coordination. Therefore hydroxy, keto, amino and aromatic moieties for example are often found structural features in energetic materials (like in NTO, ANTA, TATB and FOX-7).[2,3,7,9]

Zooming out from the chemical structure to the micro- and macroscopic shaping and formulation (different phases in solid state, co-packing, shaping of particles etc.), one component can also be manipulated in this way that it changes its characteristics. One example is PETN, which is used as secondary explosives but also can have characteristics towards external stimuli like primary explosives just by changing the particle size and shape. In general, an energetic compound can be almost as flexible in their employment as its structural variation, additionally the possibilities of mixing different components (additives, binders ect.) and formulations to design the desired properties.[2,4,7]

The characterisation of explosives materials is performed by several testing procedures. Standard procedures like shock (drop hammer), friction (friction apparatus) thermal (fast heating and slow heating tests, like different scanning calorimetry DSC) and electrostatic stimuli (electrostatic discharge ESD) are required for impression of safe manipulating and handling explosive materials.[4,6] In the case of explosives, RDX is often used as benchmark and therefore the properties of new explosives should exceed those of RDX (Table 1.1). The requirements for other kinds of energetic materials (propulsions, pyrotechnics, oxidizers etc.) are manifold, but often similar and should be discuss at the respective topic.

Testing the performance of an energetic material often needs relatively large amount of a substance. Synthesizing the required amount of a substance, especially new and scientific explosive materials, is often expensive and necessitate laborious synthetic work.[2] Consequently, the computing of detonation parameters becomes more and more important over the last decades, supported by the increased calculating power of computers and corresponding computing codes.

Table 1.1. Required values for developing new explosive materials based upon RDX.

	Required values	
Performance ^[a]	V_{det}/D	>9000 m/s
	p_{C-J}	>380 kbar
	$-U_{\text{ex}}/-Q$ ^[c]	>6200 kJ/kg
Safety ^[b]	T_{dec}	≥ 180 °C
	IS	>7 J
	FS	>120 N
	ESD	>0.2 J
Chemical	long-term stabile chemically stabile towards air and moisture stabile in formulations (towards binder and other additives) smoke-free combustion cheap and easy synthesis	
Environmental	low water solubility low toxicity (also of the decomposition products)	

[a] Performance parameters: detonation velocity V_{det} also D , detonation pressure p_{C-J} at the Chapman-Jouguet point, heat of explosion Q also U_{ex} (more detailed explanations for the values are given below); [b] safety parameters: decomposition temperature T_{dec} , impact sensitivity I_s , friction sensitivity F_s , electrostatic discharge ESD; [c] $-U_{\text{ex}} \approx -Q$ results out off $V = \text{constant}$ in the case of secondary explosives according to the explanations in the section Theoretical Background below.

Role of Silicon in the Field of Energetic Materials

Mixing secondary explosives and metals is an popular method to increase the performance data of an explosive formulation.[9] Mainly aluminium are used as additive, but also silicon or silicon alloys.[9] But silicon is mostly used under the topic of irradiation agents and decoy flairs. The advantage for these applications is in the first row the high energy release as heat and radiation (forming SiO_2) and even at oxygen deficient reaction conditions silicon reacts highly exothermic with N_2 in air (forming Si_3N_4) and also with water (SiO_2), if once ignited. The very high aza- and even more the oxophilicity of silicon and silicon containing compounds by decomposition is best seen in the pyrophoric behaviour of silanes the type $\text{Si}_n\text{H}_{n+2}$, the silicon analogues of alkanes.[10] The smallest silanes mono- (SiH_4) and disilane (Si_2H_6) for example are used to stabilize and prevent the

out-blowing of the combustion flame in scramjet propulsion engines and work as ignition aids in hydrocarbon fuels.[11] Recently, silicon based polymers (siloxanes, silicone) are under investigation for binder systems, which not loses its high flexibility in low temperature ranges (low glass transition temperature, low rubber-glass transition). This characteristic is necessary to prevent fractures by temperature fluctuations in explosive charges (for example by air-carried ammunitions), which can lead to incomplete detonation of the explosive. Several more advantages are found for silicon-based materials, like biocompatibility, good thermal and chemical stability.[12] However, silicon containing compounds are rarely found in applications concerning energetic materials till now.

In the late 1960s and early '70s several silicon based compounds with energetic moieties (nitro and nitrate moieties) were published without analytic data, their explosives behaviour were mention, but not further studied concerning their explosive characteristics were done.[13] The first investigations of silicon containing explosives were published in 2007, as Si-PETN (tetrakis(nitratomethyl)silane), a silicon analogue of the commonly used explosive PETN (pentaerythryl tetranitrate), and its azido analogue (tetrakis(azidomethyl)silane, Si-PETA) were synthesized and the strongly increased sensitivities of the sila compounds in comparison to its carbon analogues were discussed in different manners (see Figure 1.2).[14]

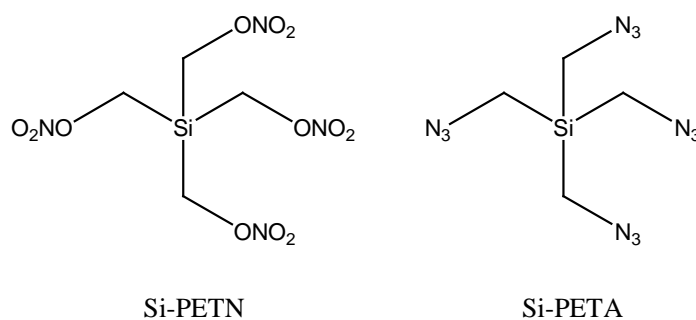


Figure 1.2. Molecular structures of the silicon analogue of PETN (Si-PETN) and its corresponding azide (Si-PETA).

Theoretical Background

For calculation and estimation of energetic values of energetic compounds the comprehension of thermodynamics behind detonation and combustion is crucial. Secondary explosives are characterized through five key criteria: heat of detonation ($\Delta_{\text{ex}}U^\circ$),

detonation temperature (T_{det}), detonation pressure ($p_{\text{C-J}}$), detonation velocity (V_{det}) and released gaseous volume (V_0).[5,6] Additionally the oxygen balance, the relative amount of oxygen which is spare or lacks for creating a balanced ratio between oxidizers and combustible components, allows a conclusion for evaluating the potential application. Along with the oxygen balance the knowledge of how much oxygen is necessary to efficiently oxidise an energetic material (negative oxygen balance) or how much is remaining to oxidise other components (positive oxygen balance). An easy calculation of the oxygen balance Ω is given below for the case of $C_aH_bN_cO_d$ containing compounds to complete oxidation to CO_2 : [4,5]

$$\Omega_{CO_2} = [d - 2a - b/2]/M \cdot 1600$$

Because of the high temperatures occurring during decomposition carbon is not fully oxidised to CO_2 , but rather to CO (Boudouard reaction).[3] Therefore, especially in the case of oxidizers often only Ω concerning CO is given (Ω_{CO}).

$$\Omega_{CO} = [d - a - b/2]/M \cdot 1600$$

To involve the Boudouard and the water-gas shift reaction, the modified Springall-Roberts-Rules help estimate the amount of oxygen used for CHNO-containing explosives.[6] These have to be applied 1 through 6 and are as follows:[4,6]

1. carbon atoms are converted to CO
2. remaining oxygen atoms oxidize hydrogen to H_2O
3. if oxygen atoms still remain, they oxidize existing CO to CO_2
4. all nitrogen is used to form N_2
5. one third of the generated CO is converted to C and CO_2 (Boudouard reaction)
6. one sixth of the originally generated CO is converted to CO_2 and H_2O (water-gas shift reaction)

Following a detonation the reaction components have to be in a state of equilibrium at the end of the reaction. This is described as the Chapman-Jouguet condition.[4,8,15] The according state corresponds to the point on the shock adiabatic curve for the reaction products. Following this postulate the Chapman-Jouguet-point (C-J-point) is described as

the tangent of the Rayleigh-line to the shock adiabatic curve at the point, which correlates with the end of the reaction. [4,5,8]

According to the first law of thermodynamics, in a closed system, the increase in internal energy equals the sum of the heat supplied to the system and the work done by the system:[16]

$$\Delta U = Q + W$$

With W defined as

$$W = -p\Delta V$$

the following modifications are permitted:

For secondary explosives $V = \text{const.}$, in close approximation, hence $\Delta U = Q_v$ and for propellants $p = \text{const.}$ applies with

$$\Delta U = Q_p - p\Delta V$$

in close approximation.[6] The enthalpy is defined as the internal energy and the pressure-volume work of a system.

$$H = U + pV$$

$$\Delta H = \Delta U + p\Delta V + \Delta pV$$

For $p = \text{const.}$ the formula $\Delta H = Q_p$ can be used.[16]

The detonation temperature (T_{det}) can be calculated from the correlation T_i (initiation temperature, commonly ambient conditions $T_i = 298 \text{ K}$) and Q as follows with ΣC_v being the sum of the molar heat capacity of all reaction products:[6]

$$T_{\text{det}} = Q / \Sigma C_v + T_i \quad (1)$$

An empirical correlation between the detonation velocity (V_{det}) and the detonation pressure (p_{C-J}) was established by Kamlet and Jacobs. Both depend on the charge density (ρ_0):[1,3,4]

$$p_{C-J} = K \cdot \rho_0^2 \cdot \Phi$$

$$V_{\text{det}} = A \cdot \Phi^2 \cdot (1 + B \cdot \rho_0)$$

with constants $K = 15.88$, $A = 1.01$ and $B = 1.30$. [4,17] Φ is defined using the following formula: [3]

$$\Phi = N \cdot \sqrt{(M \cdot Q)}$$

The parameters N (released mole of gas per gram explosive), M (mass of gas in gram per mole gas) and Q (heat of explosion) depend on the used explosive itself. [17]

Following these empirical formulas the influence to the most important values of explosives p_{C-J} and V_{det} (D respectively) are affected by four parameters:

The density ρ_0 can be obtained experimentally by pycnometer experiments, determine the crystal structure at ambient temperature or by approximation using semi-empirical formulas. [2,4,18,19] It correlates linear proportional to V_{det} values and squeric to p_{C-J} . The parameters M and Q influence the detonation velocity also in a linear proportional manner, whereas the detonation pressure is only enhanced by the square root of M and Q . M can be approximated by the sum formula of an explosive and the Springall-Roberts-Rules. [1] Q can be experimentally determined by bomb calorimetric measurements, by estimation from a decomposition assumption (Springall-Roberts-Rules) [1] and by theoretical computations (see following section). The high impact towards the detonation parameters is done by the mols of gaseous products per gram of explosive of an explosive, which can be approximately obtained by its reaction formula following the Springall-Roberts-Rules. [1] In the case of the detonation pressure the influence is linear, but the detonation velocity with the square of N . [4,6]

Performance of a rocket propellant is characterized by the specific impulse I_{sp} with $I_{sp} = I_{sp}^* = I/g$, because the specific impulse can be based on gravity acceleration and for the following discussion I_{sp} will be used as specified above, and thrust F which are connected as follows by the mass deficiency Δm per time scale Δt : [5,6,20]

$$F = I_{sp} \cdot \Delta m / \Delta t$$

The specific impulse exactly described as

$$I_{sp} = 1/g \sqrt{(2\gamma RT_c / (\gamma - 1)M)}$$

The constant γ as the ratio of the heat capacity of the gas mixture ($\gamma = C_p/C_v$). [20]

The specific impulse is also proportional to chamber temperature T_c and the mean molar mass of the combustion products M : [3,6,20]

$$I_{sp} \sim \sqrt{(T_c/M)} \quad (2)$$

An important rule of thumb is that an increase of the specific impulse of 20 s leads to duplication of the carrying capacity. [6]

Goals

The goal of this thesis is first of all to acquire the main differences between energetic molecules containing silicon and their carbon analogues. In concrete the reaction behaviour, physical properties and energetic characteristics have to be investigated in experimental and also theoretical manner. Furthermore, the influence of different energetic motifs and their compatibility towards silicon substituents have to be studied. Also a possible applications of silanes in the field of energetic materials need to be discussed.

-
- [1] S. Iyer, R. Schleyer, *Adv. Mater.* **1990**, 2,174–179.
- [2] L. E. Fried, M. R. Manaa, P. F. Pagoria, R. L. Simpson, *Annu. Rev. Mater. Res.* **2001**, 31, 291–321.
- [3] G. A. Olah, D. R. Squire in *Chemistry in Energetic Materials*, **1991**.
- [4] P. W. Cooper in *Explosives Engineering*, Wiley-VCH: New York, **1997**.
- [5] R. Meyer, J. Köhler, A. Homburg in *Explosives*, 5th ed.; Wiley-VCH: Weinheim, **2002**.
- [6] T. M. Klapötke in *Chemie der hochenergetischen Materialien*; de Gruyter: Berlin, **2009**.
- [7] J. P. Agrawal, R. D. Hodgson in *Organic Chemistry of Explosives*; John Wiley & Sons: Chichester, **2007**.
- [8] J. H. S. Lee in *The Detonation Phenomenon*, Cambridge University Press: Cambridge, **2008**.
- [9] T. Urbanzki in *Chemistry and Technology of Explosives*, Vol. 4, 1st edition; Pergamon Press: Oxford, **1984**.

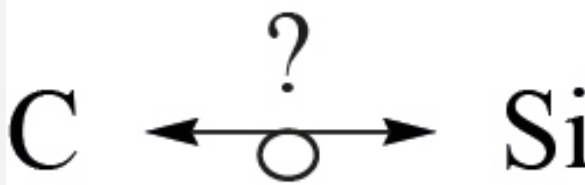
- [10] a) A. F. Hollemann, E. Wiberg, N. Wiberg in *Lehrbuch der Anorganischen Chemie*, 101. Aufl., de Gruyter: Berlin/New York, **1995**, pp.893. b) S. Patai, Z. Rappoport in *The Chemistry of Organic Silicon Compounds*, John Wiley & Sons: Chichester, 1989.
- [11] M. J. Lewis, J. S. Chang, *J. Propulsion* **2000**, 16, 365–367; b) D. Simone, C. Bruno, B. Hidding, *J. Propulsion* **2006**, 22, 1006–1011; c) V. I. Golovitchev, C. Bruno, *J. Propulsion* **1998**, 15, 92 – 96; d) D. Simone, C. Bruno, B. Hidding, *AIAA/CIRA 13th International Space Planes and Hypersonics Systems and Technologies*, **2005**, Los Angeles, AIAA 2005-3398, 1–13; e) M. Gerstein, P. R. Choudhury, *J. Propulsion* **1985**, 1, 399–402; f) J. S. Chang, M. J. Lewis, *35th AIAA/ASME/SAE/ASEE Joint Propulsion Conference and EXhibition*, **1999**, Los Angeles, AIAA 99-2252, 1–11; g) R. J. Biasca, Master Thesis: *Chemical Kinetics of SCRAMJET Propulsion*, Department of Aeronautics and Astronautics, Massachusetts Institute of Technology, **1988**.
- [12] D. S. C. dos Anjos, E. C. V. Revoredo, A. Galembeck, *Polym. Eng. Sci.* **2010**, 606–612.
- [13] a) W. Fink, U.S. Patent, US 3,127,431, **1964**. b) W. Fink, U.S. Patent, US 3,222,319, **1965**. c) Barcza, S., US 3,592,831, **1968**; d) Barcza S., US 3,585,228, **1971**.
- [14] a) T. M. Klapötke, B. Krumm, R. Ilg, D. Troegel, R. Tacke, *J. Am. Chem. Soc.* **2007**, 129, 6908-6915. b) W.-G. Liu, S. V. Zybin, S. Dasgupta, T. M. Klapötke, W. A. Goddard III, *J. Am. Chem. Soc.* **2009**, 131, 7490–7491.
- [15] W. M. Howard, L. E. Fried, P. C. Souers in *Kinetic Modeling of Non-Ideal Explosives*, International Workshop on the Modeling of Non-Ideal Explosives, Socorro, **1999**.
- [16] P. W. Atkins, J. de Paula in *Physikalische Chemie*, 4. Aufl., Wiley-VCH: Weinheim, **2006**.
- [17] U. Teipel in *Energetic Materials*, Wiley-VCH: Weinheim, **2005**.
- [18] a) J. R. Holden, Z. Du, H. L. Ammon, *J. Compt. Chem* **1993**, 14, 422–437; b) M. H. Keshavarz, *J. Hazard. Mat.* **2007**, 143, 437–442.
- [19] D. W. M. Hofmann, *Acta Cryst.* **2002**, B57, 489–493.
- [20] N. Kubota in *Propellants and Explosives: Thermochemical Aspects of Combustion*, Wiley-VCH: Weinheim, **2002**.
-

II. Summary

Energetic silanes

AnianNieder 15 - 27

Summary



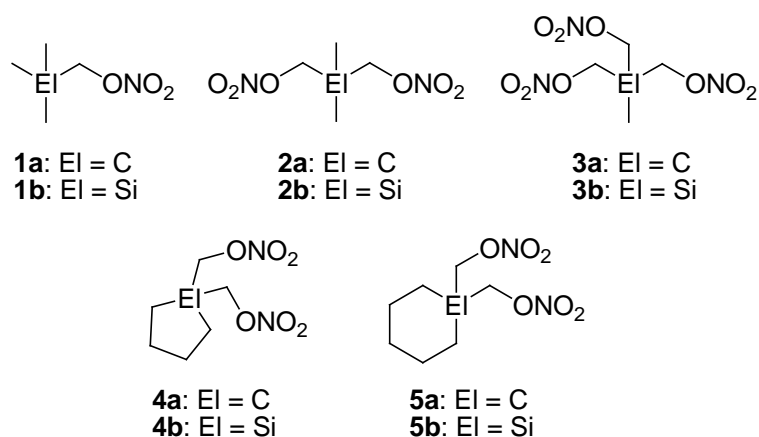
The results of the experimental and theoretical work with structurally simple silanes containing energetic or potentially energetic moieties

are presented. Each chapter is individually summarized by means of its most interesting results.

Summary

Studies on different substituted tetramethylsilane and closely related compounds are presented in summary.

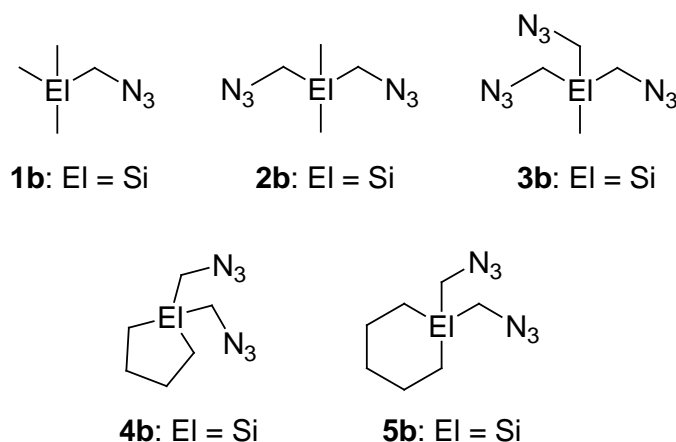
Sila-Substitution of Alkyl Nitrates (Chapter III): The influence of reducing the nitratomethyl content of Si-PETN, modifying the silicon backbone was studied and these compounds were compared to their carbon analogues. Therefore several carbon and silicon model structures (see Scheme 3.1) have been synthesized and characterized. The hitherto unknown compounds **2b–5b** were described for the first time.



Scheme 3.1. Carbon/silicon analogues **1a/1b–5a/5b** with various numbers of nitratomethyl groups bound to the central carbon or silicon atom.

The structural data of GED and X-ray diffraction experiments of the compounds **1a/b**, **2a/b**, **4a** and **5b** confirm the theoretically suggested decomposition pathway from Liu *et al.*[2] (see Scheme 5.2 top). The highly increased sensitivities of Si-PETN towards PETN concerning mechanical stimuli could also be observed by all other nitratomethyl silanes investigated in this chapter.

Azidomethyl Silanes (Chapter IV): As already mentioned by Klapötke *et al.*[1] the azido derivative Si-PETA shows lower sensitivities towards impact, friction and thermal stimuli in comparison to Si-PETN. The investigations on the azido derivatives (see Scheme 4.1) of the already mentioned model structures of the nitrate derivatives confirmed this result.



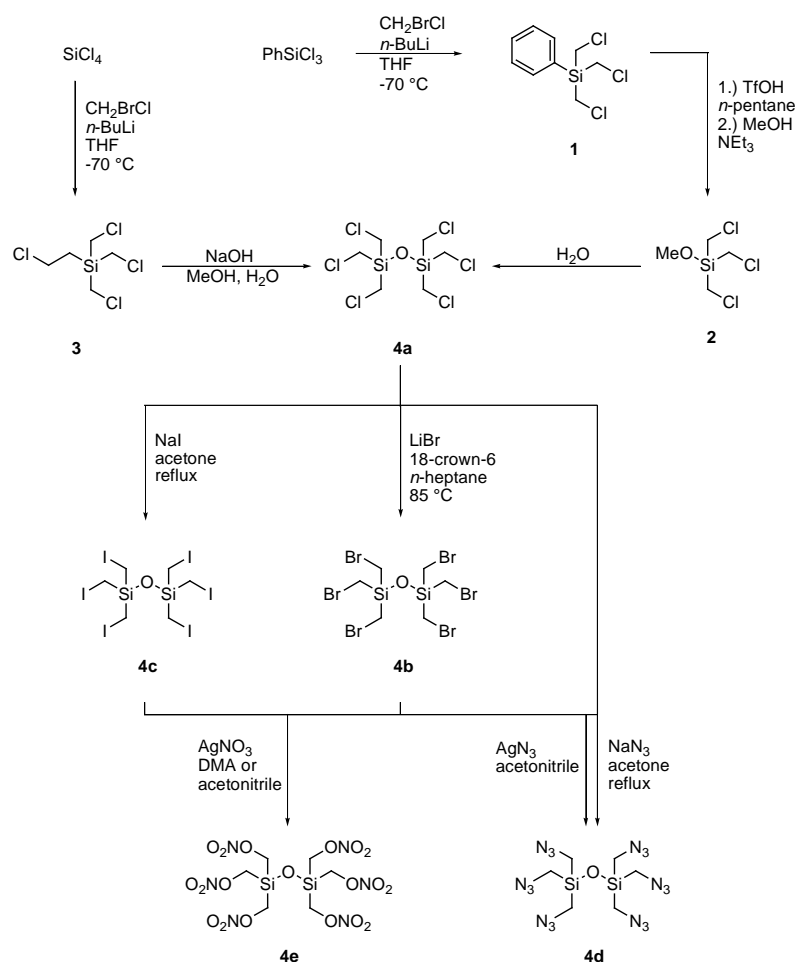
Scheme 4.1. Silicon compounds **1b–5b** with various numbers of azidomethyl groups and different alkyl substituents bound to the central silicon atom.

Azidomethyl silanes show increased sensitivities towards mechanical stimuli in comparison to their carbon derivatives, but are still much more insensitive than their nitrate derivatives. Because of the frequent use of azidomethyl silanes as precursor for further functionalized silanes and its mentioned explosive behaviour during purification, a less laborious and safer synthesis is established.

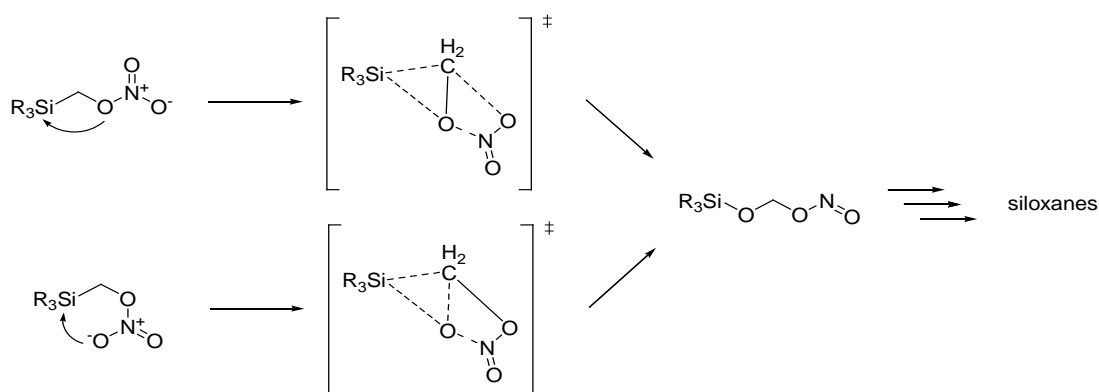
Hexa-Substituted Disiloxanes (Chapter V): The reproduction of the synthesis of hexakis(nitratomethyl)disiloxane **4e** published by Barcza in the late 1960th[3] was attempted with the goal to study its chemical and physical characteristics, in addition to structural information. It was shown that **4e** was certainly not the desired product, but more likely a mixture of several siloxane decomposition products.

Hexakis(chloromethyl)disiloxane **4a** and its bromo and iodo analogues (**4b** and **4c**) can be considered as the key compounds for several rarely studied hexa-functional

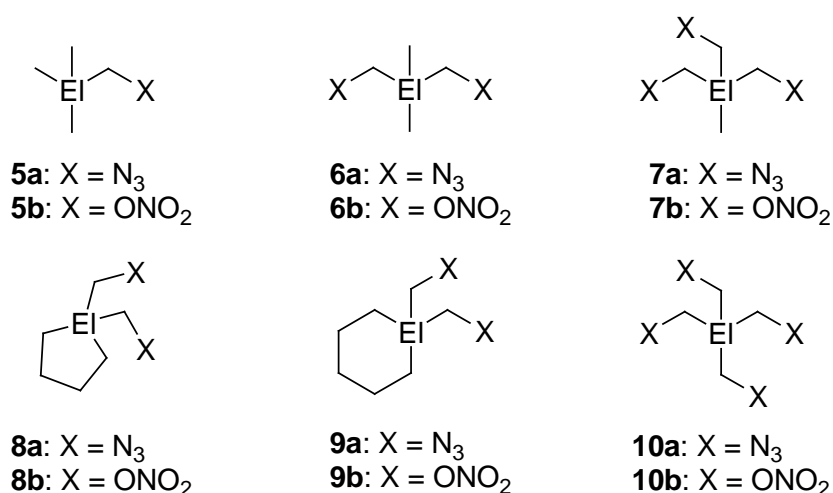
compounds. The solid state structures of the three halogeno derivatives were obtained. Furthermore the laborious synthesis to obtain these halogen derivatives using diazomethane (explosive and hazard material) was substituted by two new advanced synthetic pathways (see Scheme 5.1). The now simplified approach to hexafunctionalized disiloxanes opens the seminal class of compounds for a brought field of applications. Furthermore the formally unknown, extremely sensitive and highly explosive hexakis(azidomethyl)disiloxane **4d** was synthesized and fully characterized.



Scheme 5.1. Improved synthetic routes to hexakis(chloromethyl)disiloxane (**4a**) and further substitution reactions to the bromo (**4b**), iodo (**4c**), azido (**4d**) and nitrate derivatives (**4e**).



Scheme 5.2. The postulated decomposition mechanisms of Si-PETN calculated by Liu *et al.*[2] on M06/6-311G** level of theory (top) was supported by experimental and further theoretical computations (electron potential and NBO calculations on B3LYP level of theory). Additionally the hitherto not considered decomposition pathway based on theoretical results on MP2/6-31G* and B3LYP/cc-pVDZ level of theory (bottom) is presented.

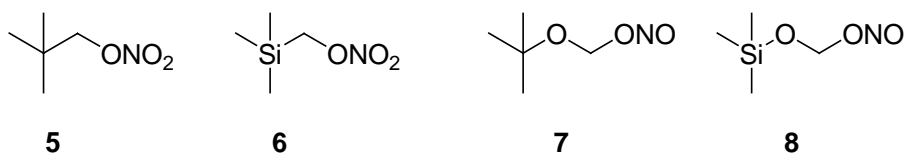


Scheme 5.3. Labeling of the calculated nitrato- and azidomethyl silanes ((nitratomethyl)- and (azidomethyl)trimethylsilane **5a/b**, 1,1-bis(nitratomethyl)- and 1,1-bis (azidomethyl)dimethylsilane **6a/b**, 1,1,1-tris(nitratomethyl)- and 1,1,1-tris(azidomethyl)methylsilane **7a/b**, 1,1-bis(nitratomethyl)- and 1,1-bis(azidomethyl)-1-sila-cyclopentane **8a/b**, 1,1-bis(nitratomethyl)- and 1,1-bis(azidomethyl)-1-sila-cyclohexane **9a/b**), Si-PETA and Si-PETN **10a/b**.

Presented computing results indicate a hitherto not considered decomposition pathway for nitratomethyl silanes in addition to the, by Liu *et al.*[2] already calculated, reactions already calculated reactions (see Scheme 5.2).

The computed energetic properties of **4d/e** and several other silanes **5a/b-10a/b** (see Scheme 5.3) show comparably good performance data like the common explosive PETN. The extreme sensitivities and the resulting consequences for a safe handling affect the justification for a common application.

Reaction Force Analysis and the Role of σ -Hole (Chapter VI): Based on the recent computing results of Liu *et al.*[2] concerning the reaction forces of Si-PETN versus PETN, Murray and Pulitzer investigated the reaction forces of the simpler (nitratomethyl)trimethylsilane **6** and its carbon analogue **5** in addition to experimental results of these compounds. The primary object in this investigation is to understand why the rearrangement in Scheme 3.2 is that facile and exothermic for the silicon derivative in contrast to its carbon analogue PETN. The energy release by building a Si-O bond is by far enough to initiate further rearrangements of this kind.



$$\Delta\text{H} (298 \text{ K}) = -79.5 \text{ kcal/mol} \quad (5)$$

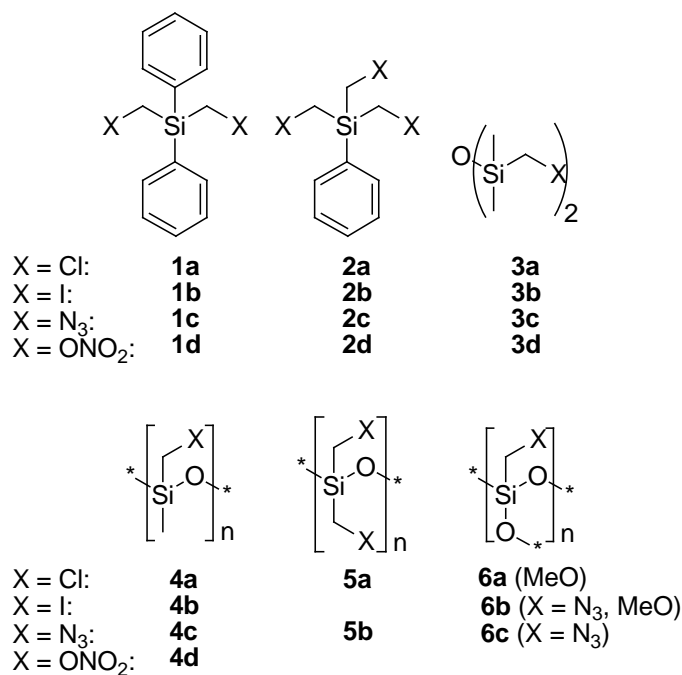


$$\Delta\text{H} (298 \text{ K}) = -112.7 \text{ kcal/mol} \quad (6)$$

Additionally, the σ -hole on the surface potential at the far side of the electron-withdrawing substituents observed for the silane **6** (in contrast to the situation in the carbon derivative **5**) increases the positive surface potential and therefore the possibility of creating a Si---O interaction. This pre-formation of the transition state is the initial step of the proposed decomposition mechanism in Scheme 5.2 (top).

Phenylsilanes and Siloxanes (Chapter VII): Beside the intermediates **2b**, **4b** and **5a**, several new energetic azidomethyl compounds **1c**, **2c**, **4a**, **5b** and **6c** were synthesized

and fully characterized (see Scheme 7.1). The corresponding nitratomethyl derivatives were however only obtained as rapid decomposing compounds in the case of **2d** and **3d**, whereas **2d** was only verified by means of NMR analysis and not further characterized as intermediate. In addition, an easy synthesis to bis-functionalized poly-siloxanes like **5b** was established.



Scheme 7.1. The labellings of diphenyl and phenyl silanes with $X = \text{Cl}$ (**1/2a**), I (**1/2b**), N_3 (**1/2c**) and ONO_2 (**1/2d**) methylene-bridged moieties, the dimeric disiloxanes $\text{O}(\text{SiMe}_2\text{CH}_2\text{X})_2$ ($X = \text{Cl}$ (**3a**), I (**3b**), N_3 (**3c**), ONO_2 (**3d**)), the two chain-like polymeric structures of $[\text{O}_{2/2}\text{SiMeCH}_2\text{X}]_n$ and $[\text{O}_{2/2}\text{Si}(\text{CH}_2\text{X})_2]_n$ ($X = \text{Cl}$ (**4/5a**), I (**4b**), N_3 (**4c/5b**), ONO_2 (**4d**)) and the methoxylated $(\text{MeO})_3\text{SiCH}_2\text{X}$ ($X = \text{Cl}$ (**6a**), N_3 (**6b**)) and polymeric $[\text{O}_{3/2}\text{SiCH}_2\text{N}_3]$ (**6c**) are shown.

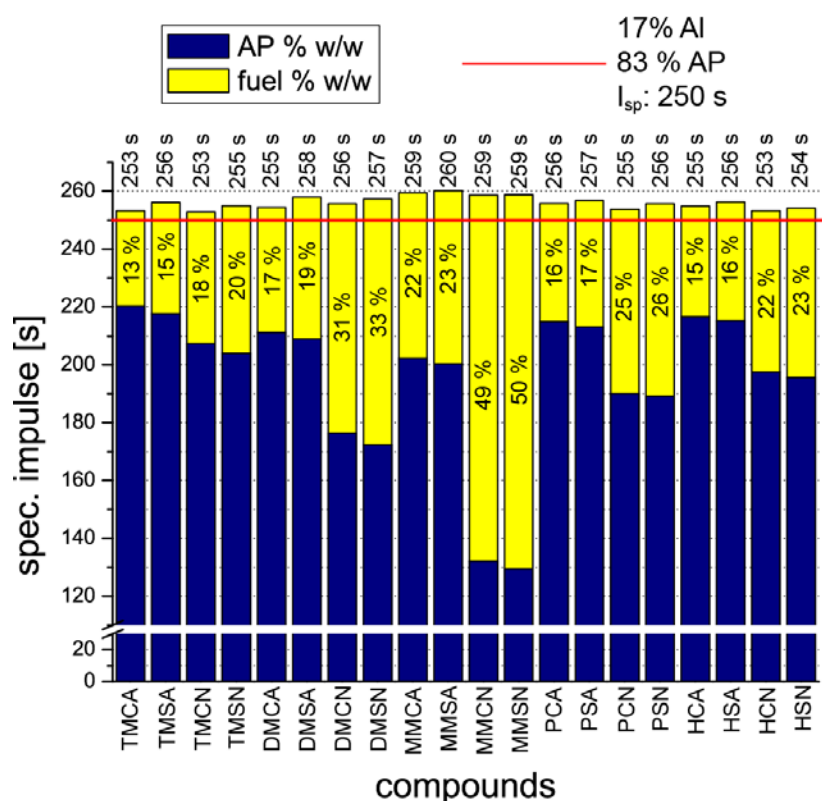


Figure 7.1. Specific impulses of several azido- and nitratomethyl silanes and their carbon analogues were computed by EXPL05 version 6.01 with an oxygen balance of $\Omega = \sim 0-1\%$ and a mixture of aluminium and AP ($\Omega = 1.2\%$) is given as bench mark (red line). The amount of fuel is given in yellow and AP in blue, in %w/w (area between 30 to 100 s is skipped for clarity). TMCA ((azidomethyl)trimethylmethane), TMSA ((azidomethyl)trimethylsilane), TMCN ((nitratomethyl)-trimethylmethane), TMSN ((nitratomethyl)trimethyl-silane), DMCA (1,1-bis(azidomethyl)dimethylmethane), DMSA (1,1-bis(azidomethyl)dimethylsilane), DMCN (1,1-bis(nitratomethyl) - dimethylmethane), DMSN (1,1-bis(nitratomethyl)dimethylsilane), MMCA (1,1,1-tris(azidomethyl)-methylmethane), MMSA (1,1,1-tris(azidomethyl)methylsilane), MMCN (1,1,1-tris(nitratomethyl)methylmethane), MMSN (1,1,1-tris(nitratomethyl)methylsilane), PCA (1,1-bis(azidomethyl)-cyclopentane), PSA (1,1-bis(azidomethyl)-1-sila-cyclopentane), PCN (1,1-bis(nitratomethyl)-cyclopentane), PSN (1,1-bis(nitratomethyl)-1-sila-cyclopentane), HCA (1,1-bis(azidomethyl)-cyclohexane), HSA (1,1-bis(azido-methyl)-1-sila-cyclohexane), HCN (1,1-bis(nitratomethyl)-cyclohexane), HSN (1,1-bis(nitratomethyl)-1-sila-cyclohexane). The nomenclature was used for comparability.

Studies on modifying the silicon backbone show, that neither electron-withdrawing (oxo, siloxo or phenyl substitutes) nor moieties, which probably react as leaving groups (like phenyl moieties) are not compatible with the nitratomethyl moiety. This

result is in good agreement with the decomposition behaviour described in Chapter V and VI. In contrast azidomethyl moieties are compatible energetic groups for all tested functionalities.

The mechanical and chemical properties of **4c**, **5b** and **6c** (or as co-polymers) show first promising results for applications as plasticizers or reactive coatings for main explosive charges.

The compounds **1c/d–3c/d** and the cyclic trimers **4c/d** show all moderate explosive parameters by computation. Even as neat compounds they have specific impulse values, which are at least on a par with the common aluminium/ammonium perchlorate formulation (Al/AP: 20/80 %w/w) with 250 s or even higher. The same is true for the carbon and silicon nitratomethyl derivatives shown in Scheme 3.1 and their azidomethyl analogues in Figure 7.1.

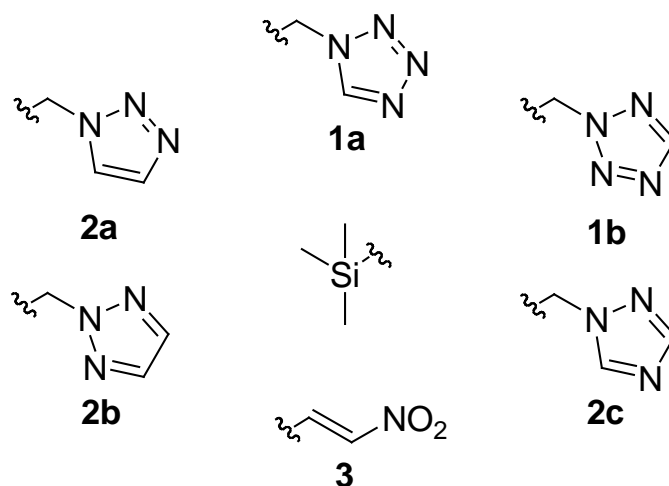
Azole and Nitro Silanes(Chapter VIII): After focusing mainly on the characteristics of nitrato- and azidomethyl silanes, several nitro, tetrazole and triazoles containing energetic motifs were studied (see Scheme 8.1).

The N-substituted azole derivatives **1a/b** and **2a–c** are synthesised in good yields, whereas the synthetic access to C-substituted tetrazolymethyltrimethylsilanes derivatives (*H*-tetrazol-5-ylmethyl)trimethylsilane (**4**, *1H*-isomer: **4^{1H}** and *2H*-isomer: **4^{2H}**) is still unfulfilled.

The synthesis of nitromethyl derivatives is still a challenge, as it is in the case of trinitroethyl ortho-silicates, due to the high oxophilicity. In addition, the susceptibility to nucleophilic substitution by cleaving Si–C bonds affects the synthesis of higher functionalized nitromethyl and azole derivatives. Nevertheless compound **3** was obtained in good yields using two synthetic routs.

The observed spontaneous ignitions of unsaturated alkene silanes like vinyl and allyl silanes while adding N₂O₄ show characteristics for a possible use in hypergolic propulsion mixtures. Additionally, the computed specific impulse values of the compounds **1a/b**, **2a–c**, **3/3^c** (**3^c**: carbon analogue of **3**), **4^{1H}/4^{2H}** and **8/8^c** (**8**:

(nitromethyl)trimethylsilane and its carbon analogue **8^c**) show impulse values similar the bench mark of Al/AP (17/83 %w/w) and even higher ones, if using other oxidizer like N₂O₄ or ammonium dinitramide (ADN, see Figure 8.1).



Scheme 8.1. Labelling of the synthesized silanes (**1a**: (1*N*-tetrazolylmethyl)trimethylsilane; **1b**: 2*N*-(tetrazolylmethyl)trimethylsilane; **2a**: 1*N*-(1,2,3-triazolylmethyl)trimethylsilane; **2b**: 2*N*-(1,2,3-triazolylmethyl)trimethylsilane; **2c**: 1*N*-(1,2,4-triazolylmethyl)trimethylsilane; **3**: *E*-(2-Nitroethyl)trimethylsilane).

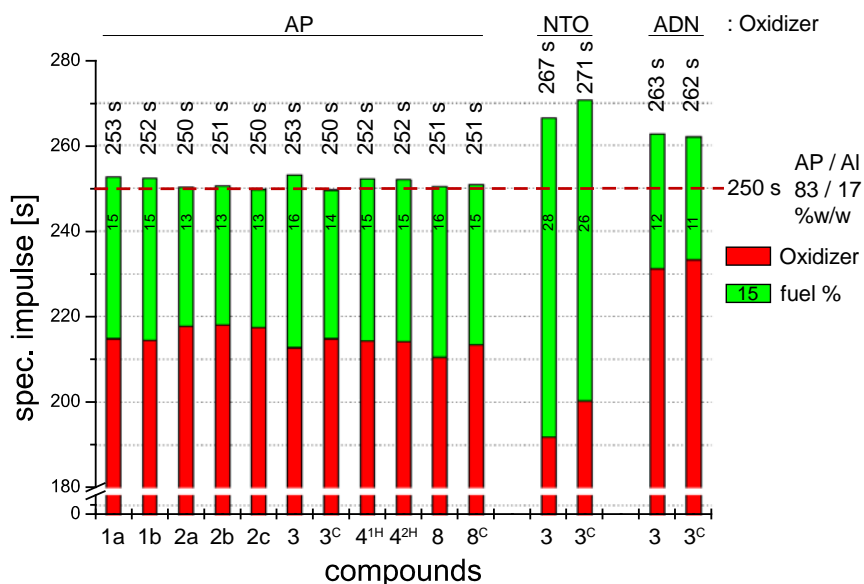
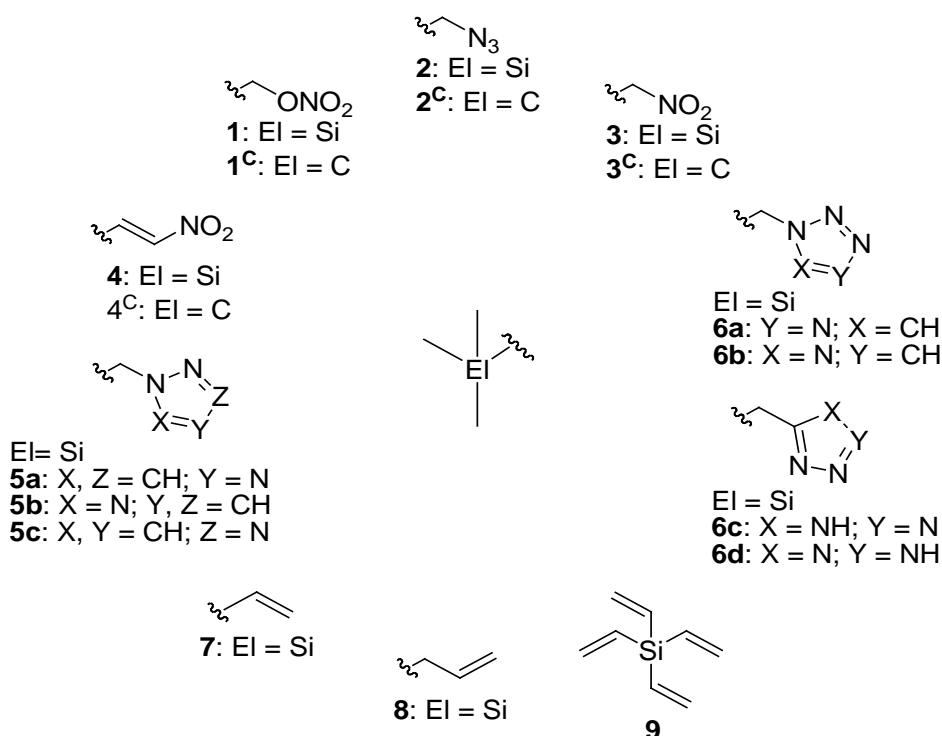


Figure 8.1. Calculated specific impulse I_{sp} of the compounds **1a/b**, **2a–c**, **3/3^c**, **4^{1H/2H}** and **8/8^c** by using the EXPL05 computing code (Model 1, advanced run). The I_{sp} of AP/Al (83/17 %w/w) is given as bench mark (red dashed line). Additionally the I_{sp} with the oxidizers NTO and ADN were calculated for **3** and **3^c**. The green bars with numbers representing the percentage amount of fuel for the optimal mixture.

Chapter IX: Theoretical Approach of Energetic Silanes

The problems occurring during the synthesis of several azoles and nitromethyl trimethylsilyl derivatives have been studied by theoretical calculations of B3LYP and MP2 level of theory. As already known from nitratomethyl silanes, intramolecular interactions between the substituent and the central silicon atom, suggested by theoretical methods, lead to the observed chemical inconsistencies described in Chapter VIII.



Scheme 9.1. Molecular structures and labels of the discussed silanes and some of their carbon analogues ((nitratomethyl)trimethylsilane **1**, [7] neopentenyl nitrate **1^c**, [7] (azidomethyl)-trimethylsilane **2**, [8] 1-azido-2,2-dimethylpropane **2^c**, (nitromethyl)trimethylsilane **3**, 2,2-dimethyl-1-nitropropane **3^c**, (*E*)-(2-nitrovinyl)trimethylsilane **4**, (*E*)-3,3-dimethyl-1-nitrobut-2-ene **4^c**, 1-((trimethylsilyl)methyl)-1*H*-1,2,4-triazole **5a**, 1-((trimethylsilyl)methyl)-2*H*-1,2,3-triazole **5b**, 1-((trimethylsilyl)methyl)-1*H*-1,2,3-triazole **5c**, 1-((trimethylsilyl)methyl)-1*H*-tetrazole **6a**, 2-((trimethylsilyl)methyl)-2*H*-tetrazole **6b**, 5-((trimethylsilyl)methyl)-1*H*-tetrazole **6c**, 5-((trimethylsilyl)methyl)-2*H*-tetrazole **6d**, trimethyl(vinyl)silane **7**, allyltrimethylsilane **8**, tetravinylsilane **9**).

To deal with the problem of the observed spontaneous ignition of alkene silanes (see Chapter VIII) further investigations were done on several model structures **4/4^c** and **7-9** shown in Scheme 9.1. All compounds were computed with higher specific

impulse values as the common bench mark of Al/AP (20/80 %w/w) with 250 s. The I_{sp} values are significantly increased by calculation using N_2O_4 , ADN or red fuming nitric acid (RFNA, see Figure 9.1). In general it was demonstrated, that the increase of the averaged molar mass of the combustion products of compounds containing the heavier silicon atom (instead of carbon) influences the computed I_{sp} insignificantly. In contrast the boosted combustion temperature observed for silicon compounds often increases the I_{sp} values in comparison to their carbon analogues.

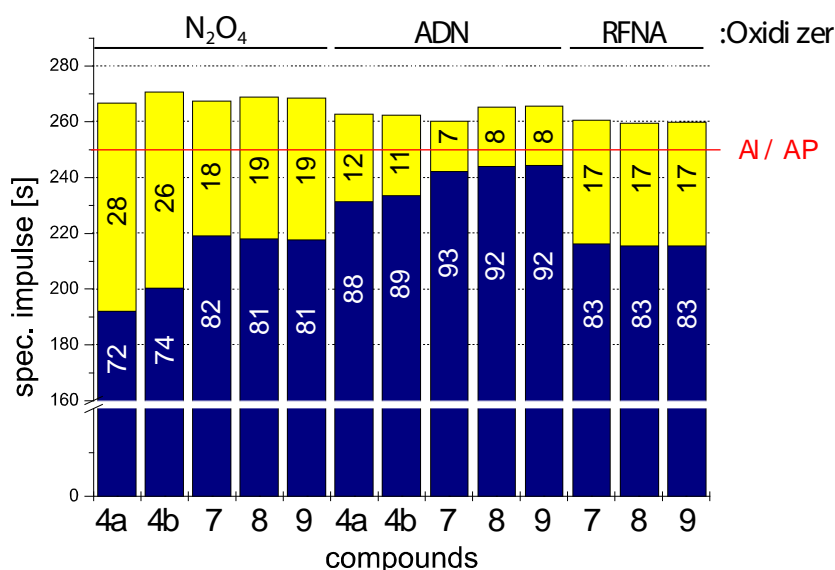


Figure 9.1. Histogram of the calculated specific impulses of the compounds **4**, **4^c** and **7–9** as fuel (% amount blue bar) and the oxidizers (% amount yellow bar) dinitrogen tetroxide (NTO), ammonium dinitamide (ADN) and red fuming nitric acid (RFNA). Aluminium/AP mixture (20/80 %w/w) is given as benchmark (250 s).

The established Springall-Roberts rules for CHNO compounds could be extended to CHNOSi compounds as described in the following:

1. all silicon atoms are converted to SiO_2 or, if no more oxygen is present, to Si_3N_4
2. if oxygen atoms remain, carbon atoms are converted to CO
3. remaining oxygen atoms oxidize hydrogen ones to H_2O
4. if still oxygen atoms remain, they oxidize existing CO to CO_2
5. still remaining nitrogen is used to form N_2
6. one third of the generated CO is converted to C and CO_2

7. one sixth of the originally generated CO is converted to CO₂ and H₂O

The knowledge about computing organo-silicon compounds in terms of energetic properties is low, therefore a general investigation of the influences of silicon onto the obtained data were done, using different computing codes and modifying the calculation strategies. EXPL05 version 6.1 and ICT Code are both suitable computing codes to calculate CHNOSi compounds, whereas EXPL05 version 6.1 allows additional modifications on the calculation modus and more detailed results.

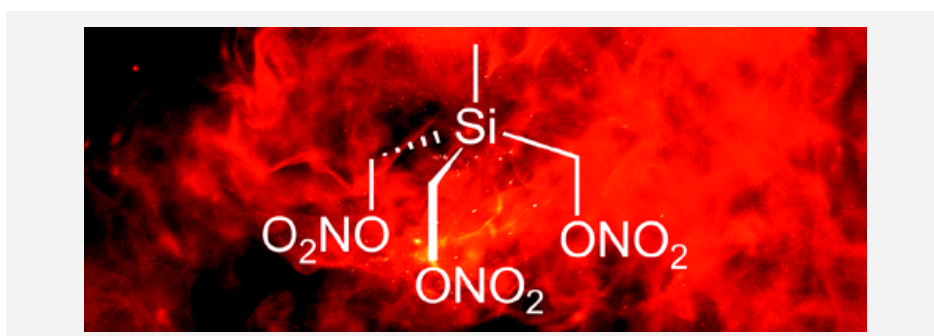
-
- [1] T. M. Klapötke, B. Krumm, R. Ilg, D. Troegel, R. Tacke, *J. Am. Chem. Soc.* **2007**, *129*, 6908-6915.
- [2] W.-G. Liu, S. V. Zybin, S. Dasgupta, T. M. Klapötke, W. A. Goddard III, *J. Am. Soc. Chem.* **2009**, *131*, 7490–7493.
- [3] Barcza, S., U.S. Patent 3,592,831, **1968**.
-

III. Sila-Substitution of Alkyl Nitrates

Energetic silanes

C. Evangelisti, T. M. Klapötke, B. Krumm, A. Nieder, R. J. F. Berger, S. A. Hayes, N. W. Mitzel,* D. Troegel, and R. Tacke* 28 - 69*

Sila-Substitution of Alkyl Nitrates: Synthesis, Structural Characterization, and Sensitivity Studies of Highly Explosive (Nitratomethyl)-, Bis(nitratomethyl)-, and Tris(nitratomethyl)silanes and Their Corresponding Carbon Analogues



A comprehensive study of silicon in detail. In addition several nitrate esters and their carbon analogues with different amounts of nitrate and with differences in the backbone structures are given. The syntheses, chemical and physical properties are discussed both the carbon and the silicon analogues.

Sila-Substitution of Alkyl Nitrates: Synthesis, Structural Characterization, and Sensitivity Studies of Highly Explosive (Nitratomethyl)-, Bis(nitratomethyl)-, and Tris(nitratomethyl)silanes and Their Corresponding Carbon Analogues

Camilla Evangelisti,^[a] Thomas M. Klapötke,^{*[a]} Burkhard Krumm,^[a] Anian Nieder,^[a]
Raphael J. F. Berger,^[b] Stuart A. Hayes,^[b] Norbert W. Mitzel,^{*[b]} Dennis Troegel,^[c] and
Reinhold Tacke^{*[c]}

Published in *Inorganic Chemistry* **2010**, *49* (11), 4865–4880.

Abstract: A series of analogous nitratomethyl compounds of carbon and silicon of the formula types Me₃ElCH₂ONO₂ (**1a/1b**), Me₂El(CH₂ONO₂)₂ (**2a/2b**), MeEl(CH₂ONO₂)₃ (**3a/3b**), (CH₂)₄El(CH₂ONO₂)₂ (**4a/4b**), and (CH₂)₅El(CH₂ONO₂)₂ (**5a/5b**) were synthesized [El = C (**a**), Si (**b**); (CH₂)₄El = (sila)cyclo-

pentane-1,1-diyl; (CH₂)₅El = (sila)cyclohexane-1,1-diyl]. All compounds were characterized by using NMR, IR, and Raman spectroscopy and mass spectrometry. In addition, the crystal structures of Me₂C(CH₂ONO₂)₂ (**2a**), (CH₂)₄C(CH₂ONO₂)₂ (**4a**), Me₂Si(CH₂ONO₂)₂ (**2b**), and (CH₂)₅Si(CH₂ONO₂)₂ (**5b**) were determined by single-crystal X-ray diffraction. The gas-phase structures of the C/Si analogues **1a** and **1b** were determined by electron diffraction and compared with the results of quantum chemical calculations at different

levels of theory. The thermal stabilities of the C/Si pairs **1a/1b–5a/5b** were investigated by using DSC. In addition, their friction and impact sensitivities were measured with standard BAM methods. The extreme compounds **1b–5b** compared to those of the corresponding carbon analogues **1a–5a** were sensitivities of the silicon discussed in terms of the structures of the C/Si analogues and possible geminal Si···O interactions.

Keywords: energetic materials • crystal structure • silanes • explosives • GED

[a] Prof. Dr. Thomas M. Klapötke
Department Chemistry
Ludwig-Maximilian-University Munich
Butenandtstr. 5–13(D)
81377 Munich, Germany
Fax: +49-89-2180-77492
E-Mail: tmk@cup.uni-muenchen.de

[b] Prof. Dr. Norbert W. Mitzel
Lehrstuhl für Anorganische Chemie und
Strukturchemie
Universität Bielefeld
Universitätsstr. 25
33615 Bielefeld, Germany
E-Mail: mitzel@uni-bielefeld.de

[c] Prof. Dr. Reinhold Tacke
Institut für Anorganische Chemie
Universität Bielefeld
Am Hubland
97074 Würzburg, Germany
E-Mail: r.tacke@uni-wuerzburg.de

Supporting information of this article (gas electron diffraction data for **1a** and **1b** and crystallographic data for **2a**, **2b**, **4a**, **5b**, **7**, and **8**) is available free of charge via the Internet at <http://pubs.acs.org>.

Introduction

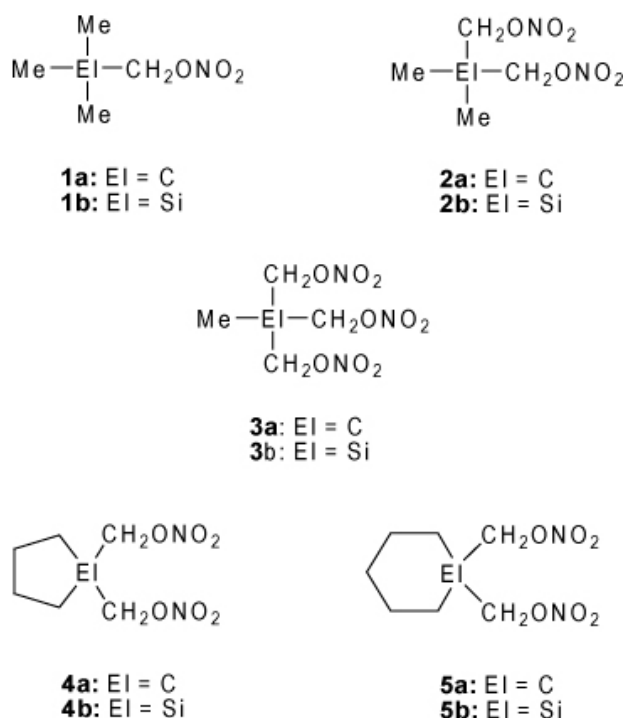
Alkyl nitrates are well-known compounds, and they are used in many different applications such as drugs, propellants, or explosives.[1,2] Since Alfred Nobel tamed nitroglycerin with kieselguhr, highly sensitive

alkyl nitrates have become manageable for industrial, military, and civil purposes.[2] One of the routinely used alkyl nitrates is pentaerythrityl tetranitrate (PETN), $C(CH_2ONO_2)_4$, as a primary explosive. A derivative also bearing a neopentane backbone is 1,1,1-tris-(nitratomethyl)ethane (also known as metriol trinitrate, **3a**; Scheme 3.1), which is used as an alternative to nitroglycerin in propellant and explosive formulations.[2] The characteristic of an explosive reaction is a fast propagating decomposition via a shock-wave mechanism. In the case of alkyl nitrate based explosives, the homolytic bond cleavage of the O-NO₂ group is mostly the first chemical step of decomposition, followed by ignition, growth of deflagration, and transition from deflagration to detonation. This initial chemical step can be initiated by different external stimuli, like shock, friction, heat, or electrostatic discharge. In some circumstances, the ignition can lead directly to detonation.[2,3]

The first sila-analogues of alkyl nitrates (C/Si exchange) were reported in 1964,[4] along with the syntheses of related compounds of the formula type $R_3ElCHClCH_2ONO_2$ (El= Si, Sn) [4] and organo siloxane-based nitrates obtained from the corresponding silanols of the formula type $(HO)_nSi(CHCl)(CH_2ONO_2)_{4-n}$ (n=2, 3).[5] The first synthesis of a silicon analogue of an alkyl nitrate with a neopentane backbone was described in a patent,⁶ where the use of $Me_3SiCH_2ONO_2$ (**1b**, Scheme 3.1) was claimed as an alternative to nitroglycerin for medical applications, and the explosive behaviour of this compound was recognized, with possible applications as an energetic material. Recently, the extremely impact- and friction-sensitive silicon analogue of PETN [$C(CH_2ONO_2)_4$], sila-PETN [$Si(CH_2ONO_2)_4$], was synthesized.[7]

The first studies of its outstanding sensitivity compared to its carbon analogue PETN were performed and different decomposition pathways of the C/Si analogues $C(CH_2ONO_2)_4$ and $Si(CH_2ONO_2)_4$ were investigated by using quantum chemical methods.[7,8] To study the characteristics and the reasons for the high instability of (nitratomethyl)silanes, several silicon compounds of this type with various numbers of nitratomethyl groups and their corresponding carbon analogues, the C/Si pairs **1a/1b-5a/5b** (Scheme 3.1), were synthesized and characterized, including their friction and impact sensitivities. The synthetic access to the precursors of the aforementioned (nitratomethyl)silanes, the corresponding (hydroxymethyl)- and (iodomethyl)silanes, and related compounds with $SiCH_2X$ groups (X = Cl, Br, N₃, SH) has been discussed extensively.[9-16] The studies on the

sila-explosives reported here represent a logical extension of related investigations dealing with sila-drugs[17] and sila-odorants.[18]



Scheme 3.1. Carbon/silicon analogues **1a/1b–5a/5b** with various numbers of nitratomethyl groups bound to the central carbon or silicon atom.

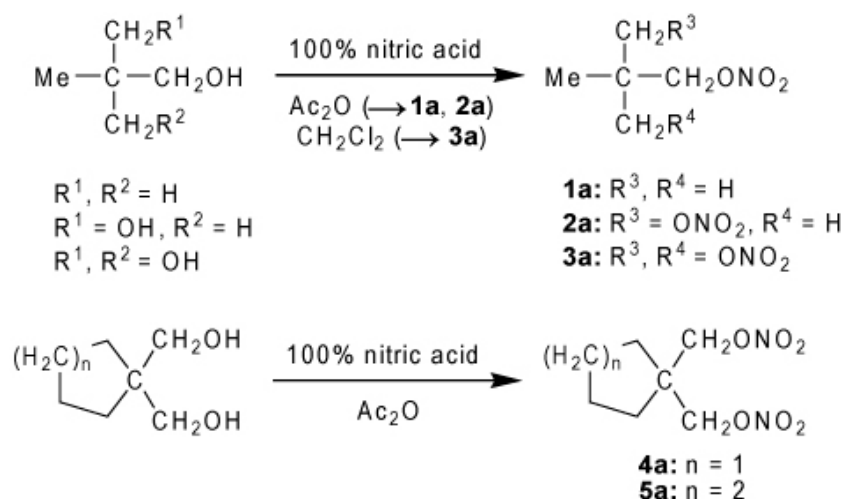
Results and Discussion

Syntheses: The acyclic carbon-based nitratomethyl compounds $\text{Me}_3\text{CCH}_2\text{ONO}_2$ [3] (**1a**), $\text{Me}_2\text{C}(\text{CH}_2\text{ONO}_2)_2$ [3] (**2a**), and $\text{MeC}(\text{CH}_2\text{ONO}_2)_3$ [3] (**3a**) were synthesized according to Scheme 3.2 by treatment of the corresponding commercially available hydroxymethyl compounds with fuming nitric acid. The related cyclic nitratomethyl compounds, $(\text{CH}_2)_4\text{C}(\text{CH}_2\text{ONO}_2)_2$ (**4a**) and $(\text{CH}_2)_5\text{C}(\text{CH}_2\text{ONO}_2)_2$ (**5a**), were obtained analogously (Scheme 3.2; for the synthesis of the corresponding hydroxymethyl compounds, $(\text{CH}_2)_4\text{C}(\text{CH}_2\text{OH})_2$ and $(\text{CH}_2)_5\text{C}(\text{CH}_2\text{OH})_2$, see ref. [35]). The nitrates **1a–5a** were synthesized by treatment of the corresponding alcohols with an excess of fuming nitric acid and acetic anhydride at 0 °C, and the reaction mixtures were then stirred at ambient temperature, followed by an aqueous workup. In the case of **3a**, the precursor $\text{MeC}(\text{CH}_2\text{OH})_3$ was treated with an excess of fuming nitric acid at 0 °C using dichloromethane as the solvent, followed by stirring of the reaction mixture at ambient temperature and subsequent aqueous workup. Compounds

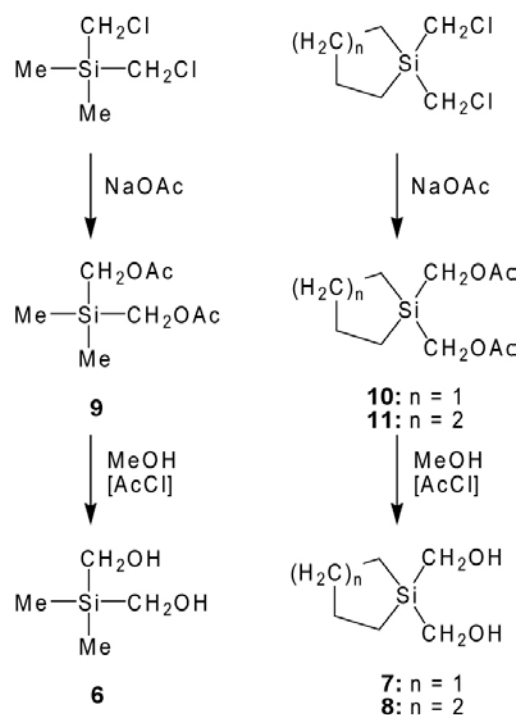
1a–5a were isolated in 82–88 % yield without any by-product. Several other syntheses of these compounds are known,[36] but in anticipation of the syntheses of their corresponding sila-analogues, this gentle and non-oxidizing synthetic route was used. For the synthesis of the (nitratomethyl)silanes **1b–5b**, the corresponding (hydroxymethyl)silanes were synthesized as precursors by using the method described in refs. [12] and [15]. The syntheses of the bis(hydroxymethyl)silanes **6–8** by using this particular synthetic pathway were not reported before and therefore shall be briefly described. Compounds **6–8** were synthesized according to Scheme 3.3, starting from the respective bis(chloromethyl) silanes.[16] Thus, treatment of $\text{Me}_2\text{Si}(\text{CH}_2\text{Cl})_2$, $(\text{CH}_2)_4\text{Si}(\text{CH}_2\text{Cl})_2$, and $(\text{CH}_2)_5\text{Si}(\text{CH}_2\text{Cl})_2$ with sodium acetate in N,N-dimethylformamide furnished the corresponding bis(acetoxymethyl)silanes **9–11** (76–87 % yield), which upon methanolysis, in the presence of acetyl chloride as a source for the formation of catalytic amounts of hydrogen chloride, yielded the corresponding bis(hydroxymethyl)silanes **6–8** (60–73 %yield).

For an alternative synthesis of the (nitratomethyl)silanes **1b–3b**, the corresponding (iodomethyl)silanes were used as precursors. $\text{Me}_3\text{SiCH}_2\text{I}$ was commercially available, and $\text{Me}_2\text{Si}(\text{CH}_2\text{I})_2$ was prepared from the commercially available bis(chloromethyl)silane $\text{Me}_2\text{Si}(\text{CH}_2\text{Cl})_2$. [37,38] $\text{MeSi}(\text{CH}_2\text{I})_3$ was synthesized as reported in the literature.[15] The silicon-based nitratomethyl compounds **1b–5b** were synthesized analogously to their corresponding carbon analogues **1a–5a** by treatment of the corresponding hydroxymethyl derivatives with an excess of fuming nitric acid and acetic anhydride (Scheme 3.4).[7] Compounds **1b–3b** were additionally prepared by treatment of the corresponding iodomethyl derivatives with an excess of silver nitrate at 0 °C using acetonitrile as the solvent, followed by stirring of the reaction mixture at ambient temperature and subsequent extraction with pentane (Scheme 3.5). In the case of **2b–5b**, the first approach (nitration of the corresponding alcohols) was found to be the best synthetic method. In contrast, for the synthesis of **1b** the second method turned out to be more advantageous. Compounds **1b–5b** were isolated in 80–96 % yield.

NMR Analyses: The carbon-based nitratomethyl compounds **1a–5a** and their corresponding sila-analogues **1b–5b** show quite similar trends in the chemical shifts of their ^1H NMR resonances.



Scheme 3.2. Synthesis of carbon-based nitratomethyl compounds **1a–5a**, starting from the corresponding hydroxymethyl derivatives.



Scheme 3.3. Synthesis of the bis(hydroxymethyl)silanes **6–8**, starting from the corresponding bis(chloromethyl)silanes.

Compared to the acyclic carbon compounds **1a–3a**, their sila-analogues **1b–3b** are high-field shifted in the ^1H NMR spectra. Especially the resonances of the methyl protons are strongly influenced by the respective R-atoms, the central carbon or silicon atom. The β -CH₂ proton resonances are strongly high-field shifted for the silicon compounds **1b–3b** compared to those of their corresponding carbon analogues **1a–3a**. The resonances of the

hydrogen atoms of the ring systems of the cyclic carbon compounds **4a** and **5a** differ from those of the sila-analogues **4b** and **5b**, respectively. For **5a** only one broad ^1H resonance signal was observed, because of overlapping of the different CH_2 resonances of the ring system, whereas in the case of **5b** three clearly defined multiplet structures were observed. In detail, the $\delta\text{-CH}_2$ ^1H resonances of **5b** are only slightly influenced compared to those of **5a**, whereas the $\beta\text{-CH}_2$ resonances are strongly high-field shifted and the $\gamma\text{-CH}_2$ resonances low-field shifted compared to those of **5a**. In the case of the C/Si analogues **4a** and **4b**, the $\beta\text{-CH}_2$ ^1H resonances are not affected by the R-atom (C or Si). However, as in the case of **5a** and **5b**, the $\beta\text{-CH}_2$ protons of **4b** show strongly high-field shifted resonances compared to those of the carbon analogue **4a**. The ^1H resonances of the exocyclic CH_2 groups are quite similar for the cyclic C/Si pairs **4a/4b** and **5a/5b**, that is, they are only slightly influenced by the R-atom (C or Si). With increasing the number of the nitratomethyl groups, the proton resonances are low-field shifted in both series of compounds. The influence of the alkyl substituents (methyl, butane-1,4-diyl, and pentane-1,5-diyl) on the proton resonances of

Table 3.1. Nitration procedures, molar equivalents of nitration agent HNO_3 , and reaction times for the syntheses of the carbon-based nitratomethyl compounds **1a–5a** as well as yields and melting, boiling, and decomposition points of **1a–5a**.

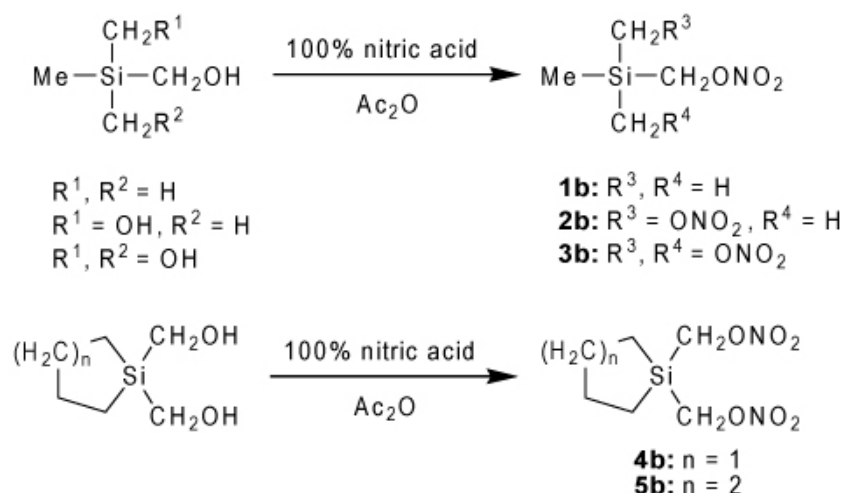
compound	1a	2a	3a	4a	5a
nitration agents	$\text{HNO}_3/\text{Ac}_2\text{O}$	$\text{HNO}_3/\text{Ac}_2\text{O}$	$\text{HNO}_3/\text{Ac}_2\text{O}$	$\text{HNO}_3/\text{Ac}_2\text{O}$	$\text{HNO}_3/\text{Ac}_2\text{O}$
molar equivalents of nitric acid ^[a]	2.1	4.2	6.3	4.2	4.2
reaction time [h]	1.5	1.5	2.0	1.5	1.5
% yield	88	82	86	83	86
mp. / bp. [°C]	- / 174	18– 23 / 178 ^[b]	-15 / 182 ^[b]	23– 25 / 190 ^[b]	- / 190 ^[b]

[a] Calculated for 1.0 mol equiv of the starting material; [b] decomposition.

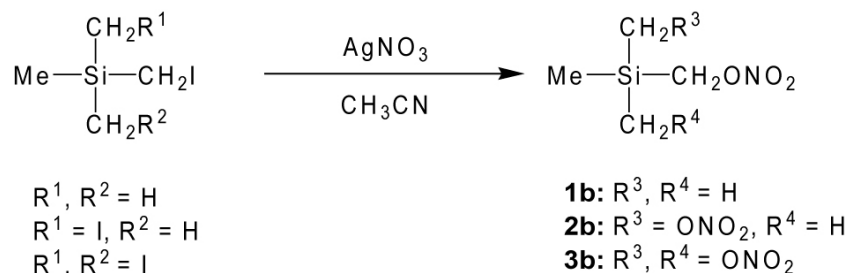
Table 3.2. Nitration procedures (methods A and B), molar equivalents of nitration agent, and reaction times for the syntheses of the silicon-based nitratomethyl compounds **1b–5b** as well as yields and melting, boiling, and decomposition points of **1b–5b**.

compound	1b	2b	3b	4b	5b
nitration procedure	B	A	A	A	A
molar equivalents of nitric acid ^[a]	2.0	4.2	6.3	4.2	4.2
reaction time [h]	1.5	1.0	1.5	1.5	1.5
% yield	86	87	80	94	96
mp. / bp. [°C]	- / 85 ^[b]	-10/ 107 ^[b]	~ -18 / 107 ^[b]	~ -18 / 97 ^[b]	~ 4 / 96 ^[b]

[a] Calculated for 1.0 mol equiv of the starting material; [b] decomposition.



Scheme 3.4. Synthesis of the silicon-based nitratomethyl compounds **1b–5b**, starting from the corresponding hydroxymethyl derivatives.



Scheme 3.5. Synthesis of the silicon-based nitratomethyl compounds **1b–3b**, starting from the corresponding iodomethyl derivatives.

the ElCH_2O groups of the bis(nitratomethyl) derivatives **2a**, **2b**, **4a**, **4b**, **5a**, and **5b** is small. In both cases ($\text{El} = \text{C}$ or Si), the ElCH_2O ^1H resonances are low-field shifted for the cyclic derivatives (**4a**, **4b**, **5a**, and **5b**) compared to the acyclic dimethyl compounds **2a** and **2b**. The ^{13}C NMR resonances of the C/Si pairs **1a/1b–5a/5b** are more influenced by the number of the nitratomethyl groups than the ^1H resonances. With increasing number of the nitratomethyl moieties, the CH_2 and CH_3 resonances exhibit a high-field shift of 3–4 ppm. In contrast, the central R-carbon atom shows a low-field shift when increasing the number of nitratomethyl groups. The ring size of the cyclic carbon compounds **4a** and **5a** exerts only a small influence on the ^{13}C NMR resonances of the CH_2O groups. The ring CH_2 groups of **4a** and **5a** are easier to distinguish in the ^{13}C than in the ^1H NMR spectra. The ^{13}C resonances of the central carbon atom (R-atom) are strongly affected by the alkyl substituents (methyl, butane-1,4-diyl, and pentane-1,5-diyl). The exchange of the central carbon by a silicon atom shifts the ^{13}C NMR resonances to higher field, with the same shifting tendencies as observed

in the series of the carbon compounds **1a–5a**. Because of hyperconjugation and β -silyl effect,[39] the ^{13}C NMR resonances of the SiCH_3 groups are high-field shifted by 0 to -10 ppm. The ^{14}N NMR resonances of the nitrate groups of the carbon compounds **1a–5a** are observed in a region between -41 and -45 ppm. The ^{14}N resonances of the corresponding sila-analogues **1b–5b** are shifted to lower field in a region between -34 and -41 ppm. In both series of compounds, high-field shifting is observed with increasing number of the nitratomethyl groups. The ring size of the C/Si pairs **4a/4b** and **5a/5b** has only a weak influence on the ^{14}N chemical shift, but a high-field shift of 3–4 ppm is observed for each additional nitratomethyl moiety. The acyclic silicon compounds **1b–3b** show ^{29}Si NMR resonances in a region between 0.1 and -5.4 ppm, and high-field shifting is observed with increasing the number of the nitratomethyl groups. The ^{29}Si resonances of the silicon compounds **2b**, **4b**, and **5b** are strongly dependent on the nature of the alkyl substituent (**2b**, -1.2 ppm; **4b**, 13.7 ppm; **5b**, -6.5 ppm).

Table 3.3. Friction and impact sensitivities measured for **1a–5a** and **1b–5b** (BAM testing).

compound	1a	2a	3a	4a	5a	1b	2b	3b	4b	5b
friction [N] ^[a]	>360	>96	>108	>108	>120	>64	<5	<5	<5	>36
impact [J] ^[b]	>100	>100	>15	>100	>100	>1	<0.5	<0.5	<0.5	<0.5

[a] Measuring range, 5 N < x < 360 N; [b] measuring range, 0.5 J < x < 100 J.

Physical Properties: The boiling, melting, and decomposition points of the C/Si pairs **1a/1b–5a/5b** were measured by differential scanning calorimetry (DSC) (Table 3.1). The acyclic carbon compounds **1a–3a** have boiling points in the temperature range 174–183 °C, but **2a** and **3a** already start to decompose at 160 °C. For the cyclic carbon compounds **4a** and **5a**, no boiling points could be determined because they start to decompose at 190 °C. For **2a** and **4a**, unexpectedly high melting points were observed (**2a**, ~ 20 °C; **4a**, 23 °C). Compound **3a** has a melting point of ~ -15 °C,[2] and **5a** becomes highly viscous upon cooling, but does not solidify at -18 °C. The silicon compounds **1b–5b** decompose violently in the temperature range 85–107 °C, which is 80–95 °C lower in temperature compared to the corresponding carbon analogues **1a–5a** (Tables 3.1 and 3.2). Interestingly, the decomposition temperatures of the cyclic silicon compounds **4b** and **5b** are slightly lower than those for the acyclic derivatives **1b–3b**. This is in contrast to the corresponding carbon analogues **1a–5a**, which show slightly higher decomposition points for the cyclic compounds **4a** and **5a** compared to their acyclic derivatives **1a–3a**. The highest

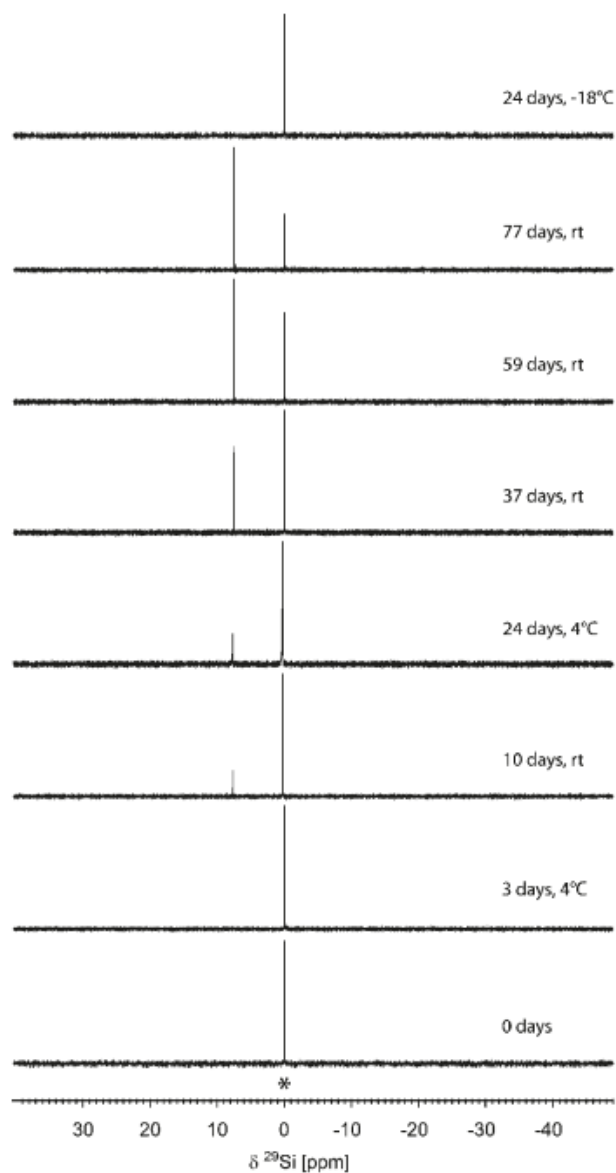


Figure 3.1. Decomposition of **1b** (*) at various temperatures (25°C , 4°C , and -18°C) and as a function of time in dry CDCl_3 as monitored by $^{29}\text{Si}\{^1\text{H}\}$ NMR spectroscopy.

decomposition points of the silicon-based nitratomethyl compounds **1b–5b** were observed for **2b** and **3b** (ca. 107°C). The boiling points of **1b–5b** could not be determined because of prior explosive decomposition. The silicon compounds **1b–5b** have lower melting points (**2b**, $\sim -10^\circ\text{C}$; **3b**, -18°C ; **4b**, -18°C ; **5b**, $\sim 4^\circ\text{C}$) than the corresponding carbon analogues, except for **5b** with a melting point of about 4°C . Only **5b** crystallized at 4°C in a refrigerator, whereas all the other compounds solidified at -18°C in the freezer, except for compound compounds can be stored at -18°C (**1b–5b**) and 4°C (**4b**, **5b**), respectively, without decomposition but decompose slowly at ambient temperature. The decomposition of **1b** in

dry trichloromethane at 25 °C, 4 °C, and -18 °C was studied by $^{29}\text{Si}\{^1\text{H}\}$ NMR spectroscopy as a function of time (Figure 3.1). The aliquots of **1b** were stored at 4 °C and -18 °C as pure substance (in air), and NMR samples were freshly prepared in dry trichloromethane after a period of time. The NMR spectra at ambient temperature were collected from one NMR sample prepared in dry trichloromethane, which was repeatedly measured after a period of time. After 10 days of storing **1b** at ambient temperature and air, about 20 % (and after 60 days about 50 %) was decomposed. The main decomposition product was unambiguously identified as hexamethyldisiloxane,[39] the formation of which is not understood at this time. At 4 °C after 24 days, about 20 % of **1b** was decomposed to give hexamethyldisiloxane, but no significant decomposition was observed upon storing at -18 °C over a period of 24 days. The NMR samples were taken from pure substances for the series at 4 °C and -18 °C.

Friction and Impact Sensitivities: The experiments concerning the friction and impact sensitivities of the C/Si pairs **1a/1b-5a/5b** were performed according to BAM (*Bundesanstalt für Materialforschung and -prüfung*) standards.[19] The parent carbon compounds **1a-5a** were found to be much less sensitive toward impact and friction of compounds (**1b**) is much higher than the highest sensitivity the silicon compounds are in the range of the critical value of compared the lowest sensitivity (impact and friction) observed for the silicon measurability of the BAM setup (<0.5 J). The number of the nitratomethyl groups is the most important factor influencing the friction sensitivity of the compounds studied. The cyclic silicon compounds **4b** and **5b** are less sensitive toward friction than the corresponding acyclic derivatives **1b-3b**, with **4b** (five-membered ring) showing a higher sensitivity toward friction than **5b** (six-membered ring). This might be due to the larger ring strain in the case of **4b**. Compounds **2a** and **4a** were measured as liquids, but spontaneous crystallization during the friction tests was observed, which would explain the higher sensitivity of the bis(nitratomethyl) compound **2a** compared to the tris(nitratomethyl) derivative **3a**.

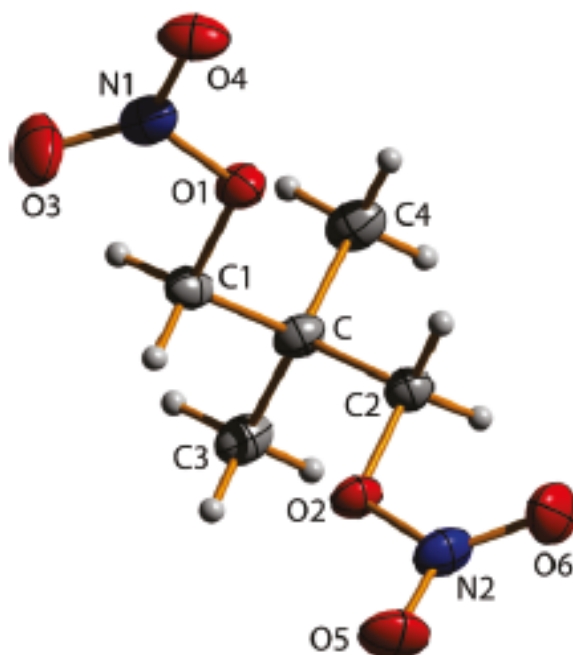


Figure 3.2. Molecular structure of **2a** in the crystal showing the atom labelling scheme. Thermal ellipsoids are shown at the 50 % probability level.

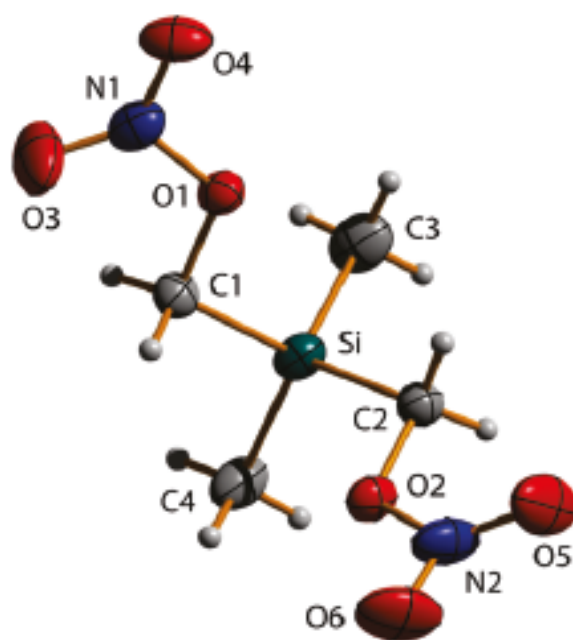


Figure 3.3. Molecular structure of **2b** in the crystal showing the atom labelling scheme. Thermal ellipsoids are shown at the 50 % probability level.

Table 3.4. Crystal data and details of the structure determinations of **2a**, **2b**, **4a** and **5b**.

	2a	2b	4a	5b
formula	C ₅ H ₁₀ N ₂ O ₆	C ₄ H ₁₀ N ₂ O ₆ Si	C ₇ H ₁₂ N ₂ O ₆	C ₇ H ₁₄ N ₂ O ₆ Si
<i>M_r</i> / g·mol ⁻¹	194.15	210.23	220.19	250.29
<i>T</i> / K	100(2)	140(2)	100(2)	200(2)
<i>λ</i> / Å	0.71073	0.71073	0.71073	0.71073
crystal system	monoclinic	monoclinic	monoclinic	monoclinic
space group	<i>P2₁/c</i>	<i>P2₁/c</i>	<i>P2₁/n</i>	<i>P2₁/c</i>
crystal size / mm	0.15×0.18×0.03	0.1×0.1×0.02	0.21×0.17×0.06	0.2×0.2×0.02
<i>a</i> / Å	7.5819(5)	7.6671(3)	7.0159(6)	10.4017(9)
<i>b</i> / Å	10.5551(6)	11.0136(4)	9.6605(9)	6.7723(6)
<i>c</i> / Å	11.5215(7)	12.0510(5)	14.7399(9)	16.6297(14)
<i>β</i> / deg	106.530(7)	105.407(5)	91.061(6)	94.726(8)
<i>V</i> / Å ⁻³	883.93(9)	981.04(7)	998.86(14)	1167.47(17)
<i>Z</i>	4	4	4	4
<i>ρ</i> _{calc.} / g·cm ⁻³	1.459	1.423	1.464	1.424
<i>μ</i> / mm ⁻¹	0.135	0.243	0.129	0.217
<i>F</i> (000)	408	440	464	528
2 <i>θ</i> range / deg	7.90–52.00	7.68–52.00	7.66–52.98	7.50–52.00
index ranges	–9 ≤ <i>h</i> ≤ 9 –13 ≤ <i>k</i> ≤ 12 –12 ≤ <i>l</i> ≤ 14	–9 ≤ <i>h</i> ≤ 9 –13 ≤ <i>k</i> ≤ 16 –14 ≤ <i>l</i> ≤ 14	–8 ≤ <i>h</i> ≤ 8 –11 ≤ <i>k</i> ≤ 11 –18 ≤ <i>l</i> ≤ 18	–12 ≤ <i>h</i> ≤ 12 –8 ≤ <i>k</i> ≤ 8 –14 ≤ <i>l</i> ≤ 20
reflections collected	4902	9722	6995	5355
reflections unique	1726 [<i>R</i> _{int} = 0.0414]	1936 [<i>R</i> _{int} = 0.0200]	1952 [<i>R</i> _{int} = 0.0379]	2254 [<i>R</i> _{int} = 0.0955]
parameters	118	128	184	145
GoF	0.959	1.180	0.859	0.990
<i>R</i> ₁ / w <i>R</i> ₂ [<i>I</i> > 2σ(<i>I</i>)]	0.0411 / 0.0756	0.0301 / 0.0825	0.0329 / 0.0678	0.0588 / 0.0814
<i>R</i> ₁ / w <i>R</i> ₂ (all data)	0.0786 / 0.0853	0.0406 / 0.0887	0.0711 / 0.0751	0.1686 / 0.1141
max / min	+0.201 / –0.172	+0.326 / –0.172	+0.151 / –0.169	+0.315 / –0.291
residual electron density / e·Å ⁻³				

Crystal Structure Analyses: The nitratomethyl compounds Me₂C(CH₂ONO₂) (**2a**), Me₂Si(CH₂ONO₂)₂ (**2b**), (CH₂)₄C(CH₂ONO₂) (**4a**), and (CH₂)₅Si(CH₂ONO₂) (**5b**) and the silicon-containing precursors (CH₂)₄Si(CH₂OH)₂ (**7**) and (CH₂)₅Si(CH₂OH)₂ (**8**) were structurally characterized by single-crystal X-ray diffraction. The crystallographic data for **2a**, **2b**, **4a**, and **5b** are given in Table 3.4. The molecular structures of these compounds in the crystal are depicted in Figures 3.2–3.5; selected bond lengths and angles are listed in Tables 3.5 and 3.6. For the crystal structure analyses of the precursors **7** and **8**, see the Supporting Information. The carbon-based nitratomethyl compound **2a** crystallizes in the monoclinic space group *P2₁/c*, with four molecules in the unit cell, a agreement with the data obtained for PETN.[40] Only the CH₂–O calculated density of 1.459 g/cm³, and a cell volume of 883.93(9) Å³. As also observed for the cyclic derivative **4a** (monoclinic, space

group $P2_1/n$, four molecules in the unit cell, density 1.464 g/cm^3), the bond lengths and angles of the C-CH₂-ONO₂ unit are in good bonds are slightly longer than a “normal” C-O single bond (1.43 \AA),[41] with bond lengths of approximately 1.46 \AA (**2a**) and 1.45 \AA (**4a**), respectively, but almost identical with the CH₂-O bond lengths observed for PETN.[40] The structure of the NO₂ group is similar to that observed for PETN and gaseous nitrogen

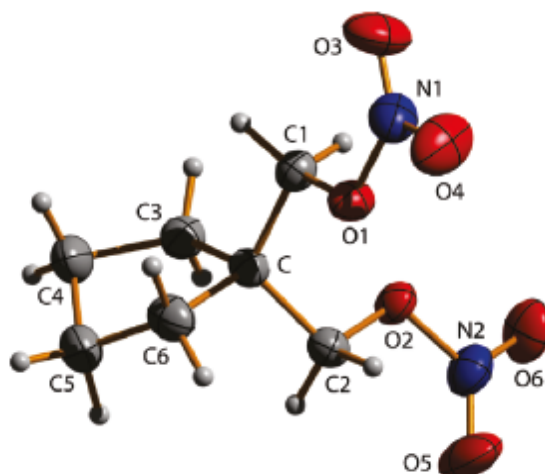


Figure 3.4. Molecular structure of **4a** in the crystal showing the atom labelling scheme. Thermal ellipsoids are shown at the 50 % probability level.

Table 3.5. Bond lengths (\AA) of **2a**, **2b**, **4a** and **5b** in the crystal.

	2a (El = C)	2b (El = Si)	4a (El = C)	5b (El = Si)
N1-O1	1.3908(19)	1.4021(13)	1.3977(16)	1.406(4)
N2-O2	1.3954(18)	1.3927(14)	1.3900(16)	1.407(4)
N1-O3/4	1.2033(19)/ 1.2096(19)	1.1878(15)/ 1.2035(14)	1.1948(18)/ 1.2001(18)	1.201(4)/ 1.205(4)
N2-O5/6	1.211(2) 1.2106(19)	1.2154(17)/ 1.2005(17)	1.1938(18)/ 1.2022(18)	1.192(4)/ 1.210(4)
C1-O1	1.460(2)	1.4512(13)	1.4541(18)	1.447(4)
C2-O2	1.457(2)	1.4495(15)	1.4535(18)	1.446(4)
El-C1/2	1.528(2)/ 1.523(2)	1.8860(12)/ 1.8892(12)	1.517(2)/ 1.514(2)	1.875(4)/ 1.883(4)
El-C3	1.535(2)	1.8489(14)	1.549(2)	1.852(4)
El-C4	1.537(3)	1.8500(13)		
El-C6			1.550(2)	
El-C7				1.850(4)
C3-C4			1.524(2)	1.532(5)
C4-C5			1.514(3)	1.523(5)
C5-C6			1.514(2)	1.513(5)
C6-C7				1.538(5)

Table 3.6. Bond angles (°) of **2a**, **2b**, **4a** and **5b** in the crystal.

	2a (El = C)	2b (El = Si)	4a (El = C)	5b (El = Si)
O3-N1-O4	129.01(17)	128.75(12)	129.24(15)	129.2(4)
O5-N2-O6	129.29(16)	129.32(13)	128.66(15)	128.7(4)
O1-N1-O3/4	118.29(16)/ 112.70 (16)	118.37(11)/ 112.88(11)	118.25(14)/ 112.51(15)	118.1(4)/ 112.6(4)
O2-N2-O5/6	118.04(17)/ 112.67(16)	112.38(12)/ 118.30(12)	118.42(15)/ 112.93(15)	118.6(4)/ 112.7(3)
N1-O1-C1	114.16(13)	114.40(9)	113.55(12)	114.5(3)
N2-O2-C2	113.92(13)	114.27(10)	113.63(13)	114.1(3)
El-C1-O1	106.55(14)	106.69(8)	106.68(13)	108.6(2)
El-C2-O2	106.61(14)	105.55(8)	107.09(13)	106.6(2)
C1-El-C2	112.02(14)	108.68(5)	112.37(12)	103.77(17)
C1-El-C3	106.75(15)	109.50(6)	107.89(14)	108.09(18)
C1-El-C4	110.16(15)	106.60(6)		
C1-El-C6			112.50(13)	
C1-El-C7				111.34(18)
C2-El-C3	110.73(15)	107.37(6)	112.09(13)	113.92(18)
C2-El-C4	106.73(15)	109.83(6)		
C2-El-C6			107.30(14)	
C2-El-C7				112.62(18)
C3-El-C4	110.49(15)	114.74(7)		
C3-El-C6			104.47(13)	
C3-El-C7				107.07(17)
El-C3-C4			105.84(15)	111.2(3)
C3-C4-C5			103.47(16)	113.6(3)
C4-C5-C6			102.34(15)	115.0(3)
C5--C6-C7				114.4(3)
El-C6-C5			104.94(14)	
El-C7-C6				110.6(3)

dioxide. The bond lengths of these compounds are similar to those of their carbon analogues. The lengths of the CH₂-O bonds of the silicon compound **2b** (1.4512(13) and 1.4495(15) Å) are marginally shorter than the corresponding bond lengths of the carbon analogue **2a** (1.457(2) and 1.460(2) Å). Also, the O-NO₂ bonds of the silicon compounds are slightly longer than those of the carbon analogues. In comparable moieties like the nitratomethyl groups of the C/Si analogues **2a** and **2b** the bond strength is inversely related to the bond length. Therefore, the O-NO₂ bonds of the silicon compound are probably slightly weaker than those of the carbon analogue, but like the situation in methyl nitrate.[42] To identify whether there are attractive interactions between the silicon atoms and the bridging oxygen atoms of **2b** and **5b**, one could be tempted to compare the distance between them with the sum of their van der Waals radii.[43] However, in the case of

geminal arrangements this is not a valid comparison. Alternatives are the use of two-bond radii of Bartell[44] or, to be preferred, the one-angle radii of Glidewell.[45]

The distances to be considered for **2b** (2.672(1)/2.690(1) Å) and **5b** (2.679(3)/2.723(3) Å) are surprisingly close to the sum of Glidewell's values for silicon (1.55 Å) and oxygen atoms (1.13 Å) at 2.68 Å. This indicates an absence of pronounced attractive Si---O interactions. Such attractive interactions between geminal silicon (acceptor) and donor atoms (O, N) are known to have significant or even dominating effects

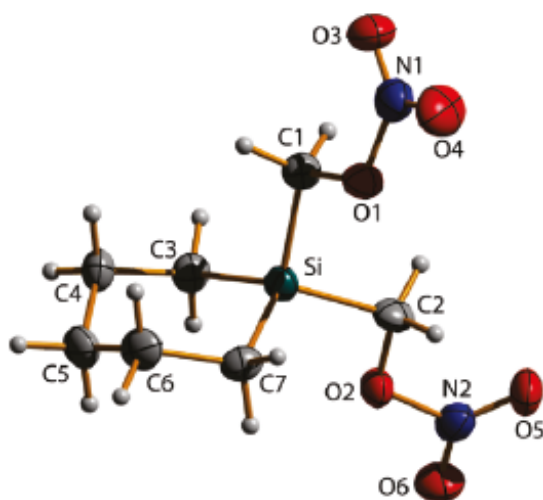


Figure 3.5. Molecular structure of **5b** in the crystal showing the atom labelling scheme. Thermal ellipsoids are shown at the 50 % probability level.

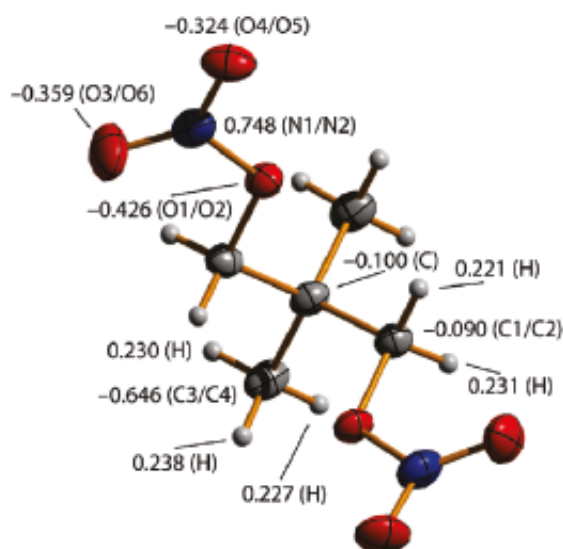


Figure 3.6. NBO charges of **2a**, calculated at the B3LYP/cc-pVDZ level of theory. All given values are in e (e = electron). The atom labels shown in parentheses (see also Figure 3.2).

on molecular structures. Examples are the structures of SiON (e.g., F₃SiONMe₂)[46] and SiNN compounds (e.g., F₃SiN--(Me)NMe₂)[47]; this effect has been coined the R-effect in silicon chemistry. However, in simple systems containing SiCO units (e.g., F₃SiCH₂OMe),[48] which are more closely related to compounds **2b** and **5b**, such pronounced interactions have not been found for the structures of the molecular ground states. The very similar Si-C-O angles of **2b** and **5b** (105.55(8)–108.6(2) °) and the analogous C-O-C angles of **2a** and **4a** (106.55(14)–107.09(13) °) do also not support the interpretation of our data in terms of such kind of interactions.

NBO analyses were performed at the B3LYP/cc-pVDZ level of theory (Figures 3.6 and 3.7). The resulting data of the C/Si analogues **2a** and **2b** show no significant evidence for intramolecular C---O and Specifically, the NBO charge of the quaternary central carbon atom of **2a** shows a negative value of -0.100 e (e = electron; -0.058 e for C(CH₃)₄). In contrast, the central silicon atom of **2b** shows a positive value of 1.754 e (1.782 e for Si(CH₃)₄). The values for the CH₃ carbon atoms of compound **2a** are clearly negative (-0.646 e), but the CH₂ carbon atoms show only a slightly negative charge (-0.090 e). The corresponding values of the silicon analogue **2b** show strongly negative charges at both the CH₃ (-1.175 e) and the CH₂ carbon atoms (-0.561 e). The NBO charges of the oxygen and nitrogen atoms of the nitrate moieties of **2a** and **2b** show almost no influence of the carbon/silicon exchange. The same holds true for the NBO charges of the hydrogen atoms of the C/Si analogues **2a** and **2b**.

The enthalpies of formation ($\Delta_f H^\circ$) of the single molecules **1a-5a** and **1b-5b** were calculated at the CBS-4 M level of theory (Table 3.7). The enthalpy changes of the isodesmic reactions ($\Delta_r H^\circ$) shown in Scheme 3.6 were obtained by the sum of $\Delta_f H^\circ$ of the products (**1a-5a**, Si(CH₃)₄) minus the sum of $\Delta_f H^\circ$ of the reactants (**1b-5b**, C(CH₃)₄). As can be seen from Table 3.7, all isodesmic reactions are exothermic ($\Delta_r H^\circ < 0$). In detail, with increasing number of nitratomethyl groups, the value of $x\Delta_r H^\circ$ increases. When comparing **1a** with **2a** and **1a** with **3a**, a doubling and a tripling, respectively, of the $\Delta_r H^\circ$ values are observed. Comparison of the acyclic molecule **2a** with the related cyclic molecule **5a** (six-membered ring) reveals similar $\Delta_r H^\circ$ values (-9.054 and -9.753 kcal/mol). In contrast, for the cyclic derivative **4a** (five-membered ring) a significantly higher $\Delta_r H^\circ$ value (-15.209 kcal/mol) is

observed. A possible explanation for this phenomenon is the increased ring strain in the case of **4a**. The intramolecular Si---O distances between the silicon atoms and the bridging oxygen atoms observed for **2b** and **5b** are 2.672(1) and 2.723(3) Å, respectively, and this is the expected range for geminal silicon and oxygen atoms.

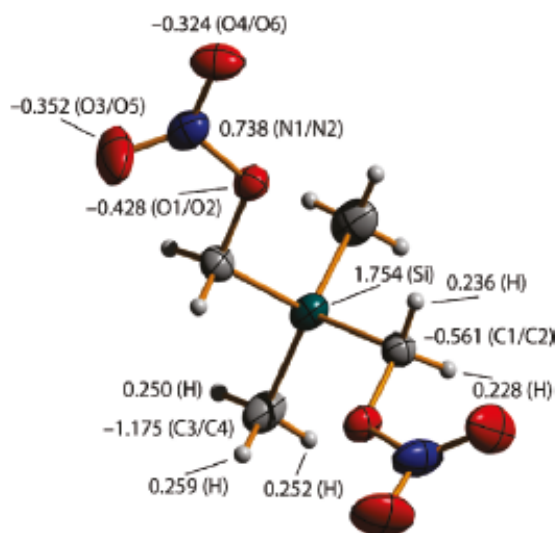


Figure 3.7. NBO charges of **2b**, calculated at the B3LYP/cc-pVDZ level of theory. All given values are in e (e = electron). The atom labels shown in parentheses (see also Figure 3.3).

Table 3.7. Enthalpies of formation ($\Delta_f H^\circ$, kcal/mol) for **1a–5a**, **1b–5b**, $C(CH_3)_4$, and $Si(CH_3)_4$ and enthalpies changes of the isodesmic reaction ($\Delta_r H^\circ$, kcal/mol) of **1b–5b** to **1a–5a** (Scheme 3.6).

reaction	$\Delta_f H^\circ$ (1b–5b)	$\Delta_f H^\circ$ ($C(CH_3)_4$)	$\Delta_f H^\circ$ (1a–5a)	$\Delta_f H^\circ$ ($Si(CH_3)_4$)	$\Delta_r H^\circ$
1b → 1a	-456720.0	-123857.1	-299182.9	-281398.6	-4.4
2b → 2a	-632040.4	-123857.1	-474507.9	-281398.6	-9.0
3b → 3a	-807358.9	-123857.1	-649830.6	-281398.6	-13.1
4b → 4a	-680527.0	-123857.1	-523000.7	-281398.6	-15.2
5b → 5a	-705155.8	-123857.1	-547624.0	-281398.6	-9.8

The proximity of these atoms makes it plausible that the first step in the decomposition reaction is the highly exothermic formation of a Si–O bond and could promote the initial step for a chain reaction. Calculations for the decomposition pathway of $Si(CH_2ONO_2)_4$ confirm this view that the initial step of this process is the formation of an Si–O bond between the bridging oxygen atom and the central silicon atom.[8] This is in contrast to the decomposition pathway known for common nitrate ester explosives, where the homolytic O–NO₂ bond cleavage is the initial step.[3] However, it is in line with the finding of very shallow Si–C–N bending potentials observed for (aminomethyl)silanes, which can also be seen as contribution to the increased reactivity of such compounds at silicon.[49]

and each individual methyl group. Finally, on the basis of the relatively small scattering intensity for hydrogen, the hydrogen atoms in the CH₂ bridge were positioned with equal El-C-H (El = C, Si) and O-C-H angles, while the C-H distance in the CH₂ bridge was assumed to be equal to that of the methyl groups. Using this combination of assumptions, the total number of internal coordinates for each compound was reduced from 54 to 14, as shown in Tables 3.8 and 3.9. The atom numbering schemes used for the molecular models, corresponding to the descriptions in Tables 3.8 and 3.9, are shown in Figures 3.9 and 3.10. The only difference between the models for the two compounds, other than in the descriptions due to the exchange of carbon for silicon, was that the C-O and N-O bond lengths were described by an average and difference for **1a**, but were included as independent parameters for **1b**.

GED Refinements: The experimental molecular-intensity and radial-distribution curves for **1a** and **1b** are shown in Figures 3.11–3.14, with the refined difference curves shown at the bottom of each figure. The refinements were performed along the lines of the SARACEN method,[50] which places flexible restraints on parameters that are not well resolved from the GED experiment, with the value of the restraint being taken from theory and the uncertainty estimated by the convergence of the calculations (a strict interpretation of the SARACEN method would require the full number of independent parameters to be included in the model, but in this case we have made use of the assumptions mentioned above). All 14 independent parameters for both **1a** and **1b** were therefore refined as shown in Tables 3.8 and 3.9. Seven of these 14 parameters were refined unrestrained for **1a** and eight in the case of **1b**, the difference being that the C-O and N-O distances for **1b** were refined independently, whereas for **1a** they were included as an average and a difference, the latter of which was restrained. Amplitudes of vibration were also refined for both molecules, but those corresponding to distances under a single peak in the respective radial-distribution curve (RDC, see Figures 3.11 and 3.13) were grouped together with fixed relative amplitudes. Restraints were also applied to all refined amplitudes, and for **1b** restraint uncertainties of 10 % of the calculated values were applied, while those for **1a** were set to 10 % for distances less than 4.5 Å and 20 % for distances greater than 4.5 Å. The full lists of interatomic distances, amplitudes of vibration, and distance corrections for the r_{h1} refinements, including details of which amplitudes were tied together, are provided as

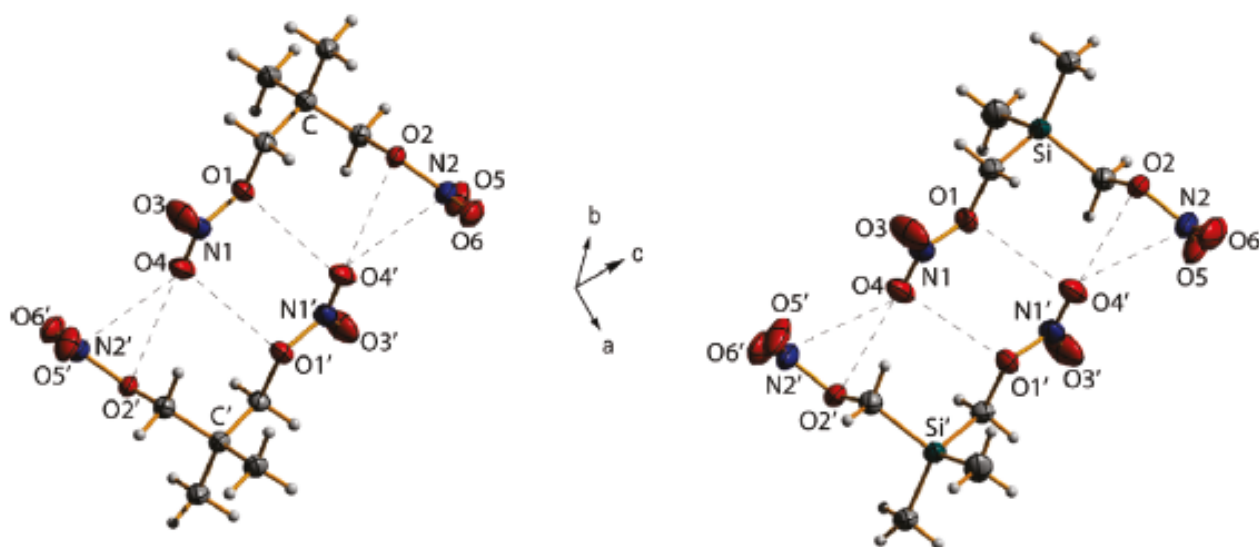


Figure 3.8. Aggregation motifs of pairs of molecules in the crystals of **2a** (left) and **2b** (right). The contacts O1---O4', O2---O4', and N2---O4' are shown in dashed lines.

Supporting Information. The refinement of **1a** yielded a good fit of the experimental to theoretical intensities for both the r_g and r_{h1} structure types, as can be seen from the low R factors (R_G) of 4.7 % and 5.2 %, respectively. In the case of **1b**, the relatively low vapor pressure at room temperature required longer exposure times and a higher beam current than have been found to be optimum, and the data are correspondingly noisier than for **1a** and in previous GED structure investigations using this combination of apparatus and refinement techniques.[26,51] The resulting R factors of 16.4 % and 14.9 % for the respective r_g and r_{h1} structure types are higher than might be expected; however, the quality of the fit can also be judged by the appearance of the molecular-intensity and radial-distribution curves (Figures 3.13 and 3.14). In particular, the residuals of the molecular intensity curves can be seen to be randomly distributed, indicating that the higher R factor is due to a lower signal-to-noise ratio rather than a refinement problem. Curiously, the standard deviations for the refined parameter values of **1a** and **1b** (Tables 3.8 and 3.9) are similar to one another, but from the preceding should be larger than those for **1a**. However, comparison of the RDCs (Figures 3.12 and 3.14) reveals that the structure of **1b** may be marginally better resolved by GED: While there are nine distinct peaks in the RDC for both compounds, the RDC for **1a** exhibits only one additional weak shoulder at about 3 Å, but the RDC for **1b** also contains two large shoulders at about 1.4 and 2.7 Å, as well as a small shoulder at 3.4 Å. Thus, the lower signal-to-noise ratio observed for **1b** is expected to be

counter-balanced by an increase in the structural information inherent in its electron diffraction pattern, compared to **1a**.

Discussion of the Gas-Phase Geometries: A selection of important geometric parameters for **1a** and **1b** are listed in Table 3.10, showing the convergence of the calculated structures, alongside the experimental GED structures, the latter being determined using both the rg and the rh1 models for vibrational motion.[52] Comparison of the calculated and experimental values indicates that the Me_3ElCH_2 groups (El = C, Si) are reasonably well described by HF theory, with only small changes in the values of these parameters when improving the theoretical treatment by applying MP2 theory. In contrast, HF theory appears to have severe limitations with regard to the treatment of the nitrate group. The terminal N–O bonds are significantly elongated by applying MP2 theory, by more than 3 pm when the geometries calculated with identical basis sets are compared. The largest discrepancy between the HF and MP2 geometries of **1a** and **1b** is in the length of the N–O3 bond, which is lengthened by 0.081 Å (**1a**) and 0.095 Å (**1b**), respectively. Such a large difference between the HF and MP2 method would normally cast doubt on the accuracy of the MP2 geometry; however, the N–O bond lengths determined by GED agree very well with those determined by the MP2 method (although the differences between the N–O5 and N–O8 distances were restrained to the MP2 values).

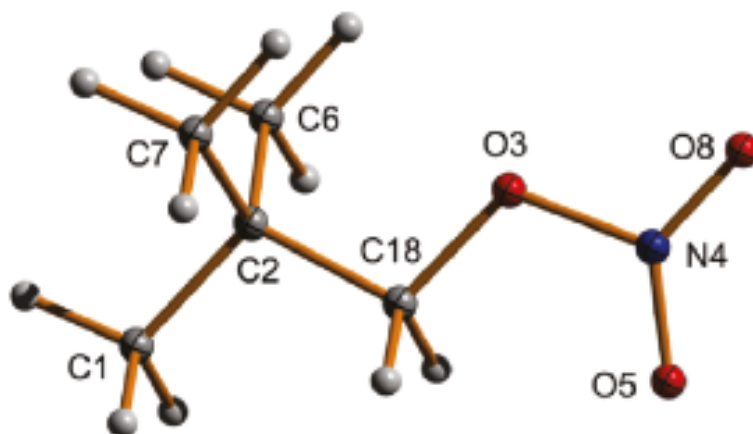


Figure 3.9. Molecular structure of **1a** in the gas phase showing the atom labelling used for the GED model.

Table 3.8. Details of the independent parameters used in the GED refinement of **1a**, refined parameter values, calculated values obtained at the RI-MP2/TZVPP level of theory, and applied restraints.^[a]

	parameter description	GED r_g	GED r_{h1}	MP2 r_e	restraint uncertainty
p_1	r C–C average	1.539(1)	1.538(1)	1.525	
p_2	r C–O, N–O3 average	1.430(2)	1.429(2)	1.422	
p_3	r –O, N–O3 difference	0.040(4)	0.035(4)	0.033	0.010
p_4	r N–O $\times 2$ mean ^[b]	1.211(1)	1.210(1)	1.208	
p_5	r C–H	1.117(2)	1.114(2)	1.090	0.010
p_6	\sphericalangle C(Me)–C–C(Me)	109.2(2)	108.7(2)	109.9	
p_7	\sphericalangle C–C–O	106.3(3)	106.9(3)	106.9	
p_8	\sphericalangle C–O–N	113.6(3)	113.2(3)	113.2	
p_9	\sphericalangle O5–N–O8	132.0(6)	128.7(6)	130.0	
p_{10}	\sphericalangle H–C–H	111.0(3)	110.8(1)	108.3	1.0
p_{11}	r C–C difference ^[c]	0.002(4)	0.003(4)	0.005	0.005
p_{12}	CMe ₃ tilt ^[d]	4.4(2)	3.7(2)	2.5	1.0
p_{13}	\sphericalangle O3–N–O difference ^[e]	4.7(5)	3.4(5)	4.4	1.0
p_{14}	r N–O $\times 2$ difference ^[f]	0.008(4)	0.004(4)	0.006	0.005
	R factor (R_G)	4.7 %	5.2 %		

[a] All distances are in Å and angles are in °. The two sets of parameter values for the GED refinement, r_g and r_{h1} , correspond to different approaches to accounting for vibrational motion. The r_g structure is a vibrational average, while the r_{h1} structure is an approximation to an equilibrium structure, r_e ; [b] average of N–O5 and N–O8; [c] C–C(Me) minus C–C18; [d] defined as a decrease in the C1–C2–C18 angle with respect to the required for C_{3v} symmetry; [e] O3–N–O5 minus O3–N–O8; [f] N–O5 minus N–O8.

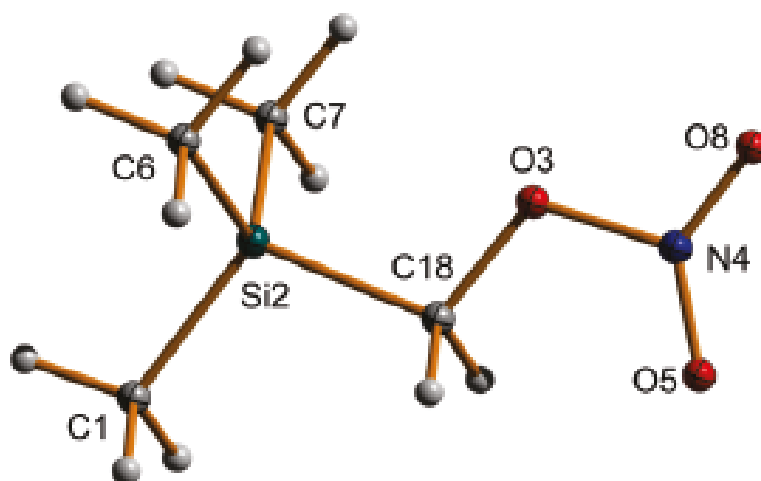
**Figure 3.10.** Molecular structure of **1b** in the gas phase showing the atom labelling used for the GED model.

Table 3.9. Details of the independent parameters used in the GED refinement of **1b**, refined parameter values, calculated values obtained at the RI-MP2/TZVPP level of theory, and applied restraints.^[a]

	parameter description	GED r_g	GED r_{h1}	MP2 r_e	restraint uncertainty
p_1	r Si-C average	1.883(1)	1.882(1)	1.879	
p_2	r C-O	1.447(5)	1.437(4)	1.433	
p_3	r N-O3	1.426(4)	1.435(3)	1.425	
p_4	r N-O $\times 2$ mean ^[b]	1.208(1)	1.206(1)	1.206	
p_5	r C-H	1.104(3)	1.103(3)	1.090	0.010
p_6	\sphericalangle C(Me)-Si-C(Me)	110.9(4)	110.7(4)	111.2	
p_7	\sphericalangle Si-C-O	107.1(3)	108.3(3)	105.4	
p_8	\sphericalangle C-O-N	113.0(4)	113.6(4)	113.4	
p_9	\sphericalangle O5-N-O8	131.6(7)	131.3(7)	130.6	
p_{10}	\sphericalangle H-C-H	109.9(4)	109.5(3)	108.0	1.0
p_{11}	r Si-C difference ^[c]	0.033(3)	0.033(3)	0.034	0.005
p_{12}	SiMe ₃ tilt ^[d]	2.8(6)	1.6(5)	1.3	1.0
p_{13}	\sphericalangle O3-N-O difference ^[e]	5.9(5)	5.2(5)	4.6	1.0
p_{14}	r N-O $\times 2$ difference ^[f] R factor (R_G)	0.006(3) 16.4 %	0.005(3) 14.9 %	0.003	0.005

[a] All distances are in Å and angles are in °. The two sets of parameter values for the GED refinement, r_g and r_{h1} , correspond to different approaches to accounting for vibrational motion. The r_g structure is a vibrational average, while the r_{h1} structure is an approximation to an equilibrium structure, r_e ; [b] average of N-O5 and N-O8; [c] Si-C18 minus Si-C(Me); [d] defined as a decrease in the C1-Si-C18 angle with respect to the required for C_{3v} symmetry; [e] O3-N-O5 minus O3-N-O8; [f] N-O5 minus N-O8.

The reliability of the GED results can be assessed by the agreement between the two models (r_g and r_{h1}) used to describe the vibrational motion, as well as the standard deviations from the least-squares fit. The agreement between the two models is reasonably good for all bond distances, the largest discrepancies for r_{C-O} being 0.009 Å (**1a**) and 0.010 Å (**1b**), respectively. There is also a good agreement for most of the angles, with discrepancies mostly less than 1 °, the exceptions being the O5-N-O8 angle for **1a** and the Si-C-O angle for **1b**, which therefore should be treated with some caution. With regard to the increased friction and impact sensitivity of the silicon compound **1b** compared to its carbon analogue **1a**, the interesting parameters are the relative lengths of the N-O3 bonds and the Si-C-O and C-C-O angles. Both the experimental and calculated structures indicate a slight for r_{N-O3} .

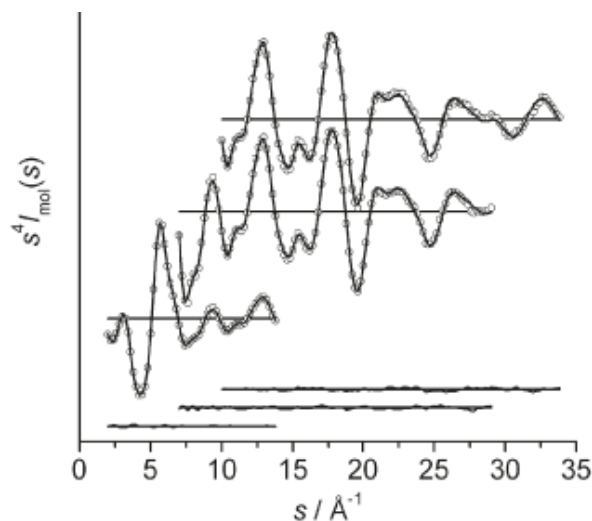


Figure 3.11. Experimental (\circ), theoretical, and difference (experimental minus theoretical) molecular-intensity curves for **1a**.

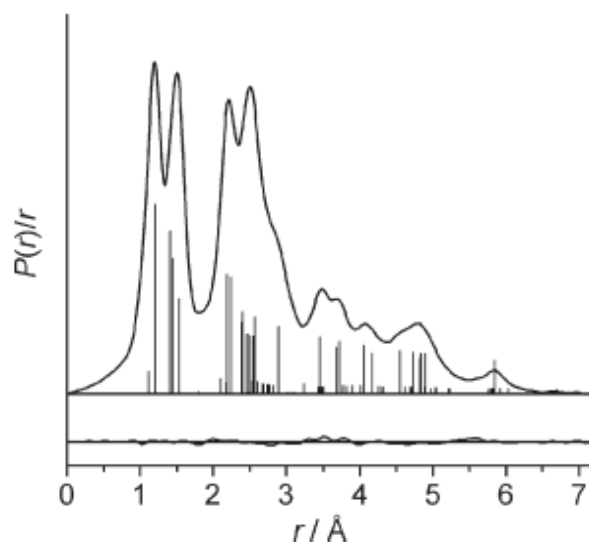


Figure 3.12. Experimental and difference (experimental minus theoretical) radial-distribution curves for **1a**. Prior to the Fourier transformation, the molecular-intensity data were multiplied by $s \cdot \exp[-0.00002s^2 / Z_N - f_N] - (Z_o - f_o)$ and the s -range was extended to 0 and to 36 \AA^{-1} by model data.

weakening of the N–O3 bond for the silicon compound **1b**, with an increase of about 0.02 \AA . The calculated structures of **1a** and **1b** also indicate a small (ca. 1°) contraction of the Si–C–O angle (**1b**) compared to the C–C–O angle (**1a**), but the experimentally established structures indicate a difference in the opposite direction. This parameter was not particularly well resolved in the GED structure of **1b**, as it was strongly dependent on the vibrational model. The observed discrepancy may be due to different dynamic behaviour for **1a** and **1b** rather than a deficiency in the theoretical model for describing the static

equilibrium geometries. In any case, the energy difference corresponding to such a small angle contraction would be minimal and the elongation of the O–NO₂ bond in **1b** is the only significant structural difference that might account for its greater instability.

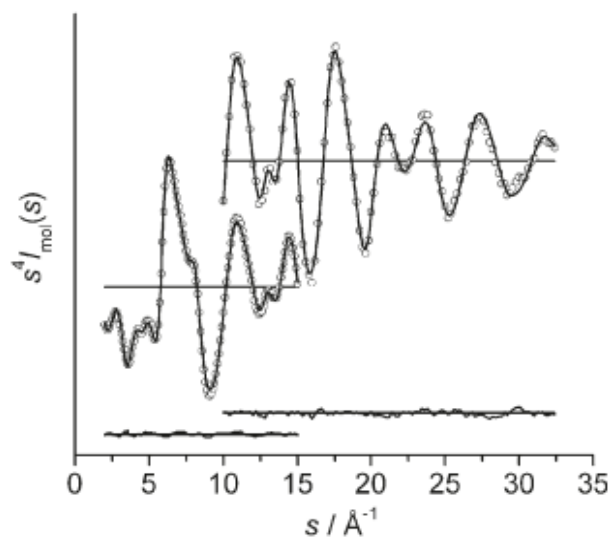


Figure 3.13. Experimental (○), theoretical, and difference (experimental minus theoretical) molecular-intensity curves for **1b**.

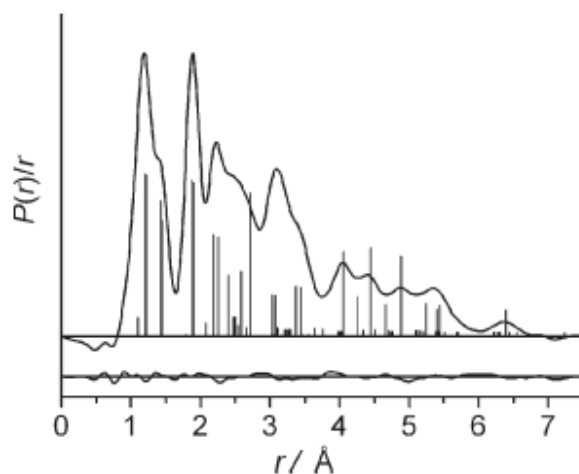


Figure 3.14. Experimental and difference (experimental minus theoretical) radial-distribution curves for **1b**. Prior to the Fourier transformation, the molecular-intensity data were multiplied by $s \cdot \exp[-0.00003s^2 / Z_N - f_N] - (Z_o - f_o)$ and the s -range was extended to 0 and to 36 \AA^{-1} by model data.

Table 3.10. Selected structural parameters for **1a** and **1b** as determined experimentally by GED and calculated by theory.

method	HF/6-31G*[b]	HF [c]	MP2 [c]	GED	
	r_e	r_e	r_e	r_g	r_{hl}
Compound 1a					
r C–H	1.085	1.083	1.090	1.117(2)	1.111(3)
r C–C(Me)	1.536	1.533	1.526	1.540(1)	1.539(1)
r C–C18	1.530	1.528	1.521	1.538(3)	1.535(3)
r C–O	1.439	1.435	1.438	1.450(3)	1.441(3)
r N–O3	1.327	1.324	1.405	1.410(2)	1.408(2)
r N–O5	1.187	1.179	1.211	1.215(2)	1.213(2)
r N–O8	1.179	1.170	1.205	1.207(2)	1.208(2)
\sphericalangle C–C–O	107.4	107.9	106.9	106.3(3)	106.9(3)
\sphericalangle C–O–N	116.5	116.7	113.2	113.6(3)	114.0(3)
\sphericalangle O5–N–O8	127.9	127.8	130.0	132.0(6)	129.7(7)
Compound 1b					
r C–H	1.086	1.084	1.090	1.104(3)	1.103(3)
r Si–C(Me)	1.886	1.877	1.870	1.875(1)	1.874(1)
r Si–C18	1.919	1.913	1.905	1.908(3)	1.907(3)
r C–O	1.439	1.435	1.433	1.447(5)	1.437(4)
r N–O3	1.333	1.330	1.425	1.426(4)	1.435(3)
r N–O5	1.185	1.177	1.207	1.211(2)	1.208(2)
r N–O8	1.179	1.171	1.204	1.205(2)	1.204(2)
\sphericalangle Si–C–O	106.6	107.4	105.4	107.1(3)	108.3(3)
\sphericalangle C–O–N	116.9	117.1	113.4	113.0(4)	113.6(4)
\sphericalangle O5–N–O8	128.0	128.0	130.6	131.6(7)	131.3(7)

[a] All distances r are in Å and angles \sphericalangle are in °, and the numbers in parentheses are one standard deviation in the last digit. For an explanation of the structure types, r_e , r_g , and r_{hl} , see ref [52]; [b] 6-31G** was used for **1a**; [c] def2-TZVPP.

Conclusion

The silicon-based nitratomethyl compounds Me₂Si(CH₂ONO₂)₂ (**2b**), MeSi(CH₂ONO₂)₃ (**3b**), (CH₂)₄Si(CH₂ONO₂)₂ (**4b**), and (CH₂)₅Si-(CH₂ONO₂)₂ (**5b**) were synthesized for the first time. In addition, the known derivative Me₃SiCH₂ONO₂ (**1b**) was resynthesized. The silicon compounds **1b–5b** were found to be much more sensitive toward friction and impact than their mostly known carbon analogues Me₃CCH₂ONO₂ (**1a**), Me₂C(CH₂ONO₂)₂ (**2a**), MeC(CH₂ONO₂)₃ (**3a**), (CH₂)₄C(CH₂ONO₂)₂ (**4a**, new), and (CH₂)₅C(CH₂ONO₂)₂ (**5a**). The thermal stabilities of the silicon compounds **1b–5b** are approximately 80–95 °C lower than those of the corresponding carbon analogues **1a–5a**. Weak O–NO₂ bonds, strong C–O bonds,

and the weaker Si-CH₂O bond of the silicon compounds are claimed to be responsible for the higher sensitivities compared to their corresponding carbon analogues. GED studies and calculations at different levels of theory established the gas phase structures of **1a** and **1b** in good agreement with the structural parameters obtained in single-crystal X-ray diffraction studies of **2a**, **2b**, **4a**, and **5b**. The carbon/silicon switch strategy has already been demonstrated to be a powerful tool for the development of novel drugs[17] and odorants[18] with unique properties. The studies presented here also clearly demonstrate the high potential of the sila-substitution concept (C/Si exchange) for the development of new silicon-based explosives (in this context see also refs. [7] and [8]), with properties that differ significantly from those of their corresponding carbon analogues.

Experimental Section

***Caution!** Many alkyl nitrates are sensitive and represent energetic materials; therefore, they must be handled with care! Since sila-analogues of alkyl nitrates are even more sensitive toward shock and friction, they must be manipulated very cautiously! During the work with alkyl nitrates, and especially with their sila-analogues, wearing leather jacket, face shield, steelreinforced Kevlar gloves, ear protection, and electrically grounded shoes is mandatory. Only electrically grounded and metal-free equipment was used during the syntheses.*

Nitric acid (100%, fuming), Me₃SiCH₂OH, Me₃SiCH₂I, Me₂Si(CH₂Cl)₂, acetonitrile (Aldrich), MeC(CH₂OH)₃, acetic anhydride (Acros Organics), Me₃CCH₂OH (Aldrich and Acros Organics), and silver nitrate (VWR) were used as received. The ¹H, ¹³C{¹H}, ¹⁴N, and ²⁹Si{¹H}NMR spectra were recorded using a Jeol 400 eclipse FT-NMR spectrometer (compounds **1a/b-5a/b**) operating at 400.2 MHz (¹H), 100.6 MHz (¹³C), 28.9 MHz (¹⁴N), and 79.5 MHz (²⁹Si) or a Bruker DRX-300 NMR spectrometer (compounds **6-11**) operating at 300.1 MHz (¹H), 75.5 MHz (¹³C), and 59.6 MHz (²⁹Si). Chemical shifts (ppm) are given with respect to TMS (¹H, ¹³C, ²⁹Si; δ 0) and MeNO₂ (¹⁴N; δ 0) as external standards (compounds **1a/b-5a/b**) or relative to internal [D₅]DMSO (¹H, δ 2.49; [D₆]DMSO), internal [D₆]DMSO (¹³C, δ 39.5; [D₆]DMSO), internal CHCl₃ (¹H, δ 7.24; CDCl₃), internal CDCl₃ (¹³C, δ 77.0; CDCl₃), or external TMS (²⁹Si, δ 0; [D₆]DMSO, CDCl₃) (compounds **6-11**). Analysis and assignment of the ¹H NMR data of **6-11** were supported by ¹H,¹H COSY, ¹³C,¹H HMQC, and ¹³C,¹H HMBC

experiments, and assignment of the ^{13}C NMR data was supported by DEPT135, $^{13}\text{C},^1\text{H}$ HMQC, and $^{13}\text{C},^1\text{H}$ HMBC experiments. Infrared (IR) spectra were recorded on a Perkin-Elmer Spectrum BXII FT-IR instrument equipped with a Diamant-ATR Dura Sampler at 25 °C. Raman spectra were recorded on a Perkin-Elmer Spectrum 2000R NIR FT-Raman instrument equipped with a Nd:YAG laser (1064 nm) with 300 mW at 25 °C, except for compound **3b**; the Raman data of **3b** were collected using a Isa Jobin-Yvon T64000 Raman instrument with CCD detector (EEV CCD115-11) equipped with a Spectra Physics Arp laser (514.5 nm) with 30 mW at 25 °C. Melting, boiling, and decomposition points were determined by differential scanning calorimetry (DSC; Perkin-Elmer Pyris 6 DSC, calibrated by standard pure indium and zinc). Measurements were performed at a heating rate of $\beta = 5\text{ °C}$ in closed aluminium containers with a hole ($1\text{ }\mu\text{m}$) on the top for gas release with a nitrogen flow of 5 mL/min. The reference sample was a closed aluminium container with air. Friction and impact sensitivities were determined by standard BAM methods.[19] A Büchi GKR-51 apparatus was used for the bulb-to-bulb distillations of **9–11**. The melting points of **7** and **8** were determined with a Büchi Melting Point B-540 apparatus using samples in sealed glass capillaries. The crystal structures were determined by using an Oxford Xcalibur CCD diffractometer (compounds **2a**, **2b**, **4a**, and **5b**) or a Stoe IPDS diffractometer (compounds **7** and **8**) and graphite-monochromated Mo-K α radiation ($\lambda=0.71073\text{ \AA}$). The structures were solved with SHELXS-97 and were refined with SHELXL-97,[21] implemented in the program package WinGX22 and finally checked using Platon.[23] Elemental analyses of the nitratomethyl compounds were not performed because of their highly sensitive and explosive properties. Mass spectrometric data were obtained from a Jeol Mstation JMS 700 spectrometer, except for **2b** and **3b**, which were too hazardous.

Electron scattering intensities were recorded at room temperature on a combination of reusable Fuji and Kodak imaging plates using a Balzers KD-G2 Gas-Eldigraph[24] (formerly operated in Tübingen by H. Oberhammer[25]). This has been equipped with an electron source built by STAIB Instruments, which was operated at 60 kV (**1a**) or 70 kV (**1b**). The accelerating voltage was monitored using a 0 to 10 V signal generated by the high-voltage supply, proportional to the variable 0 to 100 kV output, which was stable to within 0.1 to 0.2 mV during the course of the experiment. The image plates were scanned using a Fuji

BAS 1800 scanner, yielding digital 16-bit gray scale image data. Further details about the Bielefeld GED apparatus and the experimental method are published elsewhere.[26] In preparation for data reduction, the long and short nozzle-to-plate distances were remeasured after recording the short distance data and before recording the long-distance data for **1a**. The relative scaling of the two scanning directions was also recalibrated by using an exposed image plate with two pairs of pin holes, which was scanned in two orientations, approximately perpendicular to one another. The data were reduced to total intensities using Strand *et al.*'s program PIMAG27 (version 040827) in connection with a sector curve, which was based on experimental xenon scattering data and tabulated scattering factors of xenon. Further data reduction yielding molecular-intensity curves was performed by using version 2.4 of the ed@ed program,[28] using the scattering factors of Ross *et al.*[29] For both compounds the ratio of the electron wavelength to the nozzle-to-plate distances was checked using benzene data and the widely accepted r_{α} value of 1.397 Å for the C-C distance in benzene. In the determination of **1a**, the calculated electron wavelength was assumed to be correct, and the nozzle-to-plate distances were checked for consistency with the measured values leading to a small scaling being applied to the long distance. For **1b**, the data reduction was performed using the previously measured nozzle-to-plate distances, and a small scaling was applied to the electron wavelength for the data set recorded at the short distance. The electron wavelengths and nozzle-to-plate distances are provided as Supporting Information, along with other data analysis parameters including the s-limits, weighting points, R factors (RD and RG), scale factors, data correlation values, and the correlation matrix. The amplitudes of vibration, u , used in the rg and $rh1$ refinements, and the distance corrections for curvilinear perpendicular motion, $kh1$, were calculated by using the program SHRINK.[30,31] This made use of frequency calculations for **1a** and **1b**, respectively, at the RI-MP2/TZVPP and HF/6-31G* level of theory (for details of calculations, see below). The SHRINK input file for **1b** was generated using EasyInp written by K. B. Borisenko, while that for **1a** was generated using a combination of EasyInp and Q2SHRINK,[32] written by A. Zakharov.

All Hartree-Fock (HF) calculations were of the restricted type, and the second-order Møller-Plesset (MP2) calculations made use of the resolution-of-the-identity (RI) method and the default frozen-core partitioning as implemented in Turbomole.[33] The HF calculations

using the Pople-style 6-31G* basis sets were performed by using the default criteria in Gaussian 03,[34a] while those using the def2-TZVPP (herein shortened to TZVPP) basis set were performed by using Turbomole.

The theoretical calculations for structure optimization of **2a** and **2b** were performed at the B3LYP level of theory (cc-pVDZ basis sets) using Gaussian 03,[34b] and the NBO analyses were performed using the Gaussian 03 nbo5-tool. Instead, the calculations of the enthalpies of formation were performed at the CBS-4M level of theory.

General Procedure for the Nitration of the (Hydroxymethyl)alkanes and (Hydroxymethyl)cycloalkanes: For the synthesis of **1a**, **2a**, **4a**, and **5a**, the respective hydroxymethyl or bis(hydroxymethyl) compound [$\text{Me}_3\text{CCH}_2\text{OH}$, $\text{Me}_2\text{C}(\text{CH}_2\text{OH})_2$, $(\text{CH}_2)_4\text{C}(\text{CH}_2\text{OH})_2$, $(\text{CH}_2)_5\text{C}(\text{CH}_2\text{OH})_2$; 1.0 mmol (1.0 mol equiv)] was added in small portions at 20 °C to a stirred mixture of nitric acid (100 %; 2.1 and 4.2 mol equiv, respectively) and acetic anhydride (6.0 mol equiv). [For the synthesis of **3a**, the tris- (hydroxymethyl) compound, $\text{MeC}(\text{CH}_2\text{OH})_3$ was added in small portions at 0 °C to a stirred mixture of nitric acid (100 %; 3.3 mol equiv) and dichloromethane (5 mL).] The reaction mixture was then stirred at ambient temperature for 1.5 (**1a**, **2a**, **4a**, **5a**) or 2 h (**3a**), followed by the addition of ice-water (5 mL) and pentane (15 mL). The aqueous phase was separated and extracted with pentane (2 × 20 mL), and the combined organic extracts were washed with water (2 × 20 mL), neutralized by washing with a concentrated aqueous solution of sodium hydrogen carbonate, and then dried over anhydrous sodium sulphate. The solvent was removed under reduced pressure, and the residue was purified by distillation (**1a**) or by removal of the remaining solvent traces *in vacuo* (0.01 mbar, 20 °C, 3–6 h) (**2a–5a**). For further details of the syntheses, see Table 3.1.

2,2-Dimethyl-1-nitratopropane, $\text{Me}_3\text{CCH}_2\text{ONO}_2$ (1a**):** The crude product was distilled *in vacuo* (60 °C / 50 °mbar) to give **1a** 88 % yield as a colourless liquid.

^1H NMR (CDCl_3): δ = 0.97 (s, 9H, CCH_3), 4.12 (s, 2H, CCH_2O); $^{13}\text{C}\{^1\text{H}\}$ NMR (CDCl_3): δ = 26.4 (CCH_3), 31.4 (C_q), 82.1 (CCH_2O); $^{14}\text{N}\{^1\text{H}\}$ NMR (CDCl_3): δ = -41.2. Raman (300 mW): 2968 (vs), 2910 (vs), 2796 (w), 1629 (w), 1460 (m), 1365 (w), 1280 (s), 1261 (m), 1261 (w), 1045 (vw), 975 (vw), 921 (m), 868 (m), 769 (s), 696 (w), 611 (m), 478 (m), 405 (vw) cm^{-1} . IR: 2963 (w), 2875 (vw), 1621 (vs), 1479 (vw), 1467 (vw), 1279 (vs), 1219 (vw), 1043 (vw),

976 (w), 943 (vw), 924 (vw), 865 (m), 847 (m), 759 (vw), 694 (vw), 638 (vw) cm^{-1} . MS (DEI-) [m/e]: 133.1 [M⁻]. Bp.: 174 °C. Sensitivities: impact, >100 J; friction, >360 N.

2,2-Dimethyl-1,3-dinitratopropane, Me₂C(CH₂ONO₂)₂ (2a): The crude product was dried *in vacuo* (0.01 mbar, 25 °C, 3 h) to give **2a** in 82 % yield as a colourless liquid.

¹H NMR (CDCl₃): δ = 1.08 (s, 6H, CCH₃), 4.26 (s, 4H, CCH₂O); ¹³C{¹H} NMR (CDCl₃): δ = 22.1 (CCH₃), 34.7 (C_q), 76.5 (CCH₂O); ¹⁴N{¹H} NMR (CDCl₃): δ = -44.5. Raman (300 mW): 2969 (vs), 2910 (s), 2808 (vw), 2732 (vw), 1635 (w), 1467 (m), 1403 (vw), 1372 (w), 1285 (s), 1032 (w), 982 (vw), 921 (w), 870 (s), 795 (w), 693 (w), 608 (m), 475 (m), 408 (vw) cm^{-1} . IR: 2977 (w), 2900 (vw), 1826 (w), 1755 (vw), 1623 (vs), 1477 (w), 1369 (m), 1268 (vs), 1230 (w), 1122 (m), 1032 (w), 977 (s), 943 (w), 923 (w), 843 (vs), 756 (s), 718 (w), 703 (w), 637 (w) cm^{-1} . MS (DEI-) [m/e]: 193.1 [M-H]⁻. Mp.: 18-23 °C. Bp.: 178 °C (dec.). Sensitivities: impact >100 J; friction >96 N.

2-Methyl-2-nitratomethyl-1,3-dinitratopropane, MeC(CH₂ONO₂)₃ (3a): The crude product was dried *in vacuo* (0.01 mbar, 25 °C, 6 h) to give **3a** in 86 % yield as a colourless viscous liquid.

¹H NMR (CDCl₃): δ = 1.08 (s, 3H, CCH₃), 4.26 (s, 6H, CCH₂O); ¹³C NMR (CDCl₃): δ = 22.1 (CCH₃), 34.7 (C_q), 76.5 (CCH₂O); ¹⁴N NMR (CDCl₃): δ = -44.5. Raman (300 mW): 2972 (vs), 2910 (m), 2802 (vw), 2738 (vw), 1641 (m), 1467 (m), 1407 (vw), 1374 (w), 1286 (vs), 1036 (w), 994 (vw), 918 (vw), 869 (s), 639 (m), 601 (m), 465 (w), 414 (w) cm^{-1} . IR: 2962 (vw), 2907 (vw), 1825 (vw), 1753 (vw), 1626 (vs), 1473 (w), 1374 (w), 1271 (vs), 1124 (m), 1031 (w), 990 (s), 923 (w), 835 (vs), 752 (s), 724 (m), 704 (m) cm^{-1} . MS (DCI+) [m/e]: 256.1 [M + H]⁺. Mp.: -15 °C (ref 2: -15 °C). Bp.: 182 °C (dec.) (ref 2: 182 °C). Sensitivities: impact >15 J; friction >108 N.

1,1-Bis(nitratomethyl)cyclopentane, (CH₂)₄C(CH₂ONO₂)₂ (4a): The crude product was dried *in vacuo* (0.01 mbar, 25 °C, 3 h) to give **4a** in 83 % yield as a colourless liquid.

¹H NMR (CDCl₃): δ = 1.57–1.62 (m, 4H, β-CH₂), 1.67–1.72 (m, 4H, γ-CH₂), 4.33 (s, 4H, CCH₂O); ¹³C NMR (CDCl₃): δ = 24.9 (γ-CH₂), 32.8 (β-CH₂), 44.8 (C_q), 75.0 (CCH₂O); ¹⁴N NMR (CDCl₃): δ = -43.9. Raman (300 mW): 2967 (vs), 2877 (s), 1635 (w), 1454 (m), 1384 (vw), 1284 (s), 1239 (w), 1029 (w), 991 (vw), 906 (m), 869 (s), 703 (w), 607 (m), 471 (w) cm^{-1} . IR: 2958 (w), 2874 (vw), 1728 (m), 1622 (vs), 1453 (w), 1370 (vw), 1338 (vw), 1272 (vs), 1166 (w),

1130 (vw), 1024 (vw), 990 (m), 956 (w), 851 (vs), 755 (s), 700 (w), 668 (vw), 637 (vw) cm^{-1} . MS (DEI+) [m/e]: 222.3 [M + 2H]⁺. Mp.: 23–25 °C. Bp.: 190 °C (dec.). Sensitivities: impact >100 J; friction >108 N.

1,1-Bis(nitratomethyl)cyclohexane, (CH₂)₅C(CH₂ONO₂)₂ (5a): The crude product was dried *in vacuo* (0.01 mbar, 25 °C, 3 h) to give **5a** in 86 % yield as a colourless liquid.

¹H NMR (CDCl₃): δ = 1.45–1.55 (m, 10H, CCH₂C), 4.37 (s, 4H, CCH₂O); ¹³C NMR (CDCl₃): δ = 20.9 (γ -CH₂), 25.5 (δ -CH₂), 29.9 (β -CH₂), 37.2 (C_q), 74.5 (CCH₂O); ¹⁴N NMR (CDCl₃): δ = -43.5. Raman (300 mW): 2946 (vs), 2864 (s), 1635 (w), 1473 (w), 1447 (m), 1388 (vw), 1365 (w), 1283 (s), 1251 (w), 1030 (w), 988 (w), 867 (s), 852 (s), 833 (m), 684 (vw), 606 (m), 475 (m) cm^{-1} . IR: 2936 (w), 2862 (vw), 1622 (vs), 1455 (w), 1371 (vw), 1316 (vw), 1280 (vs), 1267 (vs), 1078 (vw), 1018 (vw), 988 (m), 930 (m), 930 (w), 843 (vs), 755 (s), 702 (m), 684 (vw), 636 (w) cm^{-1} . MS (DEI+) [m/e]: 235.2 [M + H]⁺. Bp.: 190 °C (dec.). Sensitivities: impact >100 J; friction, >120 N.

General Procedure of the Nitration of the (Hydroxymethyl)silanes and (Hydroxymethyl)silacycloalkanes: Method A: For the synthesis of **2b–5b**, the respective bis(hydroxymethyl) or tris(hydroxymethyl) compound [Me₂Si(CH₂OH)₂, MeSi(CH₂OH)₃, (CH₂)₄Si(CH₂OH)₂, (CH₂)₅Si(CH₂OH)₂; 1.0 mmol (1.0 mol equiv)] was added in small portions to a stirred mixture of nitric acid (100 %; 4.2 and 6.3 mol equiv, respectively) and acetic anhydride (6.0 mol equiv). The reaction mixture was stirred at ambient temperature for 1 h (**2b**) or 1.5 h (**3b–5b**), followed by the addition of ice-water (5 mL) and pentane (15 mL). The aqueous phase was separated and extracted with pentane (2 × 20 mL), and the combined organic extracts were washed with water (2 × 20 mL), neutralized by washing with a concentrated aqueous solution of sodium hydrogen carbonate, and then dried over anhydrous sodium sulphate. The solvent was removed under reduced pressure, and the residue was purified by removal of the remaining solvent traces *in vacuo* (0.01 mbar, 25 °C, 2 h). For further details of the syntheses, see Table 3.2.

Method B: For the synthesis of **1b**, the respective iodomethyl compound Me₃SiCH₂I [1.0 mmol (1.0 mol equiv)] was added at 0 °C to a stirred solution of silver nitrate (2.0 mol equiv) in acetonitrile (3 mL). The reaction mixture was then stirred at ambient temperature for 1.5 h under exclusion of light, followed by the addition of pentane (10 mL) under vigorous stirring. The pentane phase was separated, and the extraction procedure with

pentane was repeated twice. The pentane extracts were combined, and the solvent was removed by micro-distillation (40 °C, 200 mbar). For further details of the synthesis, see Table 3.2.

Trimethyl(nitratomethyl)silane, Me₃SiCH₂ONO₂ (1b): Compound **1b** was synthesized according to Method B and was isolated in 86 % yield as a colourless liquid.

¹H NMR (CDCl₃): δ = 0.10 (s, 9H, ²J(¹H,²⁹Si) = 3.4 Hz, SiCH₃), 4.04 (s, 2H, ³J(¹H,¹H) = 4.4 Hz, SiCH₂O); ¹³C NMR (CDCl₃): δ = -2.8 (¹J(¹³C,²⁹Si) = 53.0 Hz, SiCH₃), 66.8 (¹J(¹³C,²⁹Si) = 48.4 Hz, SiCH₂O); ¹⁴N NMR (CDCl₃): δ = -34.3; ²⁹Si NMR (CDCl₃): δ = 0.1. Raman (300 mW): 2961 (m), 2904 (vs), 1635 (w), 1413 (w), 1305 (m), 1248 (vw), 1213 (vw), 874 (w), 826 (m), 725 (vw), 706 (w), 649 (m), 608 (m), 554 (m) cm⁻¹. IR: 2961 (vw), 1630 (vs), 1436 (vw), 1302 (vs), 1252 (s), 1213 (vw), 977 (vw), 822 (vs), 774 (s), 754 (s), 706 (m) cm⁻¹. MS (DCI+) [m/e]: 149.2 [M⁺]. Decomp. point: 85 C. Sensitivities: impact >1 J; friction >64 N.

Dimethylbis(nitratomethyl)silane, Me₂Si(CH₂ONO₂)₂ (2b): Compound **2b** was synthesized according to Method A and was isolated in 87 % yield as a colourless oil.

¹H NMR (CDCl₃): δ = 0.29 (s, 6H, ²J(¹H,²⁹Si) = 3.5 Hz, SiCH₃), 4.18 (s, 4H, ³J(¹H,¹H) = 4.6 Hz, SiCH₂O); ¹³C NMR (CDCl₃): δ = -6.0 (¹J(¹³C,²⁹Si) = 55.4 Hz, SiCH₃), 63.6 (¹J(¹³C,²⁹Si) = 53.0 Hz, SiCH₂O); ¹⁴N NMR (CDCl₃): δ = -37.6; ²⁹Si NMR (CDCl₃): δ = -1.2. Raman (300 mW): 2971 (m), 2910 (vs), 2853 (w), 1638 (vw), 1435 (vw), 1305 (m), 1254 (vw), 1213 (vw), 979 (vw), 833 (m), 731 (vw), 671 (m), 646 (vw), 614 (vw), 551 (m) cm⁻¹. IR: 2961 (vw), 2919 (vw), 1724 (vw), 1625 (vs), 1437 (vw), 1405 (vw), 1297 (vs), 1250 (s), 1212 (w), 1163 (vw), 1072 (w), 980 (w), 817 (vs), 752 (m), 670 (m), 641 (m) cm⁻¹. Mp.: -10 °C. Decomp. point: 107 °C. Sensitivities: impact <0.5 J; friction <5 N.

Methyltris(nitratomethyl)silane, MeSi(CH₂ONO₂)₃ (3b): Compound **3b** was synthesized according to Method A and was isolated in 80 % yield as a colourless oil.

¹H NMR (CDCl₃): δ = 0.45 (s, 3H, ²J(¹H,²⁹Si) = 3.6 Hz, SiCH₃), 4.32 (s, 6H, ³J(¹H,¹H) = 4.6 Hz, SiCH₂O); ¹³C NMR (CDCl₃): δ = -8.7 (¹J(¹³C,²⁹Si) = 57.68 Hz, SiCH₃), 60.7 (¹J(¹³C,²⁹Si) = 56.2 Hz, SiCH₂O); ¹⁴N NMR (CDCl₃): δ = -40.3; ²⁹Si NMR (CDCl₃): δ = -5.4. Raman (300 mW): 2972 (s), 2921 (vs), 1639 (w), 1434 (w), 1306 (vs), 1257 (w), 1213 (vw), 989 (w), 839 (vs), 744 (w), 670 (w), 647 (w), 619 (w), 528 (m) cm⁻¹. IR: 2926 (vw), 1628 (vs), 1433 (w), 1404

(vw), 1298 (vs), 1253 (s), 1214 (m), 1098 (w), 986 (m), 811 (vs), 746 (s) cm^{-1} . Mp.: ~ -18 °C. Decomp. point: 107 °C. Sensitivities: impact <0.5 J; friction <5 N.

1,1-Bis(nitratomethyl)-1-silacyclopentane, $(\text{CH}_2)_4\text{Si}(\text{CH}_2\text{ONO}_2)_2$ (4b): Compound **4b** was synthesized according to Method A and was isolated in 94 %yield as a colourless oil.

^1H NMR (CDCl_3): $\delta = 0.80\text{--}0.86$ (m, 4H, $\beta\text{-CH}_2$), 1.63–1.69 (m, 4H, $\gamma\text{-CH}_2$), 4.28 (s, 4H, $^3\text{J}(\text{H},\text{H}) = 4.4$ Hz, SiCH_2O); ^{13}C NMR (CDCl_3): $\delta = 8.2$ ($^1\text{J}(\text{C},\text{Si}) = 54.6$ Hz, $\beta\text{-CH}_2$), 26.8 ($\gamma\text{-CH}_2$), 62.4 ($^1\text{J}(\text{C},\text{Si}) = 51.6$ Hz, SiCH_2O); ^{14}N NMR (CDCl_3): $\delta = -37.8$; ^{29}Si NMR (CDCl_3): $\delta = 13.7$. Raman (300 mW): 2942 (vs), 2923 (vs), 2861 (m), 1638 (vw), 1453 (w), 1435 (w), 1407 (w), 1303 (m), 1251 (w), 1210 (vw), 1194 (vw), 1153 (vw), 1080 (vw), 1017 (vw), 979 (vw), 944 (vw), 848 (vs), 705 (w), 655 (w), 611 (vw), 554 (m), 420 (vw) cm^{-1} . IR: 2935 (w), 2863 (vw), 1625 (vs), 1452 (vw), 1431 (vw), 1403 (vw), 1297 (vs), 1250 (s), 1212 (w), 1152 (vw), 1077 (m), 1031 (w), 1018 (w), 977 (w), 814 (vs), 744 (m), 674 (m), 639 (s) cm^{-1} . MS (FAB+) [m/e]: 235.1 [M – H]⁺. Mp.: ~ -18 °C. Decomp. point: 97 °C. Sensitivities: impact <0.5 J; friction <5 N.

1,1-Bis(nitratomethyl)-1-silacyclohexane, $(\text{CH}_2)_5\text{Si}(\text{CH}_2\text{ONO}_2)_2$ (5b): Compound **5b** was synthesized according to Method A and was isolated in 96 %yield as a colourless oil.

^1H NMR (CDCl_3): $\delta = 0.82\text{--}0.88$ (m, 4H, $\beta\text{-CH}_2$), 1.40–1.48 (m, 2H, $\delta\text{-CH}_2$), 1.67–1.77 (m, 4H, $\gamma\text{-CH}_2$), 4.24 (s, 4H, $^3\text{J}(\text{H},\text{H}) = 4.4$ Hz, SiCH_2O); ^{13}C NMR (CDCl_3): $\delta = 8.0$ ($^1\text{J}(\text{C},\text{Si}) = 53.6$ Hz, $\beta\text{-CH}_2$), 23.8 ($\delta\text{-CH}_2$), 29.0 ($\gamma\text{-CH}_2$), 62.2 ($^1\text{J}(\text{C},\text{Si}) = 51.8$ Hz, SiCH_2O); ^{14}N NMR (CDCl_3): $\delta = -37.2$; ^{29}Si NMR (CDCl_3): $\delta = -6.5$. Raman (300 mW): 2923 (vs), 2858 (s), 1641 (vw), 1450 (w), 1403 (vw), 1304 (m), 1213 (vw), 1105 (vw), 1077 (vw), 1008 (vw), 982 (vw), 909 (vw), 838 (m), 796 (w), 666 (m), 608 (vw), 553 (m) cm^{-1} . IR: 2925 (w), 2853 (w), 1718 (vw), 1628 (vs), 1460 (vw), 1447 (vw), 1434 (vw), 1403 (vw), 1297 (vs), 1251 (m), 1210 (vw), 1181 (w), 1101 (vw), 1075 (vw), 993 (w), 977 (w), 910 (m), 832 (s), 801 (s), 752 (s), 641 (s) cm^{-1} . MS (FAB+) [m/e]: 249.2 [M – H]⁺. Mp.: ~ 4 °C. Decomp. point: 96 °C. Sensitivities: impact <0.5 J; friction >36 N.

General Procedure for the Synthesis of the Bis(hydroxymethyl)silanes 6–8: Catalytic amounts of acetyl chloride were added dropwise at ambient temperature within 1 min to a stirred solution of the respective bis(acetoxymethyl)silane (compounds **9–11**) in methanol, and the resulting mixture was heated under reflux for 20 h. The solvent was removed under

reduced pressure, and the residue was purified as described in the respective protocols given below.

Bis(hydroxymethyl)dimethylsilane, $\text{Me}_2\text{Si}(\text{CH}_2\text{OH})_2$ (6**):** This compound was synthesized from **9** (9.15 g, 44.8 mmol), methanol (400 mL), and acetyl chloride (563 mg, 7.17 mmol). The crude product was purified by fractional distillation using a Vigreux column to give **6** in 73 % yield as a colourless liquid (3.96 g, 32.9 mmol). Bp.: 65–66 °C / 0.2 mbar.

^1H NMR ([D6]DMSO): $\delta = -0.03$ (s, 6H, SiCH_3), 3.17 (d, $^3\text{J}(\text{H},\text{H}) = 4.3$ Hz, 4H, SiCH_2O), 3.91 (t, $^3\text{J}(\text{H},\text{H}) = 4.3$ Hz, 2H, OH); ^{13}C NMR (CDCl_3): $\delta = -6.2$ (SiCH_3), 51.4 (SiCH_2O); ^{29}Si NMR (CDCl_3): $\delta = -2.7$. Anal. Calcd for $\text{C}_4\text{H}_{12}\text{O}_2\text{Si}$: C, 39.96; H, 10.06. Found: C, 39.9; H, 9.9.

1,1-Bis(hydroxymethyl)-1-silacyclopentane, $(\text{CH}_2)_4\text{Si}(\text{CH}_2\text{OH})_2$ (7**):** This compound was synthesized from **10** (3.15 g, 13.7 mmol), methanol (150 mL), and acetyl chloride (142 mg, 1.81 mmol). The crude product was purified by bulb-to-bulb distillation (85 °C / 0.03 mbar), and the resulting colourless liquid was crystallized from acetonitrile (4 mL; slow cooling to –20 °C and crystallization over a period of 24 h). The product was isolated by removal of the mother liquor *via* a syringe and then dried *in vacuo* (0.2 mbar, 20 °C, 2 h) to give **7** in 60 % yield as a colourless crystalline solid (1.20 g, 8.24 mmol). Mp.: 37–38 °C.

^1H NMR ([D6]DMSO): $\delta = 0.53$ – 0.59 (m, 4H, $\beta\text{-CH}_2$), 1.49– 1.54 (m, 4H, $\gamma\text{-CH}_2$), 3.27 (d, $^3\text{J}(\text{H},\text{H}) = 4.4$ Hz, 4H, SiCH_2O), 3.99 (t, $^3\text{J}(\text{H},\text{H}) = 4.4$ Hz, 2H, OH); ^{13}C NMR ([D6]DMSO): $\delta = 7.6$ ($\beta\text{-CH}_2$), 26.8 ($\gamma\text{-CH}_2$), 49.9 (SiCH_2O); ^{29}Si NMR ([D6]DMSO): $\delta = 14.2$. Anal. Calcd for $\text{C}_6\text{H}_{14}\text{O}_2\text{Si}$: C, 49.27; H, 9.65. Found: C, 49.3; H, 9.6.

1,1-Bis(hydroxymethyl)-1-silacyclohexane, $(\text{CH}_2)_5\text{Si}(\text{CH}_2\text{OH})_2$ (8**):** This compound was synthesized from **11** (6.04 g, 24.7 mmol), methanol (370 mL), and acetyl chloride (558 mg, 7.11 mmol). The crude product was crystallized from acetonitrile (15 mL; slow cooling to –20 °C and crystallization over a period of 24 h). The product was isolated by removal of the mother liquor *via* a syringe and then dried *in vacuo* (0.1 mbar, 20 °C, 3 h) to give **8** in 70 % yield as a colourless crystalline solid (2.76 g, 17.2 mmol). Mp.: 39–40 °C.

^1H NMR ([D6]DMSO): $\delta = 0.60$ – 0.64 (m, 4H, $\beta\text{-CH}_2$), 1.30– 1.38 (m, 2H, $\delta\text{-CH}_2$), 1.58– 1.67 (m, 4H, $\gamma\text{-CH}_2$), 3.25 (d, $^3\text{J}(\text{H},\text{H}) = 4.4$ Hz, 4H, SiCH_2O), 3.99 (t, $^3\text{J}(\text{H},\text{H}) = 4.4$ Hz, 2H, OH); ^{13}C

NMR ([D6]DMSO): δ = 7.9 (β -CH₂), 24.1 (δ -CH₂), 29.5 (γ -CH₂), 49.6 (SiCH₂O); ²⁹Si NMR ([D6]DMSO): δ = -7.7. Anal. Calcd for C₇H₁₆O₂Si: C, 52.45; H, 10.06. Found: C, 52.1; H, 9.8.

General Procedure for the Synthesis of the Bis(acetoxymethyl) silanes 9–11: The respective bis(chloromethyl)silane [16] was added in a single portion at ambient temperature to a stirred suspension of sodium acetate (3 mol equiv) in N,N-dimethylformamide, and the resulting mixture was then stirred under reflux for 18 h. The solvent was removed by distillation (45 °C / 10 mbar), diethyl ether (200 mL) and water (200 mL) were added to the residue, the organic layer was separated, and the aqueous phase was extracted with diethyl ether (2 × 200 mL) and then discarded. The combined organic extracts were dried over anhydrous sodium sulphate, the solvent was removed under reduced pressure, and the residue was purified by bulb-to-bulb distillation.

Bis(acetoxymethyl)dimethylsilane, Me₂Si(CH₂OAc)₂ (9): This compound was synthesized from bis(chloromethyl)dimethylsilane [16] (9.00 g, 57.3 mmol), sodium acetate (14.1 g, 172 mmol), and N,N-dimethylformamide (95 mL) to give **9** in 79 % yield as a yellowish liquid (9.29 g, 45.5 mmol).

¹H NMR (CDCl₃): δ = 0.09 (s, 6H, SiCH₃), 1.99 (s, 6H, C(O)CH₃), 3.78 (s, 4H, SiCH₂O); ¹³C NMR (CDCl₃): δ = -6.1 (SiCH₃), 20.6 (C(O)CH₃), 55.3 (SiCH₂O), 171.6 (C(O)CH₃); ²⁹Si NMR (CDCl₃): δ = -7.7. Anal. Calcd for C₈H₁₆O₄Si: C, 47.03; H, 7.89. Found: C, 46.8; H, 7.9. Bp.: 55 °C / 0.2 mbar.

1,1-Bis(acetoxymethyl)-1-silacyclopentane, (CH₂)₄Si(CH₂OAc)₂ (10): This compound was synthesized from 1,1-bis(chloromethyl)-1-silacyclopentane [16] (9.13 g, 49.8 mmol), sodium acetate (12.5 g, 152 mmol), and N,N-dimethylformamide (80 mL) to give **10** in 76 % yield as a yellowish liquid (8.77 g, 38.1 mmol).

¹H NMR (CDCl₃): δ = 0.59–0.64 (m, 4H, β -CH₂), 1.51–1.56 (m, 4H, γ -CH₂), 1.98 (s, 6H, C(O)CH₃), 3.85 (s, 4H, SiCH₂O); ¹³C NMR (CDCl₃): δ = 8.9 (β -CH₂), 20.5 (C(O)CH₃), 26.8 (γ -CH₂), 54.9 (SiCH₂O), 171.7 (C(O)CH₃); ²⁹Si NMR (CDCl₃): δ = 14.9. Anal. Calcd for C₁₀H₁₈O₄Si: C, 52.15; H, 7.88. Found: C, 52.0; H, 7.9. Bp.: 85 °C / 0.4 mbar..

1,1-Bis(acetoxymethyl)-1-silacyclohexane, (CH₂)₅Si(CH₂OAc)₂ (11): This compound was synthesized from 1,1-bis(chloromethyl)-1-silacyclohexane [16] (10.0 g, 50.7 mmol),

sodium acetate (12.5 g, 152 mmol), and N,N-dimethylformamide (80 mL) to give **11** in 87 % yield as a yellowish liquid (10.8 g, 44.2 mmol).

^1H NMR (CDCl_3): δ = 0.67–0.72 (m, 4H, β - CH_2), 1.34–1.41 (m, 2H, δ - CH_2), 1.61–1.69 (m, 4H, γ - CH_2), 1.99 (s, 6H, $\text{C}(\text{O})\text{CH}_3$), 3.87 (s, 4H, SiCH_2O); ^{13}C NMR (CDCl_3): δ = 8.5 (β - CH_2), 20.7 ($\text{C}(\text{O})\text{CH}_3$), 24.0 (δ - CH_2), 29.3 (γ - CH_2), 54.0 (SiCH_2O), 171.6 ($\text{C}(\text{O})\text{CH}_3$); ^{29}Si NMR (CDCl_3): δ = -7.7. Anal. Calcd for $\text{C}_{11}\text{H}_{20}\text{O}_4\text{Si}$: C, 54.07; H, 8.25. Found: C, 53.7; H, 8.1. Bp.: 90 °C / 0.2 mbar.

Acknowledgment

Financial support of this work by the Ludwig Maximilians University of Munich (LMU), the Fonds der Chemischen Industrie (FCI), the European Research Office (ERO) of the U.S. Army Research Laboratory (ARL), and the Armament Research, Development and Engineering Center (ARDEC) under contract nos. W911NF-09-2-0018, W911NF-09-1-0120, and W011NF-09-1-0056 is gratefully acknowledged. The authors acknowledge collaborations with Dr. Mila Krupka (OZM Research, Czech Republic) in the development of new testing and evaluation methods for energetic materials and with Dr. Muhamed Sucesca (Brodarski Institute, Croatia) in the development of new computational codes to predict the detonation and propulsion parameters of novel explosives. We are indebted to and thank Drs. Betsy M. Rice and Brad Forch (ARL, Aberdeen, Proving Ground, MD) and Dr. Gary Chen (ARDEC, Picatinny Arsenal, NJ) for many helpful and inspiring discussions and support of our work. We thank Prof. Dr. Andreas Kornath and Can Dörtbudak, M. Sc., for their support in measuring the Raman spectra. Special thanks to Dr. Matthias Scherr, Karin Lux, M. Sc., Dipl.-Chem. Franz Martin, and Dr. Christian Burschka for collecting the X-ray data sets and Stefan Huber for measuring the impact and friction sensitivities.

-
- [1] Boschan, R.; Merrow, R. T.; van Dolah, R. W. *Chem. Rev.* **1955**, *55*, 485–510.
- [2] (a) Meyer, R.; Köhler, J.; Homburg, A. *Explosives*, 5th ed.; Wiley-VCH: Weinheim, **2002**; pp 216–217. (b) Klapötke, T. M. *Chemie der hochenergetischen Materialien*; de Gruyter: Berlin, **2009**; pp 1–6.
- [3] (a) Hiskey, M. A.; Brower, K. R.; Oxley, J. C. *J. Phys. Chem.* **1991**, *95*, 3955–3960. (b) Akhavan, J. *The Chemistry of Explosives*; The Royal Society of Chemistry: Cambridge,

- 1998**; pp 63–67. (c) Klapötke, T. M. *Chemie der hochenergetischen Materialien*; de Gruyter: Berlin, **2009**; pp 87–88.
- [4] Fink, W. U.S. Patent 3,127,431, 31th March, **1964**.
- [5] Fink, W. U.S. Patent 3,222,319, 7th December, **1965**.
- [6] Barcza, S. U.S. Patent 3,592,831, 13th July, **1971**.
- [7] Klapötke, T. M.; Krumm, B.; Ilg, R.; Troegel, D.; Tacke, R. *J. Am. Chem. Soc.* **2007**, *129*, 6908–6915.
- [8] Liu, W.-G.; Zybin, S. V.; Dasgupta, S.; Klapötke, T. M.; Goddard, W. A., III *J. Am. Chem. Soc.* **2009**, *131*, 7490–7491.
- [9] Kobayashi, T.; Pannell, K. H. *Organometallics* **1991**, *10*, 1960–1964.
- [10] Anderson, W. K.; Kasliwal, R.; Houston, D. M.; Wang, Y.; Narayanan, V. L.; Haugwitz, R. D.; Plowman, J. *J. Med. Chem.* **1995**, *38*, 3789–3797.
- [11] Daiss, J. O.; Barth, K. A.; Burschka, C.; Hey, P.; Ilg, R.; Klemm, K.; Richter, I.; Wagner, S. A.; Tacke, R. *Organometallics* **2004**, *23*, 5193–5197.
- [12] Ilg, R.; Troegel, D.; Burschka, C.; Tacke, R. *Organometallics* **2006**, *25*, 548–551.
- [13] Daiss, J. O.; Burschka, C.; Mills, J. S.; Montana, J. G.; Showell, G. A.; Warneck, J. B. H.; Tacke, R. *Organometallics* **2006**, *25*, 1188–1198.
- [14] Shimizu, M.; Iwakubo, M.; Nishihara, Y.; Oda, K.; Hiyama, T. *ARKIVOC* **2007**, 29–48.
- [15] Troegel, D.; Möller, F.; Burschka, C.; Tacke, R. *Organometallics* **2009**, *28*, 5765–5770.
- [16] Apfel, U.-P.; Troegel, D.; Halpin, Y.; Tschierlei, S.; Uhlemann, U.; Görls, H.; Schmitt, M.; Popp, J.; Dunne, P.; Venkatesan, M.; Coey, M.; Rudolph, M.; Vos, J. G.; Tacke, R.; Weigand, W. *Inorg. Chem.* **2010**, *49*, 10117–10132.
- [17] Recent publications dealing with sila-drugs: (a) Büttner, M. W.; Burschka, C.; Daiss, J. O.; Ivanova, D.; Rochel, N.; Kammerer, S.; Peluso-Iltis, C.; Bindler, A.; Gaudon, C.; Germain, P.; Moras, D.; Gronemeyer, H.; Tacke, R. *ChemBioChem* **2007**, *8*, 1688–1699. (b) Tacke, R.; Popp, F.; Müller, B.; Theis, B.; Burschka, C.; Hamacher, A.; Kassack, M. U.; Schepmann, D.; Wünsch, B.; Jurva, U.; Wellner, E. *ChemMedChem* **2008**, *3*, 152–164. (c) Warneck, J. B.; Cheng, F. H. M.; Barnes, M. J.; Mills, J. S.;

- Montana, J. G.; Naylor, R. J.; Ngan, M.-P.; Wai, M.-K.; Daiss, J. O.; Tacke, R.; Rudd, J. A. *Toxicol. Appl. Pharmacol.* **2008**, *232*, 369–375. (d) Lippert, W. P.; Burschka, C.; Götz, K.; Kaupp, M.; Ivanova, D.; Gaudon, C.; Sato, Y.; Antony, P.; Rochel, N.; Moras, D.; Gronemeyer, H.; Tacke, R. *ChemMedChem* **2009**, *4*, 1143–1152. (e) Tacke, R.; Müller, V.; Büttner, M. W.; Lippert, W. P.; Bertermann, R.; Daiss, J. O.; Khanwalkar, H.; Furst, A.; Gaudon, C.; Gronemeyer, H. *ChemMedChem* **2009**, *4*, 1797–1802. (f) Johansson, T.; Weidolf, L.; Popp, F.; Tacke, R.; Jurva, U. *Drug Metab. Dispos.* **2010**, *38*, 73–83. (g) Tacke, R.; Nguyen, B.; Burschka, C.; Lippert, W. P.; Hamacher, A.; Urban, C.; Kassack, M. U. *Organometallics* **2010**, *29*, 1652–1660.
- [18] Recent publications dealing with sila-odorants: (a) Büttner, M. W.; Burschka, C.; Junold, K.; Kraft, P.; Tacke, R. *ChemBioChem* **2007**, *8*, 1447–1454. (b) Büttner, M. W.; Nätscher, J. B.; Burschka, C.; Tacke, R. *Organometallics* **2007**, *26*, 4835–4838. (c) Tacke, R.; Metz, S. *Chem. Biodiversity* **2008**, *5*, 920–941. (d) Metz, S.; Nätscher, J. B.; Burschka, C.; Götz, K.; Kaupp, M.; Kraft, P.; Tacke, R. *Organometallics* **2009**, *28*, 4700–4712. (e) Nätscher, J. B.; Laskowski, N.; Kraft, P.; Tacke, R. *ChemBioChem* **2010**, *11*, 315–319.
- [19] (a) http://www.bam.de/index_en.html. (b) *Official Journal of the European Union*, Council Regulation (EC) No. 440/2008, 30th March 2008.
- [20] Hylands, K. A.; Moodie, R. B. *J. Chem. Soc., Perkin Trans. 2* **1997**, 709–714.
- [21] Sheldrick, G. M. *SHELXL-97*, A program for the refinement of crystal structures; University of Göttingen: Göttingen, Germany, **1994**.
- [22] Farrugia, L. J. *WinGX, J. Appl. Crystallogr.* **1999**, *32*, 837–838.
- [23] Spek, A. L. *Platon*; Utrecht University: Utrecht, Netherlands, **1999**.
- [24] Zeil, W.; Haase, J.; Wegmann, L. *Z. Instrum.* **1966**, *74*, 84–88.
- [25] Oberhammer, H. in *Molecular Structure by Diffraction Methods*; Sim, G. A, Sutton, L. E., Eds.; The Chemical Society: London, **1976**; Vol. 4, pp 24–44.
- [26] Berger, R. J. F.; Mitzel, N. W. *Z. Naturforsch.* **2009**, *64b*, 1259–1268.
- [27] Gundersen, S.; Samdal, S.; Strand, T. G.; Volden, H. V. *J. Mol. Struct.* **2007**, *832*, 164–171.

- [28] Hinchley, S. L.; Robertson, H. E.; Borisenko, K. B.; Turner, A. R.; Johnston, B. F.; Rankin, D. W. H.; Ahmadian, M.; Jones, J. N.; Cowley, A. H. *Dalton Trans.* **2004**, 2469–2476.
- [29] Ross, A. W.; Fink, M.; Hilderbrandt, R. in *International Tables for Crystallography*; Wilson, A. C. J., Ed.; Kluwer Academic Publishers: Dordrecht, Netherlands, **1992**; Vol. C, pp 245–338.
- [30] Sipachev, V. A. *J. Mol. Struct., THEOCHEM* **1985**, *121*, 143–151.
- [31] Novikov, V. P.; Sipachev, V. A.; Kulikova, E. I.; Vilkov, L. V. *J. Mol. Struct.* **1993**, *301*, 29–36.
- [32] Zakharov, A. V. *Q2SHRINK version 1.3*; <http://edsoftware.sourceforge.net>.
- [33] *Turbomole version 5.7*; Ahlrichs, R.; Bär, M.; Häser, M.; Horn, H.; Kölmel, C. *Chem. Phys. Lett.* **1989**, *162*, 165–169.
- [34] (a) Frisch, M. J. *et al.*, *Gaussian 03 (revision C.02)*; Gaussian, Inc.: Wallingford, CT, **2004**. (b) Frisch, M. J. *et al.*, *Gaussian 03 (revision D.01)*; Gaussian, Inc.: Wallingford, CT, **2004**.
- [35] Domin, D.; Benito-Garagorri, D.; Mereiter, K.; Fröhlich, J.; Kirchner, K. *Organometallics* **2005**, *24*, 3957–3965.
- [36] Agrawal, J. P.; Hodgson, R. D. in *Organic Chemistry of Explosives*; John Wiley & Sons: Chichester, **2007**, pp 87–123.
- [37] Roberts, J. D.; Dev, S. *J. Am. Chem. Soc.* **1951**, *73*, 1879–1880.
- [38] Vivet, B.; Cavelier, F.; Martinez, J. *Eur. J. Org. Chem.* **2000**, 807–811.
- [39] Schraml, J. in *The Chemistry of Organic Silicon Compounds*; Rappoport, Z., Apeloig, Y., Eds.; John Wiley & Sons: Chichester, **2001**; Vol. 3, pp 223–339.
- [40] Trotter, J. *Acta Crystallogr.* **1963**, *16*, 698–699.
- [41] Cotton, F. A.; Wilkinson, G. in *Advanced Inorganic Chemistry*, 5th ed.; John Wiley & Sons: New York; **1988**, pp 321–323.
- [42] Cox, A. P.; Waring, S. *Trans. Faraday Soc.* **1971**, *67*, 3441–3450.

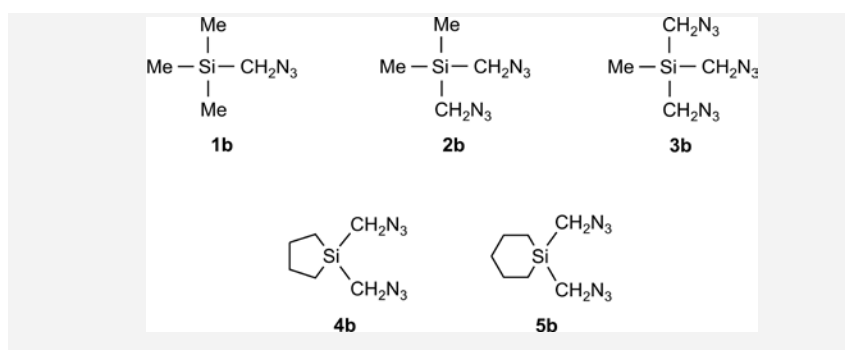
- [43] Bondi, A. *J. Phys. Chem.* **1964**, *68*, 441–451.
- [44] Bartell, L. S. *J. Chem. Phys.* **1960**, *32*, 827–831.
- [45] Glidewell, C. *Inorg. Chim. Acta* **1975**, *12*, 219–227.
- [46] (a) Mitzel, N. W.; Losehand, U. *Angew. Chem.* **1997**, *109*, 2897–2899. *Angew. Chem., Int. Ed. Engl.* **1997**, *36*, 2807–2809. (b) Losehand, U.; Mitzel, N. W. *Inorg. Chem.* **1998**, *37*, 3175–3182. (c) Mitzel, N. W.; Losehand, U. *J. Am. Chem. Soc.* **1998**, *120*, 7320–7327. (d) Mitzel, N. W.; Losehand, U.; Wu, A.; Cremer, D.; Rankin, D. W. H. *J. Am. Chem. Soc.* **2000**, *122*, 4471–4482. (e) Mitzel, N. W.; Vojinović, K.; Fröhlich, R.; Foerster, T.; Rankin, D. W. H. *J. Am. Chem. Soc.* **2005**, *127*, 13705–13713.
- [47] (a) Mitzel, N. W. *Chem. — Eur. J.* **1998**, *4*, 692–698. (b) Vojinović, K.; McLachlan, L. J.; Hinchley, S. L.; Rankin, D. W. H.; Mitzel, N. W. *Chem.; Eur. J.* **2004**, *10*, 3033–3042.
- [48] Mitzel, N. W. *Z. Naturforsch.* **2003**, *58b*, 759–763.
- [49] Mitzel, N. W.; Vojinović, K.; Foerster, T.; Robertson, H. E.; Borisenko, K. B.; Rankin, D. W. H. *Chem. — Eur. J.* **2005**, *11*, 5114–5125.
- [50] (a) Blake, A. J.; Brain, P. T.; McNab, H.; Miller, J.; Morrison, C. A.; Parsons, S.; Rankin, D. W. H.; Robertson, H. E.; Smart, B. A. *J. Phys. Chem.* **1996**, *100*, 12280–12287. (b) Mitzel, N. W.; Rankin, D. W. H. *Dalton Trans.* **2003**, 3650–3662.
- [51] Hagemann, M.; Berger, R. J. F.; Hayes, S. A.; Stammer, H.-G.; Mitzel, N. W. *Chem. — Eur. J.* **2008**, *14*, 11027–11038.
- [52] An internuclear distance obtained directly from the GED data, r_a , is the harmonic mean and can be converted to the arithmetic mean, r_g , using the root-mean-squared amplitude of vibration, u : $r_g \approx r_a + u^2/r$. Distance corrections, k , are also regularly applied in GED refinements to account for the ‘shrinkage’ effect. When the vibrational motion is considered to be harmonic with curvilinear trajectories, the resulting distances and distance corrections are termed r_{h1} and k_{h1} , respectively.
-

IV. Azidomethyl Silanes

Energetic silanes

T. M. Klapötke, B. Krumm, A. Nieder, O. Richter, D. Troegel, and R. Tacke*..... 70 - 82*

Silicon-Containing Explosives: Syntheses and Sensitivity Studies of (Azidomethyl)-, Bis(azidomethyl)-, and Tris-(azidomethyl)-silanes



Investigations for a proper and safe syntheses of several azidomethyl silanes are shown. Their nitrate-methyl analogues are compared with the

azidomethyl derivatives in terms of their chemical characteristics, thermal, friction and impact sensitivities.

Silicon-Containing Explosives: Syntheses and Sensitivity Studies of (Azidomethyl)-, Bis(azidomethyl)-, and Tris(azidomethyl)silanes

Thomas M. Klapötke,^[a] * Burkhard Krumm,^[a] Anian Nieder,^[a] Oliver Richter,^[a] Dennis Troegel,^[b] and Reinhold Tacke^[b], *

Published in *Zeitschrift für Anorganische und Allgemeine Chemie* **2012**, 638, 1075–1079.

Abstract: A series of (azidomethyl)silanes [Me₃Si-CH₂N₃ (**1b**), Me₂Si(CH₂N₃)₂ (**2b**), MeSi(CH₂N₃)₃ (**3b**), (CH₂)₄Si-(CH₂N₃)₂ (**4b**), and (CH₂)₅Si-(CH₂N₃)₂ (**5b**)] was synthesized, starting from the corresponding (chloromethyl)-silanes **1a–3a** or (iodomethyl)-silanes **4a** and **5a**.

Compounds **1b–5b** were characterized by NMR, IR, and Raman spectroscopy. The thermal stabilities of the (azidomethyl)silanes **1b–5b** were investigated by DSC, and their impact and friction sensitivities were measured with standard BAM methods. According to these

studies, the tris(azidomethyl)silane **3b** has to be classified as an extremely sensitive compound.

Keywords: azides • energetic materials • sensitivity • silanes • silicon

Introduction

Azides are important precursors for the generation of a broad range of functional groups in synthetic organic chemistry, such as amines, triazoles, and tetrazoles.[1] (Azidoalkyl)silanes of the formula type R₃Si(CH₂)_nN₃ (*n* = 1–3) are known for decades.[2] Due to serious explosions by distillation during the purification process, the explosive behaviour of (azidomethyl)silanes was discovered early.[3,4] They can serve as precursors in the synthesis of (aminomethyl)silanes, which have been used as ligands for the development of platinum-based anticancer drugs.[3–5]

Azides are commonly used as high energetic compounds in civil and military applications. Examples are the ionic lead azide and the high energetic polymeric binder GAP (glycidyl azide polymers), which contains covalently bound azido groups.[6] In general, ionic azides are often less sensitive towards friction, impact, and thermal stimuli than covalent azides. Thus, due to the covalent

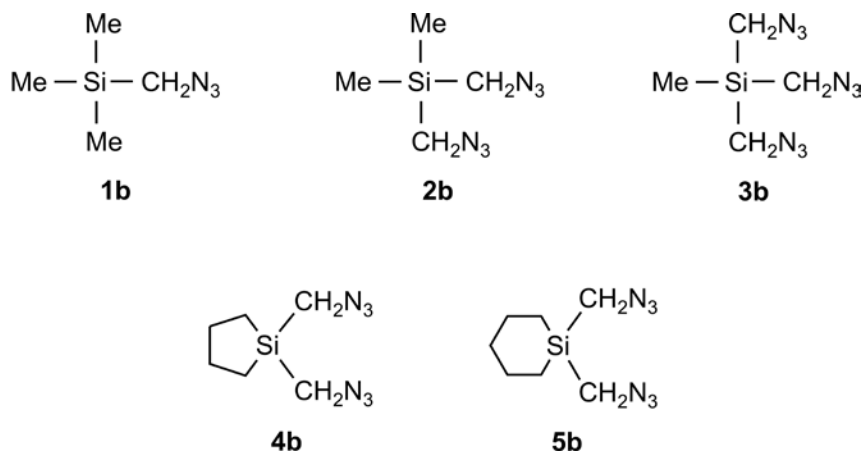
[a] *Prof. Dr. Thomas M. Klapötke
Department Chemie
Ludwig-Maximilians-Universität München
Butenandstr. 5–13(D), 81377 München, Germany
Fax: (+49-89-2180-77492
E-mail: tmk@cup.uni-muenchen.de

[b] *Prof. Dr. Reinhold Tacke
Universität Würzburg
Institut für Anorganische Chemie
Am Hubland, 97074 Würzburg, Germany
Fax: (+49-931-31-84609
E-Mail: r.tacke@uni-wuerzburg.de

Supporting information for this article (images of the NMR spectra of the compounds **1b–5b**) is available on the WWW under <http://dx.doi.org/10.1002/zaac.201100549> or from the authors.

character of (azidomethyl)silanes, high sensitivities towards friction, impact, and thermal stimuli are to be expected for this class of compounds. And indeed, (azidomethyl)trimethylsilane (**1b**), bis(azidomethyl)dimethylsilane (**2b**), and tetrakis(azido-methyl)silane $[\text{Si}(\text{CH}_2\text{N}_3)_4]$ have been reported to be hazardous explosives.[3,4,7]

In continuation of our recently published study on a series of related (nitratomethyl)silanes,[8] we have synthesized the (azidomethyl)silanes 1b–5b and have characterized these compounds systematically in terms of thermal stability as well as friction and impact sensitivity (see Scheme 4.1). The syntheses of 1b,[4,9] 2b,[3,4] 4b,[4] and 5b[5] have already been described elsewhere; however, in this study we have modified the synthetic methods.



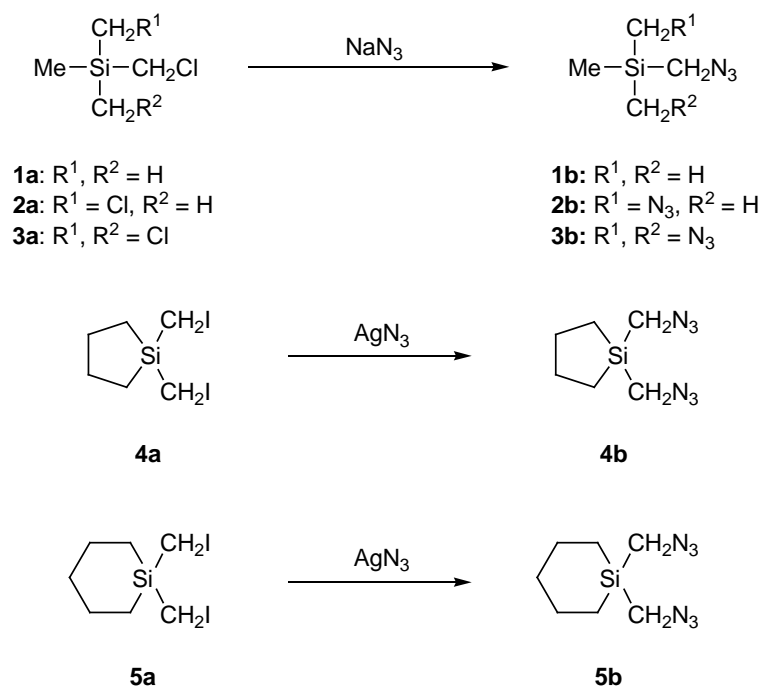
Scheme 4.1. (Azidomethyl)silanes **1b–5b** synthesized and characterized in this study.

Results and Discussion

Syntheses: The (azidomethyl)silanes **1b–5b** were synthesized according to Scheme 4.2 and Table 4.1, starting from the corresponding (chloromethyl)silanes **1a–3a** or (iodomethyl)silanes **4a** and **5a**. The (chloromethyl)silanes **1a** and **2a** were commercially available, whereas **3a** was prepared according to ref. [10]. The (iodomethyl)silanes **4a** and **5a** were also synthesized according to the literature, starting from the corresponding (chloromethyl)silanes.[10–14]

For the synthesis of (azidomethyl)silanes by reaction of the corresponding (chloromethyl)silanes with sodium azide, various aprotic solvents have been used, such as

acetone, DMF, sulfolane, HMPA, and DMPU.[3,4,7,9,15–18] In this study, the acyclic (azidomethyl)silanes **1b–3b** were synthesized by treatment of the corresponding (chloromethyl)silanes **1a–3a** with an excess of sodium azide using DMF (**1b**) or acetonitrile (**2b, 3b**) as the solvent (Scheme 4.2, Table 4.1). The cyclic (azidomethyl)silanes **4b** and **5b** were prepared by treatment of the corresponding (iodomethyl)silanes **4a** and **5a** with an excess of silver azide using acetonitrile as the solvent (Scheme 4.2, Table 4.1). In order to prevent the risk of handling the explosive compounds by extraction in a separation funnel, it is recommended to extract by stirring the reaction mixture in the reaction vessel with *n*-pentane and removing the pentane phase. The compounds **1b–5b** should not be distilled; only the solvents are removed by distillation! Compounds **1b–5b** were isolated as pure liquid products in high yields. Their identities were established by multinuclear NMR spectroscopy as well as IR and Raman spectroscopy.



Scheme 4.2. Syntheses of the (azidomethyl)silanes **1b–5b**.

Table 4.1. Syntheses of compounds **1b–5b**: Reaction conditions and yields.^[a]

Starting Material	Azide Source	Solvent	Temperature	Product	Yield
1a	NaN ₃	DMF	70 °C	1b	79%
2a	NaN ₃	CH ₃ CN	82 °C ^[b]	2b	92%
3a	NaN ₃	CH ₃ CN	82 °C ^[b]	3b	94%
4a	AgN ₃	CH ₃ CN	25 °C ^[c]	4b	96%
5a	AgN ₃	CH ₃ CN	25 °C ^[c]	5b	91%

[a] Reaction time 24 h; [b] reflux.; [c] light exclusion.

Table 4.2. ^{14}N , ^{15}N , and ^{29}Si chemical shifts of compounds **1b–5b** in CDCl_3 .^[a]

	δN_α	δN_β	δN_γ	$\delta^{29}\text{Si}$
1b	-320.2	-131.4	-173.3	3.2
2b	-321.0	-131.0	-172.6	3.3
3b	-321.8	-131.3	-170.6	1.5
4b	-321 [400]	-131 [30]	-172 [100]	18.9
5b	-320 [200]	-131 [30]	-172 [100]	-1.8

[a] δ values are given in ppm; the half-linewidth of the ^{14}N resonance signals [Hz] is given in brackets. For further details, see Experimental Section.

NMR Analyses: Compounds **1b–5b** were characterized by ^1H , ^{13}C , ^{14}N , ^{15}N (**1b–3b** only), and ^{29}Si NMR spectroscopy (see Experimental Section and Table 4.2).

The chemical shifts of the N_β atoms of the azido groups of **1b–5b** are virtually independent from the substitution pattern at the silicon atom ($\delta = -131$ ppm). The same holds true for the chemical shifts of the N_α nitrogen atoms ($\delta = -320$ to -322 ppm). The chemical shifts of the N_γ nitrogen atoms are in the range $\delta = -171$ to -173 ppm, with a small high-field shift with increasing number of azido groups.

The ^{29}Si chemical shifts of **1b** ($\delta = 3.2$ ppm) and **2b** ($\delta = 3.3$ ppm) are very similar, whereas a high-field shift was observed for the tris(azidomethyl)silane **3b** ($\delta = 1.5$ ppm). This trend fits nicely with the ^{29}Si chemical shift observed for tetrakis(azidomethyl)silane $[\text{Si}(\text{CH}_2\text{N}_3)_4]$ ($\delta = -2.1$ ppm).^[7] The large differences in the ^{29}Si chemical shifts of the acyclic bis(azidomethyl)silane **2b** ($\delta = 3.3$ ppm) and the cyclic bis(azidomethyl)silanes **4b** ($\delta = 18.9$ ppm) and **5b** ($\delta = -1.8$ ppm) are probably due to the cyclic nature of compounds **4b** and **5b** and the different geometry of their five- and six-membered ring systems.

Vibrational spectroscopy: As shown for a series of organic azides, the substituents of which cover the range of electropositive to electronegative, the strong absorption of the asymmetric azide stretching vibration in the IR spectra is found in the region of 2114 to 2083 cm^{-1} , whereas the symmetric azide stretching vibration is observed at 1297–1256 cm^{-1} .^[19] For the (azidomethyl)silanes **1b–5b**, the respective IR vibrations were found in the ranges 2089–2083 cm^{-1} (ν_{as} , strongest absorption) and 1290–1285 cm^{-1} (ν_{s}). In the Raman spectra, a weak broad emission band at 2092 cm^{-1} (ν_{as}) was observed, whereas the ν_{s}

vibration could be hardly seen as a very weak band within a group of other identified emission bands.

The thermal stabilities of the (azidomethyl)silanes **1b–5b** were studied by differential scanning calorimetry (DSC). In addition, their impact and friction sensitivities were measured with standard BAM methods.

As shown by the DSC studies, compound **1b** boils at 129 °C without decomposition, whereas **2b–5b** did not show a discrete boiling point, but decomposed in the temperature range 130–137 °C (onset point in the DSC experiments, heating rate 5 °C min⁻¹). As the decomposition areas were relatively broad, exact decomposition points cannot be given (appreciable decomposition was already observed at ca. 120 °C). Generally, the thermal stabilities of the compounds studied appear to be very similar and independent from the number of azidomethyl groups, suggesting that the decomposition is initiated at the azidomethyl moieties (for example N₂ elimination)

Table 4.3. Impact and friction sensitivities of compounds **1b–5b**.

Compound	Impact Sensitivity [J] ^[a]	Friction Sensitivity [N] ^[b]
1b	>40	192
2b	9	60
3b	<1	<5
4b	40	48
5b	>40	60

[a] The impact sensitivity tests were carried out according to STANAG 4489[20] modified instruction[21] using a BAM drophammer[22]; [b] the friction sensitivity tests were carried out according to STANAG 4487[23] modified instruction[24] using a BAM friction tester.

Physical Properties: Impact and friction sensitivity experiments are established methods to study the explosive behaviour and safety provisions of compounds. The impact and friction sensitivities of **1b–5b** are given in Table 4.3.

As can be seen from Table 4.3, the impact sensitivities of the acyclic compounds **1b–3b** strongly correlate with the number of the azidomethyl groups, the tris(azidomethyl)silane **3b** showing the highest sensitivity. Comparison of the three bis(azidomethyl)-silanes **2b**, **4b**, and **5b** reveals that the two organyl substituents also affect the impact sensitivity. The more

strained five-membered ring compound **4b** shows a higher sensitivity than the six-membered analogue **5b**.

Some of the trends observed for the impact sensitivities of compounds **1b–5b** were also found for their friction sensitivities (Table 4.3): The tris(azidomethyl)silane **3b** is much more sensitive toward friction than all the other compounds studied, and **1b** with its one azidomethyl group is much less sensitive than the bis- or tris(azidomethyl)silanes **2b–5b**. However, in contrast to the different impact sensitivities of the three bis(azidomethyl)silanes **2b**, **4b**, and **5b**, the friction sensitivities of these compounds are in the same range. In this context it is important to note that all compounds were quickly soaked by the porcelain plate that was used as the sample holder (the soaking velocity is strongly dependent on the viscosity of the test compounds). This behaviour has a significant influence on the friction sensitivity leading to a decrease in sensitivity. The unexpected low friction sensitivity of **2b** might be explained by its fast diffusion into the porcelain plate.

In summary, concerning the classification of *UN Recommendation on the Transport of Dangerous Goods*,^[25] the (azidomethyl)silane **1b** is a less sensitive compound with respect to impact and friction. The cyclic bis(azidomethyl)silanes **4b** and **5b** are both sensitive toward impact and friction, whereas the acyclic bis(azidomethyl)silane **2b** is very sensitive. The tris(azidomethyl)-silane **3b** is clearly classified as an extremely sensitive compound.

Conclusion

The (azidomethyl)silanes **1b–5b** were synthesized from the corresponding (chloromethyl)- or (iodomethyl)silanes **1a–5a** by treatment with sodium azide and silver azide, respectively. The tris(azidomethyl)silane **3b** was synthesized for the first time and was characterized as a highly sensitive energetic material. All compounds synthesized were characterized by multinuclear NMR spectroscopy as well as IR and Raman spectroscopy. The thermal decomposition pathway of **1b–5b** is supposed to be ignited at the azidomethyl groups. As all compounds studied are more or less sensitive against impact and friction (**1b**: less sensitive; **2b**: very sensitive; **4b** and **5b**: sensitive; **3b**: extremely sensitive), they should be handled with care, especially if the pure compounds are heated or are in contact with metals (catalytic decomposition can not be excluded).

Experimental Section

Caution! Azides are sensitive and represent energetic materials; therefore, they must be handled with care! During the work with (azidomethyl)silanes, wearing leather jacket, face shield, steel-reinforced Kevlar gloves, ear protection, and electrically grounded shoes is mandatory. Only electrically grounded and metal-free equipment was used during the syntheses.

Acetonitrile, DMF, *n*-pentane (Aldrich), sodium azide (ACROS ORGANICS), (chloromethyl)trimethylsilane, and bis(chloromethyl)dimethylsilane (ABCR) were used as received. Fresh silver azide was synthesized according to known procedures and was stored under light exclusion.

The ^1H , $^{13}\text{C}\{^1\text{H}\}$, ^{14}N , ^{15}N , and $^{29}\text{Si}\{^1\text{H}\}$ NMR spectra were recorded in CDCl_3 at 25 °C using a Jeol 400 Eclipse FT-NMR spectrometer operating at 400.2 (^1H), 100.6 (^{13}C), 28.9 (^{14}N), 40.6 (^{15}N), or 79.5 MHz (^{29}Si). Chemical shifts (ppm) are given with respect to TMS (^1H , ^{13}C , ^{29}Si) or MeNO_2 (^{14}N , ^{15}N). Infrared (IR) spectra were recorded at 25 °C on a Perkin-Elmer Spectrum BXII FT-IR instrument equipped with a Diamant-ATR Dura Sampler. Raman spectra were recorded at 25 °C on a Bruker RAMII Raman instrument ($\lambda = 1064$ nm, 200 mW, 25 °C) equipped with a D418-T Detector at 200 mW. Melting, boiling, and decomposition points (T_{onset}) were determined by differential scanning calorimetry (DSC; Perkin-Elmer Pyris 6 DSC, calibrated by standard pure indium and zinc, 5 °C min^{-1}). Measurements were performed at a heating rate of $\beta = 5$ °C min^{-1} in closed aluminium containers with a hole (1 μm) on the top for gas release with a nitrogen flow of 5 mL min^{-1} . The reference sample was a closed aluminium container with air. Impact and friction sensitivity experiments were performed with a drophammer setup and a friction device according to BAM standards (*Bundesanstalt für Materialforschung und -prüfung*).^[22] Elemental analyses of the (azidomethyl)silanes synthesized were not performed because of their explosive properties.

(Azidomethyl)trimethylsilane (1b): A mixture of (chloromethyl)trimethylsilane (0.25 g, 2.04 mmol), sodium azide (0.66 g, 10.2 mmol), and DMF (10 mL) was stirred at 70 °C for 24 h. After cooling the mixture to ambient temperature, water (20 mL) and *n*-pentane (10 mL) were added, and the resulting two-phase system was vigorously stirred. The *n*-

pentane phase was isolated by decantation, and the aqueous phase was extracted with *n*-pentane (4 x 10 mL; isolation of the *n*-pentane phases by decantation). The combined *n*-pentane phases were dried over anhydrous sodium sulphate, and the solvent was removed by distillation (50 °C, atmospheric pressure) to afford **1b** in 79 % yield (0.21 g) as a colourless liquid.

^1H NMR (CDCl_3): $\delta = 2.72$ (s, 2H, CH_2), 0.08 (s, 9H, $^2J_{\text{H,Si}} = 6.6$ Hz, CH_3) ppm; $^{13}\text{C}\{^1\text{H}\}$ NMR (CDCl_3): $\delta = 42.1$ (s, $^1J_{\text{C,Si}} = 51.8$ Hz, CH_2), -2.6 (s, $^1J_{\text{C,Si}} = 51.8$ Hz, CH_3) ppm; ^{14}N NMR (CDCl_3): $\delta = -131$ (N_β , $\nu_{1/2} = 24$ Hz), -174 (N_γ , $\nu_{1/2} = 64$ Hz), -321 (N_α , $\nu_{1/2} = 351$ Hz) ppm; ^{15}N NMR (CDCl_3): $\delta = -131.4$ (N_β), -173.3 (N_γ), -320.2 (N_α) ppm; $^{29}\text{Si}\{^1\text{H}\}$ NMR (CDCl_3): $\delta = 3.2$ ppm; IR (neat): $\tilde{\nu} = 2959$ (vw), 2899 (w), 2187 (w), 2089 (vs), 1410 (w), 1290 (w), 1250 (m), 839 (vs), 762 (w), 701 (w), 662 (vw), 629 (vw) cm^{-1} ; Raman: $\tilde{\nu} = 2962$ (50), 2902 (100), 2091 (6), 1417 (5), 1289 (4), 1264 (4), 1182 (4), 701 (2), 590 (10) cm^{-1} ; DSC: 128.6 °C (bp.).

Bis(azidomethyl)dimethylsilane (2b): A mixture of bis(chloromethyl)dimethylsilane (0.25 g, 1.59 mmol), sodium azide (1.04 g, 16.0 mmol), and acetonitrile (10 mL) was heated under reflux for 24 h. After cooling the mixture to ambient temperature, it was extracted with *n*-pentane (5 x 10 mL; isolation of the *n*-pentane phases by decantation). The *n*-pentane phases were combined, and the solvent was removed *in vacuo* to afford **2b** in 92 % yield (0.25 g) as a colourless liquid.

^1H NMR (CDCl_3): $\delta = 2.88$ (s, 4H), 0.18 (s, 6H, $^2J_{\text{H,Si}} = 6.2$ Hz, CH_3) ppm; $^{13}\text{C}\{^1\text{H}\}$ NMR (CDCl_3): $\delta = 39.8$ (s, $^1J_{\text{C,Si}} = 55.0$ Hz, CH_2), -5.1 (s, $^1J_{\text{C,Si}} = 52.9$ Hz, CH_3) ppm; ^{14}N NMR (CDCl_3): $\delta = -131$ (N_β , $\nu_{1/2} = 28$ Hz), -172 (N_γ , $\nu_{1/2} = 103$ Hz), -323 (N_α , $\nu_{1/2} = 198$ Hz) ppm; ^{15}N NMR (CDCl_3): $\delta = -131.0$ (N_β), -172.6 (N_γ), -321.0 (N_α) ppm; $^{29}\text{Si}\{^1\text{H}\}$ NMR (CDCl_3): $\delta = 3.3$ ppm; IR (neat): $\tilde{\nu} = 2961$ (w), 2897 (vw), 2186 (vw), 2088 (vs), 1411 (w), 1289 (w), 1257 (m), 1229 (w), 836 (m) cm^{-1} ; Raman: $\tilde{\nu} = 2964$ (45), 2904 (100), 2092 (10), 1289 (5), 1258 (4), 1225 (4), 1183 (25), 901 (4), 565 (3), 503 (7) ppm; DSC: 137.3 °C (dec.).

Tris(azidomethyl)methylsilane (3b): A mixture of tris(chloromethyl)methylsilane (0.25 g, 1.31 mmol), sodium azide (1.70 g, 26.1 mmol), and acetonitrile (10 mL) was heated under reflux for 24 h. After cooling the mixture to ambient temperature, it was extracted with *n*-pentane (5 x 10 mL; isolation of the *n*-pentane phases by decantation). The *n*-

pentane phases were combined, and the solvent was removed *in vacuo* to afford **3b** in 94 % yield (0.26 g) as a colourless liquid.

^1H NMR (CDCl_3): $\delta = 3.04$ (s, 6H, $^2J_{\text{H,Si}} = 5.5$ Hz, CH_2), 0.29 (s, 3H, $^2J(^1\text{H}, ^{29}\text{Si}) = 6.3$ Hz, CH_3) ppm; $^{13}\text{C}\{^1\text{H}\}$ NMR (CDCl_3): $\delta = 34.7$ (s, $^1J_{\text{C,Si}} = 57.1$ Hz, CH_2), -7.8 (s, $^1J_{\text{C,Si}} = 54.4$ Hz, CH_3) ppm; ^{14}N NMR (CDCl_3): $\delta = -132$ (N_β , $\nu_{1/2} = 33$ Hz), -171 (N_γ , $\nu_{1/2} = 137$ Hz), -320 (N_α , $\nu_{1/2} = 209$ Hz) ppm; ^{15}N NMR (CDCl_3): $\delta = -131.3$ (N_β), -170.6 (N_γ), -321.8 (N_α) ppm; $^{29}\text{Si}\{^1\text{H}\}$ NMR (CDCl_3): $\delta = 1.5$ ppm; IR (neat): $\tilde{\nu} = 2962$ (vw), 2890 (w), 2083 (vs), 1633 (w), 1408 (m), 1285 (m), 1260 (m), 1233 (m), 1070 (m), 911 (w), 825 (m), 802 (m) ppm; Raman: $\tilde{\nu} = 2964$ (35), 2903 (100), 2092 (15), 1413 (10), 1286 (8), 1231 (8), 1180 (10), 900 (7), 561 (8) cm^{-1} ; DSC: 136.7 °C (dec.).

1,1-Bis(azidomethyl)-1-silacyclopentane (4b): A mixture of bis(iodomethyl)-1-silacyclopentane (0.37 g, 1.01 mmol), silver azide (0.76 g, 5.07 mmol), and acetonitrile (5 mL) was stirred at ambient temperature for 24 h under light exclusion. The suspension was extracted with *n*-pentane (5 x 10 mL; isolation of the *n*-pentane phases by decantation), the *n*-pentane phases were combined, and the solvent was removed *in vacuo* to afford **4b** in 96 % yield (0.19 g) as a colourless liquid.

^1H NMR (CDCl_3): $\delta = 2.99$ (s, 4H, CH_2N_3), 1.68 – 1.62 (m, 4H, β - CH_2), 0.79 – 0.73 (m, 4H, α - CH_2) ppm; $^{13}\text{C}\{^1\text{H}\}$ NMR (CDCl_3): $\delta = 38.0$ (s, $^1J_{\text{C,Si}} = 51.9$ Hz, CH_2N_3), 26.9 (s, β - CH_2), 9.0 (s, $^1J_{\text{C,Si}} = 52.9$ Hz, α - CH_2) ppm; ^{14}N NMR (CDCl_3): $\delta = -131$ (N_β , $\nu_{1/2} = 27$ Hz), -172 (N_γ , $\nu_{1/2} = 108$ Hz), -321 (N_α , $\nu_{1/2} = 384$ Hz) ppm; $^{29}\text{Si}\{^1\text{H}\}$ NMR (CDCl_3): $\delta = 18.9$ ppm; IR (neat): $\tilde{\nu} = 2934$ (m), 2857 (w), 2084 (vs), 1452 (vw), 1406 (m), 1286 (m), 1229 (w), 1076 (m), 1030 (w), 1018 (w), 909 (vw), 858 (w), 821 (m), 787 (w) cm^{-1} ; Raman: $\tilde{\nu} = 2939$ (100), 2897 (80), 2092 (11), 1452 (8), 1409 (9), 1251 (6), 1019 (5), 945 (4), 850 (10), 580 (6), 516 (11) cm^{-1} ; DSC: 130.1 °C (dec.).

1,1-Bis(azidomethyl)-1-silacyclohexane (5b): A mixture of bis(iodomethyl)-1-silacyclohexane (0.36 g, 0.95 mmol), silver azide (0.76 g, 5.07 mmol), and acetonitrile (5 mL) was stirred at ambient temperature for 24 h under light exclusion. The suspension was extracted with *n*-pentane (5 x 10 mL; isolation of the *n*-pentane phases by decantation), the *n*-pentane phases were combined, and the solvent was removed *in vacuo* to afford **5b** in 91 % yield (0.18 g) as a colourless liquid.

^1H NMR (CDCl_3): $\delta = 2.96$ (s, 4H, CH_2N_3), 1.76–1.67 (m, 4H, $\beta\text{-CH}_2$), 1.48–1.40 (m, 2H, $\lambda\text{-CH}_2$), 0.82–0.77 (m, 4H, $\alpha\text{-CH}_2$) ppm; $^{13}\text{C}\{^1\text{H}\}$ NMR (CDCl_3): $\delta = 37.9$ (s, $^1J_{\text{C,Si}} = 52.9$ Hz, CH_2N_3), 29.4 (s, $\gamma\text{-CH}_2$), 24.1 (s, $\beta\text{-CH}_2$), 9.1 (s, $^1J_{\text{C,Si}} = 50.9$ Hz, $\alpha\text{-CH}_2$) ppm; ^{14}N NMR (CDCl_3): $\delta = -131$ (N_β , $\nu_{1/2} = 31$ Hz), -172 (N_γ , $\nu_{1/2} = 103$ Hz), -320 (N_α , $\nu_{1/2} = 187$ Hz) ppm; $^{29}\text{Si}\{^1\text{H}\}$ NMR (CDCl_3): $\delta = -1.8$ ppm; IR (neat): $\tilde{\nu} = 2918$ (m), 2855 (w), 2084 (vs), 1446 (w), 1406 (w), 1288 (m), 1230 (w), 1182 (m), 991 (w), 910 (m), 781 (m) cm^{-1} ; Raman: $\tilde{\nu} = 2934$ (98), 2886 (100), 2886 (85), 2092 (12), 1449 (8), 1408 (8), 1292 (8), 1181 (8), 1008 (7), 908 (8), 797 (10), 565 (10) cm^{-1} ; DSC: 133.9 °C (dec.).

Acknowledgements

Financial support of this work by the Ludwig-Maximilians- Universität München (LMU), the Universität Würzburg, the U.S. Army Research Laboratory (ARL), the Armament Research, Development and Engineering Center (ARDEC), the Strategic Environmental Research and Development Program (SERDP), and the Office of Naval Research (ONR Global, title: "Synthesis and Characterization of New High Energy Dense Oxidizers (HEDO) - NICOP Effort ") under contract nos. W911NF-09-2-0018 (ARL), W911NF-09-1-0120 (ARDEC), W011NF-09-1-0056 (ARDEC), and 10 WPSEED01-002/WP-1765 (SERDP) is gratefully acknowledged. The authors acknowledge collaborations with Dr. Mila Krupka (OZM Research, Czech Republic) in the development of new testing and evaluation methods for energetic materials and with Dr. Muhamed Suceca (Brodarski Institute, Croatia) in the development of new computational codes to predict the detonation and propulsion parameters of novel explosives. We are indebted to and thank Drs. Betsy M. Rice and Brad Forch (ARL, Aberdeen, Proving Ground, MD) and Mr. Gary Chen (ARDEC, Picatinny Arsenal, NJ) for many helpful and inspired discussions and support of our work. We thank Stefan Huber for measuring the impact and friction sensitivities.

-
- [1] S. Bräse, K. Banert (eds.), *Organic Azides: Syntheses and Applications*, Wiley, Chichester, **2010**.
- [2] A. Karl, W. Buder (Degussa AG), *Eur. Pat. Appl.* EP 0050768, **1982**.
- [3] R. D. Haugwitz, W. K. Anderson, J. Plowman, R. Kaslinal, D. M. Houston, V. L. Narayanan, *Appl. Organomet. Chem.* **1990**, *4*, 375–378.

- [4] W. K. Anderson, R. Kasliwal, D. M. Houston, Y.-s. Wang, V. L. Narayana, R. D. Haugwitz, J. Plowman, *J. Med. Chem.* **1995**, *38*, 3789–3797.
- [5] M. Kurono, R. Unno, Y. Matsumoto, Y. Kondo, T. Mitani, T. Jomori, H. Michishita, K. Sawai (Sanwa Kagaku Kenkyusho Co. Ltd.), *Eur. Pat. Appl.* EP 0288002, **1988**.
- [6] R. Meyer, J. Köhler, A. Homburg, *Explosives*, 5th Ed., Wiley-VCH, Weinheim, **2002**, p. 154–155 and 196–197.
- [7] T. M. Klapötke, B. Krumm, R. Ilg, D. Troegel, R. Tacke, *J. Am. Chem. Soc.* **2007**, *129*, 6908–6915.
- [8] C. Evangelisti, T. M. Klapötke, B. Krumm, A. Nieder, R. J. F. Berger, S. A. Hayes, N. W. Mitzel, D. Troegel, R. Tacke, *Inorg. Chem.* **2010**, *49*, 4865–4880.
- [9] O. Tsuge, S. Kanemasa, K. Matsuda, *Chem. Lett.* **1983**, 1131–1134.
- [10] U.-P. Apfel, D. Troegel, Y. Halpin, S. Tschierlei, U. Uhlemann, H. Görls, M. Schmitt, J. Popp, P. Dunne, M. Venkatesan, M. Coey, M. Rudolph, J. G. Vos, R. Tacke, W. Weigand, *Inorg. Chem.* **2010**, *49*, 10117–10132.
- [11] R. Ilg, D. Troegel, C. Burschka, R. Tacke, *Organometallics* **2006**, *25*, 548–551.
- [12] D. Troegel, F. Möller, C. Burschka, R. Tacke, *Organometallics* **2009**, *28*, 5765–5770.
- [13] D. Troegel, W. P. Lippert, F. Möller, C. Burschka, R. Tacke, *J. Organomet. Chem.* **2010**, *695*, 1700–1707.
- [14] D. Troegel, Dissertation, Julius-Maximilians-Universität Würzburg, **2009**.
- [15] K. Nishiyama, N. Tanaka, *J. Chem. Soc., Chem. Commun.* **1983**, 1322–1323.
- [16] W. K. Anderson, A. S. Milowsky, *J. Med. Chem.* **1986**, *29*, 2241–2249.
- [17] V. Van Dorsselaer, D. Schirlin, P. Marchal, F. Weber, C. Danzin, *Bioorg. Chem.* **1996**, *24*, 178–193.
- [18] N. Nomura, R. Ishii, Y. Yamamoto, T. Kondo, *Chem. Eur. J.* **2007**, *13*, 4433–4451.
- [19] E. Lieber, C. N. R. Rao, T. S. Chao, C. W. W. Hoffman, *Anal. Chem.* **1957**, *29*, 916–918.
- [20] *NATO standardization agreement (STANAG) on explosives, impact sensitivity tests, no. 4489*, 1st ed., **1999**.

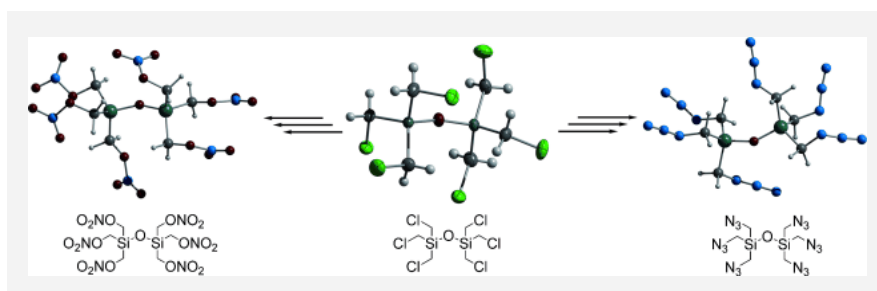
- [21] *WIWEB-Standardarbeitsanweisung 4-5.1.02, Ermittlung der Explosions-gefährlichkeit, hier der Schlagempfindlichkeit mit dem Fallhammer, 2002.*
- [22] www.bam.de (German version); www.bam.de/en/index.htm (English version).
- [23] *NATO standardization agreement (STANAG) on explosives, friction sensitivity tests, no. 4487, 1st ed., 2002.*
- [24] *WIWEB-Standardarbeitsanweisung 4-5.1.03, Ermittlung der Explosionsgefährlichkeit oder der Reibeempfindlichkeit mit dem Reibeapparat, 2002.*
- [25] *UN Recommendation on the Transport of Dangerous Goods, Manual of Tests and Criteria, Amendment 1. http://www.unece.org/trans/publications/dg_tests2011.html, 2011.*
-

V. Hexa-Substituted Disiloxanes

Energetic silanes

L. Ascherl, C. Evangelisti, T. M. Klapötke, B. Krumm, J. Nafe, A. Nieder, S. Rest, C. Schütz, M. Suceska* and M. Trunk ... 83 - 112*

Chemistry and Structures of Hexakis(halogenomethyl)-, Hexakis(azidomethyl)- and Hexakis(nitratomethyl)-disiloxanes



Hexakis(halogenomethyl)disiloxanes (see figure). Their remarkable sensitivity is discussed and a decomposition pathway is proposed. Hexakis(azidomethyl)- and hexakis(nitratomethyl) disil-

Chemistry and Structures of Hexakis(halogenomethyl)-, Hexakis(azidomethyl)- and Hexakis(nitratomethyl)disiloxanes

**Laura Ascherl,^[a] Camilla Evangelisti,^[a] Thomas M. Klapötke,^{*[a]} Burkhard Krumm,^[a]
Julia Nafe,^[a] Anian Nieder,^[a] Sebastian Rest,^[a] Christian Schütz,^[a] Muhamed
Suceska^{#[b]} and Matthias Trunk^[a]**

Published in Chemistry – A European Journal 2013, 19, 9198–9210.

Abstract: Investigations on substituted hexamethyl disiloxanes [(XCH₂)₃Si]₂O with X = F, Cl, Br, I, N₃, ONO₂) are reported in this study. New synthetic routes for the precursor hexakis(chloromethyl)disiloxane are presented. The products with X = Cl, Br, I, N₃ were characterized by NMR, IR and Raman spectroscopy. In addition, the single crystal structures of X = Cl, Br, I are discussed in detail.

The compounds containing X = F, ONO₂ were not obtained pure; instead investigations of the decomposition products reveal a conversion to intermediates. Theoretical calculations on B3LYP/cc-pVDZ, B3LYP/3-21G, MP2/6-31G* and MP2/3-21G level of theory of the gas phase structures are used to explain the chemical and physical behaviour of the compounds X = Cl, Br, I, N₃, ONO₂. A new decomposition pathway of hexakis(nitratomethyl)-

disiloxane is pointed out and used to explain the remarkable instability. Energetic properties and values of the nitrate and azide derivatives were calculated on the CBS-4M level of theory and by the improved EXPL05 computer code version 6.01.

Keywords: silanes • azides • halides • explosives • NMR spectro

Introduction

Azides and nitrate esters are commonly used energetic materials in civil and military applications.[1] The most famous examples are lead azide and nitroglycerin (glycerin trinitrate). In the late 1960th the first by nitratomethyl esters functionalized silanes were published as drug substituting glycerine trinitrate (nitroglycerin) in the field of heart

disease medication and were proposed as potential application for explosives.[2,3] The highly explosive character of this kind of compounds has been already mentioned, but not studied in detail. Since tetrakis(azidomethyl)- and tetrakis-(nitratomethyl)silane were synthesized and described as extremely sensitive compounds in 2007, first practical thoughts and studies have been

[a] Prof. Dr. Thomas M. Klapötke
Department Chemistry
Ludwig-Maximilian-University Munich
Butenandstr. 5–13(D)
81377 Munich, Germany
Fax: +49-89-2180-77492
E-Mail: tmk@cup.uni-muenchen.de

[b] Dr. Muhamed Suceska
Brodarski institut d.o.o.
Avenija Veæeslava Holjevca 20
10000 Zagreb
E-Mail: suceska@hrbi.hr

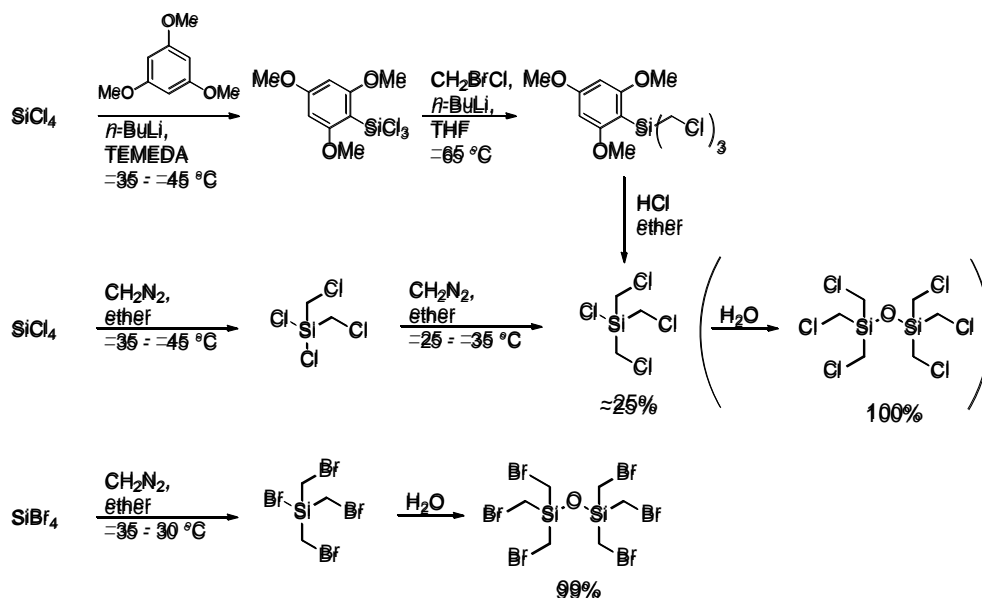
Supporting information for this article is available on the WWW under <http://www.chemeurj.org/> or from the author.

under investigation.[4] Especially the nitrate ester was mentioned as an extremely difficult to handle explosive material. A comparison with the corresponding carbon analogues shows a highly increased sensitivity for the silicon analogues towards impact, friction and thermal stimuli.[4] As a consequence, investigations on the characteristics of similar compounds with decreased numbers of energetic moieties were performed.[5]

The first azidomethyl silanes were discussed as starting materials for synthesizing aminomethyl silanes as complex ligands for Cisplatin derivatives.[6] Azidomethyl silanes have lately become an important building block for surface functionalisation, cycloadditions, amination agents of Grignard reagents and biochemical applications.[7,8,9,10] The first azidomethyl silane which was studied in terms of energetic properties was the previous mentioned tetrakis(azidomethyl)silane.[4] Similar compounds with decreased azide contents were studied elsewhere. In comparison, they show lower friction and impact sensitivities than corresponding nitratomethyl silanes.[11]

Hexakis(nitratomethyl)disiloxane was one of the first reported nitratomethyl silanes. The compound was mentioned as highly sensitive and explosive material, but no analytical data are available. To the best of our knowledge, there is no evidence for an existence of this compound. Even for the starting materials hexakis(chloromethyl)- and hexakis(iodomethyl)disiloxane there is only weak information available.[2] Some analytical data for the corresponding bromo derivative, hexakis(bromomethyl)disiloxane, is available in the literature, and it was referred to as a potential fire-resistant material.[12,13,14] The chloro and bromo derivatives are known to be synthesized (respectively the precursors tris(chloromethyl)chlorosilane and tris(bromomethyl)bromosilane, which convert easily to the product by storing at moist air) could be synthesized by using the corresponding tetrahalogenosilane and an excess of diazomethane (Scheme 5.1).[12,13] The yields are moderate to excellent, related to the corresponding halogenosilane (chloro: 25 % and bromo: 99 %), whereas the synthesis of a fluoro derivative using this synthetic route failed.[12] Because of the expensive laborious synthesis of diazomethane, in addition to the risk of handling diazomethane (explosive and toxic material) a more appropriate synthesis would be desirable.[15] Another synthesis to tris(chloromethyl)chlorosilane avoiding diazomethane was described.[16] But due to the intricate procedure, high costs and the poor overall yield (16 %), this seems not to be efficient.

In the following, the compounds hexakis(azidomethyl)- and hexakis(nitratomethyl)-disiloxane are discussed in terms of syntheses, and physical and mechanical sensitivities. In addition, the corresponding halogeno derivatives (Cl, Br, I) were synthesized by more effective and more appropriate routes for this type of compounds.

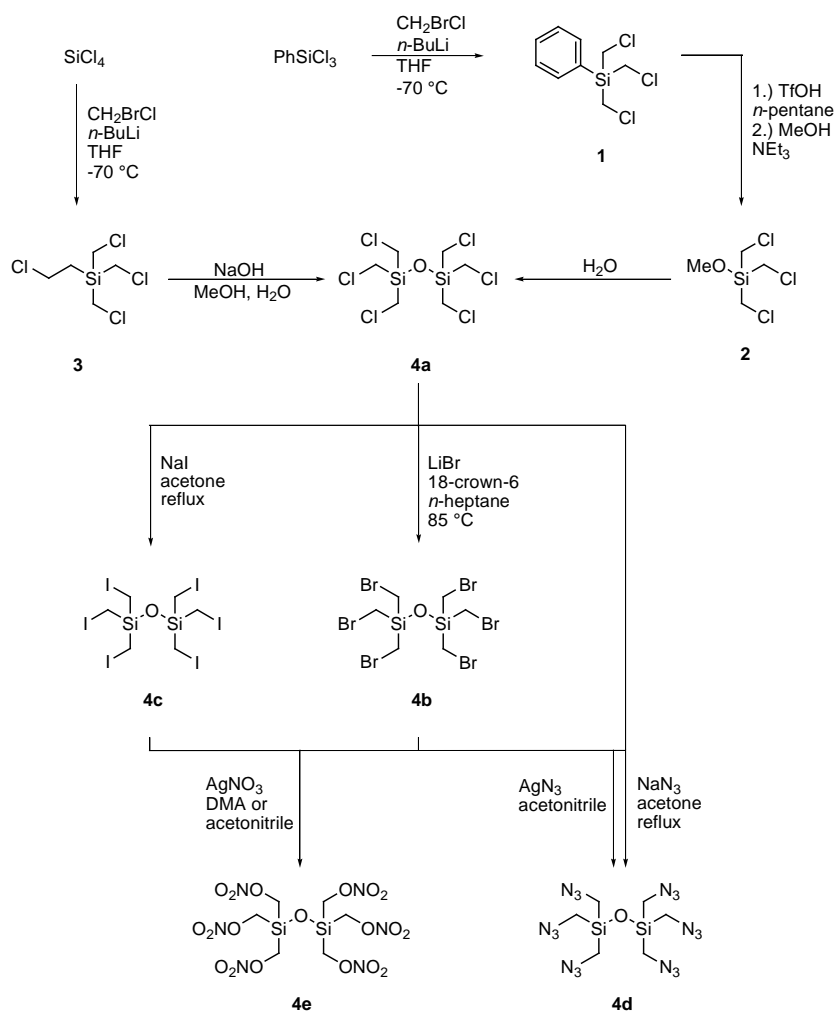


Scheme 5.1. Routes to synthesize tris(chloromethyl)chlorosilane (respectively hexakis(chloromethyl)-disiloxane) and hexakis(bromomethyl)disiloxane (yields calculated to SiCl_4 and SiBr_4).

Results and Discussion

Hexakis(chloromethyl)disiloxane (**4a**) can be obtained *via* diazomethane and tetrachlorosilane. A synthetic route to tris(chloromethyl)-chlorosilane and -methoxysilane (**2**) as precursors to give **4a** by hydrolysis, is known,[12,16] but the synthetic efforts limit an economic yield. An improved method was used to avoid diazomethane, increasing the yield and to establish an easier procedure (Scheme 5.2). Starting with the known synthesis of **1**,[17] followed by the cleavage of benzene using triflic acid in pentane, methoxylation by methanol and triethylamine, and extracting the product by *Kugelrohr* distillation leads to a 52 % yield of **2**. The disiloxane **4a** was obtained in quantitative yield by treating **2** with water in the presence of a catalytic amount of sulphuric acid. Overall, **4a** was obtained in 68 % yield (calculated from phenyltrichlorosilane) and using the direct synthetic route without purifying **2** in a one-pot synthesis. Furthermore, **4a** can be obtained by ethylene elimination (supported by hyperconjugating effect and stabilizing of β -silylcarbonium

intermediate) in chloroethylsilane derivative **3** using sodium hydroxide in methanol.[18] Compound **3** is obtained as a major side product in the synthesis of tetrakis(chloromethyl)silane.[16]



Scheme 5.2. Improved synthetic routes to hexakis(chloromethyl)disiloxane (**4a**) and further substitution reactions.

The bromo derivative **4b** was obtained as colourless solid in 92 % by treating **4a** with lithium bromide and traces of a phase transfer catalyst at 85°C in $n\text{-heptane}$ within 24 h. It is advisable to use tri(octyl)methylammonium bromide or 18-crown-6 ether, preferable the latter due to purification reasons. The compounds **4a** and **4b** are soluble in most common solvents.

The iodo derivative **4c** was obtained as a colourless solid in high yields by refluxing the chloro derivative **4a** with sodium iodide in acetone and extraction with a large amount of

diethyl ether (minimum **4c**:diethyl ether 1:1000 w/w). The solubility of **4c** in diethyl ether and DMA (dimethylacetamide) is low and even worse in ethanol, ethylacetate, acetonitrile, dioxane, *n*-pentane, *n*- and *iso*-hexane. It is well soluble in chloroform and THF.

Attempts to synthesize hexakis(fluoromethyl)disiloxane *via* several fluoride exchange reactions were unsuccessful. Treatment of **4a** with NaF, CsF, SbF₃ and AgF at ambient temperature and 50 °C leads to partially converted compounds with cleaved Si-O-Si bridge in the first two cases, which was confirmed by ¹⁹F NMR spectroscopy. From these experiments the chloride substitution seems to be much slower than the Si-O bond cleavage by fluoride ions; instead neutral tetra- and anionic penta-coordinated Si-F species were observed. In the case of SbF₃ only traces of Si-O cleavage products were found. Reactions of **4b** and **4c** with fluorides result in similar products. At ambient temperature the compounds **4a**, **4b** and **4c** react immediately with silver(I)fluoride to form elemental silver and not as hoped to silver halogenides, and many undefined higher siloxanes. Possible reaction pathways of silanes with fluorides are described in detail elsewhere.[19]

The substitution of **4a** by azide was first attempted by chloride azide exchange with sodium azide. But even at high temperature and with an excess of sodium azide (up to 30 equivalents per chloride), complete conversion was not observed, due to prior detection of decomposition side products. Treatment of the bromo derivative **4b** with silver azide in acetone at ambient temperature up to gentle heating (40 °C), also led to an uncompleted conversion. Already at ambient temperature side products were observed. Full conversion to the azido derivative **4d** without side products was only observed using the iodo derivative **4c** as a starting material. But a tenfold excess of silver azide in acetone, a reaction time of two weeks and strict exclusion of light is recommended. An extraction is very dangerous (as well as for the partially converted raw products), because the solvent has to be almost completely removed before solving the residue in a small amount of diethyl ether or pentane. The hexakis(azidomethyl)disiloxane (**4d**) should be handled only in small amounts, with extreme care and with full safety equipment! It is advisable to store this highly explosive compound as a solution in aprotic solvents such as alkanes. No decomposition is observed after one year at 4 °C, which is nicely in perfect agreement with the properties of the similar Si(CH₂N₃)₄. [4]

Table 5.1. ^1H , $^{13}\text{C}\{^1\text{H}\}$, $^{29}\text{Si}\{^1\text{H}\}$ and $^{15}\text{N}\{^1\text{H}\}$ NMR shifts of **1–3** and **4a–d** in CDCl_3 and ppm (^1H and $^{13}\text{C}\{^1\text{H}\}$ NMR values are only given for the RCH_2X moiety). $^1J_{\text{C,Si}}$ respectively $^1J_{\text{Si,C}}$ coupling constants are given in brackets [Hz] (discrepancies of the coupling constants due to resolution of the spectra).

	^1H	$^{13}\text{C}\{^1\text{H}\}$	$^{29}\text{Si}\{^1\text{H}\}$	$^{15}\text{N}\{^1\text{H}\}$ ($\text{CH}_2\text{N}_\alpha\text{N}_\beta\text{N}_\gamma$)		
1 ^[a]	3.30	24.5 (59.3)	-8.1 (59.6)			
2 ^[a]	3.07	24.1 (70.6)	-4.3 (70.2)			
3 ^[a]	3.08	24.6 (58.1)	0.1 (58.4)			
4a	3.08	24.9 (72.0)	-10.6 (72.1)			
4b	2.79	11.0 (72.7)	-11.8 (72.1)			
4c	2.45	-19.3 (67.5)	-7.6 (66.9)			
4d	3.08	37.7 (68.0)	-5.8 (68.0)	N_α -324.1	N_β -131.9	N_γ -170.8

[a] Phenyl, methoxy and chloroethyl resonances are given in the experimental section.

Hexakis(nitratomethyl)disiloxane (**4e**) was previously described as a colourless solid, which precipitates during the reaction of the iodomethyl derivative **4c** with a saturated solution of silver nitrate in acetonitrile at ambient temperature.[2] Following this procedure, a colourless precipitate was observed, which was identified by NMR spectroscopy consisting of a mixture of various unidentifiable molecular/oligomeric/polymeric siloxane derivatives with not clearly verifiable substituents in the region of below -55 ppm in the ^{29}Si NMR spectrum. In addition, nitratomethyl moieties could not be detected in the ^{14}N NMR spectrum in the area of -40 to -45 ppm, as is verified by other nitratomethyl silanes.[5] The appearance of equimolar amounts of silver iodide and the lack of the characteristic NMR signals of the starting material **4c**, indicated a complete conversion, but also a fast decomposition of the nitrate ester groups into NO_2 and siloxanes. The desired product could not be detected by this synthetic route (neither in the solution, nor in the precipitate).

However, the claimed product **4e** was characterized as highly explosive in literature![2] Even partially substituted silane nitrate esters and partially substituted siloxanes are highly sensitive and should be handled with extreme care! Consequently, it remains questionable that in ref. [2] the hexanitratomethyl derivative was isolated in a pure form. Most likely mixed *poly*-siloxanes (mainly of the type $\text{RSiO}_{3/2}$ with $\text{R} = \text{CH}_2\text{ONO}_2$ and decomposition products) were formed with variable amounts of nitratomethyl moieties. Alternatively, **4e**

was reported to be prepared in a 0.125M dimethylacetamide (DMA) solution.[2] According to our findings with DMA, during the reaction time of three days at ambient temperature under light exclusion, silver iodide precipitated with immediate formation of NO₂ (solution changed colour from colourless to bright yellow), which was identified by the ¹⁴N NMR resonance. Likely, this is similar to the proposed decomposition pathway of tetrakis(nitratomethyl)silane (Scheme 5.3).[20,21] The disadvantage of using **4c** and silver nitrate is the low solubility of **4c** in DMA (and other appropriate solvents). Therefore, **4c** was found to be an inappropriate starting material. More efficient is a reaction with the bromo derivative **4b** and silver nitrate, which leads to a fast substitution of bromide with nitrate, but also as with **4c**, the resulting nitratomethyl disiloxane groups decomposed readily within a short time in solution to NO₂ and higher siloxanes.

NMR shifts of all compounds except **4e** are given in Table 5.1. The ¹H and ¹³C NMR signals of the SiCH₂X moiety in **4a**, **4b** and **4c** (X = Cl, Br, I) show the expected high-field shifting in the order of Cl < Br < I. The ²⁹Si signals however, do not show this tendency. In the case of X = Cl and Br only a small difference is observed, in contrast the iodo derivative shows a strong low-field shift probably because of steric reasons. From our previous experience with chloro- and azido-methylsilanes, their NMR resonances are in most cases similar,[11] but not here in the case with **4a** and **4d**. In the ²⁹Si NMR spectra the strong low-field shift of **4d** compared to **4a** is likely due to mainly sterical reasons. The value of the coupling constant ¹J_{C,Si}, respectively ¹J_{Si,C}, is depending on the substituent R at the Si center of the moiety RSi(CH₂X)₃. With R = phenyl or chloroethyl, the ¹J_{C,Si} coupling constant of the CH₂X carbon was observed around 60 Hz. In the case of oxygen as the R substituent, like methoxy or disiloxanes, this coupling constant is slightly higher around 70 Hz. This confirms the fact where increased electronegativity of the substituents attached to the silicon atom results in an increase of the coupling frequencies.[22] In addition, the influence of the ¹J_{C,Si} coupling depending on the nature of X and its electronegativity seems to be negligible. The substituents iodide and azide show coupling frequencies slightly below 70 Hz. In the case of the iodo derivative **4c** the electronegativity seems to be the main factor. As known from the coupling frequencies of the compounds tris(chloromethyl)methylsilane (¹J_{C,Si} = 57.8 Hz) and its corresponding azide (¹J_{C,Si} = 57.1 Hz), a similar range is observed.[11] Comparing the coupling constants of the corresponding chloro- and azido-methyl disiloxanes **4a** and **4d**

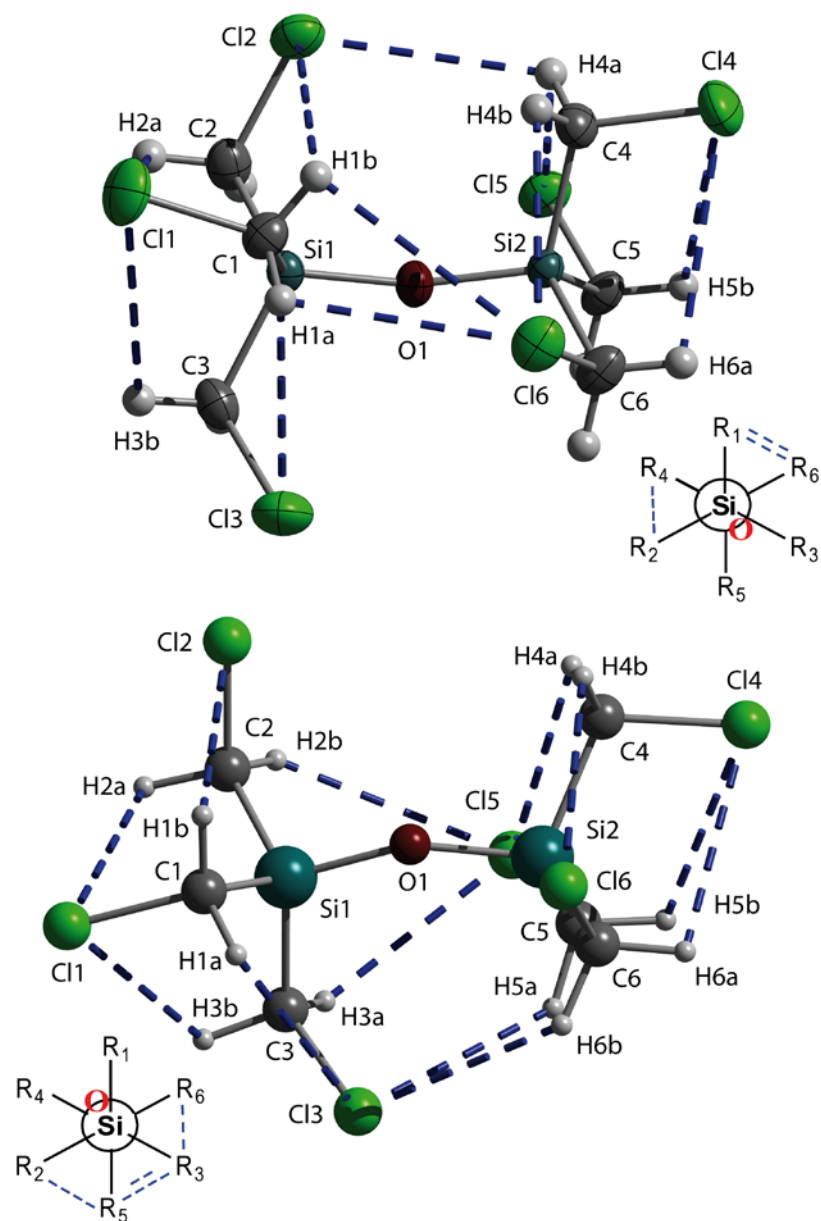


Figure 5.1. The crystallographic structure (top) and the calculated structure on the MP2 level of theory (MP2/6-31G*, bottom) of **4a**. Electrostatic attraction between the two RSi(CH₂Cl)₃ moieties, the attractions within the moieties RSi(CH₂Cl)₃ in the crystal structure and in the calculated gas phase structure are given in blue dashed lines (solid state: Cl2---H4a: 3.157(1) Å; Cl6---H1a/b: 3.202(1), 3.439(1) Å; Cl1---H3b: 3.344(2) Å; Cl1---H2aC2: 3.041(1) Å; Cl2---H1bC1: 3.326(1) Å; Cl3---H1a: 3.211(2) Å; Cl4---H5b: 3.324(2) Å; Cl4---H6aC6: 3.184(1) Å; Cl5---H4a: 3.047(1) Å; Cl6---H4bC4: 3.198(1) Å; calculated gas phase: Cl3---H5a: 3.038 Å; Cl3---H6b: 3.221 Å; Cl5---H2b: 3.220 Å; Cl5---H3a: 3.038 Å; Cl1---H2aC2: 3.228 Å; Cl1---H3bC3: 3.156 Å; Cl2---H1bC1: 3.253 Å; Cl3---H1a: 3.336 Å; Cl4---H5bC5: 3.155 Å; Cl4---H6aC6: 3.228 Å; Cl5---H4a: 3.337 Å; Cl6---H4bC4: 3.252 Å; Σ vdW(Cl,H) and Σ vdW(Cl,C) radii: 2.95 Å and 3.45 Å).[27] In addition, the Newman projection along the Si---Si axes is shown of each structure (R_i = CH₂Cl, attractions between the two RSi(CH₂Cl)₃ moieties in blue dashed lines, the position of the bridging oxygen is marked with **O**).

with 72.0 Hz and 68.0 Hz, a difference of 4 Hz was found, which can not only be explained by electronic effects, but also by sterical and structural differences. The same explanation is given for the atypical shift tendencies of the three halogeno derivatives **4a–c**. Due to the lack of structural information on **4d**, an obtuse Si–O–Si angle as it is found for **4c** (see X-ray structures below), can be postulated. The ^{15}N NMR data for **4d** are in the range of other azidomethyl silanes.[11] As mentioned before, no definite assignments of shifts in any NMR spectrum were possible for **4e**.

All three compounds **4a–c** crystallize in the monoclinic space group $P2_1/n$ with four molecules per unit cell and increasing densities from chlorine to iodine of 1.601, 2.575 respectively 3.181 g/cm³. The chloro derivative **4a** crystallizes in colourless needles just below ambient temperature ($\sim 25^\circ\text{C}$). Colourless crystalline blocks of the bromo derivative **4b** were obtained by recrystallization of the compound with *n*-pentane. Colourless crystals of iodo derivative **4c** were obtained by adding acetonitrile to a solution of **4c** in THF. Additional crystallographic data of **4a**, **4b** and **4c** are given in Table 5.2. Exemplarily, the structure of **4a** is shown in Figure 5.1; the structures of the isostructural **4b** and **4c** are shown in the Supporting Informations (Figure S1).

The bond lengths and angles of **4a–c** are given in Table 5.3. The bonding situations of all three molecules are rather similar. The Si–C bond lengths are for all three cases in average similar (**4a**: 1.861 Å, **4b**: 1.872 Å, **4c**: 1.863 Å) and in the expected range of Si–C bonds (1.87 Å).[23] The Si–O bond lengths are comparable to those in hexamethyldisiloxane (1.626 Å) for **4a–c** (1.614 Å, 1.619 Å, 1.622 Å), and consequently lie between the calculated lengths of Si–O single (1.77 Å) and double bonds (1.53 Å), but in the area of other Si–O single bonds found experimentally.[23,24] In the literature, several reasons were discussed for the significantly short Si–O bonds, which are closely related to the obtuse $\alpha(\text{Si–O–Si})$ angles discussed below.[17,22–25] In the case of **4a** and **4b** the Si–O bonds are both equal, in contrast to **4c** where one of the two Si–O bonds is slightly elongated. The C–X bonds of all three halogeno derivatives (X = Cl, Br, I) are in the expected range.

The bond angles of **4a–c** are given in Table 5.3. By comparing the angles of the X–C–Si moieties for X = Cl, Br and I, it was found, that the angles for X = Cl, Br are with 109.0° respectively 109.5° similar (on average), but significantly smaller than for X = I with 111.3° (on average). Sterical and in addition electrostatic interactions can be the reason for this

trend. The C–Si–O as well as the C–Si–C angles are almost equal on average in all three cases ($\alpha(\text{C–Si–O})$: **4a**: 108.7°, **4b**: 108.5°, **4c**: 108.5°; $\alpha(\text{C–Si–C})$: **4a**: 110.3°, **4b**: 110.4°, **4c**: 110.4°). Less space requirements of the smaller CH₂Cl in comparison to CH₂Br and CH₂I moieties, and the contrary increasing electrostatic repulsion between the chlorine relative to the bromine and iodine atoms together lead to the structural differences of compounds **4a–c**. In contrast to tetra-substituted silicon, which resemble structurally the carbon counterparts, disiloxanes show significant differences in the structures with a remarkable obtuse $\alpha(\text{Si–O–Si})$ angles in comparison to the carbon analogues.[16] Especially the angle in **4c** (169.3°) was found to be more obtuse than measured for **4a** and **4b** (161.9° respectively 163.7°). Hexakismethyldisiloxane shows an angle of 148.8° and, derived from an AB₂ system according to the Walsh diagram, the angle will be significantly obtuse for sterical and electron-withdrawing substituents at the silicon atom (increased positive charge on the silicon atom) compared to the methyl moieties.[24] In contrast, the opposite order is observed by increased obtuse angles in **4a–c** as expected from the AB₂ system in the Walsh diagram. Chlorine, the most electronegative in the halogen row of the halogens discussed here, shows the most acute angle. The opposite is found for the less electron-withdrawing halogen iodine. The percentage of ionic bonding between silicon and oxygen also has an influence on the angles and the Si–O bond.[23,25]

In each structures of **4a–c**, electrostatic attractions are observed between the two RSi(CH₂X)₃ moieties and within each RSi(CH₂X)₃ moiety. The attractions within each moiety fixed the swan-like orientation of the RCH₂Cl functions. The attractions between the halogens X₂ and X₆ of one Si(CH₂X)₃ moiety and with the CH₂ group (C₄ and C₁) located at the other Si(CH₂X)₃ moiety has influence on the twisting and bending along the Si–O–Si axes (**4a**: see Figure 5.1; **4b/c**: see Supporting Informations Figure S1). The attractions are getting weaker in the order from Cl, Br to I, because of the decreasing polarities of the halogen atoms. Due to these attractions the structures are restrained in case of rotations along the Si–Si axes and the $\alpha(\text{Si–O–Si})$ bend into the direction of the two electrostatic attractions ($\alpha(\text{Si–O–Si})$: **4a**: 163.6(2)°, **4b**: 169.4(4)°, **4c**: 161.9(1)°). Due to the increasing electrostatic attraction in the order Cl–CH₂ > Br–CH₂ > I–CH₂, the $\alpha(\text{Si–O–Si})$ becomes more acute in the same order by bending out the bridging oxygen in the direction of the C₃ and C₅.

Exemplarily for all three compounds **4a–c** the Newman projection is shown in Figure 5.1. The CH₂X moieties are ecliptically oriented along the Si---Si axes. The torsion angle $\theta(\text{C1-Si1---Si2-C4})$ (absolute values) increases from 57.9(1)° for **4a**, to 59.6(2)° for **4b** and to 60.2 (4)° for **4c** and is approximated to the idealised 60° from Cl to I (+syn-clinal). Due to the stronger C–H---X contacts, compared to the other halogens (see below), a deviation of the torsion angle of the chloro derivative occurs. On each Si atom one CH₂X moiety is \pm anti-periplanar twisted from the molecular centre (see $\theta(\text{O-Si-C-X})$ of CH₂X at the C1 and C4 atom in Table 3), whereas the other four moieties are twisted to the molecular centre (see the torsion angles in Table 3). The numbers of interactions in the crystal structures decrease in the order of Cl, Br to I derivative. Especially halogen---H₂C interactions decrease in this order. Halogen bonds (halogen---halogen) and in addition electrostatic attractions of the type CH₂---X, were found in all three structures as main intermolecular structural factor (see Figure 5.1, Table 5.4, Table S1 and Figure S1 in Supporting Information).[26]

Table 5.2. Crystallographic data of the compounds **4a–4c**.

	4a	4b	4c
formula	C ₆ H ₁₂ OSi ₂ Cl ₆	C ₆ H ₁₂ OSi ₂ Br ₆	C ₆ H ₁₂ OSi ₂ I ₆
M _r	369.05	635.80	917.76
T/K	173(2)	173(2)	173(2)
$\lambda/\text{Å}$	0.71073	0.71073	0.71073
crystal system	monoclinic	monoclinic	monoclinic
space group	<i>P2₁/n</i>	<i>P2₁/n</i>	<i>P2₁/n</i>
crystal size/mm	0.58x0.44x0.1	0.25x0.2x0.1	0.09x0.08x0.08
a/Å	9.0995(8)	9.123(5)	9.3207(7)
b/Å	13.9423(13)	14.334(5)	15.2823(12)
c/Å	12.1692(12)	12.666(5)	13.5852(10)
$\beta/^\circ$	98.259(8)	98.030(5)	97.947(7)
V/Å ³	1527.9(2)	1640.1(12)	1916.5(3)
Z	4	4	4
$\rho_{\text{calc.}}/\text{g cm}^{-3}$	1.601	2.575	3.181
μ/mm^{-1}	1.256	14.811	9.832
F(000)	744	1176	1608
2 θ range/°	8.40–50.00	8.64–54.00	8.40–52.00
index ranges	–10 ≤ <i>h</i> ≤ 9 –16 ≤ <i>k</i> ≤ 13 –13 ≤ <i>l</i> ≤ 14	–11 ≤ <i>h</i> ≤ 11 –18 ≤ <i>k</i> ≤ 18 –16 ≤ <i>l</i> ≤ 16	–8 ≤ <i>h</i> ≤ 11 –17 ≤ <i>k</i> ≤ 18 –16 ≤ <i>l</i> ≤ 11
reflections collected	6161	17425	6729
reflection unique	2686 [<i>R</i> _{int} = 0.0248]	3574 [<i>R</i> _{int} = 0.0479]	3739 [<i>R</i> _{int} = 0.0446]
parameters	136	136	136
GooF	1.044	1.031	1.056
<i>R</i> ₁ / <i>wR</i> ₂ [<i>I</i> > 2 σ (<i>I</i>)]	0.0424/0.0855	0.0451/0.0899	0.0552/0.0951
<i>R</i> ₁ / <i>wR</i> ₂ (all data)	0.0332/0.0790	0.0343/0.0846	0.0415/0.0825

V. Hexa-Substituted Disiloxanes

Table 5.3. Bond lengths, angles and selected torsion angles of compounds **4a–c** obtained by X-ray diffraction and calculated data on MP2 level of theory (MP2/6-31G*, respectively for **4c** MP2/3-21G, table is continued on the next page).

Crystal structures							
Bond [Å]	4a (X = Cl)	4b (X = Br)	4c (X = I)	Angles [°]	4a (X = Cl)	4b (X = Br)	4c (X = I)
C1–X1	1.795(3)	1.945(5)	2.140(8)	X1–C1–Si1	110.7(1)	110.2(3)	111.5(4)
C2–X2	1.798(3)	1.945(5)	2.164(8)	X2–C2–Si1	107.6(1)	107.7(3)	109.5(4)
C3–X3	1.800(3)	1.940(5)	2.144(10)	X3–C3–Si1	108.2(1)	108.6(3)	112.3(4)
C4–X4	1.793(3)	1.940(5)	2.147(9)	X4–C4–Si2	109.0(1)	109.3(3)	113.0(5)
C5–X5	1.795(3)	1.958(6)	2.150(9)	X5–C5–Si2	110.0(1)	109.7(3)	111.6(4)
C6–X6	1.806(3)	1.945(5)	2.163(8)	X6–C6–Si2	108.8(1)	108.8(3)	109.9(4)
Si1–C1	1.866(3)	1.873(5)	1.865(8)	C1–Si1–O1	108.9(1)	109.0(2)	109.1(4)
Si1–C2	1.861(3)	1.875(6)	1.882(10)	C2–Si1–O1	108.3(1)	108.3(2)	108.7(4)
Si1–C3	1.857(3)	1.864(5)	1.852(8)	C3–Si1–O1	108.3(1)	108.2(2)	108.0(4)
Si2–C4	1.864(3)	1.876(5)	1.867(9)	C4–Si2–O1	109.5(1)	109.3(2)	108.6(4)
Si2–C5	1.862(3)	1.871(5)	1.860(8)	C5–Si2–O1	108.7(1)	108.4(2)	107.8(4)
Si2–C6	1.859(3)	1.871(6)	1.850(10)	C6–Si2–O1	108.4(1)	107.9(2)	108.6(4)
Si1–O1	1.615 (2)	1.619(4)	1.615(6)	C1–Si1–C2	111.2(1)	111.6(2)	112.0(4)
Si2–O1	1.613(2)	1.618(4)	1.628(6)	C2–Si1–C3	110.3(1)	109.3(2)	108.1(4)
Torsion angles [°]				C3–Si1–C1	109.9(1)	110.3(2)	110.8(4)
X1–C1–Si1–O1	174.3(1)	174.5(2)	175.9(4)	C4–Si2–C5	110.4(1)	110.7(2)	110.9(4)
X2–C2–Si1–O1	–59.7(2)	–60.5(3)	–61.0(5)	C5–Si2–C6	108.4(1)	108.0(2)	108.0(4)
X3–C3–Si1–O1	60.9(2)	58.2(3)	55.4(5)	C6–Si2–C4	111.3(1)	112.4(2)	112.7(4)
X4–C4–Si2–O1	166.9(1)	164.4(2)	163.6(4)	Si1–O–Si2	161.9(1)	163.6 (2)	169.4(4)
X5–C5–Si2–O1	54.1(2)	52.9(3)	55.3(5)				
X6–C6–Si2–O1	–60.6(2)	–62.1(3)	–62.4(5)				
C1–Si1---Si2–C4	–57.9(1)	–59.6(2)	–60.2(4)				
MP2/6-31G* (X = I; MP2/3-21G)							
Bond [Å]	(X = Cl)	(X = Br)	(X = I)	Angles [°]	(X = Cl)	(X = Br)	(X = I)
C1–X1	1.796	1.970	2.214	X1–C1–Si1	109.5	105.7	111.8
C2–X2	1.793	1.968	2.212	X2–C2–Si1	110.4	106.3	112.5
C3–X3	1.799	1.974	2.215	X3–C3–Si1	110.3	106.7	112.2
C4–X4	1.796	1.970	2.214	X4–C4–Si2	109.5	105.7	111.9
C5–X5	1.799	1.974	2.215	X5–C5–Si2	110.3	106.6	112.2
C6–X6	1.793	1.969	2.212	X6–C6–Si2	110.4	106.2	112.5
Si1–C1	1.880	1.873	1.907	C1–Si1–O1	107.2	108.5	108.8
Si1–C2	1.885	1.880	1.910	C2–Si1–O1	109.9	107.6	110.2
Si1–C3	1.891	1.888	1.915	C3–Si1–O1	110.5	109.3	109.8
Si2–C4	1.880	1.873	1.907	C4–Si2–O1	107.2	108.3	108.6
Si2–C5	1.891	1.888	1.915	C5–Si2–O1	110.5	109.1	109.8
Si2–C6	1.885	1.881	1.910	C6–Si2–O1	109.9	107.9	110.4
Si1–O1	1.651	1.645	1.675	C1–Si1–C2	110.9	110.9	111.0
Si2–O1	1.651	1.645	1.674	C2–Si1–C3	108.2	110.5	106.7
Torsion angles θ [°]				C3–Si1–C1	110.1	110.0	110.4
X1–C1–Si1–O1	179.5	179.9	–179.7	C4–Si2–C5	110.9	109.9	110.4
X2–C2–Si1–O1	–58.4	–53.2	–58.7	C5–Si2–C6	108.2	110.9	106.7
X3–C3–Si1–O1	51.2	51.0	53.8	C6–Si2–C4	110.1	110.7	111.0
X4–C4–Si2–O1	179.6	180.0	–179.7	Si1–O1–Si2	151.1	154.1	167.8
X5–C5–Si2–O1	51.3	49.4	53.2				
X6–C6–Si2–O1	–58.3	–51.4	–58.5				
C1–Si1---Si2–C4	–93.3	–95.0	–91.4				

The CH₂X moieties (X = Cl, Br, I) at C3 and C5 are +syn-clinal faced to the central oxygen atom (see $\theta(\text{O-Si-C3/5-X3/5})$ in Table 5.3). They show a smaller torsion angle (absolute value) than the moieties of CH₂X with C2 and C6 showing intramolecular interactions, which as well are twisted from the opposite direction -syn-clinal to the central oxygen (see $\theta(\text{O-Si-C3/5-X2/6})$ in Table 5.3). Twenty C-H...Cl contacts ($\Sigma\text{vdW}(\text{Cl,H})$ and $\Sigma\text{vdW}(\text{Cl,C})$ radii: 2.95 Å and 3.45 Å; 2.823(2) Å to 3.015(1) Å)[27] and four Cl—Cl halogen bonds to ten adjacent molecules were found for one molecule in the crystal structure of **4a**. In the case of **4b**, twentysix C-H...Br contacts ($\Sigma\text{vdW}(\text{Br,H})$ and $\Sigma\text{vdW}(\text{Br,C})$ radii: 3.05 Å and 3.55 Å; 2.893(2) Å to 3.194(1) Å)[27] and six Br...Br halogen bond to eleven adjacent molecules were observed. Each molecule in the crystal structure of **4c** has sixteen I...H-C contacts ($\Sigma\text{vdW}(\text{I,H})$ and $\Sigma\text{vdW}(\text{I,C})$ radii: 3.18 Å and 3.68 Å; 3.106(1) Å to 3.334(1) Å)[27] and ten I...I halogen bonds to eleven adjacent molecules (see Table 4). The halogen bonds are often strongly influenced and disordered by additional C-H...X interactions to one hydrogen atom at the CH₂ moiety, attached to the donor halogen atom (see Table 4). Especially the halogen bonds at I5 in the structure of **4c** are strongly disordered by the I5...I4 and C-H5A...I4 interaction. As a consequence, the C-I_A...I_D (A for acceptor and D for donor) angles of the interaction C4-I_A...I5_D (145.0(2)°) and C5-I_A...I6_D (153.0(2)°) are bent to acute angles, which should be in an idealised case near 180°. As expected, chlorine has shorter and, relative to the other halogens, stronger C-H...X contacts (X = Cl, Br, I). Observed halogen bonds in the crystal structures of **4a-c** are weak for chlorine, stronger for iodine and strongest for bromine. In the case of chlorine the positive area of the surface potential is small (σ -hole).[28] Consequently, only a weak electrostatic attraction can be built to the strong negative charge on the surface. Iodine shows a large positive area on the potential surface, but only a weak negative surface potential and as a result, weak electrostatic interactions. For bromine relatively strong negative charges and large positive σ -holes were found for the surface potential and consequently the strongest interactions. In addition, the numbers of C-H...X contacts increase from Cl to Br and decrease to iodine, because of the polarity and the size of the electron donor. Due to the increasing polarisability of the halogen atoms and the increasing sphere of influence, the number of halogen halogen interactions grow from Cl to I.

Theoretical calculations on MP2/6-31G* and B3LYP/cc-pVDZ level of theory were performed with the program Gaussian09 revision C.01.[29] Compound **4c** was calculated on MP2/3-21G and B3LYP/3-21G level of theory. The structures are almost equal for **4d** and **4e** on MP2/6-31G and B3LYP/cc-pVDZ levels of theory (see Table S3 and S4 in Supporting Information). In general, MP2 perturbation theory gives often better results for electron correlation, and consequently for molecular interaction than DFT calculations and therefore only MP2 values were discussed in here.[30] In exceptional cases DFT values will be discussed additionally. The nomenclatures of the atoms are in analogy to those in the crystal structures. In the special case of **4d** and **4e**, the C1 and C4 labels were defined on the orientation of the substituent away from the Si---Si axis and show the smallest torsion angle (see $\theta(\text{C1-Si---Si2-C4})$ in Table 5.3). The calculated bond lengths in gas phase are similar as those found in the solid state. Both structures of compound **4a** are exemplarily shown for **4b** and **4c** in Figure 5.1 (see Figure S1 in Supporting Informations). The bonding situation of the two calculated structures of **4d** and **4e** are resembled to both types of the three halogen structures. The average Si-O bond lengths of the five calculated structures decrease from **4c** > **4d** > **4e** > **4a** > **4b** (1.674 Å > 1.666 Å > 1.662 Å > 1.651 Å > 1.645 Å). Sterical demanding and less electronegative atoms (respectively, less electron withdrawing

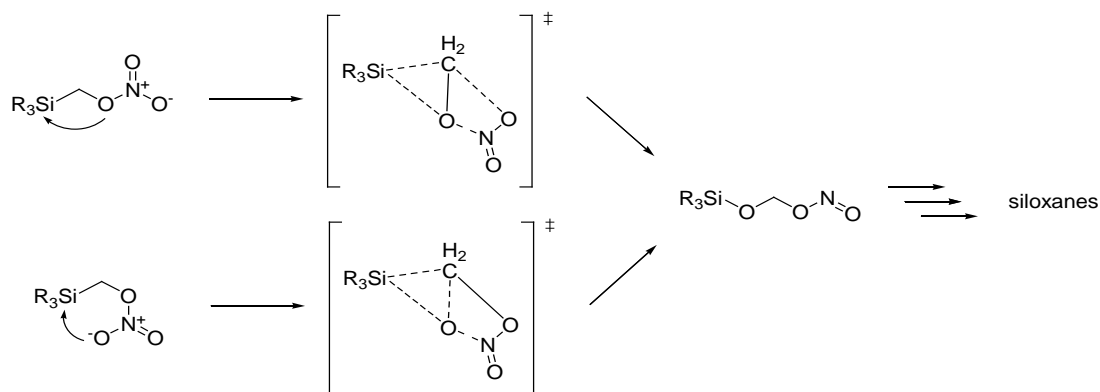
Table 5.4. Distances of donor (D) and acceptor (A) halogen atoms and corresponding angles of halogen halogen bonds in the crystal structures of **4a-c**.

D---A	D---A distance [Å]	C-X _D ---X _A angles [°]	C-X _A ---X _D angles [°]
X = Cl	$\Sigma\text{vdW}(\text{Cl,Cl}) = 3.50 \text{ \AA}[27]$		
Cl1---Cl2 [a]	3.589(2)	77.8(8)	172.9(9)
Cl2---Cl3	3.562(1)	77.2(9)	163.3(9)
X = Br	$\Sigma\text{vdW}(\text{Br,Br}) = 3.70 \text{ \AA}[27]$		
Br1---Br2 [b]	3.622(1)	80.1(1)	174.1(2)
Br2---Br3 [c]	3.666(1)	75.2(2)	161.4(1)
Br5---Br6	3.690(2)	97.5(1)	175.2(2)
X = I	$\Sigma\text{vdW}(\text{I,I}) = 3.96 \text{ \AA}[27]$		
I1---I2	3.865(1)	83.3(2)	172.4(2)
I2---I3 [d]	3.940(1)	76.1(2)	161.0(3)
I5---I4 [e]	4.117(1)	70.9(2)	145.0(2)
I5---I6 [f]	3.860(1)	104.0(2)	170.6(2)
I5---I6' [f]	4.100(1)	80.8(2)	153.0(2)

[a] influenced by C-H1a---Cl2 interaction (2.916(1) Å); [b] influenced by C-H1a---Br2 interaction (3.114(1) Å); [c] influenced by C-H2a---Br3 interaction (3.019(1) Å); [d] influenced by C-H2a---I3 interaction (3.334(1) Å); [e] influenced by C-H5a---I4 interaction (3.191(1) Å); [f] disordered by indirect interactions of the type C-H5a---I4 and I5---I4.

substituents) at the silicon, result in a Si–O bond elongation,[23] but no clear tendency was found in here. It is also in contrast to the situation in the solid state structures. The angles at Si–O–Si were calculated in the cases of **4a** and **4b** with more acute angles than found in the crystal structures, except the well fitting results of **4c** (MP2 calculation/solid state, **4a**: 151.1°/161.9(1)°; **4b**: 154.1°/163.6(2)°; **4c**: 167.8°/169.4(4)°). The calculated values for $\alpha(\text{Si–O–Si})$ of **4d** and **4e** are smaller than these found for the other structures, and consequently in disagreement to the sterical demanding azido and nitrate functions compared to the smaller halogens and their electron repulsion. The calculated structures of the halogenated disiloxanes **4a–c** show bridging oxygens, which are bent out in the opposite direction (Newman projection along Si---Si axes: oxygen between C1 and C4) than found in the crystal structures (Newman projection along Si---Si axes: oxygen between C3 and C5). The reason is based on the anti-parallel conjugation of the H₂C3X and H₂C5X moiety (X2---H₂C4 and X6---H₂C1), which should create electrostatic intramolecular interaction in gas phase. As discussed in the crystallographic part, the large amount of intermolecular interactions, which were not considered for the calculations in gas phase, was shown to be the main and most influencing factor for the differences in the structures. In the three cases of the halogen compounds **4a–c** the orientations of the substituents are rather similar in solid state and in the calculated gas phase structure. In contrast, the orientation of the calculated gas phase structure of the azide and the nitrate ester **4d** and **4e** undergoes highly structural changes compared to the halogen derivatives in both levels of theory. One CH₂X moiety of each silicon atom, which was bent to the oxygen in the halogen structures, is \pm anti-periplanar twisted to an orientation pointing away from the central oxygen (torsion angles of **4d** and **4e** $\theta(\text{O1–Si1–C2–N}_{\alpha}2/\text{O}_{\alpha}3)$ and $\theta(\text{O1–Si–C5–N}_{\alpha}5/\text{O}_{\alpha}6)$ see Figure 5.2). In the case of the calculated structure of **4d**, interactions between CH₂ moieties and nitrogen atoms were found (see Figure 5.2). But more interesting are the electrostatic attractions between the N---N, O---N and N---Si atoms. As also known from pentaerythrityl tetraazide (C(CH₂N₃)₄),[31] two types of N---N interactions are expected to be found in the structure of **4d**, a anti-parallel bidental N_γ---N_β/N_β---N_γ and a perpendicular N_β/N_β contact. Calculations on B3LYP/6-31G* level of theory already suggested N---N interactions, which were developed more precise on MP2/6-31G level of theory. Two different N---N interactions were found between N_α1---N_β3/N_α3---N_β1 and between N_α5---N_β4/ N_γ4---N_β5. This N_α---N_β/N_γ---N_α of the 4 and 5 azido moiety interactions are similar to the anti-parallel

N_γ --- N_β / N_β --- N_γ interactions already known from pentaerythryl tetraazide.[31] The interaction between the N1 and N3 azido moiety instead seems to be a mixture between an anti-parallel bidental N_α --- N_β / N_α --- N_β and a perpendicular N_β / N_β contact. The central oxygen atom O1 shows an electrostatic contact to $N_{\beta 6}$. The O1--- $N_{\beta 6}$ attraction is based on



Scheme 5.3. The postulated decomposition mechanisms of Si-PETN calculated by Liu *et al.*[2] on M06/6-311G** level of theory (top) was supported by experimental and further theoretical computations (electron potential and NBO calculations on B3LYP level of theory). Additionally the hitherto not considered decomposition pathway based on theoretical results on MP2/6-31G* and B3LYP/cc-pVDZ level of theory (bottom).

the positive surface potential of the N_β , commonly found by azide moieties and the high electron density at O1. In addition, a $N_{\alpha 2}$ ---Si2 interaction is created, which bends α (Si-O-Si) into its direction, supported by two weak N---H interactions ($N_{\alpha 2}$ ---H5 and $N_{\alpha 2}$ ---H6). Due to the $N_{\alpha 2}$ ---Si2 interaction, the angles between C4-Si-O1/C5/C6 are acute, relative to the corresponding angles at C3-Si2-O1/C1/C2 and the bond length of O1-Si2 is slightly elongated. Experimental structures could easily establish interactions between $N_\gamma 6$ to the CH_2 moieties C1H₂ and C2H₂, additionally to the weak $N_\gamma 6$ ---Si1 attraction, and consequently the angle α (Si-O-Si) becomes more obtuse as calculated in here. Due to the unusual conformation of **4d** and **4e**, intramolecular interactions of the calculated structure of **4e** are similar to those found in the structure of **4d**.

In addition to the O---N attraction and O---Si contacts, several O---H interactions were found in the computed structure of **4e**. The O---N attraction was created between O2 _{α} and N1. An additional O---N contact was built at the bridging oxygen O1 to the electron deficient N6. The main influence for the bending direction of α (Si-O-Si) was found in the O---Si interaction of O3 _{α} and O6 _{γ} to Si2, supported by O---H interactions (O3 _{γ} ---H5/H4 and O6 _{γ} ---

H2). The most significant contact, which was found by calculations on B3LYP level of theory, was built between $O_{4\beta}$ and Si1, which within a distance of 2.146 Å is a very strong interaction (respectively a weak bond, $\Sigma vdW(O,Si)$: 3.62 Å, $d(Si,O)_{crys.}$: 1.61 Å, $d(Si,O)_{calc.}$: 1.77 Å)[23,24,27] and caused a significant elongation of the Si1–O1 bond (followed by a decreased Si2–O1 bond length). In addition, the bond length of the $O_{4\beta}$ –N1 bond is elongated in comparison to all other bonds of this type in this structure. The angles $\alpha(O1-Si1-C1/C2/C3)$ decrease typically as it is known from penta-coordinated silicon atoms. In the case of the computed structure on MP2 level of theory also a short contact between $O_{\beta 4}$ –Si1 with a distance of 3.161 Å ($\Sigma vdW(O,Si)$: 3.62 Å) were found. This result will cause the remarkable high decomposition rate mentioned above in comparison to other known nitratomethyl silanes without such Si---O₂NOR contacts.[4,5] It is expected, that the initial step of the decomposition cascade will begin with a different initial step as was postulated for tetrakis(nitratomethyl)silane.[20,21] A proposal is given in Scheme 3. The decomposition mechanism for Si(CH₂ONO₂)₄ and others begin with an attraction between the Si and an O_α of a ONO₂ moiety, confirming the attraction to a covalent bonding and followed by the cleavage of the Si–C and the O–NO₂ bonds. In 4e the decomposition cascade will start with the reinforcement of the already relatively strong Si---O_γ interaction. It will result in the cleavage of the Si–C and O–NO₂ bond and simultaneously create a CO_γ bond. In total, both decomposition pathways will result in the same decomposition product (siloxanes). The structural difference of the ONO₂ syn or anti-periplanar orientation (see torsion angles $\theta(Si-C-O_{\alpha}-N)$ in Figure 5.2) seems to be the main factor for the initiation of the decomposition pathway. The $\theta(Si-C-O_{\alpha}-N)$ torsion angles of other common nitratomethylsilanes are antiperiplanar in the area of 180° and therefore favouring the already studied mechanism (see Scheme 3 top), in contrast to the case of the syn-periplanar torsion angle $\theta(Si1-C1-O1_{\alpha}-N1)$ of 9°, which probably follows a new mechanism (see Schema 3 bottom). Two additional uncommonly –anti- and –syn-clinal twisted ONO₂ moieties were found at 4e ($\theta(Si2-C4-O4_{\alpha}-N4)$: –94.3°; $\theta(Si2-C6-O6_{\alpha}-N6)$: –57.7°). The distances between the oxygens and Si2 are below $\Sigma vdW(O,Si)$: 3.62 Å[27] with the distances of $O_{4\beta}$ –Si2 (3.467 Å) and $O_{6\gamma}$ –Si2 (2.912 Å). The first one is disordered by a weak $O_{\alpha 5}$ ---N4 interaction with a distance of 3.153 Å ($\Sigma vdW(N,O)$: 3.07 Å)[27]. Deriving from the observed decomposition rates by handling different nitratomethyl silanes, the Si---O_{γ/β} initiation mechanism seems to be faster entering the decomposition cascade, which is in good

V. Hexa-Substituted Disiloxanes

B3LYP/cc-pVDZ

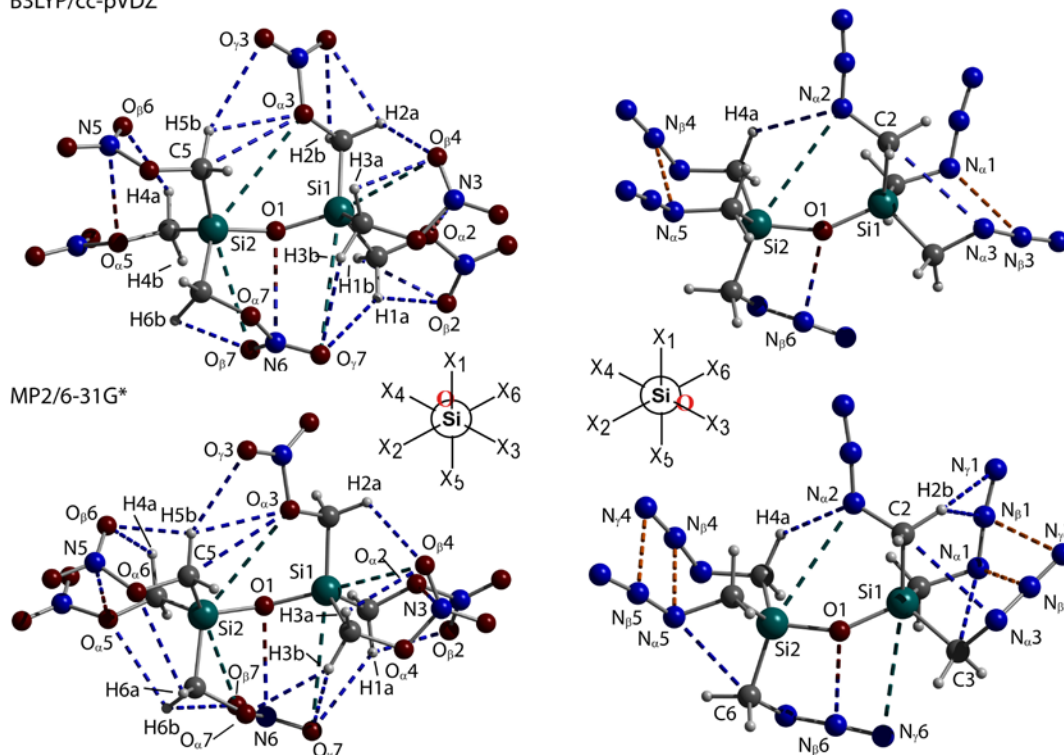
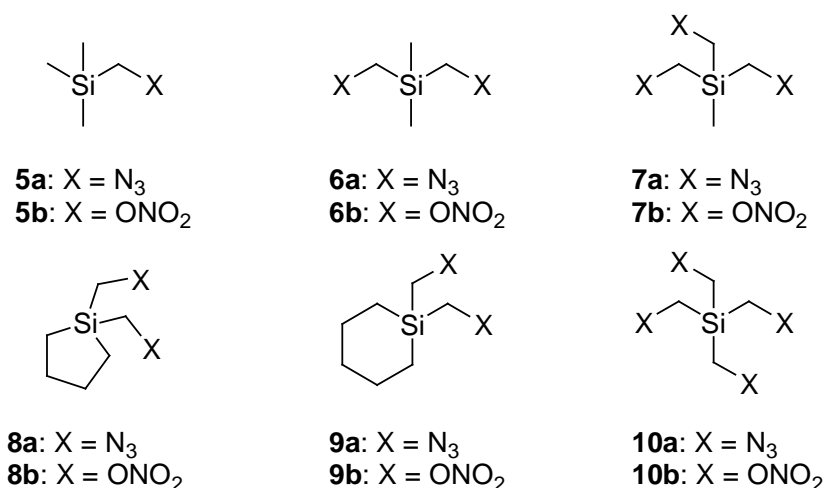


Figure 5.2. The calculated gas phase structures of **4d** (left) and **4e** (right) on the B3LYP/cc-pVDZ (top) and MP2/6-31G* (bottom) level of theory. Bending direction of the bridging oxygen (O) is shown in Newman projections along Si1---Si2 axes. Electrostatic attraction in the computed structures are given in coloured dashed lines: O/N---Si: green; N---N: orange; N---O: blue/red; N/O---H/C: blue (B3LYP/cc-pVDZ: **4d**: $N_{\alpha 2}$ ---Si2: 3.713 Å; $N_{\alpha 1}$ --- $N_{\beta 3}$: 3.341 Å; $N_{\alpha 5}$ --- $N_{\beta 4}$: 3.190 Å; $N_{\alpha 3}$ ---C2: 3.252 Å; $N_{\beta 6}$ ---O1: 3.024 Å; $N_{\alpha 2}$ ---H4a: 2.877 Å; α (Si-O-Si): 149.4 °; Torsion angles: θ (O1-Si1-C1- $N_{\alpha 1}$): -171.9 °; θ (O1-Si1-C2- $N_{\alpha 2}$): -50.6 °; θ (O1-Si1-C3- $N_{\alpha 3}$): -159.6 °; θ (O1-Si2-C4- $N_{\alpha 4}$): 172.0 °; θ (O1-Si2-C5- $N_{\alpha 5}$): -171.1 °; θ (O1-Si2-C6- $N_{\alpha 6}$): -55.5 °. **4e**: $O_{\beta 4}$ ---Si1: 3.153 Å; $O_{\gamma 7}$ ---Si1: 3.795 Å; $O_{\alpha 3}$ ---Si2: 3.721 Å; $O_{\beta 7}$ ---Si2: 3.266 Å; N_6 ---O1: 2.951 Å; $O_{\alpha 2}$ --- N_3 : 3.121 Å; $O_{\alpha 5}$ --- N_5 : 3.124 Å; $O_{\alpha 3}$ ---C5: 3.241 Å; $O_{\alpha 3}$ ---H5b: 2.595 Å; $O_{\beta 2}$ ---H1a: 2.561 Å; $O_{\beta 2}$ ---H1b: 2.564 Å; $O_{\gamma 3}$ ---H5b: 2.7734 Å; $O_{\beta 3}$ ---H2a: 2.563 Å; $O_{\beta 3}$ ---H2b: 2.612 Å; $O_{\beta 4}$ ---H3a: 2.511 Å; $O_{\beta 4}$ ---H2a: 2.482 Å; α (Si-O-Si): 152.4 °; Torsion angles: θ (O1-Si1-C1- $O_{\alpha 2}$): 171.5 °; θ (O1-Si1-C2- $O_{\alpha 3}$): 53.8 °; θ (O1-Si1-C3- $O_{\alpha 4}$): 144.2 °; θ (O1-Si2-C4- $O_{\alpha 5}$): 165.2 °; θ (O1-Si2-C5- $O_{\alpha 6}$): -173.2 °; θ (O1-Si2-C6- $O_{\alpha 7}$): 15.0 °. MP2/6-31G*: **4d**: $N_{\alpha 2}$ ---Si2: 3.517 Å; $N_{\gamma 6}$ ---Si1: 3.519 Å; $N_{\beta 1}$ --- $N_{\gamma 3}$: 3.165 Å; $N_{\alpha 1}$ --- $N_{\beta 3}$: 3.178 Å; $N_{\alpha 5}$ --- $N_{\beta 4}$: 3.091 Å; $N_{\beta 5}$ --- $N_{\gamma 4}$: 3.209 Å; $N_{\alpha 3}$ ---C2: 3.105 Å; $N_{\alpha 1}$ ---C3: 3.245 Å; $N_{\alpha 5}$ ---C6: 3.160 Å; $N_{\beta 6}$ ---O1: 2.837 Å. α (Si-O-Si): 143.2 °; Torsion angles: θ (O1-Si1-C1- $N_{\alpha 1}$): -174.7 °; θ (O1-Si1-C2- $N_{\alpha 2}$): -54.5 °; θ (O1-Si1-C3- $N_{\alpha 3}$): -153.3 °; θ (O1-Si2-C4- $N_{\alpha 4}$): 179.7 °; θ (O1-Si2-C5- $N_{\alpha 5}$): -129.8 °; θ (O1-Si2-C6- $N_{\alpha 6}$): -57.3 °. **4e**: $O_{\beta 4}$ ---Si1: 3.161 Å; $O_{\gamma 7}$ ---Si1: 3.654 Å; $O_{\alpha 3}$ ---Si2: 3.626 Å; $O_{\beta 7}$ ---Si2: 3.073 Å; N_6 ---O1: 2.837 Å; $O_{\alpha 2}$ --- N_3 : 2.776 Å; $O_{\alpha 5}$ --- N_5 : 2.772 Å; $O_{\alpha 3}$ ---C5: 3.125 Å; $O_{\beta 2}$ ---H1a: 2.453 Å; $O_{\alpha 3}$ ---H5b: 2.621 Å; $O_{\beta 4}$ ---H2a: 2.504 Å; $O_{\beta 4}$ ---H3a: 2.423 Å; $O_{\beta 6}$ ---H4a: 2.639 Å; $O_{\beta 6}$ ---H5b: 2.293 Å; $O_{\alpha 6}$ ---H6a: 2.885 Å; $O_{\alpha 5}$ ---H6b: 2.797 Å; $O_{\alpha 7}$ ---H3b: 2.560 Å; $O_{\beta 7}$ ---H1a: 2.424 Å; $O_{\gamma 7}$ ---H3b: 2.757 Å. α (Si-O-Si): 150.0 °; Torsion angles: θ (O1-Si1-C1- $O_{\alpha 2}$): 168.5 °; θ (O1-Si1-C2- $O_{\alpha 3}$): 54.9 °; θ (O1-Si1-C3- $O_{\alpha 4}$): 140.6 °; θ (O1-Si2-C4- $O_{\alpha 5}$): 166.1 °; θ (O1-Si2-C5- $O_{\alpha 6}$): -172.6 °; θ (O1-Si2-C6- $O_{\alpha 7}$): 8.8 °; Σ vdW(N,Si): 3.65 Å; Σ vdW(O,Si): 3.62 Å; Σ vdW(N,N): 3.10 Å; Σ vdW(N,O): 3.07 Å; Σ vdW(N,H): 2.75 Å; Σ vdW(N,C): 3.25 Å; Σ vdW(O,H): 2.72 Å; Σ vdW(O,C): 3.22 Å [27].

agreement with the calculated structural results. The reason for establishing a syn-periplanar torsion angle $\theta(\text{Si}-\text{C}-\text{O}_\alpha-\text{N})$ in general will probably be found in the increased positive surface potential at the silicon atom found on the averted position to the Si-O bond. Electron withdrawing moieties or atoms like O, phenyl etc. will create a stronger positive surface potential respectively σ -hole, and consequently a more attractive electrostatic interacting area for electron rich atoms such as a O_γ of a nitrate moiety.

The melting points of compounds **4a-c** obtained by DSC experiments (onset), increase as expected from ~ 25 °C to 61.6 °C and 124.7 °C. The azide **4d** does not solidify below -25 °C. The decomposition temperatures of **4a-c** are also increasing in the same order (**4a**: 170.1 °C, **4b**: 235 °C, **4c**: 331.0 °C). The azide **4d** decomposes at 143 °C, which is expectively lower than the halogen derivatives, but slightly higher than found for other known azidomethyl silanes (see Table 5).[11]



Scheme 5.4. Labeling of nitrate- and azidomethylsilanes, which were calculated in Table 5 ((nitratomethyl)- and (azidomethyl)trimethylsilane **5a/b**, 1,1-bis(nitratomethyl)- and 1,1-bis (azidomethyl)dimethylsilane **6a/b**, 1,1,1-tris(nitratomethyl)- and 1,1,1-tris(azidomethyl)methylsilane **7a/b**, 1,1-bis(nitratomethyl)- and 1,1-bis(azidomethyl)-1-sila-cyclopentane **8a/b**, 1,1-bis(nitratomethyl)- and 1,1-bis(azidomethyl)-1-sila-cyclohexane **9a/b**).[5,11].

V. Hexa-Substituted Disiloxanes

Table 5.5. Energetic properties of the compounds **4d/e** and **5–10a/b**.

	4d 4e	5a ^[p] 5b ^[p]	6a ^[p] 6b ^[p]	7a ^[p] 7b ^[p]	8a ^[p] 8b ^[p]	9a ^[p] 9b ^[p]	10a ^[q] 10b ^[q]	PETA ^[s] PETN ^[s]
formula	C ₆ H ₁₂ N ₁₈ O ₂ Si ₂ C ₆ H ₁₂ N ₆ O ₁₉ Si ₂	C ₄ H ₁₁ N ₃ Si C ₄ H ₁₁ NO ₃ Si	C ₄ H ₁₀ N ₆ Si C ₄ H ₁₀ N ₂ O ₆ Si	C ₄ H ₉ N ₉ Si C ₄ H ₉ N ₃ O ₉ Si	C ₆ H ₁₂ N ₆ Si C ₆ H ₁₂ N ₂ O ₆ Si	C ₇ H ₁₄ N ₆ Si C ₇ H ₁₄ N ₂ O ₆ Si	C ₄ H ₈ N ₁₂ Si C ₄ H ₈ N ₄ O ₁₂ Si	C ₅ H ₈ N ₁₂ C ₅ H ₈ N ₄ O ₁₂
M _r / g mol ⁻¹	408.45 528.36	129.24 149.22	170.25 210.22	211.26 271.21	196.29 236.25	210.31 250.28	252.27 332.21	236.20 316.14
IS / J [a]	<1 <1 [o]	>40 >1	>9 <0.5 [r]	<1 <0.5 [r]	<40 <0.5 [r]	>40 <0.5 [r]	<1 [o] <1 [o]	>7.5 [t] >3 [u]
FS / N [b]	<5 <5 [o]	>192 >64	>60 <5	<5 <5	>48 <5	>60 >36	<5 [o] <5 [o]	--- ---
N / % [c]	61.73 15.91	32.51 9.39	49.36 13.33	59.67 15.49	42.82 11.86	39.96 11.19	66.63 16.86	71.16 17.72
Ω _{CO2} / % [d]	-82.26 -9.08	-191.89 -134.02	-140.97 -68.50	-109.81 -32.45	-163.02 -94.81	-174.97 -108.67	-82.57 -9.11	-94.83 -10.12
T _{dec} / °C [e]	143 ---	129 (b.p.) 85	137 107	137 107	130 97	134 96	---	46 (m.p.) [t] 160 [t]
ρ / g·cm ³	---	---	---	---	---	---	---	1.44 [t] 1.78
Δ _r H ^o _M / kJ·kg ⁻¹ [f,g]	2946.1 -2361.2	-98.9 -2871.5	2133.8 -2225.2	3524.2 -1834.4	2097.6 -1824.7	1777.6 -1901.4	4508.8 -1626.8	4790 [t] -1705.0 [v]
Δ _r U ^o / kJ kg ⁻¹ [g,h]	3040.2 -2274.4	35.3 -2746.9	2250.3 -2119.1	3629.8 -1738.4	2211.2 -1796.1	1895.5 -1792.5	4607.1 -1537.2	4895.0 -1610.9
EXPLO6.01 values: ^[i]								
-Δ _{ex} U ^o / kJ·kg ⁻¹ [i]	5182 6621	3211 5548	4408 6325 (6468)	5230 6301 (6677)	4226 4899	3926 4699(4773)	5810 7010	5248 (5295) 5859(5964)
T _{det} / K[k]	3618 4850	1869 2829	2646 3818 (3814)	3284 4358 (4305)	2488 3224	2300 3015 (3005)	3843 5037	3415 (3355) 4337 (3968)
p _{cj} / kbar[l]	120.6 132.6	99.9 124.4	111.9 131.1 (154.6)	125.5 152.9 (231.2)	106.5 112.4	106.0 109.0 (133.2)	136.5 146.5	152.0 (190.2) 161.7 (320.7)
V _{det} / m·s ⁻¹ [m]	6041 6173	6163 6449	5907 6105 (6477)	6202 6504 (7371)	5823 5847	5856 5804 (6249)	6455 6471	6915 (7518) 6851 (8494)
V ₀ / L·kg ⁻¹ [n]	686.9 681.9	632.8 678.8	651.2 711.1 (685.1)	688.7 773.5 (691.9)	619.2 703.9	620.0 701.7 (681.6)	712.9 721.3	802.7 (784.2) 824.0 (746.4)

[a] impact sensitivity (according to BAM); [b] friction sensitivity (according to BAM); [c] nitrogen content; [d] oxygen balance calculated for CO₂; [e] decomposition temperature from DSC; [f] calculated heat of formation (CBS-4M); [g] for all compound calculated as liquids and by using the T_{dec} points, except: **5a** b.p. at 129 °C, **4e** with T_{dec} = 25 °C, and **10b** as solid with T_{dec} = 25 °C for T_M were used; [h] energy of formation; [i] all values were computed with a density of ρ = 1.3 g/cm³; values in parentheses were calculated with known density values obtained by x-ray diffraction; [j] energy of explosion; [k] detonation temperature; [l] detonation pressure at the Chapman-Jouguet point; [m] detonation velocity; [n] assuming volume of gaseous products; [o] expected values; [p] refs. [5,11]; [q] ref. [4]; [r]) value of <0.5 J was measured by an more precise setup and it does not mean that this compounds are more sensitive than other compounds measured with the standard setup and a value of <1 J; [s] PETA = pentaerythryl tetraazide, PETN = pentaerythryl tetranitrate; [t] ref. [35]; [u] ref. [1]; [v] ref. [36]

The impact and friction sensitivities of the azide **4d** were performed by a drop hammer and a friction apparatus by the method 'one out of six' according to BAM.[32] The impact and friction sensitivity is <1 J, respectively <5 N. Therefore both values are below the measuring range of the setups. The azide **4d** detonates immediately in the flame. For a comparison, the energetic and physical characteristics and properties of the compounds **5-9a/b** are extensively discussed elsewhere (formula given in Scheme 4); the properties of the tetrasubstituted silanes **10a/b** could not be determined, because of the extreme sensitivity and for safety reasons.[4,5,11] The sensitivity of **4d** seems to be less than for **10a**, because **4d** does not explode upon contact with an metal spatula as described.[4] Even the freshly extracted decomposition products of the failed synthesis of hexakis(nitratomethyl)disiloxane (**4e**) decompose violently in the flame. After storing the compound a few hours on air the decomposition products do not deflagrate or burn anymore in the flame. Due to their fast decomposition it is hard to obtain reliable sensitivity values. Therefore sensitivity tests of the decomposition products of the reaction leading to **4e** were not performed. As it is known, the nitrate derivatives are more sensitive than the corresponding azides.[5,11] Consequently it is expected that the nitrate **4e** and even its decomposition products will be more sensitive than the azide **4d**. The decomposition temperature of **4d** was measured in the region of other known azidomethyl silanes;[11] T_{dec} could not be determined from **4e** or its decomposition products, because of fast decomposition.

$$\Delta_f H_M^\circ(g) = H_M^\circ(g) - \sum H_{atoms}^\circ + \sum \Delta_f H_{atoms}^\circ \quad (1)$$

$$\Delta U_M = \Delta H_M - \Delta nRT \quad (2)$$

Δn = changes of moles of gaseous components

The energetic parameters of **4d**, **4e** and other related compounds (see Scheme 4), shown in Table 5, were calculated by the latest and intensively revised EXPL05 version 6.01 computer code.[33] The input values such as the energies of formation ($\text{kJ}\cdot\text{kg}^{-1}$) were calculated from the computed heat of formation. The heat of formation was calculated on the CBS-4M level of theory and the atomization method (Equation (1)) by using the program Gaussian09 revision C.01. The enthalpy of formation in the gas phase $\Delta H_m(g)$ was converted to the solid state enthalpy of formation $\Delta H_m(s)$ by using the Trouton's rule.[34]

The molar standard enthalpy of formation (ΔH_m) was used to compute the molar solid state energy of formation (ΔU_m) according to Equation (2).

Conclusion

Several new cost efficient and less laborious synthetic routes to obtain hexakis(halogenomethyl)disiloxanes with high yields were discovered. Hexakis(azidomethyl)disiloxane was synthesized the first time. In contrast hexakis(nitratomethyl)disiloxane, which is reported to be known since half a century, was not feasible. Supported by calculations on B3LYP and MP2 levels of theories, a decomposition mechanism for this nitrate was proposed. Theoretical calculations and crystal structures of the halogeno derivatives were compared and were used to discuss and interpret the possible structures of the hexakis(azidomethyl)- and the hexakis(nitratomethyl)disiloxanes. The heat of formation was calculated on CBS-4M level of theory for the azido and nitrate derivatives. As a consequence from this result, characteristic values for high energetic materials were calculated by the EXPLO5 6.01 computer code. The obtained values were compared with other already known azido- and nitratomethyl silanes. The comparison of the carbon analogues PETA and PETN, which were used as bench marks, with the sila derivatives, show the inferiority of the sila towards the carbon derivatives not only in the case of safe use, but also in the energetic parameters.

Experimental Section

Caution! Azides and nitrate esters are sensitive and represent energetic materials; therefore they must be handled with extreme care! During the work with azido- and nitrate silanes, wearing leather jacket, face shield, steel-reinforced Kevlar gloves, ear protection, and electrically grounded shoes is mandatory. Only electrically grounded and metal-free equipment was used during the syntheses.

Acetonitrile, DMA, n-pentane, n-heptane (Aldrich), sodium azide (ACROS ORGANICS), silver nitrate (VWR), were used as received. Silicon tetrachloride and trichlorophenylsilane (ABCR) were freshly distilled under argon atmosphere before using. The ^1H , $^{13}\text{C}\{^1\text{H}\}$, $^{14}\text{N}/^{15}\text{N}$, and $^{29}\text{Si}\{^1\text{H}\}$ NMR spectra were recorded in CDCl_3 at 25 °C using a Jeol 400 Eclipse FT-NMR spectrometer operating at 400.2 MHz (^1H), 100.6 MHz (^{13}C), 79.5 MHz (^{29}Si), 40.6 MHz (^{15}N), and 28.9 MHz (^{14}N). Chemical shifts (ppm) are given with respect to TMS

(^1H , ^{13}C , ^{29}Si) and MeNO_2 (^{14}N and ^{15}N). Infrared (IR) spectra were recorded on a Perkin-Elmer Spectrum BXII FT-IR instrument equipped with a Diamant-ATR Dura Sampler at 25 °C. Raman spectra were recorded on a Bruker RAMII Raman instrument ($\lambda = 1064$ nm, 200 mW, 25 °C) equipped with D418-T Detector at 200 mW at 25 °C. Melting, boiling and decomposition points (T_{onset}) were determined by differential scanning calorimetry (DSC; Perkin-Elmer Pyris 6 DSC, calibrated by standard pure indium and zinc). Measurements were performed at a heating rate of $\beta = 5$ °C in closed aluminum containers with a hole (1 μm) on the top for gas release with a nitrogen flow of 5 mL/min. The reference sample was a closed aluminum container with air. Friction and impact sensitivity experiments were performed with a friction device and a drophammer setup according to BAM standards (Bundesanstalt für Materialforschung und -prüfung). Elemental analyses of the azidomethyl and nitratomethyl compounds were not performed because of their explosive properties and the risk to damage the analyzer. Mass spectrometric data were obtained from a Jeol MStation JMS 700 spectrometer. Elemental analysis and mass spectrometry of the highly explosive and very sensitive compounds **4d** and **4e** were not performed, because of its high explosive character and to avoid potential damage to the analyzer. An Oxford Xcalibur diffractometer with a CCD area detector was employed for data collection using Mo- K_{α} radiation. The structure was solved using direct methods (SHELXS [37]) and refined by full matrix least-squares on F^2 (SHELXL [37]). All non-hydrogen atoms were refined anisotropically (Table 2). ORTEP plots are shown with thermal ellipsoids at the 50 % probability level. Crystallographic data for the structure have been deposited with the Cambridge Crystallographic Data Centre under the depository numbers CCDC-926549 – 926551 (**4a-4c**). Copies of the data can be obtained free of charge on application to The Director, CCDC, 12 Union Road, Cambridge CB2 1EZ, UK (Fax: int. code + (1223)336-033; e-mail for inquiry: fileserv@ccdc.cam.ac.uk; e-mail for deposition: deposit@ccdc.cam.ac.uk).

Tris(chloromethyl)phenylsilane (1): Tris(chloromethyl)phenylsilane was synthesized according ref. [16].

^1H NMR (CDCl_3): $\delta = 7.73$ (m, 2H, 2,6-CH), 7.55-7.48 (m, 3H, 4-CH and 3,5-CH), 3.30 (s, 6 H, CH_2Cl) ppm. $^{13}\text{C}\{^1\text{H}\}$ NMR (CDCl_3): $\delta = 134.8$ (s, 2,6-C), 134.2 (s, 1-C), 131.4 (s, 4-C), 128.6 (s, 3,5-C), 24.5 (s, $^1J_{\text{C,Si}} = 59.3$ Hz, CH_2Cl) ppm. $^{29}\text{Si}\{^1\text{H}\}$ NMR (CDCl_3): $\delta = -8.1$ (s) ppm.

Tris(chloromethyl)methoxysilane (2): Trifluoromethanesulfonic acid (0.65 g, 4.34 mmol, 1.1 eq) was added dropwise within 10 min to a solution of tris(chloromethyl)phenylsilane (1.00 g, 3.94 mmol, 1.0 eq) in *n*-pentane (5 mL) under inert atmosphere (argon). The mixture was heated under reflux for 2 h and afterwards cooled to 0 °C. A solution of triethylamine (0.40 g, 3.94 mmol, 1.0 eq) and methanol (0.14 g, 4.34 mmol, 1.1 eq) was added dropwise. The resulting solution was stirred for another 3 h. After the solvent had been removed under reduced pressure, the raw product was purified using a *Kugelrohr* distillery (90 °C, $6 \cdot 10^{-2}$ mbar). The product was obtained as a colourless liquid in 52 % yield (0.43 g).

^1H NMR (CDCl_3): δ = 3.67 (s, 3 H, OMe), 3.07 (s, 6 H, CH_2Cl) ppm. $^{13}\text{C}\{^1\text{H}\}$ NMR (CDCl_3): δ = 52.9 (s, OMe), 24.1 (s, $^1J_{\text{C,Si}}$ = 70.6 Hz, CH_2Cl) ppm. $^{29}\text{Si}\{^1\text{H}\}$ NMR (CDCl_3): δ = -4.3 (s) ppm.

Chloroethyltri(chloromethyl)silane (3): Chloroethyltri(chloromethyl)-silane was synthesized according to ref. [18].

^1H NMR (CDCl_3): δ = 3.79 (t, $^3J_{\text{H,H}}$ = 7.8 Hz, 2 H, CH_2Cl), 3.08 (s, $^3J_{\text{H,Si}}$ = 3.9 Hz, 6 H, SiCH_2Cl), 1.61 (t, $^3J_{\text{H,H}}$ = 7.8 Hz, 2 H, SiCH_2) ppm. $^{13}\text{C}\{^1\text{H}\}$ NMR (CDCl_3): δ = 41.1 (s, CH_2Cl), 24.6 (s, $^1J_{\text{C,Si}}$ = 58.1 Hz, 3 C, SiCH_2Cl), 15.0 (s, $^1J_{\text{C,Si}}$ = 54.6 Hz, SiCH_2) ppm. $^{29}\text{Si}\{^1\text{H}\}$ NMR (CDCl_3): δ = 0.1 (s) ppm.

Hexakis(chloromethyl)disiloxane (4a): Method A: **2** (400 mg, 1.92 mmol) was mixed with distilled water, a catalytic amount (one drop) of conc. sulfuric acid and stirred for 3 h. The raw product was extracted three times with diethyl ether (20 mL). After the solvent had been removed *in vacuo* ($6 \cdot 10^{-2}$ mbar), the product was obtained in quantitative yield (350 mg) as colourless solid.

Method B: Trifluoromethanesulfonic acid (980 mg, 6.5 mmol, 0.58 mL, 1.1 eq) was added dropwise within 10 min to a solution of **1** (1.50 g, 5.91 mmol, 1.0 eq) in *n*-pentane (25 mL). The mixture was heated under reflux for 2 h and afterwards cooled to 0 °C. A solution of triethylamine (660 mg, 6.5 mmol, 1.1 eq) and methanol (210 mg, 6.5 mmol, 0.26 mL, 1.1 eq) was added dropwise. The resulting solution was stirred for another 3 h and extracted five times with *n*-pentane (30 mL). The combined organic phases were concentrated by a rotary evaporator, mixed with 1 N sulfuric acid (3 mL) and stirred for 24 h. The mixture was diluted with 100 mL diethyl ether. The ether phase was washed with a saturated aqueous

solution of sodium bicarbonate (2x 30 mL) and with water (30 mL). The aqueous solution was stirred again with diethyl ether (50 mL). The organic phases were combined, diethyl ether was distilled off and the raw product was *Kugelrohr* distilled *in vacuo* ($6 \cdot 10^{-2}$ mbar, 125 °C). The product was obtained as colourless solid in a total yield of 68 % (740 mg, calculated to **1**).

Method C: **3** (1.00 g, 4.17 mmol, 1 eq) was stirred for one hour with sodium hydroxide (0.17 g, 4.17 mmol, 1 eq) and methanol (20 mL). The crude mixture was dried *in vacuo* ($6 \cdot 10^{-2}$ mbar). The residue was diluted with diethyl ether (50 mL) and washed twice with water (20 mL). The ether was distilled off and the raw product was *Kugelrohr* distilled ($6 \cdot 10^{-2}$ mbar, 125 °C) to obtain pure colourless solid in 65 % yield (500 mg).

^1H NMR (CDCl_3): $\delta = 3.08$ (s, CH_2Cl) ppm. $^{13}\text{C}\{^1\text{H}\}$ NMR (CDCl_3): $\delta = 24.9$ (s, $^1J_{\text{C,Si}} = 72.0$ Hz, CH_2Cl) ppm. $^{29}\text{Si}\{^1\text{H}\}$ NMR (CDCl_3): $\delta = -10.6$ (s) ppm. IR: $\tilde{\nu} = 2933, 1720, 1675, 1461, 1390, 1290, 1186, 1095, 811, 797, 728, 707, 660$ cm^{-1} . Raman: $\tilde{\nu} = 2986, 2937, 1393, 1198, 1088, 789, 731, 638$ cm^{-1} .

Hexakis(bromomethyl)disiloxane (4b): **4a** (400 mg, 1.08 mmol, 1.0 eq) was stirred with lithium bromide (0.75 g, 8.67 mmol, 8.0 eq) and 18-crown-6 (3 mg, 0.01 mmol, 1 mol%) in *n*-heptane (15 mL) for 24 h at 85 °C. The solvent was evaporated off and the colourless residue was washed twice with water (10 mL). The aqueous phase was removed and the residue was dried *in vacuo* ($2 \cdot 10^{-2}$ mbar, 60 °C). The residue was quickly washed with *n*-pentane (2 mL). The product was obtained as colourless crystals in 92 % yield (630 mg).

^1H NMR (CDCl_3): $\delta = 2.79$ (s, $^2J_{\text{H,Si}} = 3.3$ Hz, CH_2Br) ppm. $^{13}\text{C}\{^1\text{H}\}$ NMR (CDCl_3): $\delta = 11.0$ (s, $^1J_{\text{C,Si}} = 72.7$ Hz, CH_2Br) ppm. $^{29}\text{Si}\{^1\text{H}\}$ NMR (CDCl_3): $\delta = -11.8$ (s) ppm. IR: $\tilde{\nu} = 2999, 2940, 2857, 1466, 1385, 1367, 1154, 1129, 1103, 1050, 794, 761, 728, 654$ cm^{-1} . Raman: $\tilde{\nu} = 2999, 2942, 2874, 1380, 1142, 1054, 764, 712, 684, 651, 611, 577, 554, 509$ cm^{-1} . MS(DCI+): $m/z = 556.8$ $[\text{M}-\text{Br}]^+$; MS(DEP/EI+): $m/z = 542.33$ $[\text{M}-\text{CH}_2\text{Br}]^+$.

Hexakis(iodomethyl)disiloxane (4c): **4a** (400 mg, 1.08 mmol, 1.0 eq) was stirred with sodium iodide (0.75 g, 8.67 mmol, 8.0 eq) in acetone (15 mL) for 16 h at 65 °C. The solvent was evaporated and the colourless residue was diluted with diethyl ether (800 mL) and washed with water (3x200 mL). The water phase was extracted with diethyl ether (200 mL). The solvent of the combined organic phases was evaporated *in vacuo*. The

residue was recrystallized by diluting the raw product with hot THF (10 mL), cooled down to ambient temperature and acetonitrile (20 mL) added. The product was obtained as colourless crystals in 92 % yield (910 mg).

^1H NMR (CDCl_3): $\delta = 2.45$ (s, CH_2I) ppm. $^{13}\text{C}\{^1\text{H}\}$ NMR (CDCl_3): $\delta = -19.3$ (s, $^1J_{\text{C,Si}} = 67.5$ Hz, CH_2I) ppm. $^{29}\text{Si}\{^1\text{H}\}$ NMR (CDCl_3): $\delta = -7.6$ (s) ppm. IR: $\tilde{\nu} = 2981, 2926, 2361, 2089, 1463, 1355, 1260, 1120, 1082, 1069, 1011, 1007, 1002, 990, 783, 772, 739, 703, 668$ cm^{-1} . Raman: $\tilde{\nu} = 2989, 2929, 1363, 1091, 743, 693, 660, 567, 549, 527$ cm^{-1} . MS(EI+): $m/z = 917.3[\text{M}]^+, 790.3[\text{M}-\text{I}]^+$.

Hexakis(azidomethyl)disiloxane (4d): Method A: **4a** (100 mg, 0.27 mmol, 1.0 eq) was stirred with sodium azide (1.0 g, 15.4 mmol, 57.0 eq) in acetone (15 mL) for 24 h. The mixture was concentrated by gently evaporating off the acetone. The almost (!) dry suspension was diluted with diethyl ether (20 mL), was washed twice with water (10 mL), and dried with anhydrous sodium sulfate. The solvent was removed by allowing the solution to maintain overnight without heating, no stirring and no reduced pressure (!). The highly explosive impure compound **4d** was obtained in 92% yield (100 mg) as colourless oil.

Method B: **4b** (100 mg, 0.16 mmol, 1.0 eq) was dissolved in acetonitrile (5 ml) and powdered silver azide (150 mg, 1.00 mmol, 6.3 eq) was added at once and the reaction mixture stirred under light exclusion for 12 h. The product was extracted with *n*-pentane and decanted from the slurry residue. The pentane was evaporated by storing the solution in an open plastic beaker at ambient temperature. The impure colourless product **4d** was obtained in 96 % (65 mg) yield. The slurry (AgBr, AgN₃ residues) was decomposed adding water, sodium nitrite and dropping slowly conc. hydrochloric acid into the water phase.

Method C: **4c** (150 mg, 0.16 mmol, 1.0 eq) was dissolved in acetone (5 ml) and powdered silver azide (245 mg, 1.63 mmol, 10.0 eq) was added at once and the reaction mixture stirred under light exclusion for 14 days. The product was extracted with *n*-pentane and decanted from the slurry residue. The pentane was evaporated by storing the solution in an open plastic beaker at ambient temperature. The colourless pure product **4d** was obtained in 97 % (65 mg) yield. The slurry (AgBr, AgN₃ residues) was decomposed adding water, sodium nitrite and dropping slowly conc. hydrochloric acid into the water phase.

^1H NMR (CDCl_3): $\delta = 3.08$ (s, CH_2N_3) ppm. $^{13}\text{C}\{^1\text{H}\}$ NMR (CDCl_3): $\delta = 37.7$ (s, $^1J_{\text{C,Si}} = 68.0$ Hz, CH_2N_3) ppm. $^{14}\text{N}\{^1\text{H}\}$ NMR (CDCl_3): $\delta = -132$ (s, N_β), -170 (s, N_γ), -326 (s, N_α) ppm. ^{15}N NMR (CDCl_3): $\delta = -131.9$ (s, N_β), -170.8 (s, N_γ), -324.1 (s, N_α) ppm. $^{29}\text{Si}\{^1\text{H}\}$ NMR (CDCl_3): $\delta = -5.8$ (s) ppm. IR: $\tilde{\nu} = 2940, 2891, 2086, 1403, 1282, 1237, 1184, 1070, 910, 800$ cm^{-1} . Raman: $\tilde{\nu} = 2938, 2896, 2103, 1409, 1371, 1289, 1235, 1180, 900, 632$ cm^{-1} .

Acknowledgements

Financial support of this work by the Ludwig-Maximilian University of Munich (LMU), the U.S. Army Research Laboratory (ARL) under grant no. W911NF-09-2-0018, the Armament Research, Development and Engineering Center (ARDEC) under grant no. W911NF-12-1-0467, and the Office of Naval Research (ONR) under grant nos. ONR.N00014-10-1-0535 and ONR.N00014-12-1-0538 is gratefully acknowledged. The authors acknowledge collaborations with Dr. Mila Krupka (OZM Research, Czech Republic) in the development of new testing and evaluation methods for energetic materials. We are indebted to and thank Drs. Betsy M. Rice and Brad Forch (ARL, Aberdeen, Proving Ground, MD) for many inspired discussions. Thanks to Stefan Huber for measuring the sensitivity parameters.

-
- [1] R. Meyer, J. Köhler, A. Homburg in *Explosives*, Wiley-VCH, Weinheim, **1996**, 5th Ed..
- [2] Barcza, S., U.S. Patent 3,592,831, **1968**.
- [3] Barcza S., U.S. Patent 3,585,228, **1971**.
- [4] T. M. Klapötke, B. Krumm, R. Ilg, D. Troegel, R. Tacke, *J. Am. Chem. Soc.* **2007**, *129*, 6908-6915.
- [5] C. Evangelisti, T. M. Klapötke, B. Krumm, A. Nieder, R. J. F. Berger, S. A. Hayes, N. W. Mitzel, D. Troegel, R. Tacke, *Inorg. Chem.* **2010**, *49*, 4865–4880.
- [6] a) M. Kurono, R. Unno, Y. Matsumoto, Y. Kondo, T. Mitani, T. Jomori, H. Michishita, K. Sawai Eur. Patent 0288002, **1988**; b) R. D. Haugwitz, W. K. Anderson, J. Plowman, R. Kaslinal, D. M. Houston, V. L. Narayanan, *Appl. Organomet. Chem.* **1990**, *4*, 375–378; c) W. K. Anderson, R. Kasliwal, D. M. Houston, Y.-s. Wang, V. L. Narayana, R. D. Haugwitz, J. Plowman, *J. Med. Chem.* **1995**, *38*, 3789–3797.
- [7] T. Lummerstorfer, H. Hoffmann, *J. Phys. Chem. B* **2004**, *108*, 3963–3966.

- [8] O. Tsuge, S. Kanemasa, K. Matsuda, *Chem. Lett.* **1983**, 1131–1134.
- [9] K. Nishiyama, N. Tanaka, *J. Chem. Soc., Chem. Commun.* **1983**, 1322–1323.
- [10] V. Van Dorselaer, D. Schirlin, P. Marchal, F. Weber, C. Danzin, *Bioorg. Chem.* **1996**, *24*, 178–193.
- [11] T. M. Klapötke, B. Krumm, A. Nieder, O. Richter, D. Troegel, R. Tacke, *Z. Allg. Anorg. Chem.* **2012**, *638*, 1075–1079.
- [12] A. Y. Yakubovich, V. A. Ginsburg, *Z. Obs. Chim.* **1952**, *22*, 1783–1787.
- [13] A. Y. Yakubovich, S. P. Makarov, V. A. Ginsburg, *Dokl. Akad. Nauk. SSSR* **1950**, *172*, 69–72.
- [14] J. Z. Su, *Recent Advances in Fire Suppression Technologies: New Chemical Agents* **1999**, NRC Publication Archive, p. 8. (online: <http://www.nrc-cnrc.gc.ca/obj/irc/doc/pubs/ir/ir812/ir812.pdf>)
- [15] International Programme on Chemical Safety (IPCS), MSDS Diazomethane, state of the 4th December 2012: <http://www.inchem.org/documents/icsc/icsc/eics1256.htm>.
- [16] J. O. Daiss, K. A. Barth, C. Burschka, P. Hey, R. Ilg, K. Klemm, I. Richter, St. A. Wagner, R. Tacke, *Organometallics* **2004**, *23*, 5193–5197.
- [17] T. Weidner, N. Ballav, U. Siemeling, D. Troegel, T. Walter, R. Tacke, D. G. Castner, M. Zharnikov, *J. Phys. Chem. C* **2009**, *113*, 19609–19617.
- [18] A. R. Bassindale, P. G. Taylor in *The Chemistry of Organic Silicon Compounds* (Eds.: S. Patai, Z. Rappoport), Wiley & Sons Ltd, Chichester, **1989**, Vol. 2, part 2, pp. 898ff.
- [19] M. G. Voronkov, S. V. Kirpichenko, V. V. Keiko, V. A. Pestunovich, E. O. Tsetlina, V. Khvalovskii, Y. Vchelak, *Russ. Chem. Bull.* **1975**, *24*, 1932–1934.
- [20] W.-G. Liu, S. V. Zybin, S. Dasgupta, T. M. Klapötke, W. A. Goddard III, *J. Am. Soc. Chem.* **2009**, *131*, 7490–7493.
- [21] J. S. Murray, P. Lane, A. Nieder, T. M. Klapötke, P. Politzer, *Theor. Chem. Acc.* **2010**, *127*, 345–354.
- [22] E. A. Williams in *The Chemistry of Organic Silicon Compounds* (Eds.: S. Patai, Z. Rappoport), Wiley & Sons Ltd, Chichester, **1989**, Vol. 2, part 1, pp. 547–549.

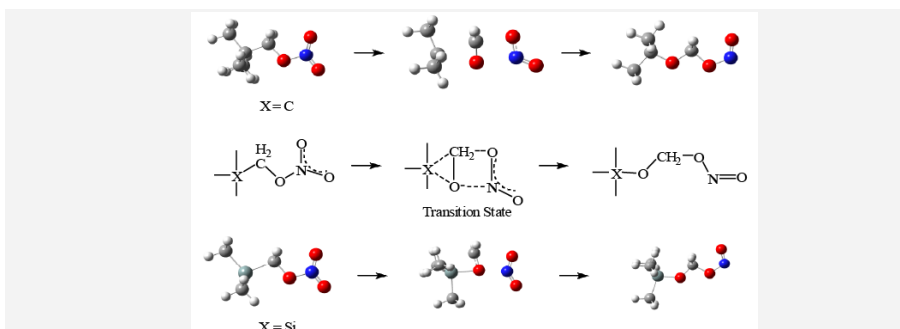
- [23] M. A. Brook in *Silicon in Organic, Organometallic, and Polymer Chemistry*, Wiley & Sons, Inc., New York, **1999**, pp. 29f.
- [24] E. A. Williams in *The Chemistry of Organic Silicon Compounds* (Eds.: S. Patai, Z. Rappoport), Wiley & Sons Ltd, Chichester, **1989**, part 1, p. 242.
- [25] M. A. Brook in *Silicon in Organic, Organometallic, and Polymer Chemistry*, Wiley & Sons, Inc. New York, **1999**, pp. 33f.
- [26] P. Politzer, P. Lane, M. C. Concha, Y. Ma, J. S. Murray, *J. Mol. Model.* **2007**, *13*, 305–311.
- [27] A. Bondi, *J. Phys. Chem.* **1964**, *68*, 441–451.
- [28] T. Clark, M. Hennemann, J. S. Murray, P. Politzer, *J. Mol. Model* **2007**, *13*, 291–296.
- [29] M. J. Frisch *et al.*, *GAUSSIAN 09 (Revision C.01)*, Gaussian Inc., Wallingford CT, **2010**.
- [30] I. N. Levine in *Quantum Chemistry*, Prentice-Hall of India, New Dehli, **2006**, pp. 563f.
- [31] K. A. Lyssenko, Y. V. Nelubina, D. V. Safronov, O. I. Haustova, R. G. Kostyanovsky, D. A. Lenev, M. Y. Antipin, *Mendeleev Comm.* **2005**, *15*, 232–234.
- [32] www.bam.de (German version), www.bam.de/en/index.htm (English version).
- [33] M. Suceška, *EXPL05 program vers. 6.01*, Zagreb, Croatia, **2012**.
- [34] M. S. Westwell, M. S. Searle, D. J. Wales, D. H. William, *J. Am. Chem. Soc.* **1995**, *117*, 5013–5015.
- [35] a) Y.-H. Joo, J. M. Shreeve, *Inorg. Chem.* **2009**, *48*, 8431–8438; b) Y.-H. Joo, J. M. Shreeve, *Chem. Commun.* **2010**, 46, 142–144.
- [36] F. Volk, H. Bathelt, *Propellants Explos. Pyrotech.* **2002**, *27*, 136–141.
- [37] SHELXS, SHELXL, G. M. Sheldrick, Universität Göttingen (Germany), **1997**.
-

VI. Reaction Force Analysis and the Role of σ -Hole

Energetic silanes

J. S. Murray, P. Lane, A. Nieder, T. M. Klapötke and P. Politzer**
 113 -133

Enhanced Detonation Sensitivities of Silicon Analogues of PETN: Reaction Force Analysis and the Role of σ -Hole Interactions



Answering the question why Si-PETN reactions in a different manner than PETN, simplified models (trimethyl mononitrate analogues) were computed, collated with the known solid and gaseous structures of other nitratomethyl sila- and carbo-

analogues. Reaction force analysis and the influences in σ -hole interactions to the reactivity and the reaction behaviour are calculated to find explanation of the anomalies between the carbon and silicon analogues.

Enhanced Detonation Sensitivities of Silicon Analogs of PETN: Reaction Force Analysis and the Role of σ -Hole Interactions

Jane S. Murray,^[a] Pat Lane, Anian Nieder,^[b] Thomas M. Klapötke^{#[b]} and Peter Politzer^{*[a]}

Published as Co-author (experimental data) in Theoretical Chemistry Accounts 2010, 127, 345–351.

Abstract: Si-pentaerythritol tetranitrate (Si-PETN), Si[CH₂ONO₂]₄, is a silicon analogue of the widely used explosive PETN, C[CH₂ONO₂]₄. Si-PETN is extremely sensitive to impact, much more so than PETN. This was attributed by Liu et al. to Si-PETN having a much lower activation barrier to decomposition, via a facile rearrangement that is not as readily available to PETN, and which releases considerable energy that can promote further steps. We have investigated computationally why the barrier to the rearrangement is so much lower

for Si-PETN than for PETN, using **5**, (H₃C)₃C-CH₂ONO₂, and **6**, (H₃C)₃Si-CH₂ONO₂, as models for PETN and Si-PETN. Reaction force analysis shows that most of the difference between the rearrangement barriers for **5** and **6** comes about in the initial (reactant) stages of the processes, in which **6** benefits from a 1,3-electrostatic interaction involving a positive σ -hole on the silicon and the negative linking oxygen. The analogous interaction is weaker in **5**, since the central carbon does not have positive σ -holes;

furthermore, this carbon is less able than silicon to temporarily expand its coordination sphere. A similar explanation involving a positive silicon σ -hole and a linking oxygen is proposed for Si-PETN. The greater exothermicity of the rearrangement of **6** (and also Si-PETN) can be rationalized, following Liu et al., in terms of the formation of the strong Si-O bond.

Keywords: PETN • Si-PETN • Reaction force • Silicon-oxygen interactions • σ -Hole interactions • Impact sensitivities • Nitrate esters • Energetic molecules

Introduction

Pentaerythritol tetranitrate (PETN, **1**) is a well-known energetic compound, in the category of nitrate esters. It can be prepared by reacting the corresponding tetrol with nitric acid. [1]

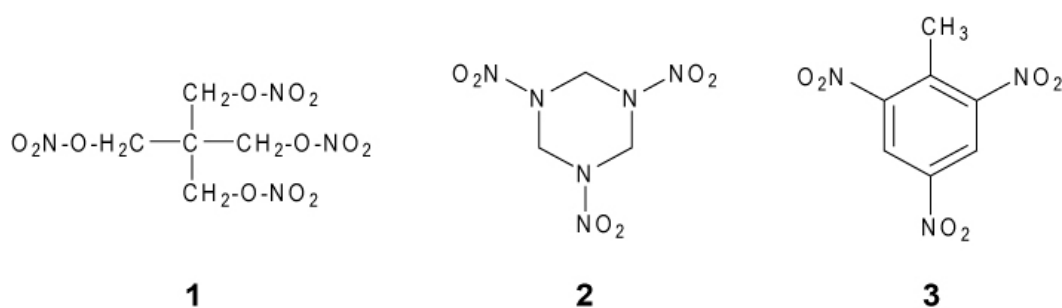
PETN has two polymorphs,[2] the less common (PETN II) occurring above 130 °C. Our focus shall be solely upon PETN I. It has a crystal density of 1.778 g/cm³ at 22 °C, with two molecules per unit cell.[2]

^{*[a]} J. S. Murray
Department of Chemistry, University of New Orleans,
New Orleans, LA 70148, USA
E-mail: jsmurray@uno.edu

^{#[b]} T. M. Klapötke
a) Department of Chemistry and Biochemistry,
Ludwig-Maximilian University of Munich,
Butenandtstr. 5-13(D), 81377 Munich, Germany
b) Departments of Mechanical Engineering and Chemistry/Biochemistry,
CECD, University of Maryland, College Park, MD 20742, USA

PETN has good detonation velocity and pressure, slightly below those of RDX (**2**) but well above TNT (**3**).[3] It has been used extensively in blasting cap fillings, detonation cords, demolition devices, industrial explosives, etc..[3, 4] However, PETN is quite sensitive to impact, more so than RDX and much more than TNT; the required impact energies for 50 % probability of ignition or explosion are about 3.5 J (PETN), 6.3 J (RDX) and 38 J (TNT).[3] (These correspond to 2.5 kg drop heights of 14, 26 and 155 cm, respectively).

An interesting feature of PETN is that its detonation behaviour has been observed to be direction-dependent within the crystal. Imposing shocks parallel to the [110] and [001] directions was found to lead to detonation, whereas parallel to the [101] and [100] did not.[5-7] Earlier work had already shown that the detonation velocities in the [110] and [001] directions differed, 8.887 versus 8.424 m/s, respectively.[1]

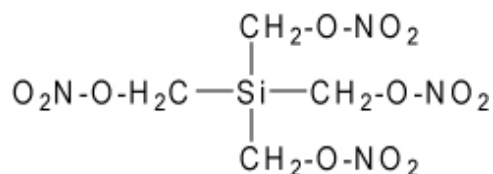


In the context of these experimental observations, Kunz demonstrated computationally that the band gap in PETN decreased with pressure imposed in either the [001] or [100] directions, but to a greater extent for the former.[8] Taken in conjunction with Gilman's hypothesis that sensitivity is related to metallization of the solid,[9] Kunz's results are consistent with direction-dependent detonation, as is also a molecular dynamics study of collision-induced PETN decomposition by Wu *et al.*[10]

Recently has been reported the preparation of Si-PETN, **4**, a silicon analogue of PETN.[11] This again involved treating the corresponding tetrol with nitric acid. A remarkable feature of Si- PETN is its extreme sensitivity: Impact is not necessary; just touching it with a spatula invariably produced an explosion!

PETN and Si-PETN decomposition: The detonation of an energetic compound is believed to proceed through its decomposition.[4, 12] Accordingly, in an effort to understand why Si-

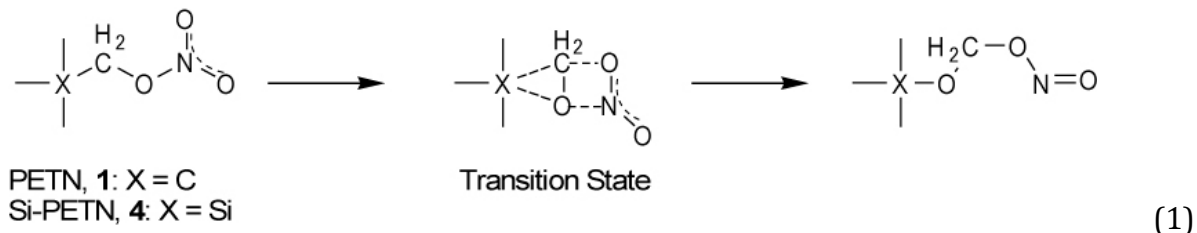
PETN is so much more sensitive that even PETN, Liu *et al.* have compared computationally several possible initial steps in PETN and Si-PETN decomposition.[13]



4

In PETN, this is generally believed to begin with rupture of an O-NO₂ bond,[10, 14–16] and Liu *et al.* did find this to be one of the two energetically preferred options, the other being HONO elimination. The corresponding processes for Si-PETN had barriers similar to those obtained for PETN, 35–40 kcal/mol.

Liu *et al.* also examined the possibility of PETN, **1**, and Si-PETN, **4**, decomposition beginning *via* the rearrangement shown in Eq. 1, in which the linking oxygen interacts with the central carbon or silicon:[13]



For PETN, the computed activation barrier for Eq. 1 was approximately double those for O-NO₂ bond cleavage and HONO elimination. For Si-PETN, however, it was 32 kcal/mol, less than for any of the other processes considered for either molecule; furthermore, the overall rearrangement was found to be quite exothermic, $\Delta H \sim -45$ kcal/mol.[13]

The results of Liu *et al.* indicate that PETN decomposes via O-NO₂ cleavage and/or HONO elimination, whereas Si-PETN does so *via* Eq. 1. They concluded that the extreme sensitivity of Si-PETN can be attributed to (a) its relatively low energy requirement for Eq. 1, significantly less than for either of the likely initiating steps in PETN, and (b) the exothermicity of the Si-PETN rearrangement, which provides energy early in the decomposition that promotes its further progress and expansion.[13]

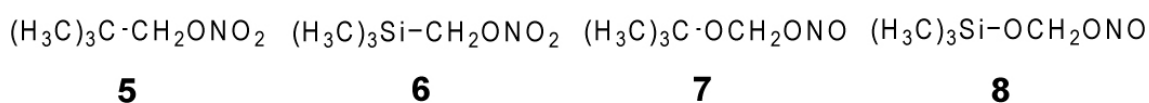
Why does Eq. 1 occur so much more readily for Si-PETN than for PETN? Liu *et al.* suggested that this is partly due to the greater size of the silicon atom compared to carbon, which facilitates, for the former, the enlargement of its coordination sphere from four to five in forming the transition state.[13] While this argument is certainly reasonable, we would like to look at the activation process in greater detail. This will be done in terms of the reaction force concept, which shall now be briefly summarized.

The reaction force: The energetics of a chemical process are commonly depicted by the variation of the potential energy $V(\mathbf{R})$ of the system along an appropriate reaction coordinate \mathbf{R} . A typical profile of $V(\mathbf{R})$ for a one-step process $A \rightarrow B$ is presented in Fig. 1a; it shows the energies of the reactants, transition state and products. Considerable additional insight can be gained from $V(\mathbf{R})$ by taking its negative gradient along \mathbf{R} , which yields the classically defined reaction force $F(\mathbf{R})$ (Fig. 1b).[17, 18]

$$F(\mathbf{R}) = \frac{\delta V(\mathbf{R})}{\delta \mathbf{R}} \quad (2)$$

\mathbf{R} is normally taken to be the intrinsic reaction coordinate. For the $V(\mathbf{R})$ in Fig. 1a, $F(\mathbf{R})$ has a minimum at α and a maximum at γ , the inflection points of $V(\mathbf{R})$. These partition the reaction, in a rigorous manner that is dictated only by the form of $V(\mathbf{R})$, into three regions. The first is prior to the $F(\mathbf{R})$ minimum, $A \rightarrow \alpha$, the second is between the minimum and maximum, $\alpha \rightarrow \gamma$, and the third is after the maximum, $\gamma \rightarrow B$.

The general characteristics of these regions have been examined in a series of studies, which include S_N2 substitution,[19–21] Markovnikov and anti-Markovnikov addition to a double bond,[22] cycloaddition to olefins,[23] bond dissociation,[24–26] proton transfer [27–32] and nitro/*aci* tautomerization [33]. It was observed that the first region, $A \rightarrow \alpha$, is usually dominated by structural changes within the reactants, such as bond stretching, rotations and angle-bending. $F(\mathbf{R})$ reflects the resistance to these changes, and is therefore increasingly retarding (i.e. negative) up to the point α , at which the system can generally be viewed as distorted states of the reactants. In the second region, $\alpha \rightarrow \gamma$, occurs the greatest part of the transition to products, emphasizing electronic factors: bonds breaking



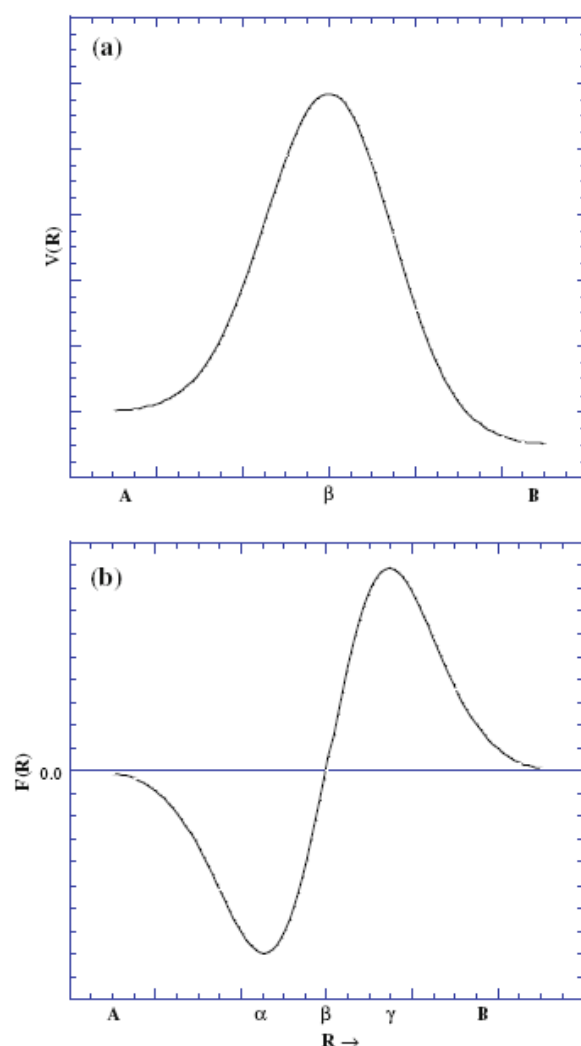


Figure 6.1. Typical profiles of a potential energy $V(\mathbf{R})$ and b the reaction force $F(\mathbf{R})$, along the intrinsic reaction coordinate \mathbf{R} . The points $\mathbf{R} = \alpha$ and $\mathbf{R} = \gamma$ correspond to the minimum and the maximum of $F(\mathbf{R})$; the transition state is at $\mathbf{R} = \beta$. The zero of $F(\mathbf{R})$ is indicated.

and new ones forming, rapid and extensive changes in properties such as electrostatic potentials and ionization energies, etc. All of this is manifested in a growing driving force; thus $F(\mathbf{R})$ increases steadily until it reaches a maximum at γ , the end of the transition region. At this point, the system can often be regarded as distorted versions of the products. Between c and B , these gradually relax to their final states. The three regions are commonly designated as reactant ($A \rightarrow \alpha$), transition ($\alpha \rightarrow \gamma$) and product ($\gamma \rightarrow B$).

A key feature of the reaction force is that it shows the activation energy to be the sum of two components—the energies needed to go (a) from the reactants to the force minimum at α , and (b) from α to the transition state at β :

$$\begin{aligned}
\Delta E_{\text{act}} &= V(\beta) - V(A) \\
&= [V(\beta) - V(\alpha)] + [V(\alpha) - V(A)] \\
&= \Delta E_{\text{act},2} + \Delta E_{\text{act},1}
\end{aligned} \tag{3}$$

$\Delta E_{\text{act},1}$ is largely the energy required to overcome the system's resistance to the structural changes in the reactant region between A and α , while $\Delta E_{\text{act},2}$ supports the first portion of the transition to products, $\alpha \rightarrow \beta$.

This division of ΔE_{act} into its two components helps to explain how external agents, such as solvents and catalysts, affect reaction rates, i.e. whether they change mainly the structural ($A \rightarrow \alpha$) or the electronic ($\alpha \rightarrow \beta$) component of ΔE_{act} or both.[20, 22, 32] For example, in the $S_{\text{N}}2$ substitution $\text{H}_2\text{O} + \text{CH}_3\text{Cl} \rightarrow \text{HCl} + \text{CH}_3\text{OH}$, the effect of aqueous solution was found to be not upon the transition state but rather in promoting the initial C-Cl bond stretching.[20] In the keto-enol tautomerization of thymine, Mg(II) acting as a catalyst also affects the first (reactant) portion of the activation process (prior to the force minimum).[32] On the other hand, in the addition of HCl to $\text{H}_3\text{C}-\text{CH}=\text{CH}_2$, chloroform solvent influences primarily the second part of the activation, $\alpha \rightarrow \beta$, approaching the transition state.[22]

An additional insight into reaction mechanisms comes from the reaction force constant $\kappa(\mathbf{R})$, which is the second derivative of $V(\mathbf{R})$:

$$\kappa(\mathbf{R}) = \frac{\partial^2 V(\mathbf{R})}{\partial \mathbf{R}^2} = -\frac{\partial F(\mathbf{R})}{\partial \mathbf{R}} \tag{4}$$

It follows from Eq. 4 that $\kappa(\mathbf{R})$ is negative throughout the entire transition region between α and γ ,[34, 35] in which $F(\mathbf{R})$ is increasing. Transition state spectroscopy led Zewail and Polanyi to conclude that a reaction has a continuum of transient, unstable configurations, a transition *region* rather than a single transition state.[36, 37] The reaction force constant $\kappa(\mathbf{R})$ reflects this continuum, and shows that it is bounded by the minimum and the maximum of $F(\mathbf{R})$, at which $\kappa(\mathbf{R}) = 0$.

Approach: Our objective is to better understand why the rearrangement in Eq. 1 is so much favoured for Si-PETN over PETN, both kinetically and thermodynamically. In order to simplify the computations, we have worked with the trimethyl mononitrate analogues of PETN and Si-PETN, i.e. **5** and **6**. Both of these are known and have been characterized.[38] The silicon compound is again by far the more sensitive; the impact energy (drop height) of **6** was reported as >1 J (>4 cm), compared to >100 J (>408 cm) for **5**. (The di- and trinitrate analogues have also been synthesized,[38] and the silicon systems are similarly much more sensitive than the carbon ones).

The optimized geometries and the enthalpies along the intrinsic reaction coordinates for the rearrangements **5** \rightarrow **7** and **6** \rightarrow **8**, Eq. 1, were calculated at the density functional B3PW91/6-311G(d,p) level using Gaussian 03.[39] In Table 6.1, our optimized geometries for **5** and **6** are compared to those obtained by electron diffraction [40] and also the molecular structure determined crystallographically for PETN.[2] Particularly pleasing is the good agreement with PETN, which provides some support for modelling Eq. 1 in terms of **5** and **6**. More will be forthcoming.

Results/Approach

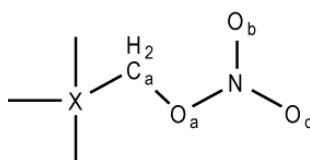
Reaction force analysis: In Table 6.2 are presented the computed structures, relative enthalpies at 298 K and key interatomic distances and angles at five points along the intrinsic reaction coordinate for the rearrangement **5** \rightarrow **7**, Eq. 1; these points correspond to the ground state of **5**, the minimum of the reaction force at a, the transition state at b, the reaction force maximum at c and the final rearrangement product **7**. Table 6.3 gives the same data for **6** \rightarrow **8**. Table 6.4 summarizes the total activation enthalpy ΔH_{act} for each process, its two components $\Delta H_{\text{act},1}$ and $\Delta H_{\text{act},2}$ corresponding to the portions of the activation before and after the $F(\mathbf{R})$ minimum, and finally the overall ΔH_{rxn} .

In terms of ΔH_{act} and ΔH_{rxn} , the rearrangements of **5** and **6** show exactly the same features as were found by Liu *et al.* for PETN and Si-PETN.[13] The activation barriers are relatively low for both silicon-containing molecules, 32–33 kcal/mol for Si-PETN and **6**, and more than twice as high for the carbon analogues. The reactions are quite exothermic for Si-PETN and **6**, with overall ΔH_{rxn} (298 K) of –40 to –45 kcal/mol, compared to just –10 to

-14 kcal/mol for PETN and **5**. These similarities between PETN and **5** and between Si-PETN and **6** are reassuring with respect to using **5** and **6** to model PETN and Si-PETN.

To analyze why the activation barrier is so much smaller for **6** than for **5**, we first look at its components in each case, $\Delta H_{\text{act},1}$ and $\Delta H_{\text{act},2}$. Table 6.4 shows that the major difference in the activation energetics of **5** and **6** is in the initial portion of the process, in the reactant region prior to the $F(\mathbf{R})$ minimum at a, which typically involves mainly structural changes. For **5**, these changes require 44.7 kcal/mol, compared to only 18.9 kcal/mol for **6**. Thus, 71 % of the difference in the overall activation barriers reflects what is happening in the respective reactant regions.

Table 6.1. Comparison of computed and experimental structures.



Distance [\AA] or angle [$^\circ$]	X = C			X = Si	
	1 , PETN (X-ray) ^[a]	5 (ED) ^[b]	5 (calc.) ^[c]	6 (ED) ^[c]	6 (calc.) ^[c]
X-C _a	1.536	1.538	1.530	1.882	1.915
C _a -O _a	1.434	---	1.440	1.437	1.435
O _a -N	1.397	---	1.404	1.435	1.416
N-O _b	1.222	1.210 ^[d]	1.203	1.206 ^[d]	1.202
N-O _c	1.207	1.210 ^[d]	1.195	1.206 ^[d]	1.195
X-C _a -O _a	107.5	106.9	107.6	108.3	106.3
C _a -O _a -N	115.9	113.2	114.4	113.6	114.5
O _b -N-O _c	128.8	128.7	129.8	131.3	130.1

[a] Crystallographic data, ref.[2]; [b] electron diffraction data, ref. [40]; [c] Present calculations, B3PW91/6-311G(d,p); [d] averages of N-O_b, N-O_c distances.

What is it that is happening? Tables 6.2 and 6.3 show a variety of structural effects for both **5** and **6** in the regions before the $F(\mathbf{R})$ minima. For **5**, the dominant ones are the stretching of two bonds: the C-C_a by 0.277 \AA and the O_a-N by fully 0.645 \AA . This requires energy. In **6**, on the other hand, the Si-C_a and O_a-N bonds lengthen by only 0.061 and 0.194 \AA in the reactant region. What is important here for **6** is that the nonbonded Si and O_a atoms move closer to each other by 0.450 \AA . This is reflected in the Si-C_a-O_a angle decreasing by 24.8 $^\circ$. The approach of O_a to Si, which will lead eventually to the formation of the Si-O_a bond, should already be accompanied by a significant release of energy, given the

strengths of Si–O bonds (see [41], and also the next section of this paper). Thus, **6** needs less energy than **5** in the reactant region (before α) because (a) it is undergoing less bond stretching, and (b) it is benefiting from the favourable Si---O_a interaction.

In the second portion of the activation process of **5**, between the $F(\mathbf{R})$ minimum at α and the transition state at β , the C–C_a and O_a–N bonds start to break and C and O_a begin to bond, as do C_a and O_b. The latter interactions bring $\Delta H_{\text{act},2}$ down to 24.6 kcal/mole for **5**. However, **6** again requires less energy. Between α and β , the breaking of the Si–C_a and O_a–N bonds in **6** proceeds rather slowly, while Si and O_a come closer by another 0.322 Å and the Si–C_a–O_a angle is reduced by 19.1 °, taking a big step toward Si–O_a bond formation. Thus, $\Delta H_{\text{act},2}$ is also less for **6** than for **5** (Table 6.4), although not nearly by as much as $\Delta H_{\text{act},1}$.

The difference in the activation barriers of **5** and **6** can therefore be attributed to their contrasting pathways from reactant $\rightarrow \alpha \rightarrow$ transition state: **5** begins with energy-consuming bond stretchings and then breakings, largely delaying energy-releasing bond formation until after the transition state. The silicon analogue **6**, on the other hand, is slower to begin the energy-demanding steps, but starts right away to benefit from the eventual formation of a strong Si–O bond.

As suggested by Liu *et al.* for Si-PETN,[13] one factor in the O_a in **6** being able to immediately move toward the silicon is the size of the latter atom, which allows it to accommodate the approaching oxygen while essentially maintaining four covalent bonds. The relatively small central carbon in **5**, on the other hand, must make room for O_a by C_a moving out of the way. But what is the driving force for the approach of O_a to Si? We believe that it is the presence of a favourable Si---O_a interaction already in the ground state of **6**. Indeed, short Si---O_a contacts have been found crystallographically in the dinitrate analogue of **6**. [38, 40] Mitzel *et al.* have observed unexpectedly small intramolecular 1,3 Si–N and Si–O distances and Si–Z–N and Si–Z–O angles in molecules such as ClH₂SiON(CH₃)₂, (F₃C)F₂SiON(CH₃)₂, and H₃SiN(CH₃)OCH₃. [42–44]

The origin of the Si---O_a interaction in **6**, as well as those observed by Mitzel *et al.*, can readily be explained. When Group IV–VII atoms form covalent bonds, the outer (non-involved) lobe of the bonding orbital undergoes a depletion in electronic density. This has

been labelled a σ -hole.[45–47] If the depletion is sufficiently great, there results a region of positive electrostatic potential with a local surface maximum. σ -Holes become more positive, and the resulting interactions stronger, for the more polarisable, i.e. larger atoms in a Group, and usually as the remainder of the molecule becomes more electron-withdrawing.[46–49]

As an example, in Fig. 2 is displayed the electrostatic potential on the molecular surface of $\text{Si}(\text{CH}_3)_3\text{CN}$, computed using the WFA Surface Analysis Suite.[50] The surface is taken to be the 0.001 au (electrons/Bohr³) contour of the electronic density, as proposed by Bader *et al.*[51] There are four positive σ -holes on the silicon surface, each corresponding to a local maximum of the electrostatic potential. The largest in magnitude is 25.7 kcal/mol on the extension of the bond from the strongly electron-withdrawing CN group; the others are 15.1 kcal/mol, on the extensions of the H_3C -Si bonds. The methyl hydrogens are also positive, with local maxima ranging from 15.8 to 20.0 kcal/mol.

A positive σ -hole can interact electrostatically with a negative site (such as O_a of **6**), either inter- or intramolecularly. There is a great deal of evidence, both experimental [52–59] and computational [45–49, 60–62], attesting to the significance of such interactions. (They are called “halogen bonds” when the σ -hole is on a halogen atom.) Very recently, complex formation between SiF_4 and di- and triamines has been interpreted in terms of electrostatic interactions between the lone pairs of the amine nitrogens and the Si σ -holes induced by the four F-Si bonds [62].

We have also computed the molecular surface electrostatic potential of **6**, which should intrinsically be quite similar to that shown for $\text{Si}(\text{CH}_3)_3\text{CN}$ in Fig. 2. However, three of the four local maxima on the silicon in **6** are masked; one of the three σ -holes on the extensions of the H_3C -Si bonds is involved in the Si--- O_a intramolecular interaction, and the other two are difficult to distinguish because of the long and bulky $-\text{CH}_2-\text{ONO}_2$ group. We are accordingly not showing the surface potential plot of **6**. The only silicon σ -hole in **6** that would clearly be seen is the strongest, 18.0 kcal/mol, on the extension of the bond from the electron-withdrawing $-\text{CH}_2-\text{ONO}_2$ group. There are also local maxima on the methyl hydrogens of **6**.

Table 6.2. Computed activation enthalpies ΔH_{act} , their components $\Delta H_{\text{act},1}$ and $\Delta H_{\text{act},2}$ and the overall enthalpy of reaction, ΔH_{rxn} , for the reaction shown in Eq.1, at 298 K.^[a]

Reaction	$\Delta H_{\text{act},1}$	$\Delta H_{\text{act},2}$	ΔH_{act}	ΔH_{rxn}
$(\text{H}_3\text{C})_3\text{CC}_a\text{H}_2\text{O}_a\text{NO}_b\text{O}_c$ (5) \rightarrow $(\text{H}_3\text{C})_3\text{CO}_a\text{C}_a\text{H}_2\text{O}_b\text{NO}_c$ (7)	44.7	24.6	69.3	-9.7
$(\text{H}_3\text{C})_3\text{SiC}_a\text{H}_2\text{O}_a\text{NO}_b\text{O}_c$ (6) \rightarrow $(\text{H}_3\text{C})_3\text{SiO}_a\text{C}_a\text{H}_2\text{O}_b\text{NO}_c$ (8)	18.9	14.1	33.0	-40.0

[a] Values are in kcal/mol. Computational level: B3PW91/6-311G(d,p).

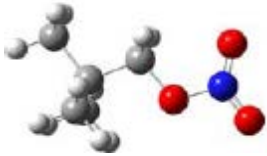
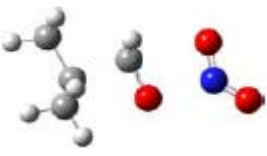
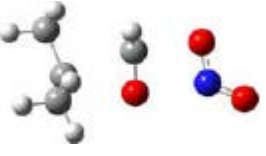
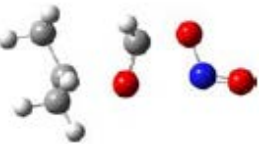
The driving force for the approach of O_a to Si in **6** is the interaction between O_a and (a) a silicon σ -hole along the extension of an H_3C -Si bond, analogous to that seen in Fig. 2, and (b) the neighbouring methyl hydrogens. The corresponding interaction is much weaker in **5**, for which we found that the central carbon, being less polarisable than silicon, has no positive σ -holes whatsoever. The strength of this interaction in **6**, and the fact that the size of the silicon atom allows it to proceed without prior stretching of other bonds, explain the low energy requirement for reaching the force minimum ($\Delta H_{\text{act},1}$ of 18.9 kcal/mol for **6** vs. 44.7 kcal/mol for **5**).

Exothermicities of rearrangements: Liu *et al.* [13] ascribed the much greater exothermicity of the Si-PETN rearrangement to the strength of the Si-O bond that is formed. We can provide some quantitative support for this explanation

If one looks only at the bonds broken and formed in the rearrangements of **5** and **6**, the differences between the two processes are breaking C-C_a versus Si-C_a and forming C-O_a versus Si-O_a. The former two bonds tend to have roughly similar dissociation enthalpies;^[41] thus, as a very crude approximation, it could be suggested that the difference in the overall ΔH_{rxn} of the two rearrangements can be estimated by comparing the ΔH for forming the C-O_a and Si-O_a bonds in **7** and **8**. Since Si-O bond enthalpies, while generally larger in magnitude, tend to be quite variable,^[41] we have computed ΔH for the formation of the C-O_a bond in **7** and the Si-O_a bond in **8**. This was done at the B3PW91/6-31++G(3d,2p) level, using B3PW91/6-311G(d,p) optimized geometries.

VI. Reaction Force Analysis and the Role of σ -Hole

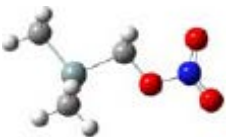
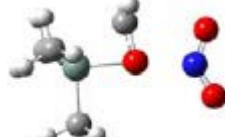
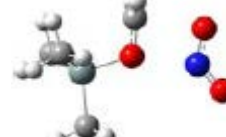
Table 6.3. Computed structures, relative enthalpies at 298 K and some interatomic distances and angles at points along the intrinsic reaction coordinate for rearrangement $(\text{H}_3\text{C})_3\text{CC}_a\text{H}_2\text{O}_a\text{NO}_b\text{O}_c$ (**5**) \rightarrow $(\text{H}_3\text{C})_3\text{CO}_a\text{C}_a\text{H}_2\text{O}_b\text{NO}_c$ (**7**), Eq.1.^[a]

	reactant	force min., α	transition state, β	force max., γ	product
Relative H (298 K)	 0.0	 44.7	 69.3	 33.8	 -9.7
interatomic distances ^[b]					
C-C _a	1.530	1.807	2.243	2.496	2.416
C-O _a	2.397	2.344	2.213	1.908	1.446
C _a -O _a	1.440	1.316	1.270	1.343	1.381
O _a -N	1.404	2.049	2.212	2.396	3.492
C _a -O _b	2.566	2.445	2.064	1.635	1.437
N-O _b	1.203	1.189	1.248	1.364	1.374
N-O _c	1.195	1.198	1.203	1.179	1.183
Angles					
C-C _a -O _a	107.6	90.0	72.2	49.1	32.1
C--O _a -C _a	37.5	50.0	74.7	98.8	117.4

[a] Enthalpies are in kcal/mol, distances in Angstroms (Å) and angles in degrees. Colours of atoms: carbons are grey, hydrogens are white, nitrogen is blue and oxygens are red; [b] The symbol C refers only to the central carbons in **5**, the structures at positions α , β and γ , and **7**.

VI. Reaction Force Analysis and the Role of σ -Hole

Table 6.4. Computed structures, relative enthalpies at 298 K and some interatomic distances and angles at points along the intrinsic reaction coordinate for rearrangement $(\text{H}_3\text{C})_3\text{SiC}_a\text{H}_2\text{O}_a\text{NO}_b\text{O}_c$ (**6**) \rightarrow $(\text{H}_3\text{C})_3\text{SiO}_a\text{C}_a\text{H}_2\text{O}_b\text{NO}_c$ (**8**), Eq.1.^[a]

	reactant	force min., α	transition state, β	force max., γ	product
					
Relative H (298 K)	0.0	18.9	33.0	17.4	-40.0
interatomic distances					
Si-C _a	1.915	1.976	2.136	2.513	2.746
Si-O _a	2.696	2.246	1.924	1.727	1.686
C _a -O _a	1.435	1.401	1.338	1.299	1.370
O _a -N	1.416	1.610	1.926	2.194	3.506
C _a -O _b	2.574	2.719	2.638	2.331	1.444
N-O _b	1.202	1.188	1.196	1.231	1.371
N-O _c	1.195	1.190	1.193	1.206	1.185
Angles					
Si-C _a -O _a	106.3	81.5	62.4	39.7	29.1
Si-O _a -C _a	43.0	60.5	79.6	111.5	127.6

[a] Enthalpies are in kcal/mol, distances in Angstroms (Å) and angles in degrees. Colours of atoms: carbons are grey, silicon are blue-grey, hydrogens are white, nitrogen is blue and oxygens are red.

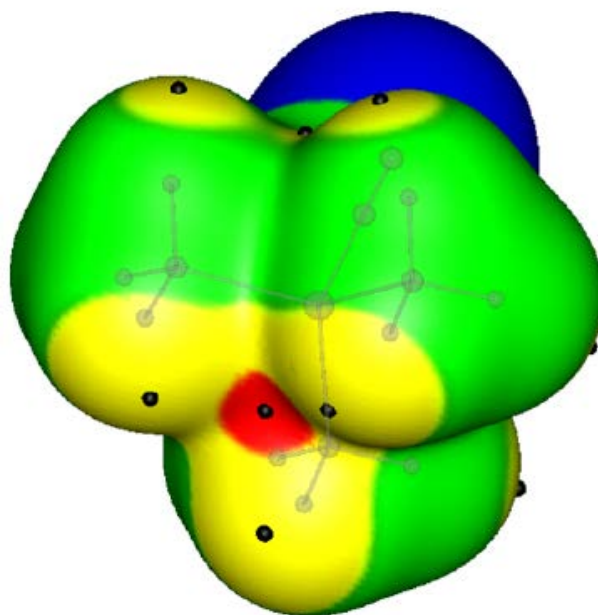
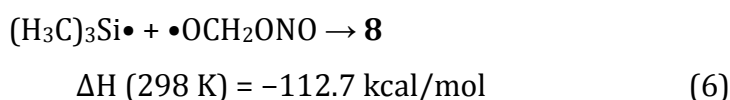
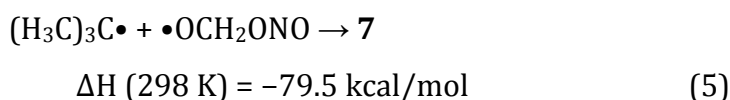


Figure 6.2. Computed electrostatic potential on the 0.001 au molecular surface of $(\text{H}_3\text{C})_3\text{Si-CN}$. The three methyl groups face the reader; the CN is pointing into the paper, the nitrogen being visible (*blue*) at the *top*. Color ranges, in kcal/mol, are: *blue* <0.0 (negative), *green* between 0.0 and 14.1, *yellow* between 14.1 and 21.3, *red* >21.3 . *Black circles* indicate local surface maxima. The most positive is a positive σ -hole (*red*), of magnitude 25.7 kcal/mol, induced on the silicon by the strongly electron-withdrawing CN group, on the extension of the NC-Si bond. One of the σ -holes on the extensions of the $\text{H}_3\text{C-Si}$ bonds, 15.1 kcal/mol, is in the upper central part of the figure. Next to both of the σ -holes shown are local maxima of 15.8–20.0 kcal/mol due to methyl hydrogens.

The results are:



Taking the difference as a measure of the relative exothermicities of the rearrangements of **5** and **6**, we have that of **6** being more exothermic by 33.2 kcal/mol. This is, perhaps fortuitously, quite close to the 30.3 kcal/mol difference between the computed ΔH_{rxn} in Table 6.4.

Discussion and summary

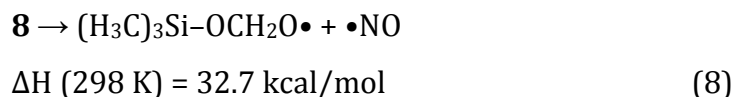
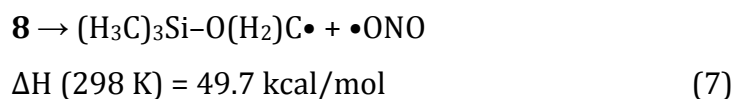
Our objective in this investigation has been to better understand why the rearrangement in Eq. 1 is so much more (a) facile and (b) exothermic for Si-PETN than for PETN. We used **5** and **6** as models for PETN and Si-PETN, which seems justified because **5** and **6** have nearly the same relative activation barriers and exothermicities for Eq. 1 as do PETN and Si-PETN.

Reaction force analysis shows that most of the difference in the activation energies of **5** and **6** reflects the greater ease with which **6** reaches the $F(\mathbf{R})$ minimum at a ; it requires only 18.9 kcal/mol in this first (reactant) region *versus* 44.7 kcal/mol for **5**. This is because the size of the silicon atom permits **6** to immediately benefit from an energy-releasing intramolecular electrostatic interaction between O_a and a positive σ -hole on the silicon plus the surrounding methyl hydrogens. The corresponding interaction in **5** is not nearly as strong because we found the central carbon to lack positive σ -holes; furthermore, the approach of O_a has to be delayed until after C_a has moved away.

We propose that analogous interactions between linking oxygens and silicon positive σ -holes are occurring in Si-PETN. There are no methyl hydrogens involved, but the silicon σ -holes in Si-PETN should be more positive because the silicon is bonded to four electron-withdrawing $-\text{CH}_2-\text{ONO}_2$ groups, rather than one as in **6**. For example, whereas the local maximum potential induced by the single $-\text{CH}_2-\text{ONO}_2$ in **6** is 18.0 kcal/mol, we found the two in the dinitrate silicon analog to each be 30.6 kcal/mol. The much lower activation barrier for Si-PETN than for PETN in Eq. 1 can therefore be explained in terms of the $\text{Si}\cdots\text{O}_a$ interaction in conjunction with the large size of silicon that allows it to progress without delay toward $\text{Si}-\text{O}_a$ bond formation.

If at least one $-\text{CH}_2-\text{ONO}_2$ group in Si-PETN undergoes the rearrangement in Eq. 1, a significant amount of energy is produced. This has been rationalized on the basis of the strength of the $\text{Si}-\text{O}$ bond that is created (see Exothermicities of Rearrangements and [13]). This energy is more than enough to allow a second $-\text{CH}_2-\text{ONO}_2$ to overcome the barrier to rearrangement. However, it might also be used for further steps involving the rearranged group. To examine this possibility, we computed the dissociation enthalpies of the OCH_2-

ONO and the O–NO bonds in **8**, which is the rearranged form of **6**. The B3PW91/6-31++G(3d,2p)//B3PW91/6-311G(d,p) procedure was again utilized. The results are:



The second of these is less than the exothermicity of the rearrangement of **6**, and could well be a follow-up step in the decomposition. This remains to be investigated.

Acknowledgements

We thank Dr. Felipe A. Bulat for his help and expertise in preparing Fig. 2 and for many useful discussions. JSM, PL and PP appreciate the support of the Defense Threat Reduction Agency, Contract No. HDTRA1-07-1-0002, Project Office Dr. William Wilson. Financial support (to TMK) of this work by LMU and the U.S. Army Research Laboratory (ARL) under Contract No. W911NF-09-2-0018 is gratefully acknowledged.

-
- [1] T. Urbański in *Chemistry and technology of explosives*, Vol 4. Pergamon Press, Oxford, **1984**.
- [2] H. H. Cady, A. C. Larson, *Acta Cryst.* **1975**, *B31*, 1864–1869.
- [3] T. R. Gibbs, A. Popolato (eds) in *LASL explosive property data*, University of California Press, Berkeley, **1980**.
- [4] R. Meyer, J. Köhler, A. Homburg in *Explosives*, 6th edn. Wiley-VCH, Weinheim, **2007**.
- [5] J. J. Dick, *Appl. Phys. Lett.* **1984**, *44*, 859–860.
- [6] J. J. Dick, *J. Appl. Phys.* **1997**, *81*, 601–612.
- [7] C.-S. Yoo, N. C. Holmes, P. C. Souers, C. J. Wu, F. H. Ree, J. J. Dick, *J. Appl. Phys.* **2000**, *88*, 70–75.
- [8] A. B. Kunz, *Mater. Res. Soc. Symp. Proc.* **1996**, *418*, 287–292.

- [9] J. J. Gilman, *Philos. Mag.* **1993**, *B67*, 207.
- [10] C. J. Wu, F. H. Ree, C.-S. Yoo, *Propellants Explos. Pyrotech.* **2004**, *29*, 296–303.
- [11] T. M. Klapötke, B. Krumm, R. Ilg, D. Troegel, R. Tacke, *J. Am. Chem. Soc.* **2007**, *129*, 6908–6915.
- [12] P. Politzer, J. S. Murray (eds) in *Energetic materials. Part 1. Decomposition, crystal and molecular properties. Part 2. Detonation, combustion*. Elsevier, Amsterdam, **2003**.
- [13] W.-G. Liu S.V. Zybin, S. Dasgupta, T. M. Klapötke, W.A.Goddard III, *J. Am. Chem. Soc.* **2009**, *131*, 7490–7491.
- [14] H. M. Hauser, J.E. Field, V. K. Mohan, *Chem. Phys. Lett.* **1983**, *99*, 66–70.
- [15] M. A. Hiskey, K. R. Brower, J. C. Oxley, *J. Phys. Chem.* **1991**, *95*, 3955–3960.
- [16] J. C. Oxley, in: P. Politzer, J. S. Murray (eds) *Energetic materials. Part I. Decomposition, crystal and molecular properties, chap 1*. Elsevier, Amsterdam, **2003**.
- [17] A. Toro-Labbé, S. Gutiérrez-Oliva J. S. Murray, P. Politzer, *Mol. Phys.* **2007**, *105*, 2619–2625.
- [18] A. Toro-Labbé, S. Gutiérrez-Oliva, P. Politzer, J. S. Murray, Chattaraj P (ed) in *Theory of chemical reactivity, chap 21*. Taylor & Francis, Boca Raton, **2008**.
- [19] P. Politzer, J. V. Burda, M. C. Concha, P. Lane, J. S. Murray, *J. Phys. Chem. A* **2006**, *110*, 756–761.
- [20] J. V. Burda, A. Toro-Labbé, S. Gutiérrez-Oliva, J. S. Murray, P. Politzer, *J. Phys. Chem. A* **2007**, *111*, 2455–2458.
- [21] E. A. Echegaray, Toro-Labbé, *J. Phys. Chem. A* **2008**, *112*, 11801–11807.
- [22] J- V. Burda, J. S: Murray, A. Toro-Labbé, S. Gutiérrez-Oliva, P. Politzer, *J. Phys. Chem. A* **2009**, *113*, 6500–6505.
- [23] P. Jaque, A. Toro-Labbé, Geerlings P, F. De Proft, *J. Phys. Chem. A* **2009**, *113*, 332–344.

- [24] P. Politzer, J. S. Murray, P. Lane, A. Toro-Labbé, *Int. J. Quantum Chem.* **2007**, *107*, 2153–2157.
- [25] P. Politzer, J. S. Murray, *Collect. Czechoslov Chem. Commun.* **2008**, *73*, 822–830.
- [26] J. S. Murray, A. Toro-Labbé, T. Clark, P. Politzer, *J. Mol. Model* **2009**, *15*, 701–706.
- [27] A. Toro-Labbé, S. Gutiérrez-Oliva, M. C. Concha, J. S. Murray, P. Politzer, *J. Chem. Phys.* **2004**, *121*, 4570–4576.
- [28] B. Herrera, A. Toro-Labbé, *J. Chem. Phys.* **2004**, *121*, 7096–7102.
- [29] P. Politzer, A. Toro-Labbé, S. Gutiérrez-Oliva, B. Herrera, P. Jaque, M. C. Concha, J. S. Murray, *J. Chem. Sci.* **2004**, *117*, 467–472.
- [30] S. Gutiérrez-Oliva, B. Herrera, A. Toro-Labbé, H. Chermette, *J. Phys. Chem. A* **2005**, *109*, 1748–1751.
- [31] E. Rincoñ, P. Jaque, A. Toro-Labbé, *J. Phys. Chem. A* **2006**, *110*, 9478–9485.
- [32] B. Herrera, A. Toro-Labbé, *J. Phys. Chem. A* **2007**, **111**, 5921–5926.
- [33] J. S. Murray, P. Lane, M. Göbel, T. M. Klapötke, P. Politzer, *Theor. Chem. Acc.* **2009**, *124*, 355–363.
- [34] P. Jaque, A. Toro-Labbé, P. Politzer, P. Geerlings, *Chem. Phys. Lett.* **2008**, *456*, 135–140.
- [35] A. Toro-Labbé, S. Gutiérrez-Oliva, J. S. Murray, P. Politzer, *J. Mol. Model* **2009**, *15*, 707–710.
- [36] J.C. Polanyi, A. H. Zewail, *Acc. Chem. Res.* **1995**, *28*, 119–132.
- [37] A. H. Zewail, *J. Phys. Chem. A* **2000**, *104*, 5660–5694.
- [38] T. M. Klapötke, B. Krumm, A. Nieder, R. Tacke, D. Troegel, *New Trends in Research of Energetic Materials, Part 1.* **2009**, Institute of Energetic Materials, University of Pardubice, Czech Republic, 262–276.

- [39] M. J. Frisch *et al.*, *Gaussian 03 (Revision E.01)*, Gaussian Inc., Wallingford CT, **2004**.
- [40] C. Evangelisti, T. M. Klapötke, B. Krumm, A. Nieder, R. J. F. Berger, S. A. Hayes, N. W. Mitzel, D. Troegel, R. Tacke, submitted.
- [41] Y-R. Luo, *Comprehensive handbook of chemical bond energies*. CRC Press, Taylor & Francis, Boca Raton, **2007**.
- [42] N. W. Mitzel, U. Losehand, *J. Am. Chem. Soc.* **1998**, *120*, 7320–7327.
- [43] N. W. Mitzel, H. Oberhammer, *Inorg. Chem.* **1998**, *37*, 3593–3598.
- [44] N. W. Mitzel, K. Vojinovic', R. Fröhlich, T. Foerster, H. E. Robertson, K. B. Borisenko, D. W. H. Rankin, *J. Am. Chem. Soc.* **2005**, *127*, 13705–13713.
- [45] T. Clark, M. Hennemann, J. S. Murray, P. Politzer, *J. Mol. Model* **2007**, *13*, 291–296.
- [46] P. Politzer, P. Lane, M. C. Concha, Y. Ma, J. S. Murray, *J. Mol. Model* **2007**, *13*, 305–311.
- [47] J. S. Murray, P. Politzer, *J. Mol. Model* **2009**, *15*, 723–729.
- [48] J. S. Murray, P. Lane, P. Politzer, *Int. J. Quantum Chem.* **2008**, *08*, 2770–2781.
- [49] K. E. Riley, J. S. Murray, M. C. Concha, P. Politzer, P. Hobza, *J. Chem. Theory Comput.* **2009**, *5*, 155–163.
- [50] F. A. Bulat, A. Toro-Labbé, T. Brinck, J. S. Murray, P. Politzer, *J. Mol. Model* **2010**, in press.
- [51] R. F. W. Bader, M. T. Carroll, J. R. Cheeseman, C. Chang, *J. Am. Chem. Soc.* **1987**, *109*, 7968–7979.
- [52] T. Di Paolo, C. Sandorfy, *Can. J. Chem.* **1974**, *52*, 3612–3622.
- [53] R. E. Rosenfeld Jr., R. Parthasarathy, J. D. Dunitz, *J. Am. Chem. Soc.* **1977**, *99*, 4860–4862.
- [54] N. Ramasabhu, R. Parthasarathy, P. Murray-Rust, *J. Am. Chem. Soc.* **1986**, *108*, 4308–4314.

- [55] F. T. Burling, B. M. Goldstein, *J. Am. Chem. Soc.* **1992**, *114*, 2313.
- [56] P. Auffinger, F. A. Hays, E. Westhof, P. Shing Ho, *Proc. Natl. Acad. Sci. USA* **2004**, *101*, 16789–16794.
- [57] P. Metrangolo, H. Neukirsch, T. Pilati, G. Resnati, *Acc. Chem. Res.* **2005**, *38*, 386–395.
- [58] F. Cheng, A. L. Hector, W. Levason, G. Reid, M. Webster, Z. Zhang, *Chem. Commun.* **2009**, 1334–1336.
- [59] A. E. A. Hassan, J. Sheng, J. Jiang, W. Zhang, Z. Huang, *Org. Lett.* **2009**, *11*, 2503–2506.
- [60] C. Bleiholder, D. B. Werz, H. Köppel, R. Gleiter, *J. Am. Chem. Soc.* **2006**, *128*, 2666.
- [61] T. Clark, J. S. Murray, P. Lane, P. Politzer, *J. Mol. Model* **2008**, *14*, 689–697.
- [62] P. Politzer, J. S. Murray, P. Lane, M. C. Concha, *Int. J. Quantum Chem.* **2009**, *109*, 3773–3780.
-

VII. Phenylsilanes and Siloxanes

Energetic silanes

T. M. Klapötke, B. Krumm, A. Nieder, A. Nordheider, O. Richter, and R. Scharf.....134 - 166*

Azidomethyl- and Nitratomethyl-Siloxanes, Disiloxanes, Silsesquioxanes and its Phenylsilane Precursors



Several nitrate and azido phenylsilanes are synthesized. They are precursors for disiloxanes, *poly*-siloxanes and *poly*-silsesquioxanes, which are interesting compounds for application as reactive silicone greases, rubbers or glasses. They combine the characteristics of silicoes and glasses with high energy release by decomposition.

Azidomethyl- and Nitratomethyl-Siloxanes, Disiloxanes, Silsesquioxanes and its Phenylsilane Precursors

Thomas M. Klapötke*, Burkhard Krumm, Anian Nieder, Andreas Nordheider, Oliver Richter, and Regina Scharf

Unpublished

Abstract: Recently several several new azido- and energetic compounds. In addition azidomethyl and nitratomethyl nitratomethylated silanes with the crystal structure of silanes were published and different kinds of backbones tris(iodomethyl)phenylsilane is studied in terms of chemical and (phenylated and oxygen discussed. physical characteristics. Herein containing substituents) are the data were completed by discussed. Especially the EXPLO5 version 6.01 calculations behaviour towards mechanical to determine their explosive and thermal stimuli is of interest performances. Furthermore, for the development of new high

Keywords: azide • nitrate
• silane • crystal structure
• explosiv

Introduction

Several silanes containing energetic moieties like azides and nitrate esters of the type $\text{Me}_x\text{Si}(\text{CH}_2\text{X})_{4-x}$ ($x = 0-4$) were studied in detail in terms of energetic properties, like impact and friction sensitivities, thermal stability and detonation parameters.[1-4] Some of them were mention to be potentially useful in pharmaceuticals, and in some cases even as explosive.[5,6] Azidomethyl silanes were studied as precursors for aminomethyl silanes, which can be used as ligands in platinum containing anticancer therapeutics.[7,8] The explosive properties were not studied in detail until Klapötke *et al.* published the properties of the sila analogues of pentaerythritol tetranitrate (PETN), a common high explosive in civil and military use, and pentaerythritol tetrazide ($\text{E}(\text{CH}_2\text{X})_4$, $\text{E} = \text{C}, \text{Si}$, $\text{X} = \text{ONO}_2, \text{N}_3$) in 2007.[1] Since then several representatives of this class of compounds differing in the amount of azide and nitrate moieties have been published elsewhere.[2-3] Furthermore, the

* T. M. Klapötke
Department of Chemistry and Biochemistry,
Ludwig-Maximilian University of Munich,
Butenandtstr. 5-13(D), 81377 Munich, Germany

superiority of silanes over their carbon analogues in term of impact, friction and thermal stimuli could be shown.[1-3]

Another class of commonly used silanes is that of phenyl silanes. Therefore several of these compounds containing different amount of phenyl, azidomethyl and nitratomethyl substituents have been synthesized and fully characterized. They are useful precursor for a broad range of compounds, like hexakis-substituted disiloxanes $[(O_{2/2}Si(CH_2X)_2)_n]$, for example $X = Cl, N_3, ONO_2$.[4] In addition, their use as potential precursors for oligomeric/polymeric siloxanes containing CH_2X moieties $[(O_{2/2}Si(CH_2X)_2)_n]$, $X = Cl, N_3, ONO_2$) by selected cleavage of the phenyl moieties [9,10] followed by hydrolysis was studied. In the same way the disiloxane $O(SiMe_2CH_2X)_2$ and polymeric silsesquioxane $[O_{3/2}SiMeCH_2X]_n$ were hypothetically obtainable.

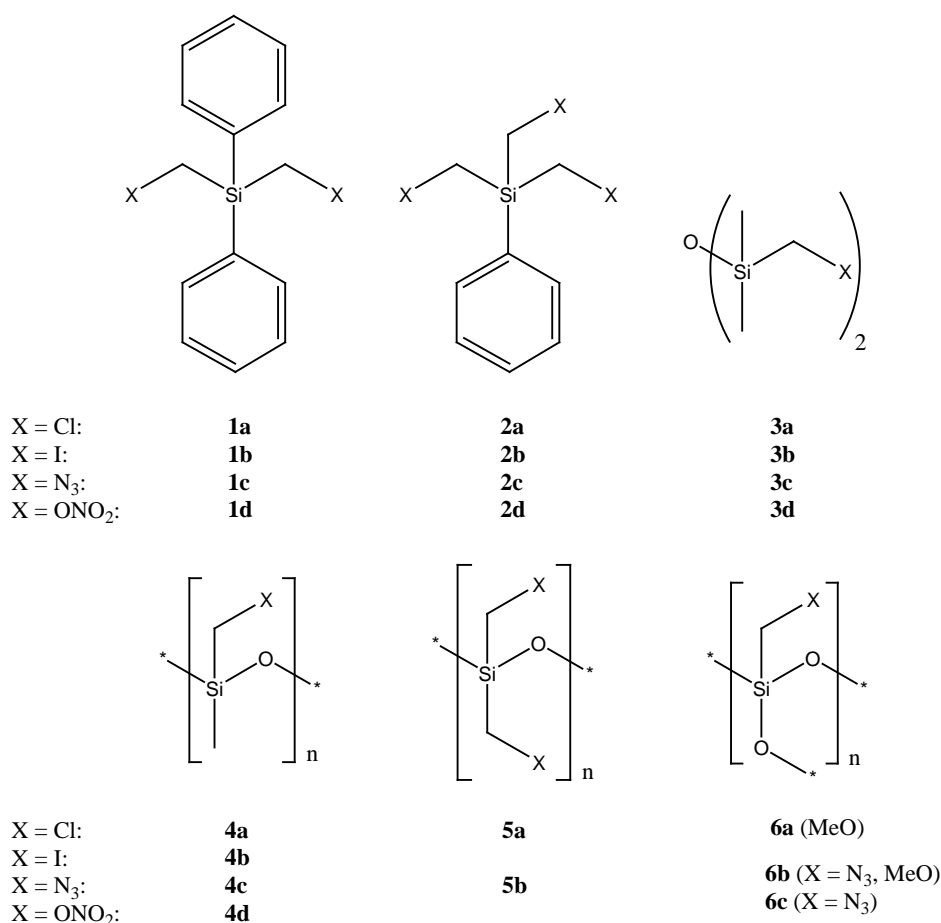
Siloxanes, from disiloxanes up to silicates, are probably the most prevalent class of silicon compounds with a high variety of structure, functionality and consequently its applications. [11] Representatively, the functionalization of surfaces should be mentioned only as one example for many easily available and powerful tool for applications and developments of siloxanes in common and industrial usage.[12,13] To the best of our knowledge, no investigations were done on applications in the topic of energetic materials, like flares, binders, coating materials etc.. The syntheses and characteristics, of several phenylsilanes and siloxanes (see Scheme 7.1) especially in terms of energetic materials, are discussed in the following.

Results and Discussion

Synthesis: Bis(chloromethyl)diphenylsilane (**1a**) and tris(chloromethyl)phenylsilane (**2a**) were synthesized by a literature known methods using the corresponding chloro phenyl silane and reacting it with *in situ* generated chloromethyl lithium ($nBuLi + BrClCH_2$).[14,15]

The compounds **1b**[16] and **2b** were obtained by Finkelstein reaction (sodium iodide in acetonitrile or acetone). Refluxing an excess of sodium azide with the corresponding chloride in acetone or acetonitrile, yield the azido analogues **1c** and **2c**. They were tried to obtain by chloride/iodide exchange using silver nitrate in acetonitrile. Precipitation of equimolare amount of silver chloride, respectively silver iodide, was observed, but the

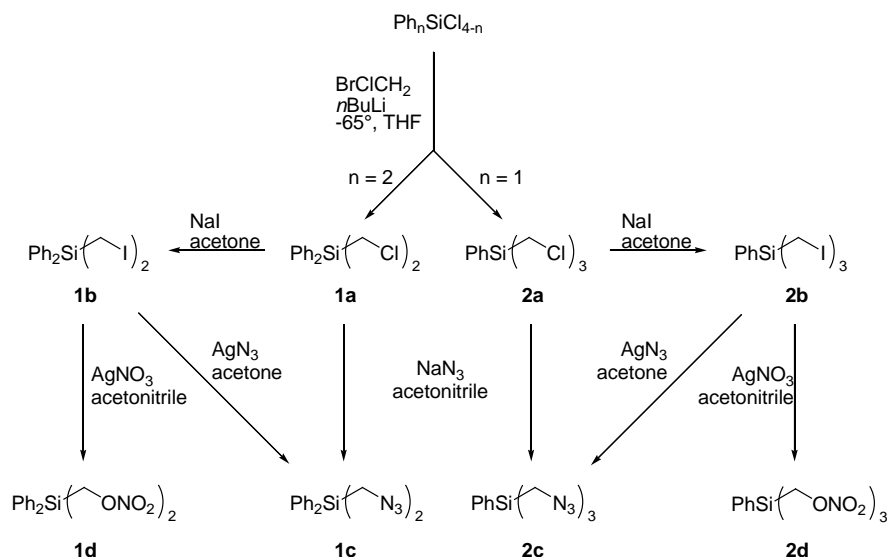
corresponding full converted nitrate ester could not be verified by NMR experiments in the case of **1d** (see NMR section). The semi-converted nitrate analogues of **2d** could be very well be observed in NMR experiments, but the fully converted nitrate **2d** could only be observed in traces and as intermediate product to following decomposition products. This case is discussed in more detail in the NMR section.



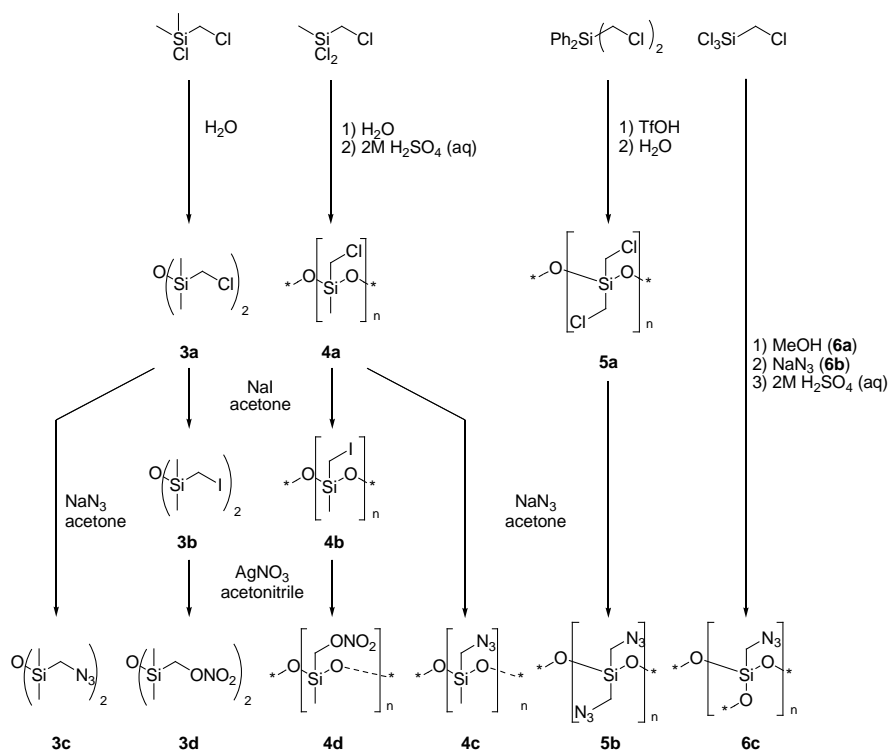
Scheme 7.1. The labelling of diphenyl and phenyl silanes with X = Cl (**1/2a**), I (**1/2b**), N₃ (**1/2c**) and ONO₂ (**1/2d**) methylene-bridged moieties, the dimeric disiloxanes O(SiMe₂CH₂X)₂ (X = Cl (**3a**), I (**3b**), N₃ (**3c**), ONO₂ (**3d**)), the two chain-like polymeric structures of [O_{2/2}SiMeCH₂X]_n and [O_{2/2}Si(CH₂X)₂]_n (X = Cl (**4/5a**), I (**4b**), N₃ (**4c/5b**), ONO₂ (**4d**)) and the methoxylated (MeO)₃SiCH₂X (X = Cl (**6a**), N₃ (**6b**)) and polymeric [O_{3/2}SiCH₂N₃] (**6c**) are shown.

The disiloxane **3a** was synthesized quantitatively by hydroxylation of commercially available chloro(chloromethyl)dimethylsilane in.[17] The iodide derivative **3b**[18] was synthesized by Finkelstein reaction *via* in acetone for 8 h. The azido compound **3c**[19] was obtained by refluxing **3a** with an excess of sodium azide at 55 °C. The synthesis of **3b** and

VII. Phenylsilanes and Siloxanes



Scheme 7.2. Syntheses of the compounds **1a-d** and **2a-d**.



Scheme 7.3. Syntheses of the compounds **3a-d**, **4a-d**, **5a/b** and **6a-c**.

3c were performed with high yields. Compound **3d** could be received by iodine exchange reaction using **3c** and treating it with an excess of silver nitrate.[6] Exclusion of light and quick purification are decisive for the outcome of the reaction. Due to rapid decomposition the compound could not be obtained free of by-products. Further information on the decomposition mechanism can be found following the discussion. The syntheses route of

the siloxanes dimer and polymers are shown in Scheme 2. The mono-functionalized polymer **4a**[20,21] was synthesized by simple hydrolysis of the commercially available dichloro(chloromethyl)methylsilane.[11] The oligomeric/polymeric chains were treated by stirring the freshly prepared compound **4a** in a 2M solution of sulphuric acid and water for three days. The growth of the molecule is always a challenge between cyclisation and chain elongation.

A comprehensive discussion of the chemical and physical influences is given elsewhere.[22] The polymerisation method used in here will lead to mainly oligomeric cyclic products (D_3 and D_4), which have the advantage in the solubility reasons and to permit a more precise comparability of experimental results and the theoretical calculations (the problem of is discussed in the theoretical section). The compound was converted into the corresponding iodide derivative by refluxing **4a** for 16 h in acetone with sodium iodide.[20,21] The azido derivative **4c** was synthesized by refluxing **4a** with an excess of sodium azide for 24 h in acetone. Storing compound **4c** for two weeks at 50 °C with or without reduced pressure leads to a colourless elastic rubber like polymer similar to commercially buyable silicone seal. Compound **4d** (also the same for the corresponding $[O_{2/2}Si(CH_2ONO_2)_2]_n$ and $[O_{3/2}SiCH_2ONO_2]_n$ polymers) was tried to be obtained by iodide nitrate exchange reaction starting from **4c** and treating it with a small excess of silver nitrate. A full conversion takes place, silver iodide precipitates quantitatively and the characteristic NMR shifting of nitratomethyl moieties is observed. Nitratomethyl derivatives decomposes rapidly to higher hydrolysed siloxane polymers, like $[O_{2/3}SiMe]_n$. The mechanism has not been studied in detail but is expected to be similar to the already investigated decomposition pathways of tetrakis(nitratomethyl)silane [23,24] and the proposed mechanism of hexakis(nitratomethyl)disiloxane [4] (Scheme 3). Most likely intermolecular interactions and not only the already discussed intramolecular interactions lead to the observed fast decomposition. For example interactions between the non-bridging nitrate oxygens O_β/O_γ to a silicon atom of another moiety, weakens the Si-R bonds of this moiety and probably followed by cleaving one of this Si-R bonds. Especially good leaving groups at the Si atom, like Ph, and high polarized Si atoms which easily coordinate to the silicon center (penta-coordination or hexa-coordination), as in disiloxanes, siloxanes and silsesquioxanes, promote the decomposition. This synthetic route was also tested for

bis(iodomethyl)-functionalized *poly*-siloxane (iodo analogues of **5a**). Substitution takes place (precipitation of AgI), but the isolation of the product fails due to rapid decomposition to silsesquioxanes and silicates (but no clear evidence of characteristic NMR signals); therefore the synthesis is not given in detail. Compound **5a** was synthesized by using **1a** as starting material and cleaving the phenyl moieties by treating **1a** with triflic acid and subsequent hydrolysis. The reaction mixture was stirred for additional three days at ambient temperature and the raw siloxane was treated by triflic acid. Polymer **5b** was synthesized in analogue manner to compound **4c** and aged by treating the polymer as already described for compound **4c**. The consistency of **5b** is less elastic and flexible in comparison to **4c**, similar to soft. The starting material for **6c** was synthesized from commercially available trichloro(chloromethyl)silane and treating with methanol.[25] The resulting trimethoxy(chloromethyl)silane (**6a**) was refluxed for 12 h in with sodium azide. After extraction of the azido derivative (**6b**), it was hydrolysed with water and 2M sulphuric acid to obtain **6c**, an in almost all common solvents insoluble, colourless solid. To obtain a colourless foil-like structure of **6c**, **6b** was diluted with a small amount of n-hexane (50–80 % of **6b**) and dropped onto a calm water surface without stirring. The solvent was evaporated over night to obtain a thin, colourless and flexible foil of **6c**.

Nuclear magnetic resonance: ^1H , $^{13}\text{C}\{^1\text{H}\}$ and $^{29}\text{Si}\{^1\text{H}\}$ NMR experiments of all mentioned compounds, and in addition $^{14}\text{N}\{^1\text{H}\}$ NMR experiments for the compounds **1–4c/d** and **5/6b** were performed (see Table 1).

In general ^1H NMR shiftings of the methylene moieties are well defined and mainly influenced on their substituent X (Cl, I, N_3 or ONO_2) and those on the silicon atom, like oxygen or phenyl. Methylene resonances in NMR experiments of the phenyl substituted compounds are shifted lower field in comparison to corresponding siloxane derivatives. The influence of the level of oxygen substitution on the silicon atom, like disiloxane (M), *poly*-siloxane (D) or silsesquioxanes (T) is low. As expected, iodide derivatives show a shifting to higher field for the methylene protons in comparison to chloro, azido and nitrate substituted molecules. In contrast to the strongest high-field shifting of the iodide derivatives (app. 2.5 ppm for phenyl, respectively 2.0 ppm for siloxanes derivatives), the nitrate analogues show the strongest low-field shifting up to app. 4.5 ppm, 4.0 ppm respectively. Chloro and azido analogues show almost the same shifting for the methylene

VII. Phenylsilanes and Siloxanes

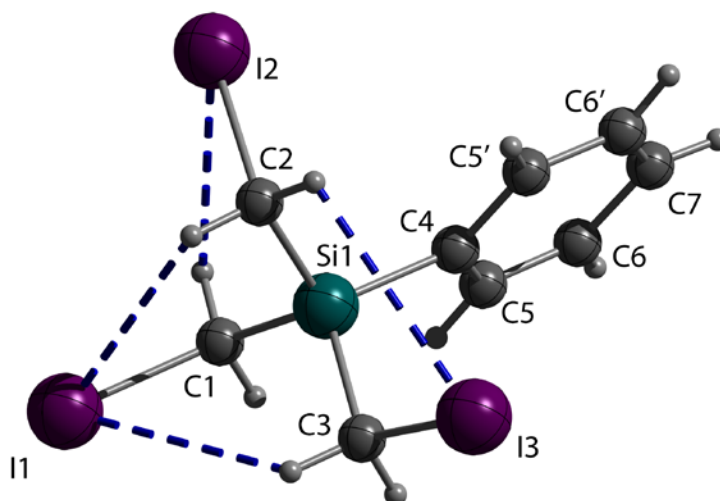
Table 7.1. NMR siftings of the SiCH₂X (X = Cl, I, N₃, ONO₂) moieties of compounds **1a–3d**, **5a/b** and **6a/b** (NMR experiments are not performed for **6c**, because of insolubility in suitable solvents); Values are given in ppm and the ¹J_{C-Si}, respectively ¹J_{Si-C}, couplings are given in parentheses in Hz (due to the resolution of the spectra small deviations can occur); Notation of the azide moieties are given by RCH₂N_αN_βN_γ.

	¹ H [a]	¹³ C{ ¹ H} [a]	²⁹ Si{ ¹ H}	¹⁴ N{ ¹ H}		
1a	3.49	26.1 (58.5)	-12.2 (73.1, 57.7)			
1b	2.65	-18.1 (57.7)	-9.4 (73.4, 58.1)			
1c	3.52	37.3 (59.4)	-14.9 (72.9, 58.3)	N _α	N _β	N _γ
				-326	-132	-171
1d	---	---	---	---		
2a	3.30	24.5 (59.3)	-8.1 (59.3)			
2b	2.51	-19.1 (59.2)	-4.6 (75.3, 59.0)			
2c	3.32	36.7 (58.1)	-9.7 (58.4)	N _α	N _β	N _γ
				-323	-132	-171
2d	~4.50	~60.5 (57.5) ^[b]	~-16.3 (71.9, 58.2) ^[b]	-39.3		
3a	2.72, 0.21	30.8 (61.2), -1.3 (62.3)	4.0 (62.7, 61.0)			
3b	2.03, 0.25	-0.3 (63.3), -12.5 (59.2)	4.6 (62.9, 58.4)			
3c	2.73, 0.19	42.3, -0.5	5.4	N _α	N _β	N _γ
				-323	-131	-173
3d	4.04, 0.23	66.4 (60.0), -0.9 (63.0)	3.2 (59.7, 63.0)	-36.0		
4a	2.72, 0.28	29.5 – 28.1 (81.0), -2.5 – -3.1 (78.9)	-28.3 – -28.6, -29.8 – -30.3			
4b	2.05, 0.41	-1.4 – -2.4, -15.0 – -16.1	-27.3 – -28.2, -29.7 – -30.3			
4c	2.77, 0.25	41.0 – 40.4, -1.5 – -1.8	-28.1 – -29.7	N _α	N _β	N _γ
				-325	-131	-173
4d	4.14 – 4.04, 0.41 – 0.30	65.1 – 64.5, -1.2 – -2.6	-25.5 – -32.7	-38.1		
5a	2.94 – 2.87	30.4 – 27.4	-35.0 – -36.0			
5b	2.76 – 2.68	38.2 – 37.8 (85.3)	-37.2 – -38.0 (85.0)	N _α	N _β	N _γ
				-326	-132	-177
6a	3.60(OMe), 2.81	50.9 (MeO), 23.6	-62.5			
6b	3.62 – 3.59, 2.89	50.9 (MeO), 36.7-35.8	-62.6	N _α	N _β	N _γ
				-327	-132	-173

[a] Resonances of phenyl moieties are given in experimental section; [b] Coupling constants were determined from SiCH₂ONO₂ moieties of the intermediate derivative PhSi(CH₂ONO₂)₂CH₂I.

moieties. But in contrast they can be clearly differed in ¹³C NMR experiments. The methylene carbons of the chloro derivatives (except **3/4a**) show resonances at app. 23–29 ppm and are consequently well separated from the corresponding signals of azidomethyl derivatives in ¹³C NMR experiments (app. 35–38 ppm). In the case of the

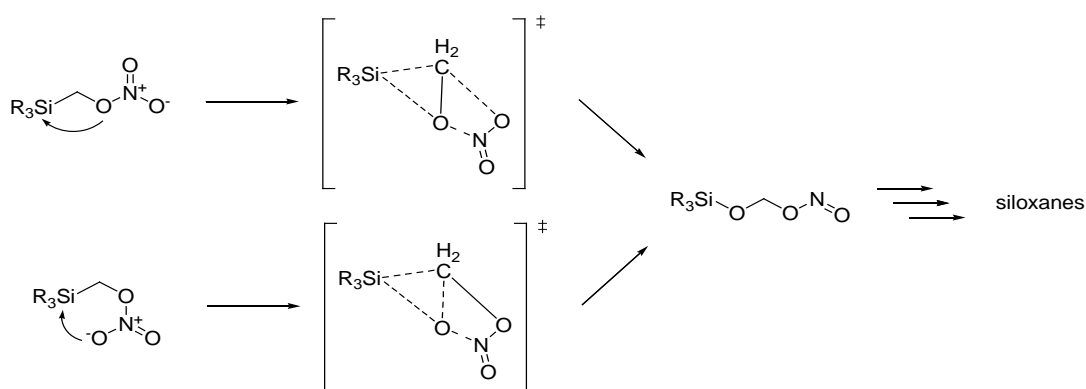
exception of **3a** and **4a**, their resonances in ^{13}C NMR spectra were found at app. 31 ppm, 29 ppm respectively, but are also well separated from their azido derivatives at 42 ppm, 41 ppm respectively. Iodide substitution leads to a strong high-field shifting, to values lower than -12 ppm (up to -19 ppm for **2b**). In addition, the increase of oxygen substitution at the silicon atom (MeO, M, D or T like substitution) results in a shift to higher field of 1–2 ppm for each introduced Si–O bond for methylene ^{13}C resonances. Methylene carbons of the discussed nitrate esters are typically found in the area of around 65 ppm in ^{13}C NMR spectra. The methyl moieties were only marginal influenced by substituents at the methylene moiety and are typically observed slightly below 0 ppm in ^{13}C NMR spectra. Resonances of ^{29}Si nuclei in NMR experiments are mainly influenced by the substituent X at the CH_2X moiety ($\text{X} = \text{Cl}, \text{I}, \text{N}_3, \text{ONO}_2$), the kind of substituent attached to the silicon atom (Me, Ph or OR) and in the case of the oligomers/polymers the surrounding bonding substitution (like in the middle of a polymeric chain/matrix, at the end of an chain or part of a cyclic oligomeric chain). These influences lead to a sometimes difficult, but very precise identification of the signals in ^{29}Si NMR experiments. The phenyl derivatives **1a–c** and **2a–c** both show a signal in the same area of slightly high-field shifted resonances between -5 ppm and -18 ppm. Disiloxanes (M), like the derivatives **3a–d**, are shifted slightly to



lower field (app. 5 ppm). The notation M (also D and T) is commonly used as description of

Figure 7.1. Labelling of the atoms in the solid state structure of **2b**. Weak intramolecular attractions influencing the twisting of the CH_2I moieties into a propeller like orientation are shown in blue dashed lines (sum of the van der Waals radii $\Sigma(\text{I},\text{H})$: 3.12 \AA , $d(\text{I}\cdots\text{H}) = 3.24\text{--}3.44 \text{ \AA}$).

siloxane chains. If nothing else is mentioned the substituents at the silicon atoms are methyl groups, as in $D_n = [O_{2/2}Si(CH_3)_2]_n$ or $D_n^R = [O_{2/2}Si(CH_3)R]_n$. ^{29}Si NMR signals of *poly*-siloxanes (D), like compounds of type **4** and **5**, were observed at higher field in the range of -18 and -38 ppm, strongly dependent of the substituent X. Influences of the length and position of one repeating unit in the polymeric chain are commonly given by the follows: D moieties near the terminus are low-field shifted in comparison to more 'central' D moieties. Cyclic oligomeric D_n (for example D_3) are strongly low-field shifted with app. -8 ppm. With increasing the ring size (D_4 , D_5 , D_6 etc.) the signal shifts to higher field and consequently into the area of the polymeric D_n resonances. Silsesquioxanes (T) like derivatives of **6a-c** were observed at higher field beginning at app. -60 and down to <-80 ppm. A problem of the polymeric silsesquioxanes is the low solubility in suitable solvents for NMR spectroscopy in solution; therefore only methoxylated or semi-methoxylated silsesquioxanes are discussed in detail in here. The influence of the substituent X at the methylene moiety is not negligible in ^{29}Si NMR resonances, but it is difficult to identify a certain pattern. The substituents of the compounds **2a-d** (range: -4.6 to app. -16.3 ppm for Cl, I, N_3 , and ONO_2) has much more influence as the disiloxanes **3a-d** (range: 3.2 to 5.2 ppm). In the case of the phenyl derivatives **1a-c** and **2a-d** the electronegativity of the substituents seems to be the main influencing factor, a minor one the sterical hindrance. In the case of siloxanes derivatives **3-6** the resonances in ^{29}Si NMR chlorido and the azido derivatives are relatively similar, but other shifting tendencies are not clearly verified without more detailed knowledge of the intramolecular interactions (halogen bonding, σ -hole interactions, electrostatic attractions etc.) as already known from other silane and siloxanes derivatives.[2,4] The $^1J_{Si-C}$ and $^1J_{C-Si}$ coupling frequencies are characteristic for each kind of carbon moiety. Methylene moieties show coupling frequencies of app. $57-59$ Hz in the cases of the phenylated silanes **1a-c** and **2a-d**, the same is true for the methylated ones. The frequencies of the $^1J_{Si-CH_2}$ are slightly smaller than the $^1J_{Si-CH_3}$ coupling frequencies. The couplings $^1J_{C-Si}$ between ^{29}Si and aromatic ^{13}C nuclei were measured with higher frequencies at about $70-75$ Hz. Even higher frequencies of app. $80-90$ Hz were found in the case of $-O-Si-$ chained ^{29}Si nuclei to methylene ^{13}C nuclei. In contrast to *poly*-siloxanes the coupling frequencies of disiloxanes are much smaller ($60-63$ Hz) but slightly larger than for the **1a-c** and **2a-d** derivatives.



Scheme 7.4. General postulated decomposition mechanisms of nitratomethyl silanes (such as **4e** and $\text{Si}(\text{CH}_2\text{ONO}_2)_4$ calculated on M06/6311G** level of theory (top, [23,24]) and postulated (bottom)).

Table 7.2. Selected bond lengths (Å), angles (°), and dihedral angles (°) for **2b** (respectively the different types A–D) with estimated standard deviations in parentheses.

2b	A	B	C	D
Distances				
Si1–C1	1.865(1)	1.873(1)	1.914(1)	1.900(1)
Si1–C2	1.886(1)	1.846(1)	1.847(1)	1.932(1)
Si1–C3	1.858(1)	1.860(1)	1.912(1)	1.878(1)
Si1–C4	1.877(1)	1.829(1)	1.862(1)	1.856(1)
C1–I1	2.130(1)	2.150(2)	2.081(1)	2.052(1)
C2–I2	2.091(1)	2.106(1)	2.104(1)	2.079(1)
C3–I3	2.148(1)	2.157(1)	2.083(1)	2.124(1)
Angles				
C1–Si1–C2	109.2(5)	109.3(6)	107.1(6)	107.6(6)
C1–Si1–C3	108.2(6)	110.3(6)	110.6(6)	110.3(6)
C1–Si1–C4	107.1(5)	105.2(6)	108.3(5)	107.7(5)
C2–Si1–C3	108.5(6)	107.4(6)	110.4(6)	110.5(6)
C2–Si1–C4	110.4(5)	111.2(6)	110.0(6)	107.9(5)
C3–Si1–C4	113.4(5)	113.5(6)	110.3(6)	112.7(6)
C5–C4–Si1	120.9(9)	123.0(9)	121.5(10)	122.1(10)
C5'–C4–Si1	119.9(9)	120.6(9)	121.9(9)	122.1(8)
Si1–C1–I1	114.3(6)	113.4(7)	114.6(6)	116.6(6)
Si1–C2–I2	115.9(6)	112.4(6)	116.2(6)	110.1(6)
Si1–C3–I3	110.1(6)	110.5(6)	111.2(6)	111.2(6)
Dihedral Angles				
C4–Si1–C1–I1	178.8(6)	–179.8(6)	179.9(6)	176.8(6)
C4–Si1–C2–I2	65.4(8)	58.9(8)	–62.3(8)	–65.3(7)
C4–Si1–C3–I3	58.7(7)	60.6(7)	–61.8(7)	–62.4(7)

The existence of **2d** was verified with regard to the frequent step by step high-field shifting of the ^{29}Si NMR resonance with ongoing I-ONO₂ exchange during the reaction (**2c**: –4.6 ppm, $\text{PhSi}(\text{CH}_2\text{I})_2\text{CH}_2\text{ONO}_2$: –8.2 ppm, $\text{PhSi}(\text{CH}_2\text{ONO}_2)_2\text{CH}_2\text{I}$: –12.1 ppm), which leads

to the conclusion that the very weak signal at -16.3 ppm is assigned to this compound. After a reaction time of 30 min only semi-converted intermediates were observed. Instantly with the first appearance of signal of the product **2d** (after 1 h), also resonances of decomposition products at > -42 ppm can be observed (related to $\text{ROSiPh}(\text{CH}_2\text{ONO}_2)\text{OR}$, minor $\text{ROSi}(\text{CH}_2\text{ONO}_2)_2\text{OR}$). Comparing the integrals of the well separated resonance populations for the aromatic phenyl protons at $7.76\text{--}7.25$ ppm (integral normalized to 5.00H) and the one of the CH_2ONO_2 moieties at $4.48\text{--}4.00$ ppm (integral of 1.52H , to compare 6.00H for **2d**) show that the CH_2ONO_2 moieties are cleaved more readily than the phenyl ones. In addition electron withdrawing moieties at the β -position to silicon increase the aptitude intramolecular phenyl migration.[26] Observations of the nitrate ester **4d** and the trials to obtain evidence of nitrate ester analogues of **5** and **6** were done in similar manner than for **2d**. Observations of the nitrate ester **4d** and the trials to obtain evidence of nitrate ester analogues of **5** and **6** were done in similar manner than for **2d**. All the above leads to the conclusion that the decomposition takes place more rapidly with the increase of the nitrate ester content and oxo-As mentioned in the synthetic section, nitratomethyl silanes are rather instable and decompose rapidly. It was possible to identify only the nitrate ester of the compounds **2–4d** by NMR experiments. Only **3d** was obtained as pure compound. Never the less **3d** decomposes within a few hours at ambient temperature under argon atmosphere. The formation of **2d** could only be verified by the observation of its intermediates in NMR experiments. The general appearance of nitrate esters during the reaction was noticed by the characteristic resonances of CH_2ONO_2 moieties in ^1H NMR at $4\text{--}4.5$ ppm, nitrate esters ^{14}N resonances at -39.3 ppm, ^{13}C signals at 63.1 ppm representatively. The existence of **2d** could be verified because the signal in the ^{29}Si NMR shifts stepwise to higher field substituents at the silicon atom. One reason can be found in the increased electron deficiency, resulting in a stronger positive charge at the silicon atom, which consequently becomes more attractive for electrostatic interactions with electron rich moieties. Due to higher polarisation and increased ionic character of Si-C bonds caused by electron withdrawing substituents at Si and C atoms, the cleavage of Si-C bonds become even more likely. Increased positive charge at the silicon atom also increases the possibility of a penta-coordination at the silicon by nucleophils, like ^-OR , ^-OH , halogenides and even the pseudohalogenide N_3^- . Penta-coordination additionally leads to a more likely cleavage of C-Si bonds and consequently decomposition derivatives of siloxanes. Former studies of

the decomposition mechanism favoure route (A) (shown in Scheme 3), but recently an additional mechanism (B) has been postulated.[4]

Crystallographic structures: Compound **2b** crystallises in the monoclinic space group Pn , with 8 molecules in the unit cell and a density of 2.528 g/cm^3 . Crystallographic data are given in Table 3.

The asymmetric unit is defined by four differently orientated molecules. The labelling of the atoms are shown in Figure 2. The representative bond lengths and angles are given in Table 2. The structure is defined by many inter- and intramolecular interactions, creating a complex network. First looking to the intramolecular molecular shaping interactions: weak intramolecular electrostatic attractions between iodine and the hydrogen atoms of a neighboured methylene moiety or more exactly with its positive surface potential leads to the twisting of the CH_2I moieties at the central Si atoms (see Figure 2). Due to the weak intramolecular interactions the CH_2I moieties are twisted more similar to a propeller-like orientation ($\text{I3}\cdots\text{HC2}$) in contrast to analogue moieties which are twisted in a swan-like orientation (swan-like orientation would be require a $\text{I3}\cdots\text{HC1}$ interaction in the structure of **2b**).[4] Due to too many intermolecular attractions in the solid state structure of **2d**, they should not be discussed all in detail. Only some attractions will be described exemplarily in the following: Intermolecular interactions can be divided into several kinds of linked networks. First of all interactions between the para-carbon (C7) of the phenyl moiety and an iodide (I2) creating an interactional dimer. The $\text{C7}\cdots\text{I2}-\text{C2H}_2$ angles are around 172° and consequently the positive surface potential is pointing to the π -electrons of the phenyl (iodine electron acceptor, phenyl π -donor).

In addition, interactions between the carbons C5 and C6 (sometimes additionally C7), respectively the electron-rich π -orbitals, of the phenyl moiety and one hydrogen of a methylene group are found. Each C1H_2 methylene moieties of the four different molecules A–D are connected to an iodine atom by intermolecular $\text{I}\cdots\text{H}$ interactions (sum of the van-der-Waal radii $\Sigma(\text{I,H})$: 3.18 \AA , $d(\text{I}\cdots\text{H}) = 3.06\text{--}3.09 \text{ \AA}$). Iodine is known to build halogen-halogen interactions,[28] which are described in the following. The iodine atoms I2, which interacts with the lipophilic phenyl back-bone, build no halogen-halogen bonds, in contrast

Table 7.3. Crystallographic data of the compound **2b**.

	2b
formula	C ₈ H ₉ SiI ₃
molecular weight	527.97
T/K	173(2)
$\lambda/\text{\AA}$	0.71073
crystal system	monoclinic
space group	<i>P n</i>
crystal size/mm	0.32x0.25x0.08
$a/\text{\AA}$	9.3107(2)
$b/\text{\AA}$	9.8931(2)
$c/\text{\AA}$	29.8234(8)
$\beta/^\circ$	98.669(2)
$V/\text{\AA}^3$	2715.70(11)
Z	8
$\rho_{\text{calc.}}/\text{g cm}^{-3}$	2.528
μ/mm^{-1}	6.953
F(000)	1816
2θ range/ $^\circ$	0.996–27.00
index ranges	$-11 \leq h \leq 9$ $-11 \leq k \leq 12$ $-38 \leq l \leq 354$
reflections collected	6161
reflection unique	8778 [$R_{\text{int}} = 0.05278$]
parameters	463
GoF	1.039
R_1/wR_2 [$I > 2\sigma(I)$]	0.0543/0.1036
R_1/wR_2 (all data)	0.0377/0.0973

to I1/3, which are highly connected to each other (see Table DDD). They create a chain-like and triangular linked network. The triangles are build out of the atoms I1C, I3C and I1A ($\Delta(\text{I1A}, \text{I3C}, \text{I1C})$, $\sphericalangle(\text{I3C}\cdots\text{I1C}\cdots\text{I1A})$: 57.8° , $\sphericalangle(\text{I1C}\cdots\text{I3C}\cdots\text{I1A})$: 60.4° , $\sphericalangle(\text{I3C}\cdots\text{I1A}\cdots\text{I1C})$: 61.8°). The chain-like interactions are mainly built out of alternated I1 and I3 chain links. The I \cdots I distances are between 3.98–4.16 \AA , which is slightly above the van-der-Waals radius (I,I: 3.96 \AA), but the interactions are well defined by their donor-acceptor angles (see Table 4). Many of the aromatic CH protons shows long-range electrostatic attractions to 2–5 iodine atoms ($d(\text{I}\cdots\text{H}_{\text{arom.}}) = 3.29\text{--}3.46 \text{\AA}$; $\sphericalangle(\text{C}\text{--}\text{I}\cdots\text{H}) = 86.8\text{--}115.2^\circ$, $\sphericalangle(\text{I}\cdots\text{H}\text{--}\text{C}_{\text{arom.}}) = 130.2\text{--}168.1^\circ$). The aromatic ring and the connected iodine atoms are, with some slightly deformations, in plane.

Table 7.4. Distances (Å) and angles (°) of I...I halogen interactions of the solid state structure of **2b** (I_D: electron donor; I_A: electron acceptor, sum of the van-der-Waals radius Σ(I,I): 3.96 Å).[27]

Interaction (I _D ---I _A)	Distances	∠(C-I _D ...I _A)	∠(I _D ...I _A -C)
I1B---I3B	4.104	114.5	168.3
I1B---I3A	4.001	102.4	171.6
I1A---I3A	4.161	113.6	166.4
I1A---I3C	3.976	121.4	176.6
I1C---I3C	4.139	113.7	167.4
I1A---I1C	4.081	114.9	171.5
I1D---I3D	4.051	120.2	162.6
Δ(I1A,I3C,I1C)	∠(I1A---I3C---I1C)	∠(I1C---I1A---I3C)	∠(I3C---I1C---I1A)
	57.8	60.4	61.8

Sensitivity and physical properties: The thermal stability was estimated by DSC experiments and in general it was found to be only minor dependent by the type and construction of the back-bone and the amount of energetic moieties at the same silicon atom. The decomposition temperatures T_{dec} of azidomethyl containing silanes compounds known in the literature[3], and of **2/3/4c** are all in a similar range at app. 135°C ±5 °C (see Table 7.5). The same is found for the nitratomethyl silanes at a temperature of app. 95 °C ±10 °C in the literature. The decomposition temperatures of the nitratomethyl derivatives discussed in here could not determined without fail, because of rapid decomposition at ambient temperature.

The sensitivities were determine by friction and impact testing apparatus according to BAM.[29] Due to the impurities and decomposition of the other compounds, only the compounds **1c**, **2c**, **3c/d**, **4c**, **5b** and **6b/c** were measured. As already mention in the literature, the amount of energetic moieties is the most important factor concerning friction and impact sensitivity.[2,3] In addition, nitratomethyl derivatives are much more sensitive towards mechanical stimuli than its azidomethyl analogues.[3,4] The aliphatic or aromatic substituents on the silicon atom show influence towards the mention sensitivities, observed at the values obtained from the phenyl derivatives **2/3c** and the values of their methyl analogues (bis(azidomethyl)dimethylsilane: IS = >9 J, FS = >60 N; tris(azidomethyl)-methylsilane: IS = <1 J, FS = <5 N)[3]. In the case of the nitrate derivative similar tendencies were expected. The only obtained value of a nitratomethyl derivative which is mentioned in here, compound **3d**, shows less sensitivity concerning mechanical stimuli than its azido analogue, which is not comprehensible. The reason is probably based on contaminations by

decomposition products, although the compound was only slightly decontaminated tested by NMR experiments (less than 10%).

It was tested, if different composition of cyclic, chain and in addition shorter or elongated fragments of compound **4c** show a significant influence to the sensitivities concerning mechanical and thermal stimuli. As result neither the structure of the polymer (cyclic or chain-like), nor the length, respectively rubber or oil-like consistence, of the polymer has a significant influence towards the tested thermal and mechanical stimuli, even so the method of polymerisation (acidic, basic catalysation or by evaporating off water). The only difference was found by thermal treating of oil-like polymers, where smaller fragments evaporated (derivatives of D₃, D₄, M₂O etc.). The content of azidomethyl moieties was variegated by adding non-functionalised dimethylsiloxane moieties into the polymer by addition of dichlorodimethylsilane during hydrolysatation or by addition of bought D₃ during the elongation process. Up to a content of 50% dimethylsiloxane moieties no significant changes concerning their behaviour towards thermal and mechanical stimuli were observed.

The increasing of the azidomethyl moieties per silicon atom leads to compound **5b**. It has increased sensitivities concerning mechanical stimuli (IS = <1 J, FS = <5 N), but almost the same thermal stability (T_{dec} = 137.4 °C) in comparison to compound **4c**, with only one azidomethyl moiety per silicon atom (T_{dec} = 138.1 °C).

Energetic properties: The energetic properties of the compounds **1c/d**, **2c/d**, and **3c/d** were calculated by the EXPL05 version 6.01 computer code.[30] The input energies of formation were calculated out off the computed heat of formation, which were obtained by calculations on CBS-4M level of theory. In the case of the compounds **4c/d** only the cyclic trimetric structure were calculated on CBS-4M level of theory, because computing time. The compounds **5b** and **6b** and its corresponding nitrate ester were not performed, because of the time consuming efforts in comparison to its profit, even for the trimeric analogues. The heat of formations were computed by the atomization method (Equation (1)) by using the program Gaussian09 revision C.01.[31] The obtained enthalpies of formation in gas phase $\Delta H_m(g)$ were converted into their enthalpies of formation in solid state $\Delta H_m(s)$ by using the

VII. Phenylsilanes and Siloxanes

Table 7.5. Energetic properties of the compounds **1c/d-3c/d** and the trimeric **4c/d**.

	1c	1d	2c	2d	3c	3d	4c	4d
formula	C ₁₄ H ₁₄ N ₆ Si	C ₁₄ H ₁₄ N ₂ O ₆ Si	C ₉ H ₁₁ N ₉ Si	C ₉ H ₁₁ N ₃ O ₉ Si	C ₆ H ₁₆ N ₆ O ₆ Si ₂	C ₆ H ₁₆ N ₂ O ₇ Si ₂	C ₆ H ₁₅ N ₉ O ₃ Si ₃	C ₆ H ₁₅ N ₃ O ₁₂ Si ₃
M /g·mol ⁻¹	294.39	334.36	273.33	333.28	244.40	284.37	345.50	405.45
IS /J [a]	>40	---	<2	---	>40	>40 ^[p]	<8	---
FS /N [b]	<108	---	<40	---	<60	<72 ^[p]	<72	---
N /% [c]	28.55	8.38	46.12	12.61	34.39	9.85	36.49	10.36
Ω _{CO2} /% ^[d]	-201.09	-148.34	-149.26	-79.21	-150.57	-95.65	-104.19	-53.27
T _{dec} /°C ^[e]	138.4	---	139.1	---	135.8	---	138.1	---
Δ _f H ^o _M	1990.0	-723.8	3139.0	-1152.4	-1261.0	-4013.9	-2694.3	-5345.9
/kJ·kg ⁻¹ ^[f,g]					(-1263.2)		(-2696.4)	
Δ _f U ^o	2074.2	-650.3	3229.7	-1066.9	-1144.3	-3904.9	-2597.5	-5254.2
/kJ·kg ⁻¹ ^[g,h]					(-1146.5)		(-2599.6)	
EXPLO6.01 values (detonation^[q], ρ = 1.0 cm³ [o]):								
-Δ _{ex} U ^o	3463	4625	4452	5241	3051	4982	2872	4285
/kJ·kg ⁻¹ [i]					(3049)		(2870)	
T _{det} /K ^[k]	2203	2888	2876	3706	2029	3024	2168	3135
					(2028)		(2167)	
p _{CJ} /kbar ^[l]	38	46	55	73	45 (45)	58	35 (35)	51
V _{det} /m·s ⁻¹ ^[m]	3867	4161	4506	5054	4130	4607	3644	4223
					(4129)		(3643)	
V ₀ /L·kg ⁻¹ ^[n]	533	596	650	749	627 (627)	691	561 (561)	640
EXPLO6.01 values (isobaric combustion^[r], ρ = 1.0 cm³ [o])^[r]:								
T _c ^[s] (neat)	3142	3142	3193	3221	3145	3150	3126	3122
I _{sp} ^[t] (neat)	252	251	255	255	252	251	246	240

[a] impact sensitivity (according to BAM method 1 of 6 with drophammer); [b] friction sensitivity (according to BAM method 1 of 6 with friction tester); [c] nitrogen content; [d] oxygen balance calculated for CO₂; [e] Decomposition temperature measured by DSC (onset); [f] calculated heat of formation (CBS-4M); [g] Decomposition temperature used for the calculations were estimated with 130 °C (azido derivatives **1c-4c**) and 100 °C (nitrate derivatives **1d-4d**); additionally the calculated values with the experimental decomposition temperatures are given in parentheses below the estimated values; [h] energy of formation; [i] all values were computed with a density of 1.0 g/cm³; [j] energy of explosion; [k] detonation temperature; [l] detonation pressure at the Chapman-Jouguet point; [m] detonation velocity; [n] assuming volume of gaseous products; [o] estimated density; [p] Sensitivities measured by slightly impure material, see text; [q] detonation settings: BKW EOS constants and co-volumes of BKWG-S, initial temperature 3600 K, Model 4, reaction products standard run; [r] isobaric combustion settings: chamber pressure 7 MPa, initial temperature 3300 K, ambient pressure 0.1 MPa, expansion through the nozzle, reaction products standard run, [s] chamber temperature T_c of the neat compound in the combustion chamber; [t] specific impulse I_{sp} of the neat compound.

$$\Delta_f H^o_M(g) = H^o_M(g) - \sum H^o_{atoms} + \sum \Delta_f H^o_{atoms} \quad (1)$$

$$\Delta U_M = \Delta H_M - \Delta nRT \quad (2)$$

Δn = changes of moles of gaseous components

Trouton's rule.[32] The molar standard enthalpies of formation were converted into the molar solid state energies of formation by using Equation (2).

Because of the deficiency of some information concerning accurate input values for computing the energetic parameter (melting, boiling decomposition point and density), the densities of each discussed compound are defined by 1.0 g/cm³. In the case of decomposing compounds like 1d–4d the boiling, respectively the decomposition point is defined by 25 °C, and for all azido derivatives 1c–4c they were estimated with 130 °C. All components were assumed to be liquids at ambient conditions. Consequently, the boiling, respectively the decomposition points were used as input for calculating the energies. Never the less the influences of the boiling and decomposition point for the calculations are low as shown elsewhere and can be also seen in the computed values of 3c with the estimated $T_{\text{dec,est.}} = 130$ °C and the experimental value $T_{\text{dec}} = 136$ °C.[4]

The studied compounds show low nitrogen contents, except 2c, which is higher than 45 %. The oxygen balances are as expected for the azido derivatives very low and low for the nitrate derivatives. The high carbon content of the two phenyl azido derivatives leads to a positive heat of formation and energy of formation (endothermic). In general the heat of formation and energy of formation is lower for azido derivatives in comparison to their nitrate analogues, due to the high positive heat of formation/energy of formation of the azido moiety.

The energy of explosion, calculated with the EXPL05 version 6.01 computer codes is lower for azido derivative and low for siloxane derivative. The same tendency is found for the heat of detonation values. The detonation pressures at the Chapman-Jouguet point are very low as a consequence of the lack of oxygen/oxidizers, which are necessary for a complete oxidation to CO₂, SiO₂, H₂O. This is also the reason for the low detonation velocities. The generated gas volume during the decomposition is lower for silicon compounds towards the carbon analogues, due to the solid SiO₂ and Si₃N₄ instead of gaseous CO₂ and N₂. The gas volumes are higher for nitrate derivatives compared to their azido analogues and also increase by increasing number of azido or nitrate moieties per molecule.

As exemplarily shown in Table 6 for a azido and a nitrate derivative (**2c** and **2d**) the main decomposition product of the highly oxygen deficient neat compounds were computed to be in both cases elemental carbon (C, carbon black), nitrogen (N₂), ammonia (NH₃),

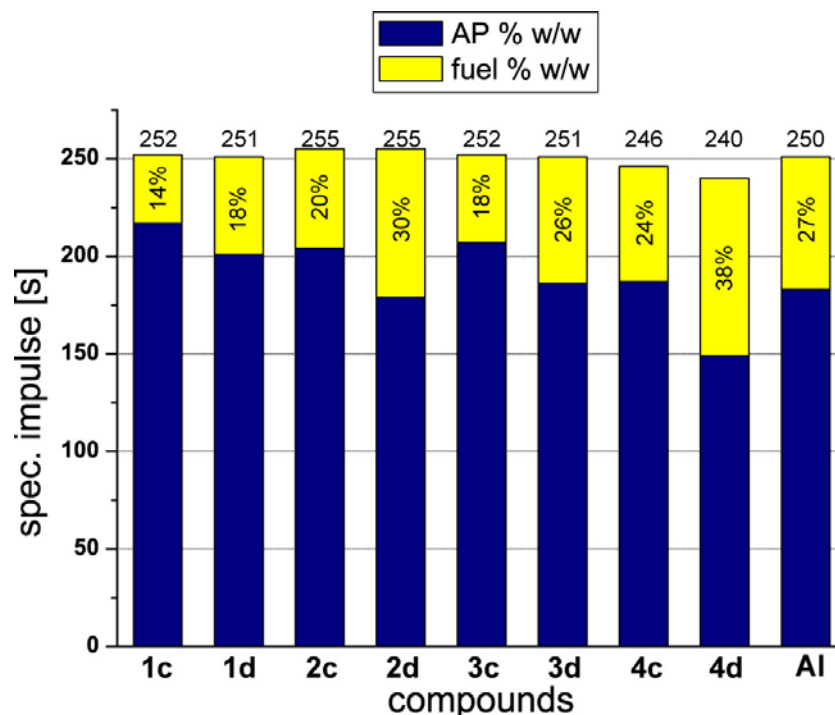


Figure 7.2. Specific impulse of the compounds **1c/d-4c/d** (in seconds) computed by EXPL05 version 6.01 with an oxygen balance of $\sim 0\%$ (slightly above 0%); mixture of aluminium and AP is given as bench mark (amount of fuel is given in yellow and AP in blue and in %w/w).

methane (CH_4), ethane (C_2H_6), hydrogen cyanide (HCN) and hydrogen (H_2). In the case of the presents of oxygen like in the nitrate or siloxane derivatives additional decomposition products were estimated: carbon monoxide/dioxide (CO/CO_2), water (H_2O), formic acid (CH_2O_2), formaldehyde (CH_2O) and methanol (CH_3OH). In contrast to carbon, the silicon decomposes almost completely to silicon nitride (Si_3N_4) in the case of oxygen deficient compounds and to silicon dioxide (SiO_2) in the case of the presents of oxygen, which is in good agreement with silicons high oxo- and azophilicity. In the cases of the addition of $\text{O}_2(\text{g})$, carbon oxidized mainly to CO and only in the second order to CO_2 . Due to the high temperatures during decomposition with oxygen addition leads to a strongly shift of the Boudouard reaction to CO . The same reason is given for the appearance of molecular gaseous SiO , which is generated by an equilibrium with elemental silicon and SiO_2 at high temperatures (similar to the Boudouard reaction), and reacts to its polymeric form $(\text{SiO})_x$ by fast cooling and further oxidation to SiO_2 at 'field conditions' (atmosphere, ambient temperature and pressure). Solid oxidizers like AN, lead to a complete oxidation of the components like the reaction of a great excess of gaseous O_2 (fuel / oxidizer:

10 / 90 %w/w). Surprisingly in all calculation for the azido derivatives SiO_2 was mainly calculated in liquid phase, in contrast to the cases for the nitrate derivatives were it was calculated in solid state, although the detonation temperatures are almost equal (T_{det} : **2c**: 5368 K, **2d**: 5149 K). The detonation pressure differs from each compounds by 20 kbar, consequently the solid state is preferred for the nitrate derivatives (lower T_{det} and higher p_{CJ}). In all calculations with the presents of oxygen or AP (except for AN) relatively high amount of NO were formed, unless the available amount of oxygen.

The compounds **1c–4c**, **3d**, **5b** and **6c** were tested by treating it with an open flame. It was performed by putting a compound on a metal spatula direct into a flame or fast heating in an open glassy capillary tube without contact to a flame (flame of a lighter was used as heat source, amount of 3–5 mg). Compound **1c** was burning relatively slow with a bright white flame. **3c** deflagrates with a bright flash. Polymer **4c** fulminates with flash and a cloud of colourless powder (SiO_2). The silsesquioxane **6c** was tested as two different kinds, first of all as colourless powder and second as transparent foil. In the first case **6c** (powder) decomposes slowly without flame to a colourless porous solid (SiO_2). In the second case the foil-like compound was rapidly burned by producing a cloud of fine powder of SiO_2 and a bright white flame. The nitrate ester **3d** detonates heavily in both descript cases of heating. In the same way the azido compounds **2c** and **5b** decomposes heavily. The polymeric compounds **4c** (also the derivatives with poly-dimethylsiloxane) and both modifications of **6c** were suitable as additive for flares, especially for silicon containing flares (for examples IR emitting flares), due to its high combustion temperatures and its IR emitting cloud of SiO_2 particles. In addition, composites for busters, where these compounds can be used as fuel, could be promising. The reason is especially found in the higher combustion temperature of sila-derivatives in contrast to carbo-derivatives.[4] The parameter for propellants is given in the specific impulse I_{sp} , which is proportional to the square root of the temperature in the combustion chamber (T_c) of a buster engine and inverse proportional to square root of the average molare mass of the decomposition products (M_{pro}).

The specific impulse values computed for the compounds **1c/d–4c/d** by using the EXPL05 version 6.01 computing code are shown in Figure 3. All tested compounds **1c/d–3c/d**, except **4c/d**, show equal or even higher I_{sp} as the bench mark of Al/AP (250 s). Inhere it is clearly seen, that the increased saturation of Si by substituted oxygen reduces

the energy releases, the chamber temperature and consequently the impulse to the lowest computed values in this testing row.

$$I_{sp} \propto \sqrt{\frac{T_c}{M_{pro}}}$$

To take a closer look to the comparison between carbon and silicon derivatives in the fact of their I_{sp} values, it can be seen that the higher chamber temperature of the silicon derivatives (ΔT_c : 60–120 K) is predominant towards the carbon derivatives and its lower molar mass of the combustion products (Figure 4). In contrast to the inferior energetic parameters in the topic of the use as explosives, silanes are superior to the carbon analogues concerning the energetic values as fuel in ammonium perchlorate based propulsion setups. The specific impulse was calculated with optimized oxygen balances (Ω_{CO_2} as positive and close as possible to 0%) by formal adding AP. A mixture of aluminium and AP was calculated the same way as for the other mixtures as bench mark (Al/AP: 27/73 %w/w, I_{sp} : 250 s, T_c : 4722 K).

In general the sila derivatives need slightly more oxidizer than their carbon derivatives, because of the Boudouard equilibrium of C, CO, CO₂ and its analogue process for Si, SiO and SiO₂, which has a much inferior importance in combustion processes than the Boudouard equilibrium. The combustion chamber temperature for the Al/AP mixture (~4700 K) was computed to be much higher as for all silicon and carbon derivatives calculated inhere (~3100 ±100 K). Due to the low amount of gaseous products the impulse of Al/AP is in the lower range of the compounds computed in here. Nevertheless the addition of common additives like binders, plasticiser etc. increases the amount of gas producing fuels and consequently the I_{sp} . A standard mixture of Al/AP and additives (70 % AP, 16 % Al, 6 % polybutadiene-acrylic acid, 6 % polybutadiene-acrylonitrile, 2 % bisphenol A ether, %w/w), which was used as solid rocket propulsion of the space shuttle missions. The computed I_{sp} value of this mixture (260 s) is as expected higher than for AP neat (157 s) and the 27/73 Al/AP mixture (250 s). The value of ~260 s is reached by several mixtures calculated inhere, but due to its known high sensitivity towards thermal and mechanical stimuli,[1,2,3,4] they are no promising candidates as pure mixtures with AP, but some of them can be probably used as additive to reduce the carbon content, which will lead to higher combustion temperatures and to modified emission of electromagnetic wavelength (pyrotechnical

application). The good compounds could be the *poly*-(azidomethyl)siloxanes based on **4c** with or with out addition of *poly*-dimethylsiloxane or *poly*-silsesquioxanes based on **6c** or methyl-*poly*-silsesquioxanes. The substitution of aluminium by silicon containing compounds also reduces the environmental pollution by toxic aluminium species (plant poisoning by hydroxo- and oxo-aluminium derivatives)[33]. The consistences of poly-silsesquioxanes make them promising candidates as reactive casts.

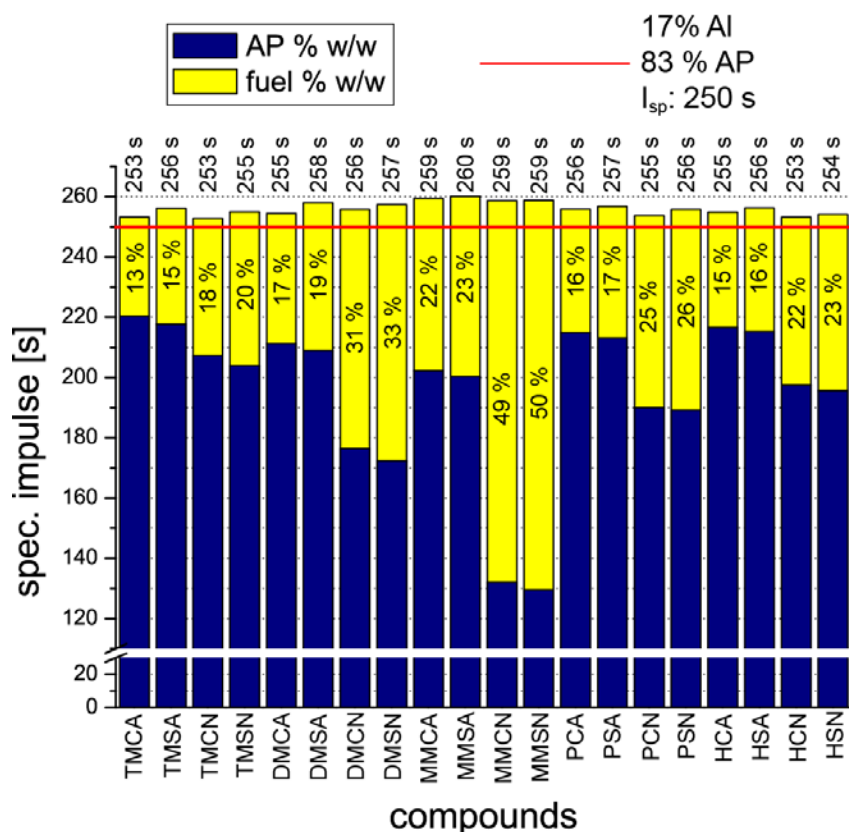


Figure 7.3. Specific impulse of several azido- and nitratomethyl silanes and its carbon analogues were computed by EXPL05 version 6.01 with an oxygen balance of $\Omega = \sim 0-1\%$ and a mixture of aluminium and AP ($\Omega = 1.2\%$) is given as bench mark (red line). The amount of fuel is given in yellow and AP in blue and in %w/w (area between 30 to 100 s is skipped for clarity). TMCA ((azidomethyl)trimethylmethane), TMSA ((azidomethyl)trimethylsilane), TMCN ((nitratomethyl)trimethylmethane), TMSN ((nitratomethyl)trimethylsilane), DMCA (1,1-bis(azidomethyl)dimethylmethane), DMSA (1,1-bis(azidomethyl)dimethylsilane), DMCN (1,1-bis(nitratomethyl) dimethylmethane), DMSN (1,1-bis(nitratomethyl)dimethylsilane), MMCA (1,1,1-tris(azidomethyl)methylmethane), MMSA (1,1,1-tris(azidomethyl)methylsilane), MMCN (1,1,1-tris(nitratomethyl)methylmethane), MMSN (1,1,1-tris(nitratomethyl)methylsilane), PCA (1,1-bis(azidomethyl)cyclopentane), PSA (1,1-bis(azidomethyl)-1-sila-cyclopentane), PCN (1,1-bis(nitratomethyl)cyclopentane), PSN (1,1-bis(nitratomethyl)-1-sila-cyclopentane), HCA (1,1-bis(azidomethyl)cyclohexane), HSA (1,1-bis(azidomethyl)-1-sila-cyclohexane), HCN (1,1-bis(nitratomethyl)cyclohexane), HSN (1,1-bis(nitratomethyl)-1-sila-cyclohexane). The nomenclature was used for comparability.

VII. Phenylsilanes and Siloxanes

Table 7.6. The main decomposition products for the compounds (exemplarily shown only for **2c** and **2d**) as neat compound and with stoichiometrical amount of gaseous oxygen.^[a]

	2c [b]			2d [b]		
	neat compound			neat compound		
O₂(g) addition ^[c]	C(s, gr) = 8.48825 31.05427 N ₂ = 2.616662 9.573059 NH ₃ = 2.405295 8.799774 H ₂ = 1.018276 3.725365 CH ₄ = 0.3760539 1.375793 Si ₃ N ₄ (s) = 0.3333332 - 1.2195 C ₂ H ₄ = 0.05382392 0.1969149 HCN = 0.02804857 0.1026157			C(s, gr) = 6.0379 18.11666 H ₂ O = 3.767468 11.30425 CO = 2.299177 6.898656 N ₂ = 1.284028 3.852713 SiO ₂ (s) = 0.9999962 3.000478 H ₂ = 0.7059735 2.118266 NH ₃ = 0.3618129 1.085616 CH ₂ O = 0.2268968 0.6808014 CO ₂ = 0.2258309 0.6776031 HCN = 0.06994518 0.2098698 CH ₄ = 0.0526976 0.1658363 C ₂ H ₄ = 0.02864544 0.08595034 CH ₃ OH = 0.02645073 0.07936514 CH ₂ O = 0.001238048 0.00371475 NO = 0.0001855455 0.0005562723		
	CO = 1.082395 16.80276 N ₂ = 0.5583996 8.66842 H ₂ = 0.3257591 5.056983 H ₂ O = 0.3130409 4.859548 SiO ₂ (l) = 0.1026977 1.594246 HCN = 0.05995134 0.9306657 CO ₂ = 0.0456393 0.7084901 NH ₃ = 0.02967176 0.4606151 Si(l) = 0.02202418 0.3418964 CH ₂ O = 0.01208303 0.1875731 SiO = 0.009203014 0.1428647 CH ₄ = 0.003513209 0.05143321 NO = 0.002491827 0.03868234 CH ₂ O = 0.001880718 0.02919568 C ₂ H ₄ = 0.001349268 0.02094561 CH ₃ OH = 0.001037282 0.01610244 O ₂ = 0.0001498747 0.002326608 Si = 0.0001264126 0.001962389			CO = 1.422708 15.52303 H ₂ O = 0.8612282 9.396774 CO ₂ = 0.2935465 3.202857 N ₂ = 0.2849716 3.102996 SiO ₂ (s) = 0.1914492 2.088883 H ₂ = 0.1504452 1.641492 CH ₂ O = 0.05463918 0.5961626 NH ₃ = 0.01013458 0.1105774 HCN = 0.009077254 0.09904101 SiO ₂ (l) = 0.005835122 0.06366643 NO = 0.004842659 0.05283776 O ₂ = 0.002001944 0.02184301 CH ₂ O = 0.000998236 0.01089165 SiO = 0.0006639308 0.007244083 CH ₃ OH = 0.0005704952 0.006224616 CH ₄ = 0.0003486568 0.003804159		
AN addition ^[d]	excess of O ₂ (g) fuel / O ₂ ratio: 10 / 90 (%ow / wv) O ₂ = 0.8106778 23.09832 CO ₂ = 0.1155614 3.292646 H ₂ O = 0.0706208 2.012171 N ₂ = 0.04501029 1.282461 NO = 0.02554116 0.7277343 SiO ₂ (l) = 0.01282513 0.3654215			O ₂ = 0.8998793 25.58069 CO ₂ = 0.09499625 2.70044 H ₂ O = 0.05805326 1.650269 N ₂ = 0.01334726 0.37942 SiO ₂ (s) = 0.01055524 0.3000517 NO = 0.004971056 0.1413112		
	H ₂ O = 2.122257 24.26341 N ₂ = 1.134269 12.96791 CO ₂ = 0.3244393 3.709261 SiO ₂ (s) = 0.03839993 0.4390201 CH ₂ O = 0.01171966 0.133989 CO = 0.009440287 0.1079293 O ₂ = 0.001949903 0.02229293 NH ₃ = 0.0001770234 0.002023879 H ₂ = 0.000157478 0.00180042			H ₂ O = 2.122257 24.26341 N ₂ = 1.134269 12.96791 CO ₂ = 0.3244393 3.709261 SiO ₂ (s) = 0.03839993 0.4390201 CH ₂ O = 0.01171966 0.133989 CO = 0.009440287 0.1079293 O ₂ = 0.001949903 0.02229293 NH ₃ = 0.0001770234 0.002023879 H ₂ = 0.000157478 0.00180042		
AP addition ^[e,f]	Composition of combustion products in chamber: Products mol/mol mol/kg Mol % H ₂ O = 1.691303 E00 1.318396 E01 36.906 HCl = 9.351504 E-01 7.289638 E00 20.407 N ₂ = 6.289212 E-01 4.902535 E00 13.724 CO ₂ = 6.222170 E-01 4.850276 E00 13.578 CO = 2.318942 E-01 1.807650 E00 5.0605 O ₂ = 1.496483 E-01 1.166531 E00 3.2657 OH = 1.340821 E-01 1.045190 E00 2.926C H ₂ = 7.912105 E-02 6.167605 E-01 1.7266 NO = 4.719737 E-02 3.679106 E-01 1.030C SiO ₂ (l) = 4.242571 E-02 3.307148 E-01 0.925E SiO = 1.425411 E-02 1.111129 E-01 0.3111 SiO ₂ = 4.246531 E-03 3.310234 E-02 0.0927 Cl ₂ = 1.920883 E-03 1.497358 E-02 0.041E SiO ₂ (s) = 3.150415 E-04 3.360397 E-04 0.0009			Composition of combustion products in chamber: Products mol/mol mol/kg Mol % H ₂ O = 1.747296 E00 1.313530 E01 37.221 HCl = 9.245681 E-01 6.950441 E00 19.695 CO ₂ = 7.399203 E-01 5.562352 E00 15.762 N ₂ = 5.131654 E-01 3.857721 E00 10.931 CO = 2.626812 E-01 1.974706 E00 5.5957 O ₂ = 1.687720 E-01 1.268743 E00 3.5952 OH = 1.412627 E-01 1.061942 E00 3.0092 H ₂ = 7.786056 E-02 5.853168 E-01 1.658E SiO ₂ (l) = 5.289640 E-02 3.976487 E-01 1.1268 NO = 4.528362 E-02 3.404197 E-01 0.964E SiO = 1.390819 E-02 1.045548 E-01 0.2963 SiO ₂ = 4.350475 E-03 3.270470 E-02 0.0927 Cl ₂ = 1.908773 E-03 1.434920 E-02 0.0407 SiO ₂ (s) = 3.150415 E-04 3.360397 E-04 0.0009		
	Composition of combustion products at the nozzle exit: Products mol/mol mol/kg Mol % H ₂ O = 1.831745 E00 1.427872 E01 41.714 HCl = 9.378628 E-01 7.310781 E00 21.357 CO ₂ = 8.500410 E-01 6.626197 E00 19.357 N ₂ = 6.512753 E-01 5.076789 E00 14.831 SiO ₂ (s) = 6.099503 E-02 4.754654 E-01 1.389C O ₂ = 4.543601 E-02 3.541805 E-01 1.0347 OH = 4.694872 E-03 3.659723 E-02 0.106E CO = 4.070204 E-03 3.172785 E-02 0.0927 NO = 2.489124 E-03 1.940309 E-02 0.0567 H ₂ = 2.016563 E-03 1.571942 E-02 0.045E Cl ₂ = 5.646938 E-04 4.401873 E-03 0.012E SiO ₂ (l) = 1.278997 E-05 9.969975 E-05 0.000C SiO ₂ = 1.037741 E-07 8.089345 E-07 0.000C SiO = 2.255724 E-08 1.758371 E-07 0.000C			Composition of combustion products at the nozzle exit: Products mol/mol mol/kg Mol % H ₂ O = 1.888716 E00 1.419842 E01 42.079C CO ₂ = 9.962664 E-01 7.489433 E00 22.196C HCl = 9.272331 E-01 6.971227 E00 20.660C N ₂ = 5.344587 E-01 4.017794 E00 11.9073 SiO ₂ (s) = 7.155386 E-02 5.379062 E-01 1.5942 O ₂ = 5.184024 E-02 3.897090 E-01 1.1550 CO = 6.335117 E-03 4.762425 E-02 0.1411 OH = 6.038722 E-03 4.539610 E-02 0.1345 NO = 2.697038 E-03 2.027499 E-02 0.0601 H ₂ = 2.007341 E-03 1.507341 E-02 0.0395 Cl ₂ = 5.262912 E-04 3.956395 E-03 0.0117 SiO ₂ (l) = 6.027551 E-05 4.531212 E-04 0.0013 SiO ₂ = 1.757187 E-07 1.320965 E-06 0.0000 SiO = 8.572980 E-08 6.444739 E-07 0.0000		

[a] EXPL05 version 6.01 calculations with the following settings (settings as in Table 7.5): Running mode 'Detonation', product activity modulation 'Model 3', reaction products 'main products', BKW EOS constants and co-volumes 'BKWG-S (default)'; [b] First column of numbers are the %mol/mol values of decomposition of 1 mol of the compounds/mixtures; second column of numbers are the mol/kg ratio by decomposing 1 kg of compounds/mixtures; [c] Calculated with addition of equimolar amount of gaseous O₂; [d] Calculated with addition of equimolar amount of ammonium nitrate (AN); [e] Amount of ammonium perchlorate (AP) was determined by empirical methods to a oxygen balance of slightly above 0 % and the following settings of the EXPL05 code: isobaric combustion, all products (advanced run), chamber pressure 7 MPa, initial temp. 3500 K, expansion through the nozzle, against ambient pressure (0.1 MPa), equilibrium expansion, Model 1; [f] For successful running calculations all combustion products with a molar content of less than 10⁻¹⁰ mol were neglected by the calculations, in addition out of our experience and to ensure a successful calculation run, only the following products were permitted: Cl₂, CO, CO₂, H₂, H₂O, HCl, N₂, NO, O₂, OH, SiO, SiO₂(g), SiO₂(l), SiO₂(s).

Conclusion

Several new compounds and syntheses of energetic silanes and its precursors were shown in detail. Especially the nitrate derivatives decompose rapidly, and some thoughts about their decomposition behaviour were done. As result it can be mention, that phenyl- and oxo-nitratomethylsilanes decomposes more readily than methyl-substituted silicon derivatives and azidomethyl analogues. First information was collected for the polymeric siloxane and silsesquioxane derivatives for preparation different modifications of the material and its application fields. The azidomethyl poly-siloxanes were proven to be good candidates as binders in pyrotechnical mixtures. Azidomethyl derivatives are as well high preferment fuel/additives for ammonium perchlorate based propellant devices.

Experimental Section

Caution! Azides and nitrate esters are sensitive and represent energetic materials; therefore, they must be handled with extreme care! During the work with azido- and nitrate silanes, wearing leather jacket, face shield, steel-reinforced Kevlar gloves, ear protection, and electrically grounded shoes is mandatory. Only electrically grounded and metal-free equipment was used during the syntheses.

Acetonitrile, npentane, sodium azide (ACROS ORGANICS), silver nitrate (VWR) and sodium iodide were used as received. Dichlorodiphenylsilane (ABCR) was freshly distilled under argon atmosphere before using.

The ^1H , $^{13}\text{C}\{^1\text{H}\}$, ^{14}N , and $^{29}\text{Si}\{^1\text{H}\}$ NMR spectra were recorded in CDCl_3 at 25 °C using a Jeol 400 Eclipse FT-NMR spectrometer operating at 400.2 MHz (^1H), 100.6 MHz (^{13}C), 79.5 MHz (^{29}Si), 40.6 MHz (^{15}N), and 28.9 MHz (^{14}N). Chemical shifts (ppm) are given with respect to TMS (^1H , ^{13}C , ^{29}Si) and MeNO_2 (^{14}N and ^{15}N). Infrared (IR) spectra were recorded on a Perkin-Elmer Spectrum BXII FT-IR instrument equipped with a Diamant-ATR Dura Sampler at 25 °C. Raman spectra were recorded on a Bruker RAMII Raman instrument ($\lambda = 1064 \text{ nm}$, 200 mW, 25 °C) equipped with D418-T Detector at 200 mW at 25 °C. Melting, boiling, and decomposition points (Tonset) were determined by differential scanning calorimetry (DSC; Perkin-Elmer Pyris 6 DSC, calibrated by standard pure indium and zinc). Measurements were performed at a heating rate of $\beta = 5 \text{ }^\circ\text{C}$ in closed aluminium containers

with a hole (1 μm) on the top for gas release with a nitrogen flow of 5 mL/min. The reference sample was a closed aluminium container with air. Friction and impact sensitivity experiments were performed with a friction device and a drophammer setup according to BAM standards (Bundesanstalt für Materialforschung und -prüfung).[29] Elemental analyses of the azidomethyl and nitratomethyl compounds were not performed because of their explosive properties and the risk of damage the analyzer. Mass spectrometric data were obtained from a Jeol Mstation JMS 700 spectrometer. Elemental analysis and mass spectrometry of the highly explosive and very sensitive compounds **4d** and **4e** were not performed, because of its high explosive character and avoid potential damage of the analyzer.

Compound **1a**, **2a** and **1b** were synthesized by literature known methods.[14,15,16]

Bis(azidomethyl)diphenylsilane (1c): Compound **1a** (0.25 g, 0.85 mmol, 1.0 eq) was refluxed with sodium azide (0.22 g, 3.40 mmol, 4.0 eq) in acetonitrile (10 mL) for 12 h. The solvent was evaporated off at reduced pressure and re-dissolved in *n*-pentane (10 mL). The organic phase was filtered and evaporating of the solvent. The product was obtained as colourless oil in a yield of 43 % (0.15 g, 0.51 mmol).

^1H NMR (CDCl_3): δ = 7.72–7.45 (m, $\text{C}_{\text{arom}}\text{H}$), 3.52 (s, CH_2N_3) ppm. ^{13}C NMR (CDCl_3): δ = 134.8 (s, *o*-CH), 130.7 (s, *p*-CH), 130.3 (s, *i*-CH), 128.1 (s, *m*-CH), 37.3 (CH_2N_3) ppm. ^{14}N NMR (CDCl_3): δ = -132 (N_β), -171 (N_γ), -326 (N_α). $^{29}\text{Si}\{^1\text{H}\}$ NMR (CDCl_3): δ = -14.9 ppm. Impact: >40 J. Friction: <108 N. T_{dec} : 138.4 °C.

Bis(nitratomethyl)diphenylsilane (1d): Compound **1b** (0.25 g, 0.54 mmol, 1.0 eq) was stirred with silver nitrate (0.73 g, 4.31 mmol, 8.0 eq) in acetonitrile (10 mL) for 4 h. The solvent was evaporated off at reduced pressure and re-dissolved in *n*-pentane (10 mL). The organic phase was filtered and evaporating of the solvent. Quantitative yield of silver iodide (0.13 g, 0.54 mmol) was obtained, but no clear evidence for the product **1d**.

Tris(iodomethyl)phenylsilane (2b): Compound **2a** (1.00 g, 3.94 mmol, 1.0 eq) was refluxed 24 h with sodium iodide (1.54 g, 23.66 mmol, 6.0 eq) in acetone. The row product was extracted with *n*-pentane (3 \times 40 mL) and washed with water (50 mL). The product was obtained with a yield of 89 % (1.85 g, 3.51 mmol) as colourless solid.

^1H NMR (CDCl_3): $\delta = 7.64\text{--}7.40$ (m, C_{aromH}), 2.52 (s, CH_2I) ppm. ^{13}C NMR (CDCl_3): $\delta = 134.7$ (s, *o*-CH), 131.0 (s, *p*-CH), 130.2 (s, *i*-CH), 128.4 (s, *m*-CH), -18.9 (s, CH_2I) ppm. $^{29}\text{Si}\{^1\text{H}\}$ NMR (CDCl_3): $\delta = -4.6$ ppm. IR: $\tilde{\nu} = 2930, 2897, 1384, 1262, 1110, 1081, 1020, 774, 755, 738, 697, 643, 531\text{ cm}^{-1}$. Raman: $\tilde{\nu} = 2981, 2938, 1382, 1163, 1082, 1000, 789, 748, 543, 512, 489\text{ cm}^{-1}$. M.p.: $94.7\text{ }^\circ\text{C}$. T_{dec} : $251.3\text{ }^\circ\text{C}$. MS(DEI+): $m/z = 527.78$ $[\text{M}]^+$, 451.0 $[\text{M}-\text{Ph}]^+$, 401.1 $[\text{M}-\text{I}]^+$, 387.1 $[\text{M}-\text{CH}_2\text{I}]^+$, 259.1 $[\text{M}-\text{CH}_2\text{I}, -\text{I}]^+$, 245.1 $[\text{M}-2\text{CH}_2\text{I}]^+$.

Tris(azidomethyl)phenylsilane (2c): Compound **2a** (0.25 g, 0.99 mmol, 1.0 eq) was refluxed 12 h with sodium azide (0.38 g, 5.91 mmol, 6.0 eq) in acetone. The raw product was extracted with *n*-pentane ($3 \times 40\text{ mL}$) and washed with water (50 mL). The product was obtained with a yield of 84 % (0.23 g, 0.83 mmol) as colourless oil.

^1H NMR (CDCl_3): $\delta = 7.59\text{--}7.43$ (m, C_{aromH}), 3.32 (s, CH_2N_3) ppm. ^{13}C NMR (CDCl_3): $\delta = 134.4$ (s, *o*-CH), 131.4 (s, *p*-CH), 129.0 (s, *i*-CH), 128.7 (s, *m*-CH), 36.7 (s, $^1\text{J}_{\text{C}-^{29}\text{Si}} = 58.1\text{ Hz}$, CH_2N_3) ppm. ^{14}N NMR (CDCl_3): $\delta = -132$ (N_β), -171 (N_γ), -323 (N_α). $^{29}\text{Si}\{^1\text{H}\}$ NMR (CDCl_3): $\delta = -9.7$ ($^1\text{J}_{\text{Si}-^{13}\text{C}} = 59.0\text{ Hz}$) ppm. Impact: $>2\text{ J}$. Friction: $>40\text{ N}$. T_{dec} $139.1\text{ }^\circ\text{C}$. Sensitivities: impact $<2\text{ J}$; friction $<40\text{ N}$.

Tris(nitratomethyl)phenylsilane (2d): Compound **2b** (0.10 g, 0.19 mmol, 1.0 eq) was stirred with silver nitrate (0.26 g, 1.52 mmol, 8.0 eq) in acetonitrile (10 mL) for 5 h. The solvent was evaporated off at reduced pressure and re-dissolved in *n*-pentane (10 mL). The organic phase was filtered and evaporating of the solvent. The product decomposes during the reaction and was not obtained pure and only observed by NMR experiments.

1,3-Bis(chloromethyl)-1,1,3,3-tetramethyldisiloxane (3a): Chloro(chloromethyl)dimethylsilane (2.00 g, 14.0 mmol, 1.0 eq) was hydrolysed by slowly adding water (20 mL) at $0\text{ }^\circ\text{C}$. The raw product was extracted with *n*-pentane ($3 \times 20\text{ mL}$) and the organic solvent was evaporated off under reduced pressure for several hours ($2 \cdot 10^{-3}\text{ mbar}$). The product was obtained with a yield of 100 % (3.23 g, 14.0 mmol) as colourless oil.

^1H NMR (CDCl_3): $\delta = 2.72$ (s, CH_2Cl), 0.21 (s, CH_3) ppm. ^{13}C NMR (CDCl_3): $\delta = 30.8$ (CH_2Cl), -1.3 (CH_3) ppm. $^{29}\text{Si}\{^1\text{H}\}$ NMR (CDCl_3): $\delta = 4.0$ ppm. Bp.: $207.4\text{ }^\circ\text{C}$. IR: $\tilde{\nu} = 2963, 2928, 1394, 1255, 1180, 1062, 842, 796, 748, 697, 655, 624\text{ cm}^{-1}$. Raman: $\tilde{\nu} = 2981, 2938, 1382, 1163, 1082, 1000, 789, 748, 543, 512, 489\text{ cm}^{-1}$.

1,3-Bis(iodomethyl)-1,1,3,3-tetramethyldisiloxane (3b): Compound **3a** (1.00 g, 4.32 mmol, 1.0 eq) was mixed with sodium iodide (1.94 g, 13.0 mmol, 3.0 eq) and was reflux for 8 h in acetone (20 mL). The solvent was evaporated off and raw product was solved in *n*-pentane (20 mL). The pentane phase was separated and washed twice with water (2 × 10 mL). The organic solvent was evaporated off and the oil was dried *in vacuo* (2·10⁻³ mbar). The product was obtained with a yield of 96 % (1.72 g, 4.15 mmol) as colourless oil.

¹H NMR (CDCl₃): δ = 2.03 (s, CH₂I), 0.25 (s, CH₃) ppm. ¹³C NMR (CDCl₃): δ = -0.3 (CH₃), -12.5 (CH₂I) ppm. ²⁹Si{¹H} NMR (CDCl₃): δ = 4.6 ppm. IR: $\tilde{\nu}$ = 2957, 2930, 1405, 1253, 1089, 1044, 832, 787, 727, 707, 654 cm⁻¹. Raman: $\tilde{\nu}$ = 2960, 2932, 1408, 1084, 711, 641, 525 cm⁻¹.

1,3-Bis(azidomethyl)-1,1,3,3-tetramethyldisiloxane (3c): Compound **3a** (0.20 g, 0.86 mmol, 1.0 eq) was mixed with sodium azide (0.17 g, 2.59 mmol, 3.0 eq) and was reflux for 16 h in acetone (10 mL). The solvent was evaporated off and raw product was solved in *n*-pentane (3 × 10 mL). The pentane phase was separated and washed twice with water (2 × 10 mL). The organic solvent was evaporated off and the oil was dried *in vacuo* (2·10⁻³ mbar). The product was obtained with a yield of 98 % (0.21 g, 0.85 mmol) as colourless gel.

¹H NMR (CDCl₃): δ = 2.73 (s, CH₂N₃), 0.19 (s, CH₃) ppm. ¹³C NMR (CDCl₃): δ = 42.3 (CH₂N₃), -0.5 (CH₃) ppm. ¹⁴N NMR (CDCl₃): δ = -131 (N_β), -173 (N_γ), -323 (N_α). ²⁹Si{¹H} NMR (CDCl₃): δ = 5.4 ppm. IR: $\tilde{\nu}$ = 2962, 2898, 2090, 1410, 1290, 1256, 1180, 1055, 837, 796, 754, 695 cm⁻¹. Raman: $\tilde{\nu}$ = 2965, 2903, 2092, 1412, 520 cm⁻¹. T_{dec} 135.8 °C. Sensitivities: impact >40 J; friction <60 N.

1,3-Bis(nitratomethyl)-1,1,3,3-tetramethyldisiloxane (3d): Compound **3c** (0.10 g, 0.24 mmol, 1.0 eq) was treated with silver nitrate (0.12 g, 1.5 mmol, 3.0 eq) in acetonitrile (5 mL) for 3 hours at ambient temperature and exclusion of light. The raw product was rapidly extracted with *n*-pentane (3 × 20 mL) and the organic solvent was evaporated off under reduced pressure (2·10⁻³ mbar). The product was obtained almost pure with a yield of 64 % (0.04 g, 0.15 mmol) calculated by ¹H NMR as colourless oil.

¹H NMR (CDCl₃): δ = 4.04 (m, CH₂ONO₂), 0.23 (s, CH₃) ppm. ¹³C NMR (CDCl₃): δ = 66.4 (CH₂ONO₂), -0.9 (CH₃) ppm. ¹⁴N{¹H} (CDCl₃): δ = -36.0 ppm. ²⁹Si{¹H} NMR (CDCl₃): δ =

3.3 ppm. IR: $\bar{\nu}$ = 2962, 1623, 1302, 1257, 1213, 1139, 1055, 799, 766, 664 cm^{-1} . Raman: $\bar{\nu}$ = 2967, 2905, 1637, 1408, 1303, 1256, 830, 687, 627 cm^{-1} . Sensitivities: impact >40 J (inpure compound); friction <72 N (inpure compound).

Poly-(chloromethyl)methylsiloxane (4a): Dichloro(chloromethyl)methylsilane (2.00 g, 12.2 mmol, 1.0 eq) was hydrolysed by slowly adding an excess of water (10 mL) at 0 °C. The raw product was extracted with *n*-pentane (3 × 20 mL). The pentane phase was separated and washed twice with water (2 × 10 mL). The organic solvent was evaporated off and the oil was dried *in vacuo* ($2 \cdot 10^{-3}$ mbar) for several hours. The product was obtained with a yield of 100 % (1.33 g, 12.2 mmol) as colourless oil. Increasing the chain length (aging) the product was stirred with 10 mL of 2M sulphuric acid for three days at ambient conditions.

^1H NMR (CDCl_3): δ = 2.72 (br, CH_2Cl), 0.28 (s, CH_3) ppm. ^{13}C NMR (CDCl_3): δ = 28.9 (CH_2Cl), -2.5 (s, CH_3) ppm. $^{29}\text{Si}\{^1\text{H}\}$ NMR (CDCl_3): δ = -28.3–28.6 (cyclic siloxanes), -29.8–30.3 ppm. IR: $\bar{\nu}$ = 2976, 2905, 1250, 1110, 850, 770, 753, 689, 660 cm^{-1} . Raman: $\bar{\nu}$ = 2977, 2935, 2908, 1402, 1103, 1087, 761, 654, 508 cm^{-1} .

Poly-(iodomethyl)methylsiloxane (4b): Compound **4a** (1.00 g, 9.21 mmol, 1.0 eq) was mixed with sodium iodide (4.14 g, 27.62 mmol, 3.0 eq) and was reflux for 16 h in acetone (20 mL). The solvent was evaporated off and raw product was solved in *n*-pentane (20 mL). The pentane phase was separated and washed twice with water (2 × 10 mL). The organic solvent was evaporated off and the oil was dried *in vacuo* ($2 \cdot 10^{-3}$ mbar). The product was obtained with a yield of 96 % (1.77 g, 8.84 mmol) as colourless oil.

^1H NMR (CDCl_3): δ = 2.06–1.95 (br, CH_2I), 0.41–0.30 (s, CH_3) ppm. ^{13}C NMR (CDCl_3): δ = -1.4--2.1 (CH_3), -15.2--15.8 (CH_2I) ppm. $^{29}\text{Si}\{^1\text{H}\}$ NMR (CDCl_3): δ = -27.3--28.2 (cyclic siloxanes), -29.3--29.7 ppm. IR: $\bar{\nu}$ = 2989, 2905, 1253, 1090, 801, 790, 731, 541, 478 cm^{-1} . Raman: $\bar{\nu}$ = 2988, 2963, 2934, 2903, 1405, 1374, 1255, 1085, 790, 728, 537, 478 cm^{-1} .

Poly-(azidomethyl)methylsiloxane (4c): Compound **4a** (0.20 g, 1.84 mmol, 1.0 eq) was mixed with sodium azide (0.36 g, 5.52 mmol, 3.0 eq) and was refluxed for 24 h in acetone (10 mL). The solvent was evaporated off and raw product was solved in *n*-pentane (3 × 10 mL). The pentane phase was separated and washed twice with water (2 × 10 mL). The organic solvent was evaporated off and the oil was dried *in vacuo* ($2 \cdot 10^{-3}$ mbar) for several

hours. For aging the viscously oil was stored in a open vessel at 50 °C for two weeks. The product was obtained with a yield of 98 % (0.21 g, 1.80 mmol) as colourless gel.

^1H NMR (CDCl_3): $\delta = 2.77$ (m, C_{aromH}), 0.25 (s, CH_2I) ppm. ^{13}C NMR (CDCl_3): $\delta = 41.0$ – 40.4 (CH_2N_3), -1.5 – -1.8 (CH_3) ppm. $^{14}\text{N}\{^1\text{H}\}$ (CDCl_3): $\delta = -131$ (N_β), -173 (N_γ), -325 (N_α) ppm. $^{29}\text{Si}\{^1\text{H}\}$ NMR (CDCl_3): $\delta = -28.1$ – -29.7 ppm. T_{dec} : 138.1 °C. Sensitivities: impact >8 J; friction <72 N

Poly-(nitratomethyl)methylsiloxane (4d): Compound **4b** (0.10 g, 0.5 mmol, 1.0 eq) was mixed with silver nitrate (0.07 g, 1.5 mmol, 3.0 eq) and was stirred in acetone (5 mL) for 2 h. The solvent was evaporated off and raw product was solved in *n*-pentane (3 × 10 mL). The pentane phase was separated. The organic solvent was evaporated off *in vacuo* ($2 \cdot 10^{-3}$ mbar). The product was decomposed, but quantitative conversion was affirmed by yielding stoicheometric amount of silveriodide (0.12 mg, 0.5 mmol). The formation of silyl nitrate esters were confirmed by NMR experiments.

^1H NMR (CDCl_3): $\delta = 4.14$ – 4.04 (br, CH_2ONO_2), 0.41 – 0.30 (s, CH_3) ppm. ^{13}C NMR (CDCl_3): $\delta = 65.1$ – 64.5 (CH_2ONO_2), -1.2 – -2.6 (CH_3) ppm. $^{14}\text{N}\{^1\text{H}\}$ (CDCl_3): $\delta = -38.1$ ppm. $^{29}\text{Si}\{^1\text{H}\}$ NMR (CDCl_3): $\delta = -25.5$ – -32.7 ppm. T_{dec} : 251.3 °C.

Poly-bis(chloromethyl)siloxane (5a): Triflic acid (0.80 g, 5.3 mmol, 3.0 eq) was slowly added at 0 °C to a solution of compound **1a** (0.50 g, 1.8 mmol, 1.0 eq) in *n*-pentane (10 mL). After adding the acid the reaction mixture was refluxed for 1 hour and cooled to 0 C. Wet methanol (10 mL, 20 % water) was slowly added to the reaction. The two phase mixture was stirred for additional three days at ambient temperature for aging the product. The aqueous phase was washed twice with *n*-pentane (10 mL), all the organic phase were combined (organic reaction phase and washing solutions) and washed once with 20 mL of water. The organic solvent was evaporated off at reduced pressure ($2 \cdot 10^{-3}$ mbar) for several hours. For aging the viscously oil was stored in an open vessel at 50 °C for several days to obtain the product in 73 % (0.19 g, 1.3 mmol) yield.

^1H NMR (CDCl_3): $\delta = 2.94$ – 2.87 (s, CH_2Cl) ppm. ^{13}C NMR (CDCl_3): $\delta = 30.4$ – 27.4 (s, CH_2Cl) ppm. $^{29}\text{Si}\{^1\text{H}\}$ NMR (CDCl_3): $\delta = -35.0$ – -36.0 ppm.

Poly-bis(azidomethyl)siloxane (5b): Compound **5a** (0.19 g, 1.3 mmol, 1.0 eq) was mixed with sodium azide (0.25 g, 3.9 mmol, 3.0 eq) and was reflux for 24 h in acetone (10 mL).

The solvent was evaporated off and raw product was solved in *n*-pentane (3 × 10 mL). The pentane phase was separated and washed twice with water (2 × 10 mL). The organic solvent was evaporated off and the oil was dried *in vacuo* (2·10⁻³ mbar) for several hours. If necessary, the product can be aged by storing the product at 50 °C for one week. The product was obtained with a yield of 90 % (0.18 g, 1.2 mmol) as colourless rubber like substance.

¹H NMR (CDCl₃): δ = 2.89 (s, CH₂N₃) ppm. ¹³C NMR (CDCl₃): δ = 36.7–35.8 (s, CH₂N₃) ppm. ¹⁴N NMR (CDCl₃): δ = -132 (N_β), -177 (N_γ), -326 (N_α). ²⁹Si{¹H} NMR (CDCl₃): δ = -37.2–-38.0 ppm. T_{dec}: 137.4 °C. Sensitivities: impact <1 J; friction <5 N

(Chloromethyl)trimethoxysilsesquioxane (6a): Trichloro(chloromethyl)silane (0.50 g, 2.7 mmol, 1.0 eq) was mixed with sodium methanolat (0.44 g, 8.2 mmol, 3.0 eq) in *n*-pentane (20 mL) under inert atmosphere (argon). The precipitate was filtered off and the solvent was evaporated off and was dried *in vacuo* (2·10⁻³ mbar). The product was obtained with a yield of 85 % (0.32 g, 1.9 mmol) as colourless oil.

¹H NMR (CDCl₃): δ = 3.60 (s, OCH₃), 2.81 (s, CH₂Cl) ppm. ¹³C NMR (CDCl₃): δ = 50.9 (OCH₃), 23.6 (s, CH₂Cl) ppm. ²⁹Si{¹H} NMR (CDCl₃): δ = -62.5 ppm. IR: $\tilde{\nu}$ = 2939, 1393, 1198, 1127, 1040, 808, 737, 668 cm⁻¹. Raman: $\tilde{\nu}$ = 2986, 2941, 2850, 1390, 1200, 1035, 802, 735, 672 cm⁻¹.

(Azidomethyl)trimethoxysilsesquioxane (6b): Compound **6a** (0.20 g, 1.2 mmol, 1.0 eq) was mixed with sodium azide (0.23 g, 3.5 mmol, 3.0 eq) and was reflux for 12 h in dry acetonitrile (10 mL) under inert gas (argon). The raw product was extracted by *n*-pentane (3 × 20 mL). The organic solvent was evaporated off and the oil was dried *in vacuo* (2·10⁻³ mbar). The product was obtained with a yield of 65 % (0.13 g, 0.8 mmol) as colourless gel.

¹H NMR (CDCl₃): δ = 3.60 (m, OCH₃), 2.81 (s, CH₂N₃) ppm. ¹³C NMR (CDCl₃): δ = 51.3 (OCH₃), 23.6 (CH₂N₃) ppm. ¹⁴N NMR (CDCl₃): δ = -132 (N_β), -173 (N_γ), -327 (N_α). ²⁹Si{¹H} NMR (CDCl₃): δ = -62.6 ppm. T_{dec}: ~165 °C. Sensitivities: impact >40 J; friction <120 N

Poly-(azidomethyl)silsesquioxane (6c): Compound **6b** (0.20 g, 1.1 mmol, 1.0 eq) was mixed with an excess of water (20 mL) and stirred for 24 h with 2M sulphuric acid (10 mL). The water was evaporated off and the raw product was washed with water (10 mL) and

diethyl ether (10 mL). The raw product was dried *in vacuo* ($2 \cdot 10^{-3}$ mbar) for several hours to obtain a colourless solid with a yield of 97 % (0.12 g, 1.1 mmol).

IR: $\tilde{\nu}$ = 2939, 1393, 1198, 1127, 1040, 808, 737, 668 cm^{-1} . Raman: $\tilde{\nu}$ = 2986, 2941, 2850, 1390, 1200, 1035, 802, 735, 672 cm^{-1} . T_{dec} : ~ 170 °C. Sensitivities: impact >40 J; friction <192 N

Acknowledgements

Financial support of this work by the Ludwig-Maximilian University of Munich (LMU), the U.S. Army Research Laboratory (ARL) under grant no. W911NF-09-2-0018, the Armament Research, Development and Engineering Center (ARDEC) under grant no. W911NF-12-1-0467, and the Office of Naval Research (ONR) under grant nos. ONR.N00014-10-1-0535 and ONR.N00014-12-1-0538 is gratefully acknowledged. The authors acknowledge collaborations with Dr. Mila Krupka (OZM Research, Czech Republic) in the development of new testing and evaluation methods for energetic materials. Also we thank Dr. M. Suceka for the many helpful discussions and information for the computer code EXPLO5 version 6.01. We are indebted to and thank Drs. Betsy M. Rice and Brad Forch (ARL, Aberdeen, Proving Ground, MD) for many inspired discussions. Thanks to Stefan Huber for measuring the sensitivity parameters.

-
- [1] T. M. Klapötke, B. Krumm, R. Ilg, D. Troegel, R. Tacke, *J. Am. Chem. Soc.* **2007**, *129*, 6908-6915.
- [2] C. Evangelisti, T. M. Klapötke, B. Krumm, A. Nieder, R. J. F. Berger, S. A. Hayes, N. W. Mitzel, D. Troegel, R. Tacke, *Inorg. Chem.* **2010**, *49*, 4865-4880.
- [3] T. M. Klapötke, B. Krumm, A. Nieder, O. Richter, D. Troegel, R. Tacke, *Z. Allg. Anorg. Chem.* **2012**, *638*, 1075-1079.
- [4] Laura Ascherl, Camilla Evangelisti, Thomas M. Klapötke, Burkhard Krumm, Julia Nafe, Anian Nieder, Sebastian Rest, Christian Schütz, Muhamed Suceka, Matthias Trunk, *Chem. Eur. J.* **2013**, submitted.
- [5] Barcza, S., US 3,592,831, **1968**.
- [6] Barcza S., US 3,585,228, **1971**.

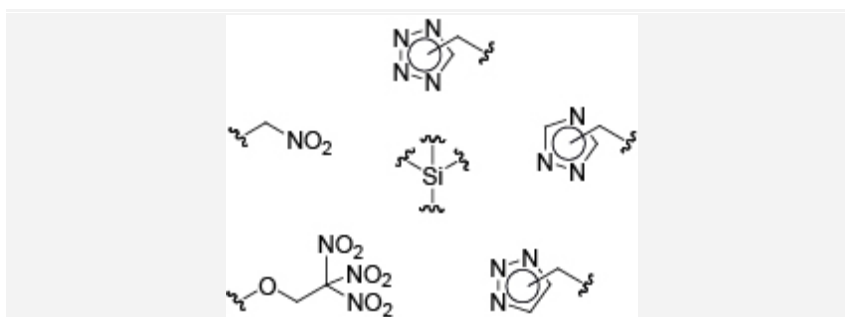
- [7] K. Alfons, W. Buder, DE 3,040,382, **1982**.
- [8] a) M. Kurono, R. Unno, Y. Matsumoto, Y. Kondo, T. Mitani, T. Jomori, H. Michishita, K. Sawai Eur. Patent 0288002, **1988**; b) R. D. Haugwitz, W. K. Anderson, J. Plowman, R. Kaslinal, D. M. Houston, V. L. Narayanan, *Appl. Organomet. Chem.* **1990**, *4*, 375–378; c) W. K. Anderson, R. Kasliwal, D. M. Houston, Y.-s. Wang, V. L. Narayana, R. D. Haugwitz, J. Plowman, *J. Med. Chem.* **1995**, *38*, 3789–3797.
- [9] J. O. Daiss, K. A. Barth, C. Burschka, P. Hey, R. Ilg, K. Klemm, I. Richter, St. A. Wagner, R. Tacke, *Organomet.* **2004**, *23*, 5193–5197.
- [10] F. Popp, J. B. Nätscher, J. O. Daiss, C. Burschka, R. Tacke, *Organomet.* **2007**, *26*, 6014–6028.
- [11] M. Alexandru, M. Cazacu, C. Racles, C. Grigoras, *Polym. Eng. Sci.* **2011**, *51*, 78–86.
- [12] a) H. Cui, M. R. Kessler, *Compo. Sci. Technol.* **2012**, *72*, 1264–1272; b) N. Hamano, Y.-C. Chiang, I. Nyamaa, H. Yamaguchi, S. Ino, R. Hickel, K.-H. Kunzelmann, *Dent. Mater.* **2012**, *28*, 894–902; c) T. Shugo, JP 2011-140677, **2011**; d) Ameron Coatings – Australasia, *Corrosion & Prevention* **2000**, *Paper 072*, 1-8. e) L. Rösch, P. John, R. Reitmeier in *Silicon Chemistry, Organic*, Ullmann's – Encyclopedia of Industrial Chemistry, Wiley-VCH Verlag GmbH&Co. KGaA, Weinheim, **2012**, *32*, 637–674.
- [13] Eugene G. Rochow in *Silicon and Silicones*, Springer-Verlag, Berlin Heidelberg, **1987**, 129ff.
- [14] D. Troegel, T. Walter, C. Burschka, R. Tacke, *Organomet.* **2009**, *28*, 2756–2761.
- [15] J. O. Daiss, K. A. Barth, C. Burschka, P. Hey, R. Ilg, K. Klemm, I. Richter, St. A. Wagner, R. Tacke, *Organomet.* **2004**, *23*, 5193–5197.
- [16] M. Shimizu, M. Iwakubo, Y. Nishihara, K. Oda, T. Hiyama, *ARKIVOC* **2007**, 29–48.
- [17] C. Däschlein, J. O. Bauer, C. Strohmam, *Angew. Chem. Int. Ed.* **2009**, *48*, 8074–8077.
- [18] R. J. Perry, M. J. O'Brien, *Energ. Fuel.* **2011**, *25*, 1906–1918.
- [19] V. van Dorsselaer, D. Schirlin, P. Marchal, F. Weber, C. Danzin, *Biorg. Chem.* **1996**, *24*, 178–193.
- [20] D. Reyx, P. Guillaume, *Makromol. Chem.* **1983**, *184*, 1179–1187.

- [21] D. Reyx, P. Guillaume, *Makromol. Chem.* **1983**, *184*, 1331–1338.
- [22] M. A. Brook in *Silicon in Organic, Organometallic, and Polymer Chemistry*, Wiley & Sons, Inc., New York, **1999**, pp. 258f.
- [23] W.-G. Liu, S. V. Zybin, S. Dasgupta, T. M. Klapötke, W. A. Goddard III, *J. Am. Soc. Chem.* **2009**, *131*, 7490–7493.
- [24] J. S. Murray, P. Lane, A. Nieder, T. M. Klapötke, P. Politzer, *Theor. Chem. Acc.* **2010**, *127*, 345–354.
- [25] R. Tacke, J. Pikies, H. Linoh, R. Rohr-Aehle, S. Gönne, *Liebigs Ann. Chem.* **1987**, 51–57.
- [26] J. M. Allen, S. L. Aprahamian, E. A. Sans, H. Shechter, *J. Org. Chem.* **2002**, *67*, 3561–3574.
- [27] A. Bondi, *J. Phys. Chem.* **1964**, *68*, 441–451.
- [28] a) P. Politzer, J. S. Murry, T. Clark, *Phys. Chem. Chem. Phys.* **2010**, *12*, 7748–7757; b) A. C. Legon, *Phys. Chem. Chem. Phys.* **2010**, *12*, 7726–7747.
- [29] www.bam.de (German version), www.bam.de/en/index.htm (English version).
- [30] M. Suceska, *EXPL05 program vers. 6.01*, Zagreb, Croatia, **2012**.
- [31] M. J. Frisch *et al.*, *GAUSSIAN 09 (Revision C.01)*, Gaussian Inc., Wallingford CT, **2010**.
- [32] M. S. Westwell, M. S. Searle, D. J. Wales, D. H. William, *J. Am. Chem. Soc.* **1995**, *117*, 5013–5015.
- [33] a) T. Mossor-Pietraszewska, *Acta Biochem. Pol.* **2001**, *48*, 673–686; b) E. Delhaize, P. R. Ryan, *Plant Physiol.* **1995**, *107*, 315–321; c) V. A. Vitorello, F. R. Capaldi, V. A. Stefanuto, *Braz. J. Plant Physiol.* **2005**, *17*, 129–143; d) P. Illés, M. Schlicht, J. Pavlovkin, I. Lichtscheidl, F. Baluška, M. Ovecka, *J. Exp. Bot.* **2006**, *57*, 4201–4213.
-

VIII. Azole and Nitro Silanes

Energetic silanes

C. Evangelisti, L. Göpfert, T. M. Klapötke, B. Krumm, J. Nafe, A. Nieder, and O. Richter ...167 – 194*

Tetrazolyl-, Triazolyl- and Nitro-Derivatives of Silanes

After recent results of azido and nitro silanes the structural similar triazoles, tetrazoles and nitro derivatives were studied. Extensive synthetic efforts to obtain different nitro derivatives, as well as di-, tri- and tetra-substituted silanes were

investigated. Possible side-reactions and decomposition pathways are discussed. Theoretical studies concerning the energetic properties were computed and possible applications of the discussed silanes were argued.

Tetrazolyl-, Triazolyl- and Nitro-Derivatives of Silanes

Camilla Evangelisti, Lisa Göpfert, Thomas M. Klapötke*, Burkhard Krumm, Julia Nafe, Anian Nieder, and Oliver Richter

Unpublished

Abstract: Several trimethylsilyl substituted N-rich heterocycles and nitro derivatives were synthesized and are discussed as potential highly energetic compounds in terms of silicon containing fuels for different propulsion applications. In general, mixtures of different

silanes with several common oxidizers (AP, ADN, N₂O₄) were calculated by using EXPLO5, version 6.01, computer code. The energies of formation were computed by Gaussian version C3 and on CBS-4M level of theory. Energetic parameters, like impact, friction and thermal

sensitivities, were obtained experimentally and are discussed.

Keywords: heterocycle • silanes • energetic material • keyword 4 • keyword

Introduction

Silanes are important and frequently used building blocks with a broad field of syntheses and applications. Recently, we reported several energetic silanes varying the backbone (methyl, phenyl and oxo substitutions) and the content of the energetic moieties (azido and nitrate).[1–3]

In the application of energetic materials other functionalities were used instead of azides and nitrates.[4] Especially tetrazoles, triazoles and nitro derivatives will be of interest. Tetrazoles and triazoles are nitrogen-rich compounds with often higher stability concerning thermal and mechanical stimuli and also better energetic performance data in comparison with azido analogues.[4,5] Nitro derivatives are known as energetic, but also often thermally and mechanically more stable compounds in comparison to the analogue nitrate esters.[4,6]

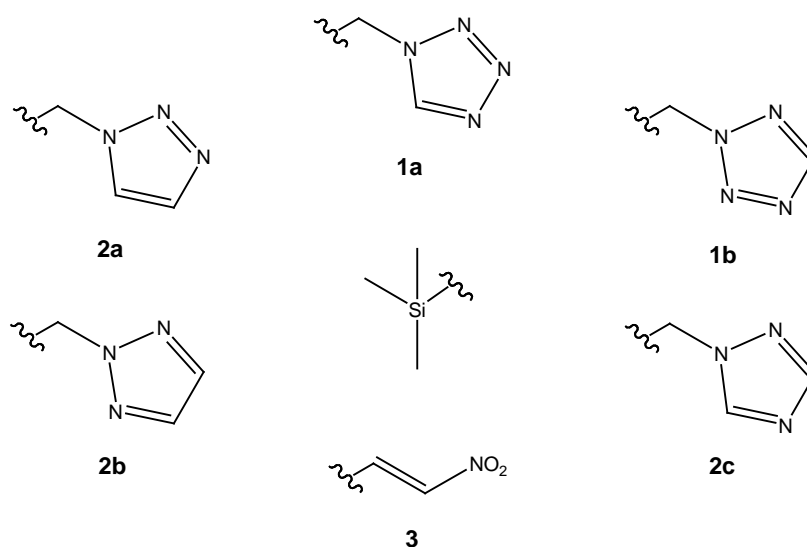
Based on this, in this work several new suitable energetic substituents were tested in the synthesis routes, chemical and physical properties for different

* T. M. Klapötke
Department of Chemistry and Biochemistry,
Ludwig-Maximilian University of Munich,
Butenandtstr. 5-13(D), 81377 Munich,
Germany

kind of silane derivatives (see Scheme 8.1). In addition, computed energetic properties were performed by different methods and additives using the EXPL05 (version 6.01) computing code.

Results and Discussion

Synthesis: The triazole and tetrazole trimethylsilyl derivatives were synthesized by a halogen exchange reaction using the corresponding azoles stirring with potassium carbonate in DMSO (Scheme 8.2).

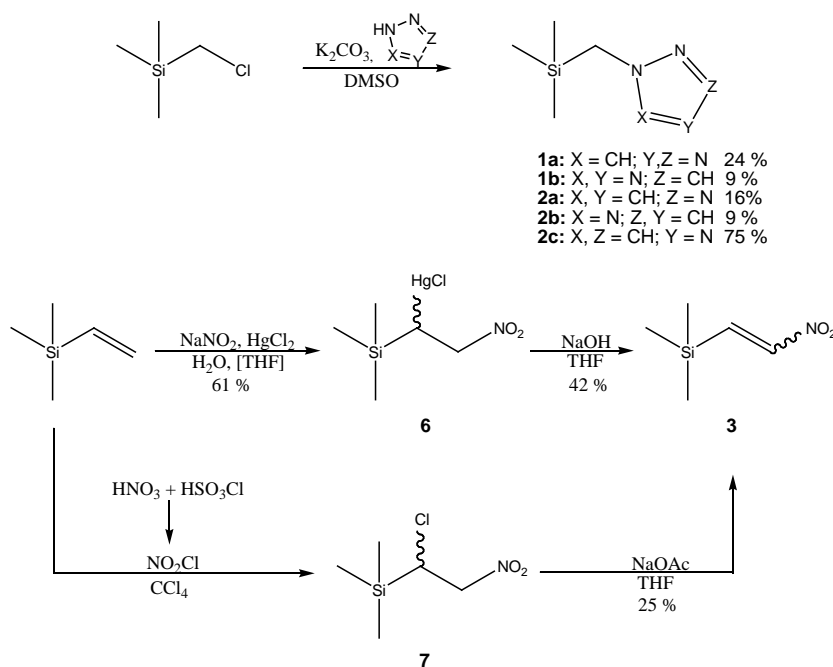


Scheme 8.1. Labeling of the synthesized silanes (**1a**: (1*N*-tetrazolylmethyl)trimethylsilane; **1b**: 2*N*-(tetrazolylmethyl)trimethylsilane; **2a**: 1*N*-(1,2,3-triazolylmethyl)trimethylsilane; **2b**: 2*N*-(1,2,3-triazolylmethyl)trimethylsilane; **2c**: 1*N*-(1,2,4-triazolylmethyl)trimethylsilane; **3**: *E*-(2-Nitroethenyl)trimethylsilane).

In the case of the tetrazole derivatives **1a**[7,8]/**1b**[7] an isomeric mixture (1.25:1) of 1*N*- and 2*N*-substitution at the tetrazole ring were obtained in 44% of total yield. Purification of the two isomers by column chromatography leads to a yield of 24 % (**1a**) and 9 %(**1b**) in total. The reason for the decreasing yield of the 2*N*-isomer is found by reacting of the compound with the silica gel. It has not been clearly verified how the compound reacts during chromatography. One possibility is cleaving off one methyl moiety, followed by creating a new Si–O–Si bridge between the silicon of the tetrazole derivatives and the silica gel. Another possible reaction is mentioned by cleaving the bond of the methylene moiety to the central silicon atom and followed by trimethylsilyl addition to an OH-moiety of the silica gel. A similar reaction with other nucleophiles is described elsewhere.[7] Computing the enthalpies of formations (CBS-4M) result in that **1b** is the thermodynamic product of the

reaction ($\Delta_f H^\circ_{\text{CBS-4M}}(\mathbf{1a}/\mathbf{1b})$: 20.2 kJ/mol). The efforts to obtain (*H*-tetrazol-5-ylmethyl)trimethylsilane (**4**, 1*H*-isomer: **4^{1H}** and 2*H*-isomer: **4^{2H}**) were unsuccessful. The Diels-Alder cyclisation using (cyanomethyl)trimethylsilane (**5**)[9,10] and azide leads to the cleavage of the Si-CH₂R bond, faster than the cyclisation occurs. Calculations on CBS-4M level of theory show that the **4^{2H}** isomer seems to be the thermodynamic product, whereas **4^{1H}** is the kinetic product ($\Delta_f H^\circ_{\text{CBS-4M}}(\mathbf{4}^{\mathbf{1H}}/\mathbf{4}^{\mathbf{2H}})$: 12.0 kJ/mol). In contrast to the tetrazole derivatives, the 1,2,4-triazole can be easily obtained as single isomers in high yield (**2c**: 75 %).[7,11,12,13] The 4*N* substituted isomer has not been observed in contrast to observations in the literature.[7,11,12,13] The synthesis towards the 1,2,3-triazolylmethyl isomers **2a** and **2b** has similar problems as the synthesis and purification of **1a** and **1b**. Isomer **2b** was obtained in higher yields (16 %) than **2a** (9 %), although **2a** is twice as much observed in ¹H NMR in comparison to **2b** before chromatographic purification. Computing results using CBS-4M calculations show that the 2*N* substituted 1,2,3-triazole derivative **2b**, like for **1b**, is the thermodynamic product of the reaction ($\Delta_f H^\circ_{\text{CBS-4M}}(\mathbf{2a}/\mathbf{2b})$: 15.6 kJ/mol). The 2*N* substituted isomer **2a** rapidly decomposes during chromatographic purification in a similar manner than already discussed for **1b**. The synthetic efforts to obtain higher azole-substituted methylsilanes were unsuccessful. During the reactions of the corresponding chloromethylsilane and sodium/potassium azolate (respectively *in situ* generation of the salt by neutral azole and potassium carbonate [12,13] in DMF), the Si-CH₂X bonds were cleaved before the second/third substitution takes place in the case of higher substituted silanes. The used potassium carbonate also has the task to catch the build acid and to prevent decomposition of the product.[12,13] Siloxanes and methylated azole derivatives were obtained as main products. In the case of the CH₂-bridged tetrazoles, silanes with two or more tetrazolylmethyl moieties could not be tested, because to the best of our knowledge the corresponding cyanomethyl silanes could not be prepared so far. Concerning the synthesis of nitromethyl silanes only a few information are known in literature. One synthesis of nitromethyltrimethylsilane (**8**) is published by Legzdins *et al.*,[14] but **8** was only mentioned as side product and not discussed in more detail. The synthesis is not suitable for larger amount, because of the high laborious efforts and the wastage of an expensive tungsten complex. The synthetic efforts to obtain **8** by palladium catalysed coupling reaction of chlorotrimethylsilane and bromonitromethane, has been published as not successful.[15] Synthesis starting from bromonitromethane and following

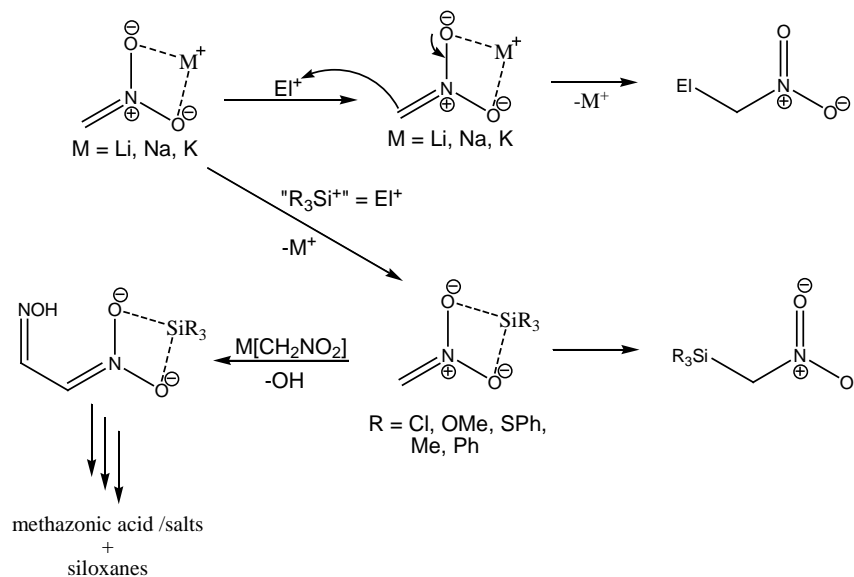
metallation by *n*-butyllithium (Mg, Zn, Li activated by 3 % Na, Li-naphthalide respectively) were not successful to obtain nitromethyl silanes by using trimethylchloride, dichlorodimethylsilane and trichloromethylsilane. The reason is given mainly by the reduction of the nitro group by some of the used metals (e.g. Zn) and the single electron transfer to radical intermediates by others (e.g. Li), which would lead to dimerisation or also to reduction of the nitro moiety. A synthesis of bis(nitromethyl)dimethylsilane is mentioned by Urbanski *et al.* using sodium nitromethanide, dichlorodimethylsilane in pyridine.[16] Reproduce the reaction by Urbanski did not lead to the desired product. Only sodium chloride, siloxanes (mainly poly-dimethylsiloxane) and other undefined products were obtained from this reaction. Using different synthetic methods (changing order, temperature, concentration, lithium nitromethanide, potassium nitromethanide) never showed a clear hint for formation of a Si-CH₂NO₂ moiety. The reactions of chlorosilanes with M[CH₂NO₂] (M = Li, Na, K)[17,18] at -30 – -78 ° and multiple lithiated nitromethanide (Li_nCH_{3-n}NO₂, n = 1, 2, 3) result in brown-reddish suspensions with no affirmation of the formation of Si-CH₂NO₂ moieties. It is known from literature that the corresponding carbon derivatives can be obtained in good yields using this methods.[19] It is supposed, that the



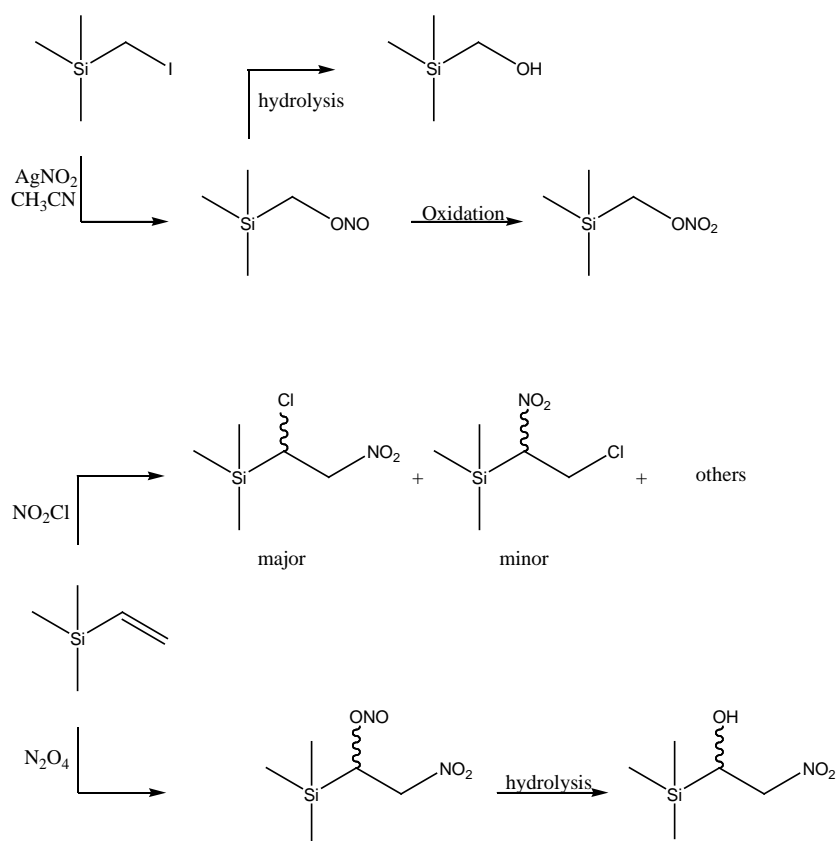
Scheme 8.2. Synthetic pathways for synthesizing (azolylmethyl)trimethylsilanes (**1a/b** and **2a-c**) and the two most efficient synthetic routes to obtain E-(nitroethylenyl)trimethylsilane (**3**) via (1-chloromercapto-2-nitroethyl)-1-trimethylsilane (**6**) or (1-chloro-2-nitroethyl)trimethylsilane (**7**).

reason for that can be found in the oxophilicity of silicon itself. The first metallation step at nitromethane results in metal nitronate species and a C=N-double bond.[17,18,20] The bonding of the Me₃Si-moiety (or other silicon species) to one of the NO₂ oxygens will stabilize the nitronate species. Consequently, if a nucleophile takes part during the reaction, the unwanted nucleophilic attack at the C=N double bond and the decomposition of the nitro moiety occurs (see Scheme 8.3). In our case by using chlorosilanes, the chloride anion should be nucleophilic enough to attack at the double bond as proposed by Urbansky.[16] Using other substituents, like thiophenolated silanes or methanolated silanes, lead to the same results. The same observation of colour and decomposition products are also an evidence for a less important role of the Si-substituents themselves (Cl, OMe, SPh etc.) as possible nucleophiles during the decomposition mechanism (lack of Cl, OMe, SPh side products). An explanation could be given by a decomposition pathway following steps to generate methanzone derivatives, which would explain the intensive colour change to brown-reddish during the reaction.[21] Further metallations with lithium leads to lithiations at the former methyl carbon and will increase the nucleophilicity of the nitromethanide carbon. It is known from literature, that multiple lithiations increase the yields of products which follow a nucleophilic attack to a carbon center.[19,22] This result for carbon centers could not be found in the case of nucleophilic attacks to a silicon centre for the silicon compounds discussed in here.

It was tried to synthesize *ortho*-silicates starting from 1,1,1-trinitroethanol and silicon tetrachloride. Also in this case a fast decomposition to silicates and dark brownish decomposition products were observed without any verified hint for formation of the desired product. Even thiophenylated and methoxylated silanes were tested to obtain the desired tetrakis(1,1,1-trinitroethanoly)-*ortho*-silicate. Reactions using trimethylsilyl and other higher substitutional silanes, like trichloromethylsilane, give the same results of decomposition. In contrast the reaction of 1-fluoro-1,1-dinitroethanol with silicon tetrachloride (also lower substitutional chlorosilanes) yielded the tetrakis(1-fluoro-1,1-dinitroethanoly)-*ortho*-silicate which is already known in literature and intensively discussed in terms of energetic properties.[23] The reason for the decomposition of the trinitro species will be probably similar to that of the nitromethane reaction described before. silver nitrite ($\text{NaNO}_2 + \text{AgNO}_3 \rightarrow \downarrow \text{AgNO}_2$) in acetonitrile. [24,25]



Scheme 8.3. The Reaction mechanisms of nitromethanides with C-based electrophiles (E^+) (upper reaction) and follow separation of the used metal ion (M^+) by yielding the corresponding salt. The reaction pathways by using oxophilic silicon derivative as electrophile (" R_3Si^+ ", bottom reaction) are dominated by the nucleophilic attack of an additional nitromethanide anion to produce methazonic acid derivatives and siloxanes.



Scheme 8.4. Reaction of (iodomethyl)trimethylsilane and silver nitrite and the main products of the addition of NO_2Cl and N_2O_4 at vinyltrimethylsilane.

In the case of the trinitromethyl moiety one nitro groups can be substituted by nucleophiles, cleaving a nitrite anion and creating a C=N double bond intermediate. In the case of the fluoro derivative, the less sterical hindrance, the stabilization of a C=N double bonded species by the electron withdrawing character of the fluorine atom and stronger C-F bond (compared to C-NO₂ bond), prevents the cleavage of a nitro or the fluoro group. Nitro alkanes also can be obtained by halogen exchange reaction using silver nitrite and a haloalkane. In the similar manner it was tried to obtain the desired nitromethyltrimethylsilane by treating iodomethyltrimethylsilane with freshly prepared and the corresponding chloromethyl silane with sodium nitrite.[24] After purification hydroxymethyltrimethylsilane and nitratomethyltrimethylsilane were obtained as main products and large amounts of elemental silver obtained out of the reduction of silver salts. The first idea was that the Ag⁺ oxidized the nitro into a nitrate moiety by an unknown reaction mechanism. But to prevent the occurrence of an Ag/Ag⁺ redox reaction, sodium nitrite and the corresponding chloromethyl silane were mixed and stirred for several hours/days at ambient and increased temperature (up to 40 °C). The reaction is slow and again only a nitrate- and hydroxymethyl silanes were obtained, but in this case with higher amount of the hydroxyl derivative in comparison to the reaction with AgNO₂. In addition, there was no analytical evidence for a nitromethyl species in all tested reactions.

The literature known (2-nitrovinyl)trimethylsilane (**3**) is easily available by different synthetic routes.[26] The first synthetic route *via* the mercury derivative (**6**)[27] and later elimination leads to compound **3** in high yield and high purity of the *E*-isomer (Scheme 8.2). The use of organic mercury compounds is economically uninteresting. The synthesis *via* the 1-chloro-2-nitro derivative **6** and elimination gives **3**, but with yields lower than using the first route. The reason is found in the isomers created by chloronitration of the vinyl moiety. It is not as stereoselective as the nitromercuration (in contrast to common organo-mercurations[28] the reaction favoured the anti-Markovnikov products[27]). In addition, by-products like the 1-nitro-2-chloro derivative, are formed by using nitrylchloride (NO₂Cl synthesized *via* ref. [29], Scheme 8.4). The synthetic efforts to obtain (1,2-dinitroethyl)trimethylsilane by reacting vinyltrimethylsilane with dinitrogen tetroxide in CCl₄ lead to (1-nitro-2-nitroethyl)trimethylsilane as main product which readily decomposes to the 1-hydroxy-2-nitro derivative during purification. The pure nitrite-nitro

derivative was not studied in more detail, because of the low stability of nitrite esters in general,[30] and even the oxidation to obtain the presumed highly sensitive nitrate-nitro derivative was not performed due to safety reasons (see below). The 1-nitro-2-hydroxy isomer is the less preferred product in comparison to the 2-nitro-1-hydroxy derivative.[30,31] The nitration of the hydroxyl group by the non-oxidizing nitration agent acetyl nitrate (from acetic acid, acetic anhydride and 100 % HNO₃) and typical purification procedure,[1] leads to a compound which ignited during evaporation off the solvent *n*-pentane (Caution!). No analytical data were obtained from this compound, but it is likely that the presumably formed (1-nitrate-2-nitroethyl)trimethylsilane decomposes spontaneously. Even the synthesis efforts of trimethylvinylsilane with N₂O₅ in CCl₄ lead to the same result during purification. Reactions of neat N₂O₄ (as liquid at 0 °C) and neat trimethylvinylsilane, tetravinylsilane and bis(allyl)dimethylsilane reacts spontaneously by ignition. Out of these results and for safety reasons the efforts to obtain pure compounds were changed in the way of using the high reactivity of the vinyl and allyl silanes as fuel for (hypergolic) propulsion mixtures with N₂O₄ (NTO) or red fuming nitric acid in a similar manner as known from NTO/MMH (monomethyl hydrazine) propulsion mixtures.[32] Theoretical studies to this issue together with propulsion mixtures of the compounds mention in Scheme 8.1 are given below.

Analytcs: ¹H, ¹³C{¹H}, ¹⁴N, ²⁹Si{¹H} and ¹⁹⁹Hg/¹⁹⁹Hg{¹H} NMR experiment were performed and the most important resonances of the compounds **1a/b**, **2a-c**, **3**, **5**, **6**, **8-10** are listed in Table 8.1.

Comparing the ¹H resonances of the tetrazole and triazole isomers **1a/b** and **2a/b** almost no changing in the shifting are observed for the trimethylsilyl proton resonances (~0.10 ppm). 1*N*-substituted compounds **1/2a** seem to be marginal more shifted to lower field than the 2*N*-substituted ones. The (azidomethyl)trimethylsilane **10** shows resonances of the methyl protons slightly shifted to higher field in comparison (0.08ppm) to the former ones. In the case of the methylene protons a significant discrepancy in their shifting is observed for the 1*N*- and 2*N*-substituted compounds, where 2*N*-substituted derivatives are shifted to lower field (**1b**: 4.18 ppm, **2b**: 4.05 ppm) compared to their 1*N*-substituted analogues (**1a**: 3.91 ppm, **2a**: 3.90 ppm). The signal of the azidomethyl moiety of **10** was observed significantly shifted to higher field (2.72 ppm) in comparison to all other

VIII. Azole and Nitro Silanes

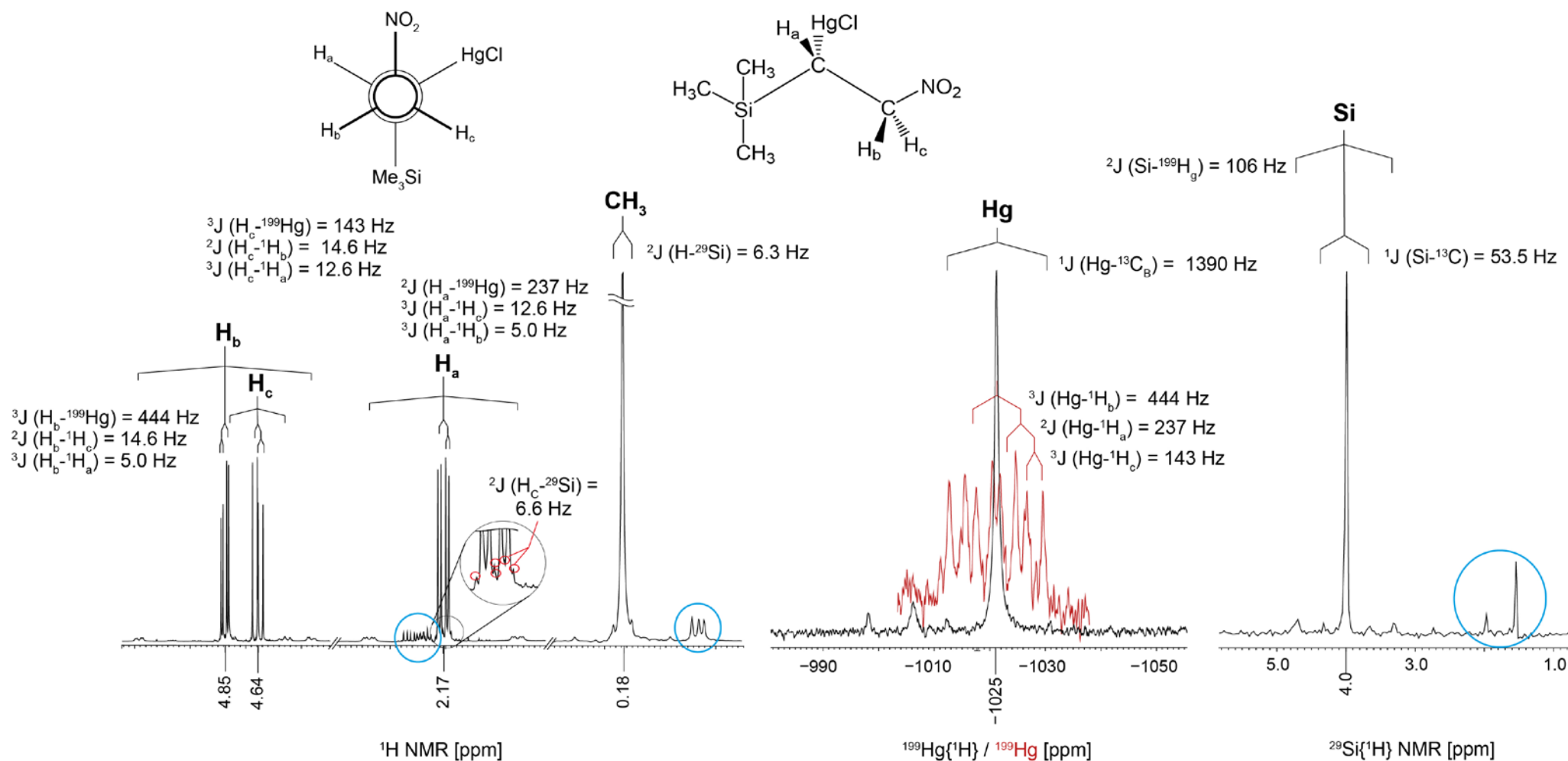


Figure 8.1. The ¹H, ²⁹Si and ¹⁹⁹Hg NMR resonance pattern of compound **6** are shown with the corresponding coupling frequencies. The ¹⁹⁹Hg{¹H} NMR spectrum is indicated in red and the resonances of the isomere are marked in blue. In addition, the molecular structure and the corresponding Newman projection of the (R)-enantiomer are illustrated exemplarily on top.

tetrazolyl- and triazolylmethyl methylene protons discussed in here. Comparing the ^{13}C NMR resonances of the 1*N*-substituted 1,2,3-triazolyl **2a** and the azide **10**, they are found similar for the CH_2 and CH_3 moieties. The ^{13}C resonances of CH_2 and CH_3 are shifted high-field for the 1*N*-substituted isomers in comparison to the resonances of the corresponding isomer **2a** and **2b**. In contrast to the compounds **1/2b** the CH_2 moieties performing ^{13}C NMR experiments always shift to higher field for the 1*N*-substituted isomers **1/2a**. The ^{29}Si resonances are similar for all azole derivatives, without the exception of the 1,2,4-triazole isomer analogue **2c**, which is shifted to higher field in comparison to the other N-heterocyclic compounds. In general, the $^1J_{\text{C-Si}}$ coupling frequencies of all discussed compounds are just below 50 Hz for the coupling to the methylene moiety and slightly above 50 Hz for the methyl moiety. In the case of the nitrovinyl derivative **3** the $^1J_{\text{C-Si}}$ coupling between Si and the vinyl CH moiety is also found above 50 Hz. The ^{29}Si resonance is shifted to higher field for compound **3** in comparison to all other discussed trimethylsilyl derivatives. An interesting molecule in NMR experiments is found to be compound **6**. Due to the manifold NMR active nuclei and the chirality, it shows a complex coupling pattern (see Figure 8.1). The couplings between ^1H and ^{199}Hg , ^{13}C and ^{199}Hg were ascertained by literature known frequency values.[33–36] Only one coupling with 106 Hz, which was observed in ^{29}Si NMR experiments could not be assigned to any known possible coupling frequency. Many references were found for $^1J_{^{29}\text{Si}-^{199}\text{Hg}}$ ($\sim 900\text{--}2000$ Hz)[34], $^2J_{^{29}\text{Si}-^{199}\text{Hg}}$ ($\sim 40\text{--}70$ Hz)[35] and $^3J_{^{29}\text{Si}-^{199}\text{Hg}}$ ($\sim 180\text{--}190$ Hz)[36] coupling frequencies and any of these fits to the observed coupling frequency. Nevertheless it is more likely that the 106 Hz assign to the $^2J_{^{29}\text{Si}-^{199}\text{Hg}}$ spin-spin coupling. The in literature described $^2J_{^{29}\text{Si}-^{199}\text{Hg}}$ coupling values seem not to be the assigned spin-spin coupling frequencies, rather the $^1J_{^{29}\text{Si}-^{13}\text{C}}$ couplings, which have the same tendencies by changing the substituents at the silicon described in the publication.[35] Unfortunately, it is not known if the coupling was observed in the ^{199}Hg NMR experiment (unlikely, because of the signal half width) or only in the ^{29}Si experiment. Consequently, to the best of our knowledge this is the first described $^2J_{^{29}\text{Si}-^{199}\text{Hg}}$ coupling of its kind. Due to the vicinal H-H and $^3J_{\text{H}-^{199}\text{Hg}}$ coupling frequencies observed for compound **6** the orientation of the substituents is likely with *anti*-orientation of the sterical hinderence of Me_3Si and NO_2 the moieties (Newman projection in Figure 8.1). In addition, the most acidic proton H_b (strongest shift to lower field) is consequently also in *anti*-position

Table 8.1. NMR resonances of the compounds **1a/b**, **2a–c**, **3**, **5**, **6** and **8–10**. Values are given in ppm and the $^1J_{C-Si}$, respectively $^1J_{Si-C}$, couplings are given in parentheses in Hz (due to the resolution of the spectra small deviations can occur); Notation of the nitrogen atoms are defined with the alkylated nitrogen N1 and common further labelling.

	1H [a]	$^{13}C\{^1H\}$ [a]	$^{29}Si\{^1H\}$	$^{14}N\{^1H\}$			
1a ^[a]	3.91	38.7 (47.0)	2.5 (47.9, 53.5)	N1	N2	N3	N4
	0.11	-3.5 (52.7)		-150	-12	9	-54
1b ^[a]	4.18	43.9 (47.9)	2.8 (48.5,	N1	N2	N3	N5
	0.10	-3.5 (53.7)	54.7)	-100	-5	-53	-77
2a ^[a]	3.90	41.9 (47.0)	2.5 (47.4, 53.5)	N1	N2/N3		
	0.10	-2.5 (52.7)		-140	-20 - -33		
2b ^[a]	4.05	46.9 (48.9)	2.5 (48.6, 53.5)	N1	N2/N5		
	0.10	-2.3 (52.7)		-127	-55		
2c ^[a]	3.69	40.0 (47.9)	1.6 (49.1, 53.5)	N1	N2	N4	
	0.10	-3.1 (55.6)		-83	-170	-132	
3	7.31	146.2	-4.0 (54.7)	-8.9			
	6.94	137.3(53.7)					
	0.20	-2.8 (54.6)					
5 ^[a]	1.57	4.9 (37.8)	4.8 (53.8, 36.0)				
	0.20	-1.9 (53.8)					
6	4.85	77.4	4.0 (53.5)	10.8			
	4.64	36.7 (42.2)					
	2.17	0.0 (53.7)					
	0.18						
8 ^[b]	4.43	---	---	---			
	0.12						
9 ^[c]	4.56	66.8 (48.2)	0.1 (48.2, 53.3)	-34.3			
	0.10	-2.8 (53.0)					
10 ^[d]	2.72	42.1 (51.8)	3.2 (52.0)	N1	N2	N3	
	0.08	-2.6 (51.8)		-321	-131	-174	

[a] Resonances of the heterocycle and the cyanide moieties are given in experimental section; [b] ref. [14] in C_6D_6 ; [c] ref. [1]; [d] ref. [2]

towards the HgCl moiety, which leads to the observed *trans*-/*E*-product **3** by elimination. As can be seen in Figure 8.1 (blue circles) there are signals of at least three more compounds which are structurally highly similar to the main product. Due to their 1H - 1H , 1H - ^{29}Si , 1H - ^{199}Hg spin-spin coupling pattern and the strongest differences found in the CH_2 moiety signals in 1H and ^{13}C NMR experiments, they likely belong to compounds with the backbone of **6**, but with different substituents R at the CH_2 moiety ($Me_3Si(HgCl)CH-CH_2R$, e.g. R = Cl, ONO, OH). In addition, at the $RHgCl$ moiety the chlorine can also be substituted by a nitrite anion which leads to an additional NMR resonance pattern of a $RHgONO$ species. The type of substituent on the mercury atom is in equilibrium between Cl and ONO

substitution.[27] After β -elimination no further side products of the type $\text{Me}_3\text{SiCH}=\text{CH}_2\text{R}$ with $\text{R} \neq \text{NO}_2$ were observed (created by $\text{Me}_3\text{Si}(\text{HgCl})\text{CH}-\text{CH}_2\text{R}$ species as starting material).

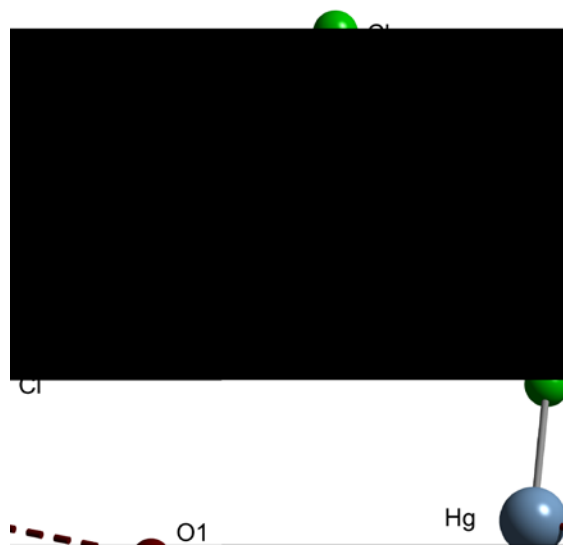


Figure 8.2. Computed molecular gas phase structure and the atom labelling of the (*R*)-enantiomer of **6** on MP2 level of theory (C,H,N,O,Si: cc-pVTZ method, Hg: quasi relativistic *ab initio* pseudopotential ECP-60-MWB method and adopt the optimized [8s 7p 6d 2f 1g]/(6s 5p 2d 2f 1g)-GTO valence basis set). The intramolecular Hg-O1 interaction is signed as red dashed line.

The gaseous structure of the (*R*)-enantiomer of **6** was calculated at the MP2 level of theory (see Figure 8.2) with Gaussian 09 revision C.01.[37] For the atoms H, C, N, O and Si the cc-pVTZ method was used. In the case of mercury the quasi relativistic *ab initio* pseudopotential ECP-60-MWB was set and adopt the optimized [8s 7p 6d 2f 1g]/(6s 5p 2d 2f 1g)-GTO valence basis set.[38] In comparison to other computed and experimentally determined structures of trimethylsilyl derivatives (see ref. 1 and Chapter IX), the structure of (*R*)-**6** shows several differences (see Table 8.2). First of all the Si-C bonds are almost similar in length ($d(\text{Si,C})$: 1.85–1.86 Å), whereas the bond between the silicon and the methyl moiety of C2 (*anti*-orientation towards the mercurychloride moiety) is computed to be the longest. As expected, the shortest length is found for the C1-Si bond. The differences are too small to take them into account, but the differences did not fit with the experience of other computed silane structures, where the longest Si-CH₃ bond is always found at the methyl moiety, which is in *anti*-position towards the substituent R ($\theta(\text{CH}_3-\text{Si}-\text{C}-\text{R})$: $\sim 180^\circ$, see Chapter IX). This result leads to the conclusion that the HgCl substituent is dominate towards the substituent CH₂NO₂ by influencing the bonding situations at the Me₃Si moiety. The average length of the CH₃-Si bonds ($d(\text{Si,C})$: 1.85 Å) is significant shorter in comparison

to the measured gas phase structure of **9** by gas electron diffraction experiments (GED: $d(\text{Si,C}): 1.88 \text{ \AA}$, MP2: $d(\text{Si,C}): 1.88 \text{ \AA}$)[1] and other computed trimethylsilyl compounds. The $\text{CH}_2\text{-Si}$ bond is elongated ($d(\text{Si,C}): 1.89 \text{ \AA}$) in comparison to the $\text{CH}_3\text{-Si}$ bonds, but not as much as computed for other trimethylsilyl compounds ($d(\text{Si,C}): 1.90\text{--}1.93 \text{ \AA}$). The angles $\alpha(\text{C4-Si-C1/3}): 108.0/108.3^\circ$ are more acute in addition with the obtuse angle of $\alpha(\text{C1-Si-C3}): 111.7^\circ$ in comparison with the C2-Si-C angles ($\alpha(\text{C2-Si-C1/3/4}): 110.0/109.7/109.1^\circ$). These results of the CH_3SiCH_2 moiety show a bending of the $\alpha(\text{C-Si-C})$ angles, which pointing to a $\text{Hg}\cdots\text{SiC1/3H}_3$ attraction, the same is true observing the $\alpha(\text{C5-C4-Si}): 111.1^\circ$, $\alpha(\text{C5-C4-Hg}): 113.0^\circ$ and $\alpha(\text{Si-C4}\cdots\text{Hg}): 104.8^\circ$ angles. But the distances compared with the van der Waals radii does not even show a weak attraction between the Hg and any SiCH_3 moiety, although the distance of Si and Hg is for structural reasons shorter than the van der Waals radii ($d(\text{Si,Hg}): 3.12 \text{ \AA}$, $\Sigma_{\text{vdW}}(\text{Si,Hg}): 3.65 \text{ \AA}$ [39]). In addition the slight deviation of the C-Hg-Cl angle ($\alpha(\text{C4-Hg-Cl}): 177.3^\circ$, expected 180°), does also not agree with an $\text{Si}\cdots\text{Hg}$ attraction. But the bending of this $\alpha(\text{C4-Hg-Cl})$ angle, together with the short distance between Hg and the O1 of the nitro group ($d(\text{O1,Hg}): 2.82 \text{ \AA}$, $\Sigma_{\text{vdW}}(\text{O,Hg}): 3.07 \text{ \AA}$ [39]) and the twisting of the NO_2 group support the appearance of a $\text{Hg}\cdots\text{O1}$ interaction ($\theta(\text{C4-C5-N-O1}): -44.7^\circ$, $\theta(\text{Hg-C4}\cdots\text{N-O1}): 13.2^\circ$). This intramolecular attraction does not result in a significant elongation of the Hg bond lengths to its neighbours ($d(\text{C4,Hg}): 2.046 \text{ \AA}$, $d(\text{Hg,Cl}): 2.287 \text{ \AA}$) compared to other C-Hg and Hg-Cl bonds found in literature.[40]

Sensitivities and physical properties: The thermal stabilities were determined by DSC experiments (onset points). All studied compounds **1a/b**, **2a-c** and **3** seem to be rather thermally stable. In contrast to known nitrate- and azidomethyl silanes, which decompose at app. 100°C (some also at ambient temperature)[1] and 135°C , respectively,[2] they are much better candidates for application. Compounds **1b** and **2b** are highly volatile. The approximate boiling points of these two substances ($\sim 175^\circ\text{C}$) could not be observed by DSC and hardly with a Büchi apparatus, because of the rapid evaporation.

The sensitivities towards mechanical stimuli (friction and impact) were measured by BAM methods.[41] The impact sensitivities (IS) of all measured compounds **1a/b**, **2a-c** are classified as insensitive ($>40 \text{ J}$) according to *UN Recommendation on the Transport of Dangerous Goods*. [42] The nitro compound **3** is classified as less sensitive material ($<40 \text{ J}$).

The friction sensitivities (FS) of the compounds **1a/b**, **2a-c** and **3** are in the range of less sensitive materials (see Table 8.3).

Table 8.2. Bond lengths, angles and selected torsion angles of compound (*R*)-**6** obtained by calculated data on MP2 level of theory and cc-pVTZ (C, H, N, o, Si) and ECP-60-MWB basis sets (Hg, pseudopotential optimized [8s 7p 6d 2f 1g]/(6s 5p 2d 2f 1g)-GTO valence basis set).

MP2/cc-pVTZ (C, H, N, O, Si), MP2/ECP-60-MWB (Hg)			
Bond length [Å]		Angles [°]	
C1–Si	1.851	C1–Si–C2	110.0
C2–Si	1.856	C1–Si–C3	111.7
C3–Si	1.854	C1–Si–C4	108.0
C4–Si	1.889	C2–Si–C3	109.7
C4–C5	1.498	C2–Si–C4	109.1
C5–N	1.504	C3–Si–C4	108.3
N–O1	1.229	C5–C4–Si	111.1
N–O2	1.229	C4–C5–N	114.4
C4–Hg	2.046	C4–Hg–Cl	177.3
Hg–Cl	2.287	C5–N–O1	119.0
O1---Hg	2.817	C5–N–O2	116.5
Torsion angles [°]		C5–C4–Hg	113.0
C1–Si–C4–C5	-173.6	Si–C4–Hg	104.8
C1–Si–C4–Hg	-51.4	N–O1---Hg	102.6
C2–Si–C4–Hg	-170.8	O1---Hg–C4	112.5
C3–Si–C4–Hg	69.7	O1---Hg–Cl	70.2
Si–C4–C5–N	172.2		
Si–C4–Hg–Cl	19.9		
C4–C5–N–O1	-41.7		
C4–C5–N–O2	139.8		
C5–C4–Hg–Cl	141.0		
N–C5–C4–Hg	54.8		
C5–N–O1---Hg	11.3		
N–O1---Hg–C4	12.9		
O2–N–C5–H _b	16.0		
Hg–C4–C5–H _b	172.1		

Energetic properties: The energetic properties of the compounds **1a/b**, **2a-c**, and **3** were calculated by the EXPL05 version 6.01 computer code.[43] The input enthalpy of formation were calculated from the computed heats of formation, which were obtained by calculations on CBS-4M level of theory. The heat of formations were computed by the atomization method (Equation (1)) by using the program Gaussian09 revision C.01.[37] The obtained enthalpies of formation in the gas phase $\Delta H_m(g)$ were converted into their enthalpies of formation in solid state $\Delta H_m(s)$ by using the Trouton's rule.[44] The molar

standard enthalpies of formation were converted into the molar solid state energies of formation by using Equation (2).

$$\Delta_f H^\circ_M(\text{g}) = H^\circ_M(\text{g}) - \sum H^\circ_{\text{atoms}} + \sum \Delta_f H^\circ_{\text{atoms}} \quad (1)$$

$$\Delta U_M = \Delta H_M - \Delta nRT \quad (2)$$

Δn = changes of moles of gaseous components

Because of the deficiency of some concrete data of the densities, the energetic values were estimated with a density of 1.0 g/cm³ (worsed case estimation). It is mainly focused on the influences of the types of energetic moieties substituted on the trimethylsilyl group.

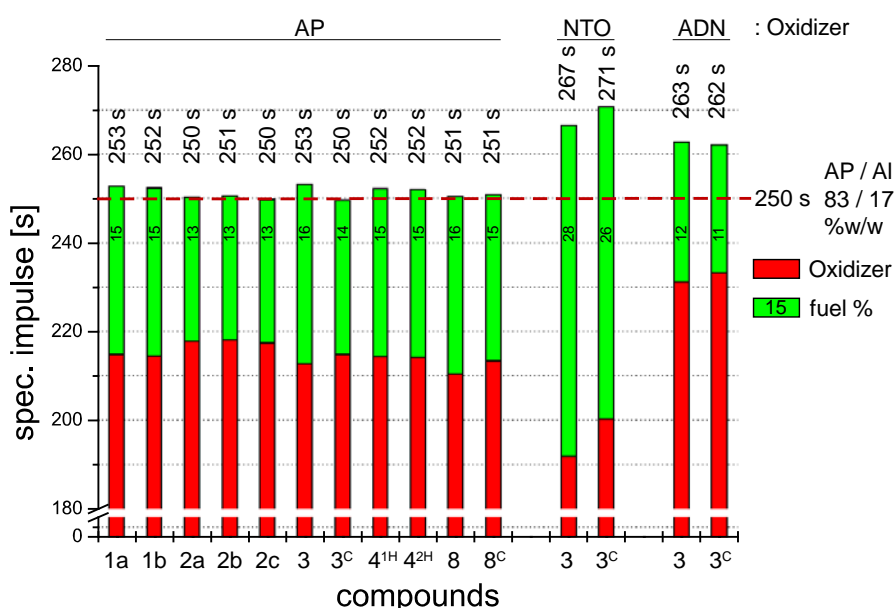


Figure 8.3. Calculated specific impulse I_{sp} of the compounds **1a/b**, **2a–c**, **3/3^c**, **4^{1H/2H}** and **8/8^c** by using the EXPLO5 computing code (Model 1, advanced run). The I_{sp} of AP/Al (83/17 %w/w) is given as bench mark (red dashed line). Additionally the I_{sp} with the oxidizers NTO and ADN were calculated for **3** and **3^c**. The green bars with numbers representing the percent amount of fuel for the optimal mixture.

More detailed studies are given in Chapter IX. In addition, for an independency of intermolecular interactions to the calculated energies of all compounds discussed inhere, the boiling- or decomposition point, respectively, were fixed at 100 °C, which show only slightly discrepancies to the values computed with the experimental physical data (ref. [3] and see Chapter IX). If certain values are known, the computed values based on the real physical properties are additionally given in parentheses in Table 8.3. The influence of the T_m , T_b or T_{dec} is insignificant and consequently almost negligible. As the first result of the computed data is the inferiority of the triazole derivatives **2a–c** in comparison to their tetrazole analogues

VIII. Azole and Nitro Silanes

Table 8.3. Energetic properties of the compounds **1a/1b, 2a-c, 3, 4^{1H}/4^{2H}** and **8**.

	1a	1b	2a	2b	2c	3	4^{1H}/4^{2H}	8
formula	C ₅ H ₁₂ N ₄ Si	C ₅ H ₁₂ N ₄ Si	C ₆ H ₁₃ N ₃ Si	C ₆ H ₁₃ N ₃ Si	C ₆ H ₁₃ N ₃ Si	C ₅ H ₁₁ NO ₂ Si	C ₅ H ₁₂ N ₄ Si	C ₄ H ₁₁ NO ₂ Si
FW /g·mol ⁻¹	156.26	156.26	155.27	155.27	155.27	145.23	156.26	133.22
IS /J [a]	>40	>40	>40	>40	>40	<40	n.n.	n.n.
FS /N [b]	120	108	92	92	144	120	n.n.	n.n.
N /% [c]	35.85	35.85	27.06	27.06	27.06	9.64	35.85	10.51
Ω _{CO2} (Ω _{CO})/% [d]	-184 (-133)	-184 (-133)	-211 (-149)	-211 (-149)	-211 (-149)	-171 (-116)	-176 (-124)	-162 (-114)
T _m , T _b , T _{dec} /°C [e]	-, 208, 208	-, 175,-	-, 216, 230	-, 175, -	-, 101, -	-, 70, 195	n.n.	n.n.
Δ _f H ^o _M /kJ·kg ⁻¹ [f,g]	-104,2 (-166.4)	-233,4 (-414.5)	-630.5 (-697.7)	-730.8 (-774.3)	-965.8 (-966,4)	-2053.8 (-2035.2)	-299.2/ -375.9	-3026.4
Δ _f U ^o /kJ·kg ⁻¹ [g,h]	-22,7 (-39.5)	-106,5 (-287.6)	-502.7 (-570.0)	-603.1 (-646.5)	-838.1 (-838,6)	-1934.3 (-1915.7)	-172.3/ -249.0	-2896.2
EXPLO5 6.01 values (detonation)^[i, o]:								
-Δ _{ex} U ^o /kJ·kg ⁻¹ [i]	2705 (2649)	2588 (2425)	2392 (2330)	2300 (2260)	2085 (1889)	5011 (5026)	2529/2460	4783
T _{det} /K [k]	1792 (1770)	1746 (1679)	1590 (1568)	1555 (1541)	1469 (1450)	2605 (2610)	1723/1693	2487
p _{CJ} /kbar [l]	49.6 (49.1)	48.6 (46.7)	45.0 (44.6)	44.2 (44.0)	41.7 (41.6)	62.4 (62.5)	48.0/47.0	66.7
V _{det} /m·s ⁻¹ [m]	4360 (4339)	4315 (4251)	4314 (4289)	4277 (4260)	4186 (4021)	5002 (5006)	4292/4265	5181
V ₀ /L·kg ⁻¹ [n]	666 (664)	662 (658)	630 (629)	628 (627)	623 (629)	659 (659)	660/659	689
EXPLO5 6.01 values AN mixtures (detonation)^[i, p]:								
AN/fuel w/w%	90/10	90/10	91/9	91/9	91/9	89/11	90/10	89/11
-Δ _{ex} U ^o /kJ·kg ⁻¹ [i]	4119	4102	4059	4050	4029	4208	4126/4126	4193
T _{det} /K [k]	2783	2795	2762	2758	2749	2845	2785/2785	2801
p _{CJ} /kbar [l]	223	229	231	231	230	226	223/223	250
V _{det} /m·s ⁻¹ [m]	7956	7947	7987	7984	7975	7883	7959/7959	8174
V ₀ /L·kg ⁻¹ [n]	1025	1025	1026	1026	1026	1012	1025/1025	1017
EXPLO5 6.01 values (isobaric combustion)^[q, r]:								
I _{sp} ^[r] (neat)	166	163	153	151	145	215	162/160	213
T _c ^[s] (neat)	1255	1228	1152	1133	1087	1904	1215/1199	1797

[a] The impact sensitivity tests according to STANAG 4489[45] modified instruction[46] using a BAM drophammer[BAM]; [b] The friction sensitivity tests according to STANAG 4487[47] modified instruction[48] using a BAM friction tester; [c] nitrogen content; [d] oxygen balance calculated for CO₂ and CO; [e] melting, boiling and decomposition temperature (T_m, T_b and T_{dec}) measured by DSC (onset point, heating rate of 5 °C/min); [f] calculated heat of formation (CBS-4M); [g] for computing ΔH^o_M decomposition temperature are used with 100 °C; additionally the calculated values with the experimental temperature values are given in parentheses below the estimated values; [h] energy of formation; [i] all values were computed with a density of 1.0 g/cm³ and T_{dec} = 100 °C; [j] energy of explosion; [k] detonation temperature; [l] detonation pressure at the Chapman-Jouguet point; [m] detonation velocity; [n] assuming volume of gaseous combustion products; [o] detonation settings: BKW EOS constants and co-volumes of BKWG-S, initial temperature 3600 K, Model 4, reaction products standard run; [p] detonation parameters of mixtures with ammonium nitrate (AN) with an almost equal oxygen balance (-1-0%); [q] isobaric combustion settings: chamber pressure 7 MPa, initial temperature 3300 K, ambient pressure 0.1 MPa, expansion through the nozzle, reaction products standard run, [r] specific impulse I_{sp} of the neat compound; [s] combustion chamber temperature T_c.

1a/b concerning the produced gas volume V_0 , detonation pressure p_{cj} and the detonation velocity. The detonation temperature T_{det} is expectedly higher for the tetrazoles as for the triazoles. Oxygen containing molecules like the nitro derivatives **3** and **8** are highly superior to the oxygen deficient compounds **1a/b**, **2a-c** and **4^{1H}/4^{2H}**, as expected. In general, these compounds are not suitable candidates for purpose without any oxygen source. Calculated fuel/oxidizer mixtures with ammonium nitrate (AN) as oxygen source show much better results. In the case of triazole or tetrazole derivatives, the computed values are relatively equal and even for the nitrovinyl compound **3**. Exceptions are the hypothetical results for the carbon substituted tetrazole derivatives **4^{1H}** and **4^{2H}**, which show the lowest results for their detonation parameters. In contrast the result for the nitromethyl derivative **8** is the best of all discussed compounds. But nevertheless the values are lower and not as good for completion of established common explosives, in addition to the still laborious synthesis of silanes. Consequently the focus will be given mainly onto the propellant parameter (specific impulse I_{sp} and the chamber temperature T_c).

In Table 8.3 the values of the neat compounds and in the histogram in Figure 8.3 the formulations for the optimized fuel/oxidizer (oxidizer: ammonium perchlorate, AP) mixture are shown. As bench mark the standard formulation aluminium/AP 17/83 w/w% is computed with I_{sp} of 250 s. In the case of **3** and its carbon analogue **3^c** additionally I_{sp} values with different oxidizers (AP, dinitrogen tetroxide NTO, ammonium dinitramide ADN) were computed with the EXPL05 computing code. In the case of the neat compounds, excluding the oxygen containing compounds **3** and **8**, compound **1a** has the most promising results (166 s), which is also the case for the AP formulation (253 s). It can be seen that the oxidizer has an important influence on the I_{sp} results for carbon *versus* silicon derivatives. Comparing the isomers **1a/b** and **2a-c**, there are only slightly differences are found, but not as much that it should be consider to use the isomeric mixtures obtained straight out of the reaction without further chromatically purification and consequently without losing great amounts of the products.

Conclusion

The two isomers 1*N*-1,2,3-triazolylmethyl)trimethylsilane and (2*N*-1,2,3-triazolylmethyl)-trimethylsilane were synthesized and characterized for the first time. In addition, the

syntheses of (1/2*H*-tetrazol-5-ylmethyl)trimethylsilane and silanes with higher content of N-rich heterocycles (triazoles, tetrazoles) were attempted, but failed for several reasons. The syntheses of nitromethyl silanes and also the synthesis of trinitroethanoxy siloxanes were not successful and the decomposition pathways were postulated and discussed. (2-Nitrovinyl)trimethylsilane was obtained by several methods and other unsaturated silanes were tried to be synthesized. The high reactivity of vinyl and allyl silanes with N₂O₄ and other oxidizers leads to the result to study them as propellant for hypergolic mixtures. All obtained compounds were fully characterized in terms of their energetic parameters. Additionally, theoretical studies of the energetic properties were determine for several compounds, whether experimentally obtained or not. The detonation values are all highly inferior towards common carbon based explosives. Calculations of the specific impulses for application as propellants are become the major scope of studying these compounds. They show similar and often better results as its carbon analogues and almost all tested mixtures show higher specific impulse values than the bench mark (Al/AP mixture).

Experimental Section

The ¹H, ¹³C{¹H}, ¹⁴N, and ²⁹Si{¹H} NMR spectra were recorded in CDCl₃ at 25 °C using a Jeol 400 Eclipse FT-NMR spectrometer operating at 400.2 MHz (¹H), 100.6 MHz (¹³C), 79.5 MHz (²⁹Si), 40.6 MHz (¹⁵N), and 28.9 MHz (¹⁴N). Chemical shifts (ppm) are given with respect to TMS (¹H, ¹³C, ²⁹Si) and MeNO₂ (¹⁴N and ¹⁵N). Infrared (IR) spectra were recorded on a Perkin-Elmer Spectrum BXII FT-IR instrument equipped with a Diamant-ATR Dura Sampler at 25 °C. Raman spectra were recorded on a Bruker RAMII Raman instrument (λ = 1064 nm, 200 mW, 25 °C) equipped with D418-T Detector at 200 mW at 25 °C. Melting, boiling, and decomposition points (T_{onset}) were determined by differential scanning calorimetry (DSC; Perkin-Elmer Pyris 6 DSC, calibrated by standard pure indium and zinc). Measurements were performed at a heating rate of β = 5 °C in closed aluminum containers with a hole (1 μm) on the top for gas release with a nitrogen flow of 5 mL/min. The reference sample was a closed aluminum container with air. Friction and impact sensitivity experiments were performed with a friction device and a drophammer setup according to BAM standards (*Bundesanstalt für Materialforschung und -prüfung*). Elemental analyses of the azidomethyl and nitratomethyl compounds were not performed because of their explosive properties

and the risk of damage the analyzer. Mass spectrometric data were obtained from a Jeol Mstation JMS 700 spectrometer.

(1*N*-Tetrazolylmethyl)trimethylsilane (1a) and (2*N*-tetrazolylmethyl)trimethylsilane (1b): (Chloromethyl)trimethylsilane (2.12 g, 15.7 mmol, 1.0 eq) was stirred with 1*H*-tetrazole (1.10 g, 17.3 mmol, 1.1 eq) and potassium carbonate (1.60 g, 18.8 mmol, 1.2 eq) in DMSO (15 mL) at ambient temperature for three days. The solvent was poured into 50 mL of ice-water. Raw product was extracted by diethyl ether (2x 50 mL). The organic phases were combined, dried with sodium sulphate, filtered and the solvent was evaporated off. The raw product containing the two isomers **1a** and **1b** (total yield: 44.0 %, **1a**: 24 %, **1b**: 20 %, estimated out of ¹H NMR integrals) were purified by column chromatography. The first (**1b**) and the second fraction (**1a**) were obtained as colourless oil in 9 % (0.22 g, 1.41 mmol) and colourless crystalline solid in 24 % (0.59 g, 3.77 mmol) total yield (calculated to chloromethyl silane), respectively.

1a: ¹H NMR (CDCl₃): δ = 8.49 (s, 1H, CH), 3.91 (s, 2H, ²J_{H-29Si} = 4.5 Hz, CH₂), 0.11 (s, 9H, ²J_{H-29Si} = 6.6 Hz, CH₃) ppm. ¹³C NMR (CDCl₃): δ = 141.9 (s, CH), 38.7 (s, ¹J_{CH₂-29Si} = 47.0 Hz, CH₂), -3.5 (s, ¹J_{CH₃-29Si} = 52.7 Hz, CH₃) ppm. ¹⁴N NMR (CDCl₃): δ = 9 (N3), -12 (N2), -54 (N4), -150 (N1). ²⁹Si{¹H} NMR (CDCl₃): δ = 2.5 (¹J_{29Si-CH₃} = 47.9 Hz, ¹J_{29Si-CH₂} = 53.5 Hz,) ppm. IR: $\tilde{\nu}$ = 3097, 2959, 2918, 2852, 2360, 1730, 1482, 1420, 1378, 1300, 1266, 1248, 1236, 1178, 11117, 1096, 1029, 973, 898, 843, 772, 732, 722, 705, 677 cm⁻¹. Raman: $\tilde{\nu}$ = 3102, 2977, 2963, 2935, 2902, 1484, 1421, 1280, 1261, 1235, 1180, 1118, 1024, 862, 733, 708, 644, 596, 328, 237, 186 cm⁻¹. B.p./T_{dec}: 208 °C. MS(EI+): *m/z* = 157.2 [M+H]⁺. Impact: >40 J. Friction: <108 N.

1b: ¹H NMR (CDCl₃): δ = 8.38 (s, 1H, ²J_{H-29Si} = 5.2 Hz, CH), 4.18 (s, 2H, CH₂), 0.10 (s, 9H, ²J_{H-29Si} = 6.6 Hz, CH₃) ppm. ¹³C NMR (CDCl₃): δ = 151.6 (s, CH), 43.9 (s, ¹J_{CH₂-29Si} = 47.9 Hz, CH₂), -3.5 (s, ¹J_{CH₃-29Si} = 53.7 Hz, CH₃) ppm. ¹⁴N NMR (CDCl₃): δ = -5 (N2), -53 (N3), -77 (N4), -100 (N1). ²⁹Si{¹H} NMR (CDCl₃): δ = 2.8 (¹J_{29Si-CH₃} = 48.5 Hz, ¹J_{29Si-CH₂} = 54.7 Hz,) ppm. IR: $\tilde{\nu}$ = 3140, 2960, 2902, 1450, 1417, 1356, 1280, 1252, 1178, 1138, 1093, 1025, 1008, 845, 773, 749, 708, 695 cm⁻¹. Raman: $\tilde{\nu}$ = 3146, 2963, 2903, 1417, 1357, 1282, 1236, 1180, 1026, 1008, 704, 600, 234, 185 cm⁻¹. M.p. 56 °C. MS(EI+): *m/z* = 157.2 [M+H]⁺. Impact: >40 J. Friction: <120 N.

(1*N*-1,2,3-Triazolylmethyl)trimethylsilane (2a) and **(2*N*-1,2,3-triazolylmethyl)-trimethylsilane (2b)**: (Chloromethyl)trimethylsilane (2.12 g, 15.7 mmol, 1.0 eq) was stirred with 1*H*-1,2,3-triazole (1.10 g, 17.3 mmol, 1.1 eq) and potassium carbonate (1.60 g, 18.8 mmol, 1.2 eq) in DMSO at ambient temperature for three days. The solvent was poured into 50 mL of ice-water. Raw product was extracted by diethyl ether (2x 50 mL). The organic phases were combined, dried with sodium sulphate, filtered and the solvent was evaporated off. The raw product containing the two isomers **2a** and **2b** (total yield: 63 %, **2a**: 42 %; **2b**: 21 %, estimated out of ¹H NMR integrals) were purified by column chromatography. The first fraction (**2b**) and the second fraction (**2a**) were obtained as colourless oil in 9 % (0.22 g, 1.41 mmol) and 16 % (0.39 g, 2.51 mmol) yield, respectively.

2a: ¹H NMR (CDCl₃): δ = 7.62 (d, 1H, ¹J_{H-H} = 1.7 Hz, C4*H*), 7.39 (d, 1H, ¹J_{H-H} = 1.7 Hz C5*H*), 3.90 (s, 2H, ²J_{H-29Si} = 4.9 Hz, CH₂), 0.09 (s, 9H, ²J_{H-29Si} = 6.6 Hz, CH₃) ppm. ¹³C NMR (CDCl₃): δ = 133.6 (CH), 123.9 (CH), 41.9 (¹J_{CH₂-29Si} = 47.0 Hz, CH₂), -2.5 (¹J_{CH₃-29Si} = 52.7 Hz, CH₃) ppm. ¹⁴N NMR (CDCl₃): δ = -20 – -33 (br, N2/1), -140 (N3). ²⁹Si{¹H} NMR (CDCl₃): δ = 2.5 (¹J_{Si-CH₂} = 47.4 Hz, ¹J_{Si-CH₃} = 53.5 Hz) ppm. IR: $\tilde{\nu}$ = 3126, 2956, 2903, 1740, 1419, 1357, 1298, 1250, 1095, 1047, 971, 963, 844, 808, 770, 753, 699, 678, 652, 621, 608 cm⁻¹. Raman: $\tilde{\nu}$ = 3143, 3128, 2960, 2902, 1421, 1361, 1242, 1191, 1081, 973, 858, 772, 752, 702, 653, 600, 366, 323, 232 cm⁻¹. B.p. 216 °C. T_{dec} 230 °C. MS(EI⁺): *m/z* = 155.2 [M]⁺. MS(FAB⁻): *m/z* = 154.1 [M-H]⁺. Impact: >40 J. Friction: <92 N.

2b: ¹H NMR (CDCl₃): δ = 7.50 (d, 2H, C3/4*H*), 4.05 (s, 2H, ²J_{H-29Si} = 4.9 Hz, CH₂), 0.10 (s, 9H, ²J_{H-29Si} = 6.6 Hz, CH₃) ppm. ¹³C NMR (CDCl₃): δ = 133.4 (CH), 46.9 (¹J_{CH₂-29Si} = 48.9 Hz, CH₂), -2.3 (¹J_{CH₃-29Si} = 52.7 Hz, CH₃) ppm. ¹⁴N NMR (CDCl₃): δ = -55 (N1/3), -127 (N2). ²⁹Si{¹H} NMR (CDCl₃): δ = 2.5 (¹J_{Si-CH₂} = 48.6 Hz, ¹J_{Si-CH₃} = 53.5 Hz) ppm. IR: $\tilde{\nu}$ = 2930, 2897, 1384, 1262, 1110, 1081, 1020, 774, 755, 738, 697, 643, 531 cm⁻¹. Raman: $\tilde{\nu}$ = 2981, 2938, 1382, 1163, 1082, 1000, 789, 748, 543, 512, 489 cm⁻¹. Raman: $\tilde{\nu}$ = 3147, 3132, 2962, 2901, 1481, 1460, 1416, 1395, 1270, 1240, 1212, 1119, 1075, 1028, 949, 850, 769, 737, 703, 640, 595, 359, 325, 234 cm⁻¹. MS(EI⁺): *m/z* = 156.2 [M+H]⁺. MS(FAB⁺): *m/z* = 156.2 [M+H]⁺. Impact: >40 J. Friction: <92 N.

(1*N*-1,2,4-Triazolylmethyl)trimethylsilane (2c): (Chloromethyl)trimethylsilane (1.10 g, 10.6 mmol, 1.50 mL, 1.1 eq) was stirred with 1*H*-tetrazole (0.67 g, 10.0 mmol, 1.0 eq) and potassium carbonate (1.60 g, 11.6 mmol, 1.2 eq) in DMSO (15 mL) at ambient temperature

for two days. The solvent was poured into 50 mL of ice-water. Raw product was extracted by diethyl ether (2x 50 mL). The organic phases were combined, washed twice with water (20 mL), dried with sodium sulphate, filtered and the solvent was evaporated off. The product was obtained as colourless oil in 75 % (1.12 g, 7.20 mmol).

^1H NMR (CDCl_3): δ = 7.87 (s, 1H, C5H), 7.77 (s, 1H, C3H), 3.69 (s, 2H, $^2\text{J}_{\text{H}-29\text{Si}}$ = 5.5 Hz, CH_2), 0.10 (s, 9H, $^2\text{J}_{\text{H}-29\text{Si}}$ = 6.6 Hz, CH_3) ppm. ^{13}C NMR (CDCl_3): δ = 150.5 (s, C3H), 142.0 (C5H), 40.0 (s, $^1\text{J}_{\text{CH}_2-29\text{Si}}$ = 47.9 Hz, CH_2), -3.1 (s, $^1\text{J}_{\text{CH}_3-29\text{Si}}$ = 55.6 Hz, CH_3) ppm. ^{14}N NMR (CDCl_3): δ = -83 (N1), -132 (N4), -170 (N2). $^{29}\text{Si}\{^1\text{H}\}$ NMR (CDCl_3): δ = 1.6 ($^1\text{J}_{29\text{Si}-\text{CH}_2}$ = 49.8, $^1\text{J}_{29\text{Si}-\text{CH}_3}$ = 53.5 Hz,) ppm. IR: $\tilde{\nu}$ = 3417, 3119, 2957, 2902, 1503, 1418, 1346, 1290, 1272, 1250, 1208, 1140, 1011, 958, 843, 768, 739, 701, 680, 661 cm^{-1} . Raman: $\tilde{\nu}$ = 3123, 2960, 2901, 1445, 1417, 1346, 1291, 1141, 1013, 702, 598, 355, 233, 184 cm^{-1} . B.p. 101 °C. MS(EI+): m/z = 155.2 [M]⁺. MS(FAB+): m/z = 156.2 [M+H]⁺. Impact: >40 J. Friction: <144 N.

***E*-(2-Nitrovinyl)trimethylsilane (3)**: Method A: Compound **6** (6.88 g, 18.0 mmol, 1.0 eq) was stirred in dichloromethane (40 mL) and a solution of sodium hydroxide (0.72 g, 18.0 mmol, 1.0 eq) in water (7.2 mL) was added at ambient temperature. After 5 min the suspension was poured onto 1 M HCl (20 mL) and the precipitate was filtered through Celite. The organic phase was washed with water (3x 20 mL), was dried with magnesium sulphate and the solvent was evaporated off. The residue was diluted with n-pentane and filtered. The Solvent was evaporated off and the product was obtained as bright yellow solid in 42 % (1.08 g, 7.47 mmol).

Method B: Similar to the method described in the literature. [nitrovinyl] Concentrated nitric acid (2.21 g, 1.46 mL, 35 mmol, 2.5 eq) was flown gently into a solution of chlorosulphuric acid (3.67 g, 2.09 mL, 31.4 mmol, 2.2 eq), diluted with conc. sulphuric acid (1 mL), under dry argon atmosphere, at 0 °C and vigorous stirring. The mixture of acids is monitored to be always cooler than 5 °C during the addition of nitric acid and afterwards. The generated NO_2Cl was passed through conc. sulphuric acid and a stirred solution of vinyltrimethylsilane (2.86 g, 4.18 mL, 28.5 mmol, 2.0 eq) in CCl_4 (40 mL) by dry argon gas flow. After the complete addition of the nitric acid, the argon gas was still bubbling through the vinyl solution for one hour. Afterwards the gas flow was stopped; the vinyl solution was poured onto ice and was extracted with n-pentane (3x 40 mL). After washing the organic solution with water (2x 20 mL) and an aqueous solution of sodium carbonate (20 mL, 2.1 g Na_2CO_3 ,

~1 M), the solvent was evaporated off and the raw product was taken up in THF and mixed with sodium acetate (2.57 g, 31.0 mmol, 1.1 eq). The solution was refluxed for 15 min and afterwards poured into a stirred mixture of 1 M HCl (20 mL) and diethyl ether (40 mL). The water phase was washed twice with diethyl ether (2x 20 mL). The ether phase was combined and the solvent was evaporated off to obtain the product in 25 % (1.52 g, 1.05 mmol) yield.

^1H NMR (CDCl_3): δ = 7.31 (d, 1H, $^3J_{\text{Hb-Ha}}$ = 15.8 Hz, CH_b), 6.94 (d, 1H, $^3J_{\text{Ha-Hb}}$ = 15.8 Hz, $^2J_{\text{H-29Si}}$ = 4.4 Hz, CH_a), 0.20 (s, 9H, $^2J_{\text{H-29Si}}$ = 6.8 Hz, CH_3) ppm. ^{13}C NMR (CDCl_3): δ = 146.2 (CH_b), 137.3 ($^1J_{\text{C-29Si}}$ = 53.7 Hz, CH_a), -2.8 ($^1J_{\text{CH}_3\text{-29Si}}$ = 54.6 Hz, CH_3) ppm. ^{14}N NMR (CDCl_3): δ = -8.9 (NO_2). $^{29}\text{Si}\{^1\text{H}\}$ NMR (CDCl_3): δ = -4.0 ($^1J_{\text{Si-CH}_3}$ = 54.7 Hz) ppm. IR: $\tilde{\nu}$ = 3089, 2960, 2902, 2865, 1602, 1524, 1418, 1349, 1295, 1252, 1187, 965, 924, 836, 790, 758, 735, 701 cm^{-1} . Raman: $\tilde{\nu}$ = 3089, 3000, 2902, 2690, 2269, 1845, 1620, 1604, 1530, 1415, 1349, 1295, 1265, 1187, 925, 848, 792, 735, 703, 618, 498, 320, 206 cm^{-1} . M.p. 70 °C. T_{dec} 195 °C. MS(EI+): m/z = 147.2 $[\text{M}+2\text{H}]^+$. MS(FAB-): m/z = 145.2 $[\text{M}]^-$. Impact: >40 J. Friction: <120 N.

(Cyanomethyl)trimethylsilane (5): Zinc granules (153 mmol, 10.0 g, 2.0 eq) were stirred with dry sand for two hours to activate the metal surface. After adding dry THF (100 mL) and chloromethylsilane (87.4 mmol, 9.50 g, 11.0 mL, 1.1 eq), chloroacetonitrile (76.5 mmol, 5.77 g, 4.85 mL, 1.0 eq) was slowly stoppered into the reaction mixture. The solution was refluxed for 24 h and quenched with water (100 mL). Mixture was extracted with diethyl ether (3x 100 mL) and washed once with water (100 mL). The organic phase was dried with anhydrous sodium sulphate, filtered and the organic solvent was evaporated off. The pure product **5** was obtained by distillation (70 °C, 29 mbar) in 59 % (5.11 g, 45.1 mmol) yield.

^1H NMR (CDCl_3): δ = 1.57 (s, 2H, $^2J_{\text{H-29Si}}$ = 7.1 Hz, CH_2), 0.20 (s, 9H, $^2J_{\text{H-29Si}}$ = 6.8 Hz, CH_3) ppm. ^{13}C NMR (CDCl_3): δ = 119.1 (CN), 4.9 ($^1J_{\text{C-29Si}}$ = 37.8 Hz, CH_2), -1.9 ($^1J_{\text{CH}_3\text{-29Si}}$ = 53.8 Hz, CH_3) ppm. ^{14}N NMR (CDCl_3): δ = -139 (CN). $^{29}\text{Si}\{^1\text{H}\}$ NMR (CDCl_3): δ = 4.8 ($^1J_{\text{Si-CH}_3}$ = 53.8 Hz, $^1J_{\text{Si-CH}_2}$ = 36.0 Hz) ppm. IR: $\tilde{\nu}$ = 2960, 2904, 2232, 1418, 1396, 1311, 1253, 1149, 952, 843, 793, 767, 702, 669, 608 cm^{-1} . Raman: $\tilde{\nu}$ = 2963, 2903, 2232, 1417, 1151, 704, 609 cm^{-1} . B.p. 165 °C. MS(EI+): m/z = 113.2 $[\text{M}]^+$.

(2-nitro-1-(trimethylsilyl)ethyl)mercury(II) chloride (6): Trimethylvinylsilane (4.00 g, 29.9 mmol, 4.34 mL, 1.0 eq) was added into a solution containing sodium nitrite (4.96 g, 71.8 mmol, 2.4 eq) and mercury(II) chloride (9.75 g, 35.9 mmol, 1.2 eq) in THF/water (0.61 mL/70 mL). The suspension was stirred for four days. The suspension was filtered, washed with water (200 mL) and dried on air for 6 h. The residue was extracted with dichloromethane (200 mL) for 20 h. The solid was filtered through Celite and the organic phase was dried with sodium sulphate. Evaporating off the solvent leads to a white crystalline solid in 61 % (6.96 g, 18.2 mmol) yield.

^1H NMR (CDCl_3): δ = 4.85 (dd, 1H, $^2J_{\text{Hb-Hc}}$ = 14.6 Hz, $^3J_{\text{Hb-Ha}}$ = 5.0 Hz, $^3J_{\text{Hb-Hg199}}$ = 444 Hz, CH_cH_b), 4.64 (dd, 1H, $^2J_{\text{Hc-Hb}}$ = 14.6 Hz, $^3J_{\text{Hc-Ha}}$ = 12.6 Hz, $^3J_{\text{Hc-Hg199}}$ = 143 Hz, CH_cH_b), 2.17 (dd, 1H, $^2J_{\text{Ha-Hg199}}$ = 237 Hz, $^2J_{\text{Ha-29Si}}$ = 6.6 Hz, $^3J_{\text{Ha-Hb}}$ = 5.2 Hz, $^3J_{\text{Ha-Hc}}$ = 12.4 Hz, CH_a), 0.18 (s, 9H, $^2J_{\text{H-29Si}}$ = 6.3 Hz, CH_3) ppm. ^{13}C NMR (CDCl_3): δ = 77.4 (CH_2NO_2), 36.7 ($^1J_{\text{CH-29Si}}$ = 42.2 Hz, $^1J_{\text{CH-199Hg}}$ = 1390 Hz), 0.0 ($^1J_{\text{CH}_3-29\text{Si}}$ = 53.7 Hz, CH_3) ppm. ^{14}N NMR (CDCl_3): δ = 10.8 (NO_2) ppm. $^{29}\text{Si}\{^1\text{H}\}$ NMR (CDCl_3): δ = 4.0 ($^1J_{\text{Si-CH}_3}$ = 53.5 Hz, $^2J_{\text{Si-199Hg}}$ = 106 Hz) ppm. $^{199}\text{Hg}\{^1\text{H}\}$ NMR (CDCl_3): -1025 ppm. ^{199}Hg NMR (CDCl_3): δ = -1025 ($^3J_{\text{Hg-Hc}}$ = 143 Hz, $^2J_{\text{Hg-Ha}}$ = 233 Hz, $^3J_{\text{Hg-Hb}}$ = 445 Hz) ppm. IR: $\tilde{\nu}$ = 2951, 1546, 1415, 1370, 1328, 1248, 1181, 1062, 1017, 962, 832, 754, 685 cm^{-1} . Raman: $\tilde{\nu}$ = 2955, 2898, 1549, 1429, 1414, 1372, 1279, 1265, 1064, 1016, 892, 774, 756, 689, 618, 534, 511, 294 cm^{-1} . Impact: >40 J. Friction: <120 N.

Acknowledgements

Financial support of this work by the Ludwig-Maximilian University of Munich (LMU), the U.S. Army Research Laboratory (ARL) under grant no. W911NF-09-2-0018, the Armament Research, Development and Engineering Center (ARDEC) under grant no. W911NF-12-1-0467, and the Office of Naval Research (ONR) under grant nos. ONR.N00014-10-1-0535 and ONR.N00014-12-1-0538 is gratefully acknowledged. The authors acknowledge collaborations with Dr. Mila Krupka (OZM Research, Czech Republic) in the development of new testing and evaluation methods for energetic materials. We are indebted to and thank Drs. Betsy M. Rice and Brad Forch (ARL, Aberdeen, Proving Ground, MD) for many inspired discussions. Thanks to Stefan Huber for measuring the sensitivity parameters.

[1] C. Evangelisti, T. M. Klapötke, B. Krumm, A. Nieder, R. J. F. Berger, S. A. Hayes, N. W. Mitzel, D. Troegel, R. Tacke, *Inorg. Chem.* **2010**, *49*, 4865–4880.

- [2] T. M. Klapötke, B. Krumm, A. Nieder, O. Richter, D. Troegel, R. Tacke, *Z. Allg. Anorg. Chem.* **2012**, *638*, 1075–1079.
- [3] L. Ascherl, C. Evangelisti, T. M. Klapötke, B. Krumm, J. Nafe, A. Nieder, S. Rest, C. Schütz, M. Sucasca, M. Trunk, *Chem. Eur. J.* **2013**, *19*, 9198–9210.
- [4] G. A. Olah, D. R. Squire in *Chemistry in Energetic Materials*, **1991**.
- [5] T.M.Klapötke in *Chemie der hochenergetischen Materialien*; de Gruyter: Berlin, **2009**.
- [6] J. P. Agrawal, R. D. Hodgson in *Organic Chemistry of Explosives*; John Wiley & Sons: Chichester, **2007**.
- [7] S. Shimizu, M. Ogata, *J. Org. Chem.* **1986**, *51*, 3897–3900.
- [8] T. Jin, S. Kamijo, Y. Yamamoto, *Tetrahedron Lett.* **2004**, 9435–9437.
- [9] W. Zarges, M. Marsch, K. Harms, G. Boche, *Chem. Ber.* **1989**, *122*, 1307–1311.
- [10] I. Matsuda, S. Murata, Y. Ishii, *J. Chem. Soc., Perkin Trans. 1* **1979**, 26–30.
- [11] S. Shimizu, M. Ogata, *Synth. Commun.* **1989**, *19*, 2219–2227.
- [12] W. K. Moberg, *US Patent*, US 4510136, **1985**.
- [13] a) W. K. Moberg, *Eur. Patent*, EP 0068813, **1982**; b) R. Lantzsch, E. Kranz, *BRD Patent*, DE 3539993, **1987**.
- [14] P. M. Graham, M. S. A. Buschhaus, R. A. Baillie, S. P. Semproni, P. Legzdins, *Organomet.* **2010**, *29*, 5068–5072.
- [15] M. Kosugi, M. Koshiha, H. Sano, T. Migita, *Bull. Chem. Soc. Jpn.* **1985**, *58*, 1075–1076.
- [16] Z. Nowak, T. Urbanski, *Biuletyn Wojskowej Akademii Technicznej imienia Jaroslawa Dabrowskiego* **1962**, *11*, 149–154.
- [17] L. A. Leites, A. P. Kurbakova, L. M. Golubinskaya, V. I. Bregadze, *J. Org. Chem.* **1976**, *122*, 1–4.
- [18] H. Feuer, C. Savides, C. N. R. Rao, *Spectrochemi. Acta* **1963**, *19*, 431–434.
- [19] T. Bug, T. Lemek, H. Mayr, *J. Org. Chem.* **2004**, *69*, 7565–7576.
- [20] G. Sanguineti, H. V. Le, B. Ganem, *Tetrahedron* **2011**, *67*, 10208–10211.

- [21] D. J. Morgan, *J. Org. Chem.* **1958**, *23*, 1069–1071.
- [22] D. Seebach, F. Lehr, *Angew. Chem.* **1976**, *88*, 540–541.
- [23] a) R. S. Neale, T. C. Williams, NTIS ADA037464, **1977**; b) R. S. Neale, NTIS ADA072559, **1979**.
- [24] a) K. Baum, D. A. Lerdal, J. S. Horn, *U.S. Patent*, US 4139403, **1979**; b) K. Baum, D. A. Lerdal, J. S. Horn, *J. Org. Chem.* **1978**, *43*, 203–209.
- [25] E. J. Pepe, *U. S. Patent*, US 2985680, **1961**.
- [26] R. F. Cunico, *Synth. Commun.* **1988**, *18*, 917–923.
- [27] G. B. Bachman, M. L. Whitehouse, *J. Org. Chem.* **1967**, *32*, 2303 – 2308; b) G. B. Bachman, M. L. Whitehouse, *US Patent*, US 3428663, **1969**; c) M. Matsuo, Y. Saito, *J. Organometal. Chem.* **1970**, *27*, C41–C43.
- [28] H. C. Brown, P. J. Geoghegan (Jr.), G. J. Lynch, J.T. Kurek, *J. Org. Chem.* **1972**, *37*, 1941–1947.
- [29] a) M. Schmeisser, H. Petri, *Z. Anorg. Allg. Chem.* **1948**, *255*, 33; b) H. Petri, M. Schmeisser, *Z. Anorg. Allg. Chem.* **1948**, *257*, 180–181; c) K. Dachlauer, Deutsches Reichspatent, DRP 509405, **1930**.
- [30] E. V. Trukhin, V. M. Berestovitskaya, G. A. Berkova, V. V. Perekalin, *Russ. J. Gen. Chem.* **1991**, *61*, 1896–1900. (Original: *Zhurnal Obshchei Khimii* **1991**, *61*, 2046–2051.)
- [31] H. Jolibois, A. Doucet, R. Perrot, *Helv. Chim. Acta* **1975**, *58*, 1801–1804.
- [32] S. Miller, S. Henderson, R. Portz, F. Lu, K. Wilson, D. Krismer, L. Alexander, J. Chapman, C. England, *Performance Optimization of Storable Bipropellant Engines to Fully Exploit Advanced Material Technologies*, 2007 NASA Science Technology Conference, College Park, Maryland, **2007**.
- [33] a) S. S. Al-Juaid, C. Eaborn, P. D. Lickiss, J. D. Smith, K. Tavakkoli, A. D. Webb, *J. Organomet. Chem.* **1996**, *510*, 143–151; b) W. Kress, D. K. Breitingner, R. Sendelbeck, *J. Organomet. Chem.* **1983**, *246*, 1–8; c) D. M. Heinekey, S. R. Stobart, *Inorg. Chem.* **1978**, *17*, 1463–1466; d) S. Al-Hashimi, J. D. Smith, *J. Organomet. Chem.* **1978**, *153*, 253–263; e) B. Wrackmeyer, K. Horchler von Locquenghien, E. Kupce, A. Sebald, *Magn.*

- Reson. Chem.* **1993**, *31*, 45–50; A. Michalides, A. Blaschette, P. G. Jones, *Z. Anorg. Allg. Chem.* **2000**, *626*, 717–721; T. M. Klapötke, B. Krumm, R. Moll, *Eur. J. Inorg. Chem.* **2011**, 422–428; T. M. Klapötke, B. Krumm, R. Moll, *Z. Anorg. Allg. Chem.* **2011**, *637*, 507–514; F. Glocking, V. B. Mahale, J. J. Sweeney, *J. Chem. Soc., Dalton Trans.* **1979**, 767–770.
- [34] a) T. N. Mitchell, H. C. Marsmann, *J. Organomet. Chem.* **1978**, *150*, 171 – 177; b) M. J. Albright, T. f. Schaaf, A. K. Hovland, J. P. Oliver, *J. Organomet. Chem.* **1983**, *259*, 37–50.
- [35] M. F. Larin, D. V. Gendin, V. A. Pestunovich, L. I. Rybin, O. A. Vyazankina, N. S. Vyazankin, *Russ. Chem. Bull.* **1983**, *9*, 2139–2140.
- [36] a) T. N. Mitchell, B. Kowall, *J. Organomet. Chem.* **1994**, *471*, 39–42; b) N. A. Daugherty, B. Schiefelbein, *J. Am. Chem. Soc.* **1969**, *91*, 4328–4329.
- [37] M. J. Frisch *et al.*, *GAUSSIAN 09 (Revision C.01)*, Gaussian Inc., Wallingford CT, **2010**.
- [38] D. Andrae, U. Häusermann, M. Dolg, H. Stoll, H. Preuss, *Theor. Chim. Acta* **1990**, *77*, 123–141.
- [39] A. Bondi, *J. Phys. Chem.* **1964**, *68*, 441–451.
- [40] a) A. Gorrane, I. Resa, D. del Rio, A. Rodriguez, E. Alvarez, K. Mereiter, E. Carmona, *Inorg. Chem.* **2007**, *46*, 4667–4676; b) P. Slavik, M. Dudic, K. Flidrova, J. Sykora, I. Cisarova, S. Böhm, P. Lhotak, *Org. Lett.* **2012**, *14*, 3628–3631.
- [41] www.bam.de (German version), www.bam.de/en/index.htm (English version).
- [42] *UN Recommendation on the Transport of Dangerous Goods, Manual of Tests and Criteria, Amendment 1*. http://www.unece.org/trans/publications/dg_tests2011.html, **2011**.
- [43] M. Suceška, *EXPLO5 program vers. 6.01*, Zagreb, Croatia, **2012**.
- [44] M. S. Westwell, M. S. Searle, D. J. Wales, D. H. Williams, *J. Am. Chem. Soc.* **1995**, *117*, 5013–5015.
- [45] *NATO standardization agreement (STANAG) on explosives, impact sensitivity tests, no. 4489*, 1st ed., **1999**.

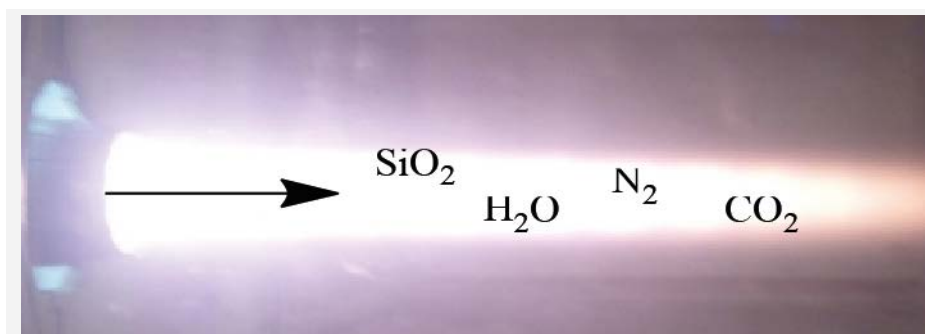
- [46] *WIWEB-Standardarbeitsanweisung 4-5.1.02, Ermittlung der Explosions-gefährlichkeit, hier der Schlagempfindlichkeit mit dem Fallhammer, 2002.*
- [47] *NATO standardization agreement (STANAG) on explosives, friction sensitivity tests, no. 4487, 1st ed., 2002.*
- [48] *WIWEB-Standardarbeitsanweisung 4-5.1.03, Ermittlung der Explosionsgefährlichkeit oder der Reibeempfindlichkeit mit dem Reibeapparat, 2002.*
-

IX. Theoretical Approach of Energetic Silanes

Energetic silanes

C. Evangelisti, L. Göpfert, T. M. Klapötke, B. Krumm, A. Nieder and M. Suceska 195 - 229*

Theoretical Approach of Nitrogen-rich Heterocycle- and Nitro-substituted Trimethylsilyl Derivatives and Their Carbon Analogues



Monosubstituted derivatives of tetramethylsilane containing different energetic moieties were studied by theoretical efforts for several reasons: First of all to get structural information, further to

calculate the specific impulse in different formulations and compare these computations by calculations using different computing codes (EXPLO5 version 6.01, ICT, CHEETAH 2.0).

Theoretical Approach of Nitrogen-rich Heterocycle- and Nitro-substituted Trimethylsilyl Derivatives and Their Carbon Analogues

Camilla Evangelisti, Lisa Göpfert, Thomas M. Klapötke*, Burkhard Krumm, Anian Nieder
and Muhamed Suceska

Unpublished

Abstract: Several trimethylsilyl substituted nitrogen-rich heterocycles (triazoles and tetrazoles), azido, nitrato, nitro derivatives are discussed as potential high energetic compounds. In general, mixtures of different silanes with several common oxidizers (AP, ADN, N₂O₄) were calculated by using EXPLO5 version 6.01, computer

codes. The results are compared with the calculations of other computing codes (ICT-Code, CHEETAH 2.0). The energies of formation were computed by Gaussian version C3 and on CBS-4M level of theory. In addition the molecular structures are computed on MP2 level of theory and their interactions and structural characteristics are

discussed to get information about their chemical and physical behavior.

Keywords: heterocycle • silanes • energetic properties • keyword 4 • keyword 5

Introduction

Recently, the computational chemistry and physics become more important, on the one hand due to the advance in computing power and precise computing codes and the laborious, time-consuming and relative expensive experiments for new compounds on the other hand.[1] In the case of hazard materials like explosive material the factory of safety is weightily. Therefore, several computing codes were written and upgraded to predict performance parameters of thought molecules and to estimate the cost-benefit ratio to start synthesizing a new compound.

One modern computer code used for this research is EXPLO5 version 6.01.[14] Other programmes, like CHEETAH 2.0 and the ICT computing code, are also common, whereas

* T. M. Klapötke
Department of Chemistry and Biochemistry,
Ludwig-Maximilian University of Munich,
Butenandtstr. 5-13(D), 81377 Munich, Germany

the first one is old-fashioned, but due to government regulation there is no newer computing code available outside the U.S.. The second one is up-to-date but only slightly information are available about its program code and also its calculation methods. The EXPL05 programme is based on the chemical equilibrium state of detonation. For gaseous detonation products the Becker-Kistiakowski-Wilson state equations (BKW EOS, Becker-Kistiakowski-Wilson equilibrium of state) are used and for solid carbon the Cowan-Fickett-equation is applied as given below. Composition of the equilibrium is based on the modified minimizing technique of the free energy by White, Johnson and Dantzig. Calculation of the respective detonation parameter is performed at the C-J-point (Chapman-Jouguet point, explanation see in the following).[14] The BKW EOS allow for the ideal gas law to be modified from (1) to (2) with the aberration from ideal gases being major.[1]

$$pV = nRT \quad (1)$$

$$pV/RT = 1 + xe^{\beta x} \quad \text{with } x = k/VT^\alpha \quad (2)$$

At extremely low temperatures the pressure would rise to infinity, so Cowan and Fickett modified the equation by changing the factor x:

$$pV/RT = 1 + xe^{\beta x} \quad \text{with } x = \kappa \sum X_i k_i / V(T + \Theta)^\alpha \quad (3)$$

Solid products are calculated using the Cowan-Fickett equation for solids, whereas the parameters for solid carbon (graphite) are given below:[1]

$$p = p_1(V) + a(V)T' + b(V)T'^2$$

$$T' = T/11605.6 \text{ K}$$

$$p_1(V) = -2.467 + 6.769\eta - 6.956\eta^2 + 3.040\eta^3 - 0.3869\eta^4$$

$$a(V) = -0.2267 + 0.2712\eta$$

$$b(V) = 0.08316 - 0.07804\eta^{-1} + 0.03068\eta^{-2}$$

and material compaction η

$$\eta = V^\circ T^\circ / V = p/p^\circ$$

The resulting $p(V)$ graph has the form of a parabola cut-out, also known as Hugoniot-curve[15] and represents all allowed states which can be assumed by the shock adiabatic curve. The C-J-point, in which the Chapman-Jouguet condition is fulfilled, is the contact point of the shock adiabatic curve of the reaction products with the Rayleigh line, characterized through the following equation:

$$p - p_0 = p_0^2 \cdot U^2(V_0 - V)$$

At the contact point the slope of the Rayleigh line and the shock adiabatic curve of the reaction products are equal and thus can be described through the following correlation:[1]

$$\delta p / \delta V = D^2 / V^2 = U^2 / V^2$$

EXPLO5 version 6.01, as well as for CHEETAH 2.0[16] and ICT-Code, calculates the detonation parameters and the chemical composition at the C-J-point with the implementation of the steady state detonation model.[11] For gases the BKW EOS is applied, using formula (3) with the parameters

$$\alpha = 0.5$$

$$\beta = 0.176$$

$$\kappa = 14.71$$

$$\theta = 6620$$

for EXPLO5 version 6.01[1] and

$$\alpha = 0.5$$

$$\beta = 0.40266$$

$$\kappa = 10.864$$

$$\theta = 5441$$

for CHEETAH 2.0[16], whereas the exact formulas for the ICT computing code are unknown.

Identification of the composition of detonation products at the equilibrium state is allowed using the minimizing internal energy according to the White-Johnson-Dantzig technique. Thermodynamic functions of the components of the system, such as enthalpy, entropy, free enthalpy and free energy, can be derived based on the state equations. These can be calculated using the following formula for reaction products at standard conditions from the enthalpy:[1]

$$(H_T^\circ - H^\circ_0) = c_0 + c_1 \cdot T + c_2 \cdot T^2 + c_3 \cdot T^3 + c_4 \cdot T^4$$

EXPLO5 calculates the Hugoniot-curve and state parameters at the shock front for reaction products between specific volumes V_0 , at the moment of explosion, and V_1 for various V_i . The C-J-point is the minimum of detonation velocity and is shown as the minimum in the derivative of the $p(V)$ -function, depicted as the Hugoniot-curve. Detonation parameters can be calculated according to the hydrodynamic detonation theory, using the conservation of mass, impulse and energy dependent on p and V , which provides the correlation for detonation velocity and impact speed:[15]

$$D = V_0 \sqrt{(p - p_0/V_0 - V)} \quad \text{and} \quad U = V_0 - V \sqrt{(p - p_0/V_0 - V)}$$

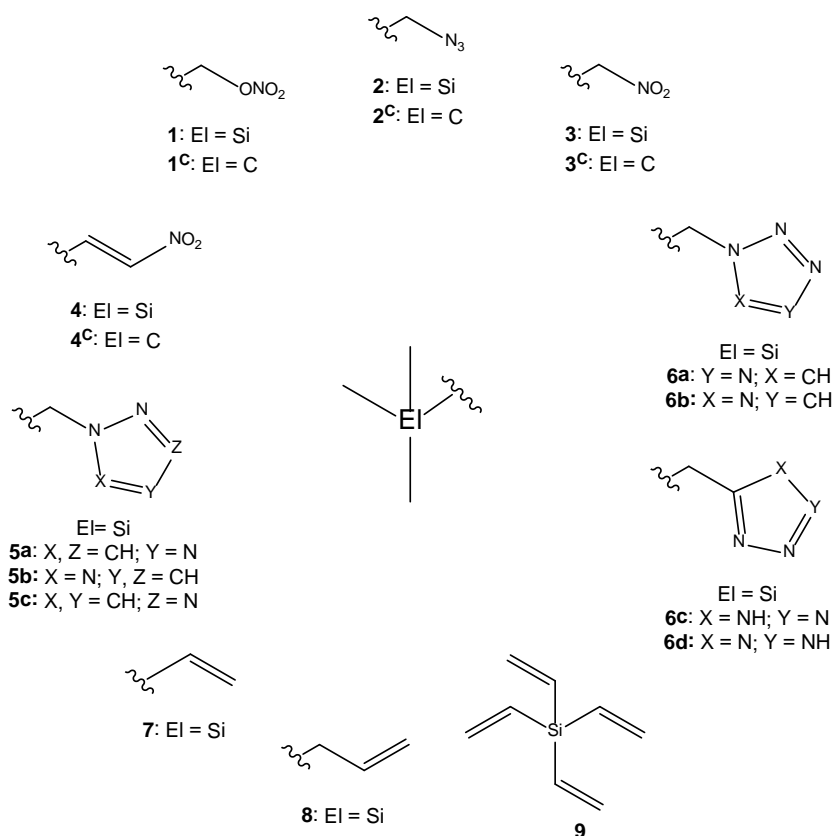
Additionally EXPLO5 and also the other mentioned computing codes CHEETAH and ICT, calculates the combustion parameters I_{sp} and T_c . For the calculation of rocket fuels $p = \text{const.}$ which leads to calculating the isobaric combustion. The following assumptions are made:[1]

1. pressure in the combustion chamber and the nozzle throat is constant,
2. conservation of energy and moment is applied,
3. velocity of the combustion products within the combustion chamber is zero,
4. temperature and velocity of the gaseous and condensed combustion products are the same,
5. the expansion into the nozzle is isentropic

In addition to the specific impulse the isobaric combustion temperature is also calculated due to the fact that according to the temperature the products and their frequency may vary, especially those of carbon monoxide, carbon dioxide and carbon as the Boudouard reaction is temperature sensitive. The water-gas shift reaction in contrast has only slightly influence to the propulsion values, because the entropy can be described as constant at the normally observed reaction conditions in the reaction chamber ($\text{CO(g)} + \text{H}_2\text{O(g)} \rightarrow \text{CO}_2\text{(g)} + \text{H}_2\text{(g)}$).[3]

In the following the main focus will be by using the EXPLO5 version 6.01 computing code. Differences of the handling and the obtained values between the three codes will be discussed. The small trimethylsilyl back-bone structure connected with methylene bridged

energetic moieties was used as comparable model structures (see Scheme 9.1). They are easy to calculate and the structural influences should be manageable. In addition the physical parameters are expected to be comparable and experimental values are often easily obtainable by experiments or already known in literature. In some cases also the carbon analogues were computed and discussed.



Scheme 9.1. Molecular structures and labels of the discussed silanes and some of their carbon analogues ((nitratomethyl)trimethylsilane **1**,[7] neopentenyl nitrate **1^c**,[7] (azidomethyl)trimethylsilane **2**, [8] 1-azido-2,2-dimethylpropane **2^c**, (nitromethyl)trimethylsilane **3**, 2,2-dimethyl-1-nitropropane **3^c**, (*E*)-(2-nitrovinyl)trimethylsilane **4**, (*E*)-3,3-dimethyl-1-nitrobut-2-ene **4^c**, 1-((trimethylsilyl)methyl)-1*H*-1,2,4-triazole **5a**, 1-((trimethylsilyl)methyl)-2*H*-1,2,3-triazole **5b**, 1-((trimethylsilyl)methyl)-1*H*-1,2,3-triazole **5c**, 1-((trimethylsilyl)methyl)-1*H*-tetrazole **6a**, 2-((trimethylsilyl)methyl)-2*H*-tetrazole **6b**, 5-((trimethylsilyl)methyl)-1*H*-tetrazole **6c**, 5-((trimethylsilyl)methyl)-2*H*-tetrazole **6d**, trimethyl(vinyl)silane **7**, allyltrimethylsilane **8**, tetravinylsilane **9**).

Results and Discussion

To the best of our knowledge no structural information is given for most of the compounds in literature except for the gas-phase structures of **1** and **1^c** by electron diffraction experiments.[7] Therefore to get an idea of the structures and its intramolecular interactions of all compounds (except **7–9**) theoretical calculation were computed on MP2/cc-pVDZ level of theory. The liquid and solid states may differ from those calculated as intermolecular interactions are present and may alter the structures, but some inferences can be possibly done. All silicon containing substances used for this research are liquid at ambient temperature and did not crystallize in a good measurable shape in the freezer. Therefore no crystal structures were obtained. The calculated structures are given in Figure 9.1 (azido derivatives), Figure 9.2 (nitro derivatives), Figure 9.3 (triazole derivatives) and Figure 9.4 (tetrazole derivatives). In addition the corresponding bond distances, angles and intramolecular interactions are given in Table 9.1 (azido derivatives), Table 9.2 (nitro derivatives), Table 9.3 (triazole derivatives) and Table 9.4 (tetrazole derivatives).

The calculated gas phase structure of the compounds **2** and **2^c** are highly similar and typical for other known computed structures of mono-substituted tetramethylsilanes and neopentyl derivatives. Also both structure show only slightly but important differences. The Si-CH₃ and C-CH₃ bond lengths are in a typical range of these types of bonding (1.888–1.892 Å, 1.534–1.535 Å respectively). In these cases the Si-C1H₃ and C-C1H₃ bond lengths are computed as slightly elongated in comparison to the other methyl bonding, whereas the elongation in structure **2^c** is more insignificant than for Si-C1H₃ bond elongation. The main difference between **2** and **2^c** is found in the bonding of the substituent. In the case of **2** the Si-CH₂ bond is elongated compared to all Si-CH₃ bond lengths (1.913 Å towards 1.888 Å in average). The bond length differences between C-CH₂ and C-CH₃ bond in **2^c** is almost negligible, but taking a closer look the inverse situation is found for the computation of **2^c** (1.533 Å towards 1.535 Å in average). The N₃-N₂-N₁-C₄-Si/C-C₁ chains are absolutely in-plane (torsion angles of always ±180 °) in both cases. Comparing the N₃CH₂- moieties of **2** and its carbon analogue **2^c**, the C-N bond is longer in the silicon derivative in contrast to the bond of its carbon analogue (1.491 Å towards 1.484 Å). The same is true for the N₁-N₂ bond lengths (1.246 Å towards 1.244 Å). N₂-N₃ bond lengths are almost equal in both cases

with 1.164 Å). To conclude the results till this point the bond length and the bond strength at N1 (C4–N1 and N1–N2) are both elongated, weaker respectively, for the computation of the silicon derivative compared to the situation of N1 in structure **2^c**. It can be derive from this situation that the ionic character is increased at N1 or intramolecular interactions degenerate the bond orders of the C4–N1 and N1–N2 bonds. The distances of possible intramolecular N1---H₃C_{2/3} or N1---C_{2/3} interactions are quite long and unlikely ($d(\text{N}---\text{H}_3\text{C})$: 2.966 Å, $\Sigma\text{vdW}(\text{N,H})$: 2.75 Å[18]; $d(\text{N}---\text{C}_{2/3})$: 3.332 Å, $\Sigma\text{vdW}(\text{N,C})$: 3.25 Å[18]), consequently a N1---Si interaction become most likely ($d(\text{N1}---\text{Si})$: 2.733 Å, $\Sigma\text{vdW}(\text{N,Si})$: 3.65 Å[18]). This is result is affirmed by the elongation of the Si–C1 bond, due to electron donation of N1 to the anti-bonding orbital of the Si–C1 bond orbital. Similar situations are expected for the following structures.

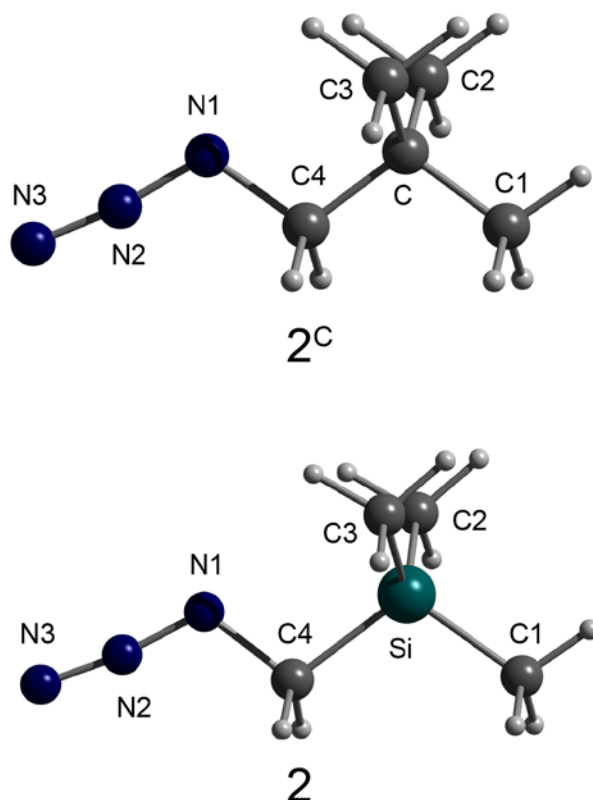


Figure 9.1. Calculated molecular gas phase structures of the compounds **2** and **2^c** on the MP2/cc-pVDZ level of theory (intramolecular interactions are given in red dashed lines).

The calculated molecular structure of **3** reveals a slightly longer bond between Si and C1 (1.889 Å, lit.: 1.88 Å[17]) than Si and C2 or C3 (1.885 Å). In contrast the bond length

between Si and C4 is elongated (1.929 Å), due to the electron withdrawing substituent at C4. In the same way the Si-C4 bond becomes longer and the C4-R bond (in this case R = NO₂, d(C4-N1): 1.486 Å, but this is also the case for other electron withdrawing substituents) is typically shortened. In comparison with its carbon analogue **3^c** the bonding situation is vice

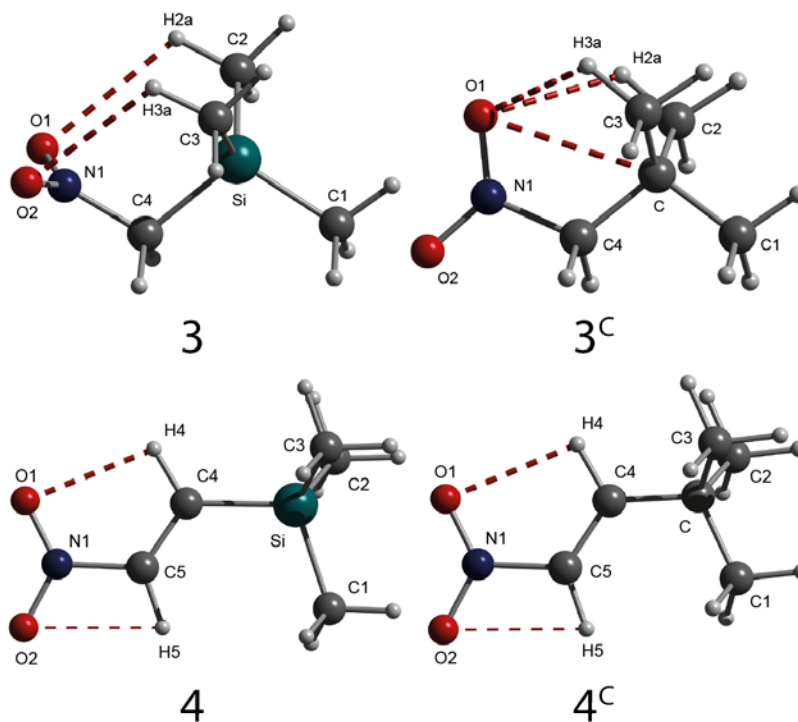


Figure 9.2. Calculated molecular gas phase structures of the compounds **3**, **3^c**, **4** and **4^c** on the MP2/cc-pVDZ level of theory (intramolecular interactions are given in red dashed lines).

versa. The carbon analogue **3^c** shows a shorter bond for C-C1 (1.536 Å) compared to C-C2/C3 (1.540 Å) and the bond length C-C4 (1.531 Å) is also shortened compared to C-C2/C3 (1.531 Å). The C-C4 bond distance is shortened in the structure of **3^c** and therefore the C4-N1 bond is expected to be elongated, which is the case (d(C4-N1): 1.508 Å). The main reason is found in the different orientation of the nitro moiety in these two analogues. For the silicon analogue **3** the nitro moiety is twisted out of the C1-Si-C4-N1 plane ($\theta(\text{O1/2-N1-C4-Si})$: $\pm 88.3^\circ$), which is fixed in position by a symmetrical intramolecular electrostatic interaction between each oxygen atom toward a hydrogen atom of two methyl groups (H2a and H3a: d(O---H2/3a): 2.739 Å, $\Sigma \text{vdW}(\text{O,H})$: 2.72 Å[18]). In the second case of the corresponding carbon analogue the oxygen atoms are in the plane of C1-C-C4-N1 ($\theta(\text{O1/2N1-C4C})$: 0/180 °) This orientation is fixed by strong interactions of O1 to the two hydrogen atoms H2a and H3a of two methyl moieties (d(O1---H2a/3a): 2.392 Å), much

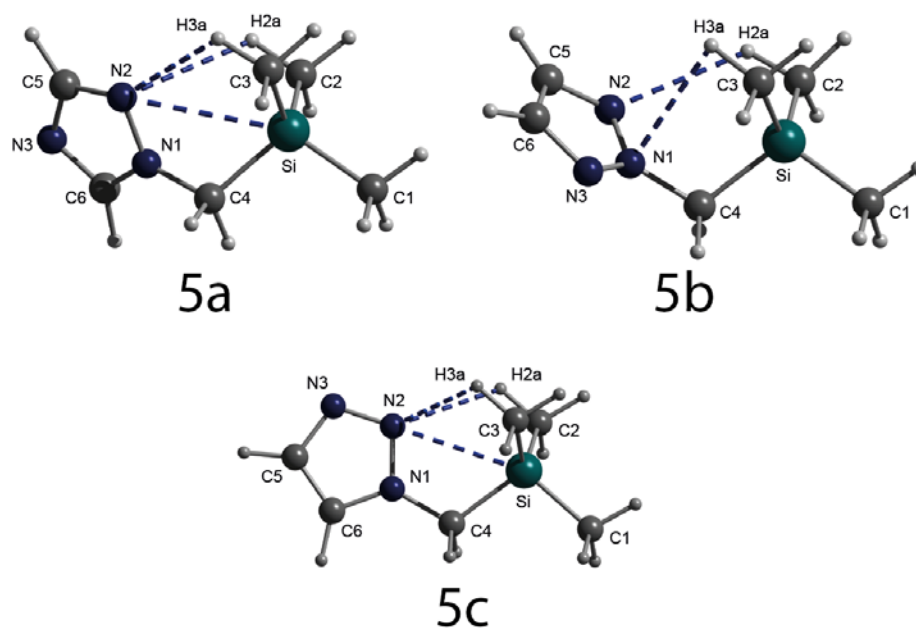


Figure 9.3. Calculated molecular gas phase structures of the compounds **5a**, **5b** and **5c** on the MP2/cc-pVDZ level of theory (intramolecular interactions are given in blue dashed lines).

stronger as found for the silicon analogue, and to the central carbon atom C ($d(\text{C}\cdots\text{O1})$: 2.852 Å, $\Sigma\text{vdW}(\text{O},\text{C})$: 3.22 Å[18]), pointing almost vertically to the C–C1 bond ($\alpha(\text{C1}-\text{C}\cdots\text{O1})$: 161.4°). The twisting in plane of R–C4–El–C1 is found for most carbon and also silicon analogues of a similar kind.[7,9] The twisting out of plane in compound **3** cannot lead to a commonly found intramolecular interaction between the substituent R and the central atom Si, but was surprisingly found for compound **3^c**. In the case of **3^c** the structural differences seem to be mainly influenced by sterical reasons, in the case of **3** it seems to be electronically (bond orbitals, electrostatic attractions etc.). The angles of the C4–Si–CH₃ moiety become more obtuse ($\alpha(\text{C4}-\text{Si}-\text{CH}_3)$: 106.8 and 107.3°) in comparison with its ideal tetrahedral Me₄Si ($\alpha(\text{C}-\text{Si}-\text{C})$: 109°), and in contrast to the situation for **3^c** ($\alpha(\text{C4}-\text{C}-\text{CH}_3)$: 110.9° and 111.6°). Consequently, the SiMe₃ trigonal pyramid becomes more flattened, which indicates in addition to the elongated C4–Si bond an increased ionic character of the Si–C bonds. Chemically it indicates a good possibility for nucleophilic attacking at the central silicon atom (not the case for **3^c**) and easy cleaving of the RCH₂–Si or a Si–CH₃ bond. Bond lengths for the nitro moieties of **3** and **3^c** are almost equal and within the expected range for bond lengths between single and double bonds ($d(\text{N1}-\text{O1}/2)$: 1.232–1.235 Å). The intramolecular interactions of the nitro moieties to hydrogen atoms of the methyl groups insignificantly influence the bonding situation of N1 to O1/2 in its lengths in **3** and **3^c**.

IX. Theoretical Approach of Energetic Silanes

Table 9.1. Bond lengths [Å], angles [°] and torsion angles [°] of the calculated gas phase structures of the nitro derivatives **1** and **1^c** on RI-MP2/TZVPP level of theory[7] (in parentheses at the bottom), the values of the computed gas phase structures **2** and **2^c** on MP2/cc-pVDZ level of theory, in addition the experimental GED values of the structures **1** and **1^c**[7] (value at the top with standard deviation in parentheses).

MP2/cc-pVDZ									
Bond length d [Å]	1 (El = Si)		1^c (El = C)		Angles α [°]	1 (El = Si)		1^c (El = C)	
	GED ^[a,b] (calc. ^[a])		GED ^[a,b] (calc. ^[a])			GED ^[a,b] (calc. ^[a])		GED ^[a,b] (calc. ^[a])	
El-C1					C1-El-C2			111.1	109.9
El-C2	1.883(1) (1.879)		1.539(1) (1.525)		C1-El-C3			111.1	109.9
El-C3					C1-El-C4	110.9(4) (111.2)	109.2(2) (109.9)	108.3	107.6
El-C4	1.906(5) (1.905)		1.536(4)		C2-El-C3			110.9	110.1
C4-O1	1.447(5) (1.433)		1.446(3) (1.422)		C2-El-C4			107.6	109.6
C4-N1				1.491	C3-El-C4			107.6	109.6
O1-N	1.426(4) (1.425)		1.411(2) (1.422)		El-C4-O1	107.1(3) (105.4)	106.3(3) (106.9)		
N-O2/3	1.208(1) (1.206)		1.211(1) (1.208)		El-C4-N1			106.2	108.9
N1-N2				1.246	C4-O1-N1	113.0(4) (113.4)	113.6(3) (113.2)		
N2-N3				1.164	C4-N1-N2			115.4	115.1
El---O1	2.729(4)(2.671)	2.392(2)			O2-N1-O3	131.2(7) (130.6)	132.0(6) (130.0)		
El---N1				2.733	N1-N2-N3			172.7	173.0
N1---C2/3				3.332	C1-El---N1			139.9	142.5
N1---H2a/3a				2.966	El---N1-N2		157.6	151.4	
				2.556					
Torsion angles θ [°]									
C1-El-C4-O5	180 (180)	180 (180)							
C1-El-C4-N1			180	180					
El-C4-N1-N2			180	180					
C4-N1-N2-N3			180	180					

[a] ref. [7]; [b] values are taken from the vibrational averaged structure.

IX. Theoretical Approach of Energetic Silanes

Table 9.2. Bond lengths [Å], angles [°] and torsion angles [°] of the calculated gas phase structures of the nitro derivatives **3**, **3^c**, **4** and **4^c** on MP2/cc-pVDZ level of theory.

MP2/cc-pVDZ									
Bond length d [Å]	3 (El = Si)	3^c (El = C)	4 (El = Si)	4^c (El = C)	Angles α [°]	3 (El = Si)	3^c (El = C)	4 (El = Si)	4^c (El = C)
El-C1	1.889	1.536	1.890	1.541	C1-El-C2	111.8	108.7	110.7	109.2
El-C2	1.885	1.540	1.888	1.541	C1-El-C3	111.8	108.7	110.3	109.7
El-C3	1.885	1.540	1.888	1.533	C1-El-C4	106.8	105.0	108.0	107.8
El-C4	1.929	1.531	1.895	1.508	C2-El-C3	111.4	110.9	110.7	109.7
C4-C5			1.344	1.343	C2-El-C4	107.3	111.6	109.0	107.8
C4-N1	1.486	1.508			C3-El-C4	107.3	111.6	108.0	112.6
C5-N1			1.479	1.468	C5-C4-El			123.3	125.9
N1-O1	1.235	1.233	1.236	1.236	El-C4-N1	109.0	117.9		
N1-O2	1.235	1.232	1.230	1.231	C4-C5-N1			121.8	120.8
O1---H2a	2.739	2.392			O1/2-N1-C4	117.2/117.2	119.8/114.9		
O1---H3a		2.392			O1/2-N1-C5			115.2/118.8	115.2/119.1
O2---H3a	2.739				O1-N1-O2	125.5	125.3	125.9	125.7
O1---H4a			2.396	2.404	C1-C---O1		161.4		
O2---H5a			2.392	2.387					
O1---C		2.852							
Torsion angles θ [°]									
C1-El-C4-C5			-120.3	121.1					
C1-El-C4-N1	180.0	180.0							
C2-El-C4-C5			0.0	-121.2					
C2-El-C4-N1	-59.9	-62.4							
C3-El-C4-C5			120.3	0.0					
C3-El-C4-N1	59.9	62.4							
O1-N1-C4-El	88.3	0	180	180					
O2-N1-C4-El	-88.3	180	0	0					
N1-C5-C4-El			180	180					

IX. Theoretical Approach of Energetic Silanes

Table 9.3. Bond lengths [Å], angles [°] and torsion angles [°] of the calculated structures of the nitro derivatives **5a–c** on MP2/cc-pVDZ level of theory.

MP2/cc-pVDZ							
Bond length d [Å]	5a	5b	5c	Angles α [°]	5a	5b	5c
Si–C1	1.894	1.892	1.897	C1–Si–C2	110.8	111.0	109.4
Si–C2	1.887	1.886	1.885	C1–Si–C3	110.2	111.6	109.8
Si–C3	1.885	1.888	1.886	C1–Si–C4	105.7	107.9	103.3
Si–C4	1.929	1.926	1.931	C2–Si–C3	111.9	107.9	112.8
C4–N1	1.460	1.462	1.461	C2–Si–C4	107.5	109.2	111.4
C5–C6		1.402	1.364	C3–Si–C4	110.5	105.7	109.8
C5–N2	1.350	1.361		C5–N2–N1	102.1		
C5–N3	1.362		1.393	C5–N3–N2		102.8	108.0
C6–N1	1.362		1.352	C5–C6–N1		108.8	103.8
C6–N3	1.338	1.360		C5–C6–N3			
N1–N2	1.350	1.337	1.331	C5–N3–C6	102.0		
N1–N3		1.336		C6–N1–N2	110.0	102.7	111.0
N2–N3			1.364	C6–C5–N3		108.7	109.3
Si---N2	3.144		3.144	N1–C6–N3	110.5		
N2---H2a	2.860	2.790	2.860	N1–N2–N3		116.9	107.9
N2---H3a	2.760		2.760	N2–C5–N3	115.4		
N1---H3a		3.142		Si–C4–N1	112.3	109.8	113.9
Torsion angles θ [°]				C4–N1–C6	129.4		129.3
C1–Si–C4–N1	-163.1	160.7	173.0	C4–N1–N2	120.6	121.5	119.7
C2–Si–C4–N1	-44.7	-78.5	-69.7	C4–N1–N3		121.3	
C3–Si–C4–N1	77.7	41.1	56.0	C1–Si---N2	156.5		157.3
C6–N1–C4–Si	-44.8		-165.7				
Si–C4–N1–N2	135.3	-104.1	15.9				
Si–C4–N1–N3		68.8					

In the case of **4** and **4^c** two interactions are found for each molecule (O1---H4 and O2---H5). They are significantly below the sum of the van der Waals radius ($\Sigma_{vdW}(O,H)$: 2.72 Å [18]; d(O1---H4): 2.392/2.396 Å and d(O2---H5): 2.387/2.404 Å). It is doubtful whether the interaction O2---H5 is a noteworthy one, because the distance is structurally rigid and has no significant influence on the N1–O2 bond distance (d(O2---H5): 1.230 Å (**4**) and 1.231 Å (**4^c**)) in contrast to the O1---H4 interaction. The O1---H4 distance is longer (d(O1---H4): 2.396/2.404 Å) compared to d(O2---H5), but it shows a significant bond elongation, due to reduced bond order by the O1---H4 interaction, which additionally creates an energetically favoured five-membered ring. In contrast to compound **3**, compound **4** has only slightly elongated Si–C4 and Si–C1 bonds. The tendencies concerning bond lengths are the same as described for compound **3**. In addition the situation is also vice versa for the carbon analogue **4^c** and consequently the same as in **3^c** (shown in Table 9.1). Both double bonds of **4** and **4^c** have almost the same distance and are in the range of typical C=C double bonds. In contrast to the N1–C4 bond lengths of **3** and **3^c** (d(C4–N1): 1.486/1.508 Å) the

IX. Theoretical Approach of Energetic Silanes

Table 9.4. Bond lengths [Å], angles [°] and torsion angles [°] of the calculated structures of the tetrazole derivatives **6a–d** on MP2/cc-pVDZ level of theory.

MP2/cc-pVDZ *									
Bond length d [Å]	6a	6b	6c	6d	Angles α [°]	6a	6b	6c	6d
Si–C1	1.893	1.894	1.892	1.892	C1–Si–C2	110.3	109.9	111.3	110.9
Si–C2	1.883	1.885	1.884	1.887	C1–Si–C3	111.0	110.2	110.8	110.7
Si–C3	1.886	1.886	1.891	1.892	C1–Si–C4	104.8	103.5	108.1	108.6
Si–C4	1.933	1.929	1.927	1.920	C2–Si–C3	112.2	112.5	110.9	110.4
C4–C5			1.489	1.489	C2–Si–C4	110.5	110.9	108.5	108.9
C4–N1	1.462	1.459			C3–Si–C4	107.7	109.5	107.0	107.3
N1–N2	1.347	1.331	1.346	1.326	Si–C4–N1	112.7	114.1		
N2–N3	1.327	1.346	1.322	1.340	Si–C4–C5			110.0	110.5
N3–N4	1.358	1.333	1.361	1.331	C4–C5–N1			127.1	123.6
N4–C5	1.333	1.353	1.337	1.363	C4–C5–N4			126.0	124.1
C5–N1	1.356	1.350	1.358	1.356	C4–N1–N2	121.0	122.1		
Si---N1			3.357	3.384	C4–N1–C5	130.8			
Si---N2	3.113	3.052			C4–N1–N4		123.5		
N2---H2/3a	2.761/ 2.807	2.756/ 2.775			C5–N1–N2	108.1	100.6	110.3	100.5
N1---H2a			2.723	2.769	C5–N4–N3	105.7	105.5	106.7	106.9
Torsion angles θ [°]					N1–C5–N4	109.0	113.6	106.8	112.2
C1–Si–C4–C5			165.8	164.1	N1–N2–N3	106.5	114.4	105.3	116.0
C1–Si–C4–N1	164.9	173.6			N2–N3–N4	110.7	105.9	111.0	104.5
C2–Si–C4–C5			-73.4	-75.1	C1–Si---N1			155.7	155.0
C2–Si–C4–N1	-76.2	-68.5			C1–Si---N2	156.5	157.0		
C3–Si–C4–C5			46.4	44.5	C2–Si---N1			76.6	77.0
C3–Si–C4–N1	46.7	56.1			C2–Si---N2	80.9	81.5		
Si–C4–C5–N1			-114.0	-109.7	C3–Si---N1			85.8	87.1
Si–C4–C5–N4			61.0	66.6	C3–Si---N2	81.6	81.8		
Si–C4–N1–N2	37.9	15.6			C4–Si---N1			48.5	47.5
Si–C4–N1–C5	-142.1				C3–Si---N2	51.8	53.5		
Si–C4–N1–N4		-166.1							

bond distance for the silicon analogue **4** ($d(\text{C5–N1})$: 1.479 Å) is not shorter than for **4^c** ($d(\text{C5–N1})$: 1.468 Å). Angles in the molecules **4** and **4^c** show exactly the same bending tendencies as already described for **3** and **3^c**. To summarize, based on the results of the computed data, for compounds **4** and **4^c**, there is no clear evidence for structural/chemical instability as found for compound **3**.

The three triazole isomers **5a–c** show an almost similar bonding situation for the $\text{Me}_3\text{SiCH}_2\text{R}$ moieties and also comparable to the structure of **3**. In all cases the Si–C1 and even more the Si–C4 bond lengths are elongated ($d(\text{Si–C1})$: 1.892–1.897 Å, $d(\text{Si–C4})$: 1.926–1.931 Å) in comparison to the Si–C2/3 bond distances ($d(\text{Si–C2/3})$: 1.885–1.887 Å). The C4–N1 bond distances are in all three cases rather similar ($d(\text{C4–N1})$: 1.460–1.462 Å), but significantly shorter than those in compound **3** ($d(\text{C4–N1})$: 1.460 Å) and **4** ($d(\text{C5–N1})$: 1.460 Å). The bond lengths of the ring are for all isomers typical for triazole derivatives between the length of single and double C–C, C–N and N–N bonds ($d(\text{C–C})$: 1.364–1.402 Å, $d(\text{C–N})$: 1.338–1.393 Å, $d(\text{N–N})$: 1.331–1.364 Å) and the rings are all planar. The angles of

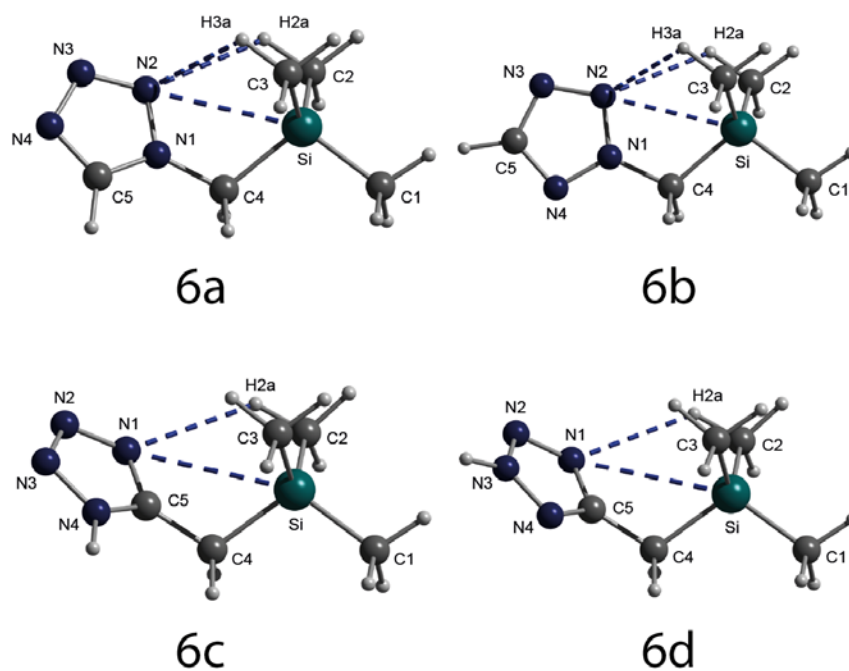


Figure 9.4. Calculated molecular gas phase structures of the compounds **6a–d** on the MP2/cc-pVDZ level of theory (intramolecular interactions are given in blue dashed lines).

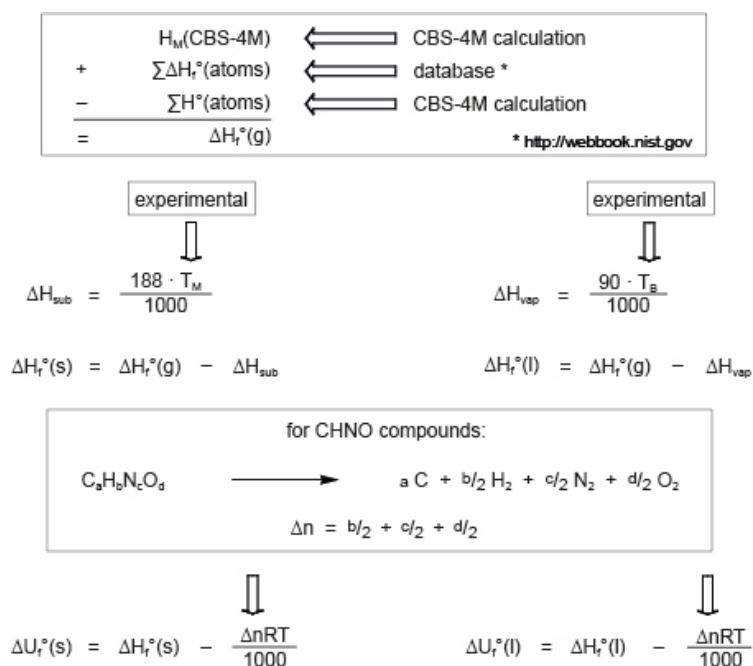
the $\text{Me}_3\text{SiCH}_2\text{R}$ moieties are similar to the situation in **3** and **4** and also mainly influenced by N–H interactions. The main difference in the structures is found in the torsion angles and orientation of the triazole moiety. The substituent R is mostly in one plane with C1–Si–C4 for each of the computed structures. In the case of **5c** the weakest ($\theta(\text{Si–C4–N1–N2})$: 15.9°) and for **5b** the strongest ($\theta(\text{Si–C4–N1–N2})$: -104.1°) anomaly was calculated. The out of plane bending results from the N---H₃C intramolecular attractions ($d(\text{N---H})$: $2.760 - 2.860 \text{ \AA}$, $\Sigma\text{vdW}(\text{N,H})$: 2.75 \AA [18]). The structure of **5b** with the strongest out of plane bending ($\theta(\text{Si–C4–N1–N2})$: -104.1°) has no Si---N interaction, which is found in all other structures, but a H3a interaction with N1 ($d(\text{N1---H3a})$: 2.897 \AA). The Si---N2 interactions of **5a** and **5c** ($d(\text{Si---N})$: both 3.144 \AA , $\Sigma\text{vdW}(\text{Si,N})$: 3.65 \AA [18]) are not vertically orientated towards the Si–C1 bond, due to the sterically demanding methyl groups ($\alpha(\text{C1–Si---N2})$: 156.5° and 157.3°). The Si–C4–N1 angle is obtuse by this repulsion ($\alpha(\text{Si–C4–N1})$: 112.3° (**5a**) and 113.9° (**5c**)) in contrast to **5b** without the repulsion between the C2/3H₃ moieties and the ring ($\alpha(\text{Si–C4–N1})$: 109.8°).

The tetrazole derivatives **6a–d** show the same bond elongations as the nitro and the triazole derivatives. The bond lengths and angles computed show no anomaly compared to other common substituted tetrazole derivatives. The main difference between the

structures of nitrogen substituted **6a/b** and carbon substituted isomers **6c/d** is found in the stronger out of plane bending of the tetrazole moieties in the case of **6c/d** (**6a/b**: $\theta(\text{Si-C4-C5-N1})$: 37.9/15.6 °, **6c/d**: $\theta(\text{Si-C4-N1-N2})$: -114.0/-109.7 °). This is a result of the missing N---H3a interaction, which is commonly created in N-substituted triazole and tetrazole derivatives (**5a-c** and **6a/b**). Pointing to the results of the triazole derivatives **5a-c**, N1---Si/H2a interactions (N2---Si/H2a interactions respectively) were found in the structures of all tetrazole derivatives as expected (see Table 9.3) in contrast to azido- and nitratomethyl silanes[7,9], where mostly an electrostatic attraction from an electron-rich atom at β -position to the silicon is formed. In the case of the triazole and tetrazole derivatives **5a-c** and **6a-d** and the nitro carbon analogue **3c** an interaction between an electron rich atom in γ -position to the central atom C or Si seems to be more common. The interpretation of these results about the chemical behaviour of the triazole and tetrazole derivatives should be rather similar. In more detail it is expected that after an attack of a nucleophile, like F⁻ or HO⁻, the highly probable following Si-C bond cleavage will be more likely to happen at the RCH₂-Si bond and the H₃C1-Si moiety. This is in good agreement with observed chemical behaviour (decomposition during column chromatography). Furthermore, the weakening of the Si-C4 and also the Si-C1 bond will be enforced by additional bonded triazolyl and tetrazolyl moieties. This is in good agreement with the results and identified decomposition products (methylated heterocycles, siloxane and silsequioxane polymers) obtained by reacting bis(chloromethyl)dimethyl silane and tris(chloromethyl)methylsilane in the same and in many different manners as described for **5a** and **5b** in the experimental section. The reasons for the unfulfilled synthetic efforts to obtain **6c** and **6d** are probably based on the reactivity of created **6c/d** towards nucleophiles, like the azide anion. In addition the starting material trimethylsilylacetonitrile is known to be not inert towards nucleophiles. The observed decomposition products (mainly acetonitrile, minor 5-methyltetrazole) point to both results.

When calculating energetic properties with EXPL05 (or even for ICT and CHEETAH 2.0) the only input apart from the molecular formula is the density and the enthalpy of formation, $\Delta_f H^\circ$. The data for the enthalpy of formation can either be measured *via* bomb calorimetry or obtained by theoretical calculations on CBS-4M level of theory. Generating data through bomb calorimetry requires larger amounts of the substances and, for more

sensitive substances, the danger involved should not be neglected. These are the reasons why, for this research, calculated data was used. The results from the CBS-4M calculation are for the gaseous phase only and therefore it was required to convert them for the liquid substances that were analysed. The conversion for liquid and solid substances can be seen in Scheme 9.2.



Scheme 9.2. Conversion of calculated CBS-4M enthalpy of formations to valuable input data for computing code (EXPLO5, CHEETAH and ICT) in liquids and solids state.

The $\Delta_f H^\circ(\text{gaseous})$ is obtained by atomization method, which is in detail the sum of $\Sigma H^\circ(\text{atoms})$ and $\Delta_f H^\circ(\text{CBS-4M})$, followed by the subtraction of $\Sigma_f H^\circ(\text{atoms})$. The values $\Sigma H^\circ(\text{atoms})$ (sum of the computed value out of each single atom) and $\Delta_f H^\circ(\text{CBS-4M})$ (computed out of the whole molecule) were both computed on CBS-4M level of theory. The $\Sigma_f H^\circ(\text{atoms})$ can be obtained from databases.[10] For liquids the ΔH_{vap} is calculated using the boiling temperature T_b or temperature of decomposition T_{dec} and the Trouton's rule [19], according to the following formula:

$$\Delta H_{\text{vap}} = 90 \cdot T_M[\text{K}]/1000$$

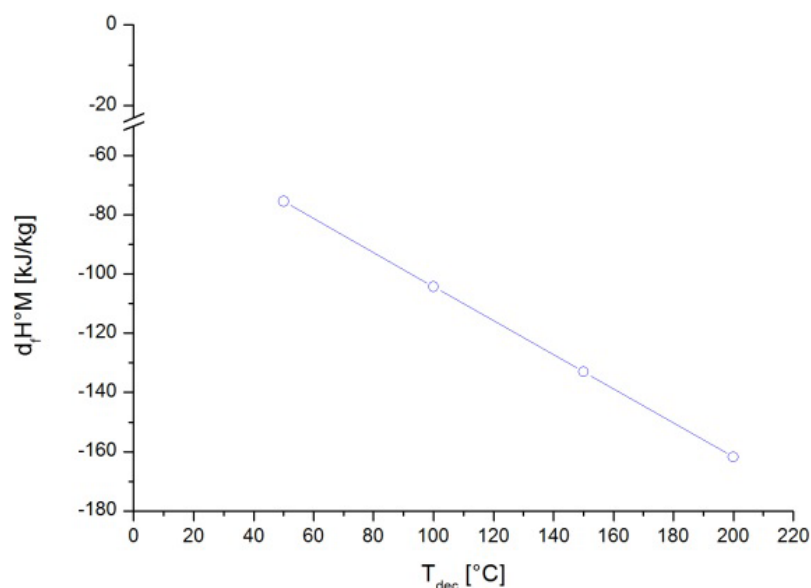


Figure 9.5. Molar enthalpy of formation $\Delta_f H^{\circ} M$ in dependency of T_{dec} exemplarily shown of the values from the liquid compound **6a** (see Supporting Information for the values of all other compounds).

According to the formula the influence of the boiling point or decomposition point to ΔH_{vap} (same for ΔH_{sub}) and $\Delta_f H^{\circ}(s,l)$ respectively, is linear inversely proportional (see Figure 9.5). The Trouton's rule states that entropy of vaporization for various kinds of liquids has the almost same value of about $90 \text{ J K}^{-1} \text{ mol}^{-1}$ [19] and can be applied for all liquids with low intermolecular interaction, whereas for example the high amount of hydrogen bonds within H_2O leads to wrong values for the entropy. $\Delta_f H^{\circ}(l)$ is then calculated by subtracting the ΔH_{vap} from the $\Delta_f H^{\circ}(g)$. Based on the $\Delta_f H^{\circ}(l)$ the internal energy $\Delta_f U(l)$ is acquired by subtracting ΔnRT (Δn as mols of gaseous products, R as the gas constant and T the ambient temperature in Kelvin) from $\Delta_f H^{\circ}(l)$. In the case of silicon containing compounds the formula for CHNO derivatives can be easily used without any restrictions ($\text{C} \rightarrow \text{C}(s)$, $\text{H} \rightarrow \text{H}_2(g)$, $\text{N} \rightarrow \text{N}_2(g)$ and $\text{O} \rightarrow \text{O}_2(g)$), because the bonded silicon is formally converted to $\text{Si}(s)$ and therefore the amount of gaseous products Δn is not influenced.

In the case of solid compounds the Trouton's rule is not suitable, but a variation of the formula can be used instead using the melting point T_m (the decomposition point respectively, if the compound decomposes before melting). The mathematical dependency of

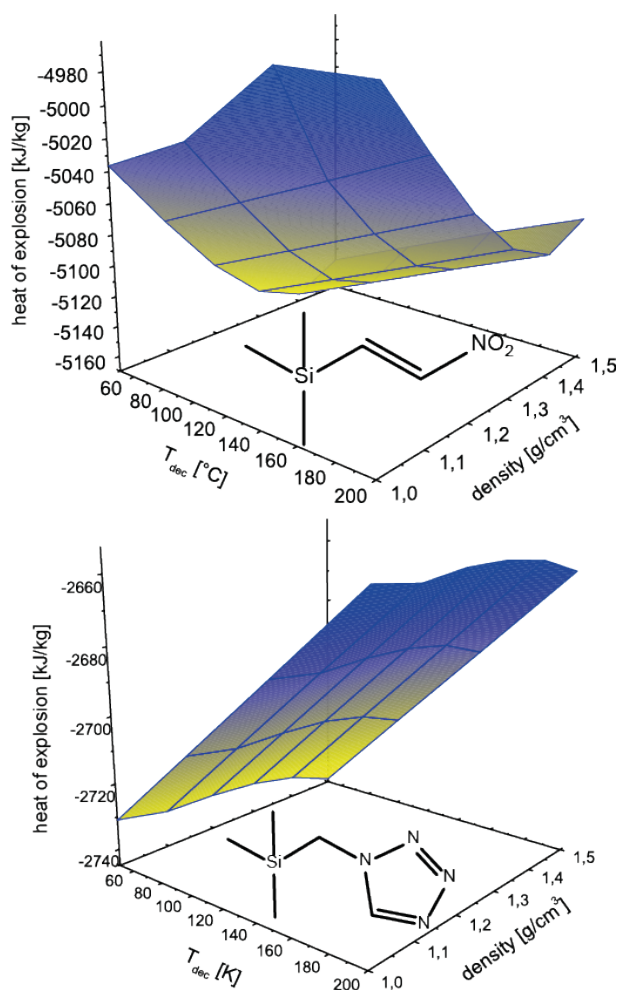


Figure 9.6. The 3D plot of the computed results of the heat of explosion $\Delta_{\text{ex}}U^{\circ}$ in dependency of T_{dec} (T_b and T_m respectively) and the density ρ of the neat compound **4** (top) and **6a** (bottom) is shown exemplarily. Blue line crossings define specific computed values. The interpolated colour distributions just illustrate the shape and gradient of the plane (yellow means lower values and blue higher values; shiny means high gradient and strong low gradient).

T_m and T_{dec} towards ΔH_{sub} , $\Delta_f H^{\circ}(s)$ respectively, is equivalent as already shown in Scheme 9.2 for the Trouton's formula and in Figure 9.5, but due to the multiplication factor 90 towards 188 for ΔH_{sub} more than twice as much as for ΔH_{vap} . In our cases all compounds are liquids and consequently the Trouton's rule is adequate and therefore only this one discussed in the following.

Based on the results of the calculations using the MP2 basic set, as previously discussed, all calculated molecules should only show few and weak intramolecular interactions, the

same is likely true for the condensed phase, which allows for the Trouton's rule, used to calculate $\Delta_f H^\circ(l)$, to be applied.

The $\Delta_f H^\circ$ is an indicator for the performance of a compound, because high $\Delta_f H^\circ$ indicates high energy difference between reactants and products. Comparison of different $\Delta_f H^\circ$ is only useful, if the products are similar, which is the case comparing different isomers. The isomers calculated are three triazoles, **5a**, **5b** and **5c** as well as four tetrazoles **6a**, **6b**, **6c** and **6d**. When looking at the triazoles the one with the highest $\Delta_f H^\circ$ is **5c** and the V_{det} is also the highest for **5c** with the other two following according to their $\Delta_f H^\circ$. The difference in $\Delta_f H^\circ$ is as large as 330 kJ/kg between **5a** and **5c**. Of the tetrazoles **6a** has the highest $\Delta_f H^\circ$ and the highest V_{det} , but the differences between the tetrazoles in $\Delta_f H^\circ$ and V_{det} are less visible, only up to 270 kJ/kg.

An important aspect of the performed calculations is the influence of the melting and boiling point (for liquids and decomposition temperature T_{dec} , respectively) and density, because for most of the compounds used in the following calculations, out of various reasons, no reliable information is available for these properties. Through getting deeper information about the influences of these parameters it was still possible to carry out different calculations and estimate their value compared to experimental data. First the influence of the T_{dec} was characterized. For this purpose different temperatures were used to generate the input data for the EXPL05 calculations (at 50 °C, 100 °C, 150 °C and 200 °C), like shown in Scheme 9.2. Then the detonation properties (heat of explosion, detonation velocity, detonation pressure, detonation temperature and gas volume) were calculated for all four temperatures.

As seen in Figure 9.5, the correlation for $\Delta_f H_M$ is approximately linear in dependency referred to T_b , respectively T_{dec} . This is conclusive with the equations used for the EXPL05 code. In addition, the differences are insignificant compared to others, like errors that occur when using the Trouton's approximation, and therefore negligible.

The next step was to look at the influence of density. For these equations density was varied (1.0–1.5 g/cm³) and different decomposition temperatures were also applied to create a more general view. As it is known from similar liquid silanes the densities are

mainly below 1.0 g/cm^3 , but interacting substituents (electrostatic interactions, hydrogen bonding etc.) increase the density up to 1.0 g/cm^3 . Computation of neat compounds with density values below 1.0 g/cm^3 leads often to inadequate results and consequently the

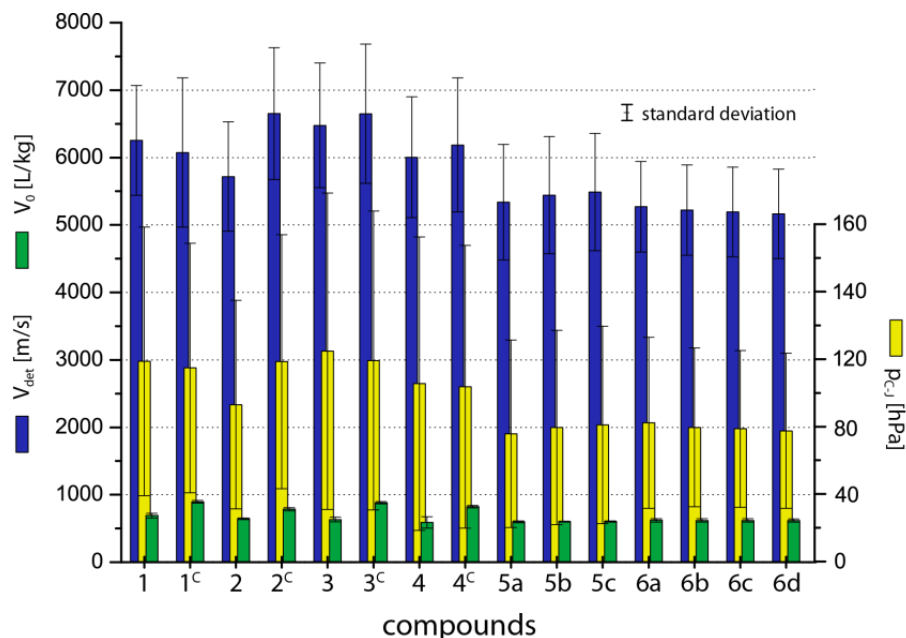


Figure 9.7. Computed predictant V_{det} (blue bar), V_0 (green bar), p_{c-J} (yellow bar) values of the compounds **1**, **1^c**, **2**, **2^c**, **3**, **3^c**, **4**, **4^c**, **5a–c** and **6a–d** with the standard deviation of the input values of $T_m/T_b/T_{dec} = 50, 100, 150$ and $200 \text{ }^\circ\text{C}$ and the density distribution of $1.0\text{--}1.5 \text{ g/cm}^3$.

computed series of density values use 1.0 g/cm^3 as lowest input. The calculations showed density values below 1.0 g/cm^3 leads often to inadequate results and consequently the computed series of density values use 1.0 g/cm^3 as lowest input. The calculations showed that the dependency of detonation temperature, detonation pressure, detonation velocity and gas volume is, according to the EXPL05 code, exponential. In contrast, the heat of explosion shows a different dependency, examples are shown in Figures 9.6. Accordingly a less laborious prediction regarding the heat of explosion cannot be made as the dependency of the heat of explosion and the volumetric work is complex. The inhomogeneous dependency of T_M and density ρ towards the heat of explosion $\Delta_{ex}U^\circ$ for the nitro and nitrate compounds **1**, **1^c**, **3**, **3^c**, **4** and **4^c** are conspicuous in contrast to the relatively homogenous plots of the azido, triazolyl and tetrazolyl derivatives **2**, **2^c**, **5a–c** and **6a–d**. Consequently the standard deviation of the computed values is increased in the case of the first group of compound towards the deviation from the second group. Never the less the dependencies of the other values like detonation temperature T_{det} and detonation velocity

V_{det} , are comparable homogenous independently of the deviation of $\Delta_{\text{ex}}U^\circ$. According to these results all following calculations were executed using $\rho = 1.0 \text{ g/cm}^3$ and $T_{\text{M}}/T_{\text{B}}/T_{\text{dec}} = 100 \text{ }^\circ\text{C}$.

In the following it is focusing on the influence of the type of substituent. As already discussed above, the standard deviation of $\Delta_{\text{ex}}U^\circ$ is higher for oxygen containing nitro or nitrate derivatives compared to the oxygen deviant nitrogen rich derivatives. There are no tendencies visible comparing silicon and carbon derivatives in their standard deviation of $\Delta_{\text{ex}}U^\circ$, although the shapes of the plots can strongly differ between the two Si and C analogues.

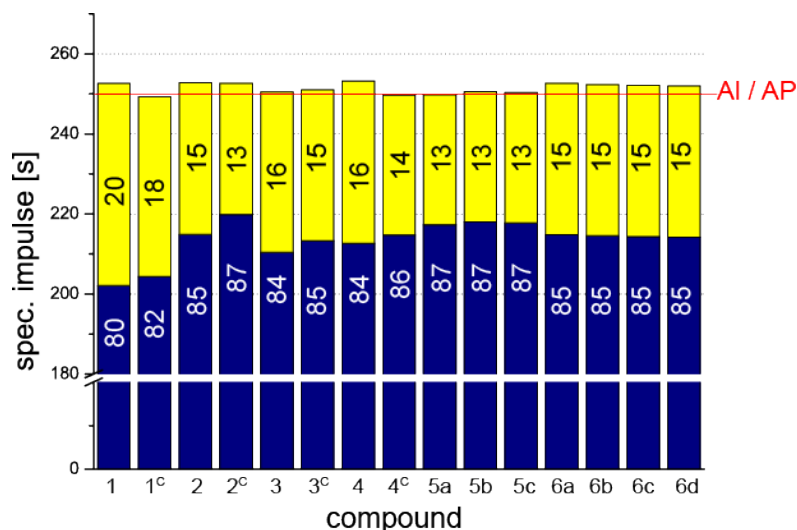


Figure 9.8. Histogram of the calculated specific impulses of the compounds **1**, **1^c**, **2**, **2^c**, **3**, **3^c**, **4**, **4^c**, **5a–c** and **6a–d** as fuel (% amount blue bar) and the oxidizer ammonium perchlorate (AP, % amount yellow bar). Aluminium/AP mixture (20/80 %w/w) is given as benchmark (250 s).

The influence of the substituent for the energetic properties is shown exemplarily for the three of the most important values of explosive characteristics computed with EXPLO5 version 6.01. The averaged values of variegating the density ($1.0\text{--}1.5 \text{ g/cm}^3$) and T_{B} (T_{dec} respectively, $50\text{--}200 \text{ }^\circ\text{C}$) are given as column (see Figure 9.7). The standard deviation is given as brackets on top of the columns. As it can be seen it is very high in the case of $p_{\text{C-J}}$, medium for V_{det} and almost insignificant for V_0 . It is lowest for the tetrazole derivative, but highest for **1^c**. In the following the standard deviation should be not from interest and instead it should just be focused on the averaged values. Comparing Si and C analogues the carbon analogues are mostly higher values of V_{det} , $p_{\text{C-J}}$ and V_0 , but in the case of **1** and **1^c** it is

the inverse situation. In the case of **3** and **4** in comparison to their carbon analogues V_{det} and V_0 are higher in the case of the carbon analogues, but in contrast p_{C-J} is slightly higher for the silicon analogues. All calculated V_0 values of the carbon derivatives are higher than the

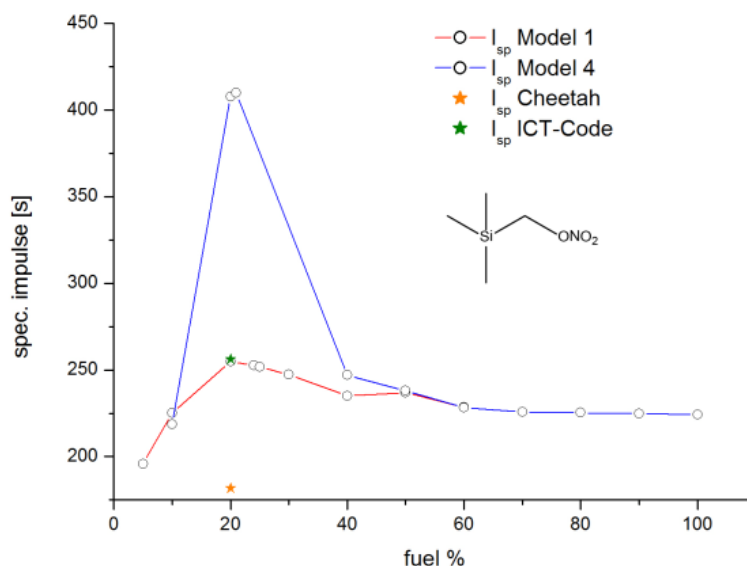


Figure 9.9. Computed I_{sp} values with different fuel/oxygen ratios, using different computing codes (EXPLO5 version 6.01, CHEETAH 2.0 and ICT) and in addition the computation using EXPLO5 Model 1 in comparison to Model 4 are exemplarily shown for compound **1**.

values of the silicon analogues, due to the increased CO/CO₂ exhaust. The best result for the tested silanes is found for the oxygen containing silanes **1**, **2** and **3**. Due to the reaction of Si with N to Si₃N₄ under hypoxic conditions, low amount of gaseous N₂ is formed, in contrast to the reaction in presence of oxygen and forming SiO₂. In the later reaction the capturing of nitrogen by Si is highly suppressed (high difference in their enthalpy of formation of Si₃N₄ and SiO₂, the burning of Si₃N₄ itself into SiO₂). In the case of p_{C-J} the best result is computed for the silane **3**. In general the p_{C-J} values are relatively low for all compounds. The detonation velocity is high for carbon derivatives, except in the case of **1/1^c**.

The best results for a silicon compound are computed for the compound **3**. It is known from other silanes, that the low values of mono substituted derivatives increases by increasing the content of substituent in one molecule. Therefore, di-, tri- or even tetra-substituted derivatives should show much better results. Especially the nitro derivatives are highly promising, because of their physical stability and good energetic properties. In

IX. Theoretical Approach of Energetic Silanes

addition due to the easy synthesis in high yield and the high performance in comparison with its isomers, the 1,2,4-triazolyl derivatives (**5c** analogues) are good candidates for reassurance. The same is true for the multiple tetrazol-1-yl substituted derivatives (**6a** analogue).

Pointing to the detonation temperature T_{det} the silicon derivatives show higher temperatures than their carbon analogues. This can be problematic for using silanes as gun propellant, because of the risk of overheating (prolongs reloading time) or deformation of the muzzle. But the profit is seen in the reduced carbon content, which reduced the building of metal carbides, which makes the muzzle frail and prim (reduced the muzzle life). In addition the influences of SiO_2 and other Si decomposition products are unknown and have to be investigated.

Table 9.5. Comparison of the reaction products in the combustion chamber for Model 1 (EXPL05 computing code) in normal run (left) and for Model 1 without the deleted products for **9** with nitrogen tetroxide (N_2O_4) as oxidizer (20% fuel and 80% oxidizer).

Model 1 normal run (product under 10^{-35} mol% were not consider)				Model 1 advanced run (product under 10^{-9} mol% were not consider)			
Composition of combustion products in chamber:				Composition of combustion products in chamber:			
Products	mol/mol	mol/kg	Mol %	Products	mol/mol	mol/kg	Mol %
N2 =	8,088961 E-01	8,220227 E00	23,5408	N2 =	8,038802 E-01	8,169255 E00	23,5660
H2O =	7,018673 E-01	7,132571 E00	20,4260	H2O =	7,018468 E-01	7,132363 E00	20,5749
CO2 =	6,494018 E-01	6,599403 E00	18,8992	CO2 =	6,197129 E-01	6,297695 E00	18,1671
CO =	5,060556 E-01	5,142678 E00	14,7274	CO =	6,357445 E-01	6,444385 E00	15,7055
O2 =	2,194549 E-01	2,230162 E00	6,3867	O2 =	2,431643 E-01	2,471104 E00	7,1284
OH =	1,674896 E-01	1,702076 E00	4,8744	OH =	1,885724 E-01	1,916325 E00	5,5281
SiO =	1,203778 E-01	1,223313 E00	3,5033	SiO =	1,218842 E-01	1,238621 E00	3,5731
NO =	9,330828 E-02	9,482248 E-01	2,7155	NO =	1,033727 E-01	1,050502 E00	3,0304
H2 =	6,411099 E-02	6,515138 E-01	1,8658	H2 =	7,045741 E-02	7,160079 E-01	2,0655
O =	4,735198 E-02	4,812041 E-01	1,3781	SiO2 =	2,245291 E-02	2,281727 E-01	0,6582
H =	3,373522 E-02	3,428268 E-01	0,9818	SiO2(l) =	7,861317 E-05	7,988890 E-04	0,0023
SiO2 =	2,347936 E-02	2,386038 E-01	0,6833	SiO2(s) =	1,652339 E-05	1,679153 E-04	0,0005
SiO2(l) =	4,415554 E-04	4,487209 E-03	0,0129	NH3 =	1,872969 E-06	1,903364 E-05	0,0001
SiO2(s) =	1,325393 E-04	1,346901 E-03	0,0039	HCN =	4,791179 E-07	4,868930 E-06	0,0000
N =	3,290184 E-05	3,343576 E-04	0,0010				
NH3 =	1,665221 E-06	1,692244 E-05	0,0000				
Si =	7,734094 E-07	7,859602 E-06	0,0000				
HCN =	3,897315 E-07	3,960561 E-06	0,0000				
SiN =	9,839426 E-08	9,999100 E-07	0,0000				
SiH =	8,517091 E-08	8,655306 E-07	0,0000				
CH4 =	1,124121 E-11	1,142363 E-10	0,0000				
CH3OH =	6,792065 E-12	6,902286 E-11	0,0000				
SiH4 =	1,289789 E-12	1,310720 E-11	0,0000				
Si(l) =	1,684423 E-15	1,711758 E-14	0,0000				
C(s,gr) =	4,691692 E-16	4,767829 E-15	0,0000				
Si(s) =	3,042591 E-16	3,091966 E-15	0,0000				
SiC(s) =	6,176300 E-21	6,276529 E-20	0,0000				
Si3N4(s) =	2,305318 E-30	2,342729 E-29	0,0000				

IX. Theoretical Approach of Energetic Silanes

Table 9.6. Comparison of the reaction products (consider products $>10^{-35}$ mol%) in the combustion chamber for Model 1 (EXPLO5 computing code) in normal run of **4** (left) and **4^C** (right) with AP as oxidizer (20% fuel and 80% oxidizer).

Products for reaction of 4 with AP 20/80				Products for reaction of 4^C with AP 20/80			
Composition of combustion products in chamber:				Composition of combustion products in chamber:			
Products	mol/mol	mol/kg	Mol %	Products	mol/mol	mol/kg	Mol %
H2O =	1,927177 E00		41,5291	H2O =	1,936322 E00		40,9179
HC1 =	7,636101 E-01		16,4552	HC1 =	7,737142 E-01		16,3499
N2 =	4,921024 E-01		10,6044	CO =	5,958450 E-01		12,5912
CO2 =	4,384678 E-01		9,4486	CO2 =	5,158522 E-01		10,9009
CO =	4,026419 E-01		8,6766	N2 =	4,966587 E-01		10,4953
H2 =	2,229035 E-01		4,8034	H2 =	2,916174 E-01		6,1624
SiO2(l) =	1,322538 E-01		2,8506	OH =	4,590297 E-02		0,9700
OH =	8,599137 E-02		1,8530	C1 =	4,038562 E-02		0,8534
C1 =	6,694326 E-02		1,4426	H =	2,148443 E-02		0,4540
SiO =	3,201254 E-02		0,6898	NO =	6,667596 E-03		0,1409
H =	2,781348 E-02		0,5994	O2 =	5,472843 E-03		0,1157
O2 =	2,213217 E-02		0,4769	O =	1,909244 E-03		0,0403
NO =	1,578295 E-02		0,3401	C12 =	2,426802 E-04		0,0051
O =	5,965345 E-03		0,1285	C10 =	9,463591 E-05		0,0020
SiO2 =	3,813818 E-03		0,0822	CC10 =	3,182110 E-05		0,0007
C12 =	4,386682 E-04		0,0095	NH3 =	1,231056 E-05		0,0003
C10 =	3,076675 E-04		0,0066	N =	1,712348 E-06		0,0000
SiO2(s) =	1,181648 E-04		0,0025	HCN =	8,925724 E-07		0,0000
CC10 =	3,253653 E-05		0,0007	CH4 =	8,540799 E-10		0,0000
NH3 =	7,849839 E-06		0,0002	CH3OH =	1,386193 E-10		0,0000
N =	3,991396 E-06		0,0001	C(s,gr) =	1,376916 E-15		0,0000
HCN =	4,259965 E-07		0,0000				
SiC14 =	1,247216 E-07		0,0000				
Si =	7,269014 E-08		0,0000				
SiH =	1,826016 E-08		0,0000				
SiN =	8,646056 E-09		0,0000				
CH4 =	1,926526 E-10		0,0000				
CH3OH =	5,207878 E-11		0,0000				
SiH4 =	4,535582 E-12		0,0000				
C(s,gr) =	5,985855 E-16		0,0000				
Si(l) =	5,939101 E-16		0,0000				
Si(s) =	1,272578 E-16		0,0000				
SiC(s) =	4,514104 E-21		0,0000				
Si3N4(s) =	6,595059 E-31		0,0000				

Producing high amounts of gaseous products and high temperatures by burning are promising key data for the use as propellant. In this case the oxygen content is not as important as for computing detonation parameters, because of the addition of an oxygen source (oxidizer). For the first series of calculations ammonium perchlorate (AP) and the computing code EXPLO5 version 6.01 were used. The results for the ideal mixture of fuel (the compounds **1** through **6d**) and oxidizer can be seen in Figure 9.8. When calculating silicon containing compounds the programme EXPLO5 in Model 1 has problems once the oxygen balance reaches the optimal value. These problems did not occur when calculating compounds without silicon, so the assumption is that the EXPLO5 computer code has problems with calculating silicon containing compounds. The calculated specific impulse reaches values of 400 s or higher, which are unrealistic for the compounds used (see Figure 9.9). These problems can be prevented by using Model 4 for the calculations or by deleting a number of molecules from the list of products. Selection was carried out by deleting all products which were calculated in an amount of less than 10^{-9} mol per mol reactant. The fourteen most frequently occurring reaction products were consequently left for calculation (see Table 9.5). Additionally the free radicals were deleted, due to the consisting occurrence

of problems during the calculations. Chemically their existence as products is only of a very short period of time as they quickly react with other molecules or radicals and their existence is consequently arguable.

Comparing the computed specific impulses indicated better values for silanes than for their carbon analogues (Figure 9.8). Due to less amount of oxidizer addition for optimized computation (high amount of fuel respectively) and high temperature in the combustion chamber boost the I_{sp} values in comparison to their carbon analogues. Especially the compounds **1**, **2** and **4** have promising results and whereas **4** is favourites, because of the less amount of expensive fuel.

Another result of the performed calculations is that the maximum specific impulse is reached once the oxygen balance is slightly negative and not at the optimum value of zero. This mainly arises from the Boudouard reaction, which shows that at high temperatures carbon dioxide and graphite react to carbon monoxide. A slightly negative oxygen balance, meaning that more oxygen is in the system than theoretically needed, allows for the carbon monoxide produced reacting with the oxygen to carbon dioxide. The silicon analogues show the same reaction behaviours, as seen in the list of products for the exemplary reaction of **4** and **4^c** with AP. An analogue of the carbon Boudouard equilibrium is also known from silicon, but as shown in Table 9.6 with highly inferior influences. This leads to the conclusion of extending the modified Springall-Roberts-Rules for silicon containing compounds. A seventh and primary rule is added and the new order is as follows:

1. all silicon atoms are converted to SiO_2 or, if no more oxygen is present, to Si_3N_4
2. if oxygen atoms remain, carbon atoms are converted to CO
3. remaining oxygen atoms oxidize hydrogen to H_2O
4. if still oxygen atoms remain, they oxidize existing CO to CO_2
5. still remaining nitrogen is used to form N_2
6. one third of the generated CO is converted to C and CO_2
7. one sixth of the originally generated CO is converted to CO_2 and H_2O

Comparison of the silicon and carbon analogues also shows a difference in the calculated values of the chamber temperature T_c . The chamber temperature for the silicon containing compounds is always higher than that of the carbon analogue which is conclusive with the higher combustion temperature reached when forming SiO_2 ($\Delta_f H^\circ(\text{s})$: -911 kJ/mol) in contrast to forming CO/CO_2 ($\Delta_f H^\circ(\text{g})$: $-111/-394$ kJ/mol).[10] Comparing the products in the combustion chamber with those at the nozzle exit it is seen that the Boudouard reaction is in place as well as its silicon analogue reaction, as seen in Table 9.7.

To compare different oxidisers more calculations were performed using the molecules (2-*E*-nitroethylen)trimethylsilane (**4**), its carbon analogue 1-nitro-3,3-dimethyl-but-1-ene (**4^C**), (vinyl)trimethylsilane (**8**), (allyl)trimethylsilane (**7**) and tetravinylsilane (**9**). These calculations revealed that for the silicon compounds and the carbon analogue nitrogen tetroxide is the best oxidizer with values of the specific impulse of up to 270 s (see Figure 9.10). This is due to the fact that N_2O_4 , in contrast to the other oxidizers, which all contain carbon and/or hydrogen and need the oxygen to react to CO/CO_2 or H_2O , only adds nitrogen, which reacts to N_2 , and oxygen to the reaction. The chamber temperature is dependent on the heat release (Q) and the heat capacity of the reaction products (C_v) (see Formula (3)). Production of a high amount of water, which will increase the mean heat capacity of the products, results in a relatively low T_c compared to compounds with lower amount of hydrogen (low amounts of water should be without prejudice). When comparing the silicon compound and the carbon analogue the carbon compound has a slightly higher specific impulse. This leads to the results that the influence of the lower molar mass of carbon analogues in relation to the lower increased T_c of silicon analogues are mainly superior. Other calculations with ammonium dinitramide (ADN) showed somewhat lower results of up to 265 s. Here also the carbon analogue gave slightly higher specific impulses, but the difference is less visible. The third tested oxidizer, red fuming nitric acid (RFNA), which is a common testing reactant for hypercolic mixtures (see Chapter VIII) gave lower results (in contrast to its low hydrogen content) and because of these values and the laborious handling of this acid further calculations, apart from the three, were not performed. As a reference the optimized composition of aluminium and ammonium perchlorate (AP) was used with a specific impulse of 250 s as common bench mark. The performed calculations allowed comparing different substances and giving a recommendation for further usage.

Compounds **8** and **9** have an almost similar specific impulse, but the production costs and the number of synthesis steps required are higher and more laborious for **9** which lead to the conclusion that **8** is the more promising compound as bipropellant liquid rocket fuel.

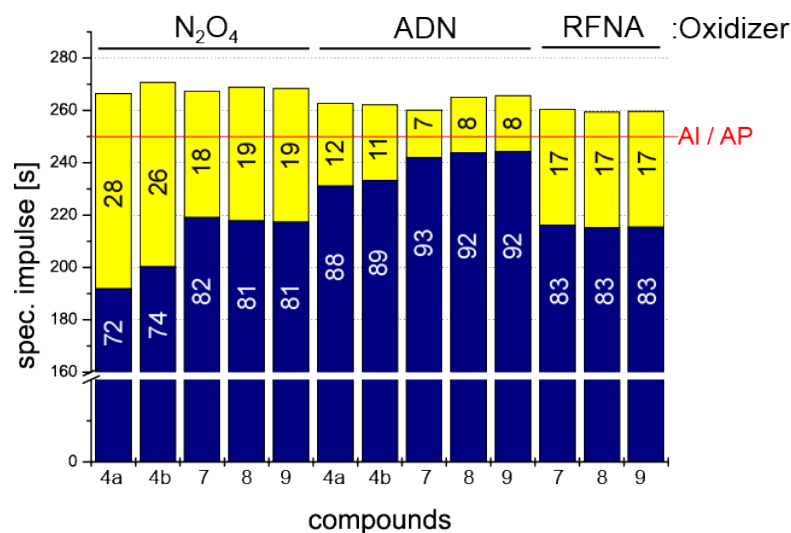


Figure 9.10. Histogram of the calculated specific impulses of the compounds **4**, **4^c** and **7–9** as fuel (% amount blue bar) and the oxidizers (% amount yellow bar) dinitrogen tetroxide (NTO), ammonium dinitamide (ADN) and red fuming nitric acid (RFNA). Aluminium/AP mixture (20/80 %w/w) is given as benchmark (250 s).

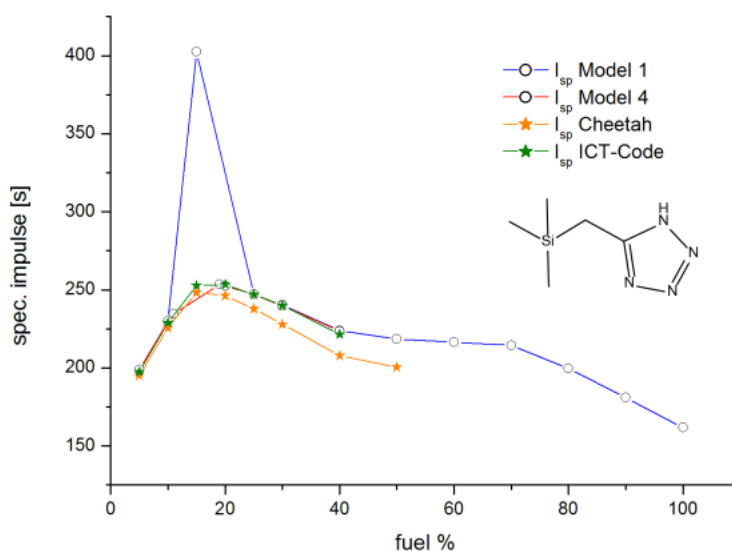


Figure 9.11. Computed I_{sp} values with different fuel/oxidizer ratios, using different computing codes (EXPL05 version 6.01, CHEETAH 2.0 and ICT) and in addition the computation using EXPL05 Model 1 in comparison to Model 4 are exemplarily shown for compound **6c**.

IX. Theoretical Approach of Energetic Silanes

Table 9.7. Comparison of the reaction products (consider products $>10^{-35}$ mol%) for Model 1 (EXPLO5 computing code, normal run) at the nozzle exit (right) and in the combustion chamber (left) of **4** with AP as oxidizer (20% fuel and 80% oxidizer).

Products for reaction of 4 with AP 20/80 in the combustion chamber				Products for reaction of 4 with AP 20/80 at the nozzle exit			
Composition of combustion products in chamber:				Composition of combustion products at the nozzle exit:			
Products mol/mol			mol/kg	Products mol/mol			mol/kg
			Mol %				Mol %
H2O =	1,927177	E00	1,577595	E01	41,5291		
HCl =	7,636101	E-01	6,250945	E00	16,4552		
N2 =	4,921024	E-01	4,028371	E00	10,6044		
CO2 =	4,384678	E-01	3,589316	E00	9,4486		
CO =	4,026419	E-01	3,296044	E00	8,6766		
H2 =	2,229035	E-01	1,824698	E00	4,8034		
SiO2(l) =	1,322838	E-01	1,082881	E00	2,8506		
OH =	8,599137	E-02	7,039290	E-01	1,8530		
Cl =	6,694326	E-02	5,480004	E-01	1,4426		
SiO =	3,201254	E-02	2,620560	E-01	0,6898		
H =	2,781348	E-02	2,276824	E-01	0,5994		
O2 =	2,213217	E-02	1,811749	E-01	0,4769		
NO =	1,578295	E-02	1,291999	E-01	0,3401		
O =	5,965345	E-03	4,883257	E-02	0,1285		
SiO2 =	3,813818	E-03	3,122008	E-02	0,0822		
Cl2 =	4,386682	E-04	3,590956	E-03	0,0095		
ClO =	3,076675	E-04	2,518579	E-03	0,0066		
SiO2(s) =	1,181648	E-04	9,673020	E-04	0,0025		
CClO =	3,253653	E-05	2,663454	E-04	0,0007		
NH3 =	7,849839	E-06	6,425912	E-05	0,0002		
N =	3,991396	E-06	3,267374	E-05	0,0001		
HCN =	4,259965	E-07	3,487225	E-06	0,0000		
SiCl4 =	1,247216	E-07	1,020977	E-06	0,0000		
Si =	7,269014	E-08	5,950446	E-07	0,0000		
SiH =	1,826016	E-08	1,494785	E-07	0,0000		
SiH =	8,646056	E-09	7,077698	E-08	0,0000		
CH4 =	1,926526	E-10	1,577063	E-09	0,0000		
CH3OH =	5,207878	E-11	4,263191	E-10	0,0000		
SiH4 =	4,535582	E-12	3,712846	E-11	0,0000		
C(s,gr) =	5,985855	E-16	4,900046	E-15	0,0000		
Si(l) =	5,939101	E-16	4,861773	E-15	0,0000		
Si(s) =	1,272578	E-16	1,041738	E-15	0,0000		
SiC(s) =	4,514104	E-21	3,695265	E-20	0,0000		
Si3N4(s) =	6,595059	E-31	5,398744	E-30	0,0000		
H =	1,036868	E00	8,487848	E00	16,4358		
H2O =	8,898227	E-01	7,284127	E00	14,1050		
CO =	7,289010	E-01	5,966815	E00	11,5541		
H2 =	6,864854	E-01	5,619598	E00	10,8818		
OH =	5,817634	E-01	4,762340	E00	9,2218		
O =	4,752390	E-01	3,890326	E00	7,5332		
N2 =	4,641256	E-01	3,799352	E00	7,3571		
Cl =	4,246462	E-01	3,476172	E00	6,7312		
HCl =	4,063509	E-01	3,326406	E00	6,4412		
O2 =	2,614655	E-01	2,140368	E00	4,1446		
SiO =	1,682279	E-01	1,377121	E00	2,6667		
CO2 =	1,122387	E-01	9,187905	E-01	1,7791		
NO =	7,155796	E-02	5,857765	E-01	1,1343		
ClO =	6,183786	E-04	5,062073	E-03	0,0098		
N =	1,904393	E-04	1,558944	E-03	0,0030		
Cl2 =	7,653375	E-05	6,265086	E-04	0,0012		
CClO =	2,953006	E-06	2,417343	E-05	0,0000		
SiO2(l) =	6,109751	E-07	5,001468	E-06	0,0000		
NH3 =	3,575561	E-07	2,926970	E-06	0,0000		
HCN =	9,096732	E-08	7,446624	E-07	0,0000		
SiO2 =	1,921350	E-08	1,572826	E-07	0,0000		
Si =	7,852747	E-09	6,428292	E-08	0,0000		
SiO2(s) =	6,443686	E-12	5,274829	E-11	0,0000		
SiN =	2,826502	E-12	2,313786	E-11	0,0000		
CH4 =	1,128322	E-12	9,236492	E-12	0,0000		
CH3OH =	7,211114	E-14	5,903049	E-13	0,0000		
SiC(s) =	4,642335	E-14	3,800235	E-13	0,0000		
SiH4 =	3,275701	E-16	2,681503	E-15	0,0000		
C(s,gr) =	4,904094	E-17	4,014512	E-16	0,0000		
SiH =	2,038417	E-19	1,668657	E-18	0,0000		
Si(l) =	1,823681	E-19	1,492873	E-18	0,0000		
Si(s) =	3,403993	E-20	2,786524	E-19	0,0000		
SiCl4 =	0,000000	E00	0,000000	E00	0,0000		
Si3N4(s) =	0,000000	E00	0,000000	E00	0,0000		

Due to the already mentioned problems computing the optimized specific impulses using EXPLO5 version 6.01 different common computing codes were compared in the following. The programmes EXPLO5 version 6.01, CHEETAH 2.0 and ICT-code are tested. As seen in Figure 9.9 and 9.11 the values of EXPLO5 and ICT-Code do not differ much, whereas the results from CHEETAH show a different and lower curve. This trend was apparent in all the calculations performed, but the values of the CHEETAH calculations went as low as 141 s for some calculations where EXPLO5 and ICT-Code gave results of 269 s (see Figure 9.9). Especially, if calculating the non-silicon containing compounds the results given by CHEETAH were lower than those computed by the other two computing codes. However for the tetrazole and triazole compounds the results by EXPLO5, CHEETAH and ICT-Code are all within the same range and only differ by up to 10 s (see Figure 9.11). It is interesting to notice, that the difference between the EXPLO5 and CHEETAH results for **6c** and **6d** varies, although the molecular formula and other parameters, apart from a slight variation in the

$\Delta_f H^\circ$ are the same. ICT-Code does not give reliable data about the chamber temperatures and therefore the following discussion is done excluding ICT-Code computed data. A closer

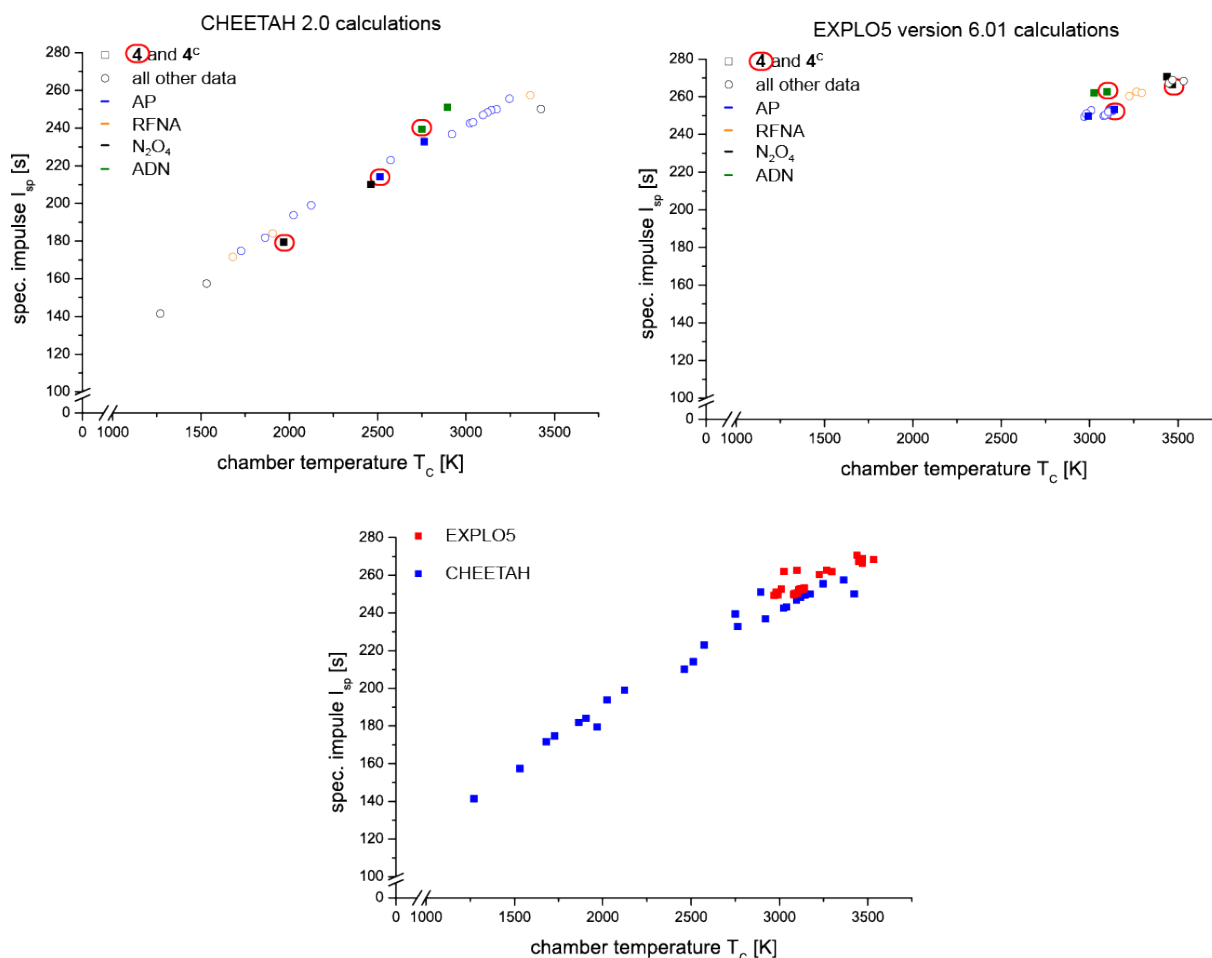


Figure 9.12. Specific impulse in correlation to chamber temperature computed with CHEETAH 2.0 (top left) and EXPLO5 version 6.01 (top right) of all discussed compounds (optimal mixtures, see Figure 9.8 and Figure 9.10). The values of 4 are market with red circles (carbon analogue 4^c without circles) and different oxidizers (blue: AP, green: ADN, black: NTO, orange RFNA). Combination of all I_{sp}/T_c relations are given of CHEETAH (blue) and EXPLO5 (red) data (bottom). The lines of best fit for Si and C derivatives are given in red and black lines in the two graphs on the top, and the line of best fit of overall data in the graph below (blue: CHEETAH data, red: EXPLO5 data)

look at the chamber temperature differences between CHEETAH and EXPLO5 reveals a higher distribution for the CHEETAH calculated T_c than EXPLO5. This is probably due to inaccuracy of the calculating code used for CHEETAH (as also seen in the passage above). In spite of the higher distribution the I_{sp} values show the dependency established in Formula (2) (see Chapter I). The almost linear progress seen in this graph (Figure 9.12) allows this

formula to be modified for this research (see below). In addition, focusing to the gradient of the line of best fit of the silicon and carbon derivatives show two different gradients of the lines. As expected the gradient of the silicon containing compound is lower than for the carbon analogues, but the amount in mol% of silicon containing decomposition products is in the case of **4** for 3.7mol% (see Table 9.6) increased by approximately 1/3 ($M(\text{CO}_2)$: 44.01 g/mol and $M(\text{CO})$: 28.01 g/mol / $M(\text{SiO}_2)$: 60.08 g/mol and $M(\text{SiO})$: 44.09 g/mol \approx 1/3). This approximation leads to the result that the influence of the increased averaged molare mass of the decomposition products of silicon derivatives is very low. The differences is mainly found in the different reaction conditions, means temperature/pressure, which strongly influence the exact composition of decomposition products by the Boudouard equilibrium and the water-gas shift reaction. As result the common used proportionality between I_{sp} an T_{c} and M can be in total for this research reduced to the following:

$$I_{\text{sp}} \sim T_{\text{c}}$$

Comparison of silicon and carbon analogue gives lower T_{c} values, calculated via CHEETAH, for the silicon compounds **1**, **3** and **4** than for the carbon analogues, but for **2** the T_{c} is higher than for **2^c** as it is expected and EXPL05 results show higher T_{c} values for the silicon compounds. The reason for this is the higher heat of formation for SiO_2 than for CO/CO_2 (see above). The specific impulse values show the same characteristics for CHEETAH calculations (**1/1^c**: 181.8/193.8 s, 1864/2024 K; **2/2^c**: 255.6/222.9 s, 3247/2574 K; **3/3^c**: 174.7/199.1 s, 1727/2124 K; **4/4^c**: 214.1/232.8 s, 2513/2764 K) whereas the EXPL05 calculated I_{sp} are higher for silicon containing compounds compared to the carbon analogues, corresponding to the results for T_{c} (**1/1^c**: 252.6/249.3 s, 3132/2971 K; **2/2^c**: 252.8/252.7 s, 3127/3009 K; **3/3^c**: 250.5/251.0 s, 3101/2981 K; **4/4^c**: 253.2/249.7 s, 3141/2993 K). Compounds **7**, **8** and **9** show for CHEETAH calculated values a wider spread than the EXPL05 calculated values with **7** giving the lowest results for I_{sp} , **8** with slightly higher values of I_{sp} and **9** gives the best results. This distribution cannot be seen for the EXPL05 calculations (see Figure 9.9). The reaction products from the different computing codes also differ. For the exemplary reaction of 10 % **2^c** with 90 % AP was calculated with EXPL05 and CHEETAH and the first five most frequent products are the

same, as seen in Table 9.7. The rest of the products not only differ in frequency but 10 out of 19 products calculated by CHEETAH cannot be found in the list of degradation products in EXPL05.

This results in the conclusion that the programme CHEETAH 2.0, in the old-fashioned version that was available for the calculations, is unreliable whereas EXPL05 and ICT-Code give more realistic, accurate and coincident results. Both the ICT-Code and EXPL05 allow the user to easily erase certain degradation products manually from the product list or only allow products to be considered over a certain frequency threshold which is not possible with CHEETAH. In addition EXPL05 is more variable as it allows different calculation models and it runs more stable in comparison to ICT-Code which often crashes in the middle of the calculation progress. Crashing during calculations is also happen using EXPL05 version 6.01, but can be mostly easily solved by using another computing model (for example Model 4) or deleting unrealistic combustion products from the product list. Both CHEETAH and ICT-Code calculate way faster than EXPL05, but the EXPL05 output contains much more and more detailed data. For example the missing of reliable T_c data of ICT calculations is enough, if ask for absolute data about I_{sp} , but not for detail studies as discussed above. In conclusion, due to the transparency of the computation, the easy modifying of parameters and its flexibility favoured EXPL05 version 6.01 as computational tool inhere.

Conclusion

The research discusses the use of silicon containing compounds as energetic materials. For the theoretical examination (nitromethyl)trimethylsilane, 2,2-dimethyl-nitropropane, (*E*)-(2-nitromethyl)trimethylsilane, 3,3-dimethyl-1-nitrobut-2-ene, 1-((trimethylsilyl)methyl)-1*H*-1,2,4-triazole, 1-((trimethylsilyl)methyl)-2*H*-1,2,3-triazole, 1-((trimethylsilyl)methyl)-1*H*-1,2,3-triazole, 1-((trimethylsilyl)methyl)-1*H*-tetrazole, 2-((trimethylsilyl)methyl)-2*H*-tetrazole, 5-((trimethylsilyl)methyl)-1*H*-tetrazole and 5-((trimethylsilyl)methyl)-2*H*-tetrazole gas phase structures are calculated using the MP2/cc-pVDZ level of theory. This allows investigating the chemical reactivity and stability of these compounds.

A theoretical approach along with no realistic decomposition or boiling temperatures and densities for the compounds used during this research made it indispensable to evaluate the influence of these characteristics on the calculation of the energetic parameters. Calculations revealed that the application of the Trouton's rule with slight errors is possible. Influence of the boiling or decomposition temperature is minor whereas density has to some extent bigger influence on the energetic parameters. The heat of explosion is an exception as the influence of the varying properties is non-homogenous and varies for each compound.

Different substituents and for some silicon containing compounds their carbon analogues were also compared. This revealed higher detonation parameters for carbon analogues compared to silicon containing compounds. Neopentyl nitrate and 2,2-dimethyl-nitropropane show the highest values but are still inferior to commercially available compounds. Tetrazole and triazole derivatives show almost identical values. Higher detonation temperature for the silicon containing compounds makes them unusable as gun propellants for various reasons. Especially the 1,2,4-triazol derivatives are the most promising compounds, because of its easy high yield synthesis and its chemical and physical stability.

Possible application as rocket fuels is also discussed. Therefore three different computing codes (EXPLO5 version 6.01, CHEETAH 2.0 and ICT-Code), different oxidizers and silicon and carbon analogues are compared. Computing codes EXPLO5 and ICT-Code give comparable results whereas the outdated CHEETAH version shows unreliable results. Problems occurring with the EXPLO5 programme can be solved by changing the calculation model or adjusting the list of reaction products. This leads to the conclusion that EXPLO5 is the most user friendly programme and therefore the most suitable one. The silicon containing compounds show higher chamber temperatures and conclusively higher specific impulses compared to their carbon analogues. Nitrogen tetroxide is the best oxidizer compared to ammonium perchlorate, ammonium dinitramide and red fuming nitric acid which in addition to giving the lowest results is very laborious to handle. Cheap and commercially available compounds trimethylvinylsilane, allyltrimethylsilane and tetravinylsilane show higher specific impulse values than all the newly synthesized and discussed silicon containing compounds. The cost benefit ratio is the highest for these

compounds and consequently the laborious and costly synthesis of new silicon containing compounds is not justified.

Acknowledgements

Financial support of this work by the Ludwig-Maximilian University of Munich (LMU), the U.S. Army Research Laboratory (ARL) under grant no. W911NF-09-2-0018, the Armament Research, Development and Engineering Center (ARDEC) under grant no. W911NF-12-1-0467, and the Office of Naval Research (ONR) under grant nos. ONR.N00014-10-1-0535 and ONR.N00014-12-1-0538 is gratefully acknowledged. The authors acknowledge collaborations with Dr. Mila Krupka (OZM Research, Czech Republic) in the development of new testing and evaluation methods for energetic materials. We are indebted to and thank Drs. Betsy M. Rice and Brad Forch (ARL, Aberdeen, Proving Ground, MD) for many inspired discussions.

-
- [1] T. M. Klapötke in *Chemie der hochenergetischen Materialien*; de Gruyter: Berlin, **2009**.
 - [2] R. Meyer, J. Köhler, A. Homburg in *Explosives*, 5th ed.; Wiley-VCH: Weinheim, **2002**.
 - [3] T. Urbanski, *Chemistry and Technology of Explosives*, Vol. 4, Pergamon Press: Oxford, **1984**.
 - [4] Barcza, S., U.S. Patent 3,592,831, **1968**.
 - [5] Barcza S., U.S. Patent 3,585,228, **1971**.
 - [6] T. M. Klapötke, B. Krumm, R. Ilg, D. Troegel, R. Tacke, *J. Am. Chem. Soc.* **2007**, *129*, 6908-6915.
 - [7] A. C. Evangelisti, T. M. Klapötke, B. Krumm, A. Nieder, R. J. F. Berger, S. A. Hayes, N. W. Mitzel, D. Troegel, R. Tacke, *Inorg. Chem.* **2010**, *49*, 4865–4880.
 - [8] T. M. Klapötke, B. Krumm, A. Nieder, O. Richter, D. Troegel, R. Tacke, *Z. Allg. Anorg. Chem.* **2012**, *638*, 1075–1079.
 - [9] L. Ascherl, C. Evangelisti, T. M. Klapötke, B. Krumm, J. Nafe, A. Nieder, S. Rest, C. Schütz, M. Sucasca, M. Trunk, *Chem. Eur. J.* **2013**, *19*, 9198–9210.

- [10] <http://webbook.nist.gov>
- [11] R. C. Weast (editor) in *Handbook of Chemistry and Physics*, 52th edition, The Chemical Rubber Co.: Cleveland, **1972**, p. D-238.
- [12] W. M. Howard, L. E. Fried, P. C. Souers in *Kinetic Modeling of Non-Ideal Explosives*, International Workshop on the Modeling of Non-Ideal Explosives, Socorro, **1999**.
- [13] P. W. Atkins, J. de Paula in *Physikalische Chemie, 4. Aufl.*, Wiley-VCH: Weinheim, **2006**.
- [14] M. Suceska, *EXPLO5 program vers. 6.01*, Zagreb (Croatia), **2012**.
- [15] N. Kubota in *Propellants and Explosives*, Wiley-VCH: Weinheim, **2002**.
- [16] J. P. Lu in *Evaluation of the Thermochemical Code – CHEETAH 2.0 for Modelling Explosives Performance*, DSTO-TR-1199, DSTO Aeronautical and Maritime Research Laboratory, Australia, **2001**.
- [17] M. A. Brook in *Silicon in Organic, Organometallic, and Polymer Chemistry*, Wiley & Sons, Inc.: New York, **1999**, p. 30.
- [18] A. Bondi, *J. Phys. Chem.* 1964, 68, 441–451.
- [19] M. S. Westwell, M. S. Searle, D. J. Wales, D. H. William, *J. Am. Chem. Soc.* **1995**, 117, 5013–5015.
-

Supporting Information

V. Sila-Substitution of Alkyl Nitrates

List of Tables and Figures

Chapter V	Hexa-Substituted Disiloxanes	S-1
Figure S1	The crystallographic structures and the calculated structures of 4b and 4c	S-2
Table S1	The X---H interactions in the crystal structures of 4a-4c	S-3
Table S2	Calculated structural data of 4a-4c on different levels of theory	S-4
Table S3	Calculated structural data of 4d and 4e on B3LYP level of theory	S-5
Table S4	Calculated structural data of 4d and 4e on MP2 level of theory	S-6
Chapter IX	Sila-Substitution of Alkyl Nitrates	S-7

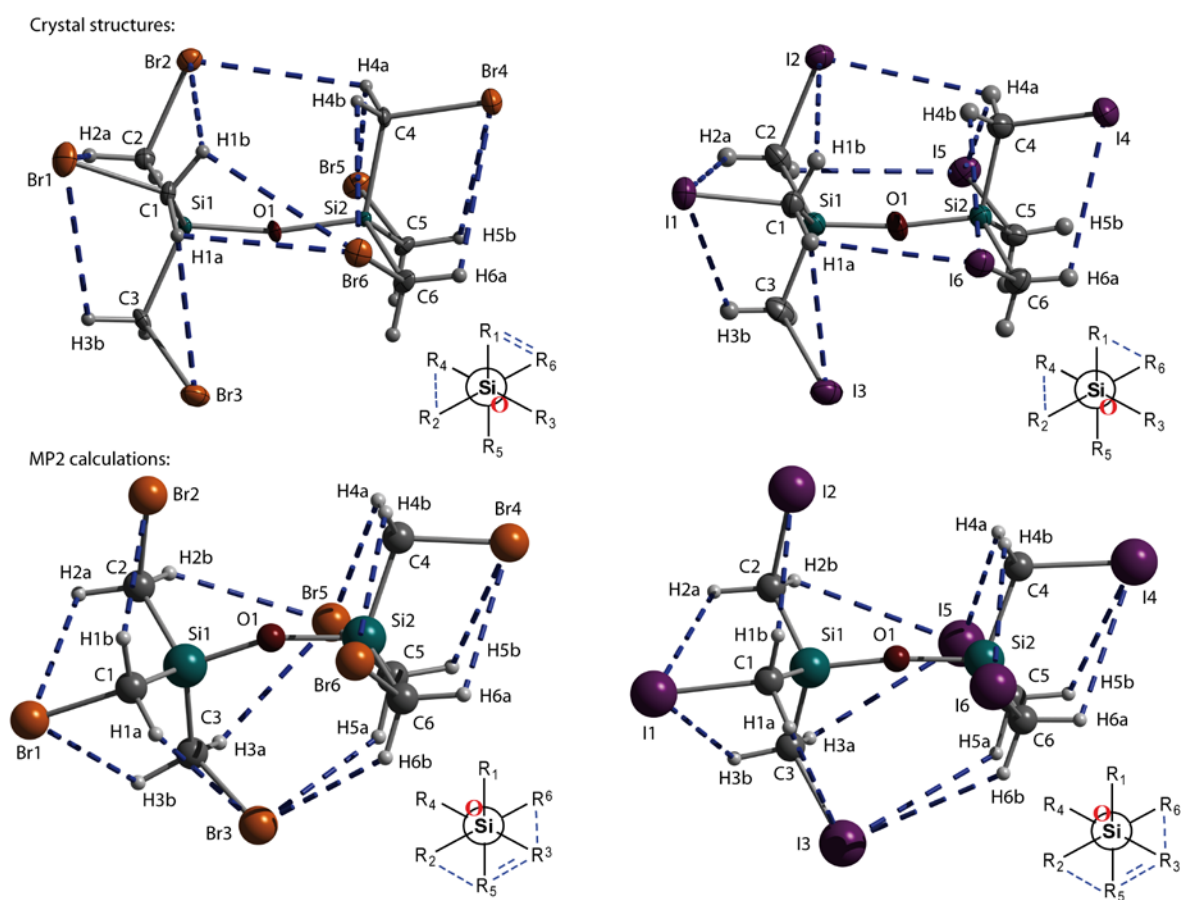


Figure S1. The crystallographic structures (top) and the calculated structures on MP2 level of theory (bottom) of **4b** (MP2/6-31G* level of theory) and **4c** (MP2/3-21G level of theory); Electrostatic attraction in the crystal and calculated gas phase structures of **4b** (X = Br) and **4c** (X = I) are shown in blue dashed lines (solid state, **4b**: Br2---H4a: 3.196(1) Å; Br6---H1a/b: 3.259(1) Å, 3.403(1) Å; Br1---H2aC2: 3.123(1) Å; Br1---H3b: 3.479(1) Å; Br2---H1b: 3.410(1) Å; Br3---H3b: 3.293(1) Å; Br4---H5b: 3.354(1) Å; Br4---H6aC6: 3.239(1) Å; Br5---H4aC4: 3.174(1) Å; Br6---H4bC4: 3.267(1) Å; **4c**: I2---H4a: 3.415(1) Å; I6---H1a: 3.371(1) Å; I1---H2a: 3.541 Å; I1---H3b: 3.414(1) Å; I2---H1b: 3.399(1); I3---H1a: 3.407(1) Å; I4---H6aC6: 3.283(1) Å; I5---H4a: 3.329(1) Å; I6---H4b: 3.501(1) Å; calculated gas phase, **4b**: Br3---H5a: 2.980 Å; Br3---H6b: 3.109 Å; Br5---H2b: 3.061 Å; Br5---H3a: 2.973 Å; Br1---H2aC2: 3.179 Å; Br1---H3bC3: 3.115 Å; Br2---H1b: 3.279 Å; Br3---H1a: 3.330 Å; Br4---H5bC5: 3.117 Å; Br4---H6aC6: 3.196 Å; Br5---H4a: 3.315 Å; Br6---H4b: 3.257 Å; **4c**: I3---H5a: 3.635 Å; I3---H6b: 3.757 Å; I5---H2b: 3.709 Å; I5---H3a: 3.618 Å; I1---H2a: 3.425 Å; I1---H3b: 3.388 Å; I2---H1b: 3.524 Å; I3---H1a: 3.577 Å; I4---H5b: 3.389 Å; I4---H6b: 3.428 Å; I5---H4a: 3.572 Å; I6---H4b: 3.520 Å; Σ vdW(Br,H) and Σ vdW(Br,C) radii: 3.05 Å and 3.55 Å; Σ vdW(I,H) and Σ vdW(I,C) radii: 3.12 Å and 3.68 Å)[27]. In addition, the Newman projection along the Si---Si axes is shown of each structure (R_i = CH₂Cl, attractions between the two RSi(CH₂Cl)₃ moieties in blue dashed lines, the position of the bridging oxygen is marked with **O**).

Table S1. The X---H interactions in the crystal structures of **4a–4c** (d(D,A) in Å).

Compound 4a : ΣvdW(Cl,H): 2.90 Å, ΣvdW(Cl,C): 3.45 Å, ΣvdW(Cl,Cl): 3.50 Å.		Compound 4b : ΣvdW(Br,H): 3.05 Å, ΣvdW(Br,C): 3.55 Å, ΣvdW(Br,Br): 3.70 Å.		Compound 4c : ΣvdW(I,H): 3.12 Å, ΣvdW(I,C): 3.68 Å, ΣvdW(I,I): 3.96 Å.	
D---A	d(D,A)	D---A	d(D,A)	D---A	d(D,A)
Cl1---H6a	3.015	Br1---H6b	3.016	I1---H6b	3.190
Cl2---H1b	2.916	Br2---H6a	3.070	I2---H6a	3.245
Cl2---H6b	2.996	Br2---H1a	3.114	I3---H2a	3.334
Cl3---H4b	2.874	Br3---H5b	2.893	I3---H4a	3.106
Cl3---H5a	2.823	Br3---H4a	2.914	I3---H5b	3.178
Cl4---H5b	2.845	Br3---H2a	3.019	I4---H2b	3.197
Cl4---H2a	2.995	Br1---H5a	3.176	I4---H3a	3.325
Cl6---H2b	2.938	Br4---H5a	2.935	I4---H5a	3.191
Cl6---H3a	2.909	Br4---H2b	2.994		
		Br6---H3a	3.193		
		Br6---H3b	3.028		
		Br6---H2a	3.074		
		Br5---H3b	3.190		

Table S2. Calculated structural data of **4a** and **4b** on MP2/6-31G* and B3LYP/cc-pVDZ, and **4c** on MP2/3-21G and B3LYP/3-21G level of theory.**MP2/6-31G* (X = I: MP2/3-21G):**

Bond [Å]	X = Cl	X = Br	X = I	Angles [°]	X = Cl	X = Br	X = I
C1–X1	1.796	1.970	2.214	X1–C1–Si1	109.5	105.7	111.8
C2–X2	1.793	1.968	2.212	X2–C2–Si1	110.4	106.3	112.5
C3–X3	1.799	1.974	2.215	X3–C3–Si1	110.3	106.7	112.2
C4–X4	1.796	1.970	2.214	X4–C4–Si2	109.5	105.7	111.9
C5–X5	1.799	1.974	2.215	X5–C5–Si2	110.3	106.6	112.2
C6–X6	1.793	1.969	2.212	X6–C6–Si2	110.4	106.2	112.5
Si1–C1	1.880	1.873	1.907	C1–Si1–O1	107.2	108.5	108.8
Si1–C2	1.885	1.880	1.910	C2–Si1–O1	109.9	107.6	110.2
Si1–C3	1.891	1.888	1.915	C3–Si1–O1	110.5	109.3	109.8
Si2–C4	1.880	1.873	1.907	C4–Si2–O1	107.2	108.3	108.6
Si2–C5	1.891	1.888	1.915	C5–Si2–O1	110.5	109.1	109.8
Si2–C6	1.885	1.881	1.910	C6–Si2–O1	109.9	107.9	110.4
Si1–O1	1.651	1.645	1.675	C1–Si1–C2	110.9	110.9	111.0
Si2–O1	1.651	1.645	1.674	C2–Si1–C3	108.2	110.5	106.7
Torsion angles [°]				C3–Si1–C1	110.1	110.0	110.4
X1–C1–Si1–O1	179.5	179.9	-179.7	C4–Si2–C5	110.9	109.9	110.4
X2–C2–Si1–O1	-58.4	-53.2	-58.7	C5–Si2–C6	108.2	110.9	106.7
X3–C3–Si1–O1	51.2	51.0	53.8	C6–Si2–C4	110.1	110.7	111.0
X4–C4–Si2–O1	179.6	180.0	-179.7	Si1–O1–Si2	151.1	154.1	167.8
X5–C5–Si2–O1	51.3	49.4	53.2				
X6–C6–Si2–O1	-58.3	-51.4	-58.5				
C1–Si1---Si2–C4	-93.3	-95.0	-91.4				

B3LYP/cc-pVDZ (X = I: B3LYP/3-21G)

Bond [Å]	X = Cl	X = Br	X = I	Angles [°]	X = Cl	X = Br	X = I
C1–X1	1.826	1.983	2.223	X1–C1–Si1	109.1	109.9	111.7
C2–X2	1.822	1.981	2.222	X2–C2–Si1	110.6	111.2	112.7
C3–X3	1.828	1.986	2.226	X3–C3–Si1	110.7	111.5	112.5
C4–X4	1.826	1.983	2.223	X4–C4–Si2	109.1	109.9	111.6
C5–X5	1.828	1.985	2.225	X5–C5–Si2	110.7	111.5	112.3
C6–X6	1.822	1.981	2.222	X6–C6–Si2	110.6	111.2	112.7
Si1–C1	1.892	1.889	1.900	C1–Si1–O1	107.3	107.2	109.0
Si1–C2	1.898	1.896	1.904	C2–Si1–O1	109.4	109.1	109.9
Si1–C3	1.903	1.900	1.909	C3–Si1–O1	110.6	110.4	109.7
Si2–C4	1.892	1.889	1.901	C4–Si2–O1	107.2	107.1	109.1
Si2–C5	1.903	1.900	1.909	C5–Si2–O1	110.6	110.3	109.6
Si2–C6	1.898	1.900	1.904	C6–Si2–O1	109.5	109.2	109.8
Si1–O1	1.671	1.669	1.653	C1–Si1–C2	110.9	111.5	111.1
Si2–O1	1.671	1.669	1.652	C2–Si1–C3	108.0	107.4	106.6
Torsion angles [°]				C3–Si1–C1	110.6	111.3	110.6
X1–C1–Si1–O1	-179.9	-179.9	-178.4	C4–Si2–C5	110.6	111.3	110.3
X2–C2–Si1–O1	-57.3	-57.4	-62.4	C5–Si2–C6	108.0	107.4	106.8
X3–C3–Si1–O1	53.5	55.2	52.0	C6–Si2–C4	110.9	111.5	111.2
X4–C4–Si2–O1	-179.9	-179.8	179.6	Si1–O1–Si2	155.5	160.0	170.4
X5–C5–Si2–O1	53.1	54.9	50.6				
X6–C6–Si2–O1	-57.1	-57.4	-60.7				
C1–Si1---Si2–C4	-95.0	-94.5	-89.2				

Table S3. Calculated structural data of **4d** and **4e** on B3LYP/cc-pVDZ level of theory.**Compound 4d on B3LYP/cc-pVDZ level of theory:**

Bonds [Å]				Angles [°]			
C1–N _α 1	1.495	N _α 1–N _β 1	1.248	X1–C1–Si1	104.7	N _α 1–N _β 1–N _γ 1	173.1
C2–N _α 2	1.489	N _α 2–N _β 2	1.247	X2–C2–Si1	103.8	N _α 2–N _β 2–N _γ 2	171.8
C3–N _α 3	1.494	N _α 3–N _β 3	1.250	X3–C3–Si1	110.9	N _α 3–N _β 3–N _γ 3	173.2
C4–N _α 4	1.491	N _α 4–N _β 4	1.247	X4–C4–Si2	108.4	N _α 4–N _β 4–N _γ 4	172.9
C5–N _α 5	1.493	N _α 5–N _β 5	1.243	X5–C5–Si2	104.9	N _α 5–N _β 5–N _γ 5	171.6
C6–N _α 6	1.487	N _α 6–N _β 6	1.249	X6–C6–Si2	107.9	N _α 6–N _β 6–N _γ 6	172.8
Si1–C1	1.891	N _β 1–N _γ 1	1.164	C1–Si1–O1	112.4	C1–N _α 1–N _β 1	115.0
Si1–C2	1.896	N _β 2–N _γ 2	1.165	C2–Si1–O1	107.2	C2–N _α 2–N _β 2	115.0
Si1–C3	1.892	N _β 3–N _γ 3	1.163	C3–Si1–O1	109.9	C3–N _α 3–N _β 3	116.3
Si2–C4	1.892	N _β 4–N _γ 4	1.164	C4–Si2–O1	112.3	C4–N _α 4–N _β 4	115.0
Si2–C5	1.889	N _β 5–N _γ 5	1.167	C5–Si2–O1	109.8	C5–N _α 5–N _β 5	115.3
Si2–C6	1.890	N _β 6–N _γ 6	1.163	C6–Si2–O1	104.1	C6–N _α 6–N _β 6	117.4
Si1–O1	1.663			C1–Si1–C2	108.3	Torsions angles [°]	
Si2–O1	1.668			C2–Si1–C3	109.6	X1–C1–Si1–O1	-174.7
				C3–Si1–C1	109.3	X2–C2–Si1–O1	-54.5
				C4–Si2–C5	111.0	X3–C3–Si1–O1	-129.8
				C5–Si2–C6	111.5	X4–C4–Si2–O1	179.7
				C6–Si2–C4	107.9	X5–C5–Si2–O1	-153.3
				Si1–O1–Si2	143.2	X6–C6–Si2–O1	-57.3
						C1–Si1---Si2–C4	-28.8

Compound 4e on B3LYP/cc-pVDZ level of theory:

Bonds [Å]				Angles [°]			
C1–O _α 1	1.441	N1–O _{β/γ} 1	1.217/1.214	X1–C1–Si1	100.7	C1–O _α 2–N1	113.1
C2–O _α 2	1.444	N2–O _{β/γ} 2	1.218/1.218	X2–C2–Si1	101.3	C2–O _α 3–N2	113.3
C3–O _α 3	1.453	N3–O _{β/γ} 3	1.217/1.225	X3–C3–Si1	111.6	C3–O _α 4–N3	112.9
C4–O _α 4	1.442	N4–O _{β/γ} 4	1.217/1.214	X4–C4–Si2	100.3	C4–O _α 5–N4	113.1
C5–O _α 5	1.460	N5–O _{β/γ} 5	1.224/1.217	X5–C5–Si2	107.5	C5–O _α 6–N5	113.3
C6–O _α 6	1.459	N6–O _{β/γ} 6	1.225/1.224	X6–C6–Si2	109.9	C6–O _α 7–N6	112.2
Si1–C1	1.891	N1–O _α 1	1.462	C1–Si1–O1	108.7	O _α 2–N1–O _{β/γ} 2	116.4/111.6
Si1–C2	1.893	N2–O _α 2	1.450	C2–Si1–O1	106.6	O _α 3–N2–O _{β/γ} 3	116.8/111.8
Si1–C3	1.903	N3–O _α 3	1.422	C3–Si1–O1	108.8	O _α 4–N3–O _{β/γ} 4	117.1/112.5
Si2–C4	1.890	N4–O _α 4	1.462	C4–Si2–O1	108.9	O _α 5–N4–O _{β/γ} 5	116.4/111.6
Si2–C5	1.897	N5–O _α 5	1.429	C5–Si2–O1	112.3	O _α 6–N5–O _{β/γ} 6	117.5/112.1
Si2–C6	1.911	N6–O _α 6	1.411	C6–Si2–O1	107.6	O _α 7–N6–O _{β/γ} 7	117.7/112.5
Si1–O1	1.664			C1–Si1–C2	110.1	O _β 2–N1–O _γ 2	132.0
Si2–O1	1.660			C2–Si1–C3	107.4	O _β 3–N1–O _γ 3	131.4
				C3–Si1–C1	115.3	O _β 4–N1–O _γ 4	130.4
				C4–Si2–C5	111.6	O _β 5–N1–O _γ 5	132.0
				C5–Si2–C6	109.6	O _β 6–N1–O _γ 6	130.3
				C6–Si2–C4	106.7	O _β 7–N1–O _γ 7	129.8
				Si1–O1–Si2	150.0		
Torsions angles [°]							
X1–C1–Si1–O1			168.5				
X2–C2–Si1–O1			54.9				
X3–C3–Si1–O1			140.6				
X4–C4–Si2–O1			166.1				
X5–C5–Si2–O1			-172.6				
X6–C6–Si2–O1			8.8				
C1–Si1---Si2–C4			-50.2				
X1–C1–Si1–O1			168.5				

Table S4. Calculated structural data of **4d** and **4e** on MP2/6-31G* level of theory.**Compound 4d on MP2/6-31G* level of theory:**

Bonds [Å]				Angles [°]			
C1–N _α 1	1.495	N _α 1–N _β 1	1.248	X1–C1–Si1	104.7	N _α 1–N _β 1–N _γ 1	173.1
C2–N _α 2	1.489	N _α 2–N _β 2	1.247	X2–C2–Si1	103.8	N _α 2–N _β 2–N _γ 2	171.8
C3–N _α 3	1.494	N _α 3–N _β 3	1.250	X3–C3–Si1	110.9	N _α 3–N _β 3–N _γ 3	173.2
C4–N _α 4	1.491	N _α 4–N _β 4	1.247	X4–C4–Si2	108.4	N _α 4–N _β 4–N _γ 4	172.9
C5–N _α 5	1.493	N _α 5–N _β 5	1.243	X5–C5–Si2	104.9	N _α 5–N _β 5–N _γ 5	171.6
C6–N _α 6	1.487	N _α 6–N _β 6	1.249	X6–C6–Si2	107.9	N _α 6–N _β 6–N _γ 6	172.8
Si1–C1	1.891	N _β 1–N _γ 1	1.164	C1–Si1–O1	112.4	C1–N _α 1–N _β 1	115.0
Si1–C2	1.896	N _β 2–N _γ 2	1.165	C2–Si1–O1	107.2	C2–N _α 2–N _β 2	115.0
Si1–C3	1.892	N _β 3–N _γ 3	1.163	C3–Si1–O1	109.9	C3–N _α 3–N _β 3	116.3
Si2–C4	1.892	N _β 4–N _γ 4	1.164	C4–Si2–O1	112.3	C4–N _α 4–N _β 4	115.0
Si2–C5	1.889	N _β 5–N _γ 5	1.167	C5–Si2–O1	109.8	C5–N _α 5–N _β 5	115.3
Si2–C6	1.890	N _β 6–N _γ 6	1.163	C6–Si2–O1	104.1	C6–N _α 6–N _β 6	117.4
Si1–O1	1.663			C1–Si1–C2	108.3	Torsions angles [°]	
Si2–O1	1.668			C2–Si1–C3	109.6	X1–C1–Si1–O1	-174.7
				C3–Si1–C1	109.3	X2–C2–Si1–O1	-54.5
				C4–Si2–C5	111.0	X3–C3–Si1–O1	-129.8
				C5–Si2–C6	111.5	X4–C4–Si2–O1	179.7
				C6–Si2–C4	107.9	X5–C5–Si2–O1	-153.3
				Si1–O1–Si2	143.2	X6–C6–Si2–O1	-57.3
						C1–Si1---Si2–C4	-28.8

Compound 4e on MP2/6-31G* level of theory:

Bonds [Å]				Angles [°]			
C1–O _α 1	1.441	N1–O _{β/γ} 1	1.217/1.214	X1–C1–Si1	100.7	C1–O _α 2–N1	113.1
C2–O _α 2	1.444	N2–O _{β/γ} 2	1.218/1.218	X2–C2–Si1	101.3	C2–O _α 3–N2	113.3
C3–O _α 3	1.453	N3–O _{β/γ} 3	1.217/1.225	X3–C3–Si1	111.6	C3–O _α 4–N3	112.9
C4–O _α 4	1.442	N4–O _{β/γ} 4	1.217/1.214	X4–C4–Si2	100.3	C4–O _α 5–N4	113.1
C5–O _α 5	1.460	N5–O _{β/γ} 5	1.224/1.217	X5–C5–Si2	107.5	C5–O _α 6–N5	113.3
C6–O _α 6	1.459	N6–O _{β/γ} 6	1.225/1.224	X6–C6–Si2	109.9	C6–O _α 7–N6	112.2
Si1–C1	1.891	N1–O _α 1	1.462	C1–Si1–O1	108.7	O _α 2–N1–O _{β/γ} 2	116.4/111.6
Si1–C2	1.893	N2–O _α 2	1.450	C2–Si1–O1	106.6	O _α 3–N2–O _{β/γ} 3	116.8/111.8
Si1–C3	1.903	N3–O _α 3	1.422	C3–Si1–O1	108.8	O _α 4–N3–O _{β/γ} 4	117.1/112.5
Si2–C4	1.890	N4–O _α 4	1.462	C4–Si2–O1	108.9	O _α 5–N4–O _{β/γ} 5	116.4/111.6
Si2–C5	1.897	N5–O _α 5	1.429	C5–Si2–O1	112.3	O _α 6–N5–O _{β/γ} 6	117.5/112.1
Si2–C6	1.911	N6–O _α 6	1.411	C6–Si2–O1	107.6	O _α 7–N6–O _{β/γ} 7	117.7/112.5
Si1–O1	1.664			C1–Si1–C2	110.1	O _β 2–N1–O _γ 2	132.0
Si2–O1	1.660			C2–Si1–C3	107.4	O _β 3–N1–O _γ 3	131.4
				C3–Si1–C1	115.3	O _β 4–N1–O _γ 4	130.4
				C4–Si2–C5	111.6	O _β 5–N1–O _γ 5	132.0
				C5–Si2–C6	109.6	O _β 6–N1–O _γ 6	130.3
				C6–Si2–C4	106.7	O _β 7–N1–O _γ 7	129.8
				Si1–O1–Si2	150.0		
Torsions angles [°]							
X1–C1–Si1–O1			168.5				
X2–C2–Si1–O1			54.9				
X3–C3–Si1–O1			140.6				
X4–C4–Si2–O1			166.1				
X5–C5–Si2–O1			-172.6				
X6–C6–Si2–O1			8.8				
C1–Si1---Si2–C4			-50.2				
X1–C1–Si1–O1			168.5				

V. Sila-Substitution of Alkyl Nitrates

List of Tables and Figures

Chapter IX	Theoretical Approach of Energetic Silanes	
1.	(Nitratomethyl)trimethylsilane (1)	S-12
Table S1:	Detonation parameter of 1 in dependency of T_{dec} and density	S-12
Figure S1:	Graph of heat of explosion of 1 in dependency to T_{dec} and density	S-12
Table S2:	Propulsion parameters of 1 computed with EXPL05 (Model 1) with ammonium perchlorate (AP)	S-13
Table S3:	Propulsion parameters of 1 computed with EXPL05 (Model 4) with AP	S-13
Figure S2:	Specific impulse values verses different amounts of AP calculated of 1 with different computer codes	S-13
2.	Neopentyl nitrate (1^c)	S-14
Table S4:	Detonation parameter of 1^c in dependency of T_{dec} and density	S-14
Figure S3:	Graph of heat of explosion of 1^c in dependency to T_{dec} and density	S-14
Table S5:	Propulsion parameters of 1^c computed with EXPL05 (Model 1) with AP	S-15
Figure S4:	Specific impulse values verses different amounts of AP calculated of 1^c with different computer codes	S-15
3.	(Azidomethyl)trimethylsilane (2)	S-16
Table S6:	Detonation parameter of 2 in dependency of T_{dec} and density	S-16
Figure S5:	Graph of heat of explosion of 2 in dependency to T_{dec} and density	S-16
Table S7:	Propulsion parameters of 2 computed with EXPL05 (Model 1) with AP	S-17
Table S8:	Propulsion parameters of 2 computed with EXPL05 (Model 4) with AP	S-17
Figure S6:	Specific impulse values verses different amounts of AP calculated of 2 with different computer codes	S-17
4.	1-Azido-2,2-dimethylpropane (2^c)	S-18
Table S9:	Detonation parameter of 2^c in dependency of T_{dec} and density	S-18
Figure S7:	Graph of heat of explosion of 2^c in dependency to T_{dec} and density	S-18
Table S10:	Propulsion parameters of 2^c computed with EXPL05 (Model 1) with AP	S-19

Figure S8:	Specific impulse values verses different amounts of AP calculated of 2^c with different computer codes	S-19
5.	(Nitromethyl)trimethylsilane (3)	S-20
Table S11:	Detonation parameter of 3 in dependency of T_{dec} and density	S-20
Figure S9:	Graph of heat of explosion of 3 in dependency to T_{dec} and density	S-20
Table S12:	Propulsion parameters of 3 computed with EXPL05 (Model 1) with AP	S-21
Table S13:	Propulsion parameters of 3 computed with EXPL05 (Model 4) with AP	S-21
Figure S10:	Specific impulse values verses different amounts of AP calculated of 3 with different computer codes	S-21
6.	2,2-Dimethyl-1-nitropropane (3^c)	S-22
Table S14:	Detonation parameter of 3^c in dependency of T_{dec} and density	S-22
Figure S11:	Graph of heat of explosion of 3^c in dependency to T_{dec} and density	S-23
Table S15:	Propulsion parameters of 3^c computed with EXPL05 (Model 1) with AP	S-23
Figure S12:	Specific impulse values verses different amounts of AP calculated of 3^c with different computer codes	S-23
7.	(E)-(2-Nitrovinyl)trimethylsilane (4)	S-24
Table S16:	Detonation parameter of 4 in dependency of T_{dec} and density	S-24
Figure S13:	Graph of heat of explosion of 4 in dependency to T_{dec} and density	S-24
Table S17:	Propulsion parameters of 4 computed with EXPL05 (Model 1) with AP	S-25
Table S18:	Propulsion parameters of 4 computed with EXPL05 (Model 4) with AP	S-25
Figure S14:	Specific impulse values verses different amounts of AP calculated of 4 with different computer codes	S-25
Table S19:	Propulsion parameters of 4 computed with EXPL05 (Model 1) with ammonium dinitramide (ADN)	S-26
Figure S15:	Specific impulse values verses different amounts of ADN calculated of 4 with different computer codes	S-26
Table S20:	Propulsion parameters of 4 computed with EXPL05 (Model 1) with nitrogen tetroxide (N_2O_4)	S-27
Figure S16:	Specific impulse values verses different amounts of N_2O_4 calculated of 4 with different computer codes	S-27
8.	(E)-3,3-Dimethyl-1-nitrobut-2-ene (4^c)	S-28
Table S21:	Detonation parameter of 4^c in dependency of T_{dec} and density	S-28

Figure S17:	Graph of heat of explosion of 4^c in dependency to T_{dec} and density	S-28
Table S22:	Propulsion parameters of 4^c computed with EXPL05 (Model 1) with AP	S-29
Figure S18:	Specific impulse values verses different amounts of AP calculated of 4^c with different computer codes	S-29
Table S23:	Propulsion parameters of 4^c computed with EXPL05 (Model 1) with ADN	S-30
Figure S19:	Specific impulse values verses different amounts of ADN calculated of 4^c with different computer codes	S-30
Table S24:	Propulsion parameters of 4^c computed with EXPL05 (Model 1) with N_2O_4	S-31
Figure S20:	Specific impulse values verses different amounts of N_2O_4 calculated of 4^c with different computer codes	S-31
9.	1-((Trimethylsilyl)methyl)-1<i>H</i>-1,2,4-triazole (5a)	S-32
Table S25:	Detonation parameter of 5a in dependency of T_{dec} and density	S-32
Figure S21:	Graph of heat of explosion of 5a in dependency to T_{dec} and density	S-32
Table S26:	Propulsion parameters of 5a computed with EXPL05 (Model 1) with AP	S-33
Table S27:	Propulsion parameters of 5a computed with EXPL05 (Model 4) with AP	S-33
Figure S22:	Specific impulse values verses different amounts of AP calculated of 5a with different computer codes	S-33
10.	1-((Trimethylsilyl)methyl)-2<i>H</i>-1,2,3-triazole (5b)	S-34
Table S28:	Detonation parameter of 5b in dependency of T_{dec} and density	S-34
Figure S23:	Graph of heat of explosion of 5b in dependency to T_{dec} and density	S-34
Table S29:	Propulsion parameters of 5b computed with EXPL05 (Model 1) with AP	S-35
Table S30:	Propulsion parameters of 5b computed with EXPL05 (Model 4) with AP	S-35
Figure S24:	Specific impulse values verses different amounts of AP calculated of 5b with different computer codes	S-35
11.	1-((Trimethylsilyl)methyl)-1<i>H</i>-1,2,3-triazole (5c)	S-36
Table S31:	Detonation parameter of 5c in dependency of T_{dec} and density	S-36
Figure S25:	Graph of heat of explosion of 5c in dependency to T_{dec} and density	S-36
Table S32:	Propulsion parameters of 5c computed with EXPL05 (Model 1) with AP	S-37

Table S33:	Propulsion parameters of 5c computed with EXPL05 (Model 4) with AP	S-37
Figure S26:	Specific impulse values verses different amounts of AP calculated of 5c with different computer codes	S-37
12.	1-((Trimethylsilyl)methyl)-1H-tetrazole (6a)	S-38
Table S34:	Detonation parameter of 6a in dependency of T_{dec} and density	S-38
Figure S27:	Graph of heat of explosion of 6a in dependency to T_{dec} and density	S-38
Table S35:	Propulsion parameters of 6a computed with EXPL05 (Model 1) with AP	S-39
Table S36:	Propulsion parameters of 6a computed with EXPL05 (Model 4) with AP	S-39
Figure S28:	Specific impulse values verses different amounts of AP calculated of 6a with different computer codes	S-39
13.	1-((Trimethylsilyl)methyl)-2H-tetrazole (6b)	S-40
Table S37:	Detonation parameter of 6b in dependency of T_{dec} and density	S-40
Figure S29:	Graph of heat of explosion of 6b in dependency to T_{dec} and density	S-40
Table S38:	Propulsion parameters of 6b computed with EXPL05 (Model 1) with AP	S-41
Table S39:	Propulsion parameters of 6b computed with EXPL05 (Model 4) with AP	S-41
Figure S30:	Specific impulse values verses different amounts of AP calculated of 6b with different computer codes	S-41
14.	5-((Trimethylsilyl)methyl)-1H-tetrazole (6c)	S-42
Table S40:	Detonation parameter of 6c in dependency of T_{dec} and density	S-42
Figure S31:	Graph of heat of explosion of 6c in dependency to T_{dec} and density	S-42
Table S41:	Propulsion parameters of 6c computed with EXPL05 (Model 1) with AP	S-43
Table S42:	Propulsion parameters of 6c computed with EXPL05 (Model 4) with AP	S-43
Figure S32:	Specific impulse values verses different amounts of AP calculated of 6c with different computer codes	S-43
15.	5-((Trimethylsilyl)methyl)-2H-tetrazole (6d)	S-44
Table S43:	Detonation parameter of 6d in dependency of T_{dec} and density	S-44
Figure S33:	Graph of heat of explosion of 6d in dependency to T_{dec} and density	S-44

Table S44:	Propulsion parameters of 6d computed with EXPL05 (Model 1) with AP	S-45
Table S45:	Propulsion parameters of 6d computed with EXPL05 (Model 4) with AP	S-45
Figure S34:	Specific impulse values verses different amounts of AP calculated of 6d with different computer codes	S-45
16.	Trimethylvinylsilane (7)	S-46
Table S46:	Propulsion parameters of 7 computed with EXPL05 (Model 1) with N ₂ O ₄	S-46
Figure S35:	Specific impulse values verses different amounts of N ₂ O ₄ calculated of 7 with different computer codes	S-46
Table S47:	Propulsion parameters of 7 computed with EXPL05 (Model 1) with red fuming nitric acid (RFNA)	S-47
Figure S36:	Specific impulse values verses different amounts of RFNA calculated of 7 with different computer codes	S-47
17.	Allyltrimethylsilane (8)	S-48
Table S48:	Propulsion parameters of 8 computed with EXPL05 (Model 1) with N ₂ O ₄	S-48
Figure S37:	Specific impulse values verses different amounts of N ₂ O ₄ calculated of 8 with different computer codes	S-48
Table S49:	Propulsion parameters of 8 computed with EXPL05 (Model 1) with red fuming nitric acid (RFNA)	S-49
Figure S38:	Specific impulse values verses different amounts of RFNA calculated of 8 with different computer codes	S-49
18.	Tetravinylsilane (9)	S-50
Table S50:	Propulsion parameters of 9 computed with EXPL05 (Model 1) with N ₂ O ₄	S-50
Figure S39:	Specific impulse values verses different amounts of N ₂ O ₄ calculated of 9 with different computer codes	S-50
Table S51:	Propulsion parameters of 9 computed with EXPL05 (Model 1) with RFNA	S-51
Figure S40:	Specific impulse values verses different amounts of RFNA calculated of 9 with different computer codes	S-51
19.	CHEETAH 2.0 values	S-52
Table S52:	Propulsion parameters computed with CHEETAH 2.0 for different compounds and oxidizers	S-52
20.	ICT-Code values	S-52
Table S53:	Propulsion parameters computed with ICT-Code for different compounds and oxidizers	S-52

1. Nitratomethyl)trimethylsilane (1)

Table S1: Detonation parameter (heat of explosion $\Delta_{\text{ex}}U^\circ$, detonation temperature T_{det} , detonation pressure p_{cl} , detonation velocity V_{det} and gas volume V_0) of **1** in dependency of T_{dec} and density

T_{dec} [°C]	density [g/cm ³]	$\Delta_{\text{ex}}U^\circ$ [kJ·kg ⁻¹]	T_{det} [K]	p_{cl} [kbar]	V_{det} [m·s ⁻¹]	V_0 [L·kg ⁻¹]
50	1.0	-5407.232	2876.152	6.92017	5140.971	747.0042
	1.1	-5471.625	2869.367	8.444506	5542.092	722.0688
	1.2	-5523.917	2856.900	10.28971	5977.626	699.3983
	1.3	-5566.975	2835.382	12.45399	6454.446	679.2231
	1.4	-5604.012	2812.682	15.26069	6969.907	658.9127
1.5	-5632.726	2781.642	18.59138	7511.304	638.6118	
100	1.0	-5379.654	2861.76	6.832355	5133.142	747.0168
	1.1	-5444.753	2859.666	8.422148	5534.592	721.4100
	1.2	-5496.644	2847.019	10.25652	5970.375	698.8741
	1.3	-5539.561	2824.195	12.37468	6447.328	678.9189
	1.4	-5576.566	2803.428	15.22961	6963.129	658.4948
1.5	-5605.446	2772.474	18.55383	7504.635	638.2442	
150	1.0	-5353.170	2851.958	6.810142	5125.599	746.3171
	1.1	-5417.877	2849.928	8.399351	5527.074	720.7548
	1.2	-5469.492	2837.183	10.22881	5962.941	698.2823
	1.3	-5512.167	2813.457	12.31114	6440.177	678.5532
	1.4	-5549.355	2787.906	14.96904	6956.110	658.9550
1.5	-5578.074	2763.429	18.52142	7498.078	637.9177	
200	1.0	-5326.755	2842.211	6.789841	5117.954	745.5834
	1.1	-5390.976	2840.302	8.376722	5519.623	720.0961
	1.2	-5442.334	2827.629	10.20373	5955.627	697.6653
	1.3	-5484.852	2803.984	12.28426	6432.976	678.004
	1.4	-5521.996	2778.577	14.93812	6949.115	658.4823
1.5	-5550.750	2754.319	18.48842	7491.390	637.5585	

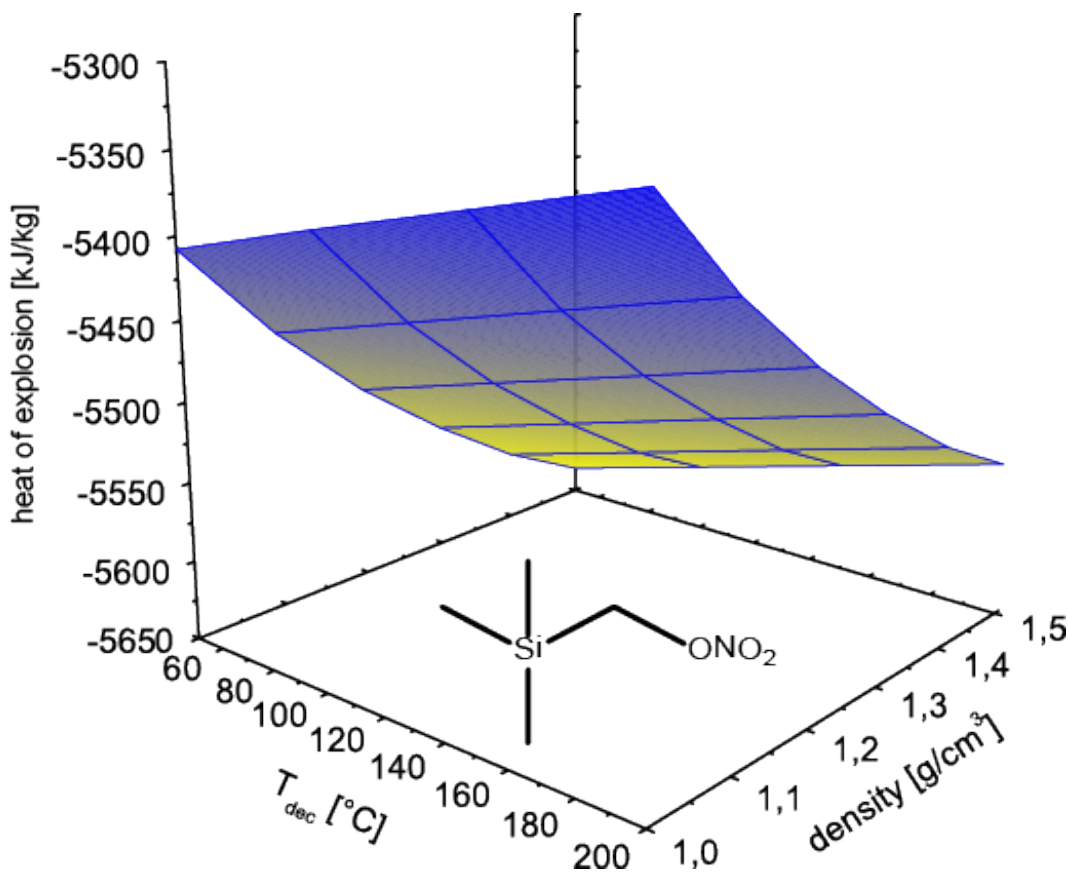
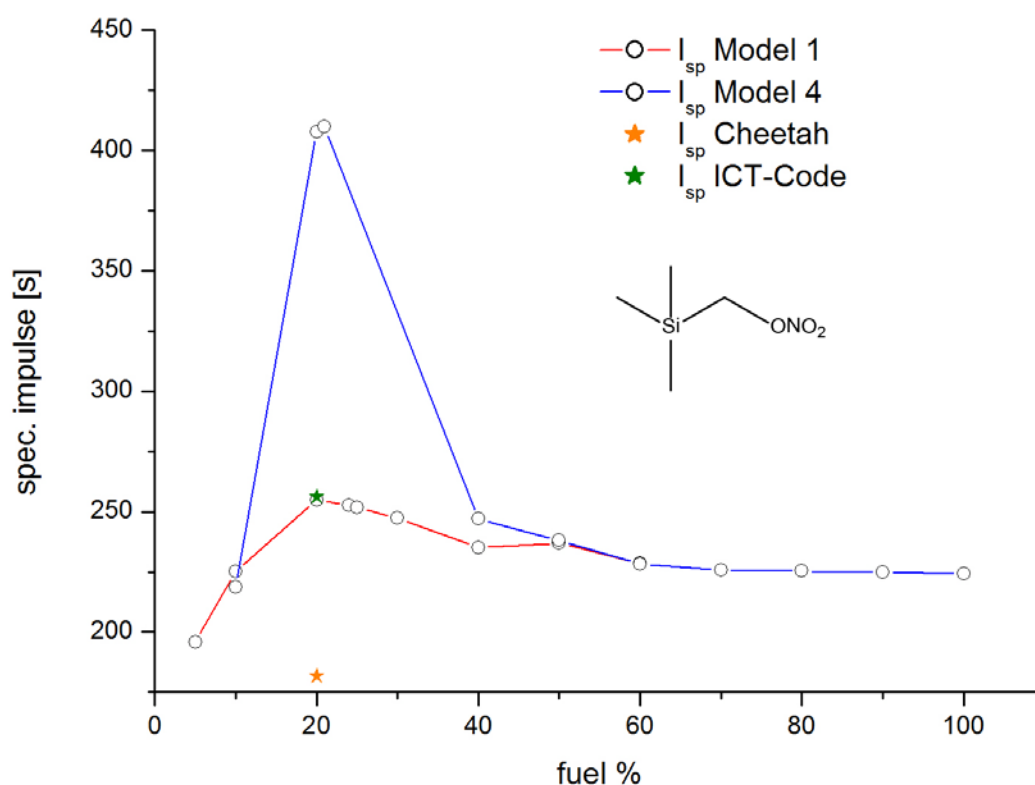
**Figure S1:** Graph of heat of explosion of **1** in dependency to T_{dec} and density

Table S2: Propulsion parameters (chamber temperature T_c , specific impulse I_{sp} and oxygen balance) of **1** computed with EXPL05 (Model 1) with AP (ammonium perchlorate)

T_{dec} [°C]	T_c [K]	I_{sp} [s]	Oxygen balance [atm] in %	1 / AP
100	2553.1	218.72	17.23593	10 / 90
	3111.4	407.81	0.4294036	20 / 80
	3127.3	409.90	-1.251252	21 / 79
	2738.6	247.03	-33.18365	40 / 60
	2412.1	238.13	-49.99018	50 / 50
	2065.7	228.30	-66.79671	60 / 40
	1980.5	225.76	-83.60325	70 / 30
	1983.6	225.34	-100.4098	80 / 20
	1986.2	224.96	-117.2163	90 / 10
	1988.1	224.22	-134.0228	100 / 0

Table S3: Propulsion parameters (T_c , I_{sp} and oxygen balance) of **1** computed with EXPL05 (Model 4) with AP

T_{dec} [°C]	T_c [K]	I_{sp} [s]	Oxygen balance [atm] in %	1 / AP
100	2109.5	195.97	24.23395	5 / 95
	2668.3	225.05	14.42544	10 / 90
	3146.2	254.83	-5.191571	20 / 80
	3084.8	252.66	-13.03838	24 / 76
	3055.1	251.89	-15.00008	25 / 75
	2865.3	247.34	-24.80858	30 / 70
	2421.3	235.04	-44.42559	40 / 60
	2414.0	236.90	-49.99018	50 / 50
	2118.0	228.50	-66.79671	60 / 40
	2109.5	195.97	24.23395	5 / 95

**Figure S2:** Specific impulse values versus different amounts of AP calculated of **1** with different computer codes

2. Neopentyl nitrate (1^c)**Table S4:** Detonation parameter ($\Delta_{\text{ex}}U$, T_{det} , p_{CJ} , V_{det} and V_0) of 1^c in dependency of T_{dec} and density

T_{dec} [°C]	density [g/cm ³]	$\Delta_{\text{ex}}U^{\circ}$ [kJ·kg ⁻¹]	T_{det} [K]	p_{CJ} [kbar]	V_{det} [m·s ⁻¹]	V_0 [L·kg ⁻¹]
50	1.0	-3705.157	2190.299	6.70376	5157.994	930.3107
	1.1	-3744.499	2188.554	8.27274	5568.620	911.1451
	1.2	-3772.464	2178.093	10.08087	6010.008	895.0609
	1.3	-3792.295	2157.562	12.11142	6493.208	883.1689
	1.4	-3806.537	2132.486	14.55836	7027.729	875.3260
1.5	-3817.914	2103.66	17.53731	7610.552	870.1565	
100	1.0	-3735.507	2201.595	6.734016	5169.621	931.1776
	1.1	-3775.731	2199.749	8.307166	5580.195	911.8658
	1.2	-3804.227	2189.381	10.12053	6021.818	895.6771
	1.3	-3824.427	2168.775	12.15596	6505.139	883.6784
	1.4	-3838.897	2143.40	14.60742	7039.560	875.7438
1.5	-3850.301	2114.484	17.59340	7622.712	870.5486	
150	1.0	-3674.800	2179.035	6.673613	5146.383	929.4363
	1.1	-3713.188	2173.926	8.180056	5556.526	910.6812
	1.2	-3740.722	2166.616	10.04048	5997.954	894.4347
	1.3	-3760.172	2146.335	12.06675	6481.225	882.6547
	1.4	-3774.257	2121.302	14.50795	7039.560	874.8793
1.5	-3785.394	2095.207	17.57950	7598.315	869.7626	
200	1.0	-3644.444	2167.655	6.643251	5134.641	928.5592
	1.1	-3682.035	2162.438	8.144853	5544.556	909.9279
	1.2	-3708.935	2155.358	10.00079	5986.087	893.8197
	1.3	-3728.017	2135.216	12.02245	6469.316	882.1497
	1.4	-3741.951	2110.234	14.45796	7003.454	874.4409
1.5	-3753.028	2084.327	17.52149	7586.046	869.3630	

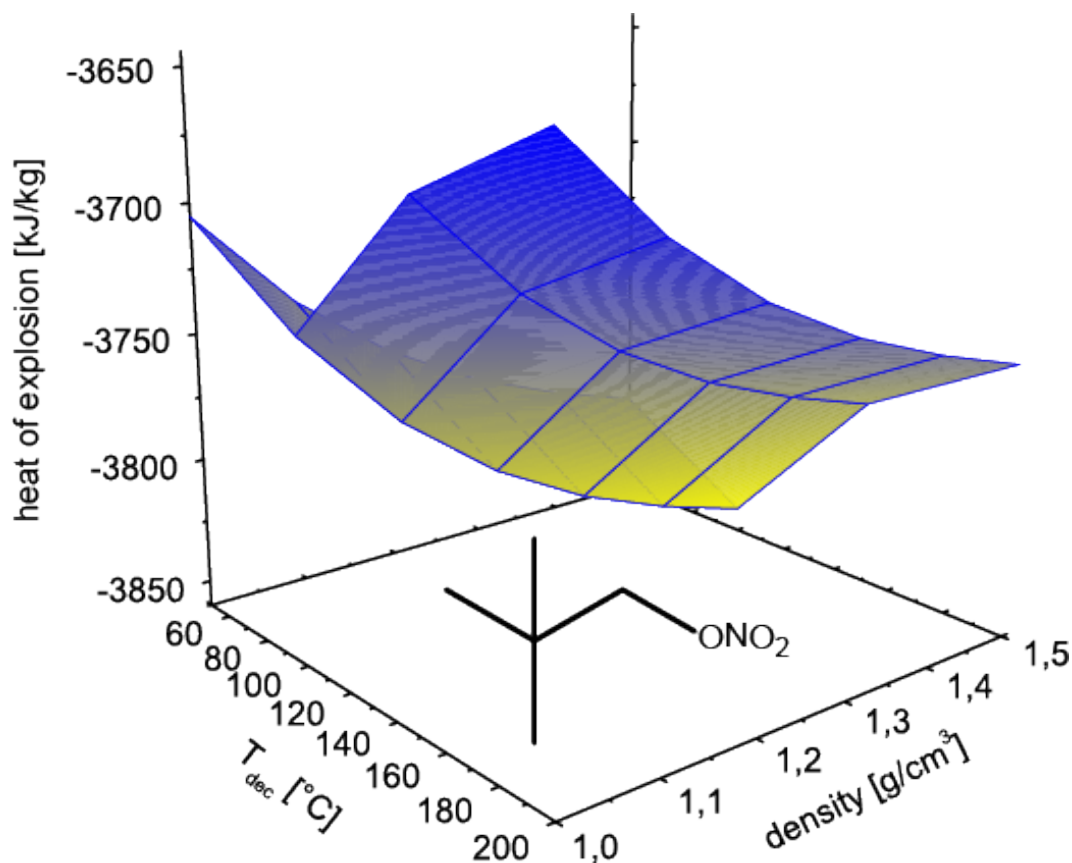
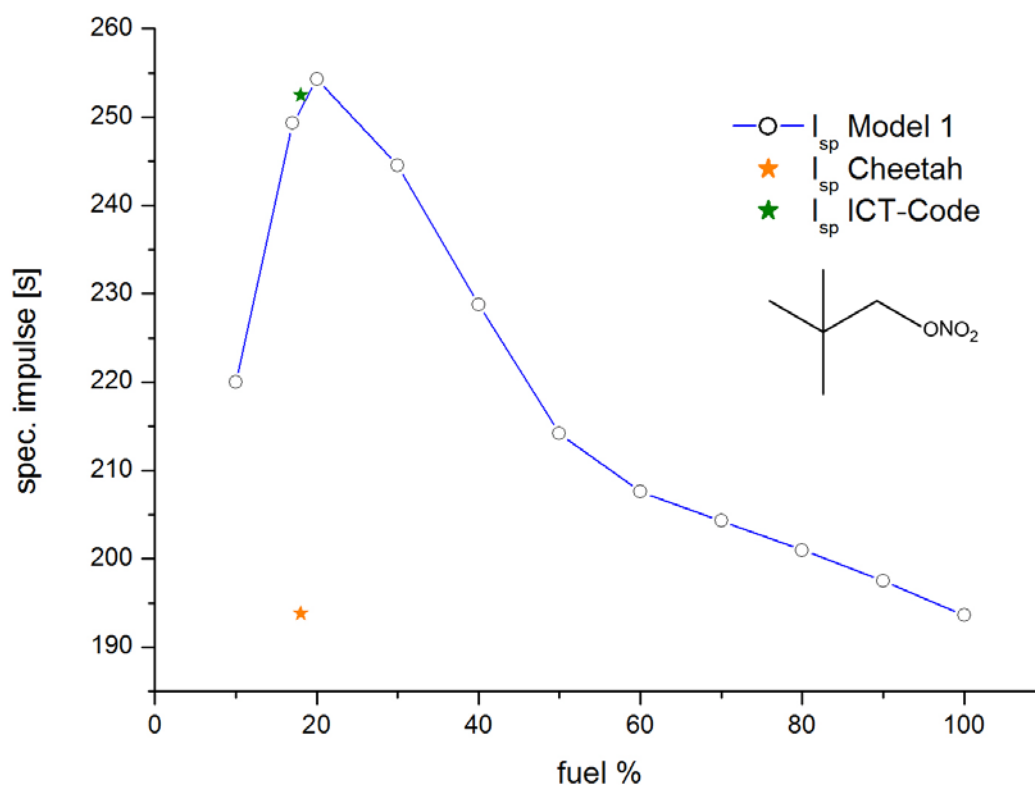
**Figure S3:** Graph of heat of explosion of 1^c in dependency to T_{dec} and density

Table S5: Propulsion parameters (T_c , I_{sp} and oxygen balance) of **1^c** computed with EXPL05 (Model 1) with AP

T_{dec} [°C]	T_c [K]	I_{sp} [s]	Oxygen balance [atm] in %	1^c / AP
100	2532.7	220.00	15.61771	10 / 90
	3028.8	254.28	-2.807043	20 / 80
	2719.4	244.52	-21.23179	30 / 70
	2190.4	228.80	-39.65654	40 / 60
	1679.0	214.21	-58.08129	50 / 50
	1374.7	207.63	-76.50602	60 / 40
	1318.8	204.30	-94.93079	70 / 30
	1290.5	200.98	-113.3555	80 / 20
	1264.0	197.54	-131.7803	90 / 10
	1238.9	193.62	-150.205	100 / 0

**Figure S4:** Specific impulse values versus different amounts of AP calculated of **1^c** with different computer codes

3. (Azidomethyl)trimethylsilane (2)

Table S6: Detonation parameter ($\Delta_{\text{ex}}U$, T_{det} , p_{CJ} , V_{det} and V_0) of **2** in dependency of T_{dec} and density

T_{dec} [°C]	density [g/cm ³]	$\Delta_{\text{ex}}U^\circ$ [kJ·kg ⁻¹]	T_{det} [K]	p_{CJ} [kbar]	V_{det} [m·s ⁻¹]	V_0 [L·kg ⁻¹]
50	1.0	-3212.035	1926.87	5.469373	4635.399	685.2399
	1.1	-3229.000	1917.042	6.697492	5014.087	664.3095
	1.2	-3244.853	1901.531	8.083555	5432.719	647.6891
	1.3	-3261.084	1884.815	9.790883	5904.353	634.8713
	1.4	-3277.639	1866.393	11.90223	6431.465	625.3456
1.5	-3292.469	1847.797	14.62634	7004.545	617.9815	
100	1.0	-3181.070	1915.688	5.443464	4624.406	684.1684
	1.1	-3197.332	1906.751	6.68541	5002.688	663.2688
	1.2	-3212.807	1890.591	8.052132	5420.930	646.9203
	1.3	-3228.771	1871.631	9.68405	5892.233	634.4371
	1.4	-3245.022	1852.545	11.75076	6419.067	625.0180
1.5	-3259.536	1837.006	14.57109	6991.998	617.6323	
150	1.0	-3150.081	1904.478	5.417492	4613.361	683.1016
	1.1	-3166.020	1893.652	6.616944	4991.128	662.6533
	1.2	-3180.778	1879.161	8.01421	5408.830	646.1777
	1.3	-3196.297	1860.656	9.644089	5880.063	633.8369
	1.4	-3212.305	1841.517	11.7084	6406.259	624.5268
1.5	-3226.587	1826.083	14.51604	6979.208	617.2827	
200	1.0	-3119.379	1891.385	5.362605	4602.042	682.3291
	1.1	-3134.283	1883.624	6.612127	4979.539	661.5535
	1.2	-3148.724	1867.453	7.963302	5396.975	645.5172
	1.3	-3163.864	1849.356	9.602858	5867.480	633.2217
	1.4	-3179.516	1830.412	11.66061	6393.514	624.0606
1.5	-3193.607	1815.258	14.46445	6966.364	616.9290	

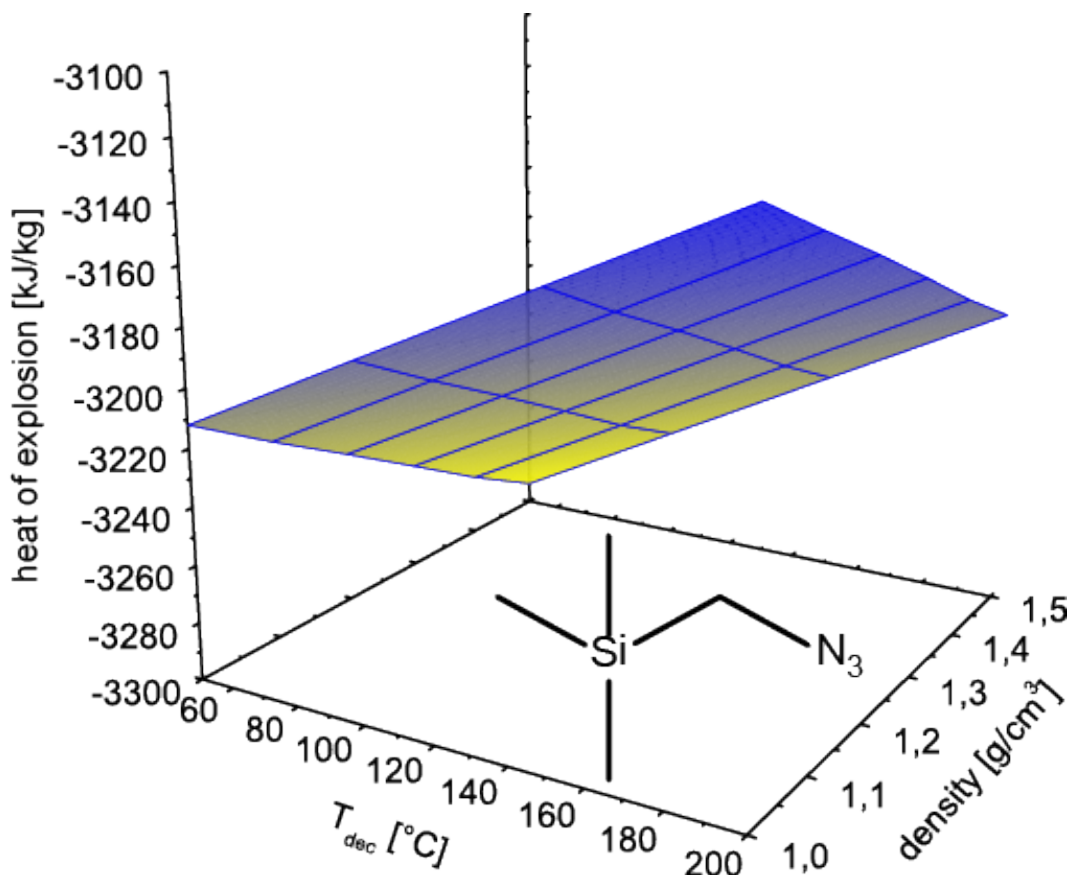
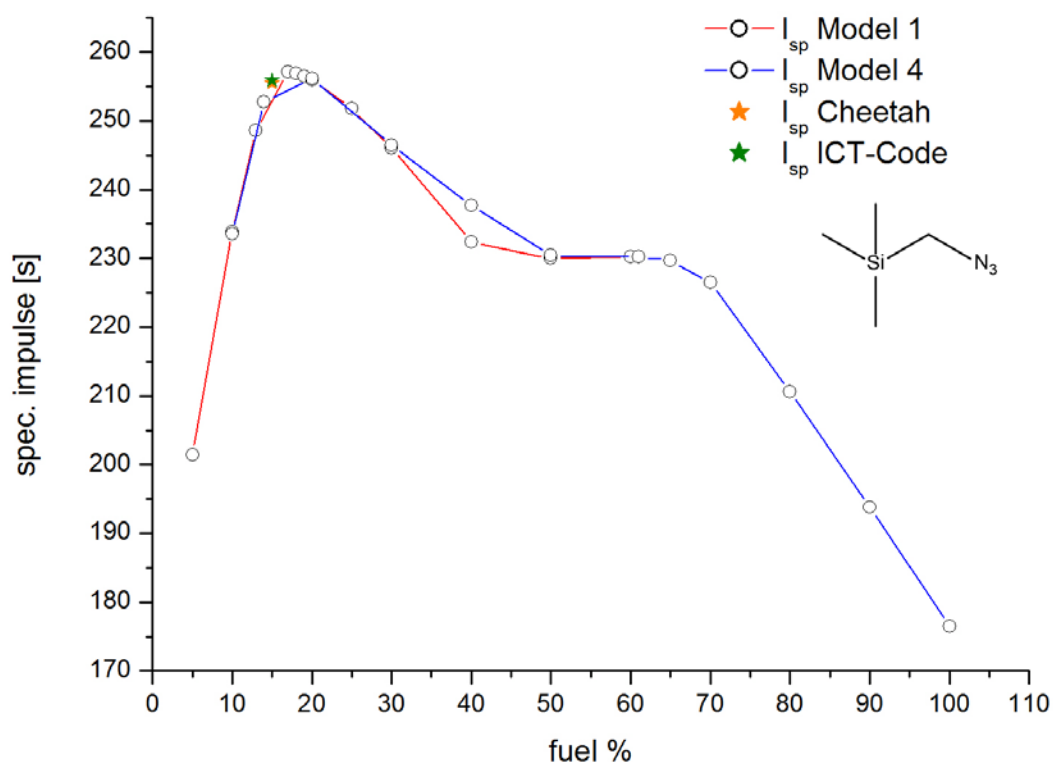
**Figure S5:** Graph of heat of explosion of **2** in dependency to T_{dec} and density

Table S7: Propulsion parameters (T_c , I_{sp} and oxygen balance) of **2** computed with EXPLO5 (Model 1) with AP

T_{dec} [°C]	T_c [K]	I_{sp} [s]	Oxygen balance [atm] in %	2 / AP
100	1327	176.5	-191.882	100 / 0
	2821	233.6	11.45001	10 / 90
	3127	252.8	2.413026	14 / 86
	3119	256.2	-11.14244	20 / 80
	2694	246.5	-33.73489	30 / 70
	2226	237.7	-56.32734	40 / 60
	2090	230.4	-78.91978	50 / 50
	2025	230.2	-103.7715	61 / 39
	1983	229.7	-112.8085	65 / 35
	1920	226.5	-124.1047	70 / 30
	1744	210.6	-146.6971	80 / 20
	1518	193.8	-169.2896	90 / 10

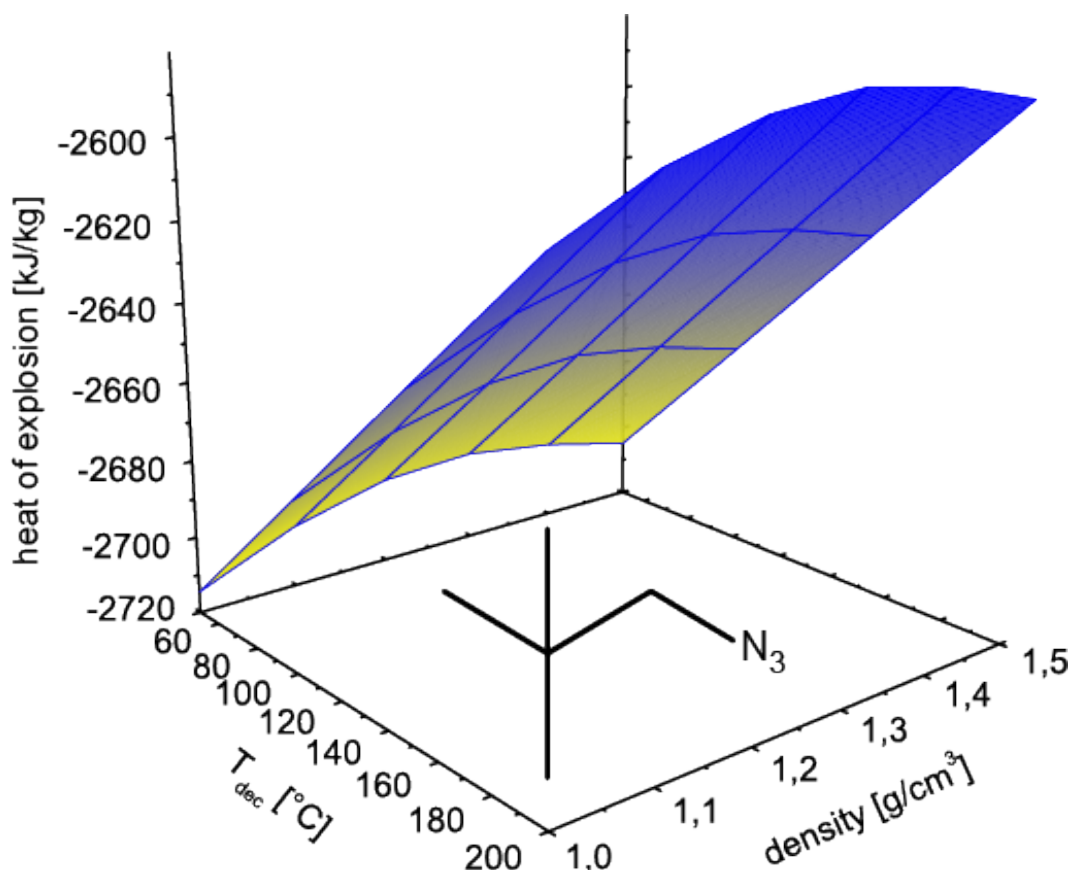
Table S8: Propulsion parameters (T_c , I_{sp} and oxygen balance) of **2** computed with EXPLO5 (Model 4) with AP

T_{dec} [°C]	T_c [K]	I_{sp} [s]	Oxygen balance [atm] in %	2 / AP
100	2213	201.5	22.74623	5 / 95
	2828	233.8	11.45001	10 / 90
	3097	248.6	4.672271	13 / 87
	3174	257.2	-4.364708	17 / 83
	3173	256.9	-6.623952	18 / 82
	3163	256.5	-8.883196	19 / 81
	3143	255.9	-11.14244	20 / 80
	2962	251.8	-22.43867	25 / 75
	2725	246.0	-33.73489	30 / 70
	2252	232.4	-56.32734	40 / 60
	2132	230.0	-78.91978	50 / 50
	2090	230.3	-101.5122	60 / 40

**Figure S6:** Specific impulse values versus different amounts of AP calculated of **2** with different computer codes

4. 1-Azido-2,2-dimethylpropane (2^c)**Table S9:** Detonation parameter ($\Delta_{\text{ex}}U$, T_{det} , p_{CJ} , V_{det} and V_0) of 2^c in dependency of T_{dec} and density

T_{dec} [°C]	density [g/cm ³]	$\Delta_{\text{ex}}U^\circ$ [kJ·kg ⁻¹]	T_{det} [K]	p_{CJ} [kbar]	V_{det} [m·s ⁻¹]	V_0 [L·kg ⁻¹]
50	1.0	-2714.503	1672.897	7.213625	5383.795	826.4415
	1.1	-2703.933	1651.466	8.757018	5806.551	802.4953
	1.2	-2697.510	1622.944	10.44672	6288.547	785.1631
	1.3	-2696.105	1589.381	12.38975	6852.030	773.8521
	1.4	-2699.236	1557.329	14.92453	7509.980	767.3096
1.5	-2704.864	1532.402	18.56689	8245.302	763.6699	
100	1.0	-2677.126	1660.248	7.171792	5368.162	825.6667
	1.1	-2666.581	1636.559	8.656734	5789.711	802.2217
	1.2	-2659.929	1606.257	10.27291	6270.866	785.1512
	1.3	-2657.710	1574.261	12.22865	6833.754	773.6462
	1.4	-2660.349	1545.131	14.84927	7491.020	767.0261
1.5	-2665.917	1516.265	18.26468	8225.700	763.4908	
150	1.0	-2639.733	1647.619	7.129661	5352.502	824.9022
	1.1	-2628.569	1624.008	8.607354	5773.175	801.6035
	1.2	-2621.520	1593.471	10.21426	6252.938	784.6436
	1.3	-2618.940	1562.352	12.17925	6815.382	773.2322
	1.4	-2621.435	1533.136	14.77496	7472.254	766.7505
1.5	-2626.871	1504.361	18.17694	8205.918	763.2880	
200	1.0	-2602.708	1633.760	7.068012	5336.497	824.3434
	1.1	-2590.595	1611.138	8.553533	5756.335	801.0128
	1.2	-2583.214	1580.24	10.13661	6235.296	784.2385
	1.3	-2580.272	1549.239	12.09459	6796.563	772.8837
	1.4	-2582.554	1520.378	14.68465	7452.622	766.4735
1.5	-2587.806	1492.415	18.08847	8185.926	763.0887	

**Figure S7:** Graph of heat of explosion of 2^c in dependency to T_{dec} and density

5. (Nitromethyl)trimethylsilane (3)

Table S11: Detonation parameter ($\Delta_{\text{ex}}U$, T_{det} , p_{Cl} , V_{det} and V_0) of **3** in dependency of T_{dec} and density

T_{dec} [°C]	density [g/cm ³]	$\Delta_{\text{ex}}U^\circ$ [kJ·kg ⁻¹]	T_{det} [K]	p_{Cl} [kbar]	V_{det} [m·s ⁻¹]	V_0 [L·kg ⁻¹]
50	1.0	-4809.745	2496.136	6.684980	5188.783	690.4351
	1.1	-4854.194	2486.478	8.414590	5661.070	663.0180
	1.2	-4894.190	2474.450	10.45244	6173.049	639.0287
	1.3	-4919.660	2457.861	13.15273	6719.829	617.6514
	1.4	-4924.349	2429.785	16.38670	7291.763	600.7849
1.5	-4896.457	2391.000	20.35979	7880.988	588.5481	
100	1.0	-4782.684	2486.779	6.665058	5181.045	689.2043
	1.1	-4827.061	2480.075	8.391241	5653.211	661.9019
	1.2	-4866.769	2465.311	10.42721	6165.431	638.0964
	1.3	-4892.147	2448.883	13.12462	6712.645	616.9193
	1.4	-4896.530	2421.402	16.36941	7285.291	600.2166
1.5	-4869.339	2382.439	20.33404	7875.029	588.1137	
150	1.0	-4755.807	2477.152	6.644516	5173.055	687.9322
	1.1	-4800.737	2467.589	8.289252	5645.197	661.3295
	1.2	-4839.323	2456.146	10.40134	6157.781	637.1688
	1.3	-4866.269	2437.361	12.99383	6705.298	616.5284
	1.4	-4807.062	2411.727	16.29768	7278.537	599.7311
1.5	-4842.306	2373.949	20.29889	7869.193	587.6995	
200	1.0	-4729.563	2463.938	6.547935	5165.291	687.4155
	1.1	-4773.469	2458.267	8.266134	5637.320	660.2229
	1.2	-4811.762	2447.100	10.37576	6150.204	636.2548
	1.3	-4838.640	2428.416	12.97312	6697.890	615.7583
	1.4	-4843.742	2401.86	16.21621	7271.747	599.2632
1.5	-4815.334	2365.358	20.26428	7863.280	587.2905	

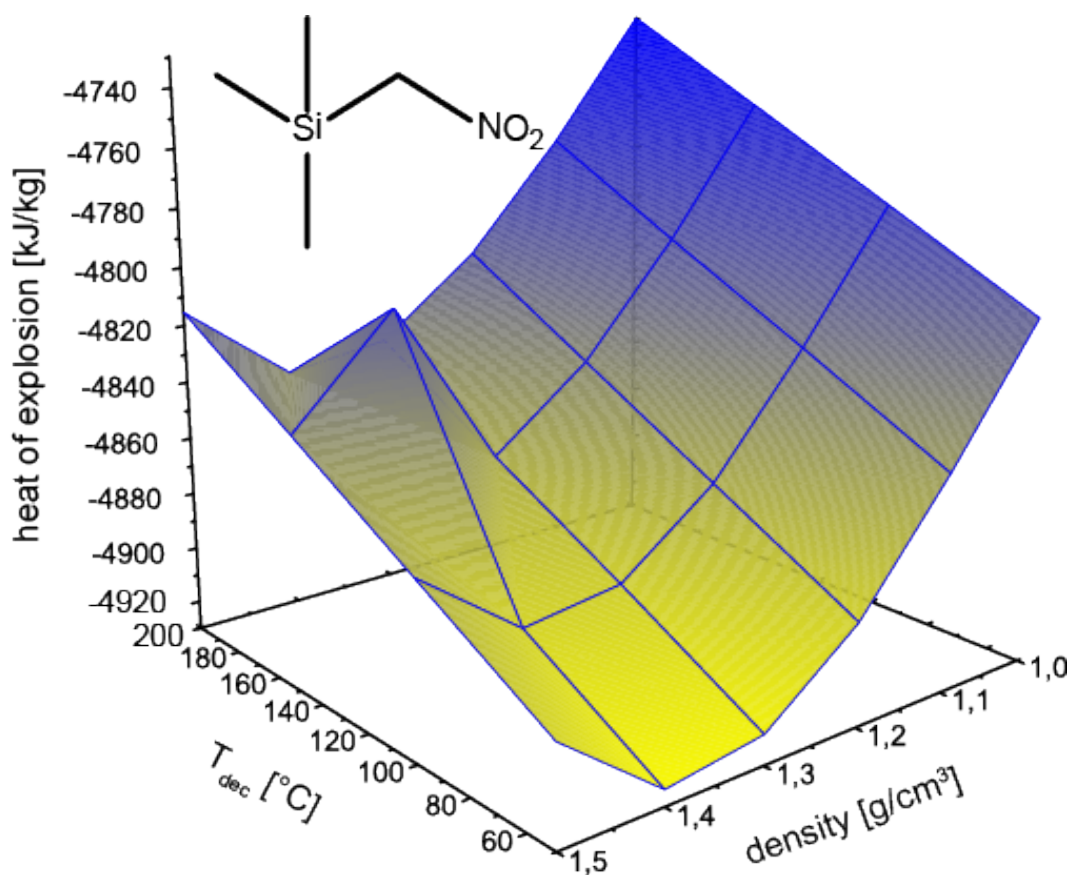
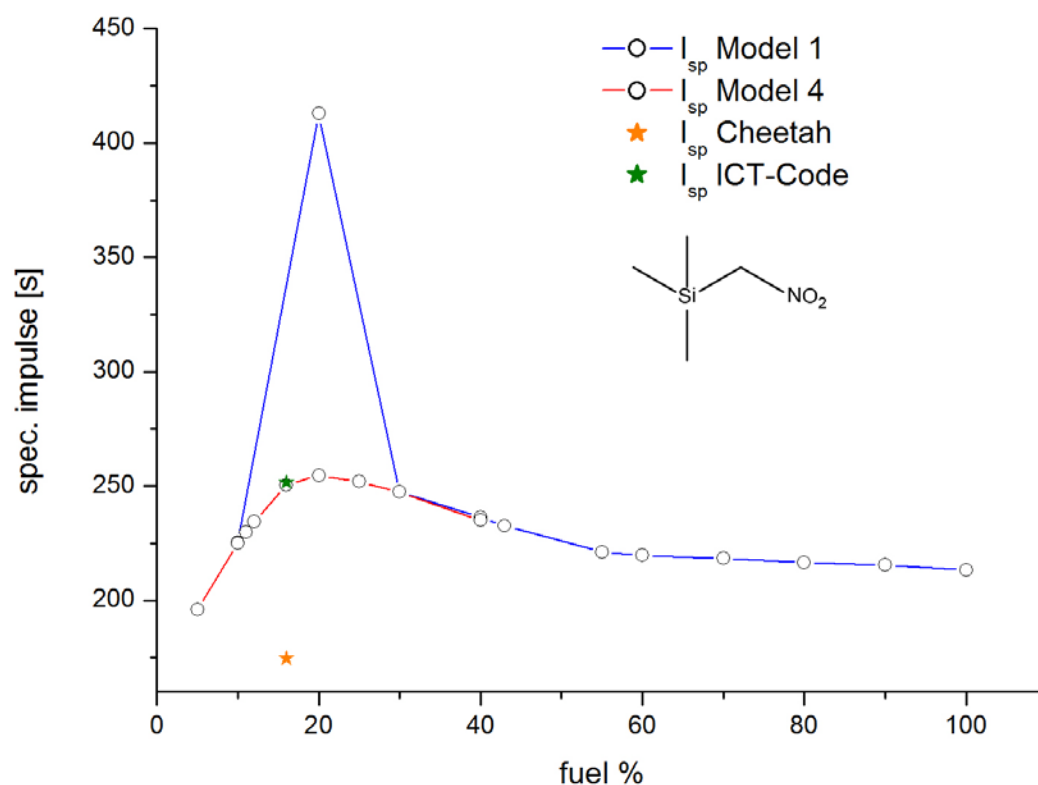
**Figure S9:** Graph of heat of explosion of **3** in dependency to T_{dec} and density

Table S12: Propulsion parameters (T_c , I_{sp} and oxygen balance) of **3** computed with EXPL05 (Model 1) with AP

T_{dec} [°C]	T_c [K]	I_{sp} [s]	Oxygen balance [atm] in %	3 / AP
100	2671.1	225.17	14.42544	10 / 90
	3101.0	250.50	2.655234	16 / 84
	3112.1	412.86	-5.19157	20 / 80
	2825.4	247.46	-24.80858	30 / 70
	2421.8	236.27	-44.42559	40 / 60
	2289.5	232.64	-50.3107	43 / 57
	1870.3	221.04	-73.85112	55 / 45
	1866.4	219.69	-83.65962	60 / 40
	1860.5	218.38	-103.2766	70 / 30
	1855.3	216.61	-122.8937	80 / 20
	1850.6	215.36	-142.5107	90 / 10
	1796.8	213.14	-162.1277	100 / 0

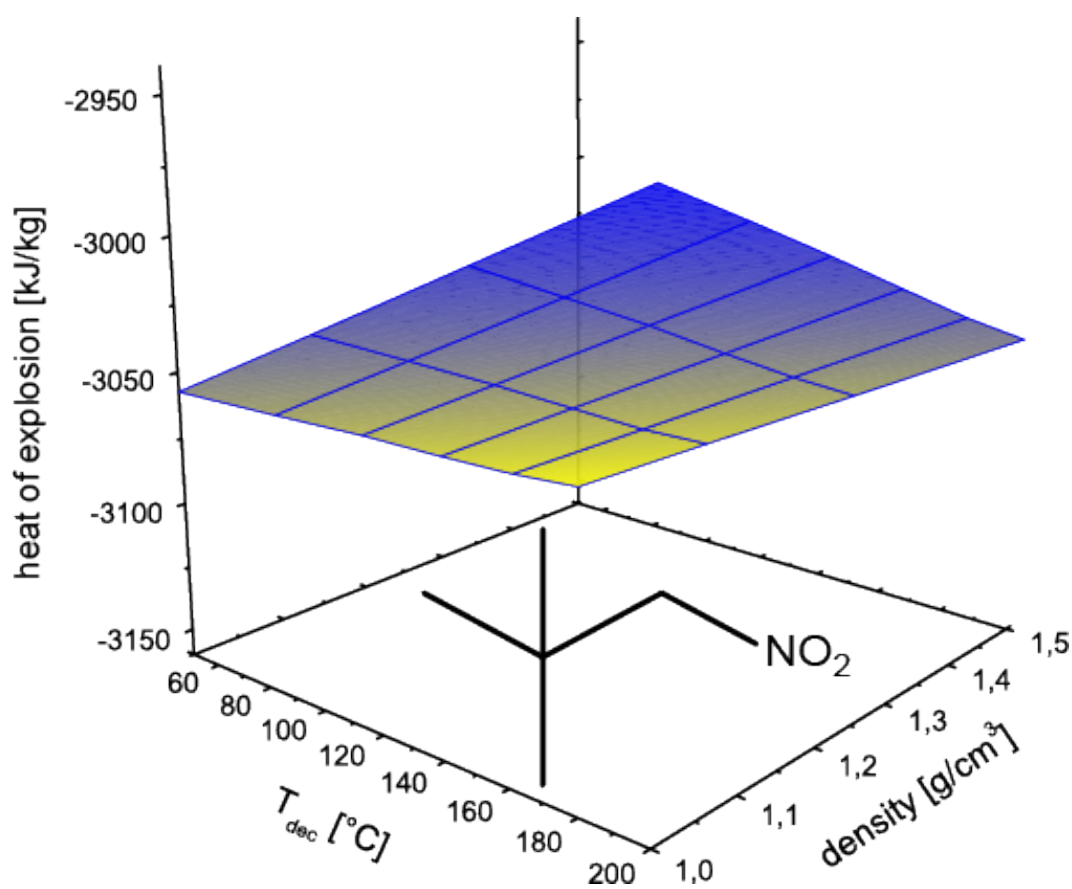
Table S13: Propulsion parameters (T_c , I_{sp} and oxygen balance) of **3** computed with EXPL05 (Model 4) with AP

T_{dec} [°C]	T_c [K]	I_{sp} [s]	Oxygen balance [atm] in %	3 / AP
100	2109.5	195.98	24.23395	5 / 95
	2668.3	225.06	14.42544	10 / 90
	2760.0	230.00	12.46374	11 / 89
	2845.0	234.30	10.50204	12 / 88
	3146.0	254.80	-5.19157	20 / 80
	3055.1	251.89	-15.00008	25 / 75
	2865.3	247.34	-24.80858	30 / 70
	2421.8	235.07	-44.42559	40 / 60

**Figure S10:** Specific impulse values versus different amounts of AP calculated of **3** with different computer codes

6. 2.2-Dimethyl-1-nitropropane (3^c)**Table S14:** Detonation parameter ($\Delta_{\text{ex}}U$, T_{det} , p_{Cl} , V_{det} and V_0) of 3^c in dependency of T_{dec} and density

T_{dec} [°C]	density [g/cm ³]	$\Delta_{\text{ex}}U^\circ$ [kJ·kg ⁻¹]	T_{det} [K]	p_{Cl} [kbar]	V_{det} [m·s ⁻¹]	V_0 [L·kg ⁻¹]
50	1.0	-3057.299	1826.578	6.556330	5259.490	909.1172
	1.1	-3076.359	1811.785	8.088911	5754.658	894.7487
	1.2	-3095.281	1797.436	10.04974	6310.754	883.9421
	1.3	-3115.076	1781.545	12.50967	6922.992	875.3912
	1.4	-3134.378	1768.038	15.75366	7578.803	867.7184
1.5	-3152.062	1747.934	19.59596	8270.752	860.5371	
100	1.0	-3022.867	1814.37	6.521162	5245.365	907.8935
	1.1	-3041.433	1799.631	8.047442	5739.888	893.6717
	1.2	-3059.954	1785.577	10.00159	6259.618	883.0089
	1.3	-3079.426	1769.867	12.45297	6907.284	874.5883
	1.4	-3098.450	1756.568	15.68643	7562.613	867.0410
1.5	-3115.773	1737.676	19.56539	8254.156	859.9936	
150	1.0	-2988.336	1802.415	6.486740	5231.481	906.6975
	1.1	-3006.450	1787.745	8.006809	5725.379	892.6092
	1.2	-3024.612	1773.688	9.953199	6280.368	882.0786
	1.3	-3043.781	1758.157	12.39592	6891.442	873.7795
	1.4	-3062.461	1745.104	15.61906	7546.357	866.3817
1.5	-3079.874	1722.032	19.27254	8237.254	859.5007	
200	1.0	-2953.912	1790.124	6.451223	5217.162	905.4670
	1.1	-2971.464	1775.683	7.965512	5710.595	891.5465
	1.2	-2989.537	1758.757	9.819589	6265.080	881.1758
	1.3	-3008.112	1746.287	12.33496	6875.447	872.9791
	1.4	-3026.585	1732.53	15.50980	7529.769	865.7032
1.5	-3043.605	1710.733	19.19305	8220.248	858.9715	

**Figure S11:** Graph of heat of explosion of 3^c in dependency to T_{dec} and density

7. (E)-(2-Nitrovinyl)trimethylsilane (4)

Table S16: Detonation parameter ($\Delta_{\text{ex}}U$, T_{det} , p_{Cl} , V_{det} and V_0) of 4 in dependency of T_{dec} and density

T_{dec} [°C]	density [g/cm ³]	$\Delta_{\text{ex}}U^\circ$ [kJ·kg ⁻¹]	T_{det} [K]	p_{Cl} [kbar]	V_{det} [m·s ⁻¹]	V_0 [L·kg ⁻¹]
50	1.0	-5036.388	2613.815	6.255987	5008.981	659.6226
	1.1	-5080.407	2606.947	7.836051	5462.429	632.5917
	1.2	-5120.853	2594.907	9.754629	5954.721	607.5617
	1.3	-5150.946	2581.164	12.27678	6484.089	584.1964
	1.4	-5164.842	2555.329	15.24636	7041.699	564.8605
1.5	-5148.485	2520.398	18.97596	7620.235	549.8001	
100	1.0	-5011.492	2604.979	6.239705	5002.137	658.5135
	1.1	-5055.411	2598.116	7.816329	5455.528	631.5881
	1.2	-5095.746	2586.285	9.732494	5947.961	606.6656
	1.3	-5126.197	2571.844	12.22150	6477.576	583.6024
	1.4	-5139.622	2547.151	15.22009	7035.828	564.2882
1.5	-5123.466	2512.336	18.94979	7614.979	549.3793	
150	1.0	-4962.116	2596.099	6.222857	4995.257	657.4103
	1.1	-5030.450	2589.416	7.796676	5448.665	630.5522
	1.2	-5070.607	2577.548	9.710148	5941.128	605.7876
	1.3	-5101.036	2563.386	12.19704	6471.091	582.8463
	1.4	-5114.266	2538.933	15.19555	7029.957	563.7478
1.5	-5098.787	2504.05	18.9096	7609.688	548.9791	
200	1.0	-4962.419	2584.861	6.161718	4988.369	656.7926
	1.1	-5005.350	2580.488	7.770629	5441.866	7.311259
	1.2	-5045.435	2568.953	9.688007	5934.352	604.8975
	1.3	-5075.767	2554.84	12.17258	6464.598	582.1323
	1.4	-5089.482	2530.188	15.15101	7023.870	563.2106
1.5	-5075.789	2494.717	18.80191	7604.355	548.6776	

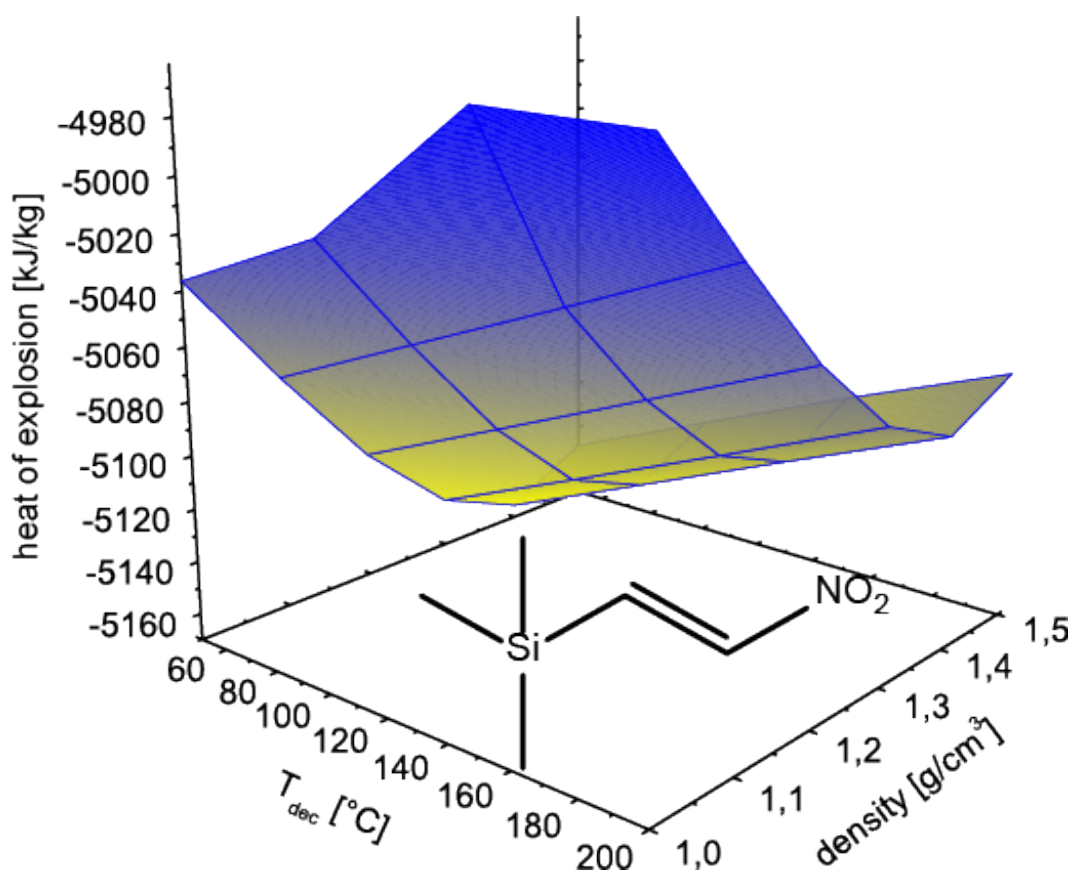
Figure S13: Graph of heat of explosion of 4 in dependency to T_{dec} and density

Table S19: Propulsion parameters (T_c , I_{sp} and oxygen balance) of **4** computed with EXPL05 (Model 1) with ammonium dinitramide (ADN)

T_{dec} [°C]	T_c [K]	I_{sp} [s]	Oxygen balance [atm] in %	4 / ADN
100	2620	232.8	15.96509	5 / 95
	2997	419.7	6.137828	10 / 90
	3013	255.5	6.137828	10 / 90
	3099	262.7	2.106923	12 / 88
	3149	266.5	-3.689443	15 / 85
	3067	263.2	-13.5167	20 / 80
	2908	258.4	-23.34397	25 / 75
	2718	252.7	-33.17124	30 / 70
	2324	238.9	-52.82576	40 / 60
	1979	229.1	-72.48029	50 / 50
	1985	226.5	-92.13483	60 / 40
	1990	224.4	-111.7894	70 / 30
	1993	222.0	-131.4439	80 / 20
	1989	219.4	-151.0984	90 / 10

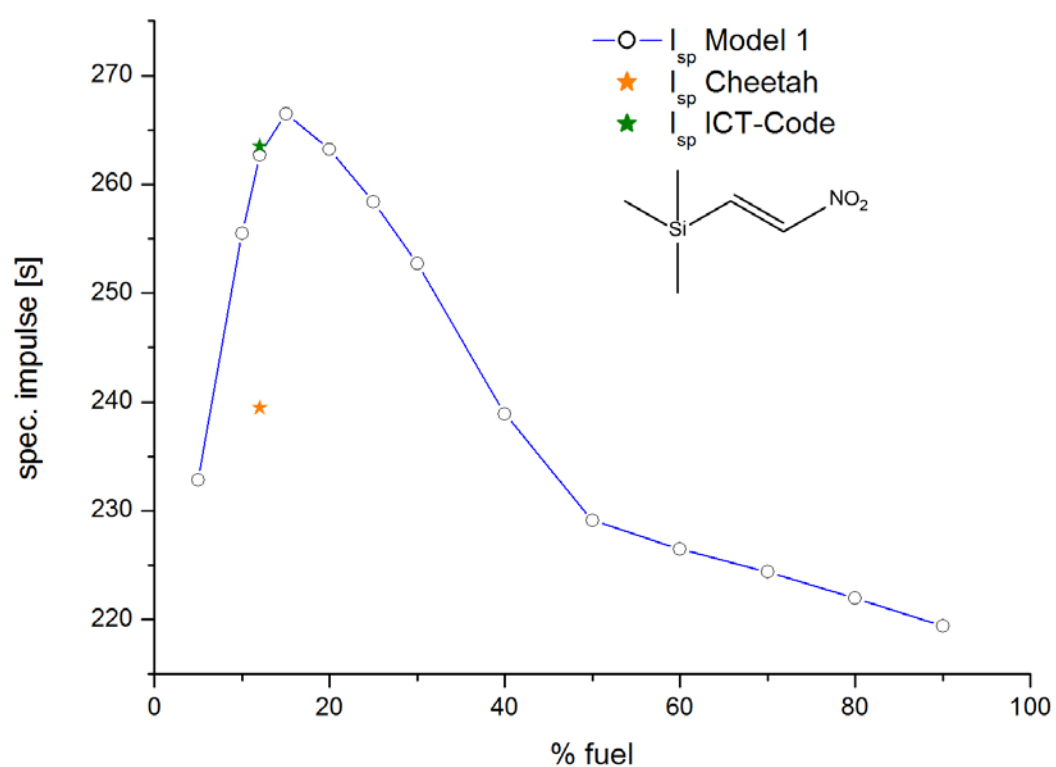
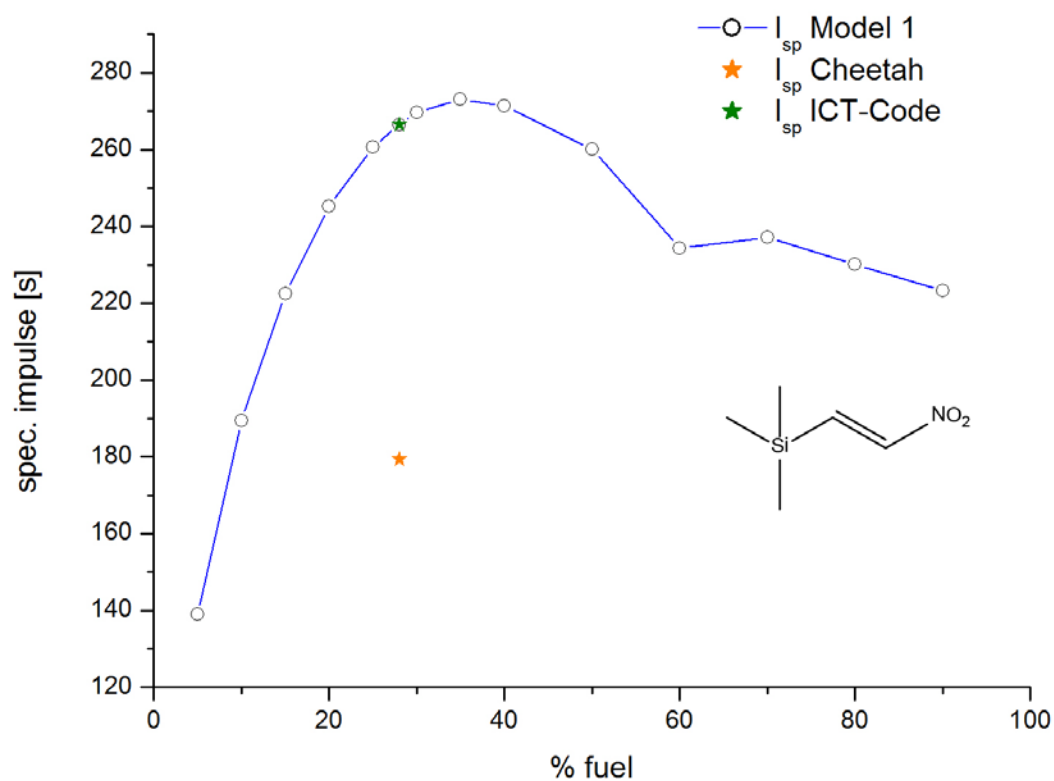
**Figure S15:** Specific impulse values versus different amounts of ADN calculated of **4** with different computer codes

Table S20: Propulsion parameters (T_c , I_{sp} and oxygen balance) of **4** computed with EXPL05 (Model 1) with nitrogen tetroxide (N_2O_4)

T_{dec} [°C]	T_c [K]	I_{sp} [s]	Oxygen balance [atm] in %	4 / N_2O_4
100	1324	138.9	57.53656	5 / 95
	2263	189.4	45.52132	10 / 90
	2914	222.4	33.50608	15 / 85
	3268	245.1	21.49085	20 / 80
	3405	402.6	9.475603	25 / 75
	3435	260.6	9.475603	25 / 75
	3468	266.5	2.266463	28 / 72
	3473	269.6	-2.539627	30 / 70
	3400	273.0	-14.55486	35 / 65
	3239	271.3	-26.57011	40 / 60
	2811	260.2	-50.60058	50 / 50
	2112	234.4	-74.63105	60 / 40
	2159	237.1	-98.66153	70 / 30
	2111	230.2	-122.692	80 / 20
	2036	223.2	-146.7225	90 / 10

**Figure S16:** Specific impulse values versus different amounts of N_2O_4 calculated of **4** with different computer codes

8. (E)-3,3-Dimethyl-1-nitrobut-2-ene (4^c)Table S21: Detonation parameter ($\Delta_{\text{ex}}U$, T_{det} , p_{CJ} , V_{det} and V_0) of 4^c in dependency of T_{dec} and density

T_{dec} [°C]	density [g/cm ³]	$\Delta_{\text{ex}}U^{\circ}$ [kJ·kg ⁻¹]	T_{det} [K]	p_{CJ} [kbar]	V_{det} [m·s ⁻¹]	V_0 [L·kg ⁻¹]
50	1.0	-3422.502	1985.378	6.265391	5110.718	847.7492
	1.1	-3446.648	1977.708	7.824596	5581.407	831.0560
	1.2	-3468.283	1961.331	9.607153	6108.433	818.3571
	1.3	-3489.406	1945.659	11.94083	6695.812	808.3416
	1.4	-3510.649	1927.891	14.86832	7334.163	799.6210
1.5	-3530.759	1909.231	18.60737	8011.957	791.2239	
100	1.0	-3391.458	1974.211	6.236392	5098.877	846.6405
	1.1	-3415.050	1966.706	7.790931	5569.387	830.0790
	1.2	-3436.371	1950.303	9.567838	6095.921	817.4861
	1.3	-3457.167	1934.938	11.89344	6683.260	807.6008
	1.4	-3478.244	1917.345	14.81559	7321.145	798.0618
1.5	-3498.243	1898.011	18.5034	7998.604	790.6822	
150	1.0	-3360.328	1963.419	6.210557	5087.249	845.5271
	1.1	-3383.534	1954.666	7.734657	5557.259	829.1667
	1.2	-3404.400	1939.436	9.529027	6083.544	816.6311
	1.3	-3424.969	1924.186	11.84811	6670.512	806.8414
	1.4	-3445.822	1906.779	14.76261	7308.044	798.3065
1.5	-3465.540	1888.548	18.48217	7985.32	790.1292	
200	1.0	-3329.286	1952.028	6.178759	5075.262	844.4191
	1.1	-3351.889	1943.609	7.700880	5545.087	828.2008
	1.2	-3372.443	1928.507	9.489914	6071.046	815.7693
	1.3	-3392.957	1910.710	11.71273	6657.679	806.1097
	1.4	-3413.355	1896.872	14.73098	7295.056	797.6434
1.5	-3432.975	1877.245	18.37791	7971.705	789.5982	

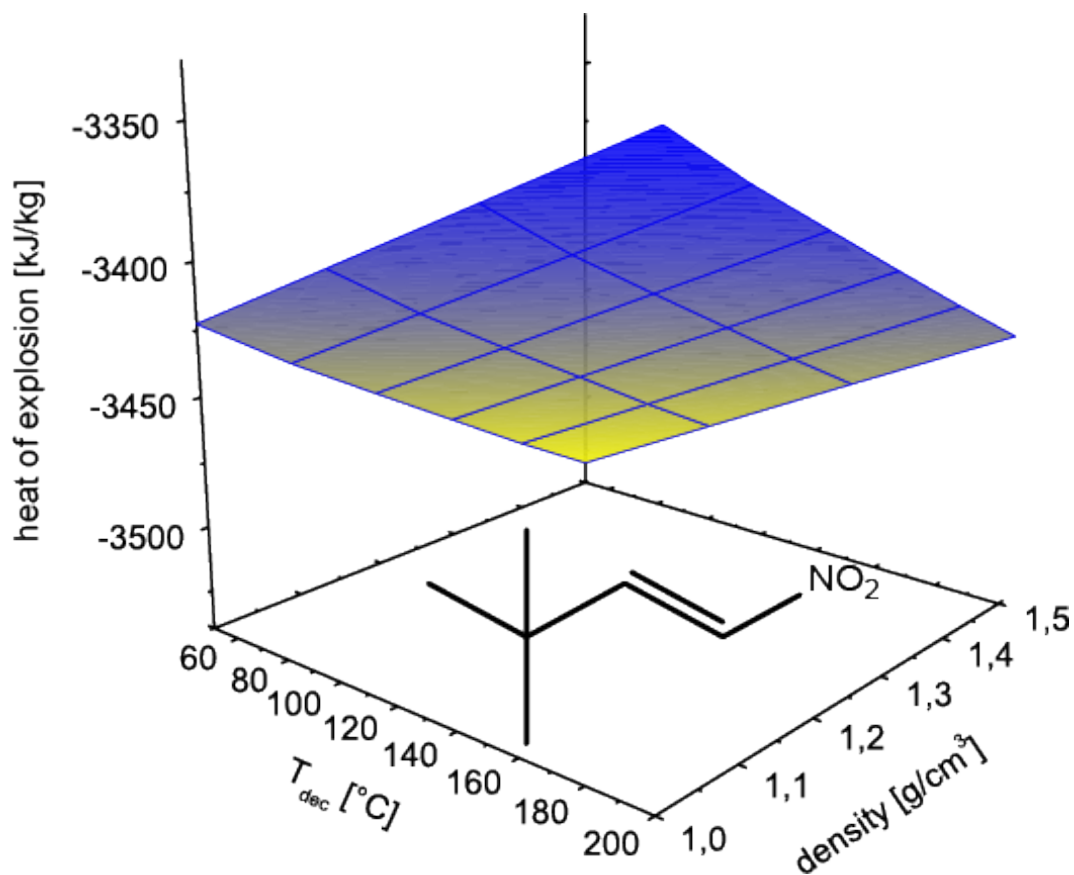
Figure S17: Graph of heat of explosion of 4^c in dependency to T_{dec} and density

Table S22: Propulsion parameters (T_c , I_{sp} and oxygen balance) of 4^c computed with EXPL05 (Model 1) with AP

T_{dec} [°C]	T_c [K]	I_{sp} [s]	Oxygen balance [atm] in %	4^c / AP
100	2734.1	230.71	11.43753	10 / 90
	2993.0	249.70	2.39556	14 / 86
	2985.9	250.97	-11.1674	20 / 80
	2402.5	233.86	-33.772332	30 / 70
	1756.8	214.49	-56.37725	40 / 60
	1389.7	206.72	-78.98219	50 / 50
	1349.9	202.39	-101.5871	60 / 40
	1315.4	198.07	-124.192	70 / 30
	1283.4	193.61	-146.797	80 / 20
	1252.7	188.98	-169.4019	90 / 10
	1222.5	183.74	-192.0068	100 / 0

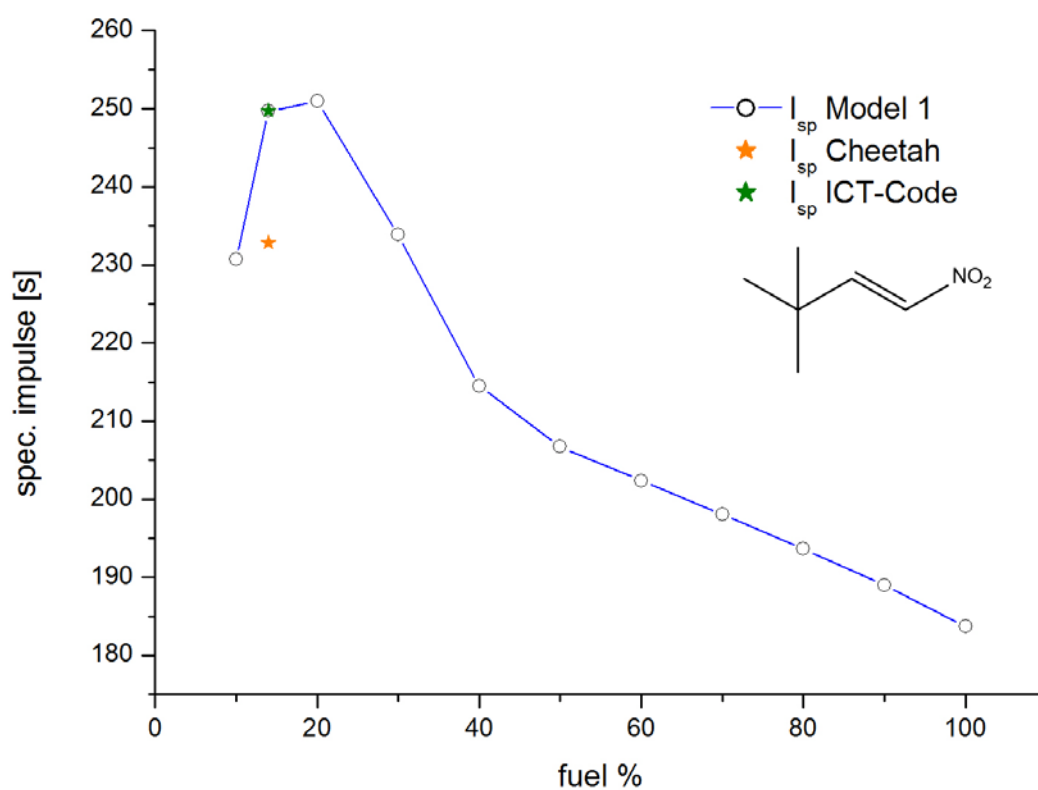
**Figure S18:** Specific impulse values versus different amounts of AP calculated of 4^c with different computer codes

Table S23: Propulsion parameters (T_c , I_{sp} and oxygen balance) of 4^c computed with EXPL05 (Model 1) with ADN

T_{dec} [°C]	T_c [K]	I_{sp} [s]	Oxygen balance [atm] in %	4^c / ADN
100	2622	234.1	14.9024	5 / 95
	2986	258.1	4.012443	10 / 90
	3026	262.1	1.834449	11 / 89
	3063	263.5	-6.877516	15 / 85
	2874	256.8	-17.76748	20 / 80
	2589	248.0	-28.65743	25 / 75
	2288	237.9	-39.54739	30 / 70
	1696	219.2	-61.32731	40 / 60
	1397	211.1	-83.10722	50 / 50
	1357	205.9	-104.8871	60 / 40
	1320	200.5	-126.6671	70 / 30
	1286	195.1	-148.447	80 / 20
	1254	189.6	-170.2269	90 / 10

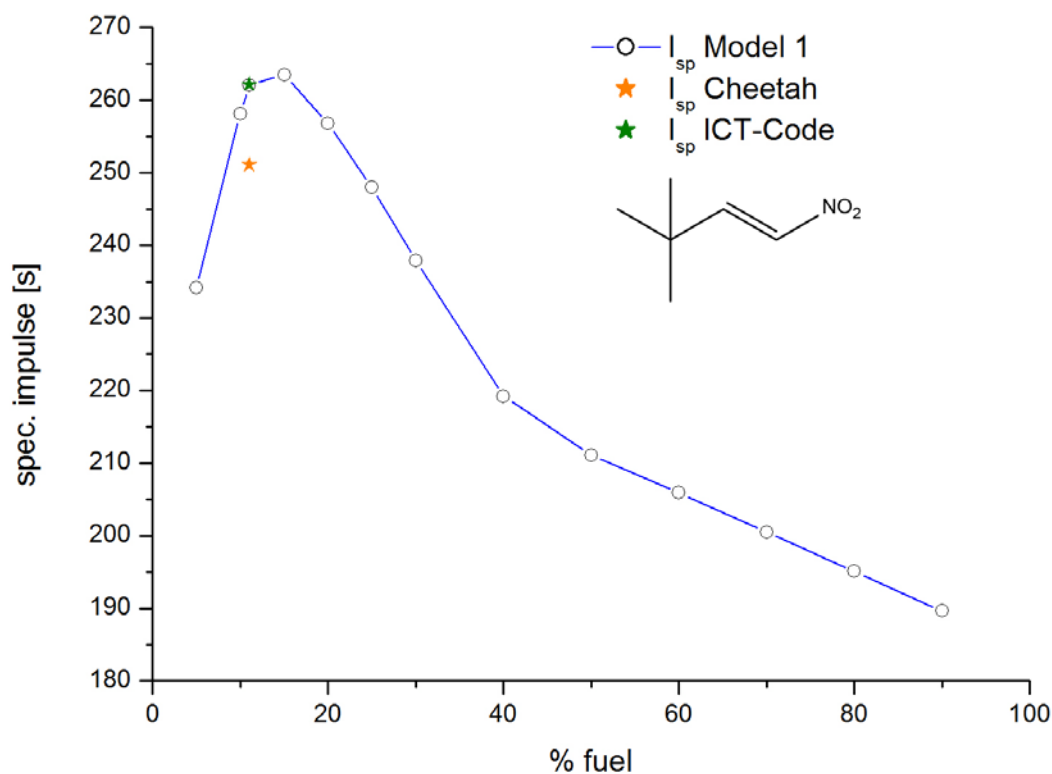
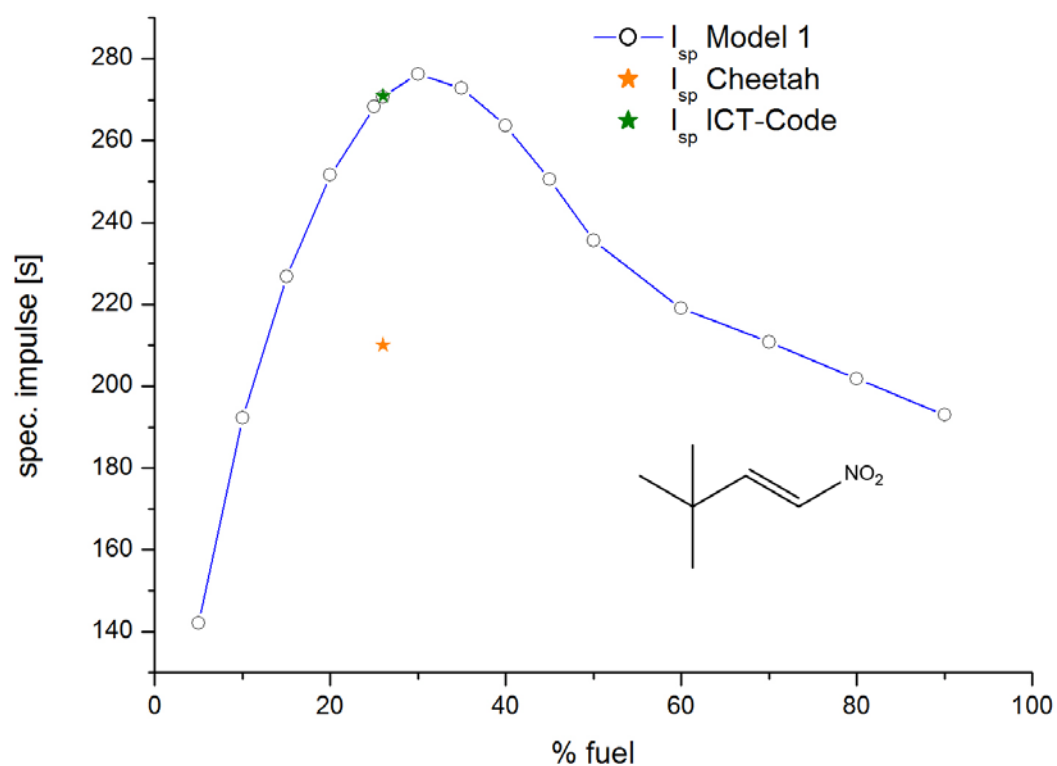
**Figure S19:** Specific impulse values versus different amounts of ADN calculated of 4^c with different computer codes

Table S24: Propulsion parameters (T_c , I_{sp} and oxygen balance) of **4^c** computed with EXPL05 (Model 1) with N_2O_4

T_{dec} [°C]	T_c [K]	I_{sp} [s]	Oxygen balance [atm] in %	4^c / N_2O_4
100	1341	142.2	56.47387	5 / 95
	2279	192.2	43.39594	10 / 90
	2915	226.8	30.018	15 / 85
	3250	251.6	17.24007	20 / 80
	3418	268.3	4.162143	25 / 75
	3438	270.7	1.546549	26 / 74
	3472	276.3	-8.915784	30 / 70
	3378	272.8	-21.99372	35 / 65
	3083	263.6	-35.07165	40 / 60
	2669	250.6	-48.14958	45 / 55
	2232	235.6	-61.2275	50 / 50
	1586	219.0	-87.38337	60 / 40
	1449	210.8	-113.5392	70 / 30
	1360	201.8	-139.6951	80 / 20
	1288	193.0	-165.8509	90 / 10

**Figure S20:** Specific impulse values versus different amounts of N_2O_4 calculated of **4^c** with different computer codes

9. 1-((Trimethylsilyl)methyl)-1H-1.2.4-triazole (5a)

Table S25: Detonation parameter ($\Delta_{\text{ex}}U$, T_{det} , p_{CJ} , V_{det} and V_0) of 5a in dependency of T_{det} and density

T_{det} [°C]	density [g/cm ³]	$\Delta_{\text{ex}}U^\circ$ [kJ·kg ⁻¹]	T_{det} [K]	p_{CJ} [kbar]	V_{det} [m·s ⁻¹]	V_0 [L·kg ⁻¹]
50	1.0	-2111.706	1481.138	4.223193	4197.194	623.6306
	1.1	-2110.387	1472.375	5.285031	4589.61	609.5233
	1.2	-2111.767	1457.738	6.472395	5029.817	599.1839
	1.3	-2116.1	1447.783	8.105682	5532.559	591.6929
	1.4	-2123.117	1428.406	9.891768	6093.277	587.2801
1.5	-2130.114	1412.45	1412.45	12.33947	6702.893	583.9991
100	1.0	-2085.474	1469.075	4.17072	4185.757	623.28
	1.1	-2085.513	1451.738	5.050481	4579.335	610.4716
	1.2	-2084.272	1447.364	6.438362	5016.576	598.6581
	1.3	-2088.23	1437.518	8.06608	5519.027	591.4531
	1.4	-2095.062	1418.225	9.843662	6078.442	586.869
1.5	-2101.825	1402.401	12.2834	6688.071	583.8954	
150	1.0	-2059.205	1457.033	4.118999	4174.514	623.0203
	1.1	-2058.367	1441.457	5.023383	4567.034	609.9791
	1.2	-2056.681	1436.985	6.405049	5003.581	598.3557
	1.3	-2060.573	1423.008	7.904379	5503.841	591.2864
	1.4	-2066.976	1405.453	9.70725	6063.805	586.7021
1.5	-2073.536	1391.968	12.21025	6672.844	583.6749	
200	1.0	-2031.555	1450.099	4.153948	4162.643	621.7319
	1.1	-2031.192	1431.04	4.995902	4554.524	609.4584
	1.2	-2029.177	1426.549	6.370231	4989.962	597.7106
	1.3	-2032.697	1412.644	7.864013	5489.77	590.9529
	1.4	-2038.86	1395.202	9.65984	6048.979	586.4402
1.5	-2045.224	1384.943	12.28317	6657.72	583.4337	

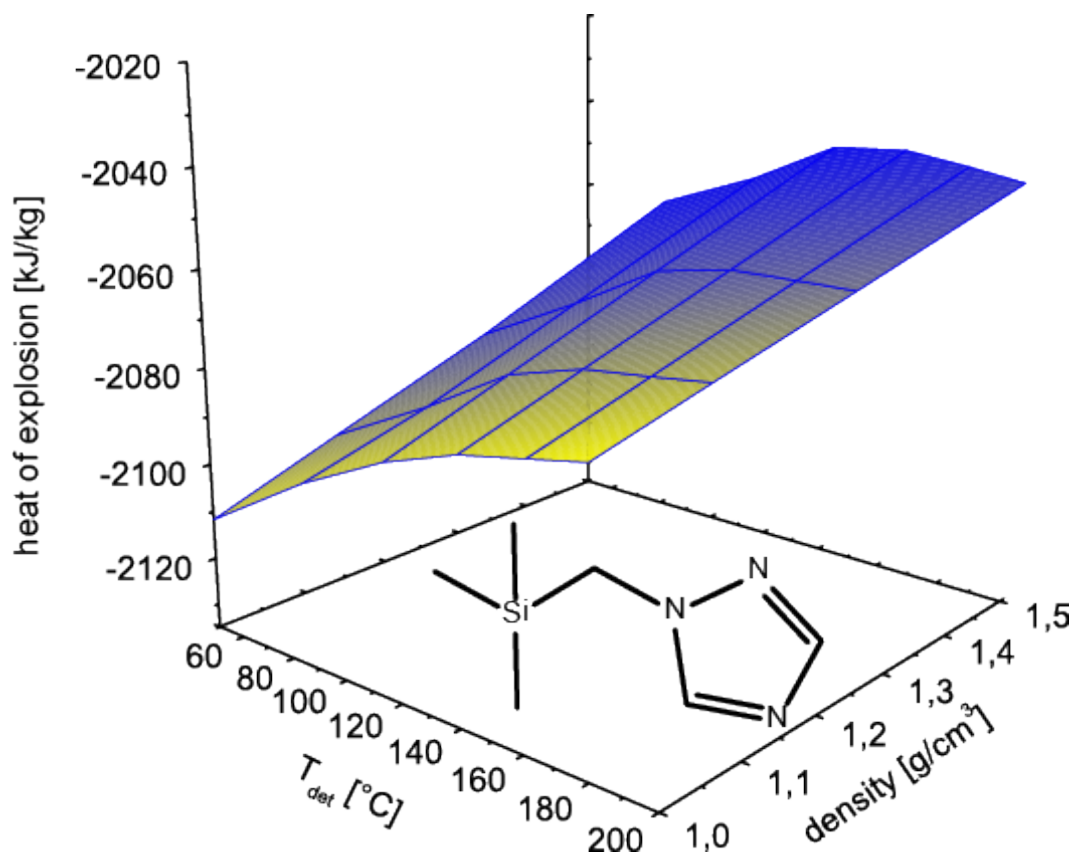
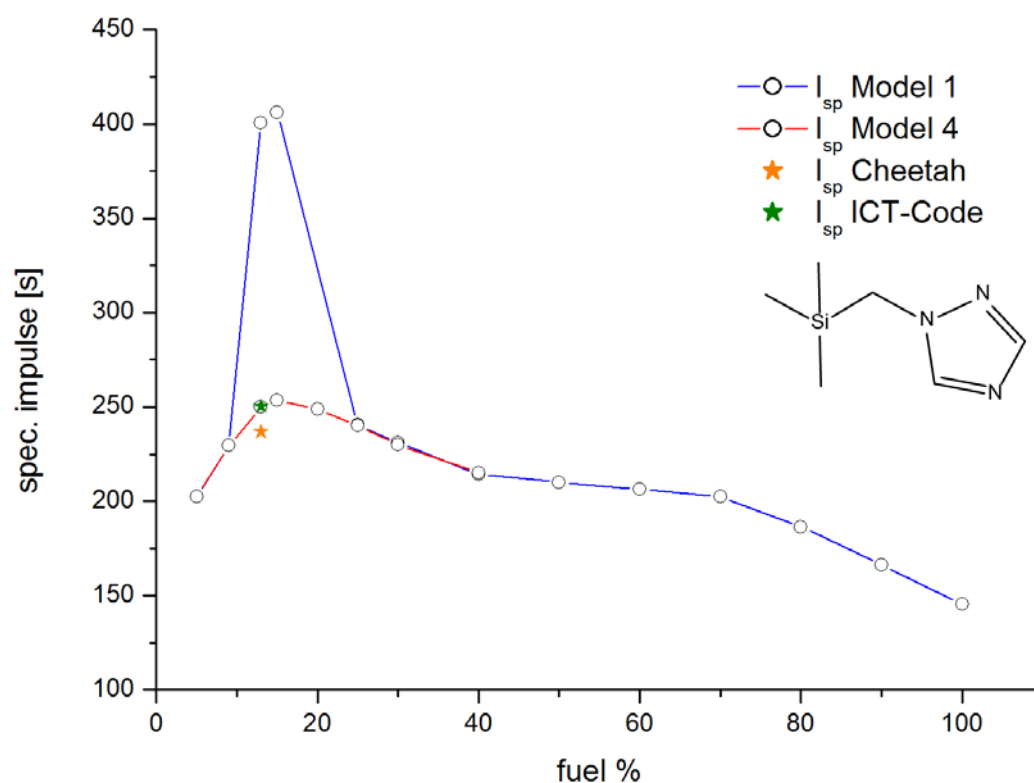
Figure S21: Graph of heat of explosion of 5a in dependency to T_{det} and density

Table S26: Propulsion parameters (T_c , I_{sp} and oxygen balance) of **5a** computed with EXPL05 (Model 1) with AP

T_{dec} [°C]	T_c [K]	I_{sp} [s]	Oxygen balance [atm] in %	5a / AP
100	1087.3	145.23	-211.2263	100 / 0
	2235.2	202.37	21.77902	5 / 95
	2746.4	229.40	11.96827	9 / 91
	3079.0	249.80	2.15752	13 / 87
	3035.1	400.67	2.157523	13 / 87
	3081.3	406.33	-2.747854	15 / 85
	2684.0	240.49	-27.27473	25 / 75
	2377.1	230.93	-39.53817	30 / 70
	1779.7	214.28	-64.06504	40 / 60
	1755.7	210.05	-88.59191	50 / 50
	1735.5	206.21	-113.1188	60 / 40
	1718.3	202.53	-137.6456	70 / 30
	1482.3	186.39	-162.1725	80 / 20
	1262.8	166.30	-186.6994	90 / 10

Table S27: Propulsion parameters (T_c , I_{sp} and oxygen balance) of **5a** computed with EXPL05 (Model 4) with AP

T_{dec} [°C]	T_c [K]	I_{sp} [s]	Oxygen balance [atm] in %	5a / AP
100	2234.0	202.51	21.77902	5 / 95
	2759.5	229.43	11.96827	9 / 91
	3103.9	236.97	-2.747854	15 / 85
	3160.0	253.70	-2.747854	15 / 85
	2987.7	248.63	-15.01129	20 / 80
	2699.5	240.16	-27.27473	25 / 75
	2377.7	229.89	-39.53817	30 / 70
	1889.9	215.20	-64.06504	40 / 60
	1405.2	186.79	-162.1725	80 / 20
	1079.6	156.86	-198.9628	95 / 5

**Figure S22:** Specific impulse values versus different amounts of AP calculated of **5a** with different computer codes

10. 1-((Trimethylsilyl)methyl)-2H-1.2.3-triazole (**5b**)**Table S28:** Detonation parameter ($\Delta_{\text{ex}}U$, T_{det} , p_{Cl} , V_{det} and V_0) of **5b** in dependency of T_{dec} and density

T_{dec} [°C]	density [g/cm ³]	$\Delta_{\text{ex}}U^\circ$ [kJ·kg ⁻¹]	T_{det} [K]	p_{Cl} [kbar]	V_{det} [m·s ⁻¹]	V_0 [L·kg ⁻¹]
50	1.0	-2326.755	1565.792	4.444797	4287.561	628.7264
	1.1	-2329.863	1554.416	5.498380	4685.517	614.0948
	1.2	-2334.266	1540.279	6.738401	5132.136	602.8441
	1.3	-2341.343	1525.584	8.296886	5639.490	594.8527
	1.4	-2350.209	1513.352	10.39642	6206.003	589.3545
1.5	-2358.766	1495.554	12.90718	6819.563	585.5807	
100	1.0	-2300.347	1555.349	4.417499	4276.523	628.0588
	1.1	-2302.859	1544.461	5.471558	4674.075	613.5218
	1.2	-2306.894	1530.26	6.706255	5119.879	602.3671
	1.3	-2313.665	1515.656	8.260741	5626.542	594.4655
	1.4	-2322.262	1503.463	10.35148	6192.574	589.0687
1.5	-2330.626	1485.805	12.85458	6805.653	585.3752	
150	1.0	-2273.813	1545.209	4.394776	4265.510	627.3668
	1.1	-2275.859	1534.361	5.444331	4662.431	612.9481
	1.2	-2279.524	1520.089	6.673230	5107.406	601.8904
	1.3	-2285.932	1505.794	8.223094	5613.706	594.0957
	1.4	-2294.312	1491.517	10.23411	6178.840	588.8326
1.5	-2302.468	1476.024	12.80163	6791.621	585.1719	
200	1.0	-2247.810	1532.802	4.332145	4254.498	627.0652
	1.1	-2248.821	1524.271	5.417104	4650.758	612.3852
	1.2	-2252.113	1509.981	6.641036	5094.922	601.4210
	1.3	-2258.036	1499.751	8.307788	5601.108	593.5383
	1.4	-2266.334	1481.143	10.17402	6165.119	588.5609
1.5	-2274.305	1466.137	12.75133	6777.230	584.9664	

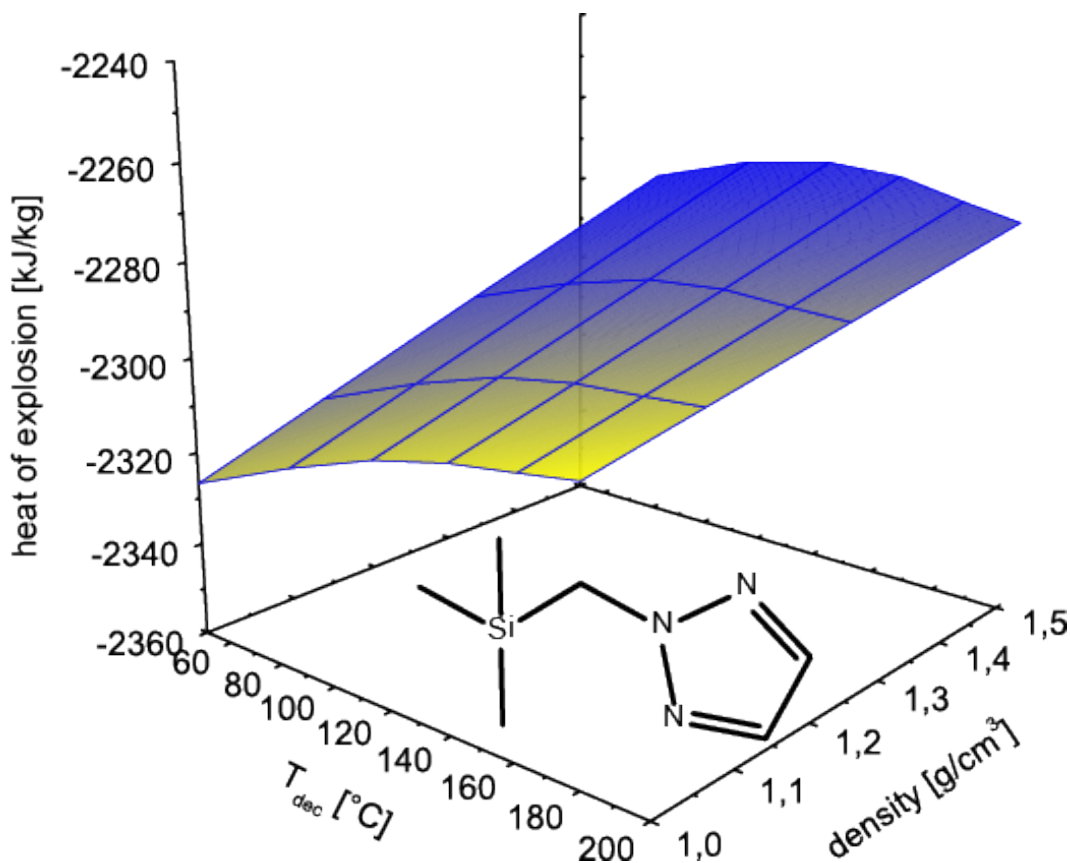
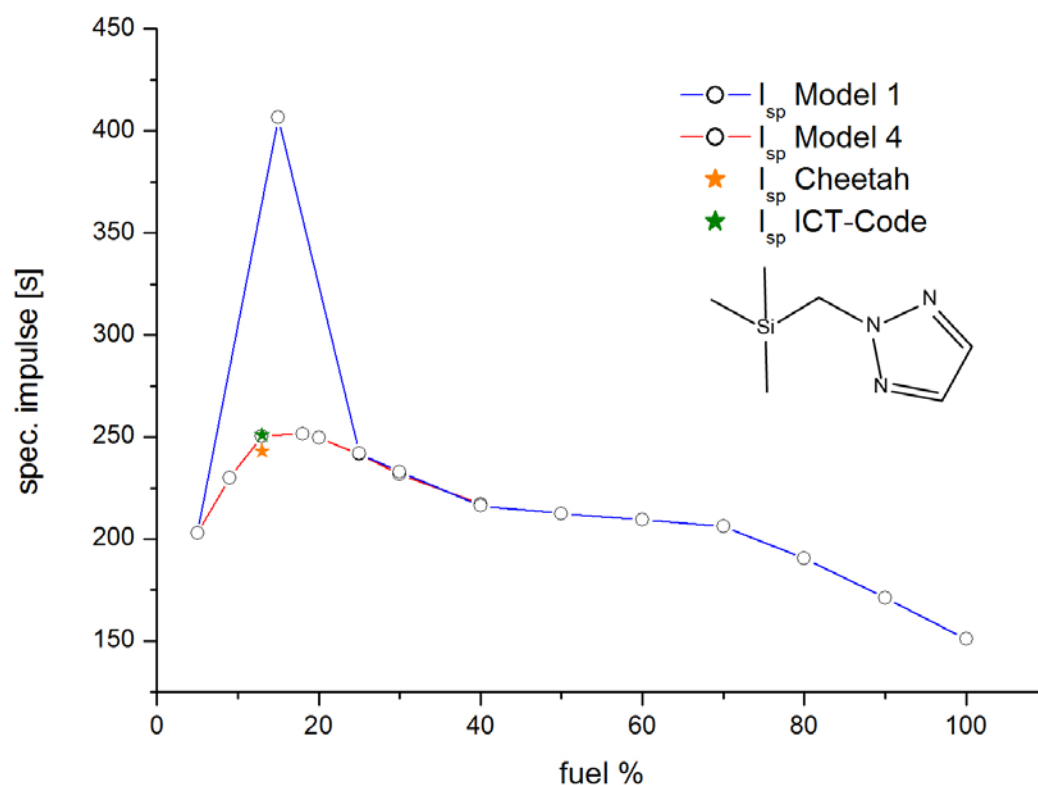
**Figure S23:** Graph of heat of explosion of **5b** in dependency to T_{dec} and density

Table S29: Propulsion parameters (T_c , I_{sp} and oxygen balance) of **5b** computed with EXPL05 (Model 1) with AP

T_{dec} [°C]	T_c [K]	I_{sp} [s]	Oxygen balance [atm] in %	5b / AP
100	2241.6	202.78	21.77902	5 / 95
	3087.0	250.30	2.157523	13 / 87
	3089.3	406.77	-2.747854	15 / 85
	2707.3	241.88	-27.27473	25 / 75
	2411.1	232.92	-39.53817	30 / 70
	1820.9	216.34	-64.06504	40 / 60
	1803.0	212.60	-88.59191	50 / 50
	1788.0	209.40	-113.1188	60 / 40
	1775.0	206.30	-137.6456	70 / 30
	1532.0	190.40	-162.1725	80 / 20
	1307.0	171.30	-186.6994	90 / 10
	1133.0	150.90	-211.2263	100 / 0

Table S30: Propulsion parameters (T_c , I_{sp} and oxygen balance) of **5b** computed with EXPL05 (Model 4) with AP

T_{dec} [°C]	T_c [K]	I_{sp} [s]	Oxygen balance [atm] in %	5b / AP
100	2240.0	202.76	21.77902	5 / 95
	2769.0	229.92	11.96827	9 / 91
	3082.8	251.66	-10.10592	18 / 82
	3005.2	249.60	-15.01129	20 / 80
	2726.8	241.59	-27.27473	25 / 75
	2412.2	231.70	-39.53817	30 / 70
	1925.9	217.22	-64.06504	40 / 60

**Figure S24:** Specific impulse values versus different amounts of AP calculated of **5b** with different computer codes

11. 1-((Trimethylsilyl)methyl)-1*H*-1.2.3-triazole (**5c**)**Table S31:** Detonation parameter ($\Delta_{\text{ex}}U$, T_{det} , p_{CJ} , V_{det} and V_0) of **5c** in dependency of T_{dec} and density

T_{dec} [°C]	density [g/cm ³]	$\Delta_{\text{ex}}U^{\circ}$ [kJ·kg ⁻¹]	T_{det} [K]	p_{CJ} [kbar]	V_{det} [m·s ⁻¹]	V_0 [L·kg ⁻¹]
50	1.0	-2418.278	1600.825	4.533729	4324.566	631.0710
	1.1	-2422.708	1591.187	5.634211	4725.178	615.8925
	1.2	-2428.783	1575.799	6.875447	5173.901	604.4355
	1.3	-2437.026	1560.992	8.458662	5683.565	596.1483
	1.4	-2446.825	1547.491	10.55847	6251.543	590.3601
1.5	-2456.024	1531.028	13.17031	6866.747	586.2800	
100	1.0	-2392.057	1589.954	4.495187	4313.860	630.4982
	1.1	-2395.803	1581.247	5.607606	4713.886	615.289
	1.2	-2401.573	1564.937	6.817350	5162.112	604.0416
	1.3	-2409.419	1550.858	8.413691	5670.96	595.7648
	1.4	-2418.938	1537.817	10.51488	6238.626	590.0651
1.5	-2427.968	1521.192	13.11766	6853.008	586.0626	
150	1.0	-2365.567	1580.094	4.476856	4302.996	629.7357
	1.1	-2369.282	1568.962	5.532076	4702.524	615.0060
	1.2	-2374.276	1554.836	6.786098	5149.806	603.5388
	1.3	-2381.785	1540.251	8.354288	5658.310	595.4154
	1.4	-2391.038	1527.757	10.46166	6225.444	589.7781
1.5	-2399.862	1511.674	13.06655	6839.642	585.8549	
200	1.0	-2339.003	1570.419	4.455170	4292.562	629.0509
	1.1	-2342.260	1559.336	5.511669	4691.155	614.3824
	1.2	-2346.930	1544.885	6.753181	5137.760	603.0618
	1.3	-2354.143	1530.26	8.316345	5645.446	595.0237
	1.4	-2363.135	1515.068	10.31479	6212.116	589.5589
1.5	-2371.756	1500.042	12.93137	6825.950	585.6798	

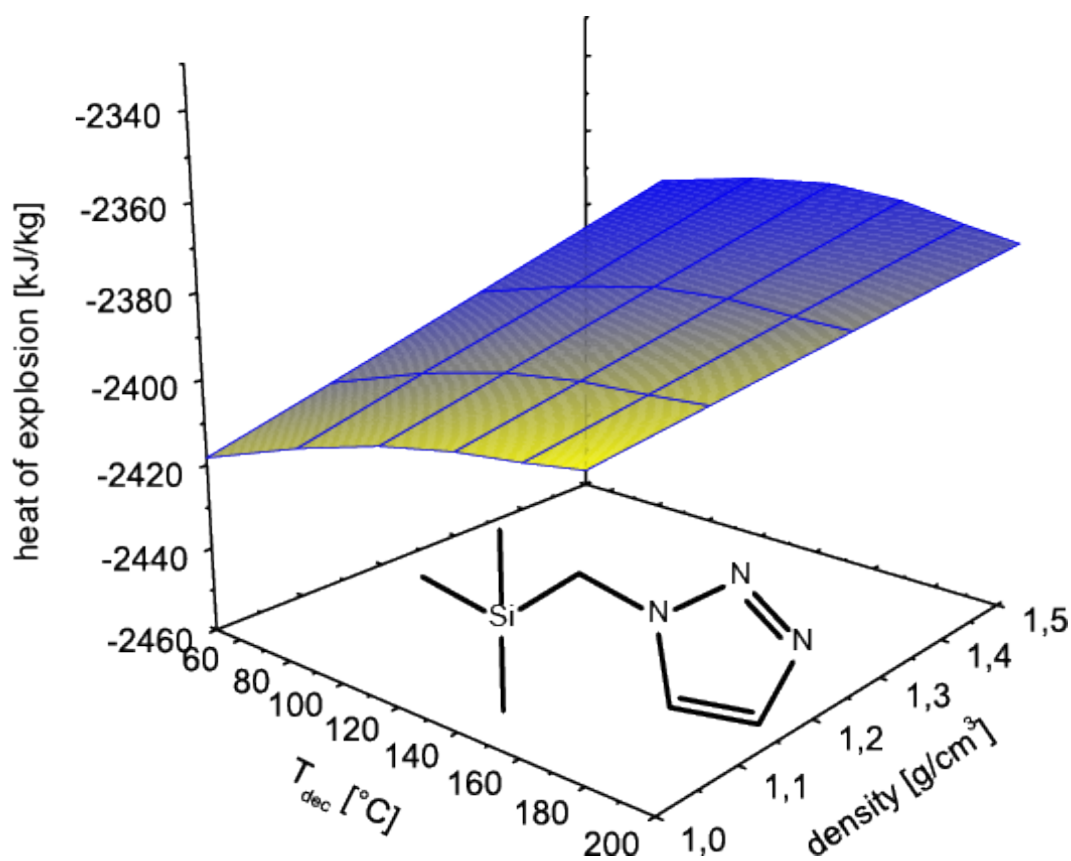
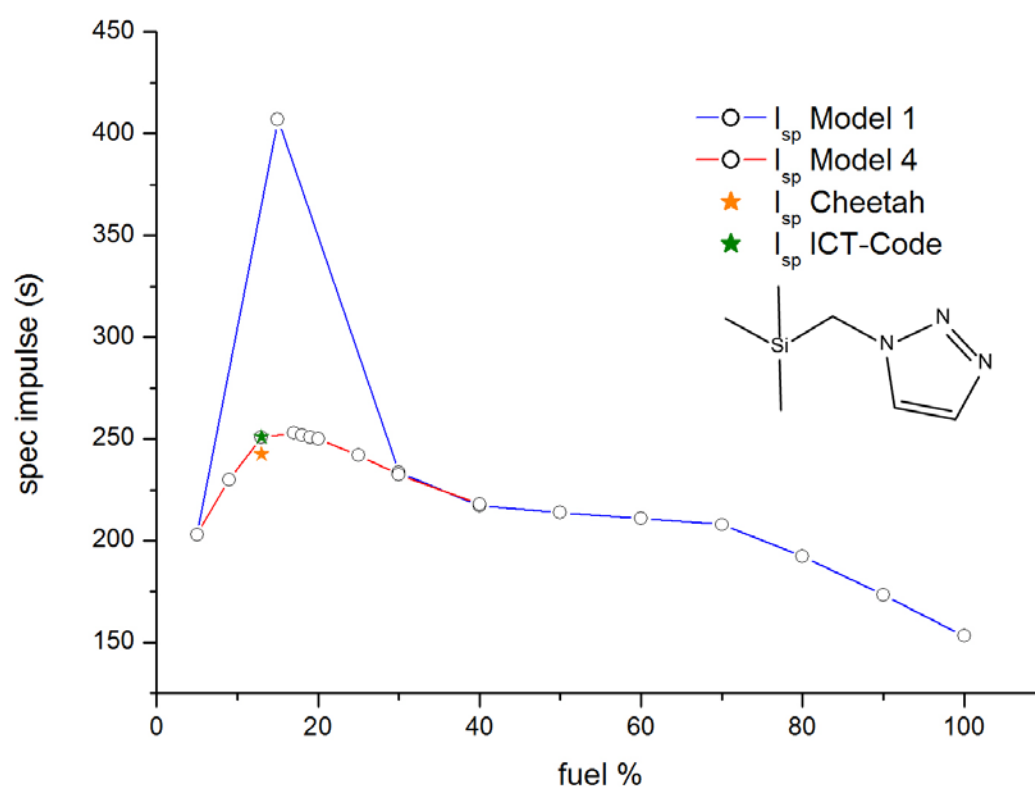
**Figure S25:** Graph of heat of explosion of **5c** in dependency to T_{dec} and density

Table S32: Propulsion parameters (T_c , I_{sp} and oxygen balance) of **5c** computed with EXPL05 (Model 1) with AP

T_{dec} [°C]	T_c [K]	I_{sp} [s]	Oxygen balance [atm] in %	5c / AP
100	2244.4	202.91	21.77902	5 / 95
	3090.0	250.60	2.157523	13 / 87
	3092.5	406.95	-2.747861	15 / 85
	2425.0	233.63	-39.53817	30 / 70
	1838.7	217.29	-64.06504	40 / 60
	1823.5	213.77	-88.59191	50 / 50
	1810.0	210.83	-113.1188	60 / 40
	1799.3	207.84	-137.6456	70 / 30
	1553.9	192.25	-162.1725	80 / 20
	1326.4	173.31	-186.6994	90 / 10
1152.4	153.23	-211.2263	100 / 0	

Table S33: Propulsion parameters (T_c , I_{sp} and oxygen balance) of **5c** computed with EXPL05 (Model 4) with AP

T_{dec} [°C]	T_c [K]	I_{sp} [s]	Oxygen balance [atm] in %	5c / AP
100	2242.6	202.99	21.77902	5 / 95
	2772.6	230.14	11.96827	9 / 91
	3111.5	252.97	-7.653229	17 / 83
	3088.5	252.02	-10.10592	18 / 82
	3054.6	250.91	-12.5586	19 / 81
	3012.4	250.02	-15.01129	20 / 80
	2738.2	242.19	-27.27473	25 / 75
	2426.8	232.47	-39.53817	30 / 70
	1941.2	218.07	-64.06504	40 / 60

**Figure S26:** Specific impulse values versus different amounts of AP calculated of **5c** with different computer codes

12. 1-((Trimethylsilyl)methyl)-1H-tetrazole (6a)

Table S34: Detonation parameter ($\Delta_{\text{ex}}U$, T_{det} , p_{Cl} , V_{det} and V_0) of **6a** in dependency of T_{dec} and density

T_{dec} [°C]	density [g/cm ³]	$\Delta_{\text{ex}}U^\circ$ [kJ·kg ⁻¹]	T_{det} [K]	p_{Cl} [kbar]	V_{det} [m·s ⁻¹]	V_0 [L·kg ⁻¹]
50	1.0	-2730.912	1803.024	4.999796	4369.813	666.1612
	1.1	-2733.924	1793.314	6.103676	4695.063	644.2411
	1.2	-2734.234	1780.167	7.359192	5040.299	625.1776
	1.3	-2735.393	1759.411	8.691048	5420.626	610.3686
	1.4	-2738.400	1735.312	10.22266	5852.321	599.3597
1.5	-2743.982	1710.034	12.09095	6346.617	591.7657	
100	1.0	-2704.91	1792.951	4.977321	4359.98	665.3474
	1.1	-2707.426	1783.191	6.076963	4684.777	643.5532
	1.2	-2707.371	1769.664	7.320209	5029.531	624.6598
	1.3	-2708.111	1749.244	8.655010	5409.375	609.8864
	1.4	-2710.868	1725.335	10.18244	5840.797	598.9612
1.5	-2716.270	1700.106	14.04555	6334.690	591.4448	
150	1.0	-2678.901	1782.859	4.954812	4350.110	664.5364
	1.1	-2680.914	1773.043	6.050180	4674.442	642.8689
	1.2	-2680.453	1759.427	7.287227	5018.719	624.0915
	1.3	-2681.029	1738.021	8.590054	5398.101	609.5468
	1.4	-2683.331	1715.271	10.14179	5829.128	598.5627
1.5	-2688.627	1688.578	11.94102	6322.623	591.1986	
200	1.0	-2652.816	1773.062	4.937140	4340.231	663.6609
	1.1	-2654.972	1760.557	5.981135	4664.061	642.6337
	1.2	-2653.463	1749.249	7.257136	5007.816	623.5130
	1.3	-2653.752	1727.863	8.553971	5386.752	609.0594
	1.4	-2655.783	1705.182	10.10097	5817.385	598.1663
1.5	-2660.886	1678.724	11.89585	6310.655	590.8828	

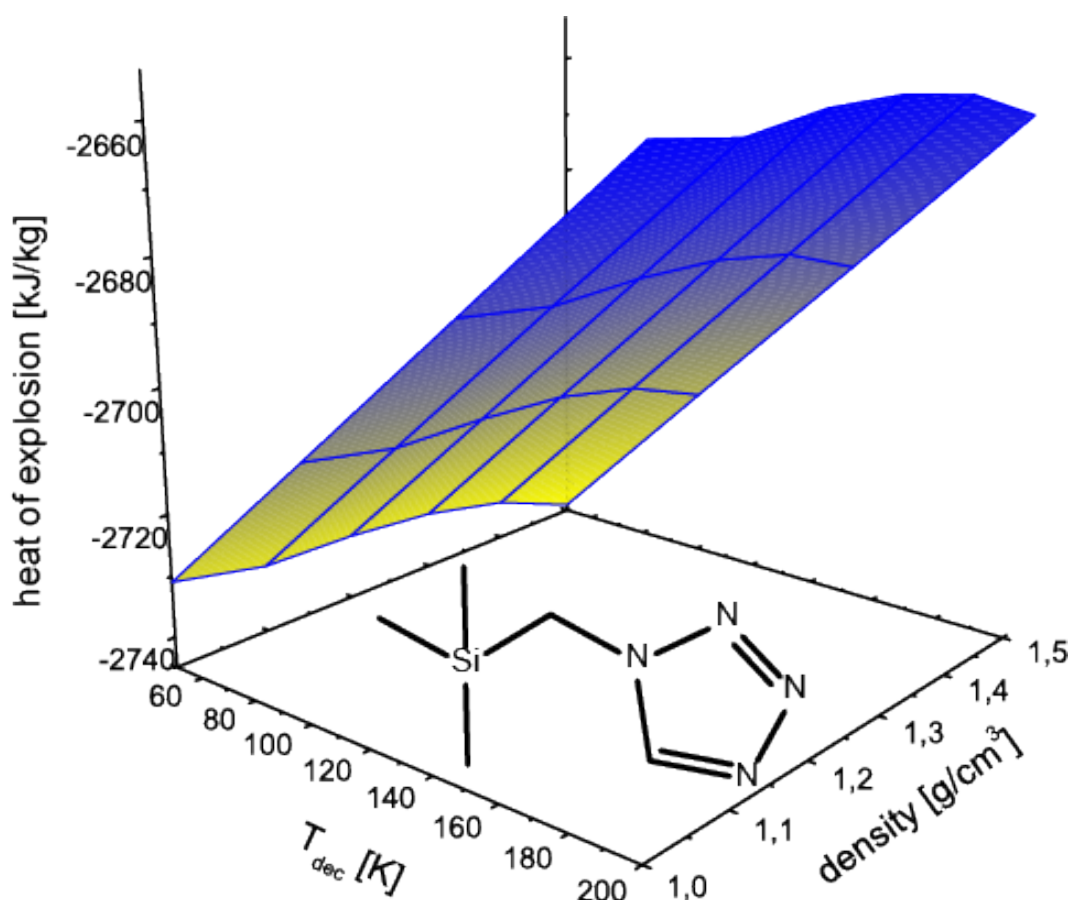
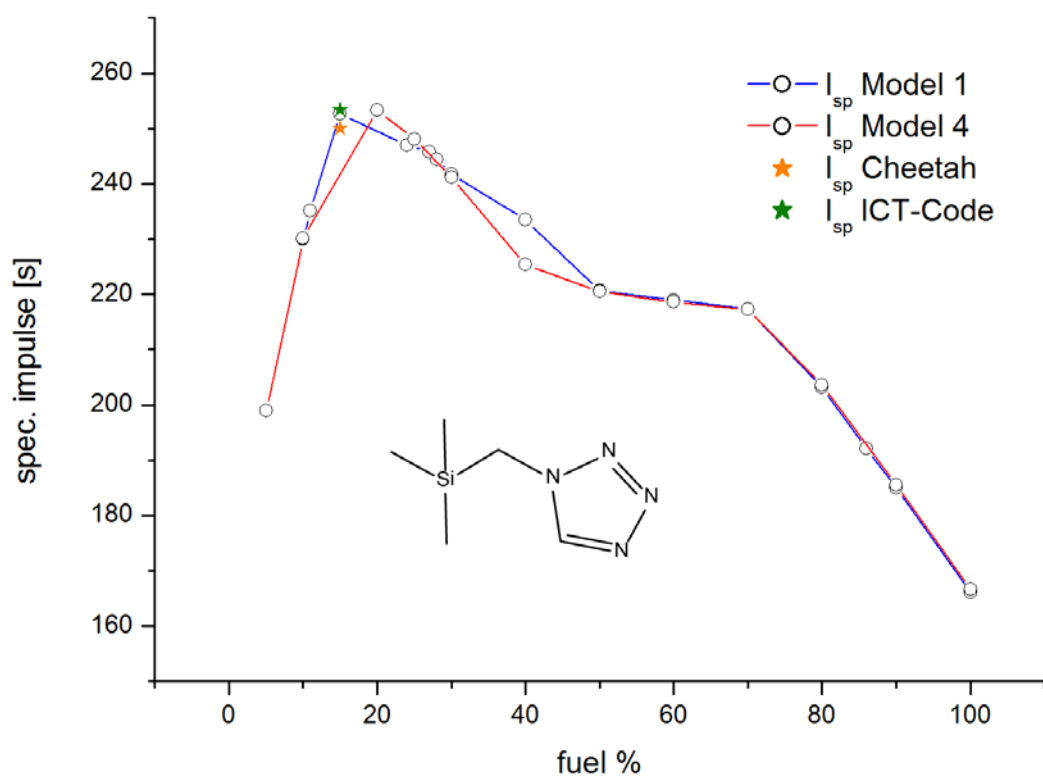
Figure S27: Graph of heat of explosion of **6a** in dependency to T_{dec} and density

Table S35: Propulsion parameters (T_c , I_{sp} and oxygen balance) of **6a** computed with EXPL05 (Model 1) with AP

T_{dec} [°C]	T_c [K]	I_{sp} [s]	Oxygen balance [atm] in %	6a / AP
100	2758.5	230.04	12.20901	10 / 90
	2850.2	235.08	10.02567	11 / 89
	3117.0	252.70	1.292289	15 / 85
	2837.0	246.99	-22.72449	24 / 76
	2793.0	245.79	-24.90784	27 / 73
	2747.6	244.49	-27.09118	28 / 72
	2654.0	241.73	-31.45787	30 / 70
	2134.1	233.48	-53.29132	40 / 60
	1969.9	220.67	-75.12475	50 / 50
	1971.7	218.99	-96.9582	60 / 40
	1895.7	217.37	-118.7916	70 / 30
	1697.4	203.15	-140.6251	80 / 20
	1547.3	192.14	-153.7251	86 / 14
	1452.0	184.99	-162.4585	90 / 10
	1255.2	166.14	-184.292	100 / 0

Table S36: Propulsion parameters (T_c , I_{sp} and oxygen balance) of **6a** computed with EXPL05 (Model 4) with AP

T_{dec} [°C]	T_c [K]	I_{sp} [s]	Oxygen balance [atm] in %	6a / AP
100	2167.4	198.99	23.12573	05 / 95
	2772.3	230.12	12.20901	10 / 90
	3114.0	253.32	-9.624429	20 / 80
	2927.4	248.14	-20.54115	25 / 75
	2673.0	241.21	-31.45787	30 / 70
	2160.1	225.43	-53.29132	40 / 60
	1989.3	220.54	-75.12475	50 / 50
	1966.7	218.64	-96.9582	60 / 40
	1916.0	217.34	-118.7916	70 / 30
	1656.7	203.58	-140.6251	80 / 20
	1373.2	185.52	-162.4585	90 / 10
	1158.5	166.63	-184.292	100 / 0

**Figure S28:** Specific impulse values versus different amounts of AP calculated of **6a** with different computer codes

13. 2-((Trimethylsilyl)methyl)-2H-tetrazole (**6b**)Table S37: Detonation parameter ($\Delta_{\text{ex}}U$, T_{det} , p_{Cl} , V_{det} and V_0) of **6b** in dependency of T_{dec} and density

T_{dec} [°C]	density [g/cm ³]	$\Delta_{\text{ex}}U^\circ$ [kJ·kg ⁻¹]	T_{det} [K]	p_{Cl} [kbar]	V_{det} [m·s ⁻¹]	V_0 [L·kg ⁻¹]
50	1.0	-2615.181	1753.799	4.838865	4325.168	663.3075
	1.1	-2615.485	1745.495	5.941541	4648.597	641.6324
	1.2	-2613.487	1733.538	7.200846	4991.403	622.7191
	1.3	-2613.125	1712.699	8.500082	5369.757	608.3523
	1.4	-2614.788	1690.131	10.03992	5799.779	597.5811
1.5	-2619.641	1663.582	11.82622	6292.158	590.4053	
100	1.0	-2588.353	1746.489	4.859123	4315.335	661.9699
	1.1	-2588.950	1735.244	5.916710	4637.900	640.9186
	1.2	-2587.040	1721.098	7.119509	4980.446	622.5410
	1.3	-2585.800	1702.473	8.463670	5358.243	607.8779
	1.4	-2587.296	1679.201	9.971338	5787.881	597.2708
1.5	-2591.850	1653.674	11.78050	6279.984	590.0995	
150	1.0	-2562.326	1736.17	4.836195	4305.142	661.1663
	1.1	-2562.230	1725.448	5.897236	4627.389	640.1884
	1.2	-2560.044	1710.82	7.087823	4969.351	621.9782
	1.3	-2558.463	1692.219	8.427112	5346.658	607.4064
	1.4	-2559.905	1667.362	9.884384	5775.485	596.9938
1.5	-2564.075	1643.570	11.73262	6267.559	589.7903	
200	1.0	-2536.217	1725.952	4.813489	4295.024	660.3867
	1.1	-2535.657	1715.167	5.870157	4616.752	639.5222
	1.2	-2533.035	1700.516	7.056030	4958.193	621.4191
	1.3	-2531.138	1681.898	8.385442	5335.181	606.9708
	1.4	-2532.292	1657.227	9.843175	5763.433	596.6105
1.5	-2536.301	1633.447	11.68684	6254.969	589.4755	

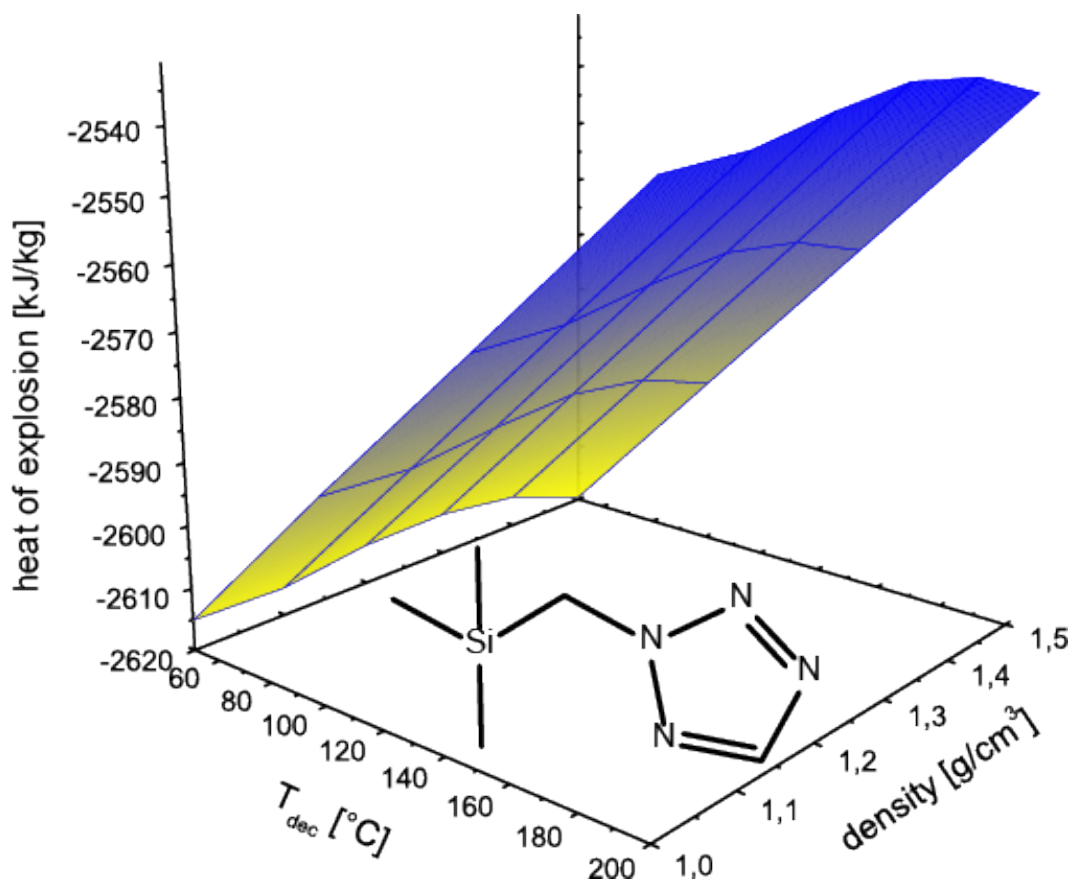
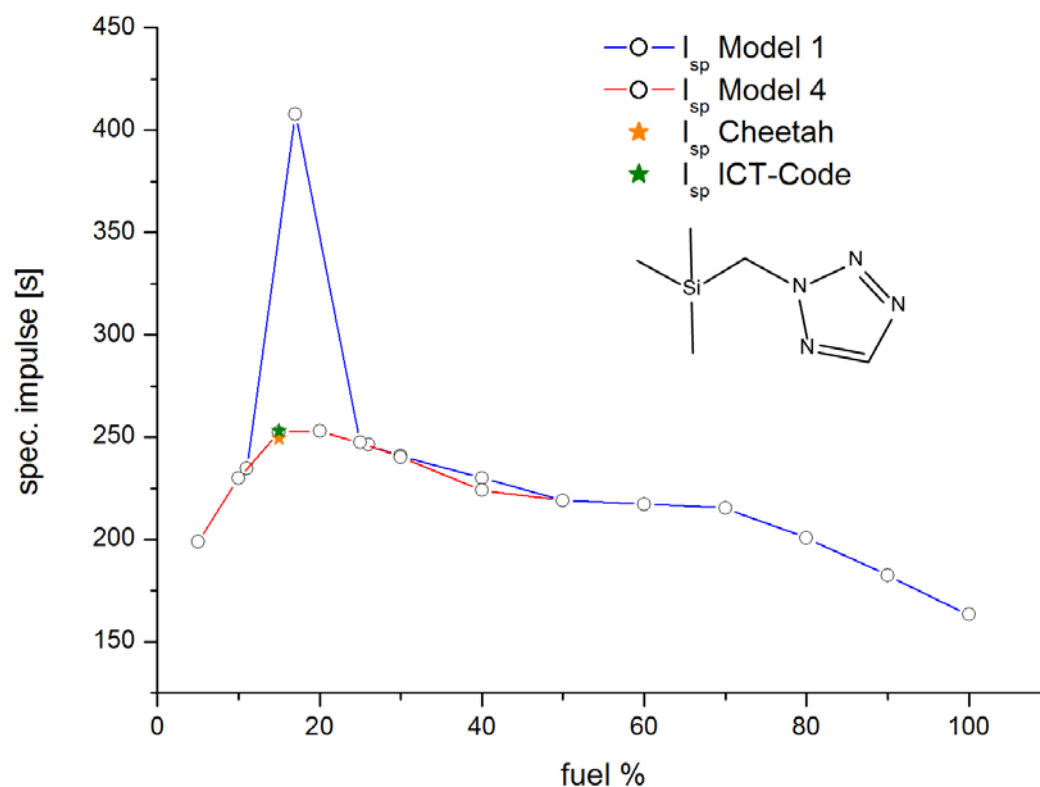
Figure S29: Graph of heat of explosion of **6b** in dependency to T_{dec} and density

Table S38: Propulsion parameters (T_c , I_{sp} and oxygen balance) of **6b** computed with EXPL05 (Model 1) with AP

T_{dec} [°C]	T_c [K]	I_{sp} [s]	Oxygen balance [atm] in %	6b / AP
100	2753.9	229.79	12.20901	10 / 90
	2844.9	234.77	10.02567	11 / 89
	3112.0	252.40	1.292289	15 / 85
	3101.8	407.79	-3.074392	17 / 83
	2865.9	247.49	-20.54115	25 / 75
	2826.1	246.25	-22.72449	26 / 74
	2638.9	240.83	-31.45787	30 / 70
	2108.2	230.03	-53.29132	40 / 60
	1943.4	219.18	-75.12475	50 / 50
	1942.9	217.26	-96.9582	60 / 40
	1880.5	215.38	-118.7916	70 / 30
	1669.8	200.80	-140.6251	80 / 20
	1422.0	182.39	-162.4585	90 / 10
	1228.3	163.33	-184.292	100 / 0

Table S39: Propulsion parameters (T_c , I_{sp} and oxygen balance) of **6b** computed with EXPL05 (Model 4) with AP

T_{dec} [°C]	T_c [K]	I_{sp} [s]	Oxygen balance [atm] in %	6b / AP
100	2163.2	198.79	23.12573	5 / 95
	2766.4	229.80	12.20901	10 / 90
	3106.3	252.83	-9.624429	20 / 80
	2914.2	247.43	-20.54115	25 / 75
	2655.5	240.29	-31.45787	30 / 70
	2136.7	224.21	-53.29132	40 / 60
	1962.0	219.10	-75.12475	50 / 50

**Figure S30:** Specific impulse values versus different amounts of AP calculated of **6b** with different computer codes

14. 5-((Trimethylsilyl)methyl)-1H-tetrazole (**6c**)Table S40: Detonation parameter ($\Delta_{\text{ex}}U$, T_{det} , p_{CJ} , V_{det} and V_0) of **6c** in dependency of T_{dec} and density

T_{dec} [°C]	density [g/cm ³]	$\Delta_{\text{ex}}U^\circ$ [kJ·kg ⁻¹]	T_{det} [K]	p_{CJ} [kbar]	V_{det} [m·s ⁻¹]	V_0 [L·kg ⁻¹]
50	1.0	-2554.865	1733.415	4.930059	4302.41	660.9557
	1.1	-2554.677	1722.529	5.889552	4624.373	639.9996
	1.2	-2552.370	1707.895	7.078799	4966.187	621.8189
	1.3	-2550.692	1689.301	8.416697	5343.354	607.2729
	1.4	-2552.069	1664.416	9.872419	5771.988	596.8817
1.5	-2556.182	1640.665	11.71789	6264.008	589.7039	
100	1.0	-2528.951	1722.554	4.799474	4292.090	660.2571
	1.1	-2528.100	1712.24	5.862451	4613.721	639.3348
	1.2	-2525.357	1697.583	7.049760	4955.011	621.2609
	1.3	-2523.370	1678.921	8.374807	5331.797	606.8358
	1.4	-2524.446	1654.322	9.831351	5759.970	596.5008
1.5	-2528.410	1630.487	11.67309	6251.290	589.3855	
150	1.0	-2503.485	1710.078	4.742301	4281.795	659.9229
	1.1	-2501.497	1701.925	5.835285	4603.019	638.6780
	1.2	-2498.711	1685.686	6.981759	4943.792	620.9693
	1.3	-2496.030	1668.426	8.337285	5319.839	606.3629
	1.4	-2496.885	1643.628	9.780354	5727.507	596.1342
1.5	-2500.597	1620.238	11.61676	6238.812	589.0978	
200	1.0	-2477.375	1699.804	4.719617	4271.542	659.1456
	1.1	-2474.880	1691.582	5.808038	4592.260	638.0261
	1.2	-2471.675	1675.322	6.949831	4932.476	620.4185
	1.3	-2468.635	1658.134	8.300423	5308.066	605.9054
	1.4	-2469.305	1633.049	9.724480	5735.347	595.7966
1.5	-2472.790	1610.08	11.56941	6226.082	588.7917	

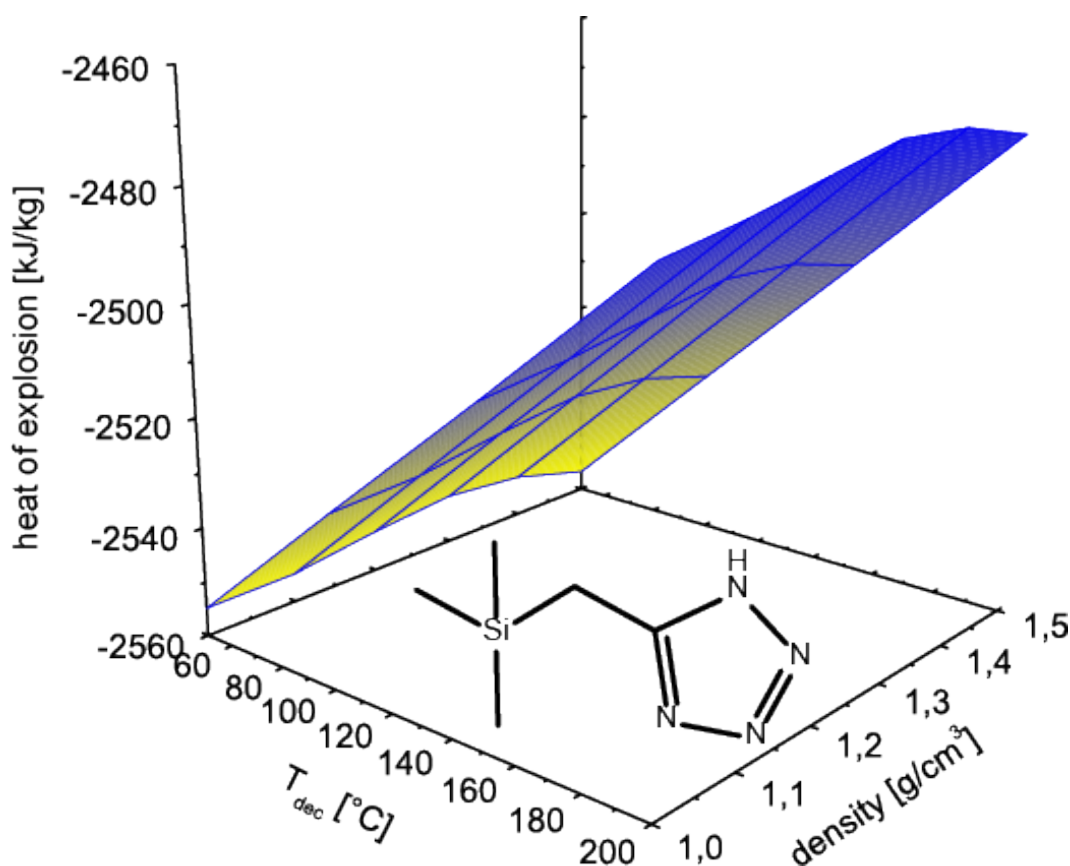
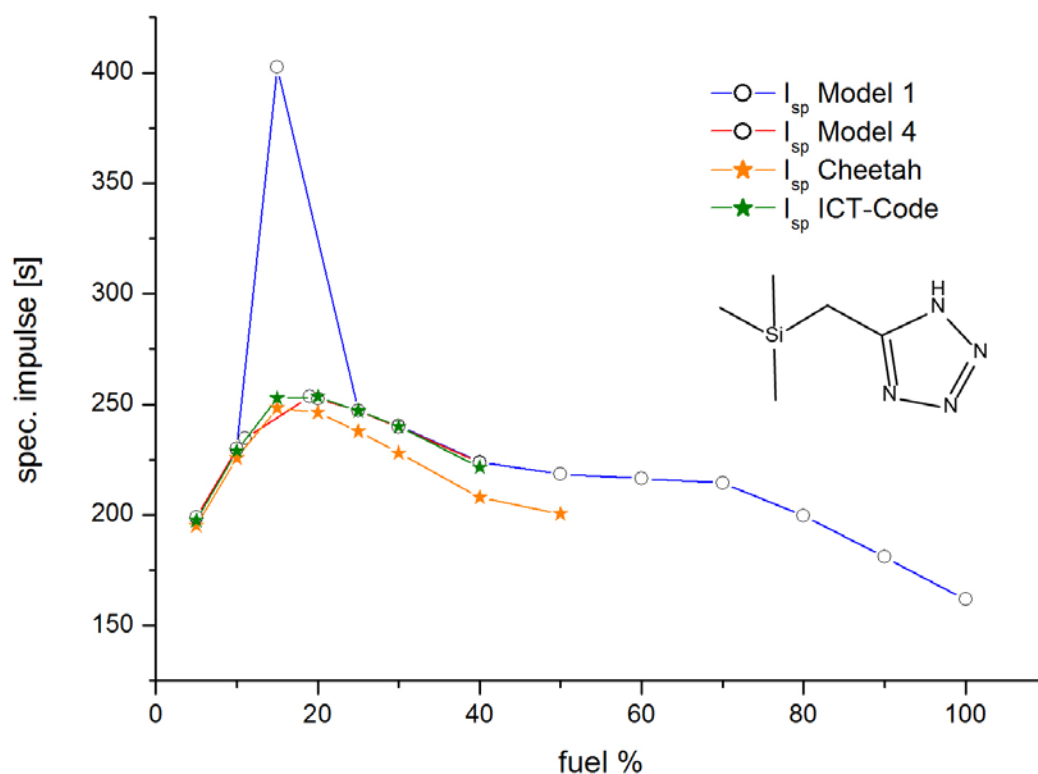
Figure S31: Graph of heat of explosion of **6c** in dependency to T_{dec} and density

Table S41: Propulsion parameters (T_c , I_{sp} and oxygen balance) of **6c** computed with EXPL05 (Model 1) with AP

T_{dec} [°C]	T_c [K]	I_{sp} [s]	Oxygen balance [atm] in %	6c / AP
100	2163	198.6	23.12573	5 / 95
	2751	229.7	12.20901	10 / 90
	3110	252.2	1.292289	15 / 85
	3066	402.7	1.292289	15 / 85
	2860	247.1	-20.54115	25 / 75
	2361	240.3	-31.45787	30 / 70
	2095	224.0	-53.29132	40 / 60
	1929	218.4	-75.12475	50 / 50
	1928	216.5	-96.9582	60 / 40
	1872	214.4	-118.7916	70 / 30
	1655	199.6	-140.6251	80 / 20
	1407	181.0	-162.4585	90 / 10
1215	161.8	-184.292	100 / 0	

Table S42: Propulsion parameters (T_c , I_{sp} and oxygen balance) of **6c** computed with EXPL05 (Model 4) with AP

T_{dec} [°C]	T_c [K]	I_{sp} [s]	Oxygen balance [atm] in %	6c / AP
100	2162	198.8	23.12573	5 / 95
	2759	229.9	12.20901	10 / 90
	2863	234.6	10.02567	11 / 89
	3121	253.4	7.441081	19 / 81
	3102	252.6	-9.624429	20 / 80
	2907	247.1	-20.54115	25 / 75
	2646	239.8	-31.45787	30 / 70
	2125	223.6	-53.29132	40 / 60

**Figure S32:** Specific impulse values versus different amounts of AP calculated of **6c** with different computer codes

15. 5-((Trimethylsilyl)methyl)-2H-tetrazole (**6d**)**Table S43:** Detonation parameter ($\Delta_{\text{ex}}U$, T_{det} , p_{CJ} , V_{det} and V_0) of **6d** in dependency of T_{dec} and density

T_{dec} [°C]	density [g/cm ³]	$\Delta_{\text{ex}}U^\circ$ [kJ·kg ⁻¹]	T_{det} [K]	p_{CJ} [kbar]	V_{det} [m·s ⁻¹]	V_0 [L·kg ⁻¹]
50	1.0	-2486.210	1703.283	4.727298	4275.017	659.4080
	1.1	-2483.887	1695.084	5.817265	4595.906	638.2461
	1.2	-2480.823	1678.832	6.960646	4936.312	620.6046
	1.3	-2477.932	1661.466	8.312374	5311.886	606.0518
	1.4	-2478.620	1636.813	9.749116	5739.484	595.8940
1.5	-2482.201	1613.521	11.58546	6230.401	588.8944	
100	1.0	-2460.090	1692.991	4.704576	4264.73	658.6343
	1.1	-2457.261	1684.723	5.789965	4585.109	637.5972
	1.2	-2453.803	1668.366	6.928364	4924.852	620.0478
	1.3	-2450.546	1651.121	8.272035	5300.188	605.6212
	1.4	-2451.261	1624.266	9.636600	5727.077	595.7097
1.5	-2454.372	1603.166	11.53140	6217.577	588.6030	
150	1.0	-2433.953	1682.672	4.681798	4254.394	657.8663
	1.1	-2430.619	1674.333	5.762583	4574.254	636.9531
	1.2	-2426.061	1660.528	6.949708	4913.608	619.1043
	1.3	-2423.121	1640.909	8.238001	5288.311	605.1506
	1.4	-2423.627	1613.951	9.594550	5714.568	595.3287
1.5	-2426.661	1591.07	11.41425	6204.493	588.3768	
200	1.0	-2408.128	1671.25	4.642416	4243.981	657.3182
	1.1	-2403.996	1663.813	5.735246	4563.200	636.2960
	1.2	-2398.981	1650.082	6.917285	4902.133	618.5656
	1.3	-2396.188	1628.166	8.143109	5276.007	604.9763
	1.4	-2395.959	1603.676	9.552561	5702.049	594.9561
1.5	-2398.813	1580.908	11.36906	6191.468	588.0742	

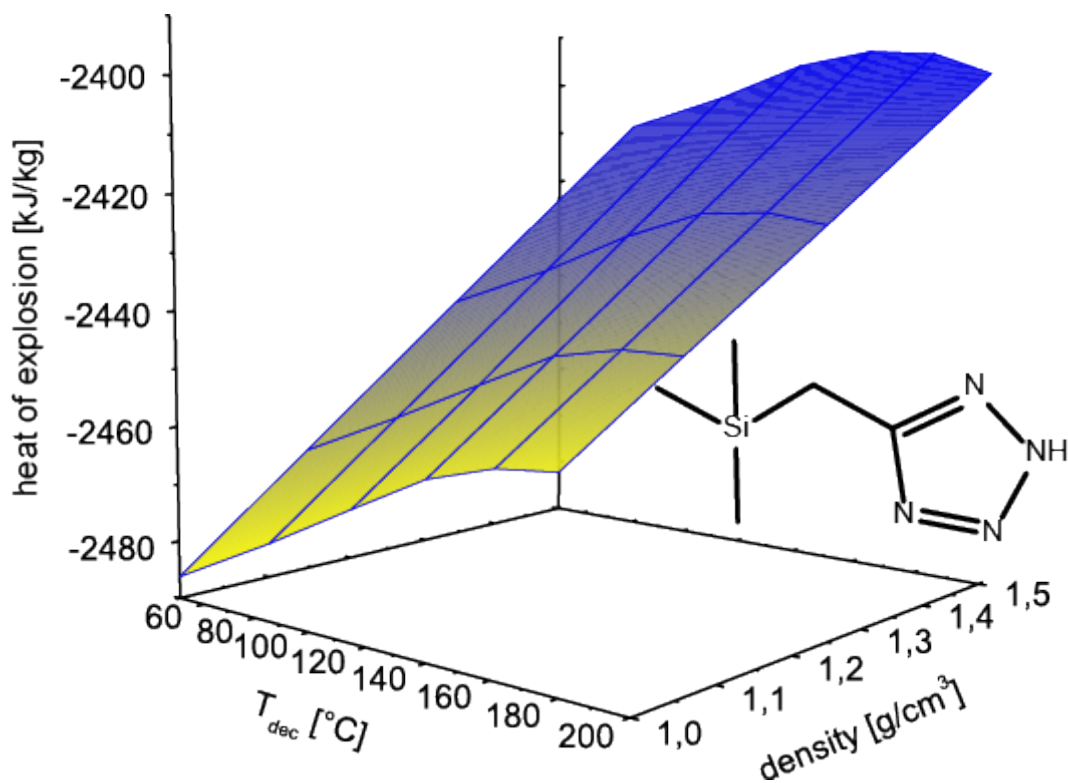
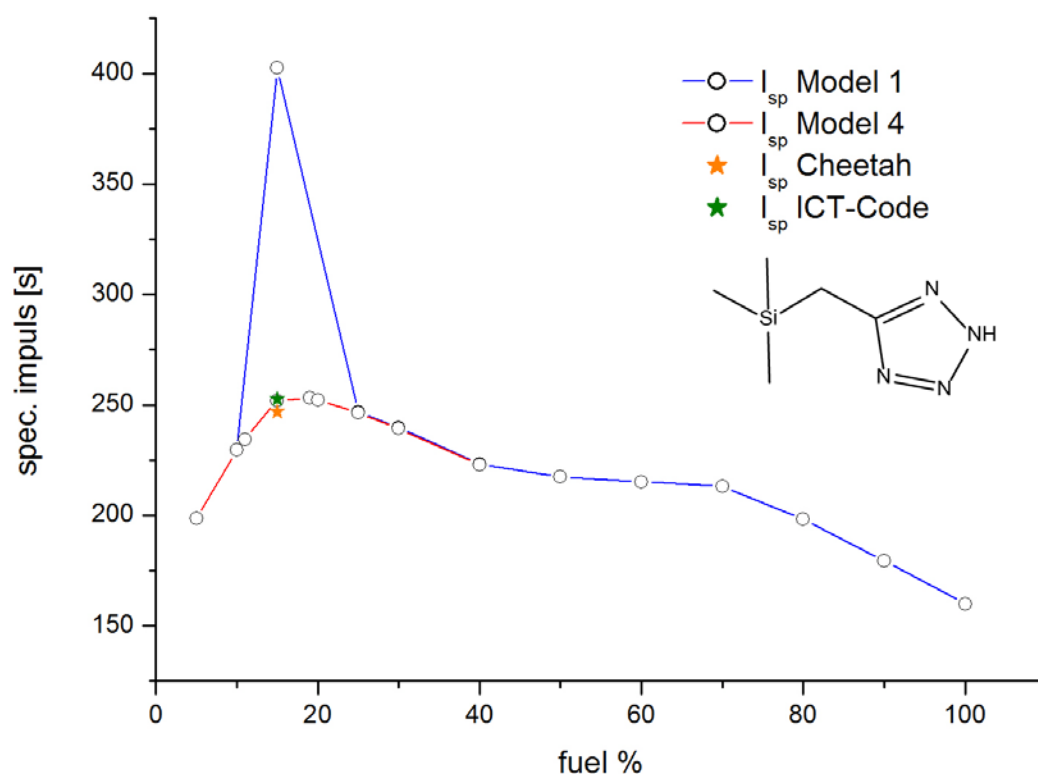
**Figure S33:** Graph of heat of explosion of **6d** in dependency to T_{dec} and density

Table S44: Propulsion parameters (T_c , I_{sp} and oxygen balance) of **6d** computed with EXPL05 (Model 1) with AP

T_{dec} [°C]	T_c [K]	I_{sp} [s]	Oxygen balance [atm] in %	6d / AP
100	2748	229.5	12.20901	10 / 90
	3107	252.0	1.292293	15 / 85
	3063	402.5	1.292293	15 / 85
	2854	246.7	-20.54115	25 / 75
	2622	239.8	-31.45787	30 / 70
	2080	223.2	-53.29132	40 / 60
	1913	217.5	-75.12475	50 / 50
	1910	215.3	-96.9582	60 / 40
	1863	213.2	-118.7916	70 / 30
	1639	198.2	-140.6251	80 / 20
	1390	179.4	-162.4585	90 / 10
1199	160.0	-184.292	100 / 0	

Table S45: Propulsion parameters (T_c , I_{sp} and oxygen balance) of **6d** computed with EXPL05 (Model 4) with AP

T_{dec} [°C]	T_c [K]	I_{sp} [s]	Oxygen balance [atm] in %	6d / AP
100	2160	198.5	23.12573	5 / 95
	2754	229.7	12.20901	10 / 90
	2860	234.5	10.02567	11 / 89
	3117	253.1	-7.441082	19 / 81
	3097	252.3	-9.624429	20 / 80
	2900	246.6	-20.54115	25 / 75
	2635	239.3	-31.45787	30 / 70
	2111	222.9	-53.29132	40 / 60

**Figure S34:** Specific impulse values versus different amounts of AP calculated of **6d** with different computer codes

16. Trimethylvinylsilane (7)

Table S46: Propulsion parameters (T_c , I_{sp} and oxygen balance) of **7** computed with EXPL05 (Model 1) with N_2O_4

T_{dec} [°C]	T_c [K]	I_{sp} [s]	Oxygen balance [atm] in %	7 / N_2O_4
55	1826	168.2	51.70844	5 / 95
	2908	223.0	33.86507	10 / 90
	3365	254.0	16.02172	15 / 85
	3470	268.9	1.747033	19 / 81
	3474	271.3	-1.821646	20 / 80
	3364	275.8	-19.66501	25 / 75
	3058	270.6	-37.50837	30 / 70
	2260	248.6	-73.19509	40 / 60
	2140	239.5	-108.8818	50 / 50
	2052	230.6	-144.5685	60 / 40
	1855	218.4	-180.2553	70 / 30
	1470	189.6	-215.942	80 / 20
	1064	148.0	-251.6287	90 / 10

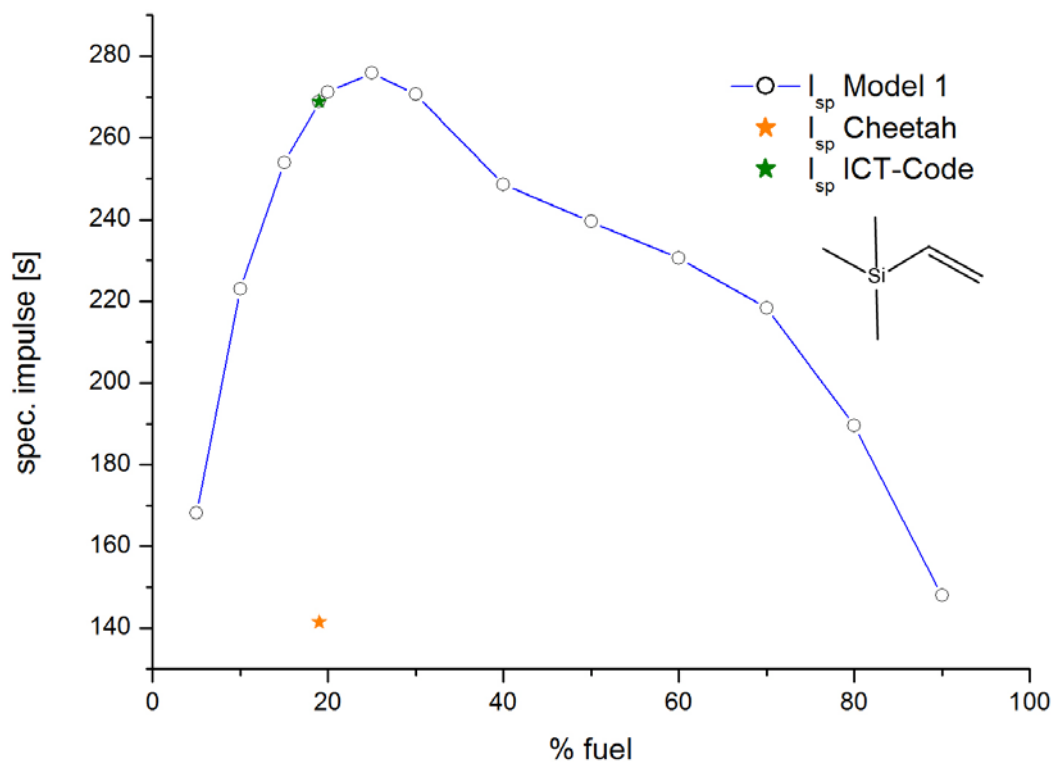
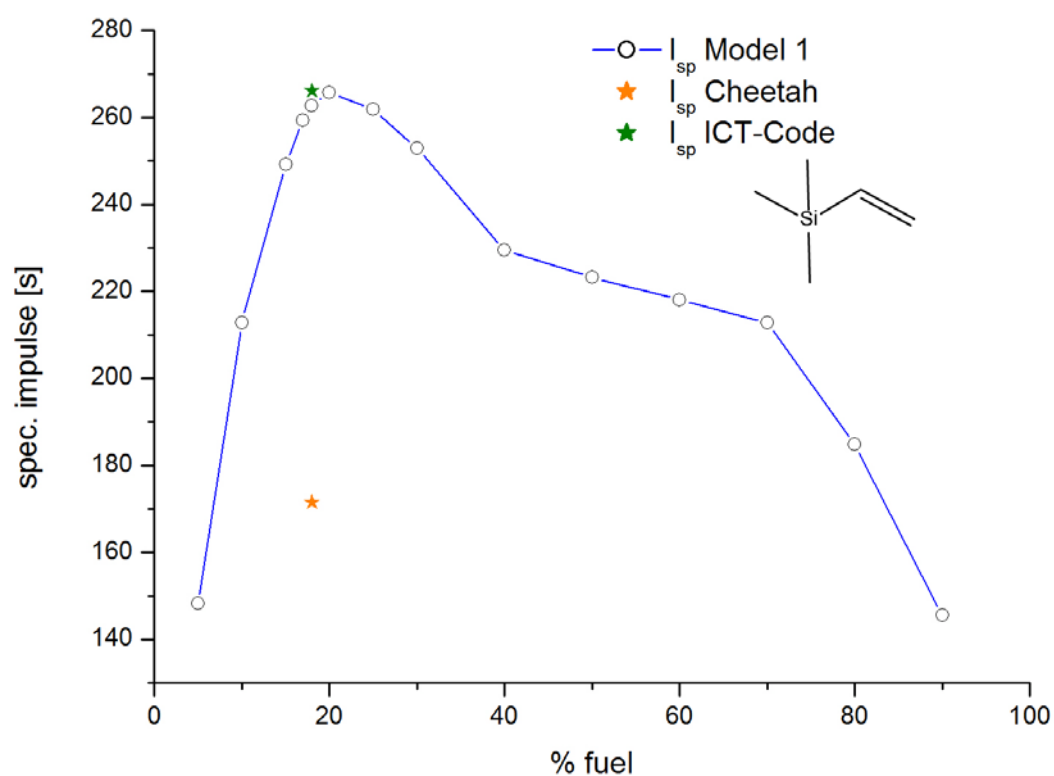
**Figure S35:** Specific impulse values versus different amounts of N_2O_4 calculated of **7** with different computer codes

Table S47: Propulsion parameters (T_c , I_{sp} and oxygen balance) of **7** computed with EXPL05 (Model 1) with red fuming nitric acid (RFNA)

T_{dec} [°C]	T_c [K]	I_{sp} [s]	Oxygen balance [atm] in %	7 / RFNA
55	1305	148.2	45.53767	5 / 95
	2478	212.9	28.01908	10 / 90
	3122	249.3	10.5005	15 / 85
	3236	259.4	3.49307	17 / 83
	3266	262.8	-0.01065154	18 / 82
	3279	265.8	-7.018087	20 / 80
	3072	261.8	-24.53667	25 / 75
	2737	253.0	-42.05526	30 / 70
	2252	229.5	-77.09242	40 / 60
	1871	223.2	-112.1296	50 / 50
	1818	218.1	-147.1667	60 / 40
	1757	212.8	-182.2039	70 / 30
	1400	184.8	-217.2411	80 / 20
	1038	145.5	-252.2782	90 / 10

**Figure S36:** Specific impulse values versus different amounts of RFNA calculated of **7** with different computer codes

17. Allyltrimethylsilane (**8**)**Table S48:** Propulsion parameters (T_c , I_{sp} and oxygen balance) of **8** computed with EXPLO5 (Model 1) with N_2O_4

T_{dec} [°C]	T_c [K]	I_{sp} [s]	Oxygen balance [atm] in %	8 / N_2O_4
85	1833	168.6	51.37156	5 / 95
	2911	223.8	33.19133	10 / 90
	3360	255.1	15.01109	15 / 85
	3449	267.3	4.102948	18 / 82
	3459	272.3	-3.169144	20 / 80
	3325	275.1	-21.34939	25 / 75
	3001	268.2	-39.52962	30 / 70
	2191	244.7	-75.8901	40 / 60
	2103	233.2	-112.2506	50 / 50
	1937	223.3	-148.611	60 / 40
	1787	213.6	-184.9715	70 / 30
	1421	187.1	-221.332	80 / 20
	1047	147.3	-257.6924	90 / 10

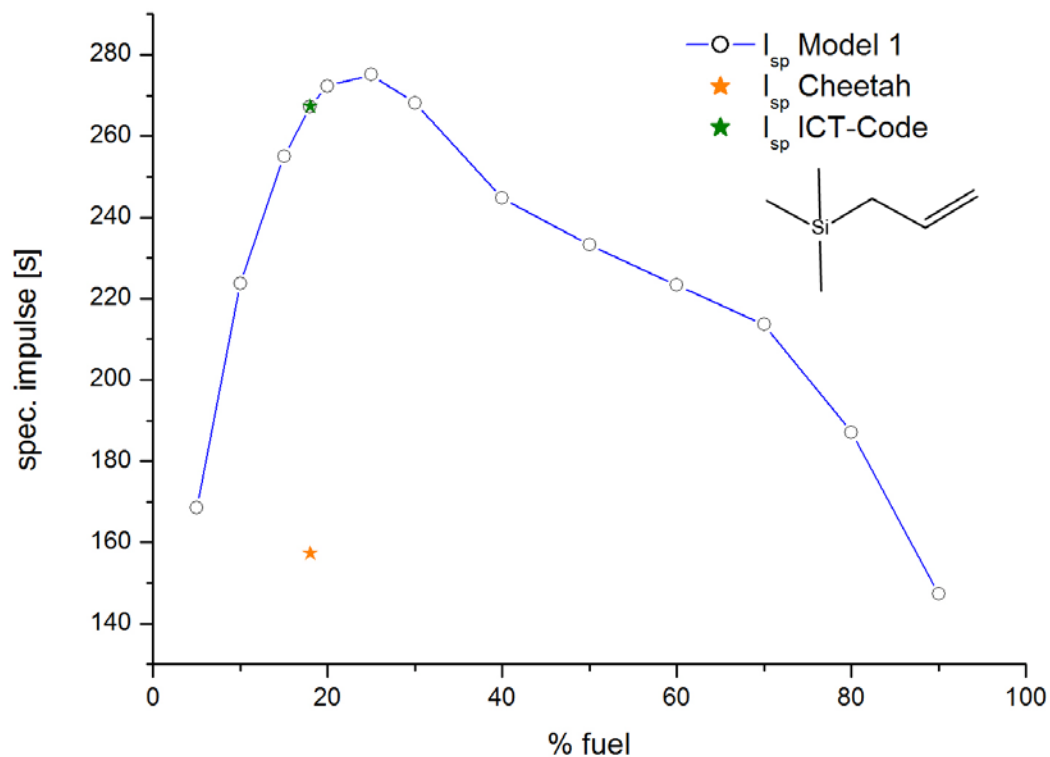
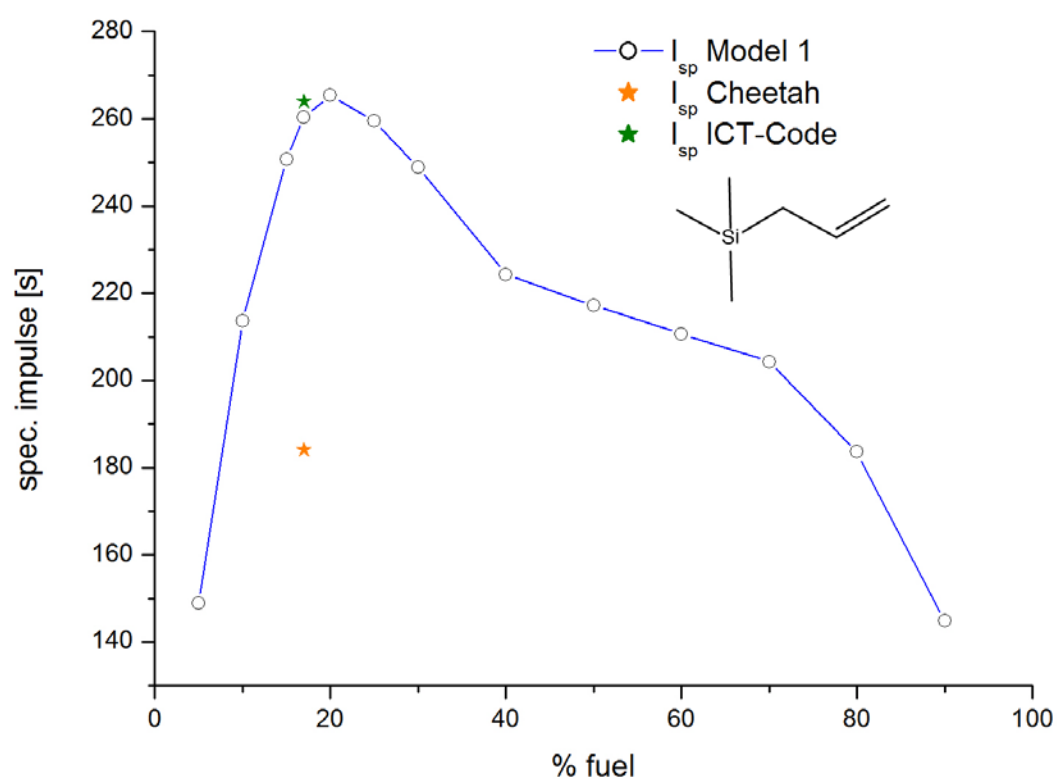
**Figure S37:** Specific impulse values versus different amounts of N_2O_4 calculated of **8** with different computer codes

Table S49: Propulsion parameters (T_c , I_{sp} and oxygen balance) of **8** computed with EXPL05 (Model 1) with RFNA

T_{dec} [°C]	T_c [K]	I_{sp} [s]	Oxygen balance [atm] in %	8 / RFNA
85	1311	148.9	45.20079	5 / 95
	2485	213.7	27.34534	10 / 90
	3121	250.8	9.489878	15 / 85
	3225	260.4	2.347686	17 / 83
	3252	265.4	-8.365583	20 / 80
	3008	259.5	-26.22105	25 / 75
	2633	248.9	-44.0765	30 / 70
	1797	224.3	-79.78741	40 / 60
	1711	217.2	-115.4983	50 / 50
	1650	210.7	-151.2092	60 / 40
	1601	204.3	-186.9202	70 / 30
	1371	183.6	-222.6311	80 / 20
	1021	144.9	-258.342	90 / 10

**Figure S38:** Specific impulse values versus different amounts of RFNA calculated of **8** with different computer codes

18. Tetravinylsilane (9)

Table S50: Propulsion parameters (T_c , I_{sp} and oxygen balance) of **9** computed with EXPL05 (Model 1) with N_2O_4

T_{dec} [°C]	T_c [K]	I_{sp} [s]	Oxygen balance [atm] in %	9 / N_2O_4
130	1862	168.7	51.98459	5 / 95
	2974	223.8	34.41737	10 / 90
	3412	255.1	16.85016	15 / 85
	3532	268.4	2.796393	19 / 81
	3564	270.9	-0.717049	20 / 80
	3526	277.5	-18.28426	25 / 75
	3242	274.9	-35.85147	30 / 70
	2345	255.6	-70.9859	40 / 60
	2583	248.4	-106.1203	50 / 50
	2150	237.5	-141.2548	60 / 40
	2079	227.3	-176.3892	70 / 30
	1931	213.4	-211.5236	80 / 20
	1601	186.9	-246.658	90 / 10

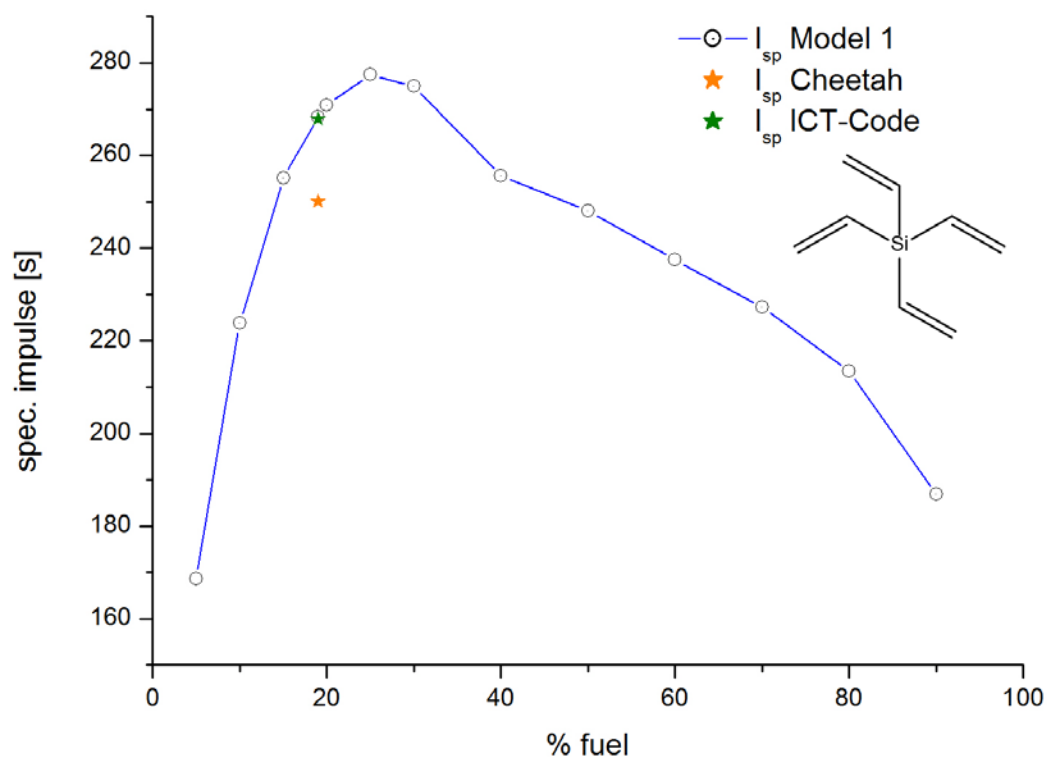
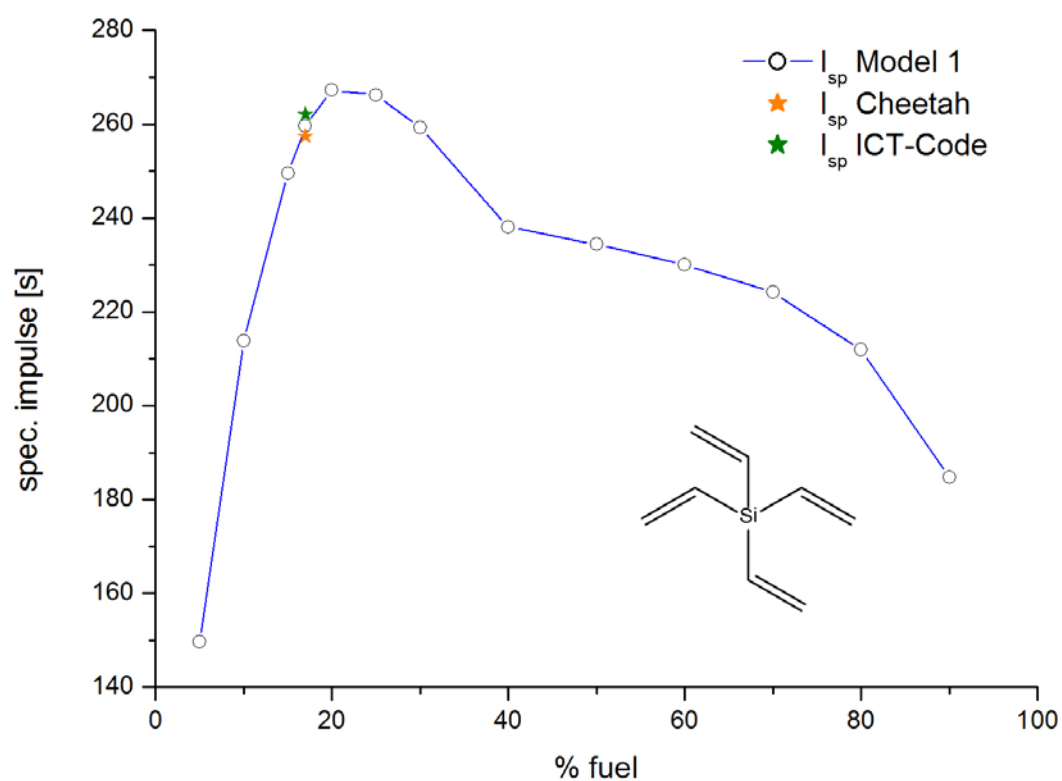
**Figure S39:** Specific impulse values versus different amounts of N_2O_4 calculated of **8** with different computer codes

Table S51: Propulsion parameters (T_c , I_{sp} and oxygen balance) of **9** computed with EXPL05 (Model 1) with RFNA

T_{dec} [°C]	T_c [K]	I_{sp} [s]	Oxygen balance [atm] in %	9 / RFNA
130	1333	149.6	45.81382	5 / 95
	2538	213.9	28.57138	10 / 90
	3178	249.5	11.32895	15 / 85
	3296	262.0	1.640483	17 / 83
	3342	267.3	-5.913486	20 / 80
	3209	266.3	-23.15593	25 / 75
	2930	259.3	-40.39836	30 / 70
	2201	238.1	-74.88323	40 / 60
	2178	234.4	-109.3681	50 / 50
	2132	230.1	-143.853	60 / 40
	2057	224.2	-178.3378	70 / 30
	1897	211.9	-212.8227	80 / 20
	1558	184.7	-247.3076	90 / 10

**Figure S40:** Specific impulse values versus different amounts of RFNA calculated of **9** with different computer codes

19. CHEETAH 2.0 values

Table S52: Propulsion values (I_{sp} and T_c) computed with CHEETAH 2.0 for different compounds (X) and oxidizers (ox)

compound	T_{dec} [°C]	T_c [K]	I_{sp} [s]	X / Ox	oxidizer
1	100	1864	181.81	20 / 80	AP
1c	100	2025	193.83	18 / 82	AP
2	100	3247	255.56	15 / 85	AP
2c	100	2574	222.93	13 / 87	AP
3	100	1727	174.73	16 / 84	AP
3c	100	2124	199.07	15 / 85	AP
4	100	2513	214.10	16 / 84	AP
4c	100	2764	232.84	14 / 86	AP
5a	100	2920	236.87	13 / 87	AP
5b	100	3040	243.18	13 / 87	AP
5c	100	3023	242.59	13 / 87	AP
6a	100	3174	250.07	15 / 85	AP
6b	100	3143	249.49	15 / 85	AP
6c	100	3122	248.32	15 / 85	AP
6d	100	3096	246.93	15 / 85	AP
4	100	2750	239.49	12 / 88	ADN
4c	100	2894	251.11	11 / 89	ADN
4	100	1968	179.39	28 / 72	N ₂ O ₄
4c	100	2461	210.10	26 / 74	N ₂ O ₄
7	55	1270	141.45	19 / 81	N ₂ O ₄
8	85	1532	157.36	18 / 82	N ₂ O ₄
9	130	3423	250.14	19 / 81	N ₂ O ₄
7	55	1680	171.58	18 / 82	RFNA
8	85	1905	184.12	17 / 83	RFNA
9	130	3364	257.45	17 / 83	RFNA

20. ICT-Code values

Table S53: Propulsion values (I_{sp}) computed with ICT-Code for different compounds (X) and oxidizers (ox)

compound	T_{dec} [°C]	I_{sp} [s]	X / Ox	oxidizer
1	100	256.3	20 / 80	AP
1c	100	252.5	18 / 82	AP
2	100	256.0	15 / 85	AP
2c	100	252.8	13 / 87	AP
3	100	251.7	16 / 84	AP
3c	100	251.2	15 / 85	AP
4	100	254.1	16 / 84	AP
4c	100	249.7	14 / 86	AP
5a	100	250.4	13 / 87	AP
5b	100	251.0	13 / 87	AP
5c	100	251.1	13 / 87	AP
6a	100	253.4	15 / 85	AP
6b	100	253.1	15 / 85	AP
6c	100	253.0	15 / 85	AP
6d	100	253.7	15 / 85	AP
4	100	263.5	12 / 88	ADN
4c	100	262.2	11 / 89	ADN
4	100	266.6	28 / 72	N ₂ O ₄
4c	100	270.9	26 / 74	N ₂ O ₄
7	55	268.9	19 / 81	N ₂ O ₄
8	85	267.4	18 / 82	N ₂ O ₄
9	130	267.9	19 / 81	N ₂ O ₄
7	55	266.2	18 / 82	RFNA
8	85	264.0	17 / 83	RFNA
9	130	262.2	17 / 83	RFNA